1141

RESEARCH IN

THE GEYSERS–CLEAR LAKE GEOTHERMAL AREA,

NORTHERN CALIFORNIA

[illegible]
DEPOSITORY 376

GEOLOGICAL SURVEY PROFESSIONAL PAPER 1141

I 19.16:

COVER

View southeastward at geothermal development in the Geysers steam field. Large steam plumes rise from condensing towers of numerous electrical powerplants; smaller plumes rise from geothermal wellheads. Northwest-flowing Big Sulphur Creek has excavated the canyon that transects the photograph from upper right to lower left. Hydrothermal leakage from the steam reservoir occurs along faults that cut rocks of the Franciscan assemblage along the northeast side of Big Sulphur Creek canyon. The altered rocks are prone to extensive landslides, many of which are visible here. Prominent flat-topped peak on the central horizon is Cobb Mountain, a 1.1-million-year-old silicic volcanic center of the Clear Lake Volcanics.

RESEARCH IN THE GEYSERS-CLEAR LAKE GEOTHERMAL AREA, NORTHERN CALIFORNIA

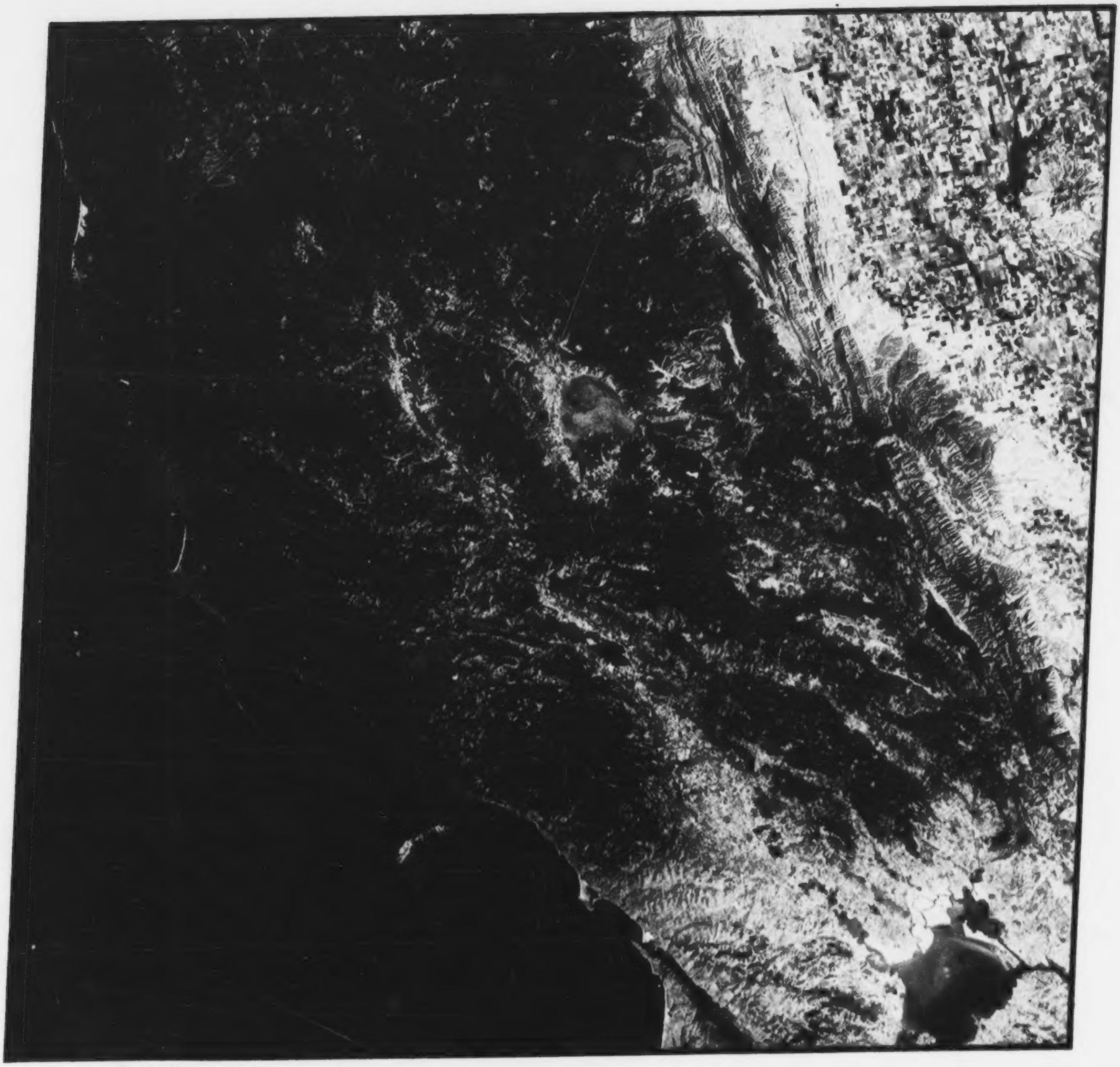

Landsat image of a part of northwestern California, showing Clear Lake in the center, Lake Berryessa to the southeast, Suisun Bay still farther south (lower right corner), and the Pacific Ocean to the west. Agricultural development in the western Sacramento Valley is visible northeast of Clear Lake. Two smaller closed valleys, visible west of Clear Lake, that are alined along a northwestward trend are Little Lake Valley to the northwest and Ukiah Valley with Lake Mendocino on the southeast. The present area of geothermal development in the Geysers steam field is encircled. Northwest-trending hogback ridges, composed of late Mesozoic sedimentary rocks of the Sacramento Valley that mark the west side of the Great Valley physiographic province, contrast with the more heterogeneous intricately dissected terrane of the Coast Range province to the west. Sutter Buttes, a center of late Cenozoic volcanism in the center of Sacramento Valley, is visible in the upper right corner. Along the southwest coast can be seen the rift of the San Andreas fault, trending southeast from Point Arena and passing through Bodega Head and Tomales Bay in the lower part of the photograph.

Research in the Geysers-Clear Lake Geothermal Area, Northern California

ROBERT J. McLAUGHLIN *and* JULIE M. DONNELLY-NOLAN, *Editors*

GEOLOGICAL SURVEY PROFESSIONAL PAPER 1141

Contributions from:

Cascadia Exploration Corporation, Consulting Geologists
Simon Fraser University
Stanford University
U.S. Department of the Interior, Geological Survey
University of California, Berkeley
University of California, Davis
University of Texas, Dallas

March 3, 1849

UNITED STATES GOVERNMENT PRINTING OFFICE, WASHINGTON : 1981

UNITED STATES DEPARTMENT OF THE INTERIOR
JAMES G. WATT, *Secretary*

GEOLOGICAL SURVEY
Doyle G. Frederick, *Acting Director*

Research in the Geysers-Clear Lake geothermal area, northern California.

(Geological Survey professional paper ; 1141)

Supt. of Docs. no.: I 19.16.1141
1. Geology--California--The Geysers region. 2. Geothermal resources--
California--The Geysers region. I. McLaughlin, Robert J.
II. Donnelly-Nolan, Julie M. III. Cascadia Exploration Corporation.
IV. Series: United States. Geological Survey. Professional Paper
1141.
QE90.G45R45 557.94 80-607169

For sale by the Superintendent of Documents, U.S. Government Printing Office
Washington, D.C. 20402

CONTENTS

Page

Introduction, by R. J. McLaughlin and J. M. Donnelly-Nolan, U.S. Geological Survey 1

Tectonic setting of pre-Tertiary rocks and its relation to geothermal resources in the Geysers-Clear Lake area, by Robert J. McLaughlin, U.S. Geological Survey 3

The Clear Lake Volcanics: Tectonic setting and magma sources, by B. Carter Hearn, Jr., Julie M. Donnelly-Nolan, and Fraser E. Goff, U.S. Geological Survey 25

Geochronology and evolution of the Clear Lake Volcanics, by Julie M. Donnelly-Nolan and B. Carter Hearn, Jr., U.S. Geological Survey, and Garniss H. Curtis and Robert E. Drake, University of California at Berkeley 47

Strontium isotopes in the Clear Lake Volcanics, by Kiyoto Futa, Carl E. Hedge, B. Carter Hearn, Jr., and Julie M. Donnelly-Nolan, U.S. Geological Survey 61

Paleomagnetism of the Clear Lake Volcanics and new limits on the age of the Jaramillo normal-polarity event, by E. A. Mankinen, J. M. Donnelly-Nolan, C. S. Grommé, and B. C. Hearn, Jr., U.S. Geological Survey 67

Geophysical overview of The Geysers, by William F. Isherwood, U. S. Geological Survey 83

Large teleseismic *P*-wave delays in the Geysers-Clear Lake geothermal area, by H. M. Iyer, David H. Oppenheimer, Tim Hitchcock, Jeffrey N. Roloff, and John M. Coakley, U.S. Geological Survey 97

Seismic-reflection investigations at Castle Rock Springs in the Geysers geothermal area, by Roger P. Denlinger and Robert L. Kovach, Stanford University 117

Seismicity of the Geysers-Clear Lake region, by C. G. Bufe, S. M. Marks, F. W. Lester, R. S. Ludwin, and M. C. Stickney, U.S. Geological Survey 129

Monitoring crustal deformation in the Geysers-Clear Lake region, by Ben E. Lofgren, U.S. Geological Survey 139

Attenuation of teleseismic *P* waves in the Geysers-Clear Lake region, by Chi Yuh Young and Ronald W. Ward, University of Texas, Dallas 149

A detailed gravity survey of the Wilbur Springs area, California, by John M. Harrington and Kenneth L. Verosub, University of California at Davis 161

Seismic-refraction measurements of crustal structure near Santa Rosa and Ukiah, California, by David H. Warren, U.S. Geological Survey 167

Chemical analyses of waters from springs and wells in the Clear Lake volcanic area, by J. M. Thompson, F. E. Goff, and J. M. Donnelly-Nolan, U.S. Geological Survey 183

Variability and sources of hydrogen sulfide and other gases in steam at The Geysers, by Charles A. Brook, U.S. Geological Survey 193

Gases from springs and wells in the Geysers-Clear Lake area, by Nancy L. Nehring, U.S. Geological Survey 205

Carbon-13 isotope values for carbon dioxide gas and dissolved carbon species in springs and wells in the Geysers-Clear Lake region, by Mark Huebner, U.S. Geological Survey 211

Chemical composition of water and gas from five nearshore subaqueous springs in Clear Lake, by J. M. Thompson, J. D. Sims, Sandhya Yadav, and M. J. Rymer, U.S. Geological Survey 215

Late Pleistocene stratigraphy and palynology of Clear Lake, by John D. Sims, David P. Adam, and Michael J. Rymer, U.S. Geological Survey 219

Pliocene and Pleistocene fishes from the Clear Lake area, by Richard W. Casteel, Simon Fraser University, and Michael J. Rymer, U.S. Geological Survey 231

Mercury in the sediments of Clear Lake, by John D. Sims and Donald E. White, U.S. Geological Survey 237

Faulting and ore controls at the Culver-Baer mine, Sonoma County, California, by Eugene V. Ciancanelli, Cascadia Exploration Corporation 243

Preliminary investigation of accessory zircons from volcanic and sedimentary rocks from Clear Lake, by Frederick A. Wilson, U.S. Geological Survey 251

ILLUSTRATIONS

Page

FRONTISPIECE. Landsat image of a part of northwestern California

FIGURE 1. Map showing generalized regional geology of northern Coast Ranges of California and location of the Geysers steam field 4

2. Schematic drawings showing plate-tectonic reconstruction for North American plate margin from 40 m.y. ago to present 7

3. Map of northern California showing northward progression of Tertiary and Quaternary volcanism with time, major northwest-trending faults of San Andreas fault system, and extrapolated positions of Mendocino fracture zone between 3 and 5 m.y. ago 8

Page

FIGURE 4. Schematic drawing showing major crustal features of northern California and their relation to emplacement of magma beneath the Geysers-Clear Lake area 10
5. Generalized geologic map and cross sections of the Geysers steam field 12
6. Structural model for the Geysers geothermal system 14
7. Map and diagram showing pattern of faulting over the Geysers steam reservoir 16
8. Block diagram illustrating relation of open fault and fracture networks of the Geysers steam reservoir to principal vectors of regional horizontal compression and extension 17
9. Map showing complex structural high associated with the Castle Rock Springs area of the Geysers steam field 18
10. Map showing geology of The Geysers Resort area 19
11. Diagram showing hypothetical open fractures in structural highs produced by horizontal extension and by horizontal compression 20
12. Geologic map and cross section of diapiric structure associated with unproductive exploratory wells in the Geysers steam field 21
13. Map showing age and distribution of volcanic rocks, central Coast Ranges 26
14. Geologic map and outline of present magma chamber 28
15. Fault map showing Clear Lake Volcanics 30
16. Maps showing distribution of young volcanic rocks, Clear Lake area 32
17. SiO_2 variation diagrams for Clear Lake Volcanics and other rocks 34
18. AFM diagrams for Clear Lake Volcanics and other rocks 38
19. Graph showing patterns of rare-earth elements 39
20. Location map of samples for potassium-argon dating 49
21. Generalized correlation chart showing Clear Lake Volcanics 52
22. Graph showing volumes of lava erupted during each period of activity 57
23. Graph of total erupted volumes of lava 57
24. Map showing sample localities in the Clear Lake Volcanics 62
25-28. Graphs showing:
  25. $^{87}Sr/^{86}Sr$ ratios versus K-Ar ages 64
  26. Rubidium versus strontium concentrations 64
  27. $^{87}Sr/^{86}Sr$ ratios versus rubidium concentrations 64
  28. $^{87}Sr/^{86}Sr$ ratios versus strontium concentrations 65
29. Map of Clear Lake area showing prominent topographic features and sample localities 68
30-35. Diagrams showing:
  30. Stratigraphic relations, K-Ar ages, and magnetic polarity of units related to Jaramillo normal-polarity event 70
  31. Average remanent magnetization directions for older lavas of Mount Hannah area 71
  32. Average remanent magnetization directions for younger lavas of Mount Hannah area 71
  33. Average remanent magnetization directions showing sequence of eruption for andesite of Split-Top Ridge, andesite of Poison Smith Spring, and dacite of Harrington Flat 72
  34. Average remanent magnetization directions for localities sampled in rhyolite of Alder Creek 75
  35. Four types of strong-field thermomagnetic curves 76
36. Histograms showing NRM intensity, susceptibility, and Koenigsberger ratio for rock types of Clear Lake Volcanics 78
37. Chart showing polarity and K-Ar ages of Clear Lake Volcanics 79
38. Map showing VGP positions for transitional lavas from Clear Lake and Matuyama-Brunhes polarity transition from Lake Tecopa, Calif. 80
39-44. Maps of the Geysers area showing:
  39. Residual gravity 84
  40. Upward-continued magnetic field 85
  41. Pseudogravity derived from filtered aeromagnetic data 87
  42. Generalized geology and apparent resistivity 89
  43. Generalized horizontal ground movement, 1972-77 92
  44. Gravity changes between July 1974 and February 1977 93
45. Graph and section showing correlation between subsidence, gravity decrease, and pressure decline at The Geysers 93
46. Map showing generalized volcanism and plate tectonics of Western United States 93
47. Diagram of proposed evolution of Clear Lake Volcanics from severed limb of subducting Farallon plate 94
48. Generalized geologic map of the Geysers-Clear Lake geothermal area 98
49. Residual gravity map of the Geysers-Clear Lake region 99
50. Map showing inferred approximate outlines of vapor-dominated and steam-production zones in the Geysers-Clear Lake region 99
51. Seismogram showing two typical teleseisms recorded by telemetered network in the Geysers-Clear Lake region 101
52. Illustrations showing computer manipulation of seismograms 102
53. Graphs showing variation of relative residuals as a function of distance and azimuth 107
54. Relative residual contour maps 108
55. Profile of northwest and southeast residual values and gravity along line *A-A'* 110
56. Map showing calculated depth to bottom of anomalous body 112

Page

FIGURE 57. Map showing composite of figure 56 ... 114
58. Conceptual model of subsurface structure and percentage decrease in velocity in the Geysers-Clear Lake region ... 115

59-61. Maps showing:

59. Regional geology and structure of the Geysers-Castle Rock Springs geothermal area ... 118
60. Regional geology and structure of study area ... 119
61. Locations of seismic stations and producing steam wells in study area ... 120
62. Stacked seismic section along line two showing reflection profile and two-way traveltime ... 121
63. Geologic section along reflection line two ... 124
64. Interval velocity section calculated for seismic line two ... 124
65. Stacked seismic section along line one showing reflection profile and two-way traveltime ... 125
66. Geologic section along reflection line one ... 128
67. Interval velocity section calculated for seismic line one ... 128

67-72. Maps showing:

68. Evolution of the U.S. Geological Survey seismograph network north of San Francisco Bay ... 129
69. Preliminary epicenters of earthquakes north of San Francisco Bay 1969-78 ... 131
70. Earthquake events in the Geysers geothermal area ... 132
71. Two main clusters of microearthquakes recognized at The Geysers ... 134
72. Representative focal-plane solutions for earthquakes in the Geysers-Clear Lake region ... 136
73. Diagrams showing temporal changes in stress orientation from focal-plane solutions in the Geysers region ... 137
74. Map showing regional setting of the Geysers geothermal production area and network of first-order leveling in the Geysers-Clear Lake area ... 141
75. Map showing network of precise horizontal control in the Geysers-Clear Lake geothermal area in relation to areas of present and potential geothermal production and major fault systems ... 142
76. Graph of measured vertical changes in the Geysers area, 1973-77, relative to bench mark R1243 ... 143
77. Profiles of vertical change through the geothermal production area, 1973-77 ... 144
78. Graph of relation of subsidence to reservoir pressure along line *A-A'* ... 144
79. Profiles of vertical change southwesterly across the Mayacmas Mountains, 1973-77 ... 145
80. Graph of generalized horizontal ground movement in the Geysers-Clear Lake area, 1972-77 ... 146
81. Graph of changing rates of ground movement on lines spanning the geothermal production area ... 147
82. Generalized geologic and structural map of the Geysers-Clear Lake area showing location of seismic array ... 150
83. Diagram showing sample *P*-wave seismograms recorded by the Geysers-Clear Lake array for three events ... 152
84. Diagram of teleseismic *P* wave incident beneath a model geothermal system ... 153
85. Graphs showing power density spectra and spectral ratios from the Geysers-Clear Lake array for a typical event ... 154
86. Graph showing dominant frequencies of *P* phases along northwest-southeast line ... 155
87. Graphs showing differential attenuation for each station as a function of distance and azimuth ... 155
88. Maps showing two-dimensional contoured surface fitted to averaged δt^* ... 156
89. Graph showing simplified *Q* model for the Geysers-Clear Lake area ... 158
90. Bouguer gravity map of the Geysers-Clear Lake area over area of seismic-attenuation study ... 159
91. Map showing location of Wilbur Springs study area and Clear Lake volcanic field ... 162
92. Map showing generalized geology of Wilbur Springs quadrangle ... 163
93. Residual Bouguer gravity map of Wilbur Springs area ... 164
94. Map showing locations of seismic recording stations, shotpoints, and faults, Santa Rosa-Ukiah area ... 168
95. Traveltime plots and velocity profile for southwesterly shots ... 171
96. Traveltime plots and velocity profile for northeasterly shots ... 172
97. Traveltime plot for northeasterly profile through The Geysers ... 174
98. Record sections for Roblar shotpoint ... 175
99. Record sections for Geysers shotpoint ... 178
100. Plots of time squared versus distance squared for Roblar and Skaggs Springs shotpoints ... 180
101. Map showing generalized geologic setting of the Geysers steam field ... 194
102. Diagram of conceptual model of fluid movement in a vapor-dominated geothermal system ... 195
103. Map showing sampling sites in the Geysers-Clear Lake area ... 205
104. Chromatograms of hydrocarbon gas analyses ... 208
105. Map showing sampling sites in the Geysers-Clear Lake region ... 211
106. Graph showing carbon isotope composition of samples from the Geysers-Clear Lake region compared with isotopic compositions of possible sources ... 212
107. Generalized map of Clear Lake and vicinity, showing location of sample sites ... 215
108. Plot of lithium versus chloride ... 218
109. Map showing location of Clear Lake and core sites ... 219
110. Diagram showing ash-bed correlations in eight cores from Clear Lake ... 222
111. Chart showing age-depth relation in cores 4 and 7, Clear Lake, and in Lake Biwa, Japan ... 224
112. Diagrams showing oak, pine, and TCT pollen frequencies for cores 4 and 7 ... 225
113. Diagram showing oak-pollen frequency curve from Clear Lake and ^{18}O curve from Pacific Ocean ... 228
114. Map showing fossil-fish localities in the Cache, Lower Lake, and Kelseyville Formations, Lake County, Calif. ... 231

Page

FIGURE 115. Photographs of fossil otoliths from the Kelseyville Formation 235
116. Map showing location of cores 6 and 10 in Oaks Arm of Clear Lake with respect to Sulphur Bank mercury mine 237
117. Diagram showing summary of data from core 6 239
118. Geologic map of the Geysers and Culver-Baer mine area 244
119. Diagrammatic cross section of part of Mercuryville fault zone as exposed in Culver-Baer mine 245
120. Geologic sketch map of Field stope area of Culver-Baer mine 246
121. Geologic map and cross section of Culver-Baer mine 248
122. Geologic map showing location of samples, Clear Lake 252
123. Histograms of crystal type, idiomorphism, and inclusions of zircon from rocks from Clear Lake 253
124-128. Graphs showing data comparing zircon sample populations of rocks from Clear Lake:
  124. Reduced major axes 255
  125. Scatter plots 256
  126. Elongation-frequency curves 256
  127. Length-frequency curves 256
  128. Breadth-frequency curves 257

TABLES

Page

TABLE 1. K-Ar dates and analytical data, Clear Lake Volcanics 50
2. Rubidium and strontium concentrations and $^{87}Sr/^{86}Sr$ ratios, Clear Lake Volcanics 63
3. Paleomagnetic results and K-Ar ages 69
4. Magnetic properties of Clear Lake volcanic rocks 77
5. Geographic information on and periods of operation of the seismic stations located south of Clear Lake 100
6. List of teleseisms 104
7. Mean relative residuals and their standard deviations for three azimuth groups 104
8. Descriptions of earthquakes shown on figure 72 137
9. List of teleseismic events used in this study 152
10. List of differential attenuation δt^*, in milliseconds, for each station 156
11. Comparison of gravity stations 163
12. Descriptions of shots and shotpoints 167
13. Traveltime data 169
14. Equations of traveltime curves 173
15. Calculated crustal structure 173
16. Reflection investigation 174
17. Chemical analyses of thermal water samples from Clear Lake volcanic field 184
18. Composition (weight percent) of steam from wells at The Geysers 193
19. Initial gas concentrations in steam entries encountered during drilling of wells in the southern part of the Geysers steam field 197
20. Average incoming H_2S concentrations at full steam flow for generating units at the Geysers powerplant 198
21. Major-gas analyses of the Geysers-Clear Lake area 206
22. Residual-gas analyses of the Geysers-Clear Lake area 207
23. Hydrocarbon-gas analyses of the Geysers-Clear Lake area 207
24. Carbon-13 isotope values for CO_2 (gas) and dissolved carbon species in springs and wells in the Geysers-Clear Lake region 212
25. Chemical analyses of spring water along the shore of Clear Lake 217
26. Chemical analyses of spring gases along the shore of Clear Lake 217
27. Total length and recovery and the number of ash beds and estimated maximum age for eight cores from Clear Lake 219
28. Descriptions of cores from Clear Lake 221
29. Grain-size analyses from core 4, Clear Lake 221
30. Radiocarbon dates from Clear Lake cores 4 and 7 223
31. Location, specific distribution, and listing of fossil fish parts recovered in the Cache, Lower Lake, and Kelseyville Formations 232
32. Specific distribution of fossil fish in the Cache, Lower Lake, and Kelseyville Formations and in cores from Clear Lake, and present-day Clear Lake 234
33. Mercury analyses for cores 6 and 10, Clear Lake 240
34. Sample locations 253
35. Statistical size data for zircon samples, Clear Lake 254
36. Z tests of reduced major axes of zircons from Clear Lake 254

RESEARCH IN THE GEYSERS-CLEAR LAKE GEOTHERMAL AREA, NORTHERN CALIFORNIA

INTRODUCTION

By R. J. McLaughlin and J. M. Donnelly-Nolan

The Geysers-Clear Lake area is one of two places in the world where major vapor-dominated hydrothermal reservoirs are commercially exploited for electric power production. Because energy can be extracted more efficiently from steam than from hot water, vapor-dominated systems are preferable for electric power generation, although most geothermal electric power facilities tap water-dominated systems. The Geysers-Clear Lake geothermal system has therefore been of great interest to the geothermal industry.

This geothermal area straddles the deeply dissected Mayacmas Mountains, which rise to over 1,500 meters (4,600 feet) on the southwest, and other northwest-trending ridges of the Coast Ranges that range in elevation from 1,800 m (6,000 ft) to less than 600 m (2,000 ft) to the north, east, and south. Clear Lake basin is a volcanotectonic depression bounded by these elevated areas. The climate and vegetation of this part of the Coast Ranges is typical of the Mediterranean area, with moderate to heavy annual precipitation that locally exceeds 250 centimeters (100 inches) in the Mayacmas Mountains, but is as low as 50 cm (20 in.) in Clear Lake basin. Most precipitation occurs between the months of October and May, commonly accompanied by snow above 900-m elevations. Mean annual temperatures are about 15°C (60°F), with summer temperatures ranging to well above 37°C (100°F) and winter temperatures locally reaching well below freezing. Vegetation patterns are affected by climate, elevation, and soil type. Grassland, scrub oak, stands of cypress, manzanita, and other chaparral-type plants are distributed between the lowlands and the moderately high ridges. Evergreen conifers and some deciduous plants, such as dogwood, are restricted to higher elevations and often are specific to soils developed on certain rock types, such as serpentinite and rhyolite.

The Geysers-Clear Lake area was famous for its thermal springs long before interest in geothermal development. From the late 1860's to the early 1900's, when mineral baths and spas were in their heyday in the United States, those in Lake and Sonoma Counties were known internationally, including The Geysers Resort. Present tourism in the area now revolves around interest in the geothermal industry, although there has been a recent revival in the recreational use of some hot springs. Generating electricity from natural steam was seriously considered as early as the 1920's by the Geysers Development Company. Allen and Day demonstrated the feasibility of such a venture by drilling the first wells at The Geysers Resort in 1927. However, the technology for large-scale transport of steam for production of electrical energy did not then exist in the United States, and it was not until the late 1950's that Magma Power Company and Thermal Power Company entered into an agreement with Pacific Gas and Electric Company and built a commercially competitive geothermal power plant at The Geysers, which went into production in 1960. Since then, many private companies have been involved in exploration and expansion of the Geysers steam field. Presently, proven steam resources underlie an area of approximately 600 square kilometers defined by more than 130 productive steam wells that produce about 700 megawatts of electricity. By 1983, production will reach 1,238 megawatts.

Geologic investigations that largely predate the U.S. Geological Survey's geothermal research program in the Geysers-Clear Lake area began at least as early as the quicksilver investigations of G. F. Becker in 1888. Later, more thorough investigations of mercury deposits in the Mayacmas Mountains and Clear Lake area include those of Bailey, Yates, and Hilpert in 1946, A. N. Moisseeff in 1966, and papers by D. E. White and various coworkers in the 1960's. A paper by C. A. Anderson, published in 1936, is perhaps the most comprehensive study of the chemistry, petrography, and geologic relations of the Clear Lake Volcanics before the recent investigations by the U.S. Geological Survey. The geochronologic and paleomagnetic work of E. A. Mankinen on the Sonoma Volcanics in 1972 remains a chief reference for these rocks. Previous regional investigations of similar geologic and tectonic significance include that of J. C. Brice in 1953, several short papers and maps by J. R. McNitt in the 1960's, and a paper by Win Swe and W. R. Dickinson in 1970. Important published investigations of the geochemistry of thermal and mineral springs include those of G. A. Waring in 1951 and 1968, and many papers by Ivan Barnes, D. E. White, and their coworkers in the 1960's and 1970's. These previous investigations are cited throughout this volume.

The U.S. Geological Survey began a long-term research program in the Geysers-Clear Lake area in 1972 under the direction of L. J. P. Muffler and later by R. L. Christiansen and W. A. Duffield, coordinators of all geothermal research for the Geologic Division of the U.S.G.S. from 1972 to 1980. The range of this program is evident in the table of contents of this volume. Papers in this volume present many of the main results of this endeavor as well as contributions from researchers outside the U.S. Geological Survey. Some papers are not directly related to geothermal research but nevertheless characterize important aspects of the geologic history and tectonics of the Geysers-Clear Lake area.

In most respects the reader will find agreement among the various authors about the nature and extent of the geothermal system and its heat source. However, in detail, the reader will find differences in geophysical and geologic models. We hope that such differences in interpretation will stimulate further research to test various hypotheses. The models presented here to explain different aspects of the Geysers-Clear Lake geothermal system are by no means the only ones that can explain the data, and they will undoubtedly be tested and improved with further exploration and development in the area. The validity of such models and their endurance in the literature depend respectively on the present data upon which the models are based and on how they hold up under the accumulation of new data and theories that will surely follow publication of these papers.

Any use of trade names or trademarks in this publication is for descriptive purposes only and does not constitute endorsement by the U.S. Geological Survey.

TECTONIC SETTING OF PRE-TERTIARY ROCKS AND ITS RELATION TO GEOTHERMAL RESOURCES IN THE GEYSERS-CLEAR LAKE AREA

By Robert J. McLaughlin

ABSTRACT

The Geysers-Clear Lake geothermal area lies within the central belt of the Franciscan assemblage in northern California. The structure of this terrane is characterized by northeast-dipping imbricate thrust slices that have been warped and cut by steeply dipping strike-slip and normal faults. Introduction of magma into the crust beneath the Geysers-Clear Lake area can be related to east-southeast extension accompanying northward propagation of the San Andreas transform system between the Clear Lake region and Cape Mendocino within the last 3 million years. The initiation of strike-slip faulting during this time terminated subduction of elements of the Farallon plate beneath North America as strike-slip motion was taken up along the Pacific-North American plate boundary. The mechanism for magma generation appears to require a heat source in the mantle that mixed mantle-derived melts with various crustal rocks. These crustal rocks may have included the Franciscan central and coastal belts, ophiolite, Great Valley sequence, and possibly middle and late Tertiary rocks subducted before initiation of strike-slip faulting.

The Geysers steam reservoir is on the northeast limb of a major southeast-plunging antiform in late Mesozoic rocks of the Franciscan assemblage. The reservoir also coincides with the southwest side of a major negative gravity anomaly interpreted to delineate the presence of magma within the upper crust. The most significant factors limiting the extent of the steam reservoir seem to be the distribution of heat and open-fracture networks, the presence of cap rocks that retain fluid in the reservoir rocks, and the presence of areas of adequate hydrothermal leakage that allow the system to remain vapor-dominated.

The orientation of regional stress determined from earthquake studies in the Geysers area implies that north- to northeast-oriented steeply dipping faults and fractures should produce maximum horizontal extension in the steam reservoir. Vertical extension may also be significant in gently dipping or subhorizontal fractures in the axial regions of anticlinal warps and horstlike structures. Local structures of probable significance to steam production include a structural high associated with the Castle Rock Springs area, and southeast-plunging folds in Franciscan rocks overthrust by serpentinite near The Geysers Resort.

Specific areas and mechanisms of natural recharge to the Geysers steam reservoir are poorly known. However, the vent areas for rhyolite and dacite that cap Cobb Mountain may provide conduits that allow deep circulation into the reservoir rocks. Northeast of the steam field, the numerous vents underlying a thick cover of volcanic rocks may have promoted the development of a hot-water-dominated geothermal system due to an excess of recharge.

INTRODUCTION

The Geysers steam field of northern California is the world's largest commercial geothermal development exploited for the purpose of electrical production. The area of commercial development lies within a roughly circular 600-km^2 area over which young volcanism and active hydrothermal manifestations are apparent. The vapor-dominated Geysers steam reservoir occupies about 300 km^2 along the southwest side of the geothermal region, extending to unknown depths below about 3 km. The steam reservoir is entirely within an allochthonous basement of complexly deformed and metamorphosed marine sedimentary and igneous rocks assigned to the Franciscan assemblage and to the largely coeval Great Valley sequence.

The structure of these late Mesozoic and early Tertiary rocks and present regional tectonics strongly influence the geothermal system. In this report I describe these structural and tectonic relations, with particular reference to the recent studies of the U.S. Geological Survey and to plate-tectonic concepts.

TECTONIC SETTING OF THE GREAT VALLEY SEQUENCE AND THE FRANCISCAN ASSEMBLAGE

The northern California Coast Ranges east of the San Andreas fault (fig. 1) consist mainly of two approximately coeval units now separated by a great regional thrust referred to as the Coast Range thrust (Bailey and others, 1970). The upper plate of the Coast Range thrust consists of a fragmented ophiolite complex of Late Jurassic age (the Coast Range ophiolite), considered to represent oceanic crust (Bailey and others, 1970; McLaughlin and Pessagno, 1978), overlain depositionally by moderately deformed marine sedimentary rocks referred to as the Great Valley sequence (Bailey and others, 1964). The Great Valley sequence ranges in age from Late Jurassic to Late Cretaceous and consists of coarse ophiolite breccia or tuff near the base (McLaughlin and Pessagno, 1978) overlain by conglomerate, mudstone, and sandstone. The Great Valley sequence is interpreted to represent arc-trench gap or fore-arc basin deposits that were derived from Klamath and Sierran island-arc terranes as a series of coalescing submarine fans (Dickinson, 1970; Ingersoll

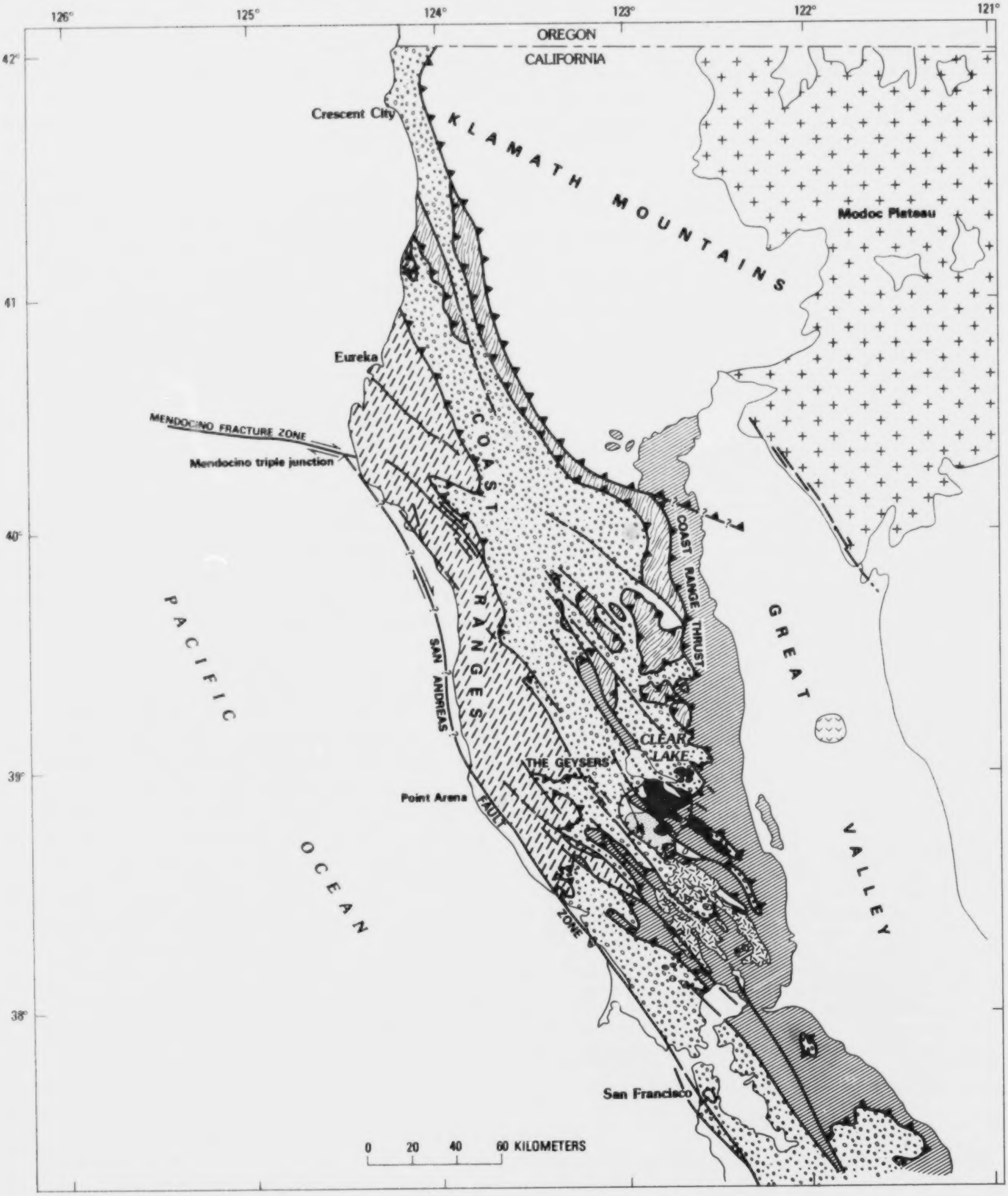
126°
125°
124°
123°
122°
121°
42°
41°
40°
39°
38°
OREGON
CALIFORNIA
Crescent City
KLAMATH MOUNTAINS
Modoc Plateau
Eureka
MENDOCINO FRACTURE ZONE
Mendocino triple junction
COAST RANGES
COAST RANGE THRUST
GREAT VALLEY
PACIFIC OCEAN
SAN ANDREAS FAULT ZONE
CLEAR LAKE
THE GEYSERS
Point Arena
San Francisco
0 20 40 60 KILOMETERS

and others, 1977). The basal part of the Great Valley sequence was largely derived from the depositionally underlying Coast Range ophiolite (McLaughlin and Pessagno, 1978).

Rocks in the lower plate of the Coast Range thrust have been assigned to the Franciscan assemblage (or Franciscan Complex of Berkland and others, 1972) and consist of a heterogeneous assemblage of intensely deformed and mildly to moderately metamorphosed sandstone, shale, chert, and mafic igneous rocks. Serpentinite, limestone, amphibolite, eclogite, and high-grade blueschist are minor but significant constituents. Franciscan rocks and their equivalents are now known to extend along the Pacific coast of North America at least from Baja California, Mexico, to southern Alaska (Jones and others, 1977). Initial deformation and metamorphism of these rocks apparently occurred in Cretaceous and early Tertiary time, as the result of oblique northeast-directed subduction and strike-slip. Popular plate-tectonic models (Hamilton, 1969; Dickinson, 1970; Blake and Jones, 1974) interpreted rocks of the Franciscan assemblage to have been deposited in a trench over an east-dipping subduction zone located to the west of the fore-arc basin of the Great Valley sequence. However, paleomagnetic evidence presented recently by Jones and others (1977) and Alvarez and others (1979), and arguments put forth by McLaughlin and Pessagno (1978), suggested that this model is overly simplistic. The paleomagnetic data indicate that as much as 30° of northward translation of Mesozoic plate elements occurred along the Pacific margin in pre-Late Cretaceous time (Jones and others, 1977). The data of Alvarez and others (1979) imply 56°–57° of late Cretaceous or younger northward translation. It is not clear what the relative importance of transforms and oblique subduction were in these displacements, but by implication, elements of the Franciscan assemblage and possibly even the Great Valley sequence may have sustained large-scale northward displacement from their original sites of deposition before, during, or after periods of pre-Late Cretaceous subduction.

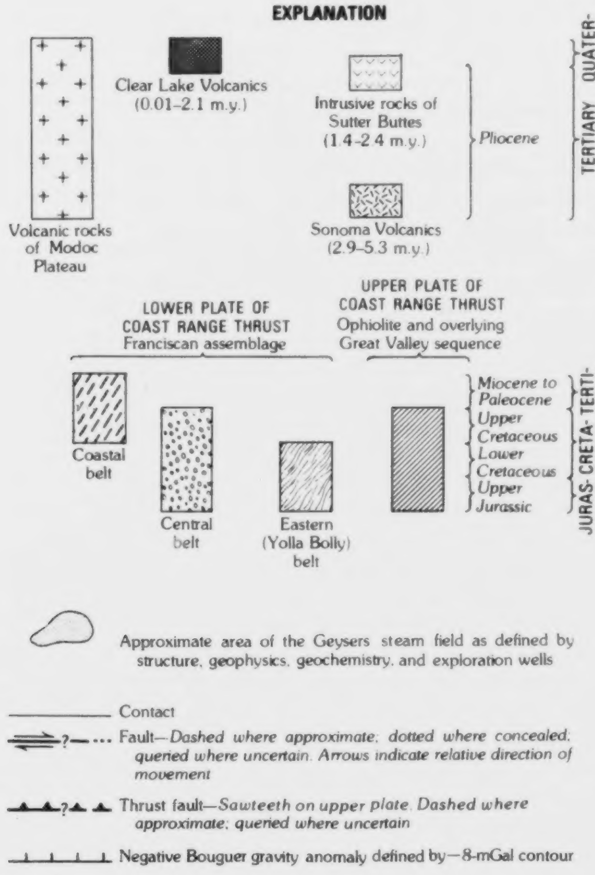
EXPLANATION
Clear Lake Volcanics (0.01–2.1 m.y.)
Intrusive rocks of Sutter Buttes (1.4–2.4 m.y.)
Sonoma Volcanics (2.9–5.3 m.y.)
Pliocene
TERTIARY
QUATERNARY
Volcanic rocks of Modoc Plateau
LOWER PLATE OF COAST RANGE THRUST
Franciscan assemblage
UPPER PLATE OF COAST RANGE THRUST
Ophiolite and overlying Great Valley sequence
Coastal belt
Central belt
Eastern (Yolla Bolly) belt
Miocene to Paleocene
Upper Cretaceous
Lower Cretaceous
Upper Jurassic
TERTIARY
CRETACEOUS
JURASSIC
Approximate area of the Geysers steam field as defined by structure, geophysics, geochemistry, and exploration wells
Contact
Fault—Dashed where approximate; dotted where concealed; queried where uncertain. Arrows indicate relative direction of movement
Thrust fault—Sawteeth on upper plate. Dashed where approximate; queried where uncertain
Negative Bouguer gravity anomaly defined by −8-mGal contour

FIGURE 1.—Generalized regional geology of northern Coast Ranges of California, showing location of the Geysers steam field.

In northern California, the Franciscan assemblage has been divided into broad northwest-trending thrust-fault-bounded structural belts by Berkland and others (1972), Blake and Jones (1974), and Jones, Blake, Bailey, and McLaughlin (1978). (1) The eastern (Yolla Bolly) belt of Late Jurassic and Early Cretaceous age (fig. 1) is composed of intact lawsonite-grade metamorphosed sandstone, with minor interbedded chert and very minor interbedded metamorphosed igneous rocks. (2) The somewhat younger central belt to the west is composed of rocks of Late Jurassic to Late Cretaceous age that were probably deformed into extensive melanges and broken formations in later Cretaceous time. The broken formations of the central belt consist of pumpellyite to lawsonite-grade metamorphosed sandstone and argillite, basaltic igneous rocks, and chert; they differ from the melanges in displaying local stratal continuity, in being significantly less penetratively sheared, in having less argillite in relation to sandstone, and generally in not containing exotic blocks such as eclogite, amphibolite, high-grade blueschist, or serpentinite. (3) The youngest western (coastal) belt of Late Cretaceous to Miocene age consists mainly of broken formations of K-feldspar-bearing laumontite-grade arkosic sandstone and shale. Basaltic igneous rocks, blueschist, eclogite, amphibolite, limestone, and chert are rare in the coastal belt. These various belts of Franciscan rocks have probably sustained large components of strike-slip movement relative to one another and to the upper plate of the Coast Range thrust, in addition to major crustal shortening associated with subduction.

BLUESCHIST METAMORPHISM AND EMPLACEMENT OF THE COAST RANGE THRUST

Two principal occurrences of blueschist are recognized in the Franciscan assemblage: (1) displaced blocks of high-grade fine-grained to coarsely crystalline blueschist that were derived from metamorphosed basalt, eclogite, amphibolite, or rocks with more siliceous protoliths; and (2) extensive intact terranes of graywacke and minor interbedded chert and igneous rocks that have been metamorphosed to blueschist grade and contain lawsonite. The first type of blueschist is most common as blocks in melange terranes, especially along the west side of the central belt. High-grade blueschist blocks are rare in the coastal belt but occur sporadically in some melanges in the eastern Franciscan belt. The second type of blueschist is typical of most of the eastern belt and also occurs in several large slabs in the central belt.

The unusual depressed temperature and high pressure gradients necessary to produce blueschist mineral assemblages (Coleman and Lee, 1963; Bailey and others, 1964) are widely regarded as indicative of conditions encountered in subduction zones (Bailey and others, 1970; Ernst, 1970, 1971; Platt, 1975). The age of this blueschist metamorphism is thought to constrain the timing of subduction. Coleman and Lanphere (1971) dated glaucophane and white mica from high-grade blueschist blocks in the Franciscan assemblage by K-Ar methods and demonstrated that the metamorphism took place in the Late Jurassic, about 150 m.y. ago. In contrast, dating of highly reconstituted blueschist-grade metamorphosed graywacke from the South Fork Mountain Schist of the eastern belt by conventional and ^{40}Ar/^{39}Ar methods (Lanphere and others, 1978) suggests a metamorphic age of 115–120 m.y. for these rocks. Suppe and Armstrong (1972) found a wide age range of 150 to 70 m.y. for blueschist metamorphism of eastern and central belt rocks, and they interpreted this wide age range to indicate that subduction occurred in the Late Jurassic and sporadically throughout most of the Cretaceous simultaneously with sedimentation.

Blake, Irwin, and Coleman (1967) documented a regional increase in the degree of schistosity in graywackes of the eastern Franciscan belt that corresponds to an increase in abundance of blueschist minerals such as lawsonite. It was found that both degree of schistosity and development of high-pressure mineral assemblages increase structurally upward toward the Coast Range thrust. This inverted metamorphic zonation was related by them to emplacement of the Coast Range thrust. Bailey, Blake, and Jones (1970) later interpreted the Coast Range thrust as the hanging wall of a subduction zone. By this interpretation, the age of blueschist metamorphism gave a maximum age of 115–120 m.y. for emplacement of the Coast Range thrust above rocks of the eastern Franciscan belt (about Aptian or Albian time). However, in the Geysers-Clear Lake area inverted metamorphic zonation adjacent to the Coast Range thrust cannot be demonstrated except locally because of postmetamorphic imbrication of eastern belt rocks with central belt rocks. Furthermore, paleontologic evidence from the Geysers area demonstrates that emplacement of the Coast Range ophiolite above the Franciscan central belt occurred no earlier than Cenomanian time, or less than about 96 m.y. ago in that area (McLaughlin and Pessagno, 1978).

SOURCE TERRANES FOR THE FRANCISCAN ASSEMBLAGE

The source areas for Franciscan detritus have been eliminated by subduction or transform faulting or both. The original location and composition of these source areas are unknown, although some insights can be obtained from study of the petrology and sedimentology of Franciscan sandstone and conglomerate.

In spite of the association of Franciscan sandstone with mafic igneous rocks and chert of oceanic affinity, the sandstone compositions reflect island-arc or continental sources. These sandstones are arkosic to subarkosic in composition, although some are also volcanic-lithic (R. J. McLaughlin and H. N. Ohlin, unpub. data; Blake and Jones, 1978). The ages of radiolarians present in abundant chert detritus in conglomerate of the central belt indicate that the chert detritus is derived partly from older Franciscan chert interbedded with graywacke and greenstone of the central belt (McLaughlin and Pessagno, 1978) and partly from older Mesozoic sources (Seiders and others, 1979). More than 20 percent K-feldspar is typically found in sandstone of the coastal belt, 0–6 percent is typical of sandstone along the west side of the central Franciscan belt, and usually only 1 percent or less in the sandstone in the main part of the central and eastern belt. This eastward regional decrease in K-feldspar may be partly due to development of white mica at the expense of K-feldspar with increasing metamorphism.

The presence of early Mesozoic hypabyssal silicic and intermediate plutonic rocks and of pelagic sedimentary clasts in several conglomerates in the central Franciscan belt and lower part of the Great Valley sequence led Seiders, Pessagno, and Harris (1979) to suggest the Calaveras Formation and its equivalents in the Sierra Nevada and Klamath Mountains as possible sources for this detritus. An island arc active to the west in the early Tertiary has been proposed by Beutner (1977) to explain the bimodal compositions of andesitic and quartzofeldspathic graywacke sequences in the Franciscan coastal belt. Other island-arc terranes, including Early Cretaceous arc-related rocks at Trinidad Head in northern California and an arc thought to have been the source for the Late Jurassic Otter Point Formation in southwestern Oregon (Blake and Jones, 1978), are also possible sources of Franciscan sandstone detritus.

The provenance of the blocks of amphibolite and eclogite present in melange of the Franciscan central belt is unknown. The high temperatures and pressures of formation of the mineral assemblages in these rocks suggest that they are displaced from lower crust and upper mantle levels. Many of the blocks have sheared and polished rinds of actinolite and serpentinite, and other blocks contain retrograde blueschist mineral assemblages. Emplacement of these rocks into the melanges must have involved large vertical displacements and at least partial transport within serpentinite, possibly accompanied by large-scale gravity or submarine sliding.

TERTIARY AND QUATERNARY TECTONICS

Plate-tectonic reconstructions (fig. 2) by Atwater (1970) and Blake and others (1978) trace the evolution of the San Andreas transform fault system from the time that the North American plate came into contact with the Pacific and Farallon oceanic plates about 40 m.y. ago. This triple junction (the Mendocino triple junction) migrated north along the North American plate margin from southern California to its present position at Cape Mendocino in northern California, terminating subduction that was occurring north of the triple junction and initiating a broad right-lateral transform shear (the San Andreas fault system) southeast of the propagating transform front.

The western part of the North American plate now consists largely of elements of the Farallon plate that were accreted by subduction and strike-slip during the Late Cretaceous and Tertiary before passage of the Mendocino triple junction. The Franciscan coastal belt and at least part of the Franciscan central belt probably consist of elements of the Farallon plate.

Data of E. A. Silver (published by Blake and others, 1978) show that the azimuth of shear between the Pacific and North American plates (fig. 2*B*) shifted westward between about 10 m.y. ago and the present, resulting in a slightly extensional regime along and within the San Andreas fault system. This change in motion facilitated creation of extensional basins within the San Andreas fault system and in the northern Coast Ranges. Examples of these basins in northern California are Ukiah and Little Lake Valleys, Round Valley, and Clear Lake basin, all of which are typical of the types of extensional basins proposed by Crowell (1974a, b) to lie within a major strike-slip fault system.

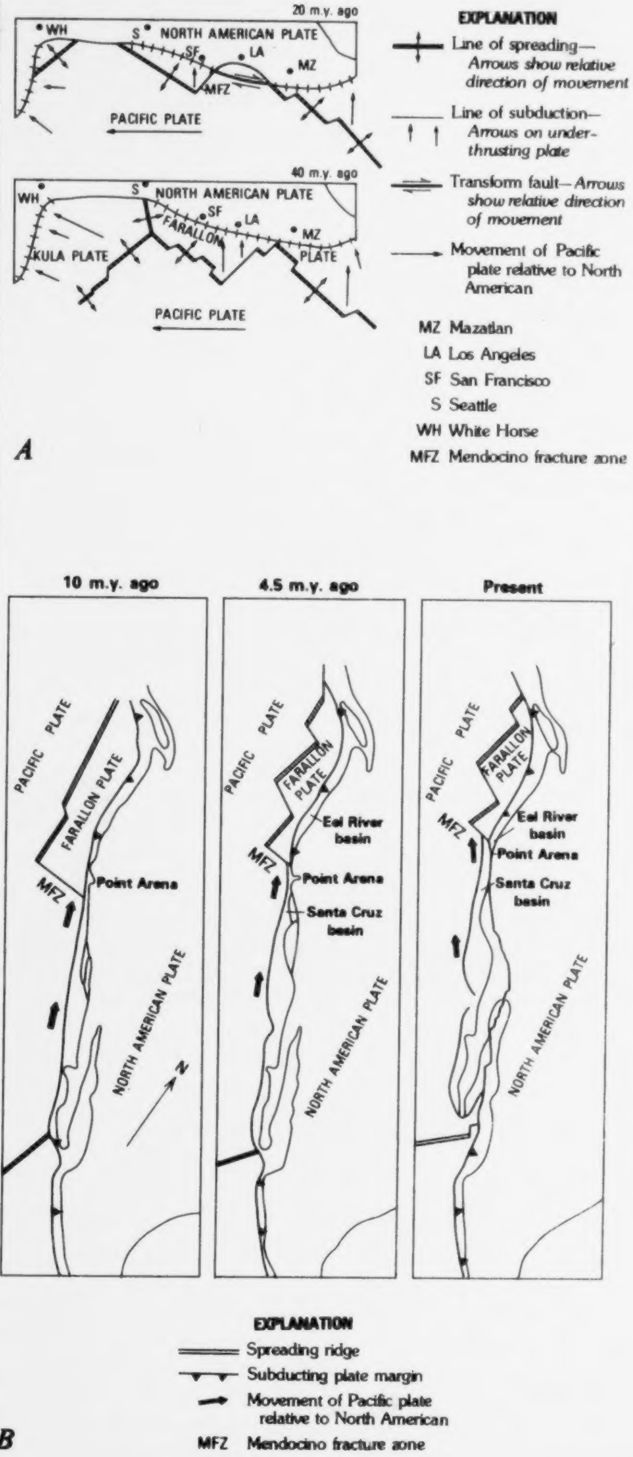
20 m.y. ago
WH
S
NORTH AMERICAN PLATE
SF
LA
MZ
MFZ
PACIFIC PLATE
40 m.y. ago
WH
S
NORTH AMERICAN PLATE
SF
LA
FARALLON
PLATE
MZ
KULA PLATE
PACIFIC PLATE
A
EXPLANATION
Line of spreading—Arrows show relative direction of movement
Line of subduction—Arrows on underthrusting plate
Transform fault—Arrows show relative direction of movement
Movement of Pacific plate relative to North American
MZ Mazatlan
LA Los Angeles
SF San Francisco
S Seattle
WH White Horse
MFZ Mendocino fracture zone
10 m.y. ago
4.5 m.y. ago
Present
PACIFIC PLATE
FARALLON PLATE
MFZ
Point Arena
NORTH AMERICAN PLATE
N
PACIFIC PLATE
FARALLON PLATE
Eel River basin
MFZ
Point Arena
Santa Cruz basin
NORTH AMERICAN PLATE
PACIFIC PLATE
FARALLON PLATE
MFZ
Eel River basin
Point Arena
Santa Cruz basin
NORTH AMERICAN PLATE
B
EXPLANATION
Spreading ridge
Subducting plate margin
Movement of Pacific plate relative to North American
MFZ Mendocino fracture zone

FIGURE 2.—Plate-tectonic reconstruction of North American plate margin from 40 m.y. ago to present, using reconstructions of: *A*, Atwater (1970) from 40 to 20 m.y. ago; and *B*, those of Blake and others (1978) from 10 m.y. ago to present.

Plate reconstructions by Silver further indicated that subduction terminated and that the San Andreas system was initiated in the northern Coast Ranges between Point Arena and Cape Mendocino within the last 10 m.y. (fig. 2*B*). The average rate of right-lateral motion for the last 4–6 m.y. between the Pacific and North American plates is estimated at about 5.5 cm/yr (Atwater and Molnar, 1973). Extrapolation of the Mendocino triple junction backward in time along the present boundary between the North American and

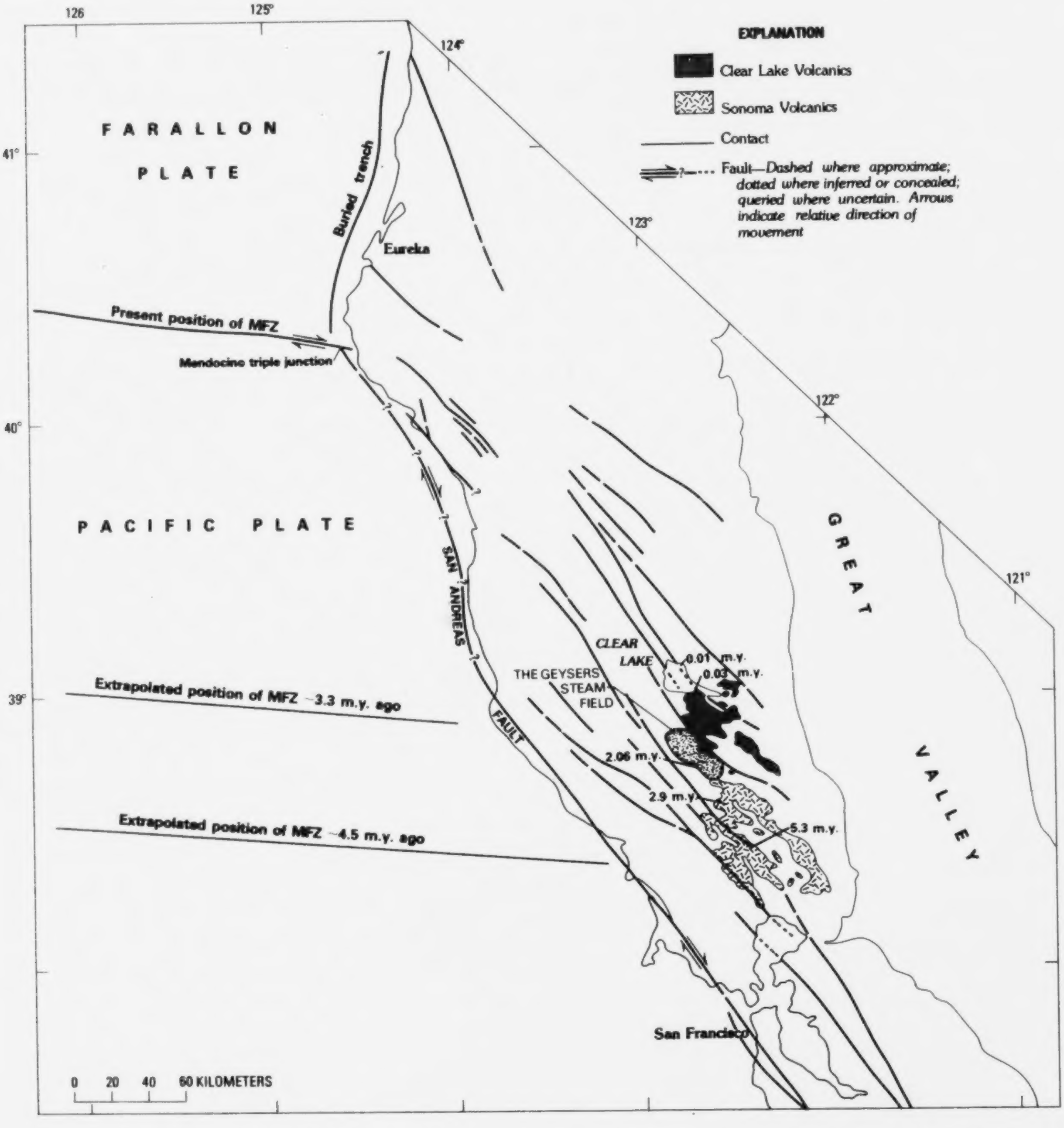
126
125°
124°
123°
122°
121°
41°
40°
39°
EXPLANATION
Clear Lake Volcanics
Sonoma Volcanics
Contact
Fault—Dashed where approximate; dotted where inferred or concealed; queried where uncertain. Arrows indicate relative direction of movement
FARALLON PLATE
Buried trench
Eureka
Present position of MFZ
Mendocino triple junction
PACIFIC PLATE
SAN ANDREAS FAULT
GREAT VALLEY
CLEAR LAKE
THE GEYSERS STEAM FIELD
0.01 m.y.
0.03 m.y.
2.06 m.y.
2.9 m.y.
5.3 m.y.
Extrapolated position of MFZ ~3.3 m.y. ago
Extrapolated position of MFZ ~4.5 m.y. ago
San Francisco
0 20 40 60 KILOMETERS

FIGURE 3.—Northward progression of Tertiary and Quaternary volcanism with time, major northwest-trending faults of San Andreas fault system, and extrapolated positions of Mendocino fracture zone (MFZ) between 3 and 5 m.y. ago. Ages of volcanic rocks from Donnelly-Nolan, Hearn, Curtis, and Drake (this volume) and Mankinen (1972).

Pacific plates (the San Andreas fault) at this rate suggests that the triple junction was opposite the latitude of the Geysers-Clear Lake area approximately 3 m.y. ago (fig. 3). Significant components of Pacific-North American plate motion apparently are also taken up by subsidiary faults in the strike-slip system east of the main San Andreas fault (fig. 3; Herd, 1979). This implies that Clear Lake basin and several other San Andreas-related extensional basins between Clear Lake and Cape Mendocino are less than 3 m.y. old. The orientation and position of the present Eel River basin north of Cape Mendocino (Ogle, 1953) suggests that it may be one of the basins suggested by Blake and others (1978) to have formed in front of the northward-propagating Mendocino triple junction (figs. 2*B*, 3, and 4).

The timing of Clear Lake volcanism indicates that it closely followed passage of the Mendocino triple junction and propagation of San Andreas-related extensional structures. Propagation of the triple junction past the Clear Lake area appears to have preceded the changeover from Sonoma to Clear Lake volcanism between 2.9 and 2.1 m.y. ago. Hearn, Donnelly-Nolan, and Goff (this volume) argue that volcanism in the northern Coast Ranges shifted northward with time (fig. 3) as the North American plate passed over a stationary mantle plume or hot spot.

I favor a model for emplacement of magma into the crust beneath the Geysers-Clear Lake area that is closely tied to passage of the Mendocino triple junction and crustal extension within the San Andreas fault system (McLaughlin, 1977a). Donnelly (1977) also related late Cenozoic volcanism and magma emplacement to propagation of the San Andreas fault system. Sonoma and Clear Lake volcanism might thus be characterized as magma leakage along a propagating land-bound transform fault system. North- to northeast-oriented normal faults associated with right-lateral shear couples within the San Andreas system apparently acted as the conduits for venting of the Clear Lake magmas (Hearn and others, this volume).

Magma sources for the region are highly conjectural, but strontium isotope and trace-element studies of the Clear Lake Volcanics (Futa and others, and Hearn and others, this volume) suggest that the lavas are derived at least in part from primitive mantle material that underwent considerable mixing with various crustal rocks, in addition to fractional crystallization and assimilation at different levels in the crust. A stationary hot spot or mantle plume might have provided the heat for these melts (Hearn and others, this volume). However, absolute motion of North America derived from assuming the presence of a mantle-stationary hot spot is significantly more complex than suggested in the simple hot-spot model of Morgan (1972), and crustal characteristics suggested by Morgan to be associated with most hot spots apparently cannot be applied to the Geysers-Clear Lake area.

In an alternative model to the hot-spot concept, mantle rocks are emplaced into the crust through extension near or at the propagating end of the San Andreas transform. Extension would thus allow rapid upward emplacement of mantle material into the crust, accompanied by pressure release, which would in turn allow the crust and mantle rocks to melt. Dickinson and Snyder (1979) demonstrated that triangular areas of extension can be left in the wake of an unstable migratory triple junction like the Mendocino triple junction.

In figure 4, I attempt to show the relations of regional tectonics and deep crustal conditions to the presence of magma beneath the Geysers-Clear Lake area. Clear Lake magmas have passed upward through the Franciscan central belt and rocks in the upper plate of the Coast Range thrust; they may also have passed through the Franciscan coastal belt and younger Tertiary rocks subducted with the Farallon plate before the onset of strike-slip.

THE GEYSERS STEAM RESERVOIR

GEOLOGIC SETTING

The Geysers steam reservoir occupies the northeast limb of a complexly faulted southeast-plunging antiform that forms the core of the Mayacmas Mountains (McLaughlin, 1975). The southwest limb of this antiform is sheared right-laterally along several Tertiary and Quaternary faults. The Maacama fault zone, a major active right-lateral fault of the San Andreas system, is the furthest southwest of the faults that bound the Mayacmas antiform. The northeast side of the Mayacmas uplift is bounded by the Collayomi fault zone, another major northwest-trending member of the San Andreas fault system. Major uplift of the Mayacmas Mountains between the Maacama and Collayomi fault zones is due to north-northeast-oriented compression.

Broad, southeast-plunging folds in the Geysers region trend somewhat more westerly than the San Andreas-related strike-slip faults. These folds are in large part the result of late Tertiary and Quaternary north-south compression that either preceded or accompanied strike-slip faulting. Contemporaneous sets of subtle east-trending warps are locally present in uplifted areas between east-west-trending normal and thrust faults (see structural section *A–A′* between geothermal wells CA-1862 and CA-956-1 in fig. 5).

The southeast-plunging folded regional structure of

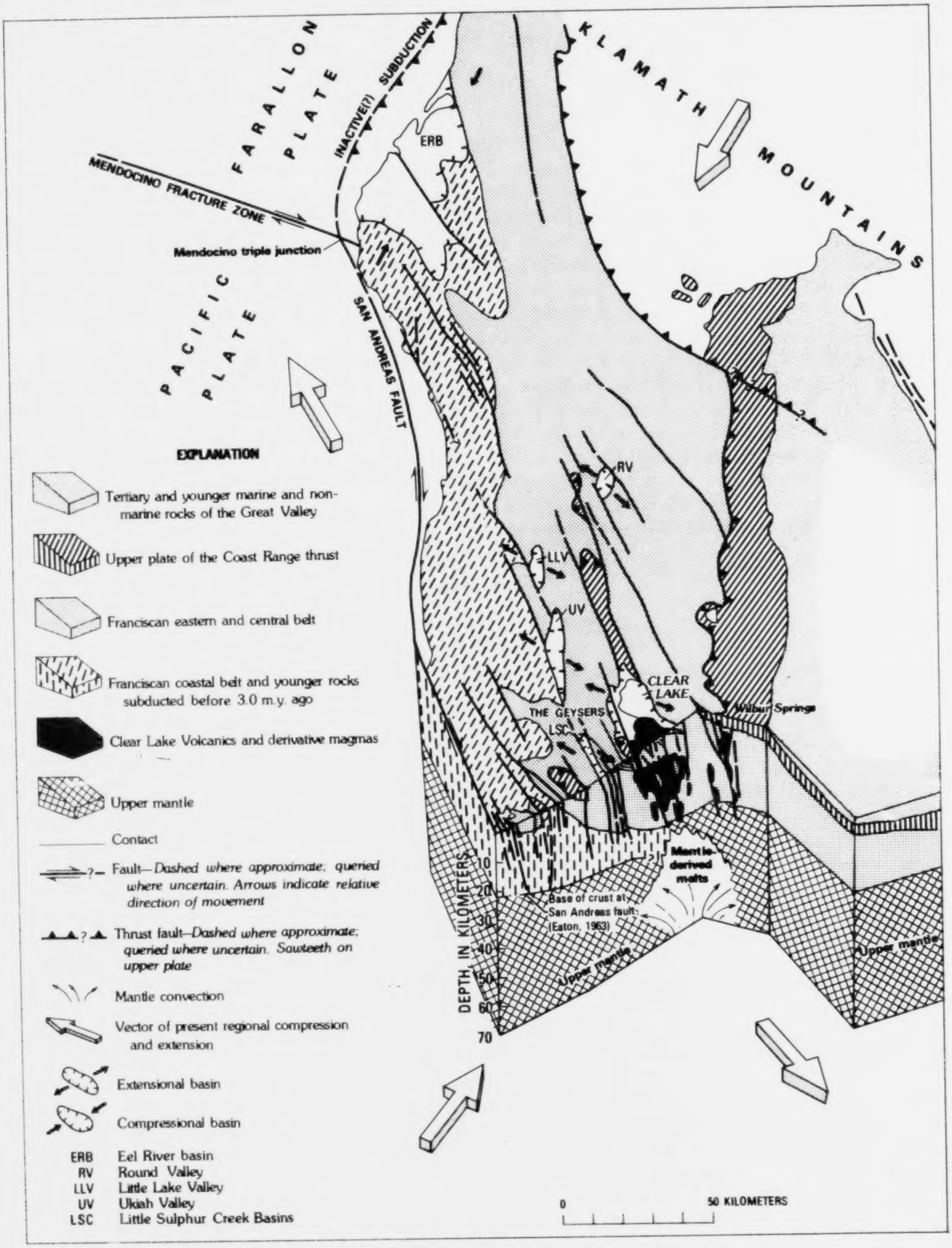
FARALLON PLATE
INACTIVE(?) SUBDUCTION
KLAMATH MOUNTAINS
ERB
MENDOCINO FRACTURE ZONE
Mendocino triple junction
PACIFIC PLATE
SAN ANDREAS FAULT
RV
LLV
UV
CLEAR LAKE
THE GEYSERS
LSC
Wilbur Springs
Mantle-derived melts
Base of crust at San Andreas fault (Eaton, 1963)
Upper mantle
Upper mantle
DEPTH, IN KILOMETERS
10
20
30
40
50
60
70
0
50 KILOMETERS
EXPLANATION
Tertiary and younger marine and nonmarine rocks of the Great Valley
Upper plate of the Coast Range thrust
Franciscan eastern and central belt
Franciscan coastal belt and younger rocks subducted before 3.0 m.y. ago
Clear Lake Volcanics and derivative magmas
Upper mantle
Contact
Fault—Dashed where approximate; queried where uncertain. Arrows indicate relative direction of movement
Thrust fault—Dashed where approximate; queried where uncertain. Sawteeth on upper plate
Mantle convection
Vector of present regional compression and extension
Extensional basin
Compressional basin
ERB Eel River basin
RV Round Valley
LLV Little Lake Valley
UV Ukiah Valley
LSC Little Sulphur Creek Basins

FIGURE 4.—Major crustal features of northern California and their relation to emplacement of magma beneath the Geysers-Clear Lake area.

the area is apparent in the distribution of ophiolite in the upper plate of the Coast Range thrust, and the depositionally overlying strata of the Great Valley sequence (black areas in index map, fig. 5). A thick, folded, and imbricated section of ophiolite and Great Valley sequence is present northeast of the Collayomi fault zone, covered to a large extent by the Clear Lake Volcanics (fig. 5). The ophiolite and Great Valley sequence wrap over Franciscan rocks several kilometers southeast of the map area shown in figure 5 (see McLaughlin and Stanley, 1976) and over the crest of the Mayacmas Mountains just northwest of the summit of Mount St. Helena. On the southwest side of Mount St. Helena, the ophiolite is sheared and fragmented right-laterally along the broad Mercuryville-Geyser Peak-Maacama fault zones. One large mass of ophiolite, which composes Geyser Peak and Black Mountain, is separated right-laterally along this fault system about 18 km from the Mount St. Helena mass. A post-Pliocene right-lateral offset of about 20 km along the Mercuryville-Geyser Peak-Maacama fault zones is also implied by offset of the Sonoma Volcanics along the Maacama fault zone, although at least part of the apparent offset may be due to uplift across the fault zones.

FRANCISCAN ROCKS ASSOCIATED WITH THE STEAM RESERVOIR

Rocks of the central and eastern Franciscan belts compose the uplifted core of the Mayacmas antiform and underlie the entire area of the Geysers steam field. In the Geysers area, these Franciscan rocks are subdivided into several fault-bounded slablike units on the basis of their lithology and their degree of metamorphism (fig. 5). The structurally lowest unit in the area may merely be an intact sandstone slab within the Franciscan central belt. The unit, which is exposed in the core of the Mayacmas antiform between the Mercuryville and Geyser Peak fault zones, consists of well-bedded fine- to coarse-grained graywacke and minor shale with a very weak metamorphic fabric (textural zone 1 of Blake and others, 1967). The rocks of this unit are penetratively sheared and well fractured and constitute a broken formation. The unit is characterized by weak metamorphism (pumpellyite grade) and an absence of chert, greenstone, polymict conglomerate, or exotic blocks. The lower unit extends at depth beneath the area of steam production and probably constitutes part of the reservoir rocks.

The lower structural unit is overlain on the northeast and southwest by an intermediate structural unit consisting in part of large slabs of conglomeratic and lithic graywacke interbedded with chert and basalt flows. These slabs are interleaved with melanges containing sporadic blocks of blueschist, amphibolite, and eclogite, in addition to chert, basalt, and graywacke. The graywacke of the intermediate structural unit is reconstituted to textural zones 1 and 2 of Blake, Irwin, and Coleman (1967) and contains pumpellyite and local lawsonite. Also intercalated in this intermediate structural unit is a thick northeast-dipping slab of actinolitic serpentinite extending about 10 km along strike and traceable northeastward in the subsurface for about 1.5 km from its surface exposure along Big Sulphur Creek (fig. 5). The serpentinite body, along with other highly sheared rocks of the intermediate structural unit, compose a series of thick, northeast-dipping impermeable cap rocks. The interleaved fractured slabs of graywacke in the intermediate structural unit apparently act as reservoir rocks at several different structural levels.

The structurally highest Franciscan rocks in the steam field locally consist of highly reconstituted lawsonitic metagraywacke (textural zone 2 to 3 of Blake and others, 1967) and minor metachert and metavolcanic rocks that may be correlative with the eastern (Yolla Bolly) belt. The metagraywacke of this upper structural unit is extensively recrystallized and may contain jadeite or glaucophane in addition to lawsonite. These rocks have a penetrative schistosity that makes them poorer reservoir rocks than structurally lower, less metamorphosed graywackes.

Large imbricate thrusts of Late Cretaceous and Tertiary age in the map area have juxtaposed rocks of the intermediate and upper Franciscan structural units with ophiolitic rocks in the upper plate of the Coast Range thrust. The lower ultramafic part of the ophiolite has in several places been downdropped along these thrusts and sheared laterally along the thrust boundaries, so that the original base of the upper plate of the Coast Range thrust is difficult or impossible to recognize in many places (fig. 5). These later thrusts may represent transitional structures produced during changes in plate motion from northeast-directed subduction to strike-slip fault movement. The late thrusts formed after initial emplacement of the Coast Range thrust and formation of melanges in the Franciscan central belt, and they include nearly all the thrusts that now separate major structural units in the Geysers area.

BOUNDARIES OF THE STEAM RESERVOIR

The Geysers steam reservoir is apparently confined to the northeast limb of the Mayacmas antiform (fig. 6). It is bounded on the southwest side by the northwest-trending Mercuryville fault zone and on the northeast by the Collayomi fault zone. A hot-water-dominated reservoir whose extent is unknown in detail is present

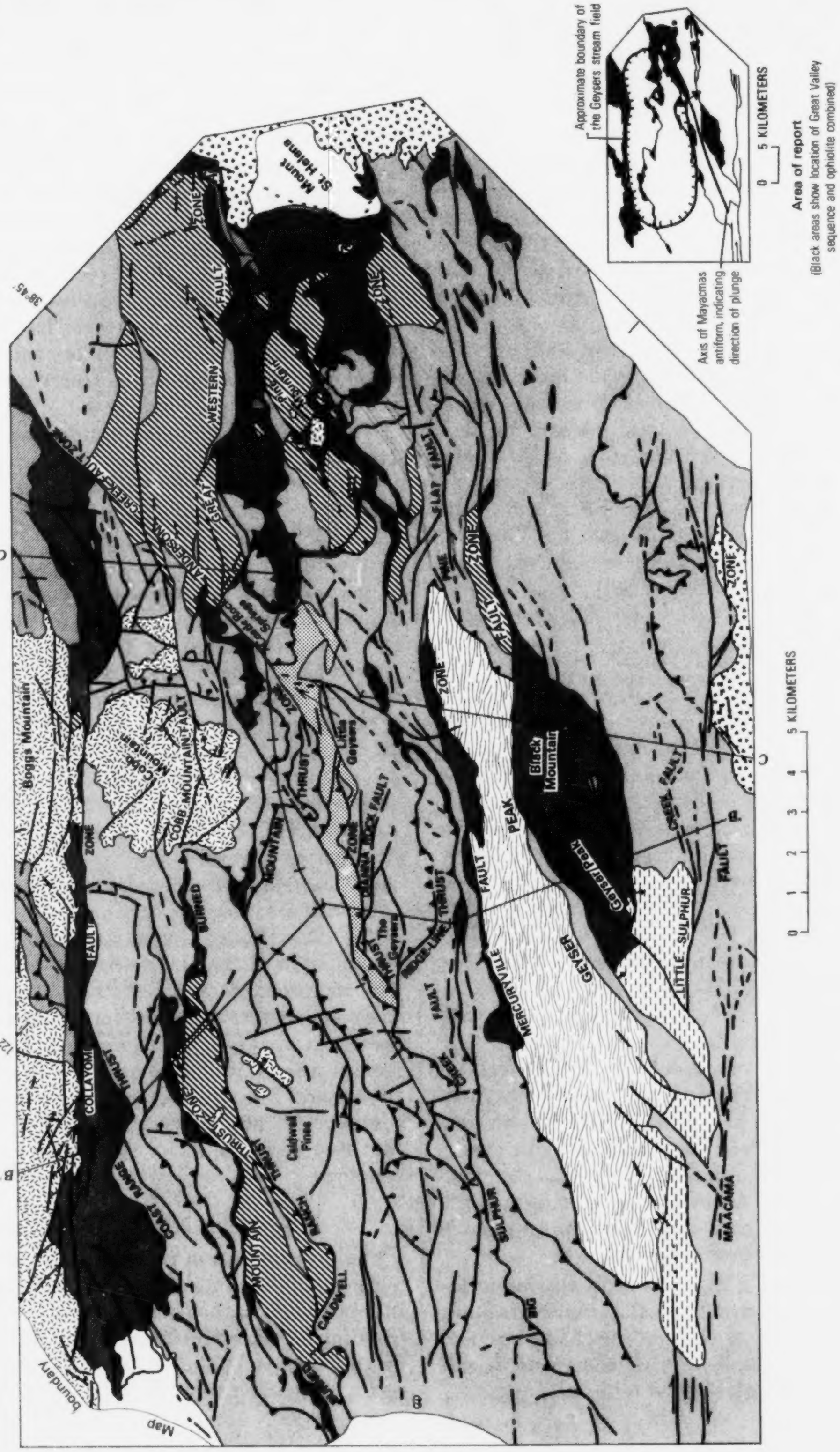
Mount St Helena
WESTERN GREAT VALLEY FAULT ZONE
ANDERSON CREEK FAULT ZONE
PINE FLAT FAULT ZONE
Castle Rock Springs
38°45'
C'
Boggs Mountain
Cobb Mountain
COBB MOUNTAIN FAULT
Little Geysers
MOUNTAIN THRUST ZONE
BURNED
The Geysers
RIDGE LINE THRUST
FAULT ZONE
Black Mountain
Geyser Peak
GEYSER PEAK FAULT
MERCURYVILLE
C
COLLAYOMI FAULT ZONE
THRUST
122°45'
B'
COAST RANGE THRUST ZONE
Caldwell Pines
MOUNTAIN
CALDWELL
BIG SULPHUR CREEK
LITTLE SULPHUR CREEK FAULT ZONE
MAACAMA
B
Map boundary
0 1 2 3 4 5 KILOMETERS
Approximate boundary of the Geysers steam field
Axis of Mayacmas antiform, indicating direction of plunge
0 5 KILOMETERS
Area of report
(Black areas show location of Great Valley sequence and ophiolite combined)

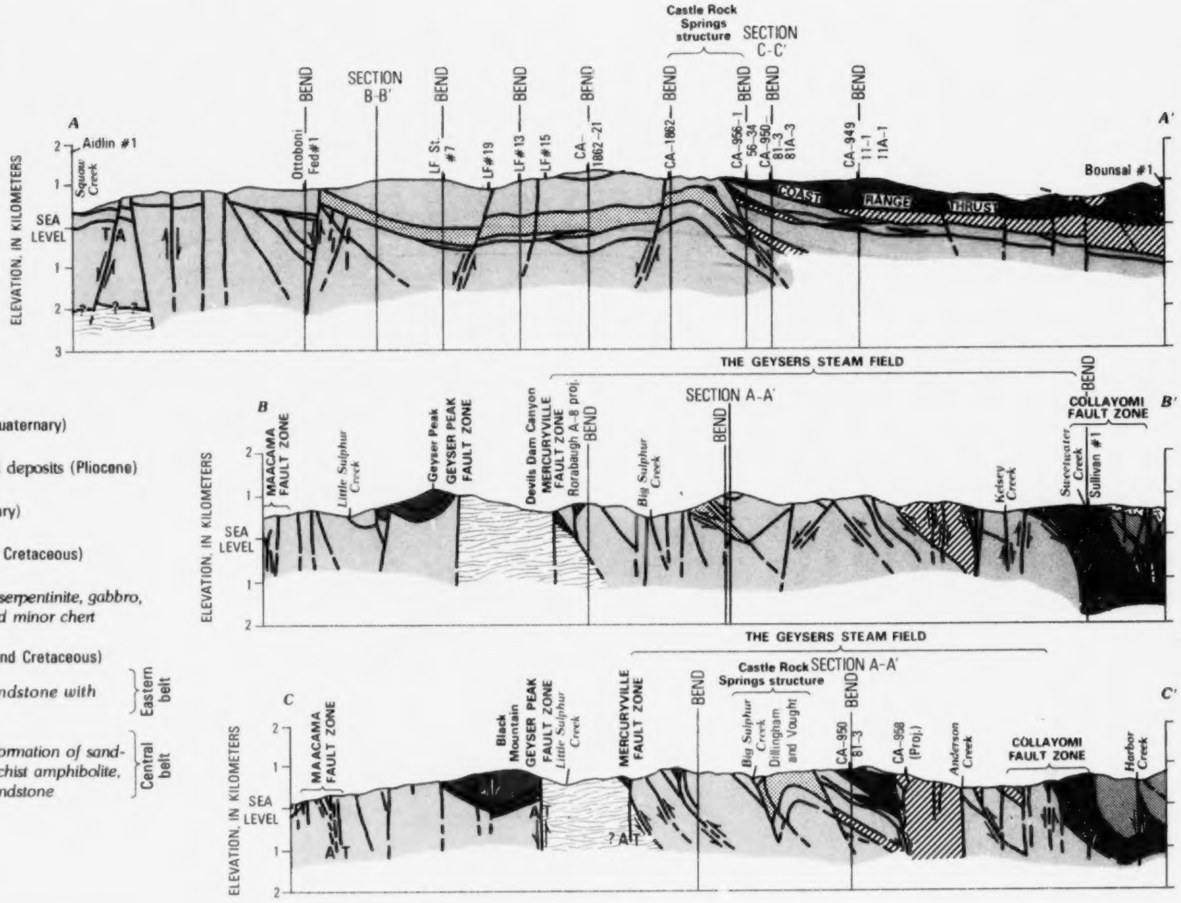
A
A'
Aidlin #1
Squaw Creek
Ottoboni Fed#1 — BEND
SECTION B-B'
LF St. #7 — BEND
LF#19
LF#13 — BEND
LF#15
CA-1862-21 — BEND
CA-1862 — BEND
Castle Rock Springs structure
SECTION C-C'
CA-956-1 — BEND
56-34
CA-950 — BEND
81-3
81A-3
CA-949 — BEND
11-1
11A-1
Bounsal #1
COAST RANGE THRUST
ELEVATION, IN KILOMETERS
SEA LEVEL
THE GEYSERS STEAM FIELD
B
B'
MAACAMA FAULT ZONE
Little Sulphur Creek
Geyser Peak
GEYSER PEAK FAULT ZONE
Devils Dam Canyon
MERCURYVILLE FAULT ZONE
Rorabaugh A-8 proj.
BEND
Big Sulphur Creek
SECTION A-A'
BEND
Kelsey Creek
Sweetwater Creek
Sullivan #1
COLLAYOMI FAULT ZONE
BEND
C
C'
MAACAMA FAULT ZONE
Black Mountain
GEYSER PEAK FAULT ZONE
Little Sulphur Creek
MERCURYVILLE FAULT ZONE
BEND
Castle Rock Springs structure
SECTION A-A'
Big Sulphur Creek
Dillingham and Vaught
CA-950 — BEND
81-3
CA-958 (Proj.)
Anderson Creek
COLLAYOMI FAULT ZONE
Harbor Creek
T A
A T
? A T
2
1
1
2
3

EXPLANATION

▨ Clear Lake Volcanics (late Tertiary and Quaternary)

▨ Sonoma Volcanics and associated alluvial deposits (Pliocene)

▨ Fluvial and lacustrine deposits (late Tertiary)

▨ Great Valley sequence (Late Jurassic and Cretaceous)

■ Ophiolite (Late Jurassic)—*Composed of serpentinite, gabbro, diabase, basalt flows, mafic breccia, and minor chert*

Franciscan assemblage (Late Jurassic and Cretaceous)

▨ Structural unit 3—*Lawsonitic metasandstone with minor metachert and metagreenstone* } Eastern belt

☐ Structural unit 2—*Melange and broken formation of sandstone, shale, greenstone, chert, blueschist amphibolite, eclogite, and minor lawsonitic metasandstone* } Central belt

▨ Structural unit 1—*Sandstone and shale*

▨ Actinolitic serpentinite

— Contact

⇄ Fault—*Dashed where approximately located; dotted where concealed. Bar and ball on downthrown side; arrow shows relative horizontal movement. In cross section, T indicates movement toward observer, A movement away from observer*

▲▲▲ Thrust fault—*Sawteeth on upper plate; dashed where approximately located.*

CA-1862 Surface location and names of geothermal well along line of cross section

FIGURE 5.—Generalized geologic map and cross sections of the Geysers steam field.

northeast of the Collayomi fault zone (Goff and others, 1977). On the northwest and southeast, the steam reservoir boundaries are less well determined. It is thought to extend no farther to the northwest than Tyler Valley. On the southeast, the reservoir may extend to the vicinity of the Helen-Wallstreet mercury mines of Dry Creek Canyon. Local inactive hydrothermal areas and several small rhyolite and dacite intrusions (including Pine Mountain and Pilot Knob) are present near the crest of the Mayacmas Mountains southwest of the Helen-Wallstreet mines. These areas may lie near the southeast boundary of the steam reservoir.

The Geysers-Clear Lake geothermal area is believed to be heated by a silicic magma body centered below 10 km depth, the top of which is within about 7 km of the surface (Isherwood, this volume). The distribution of this magma at depth is probably the most significant factor controlling the northwest, southeast, and southwest boundaries of the steam reservoir. Outside the area of potent heat conductance, the steam system presumably passes into a hot- and then cold-water-dominated system, except in areas where it is prevented from doing so by a lack of permeability. The presence and regional distribution of the magma is suggested geophysically by closure on a large-scale −30-mGal Bouguer gravity anomaly centered beneath the Clear Lake Volcanics, and by large delays in the traveltime of teleseismic *P* waves (Iyer and others, this volume). The Geysers steam field lies along the

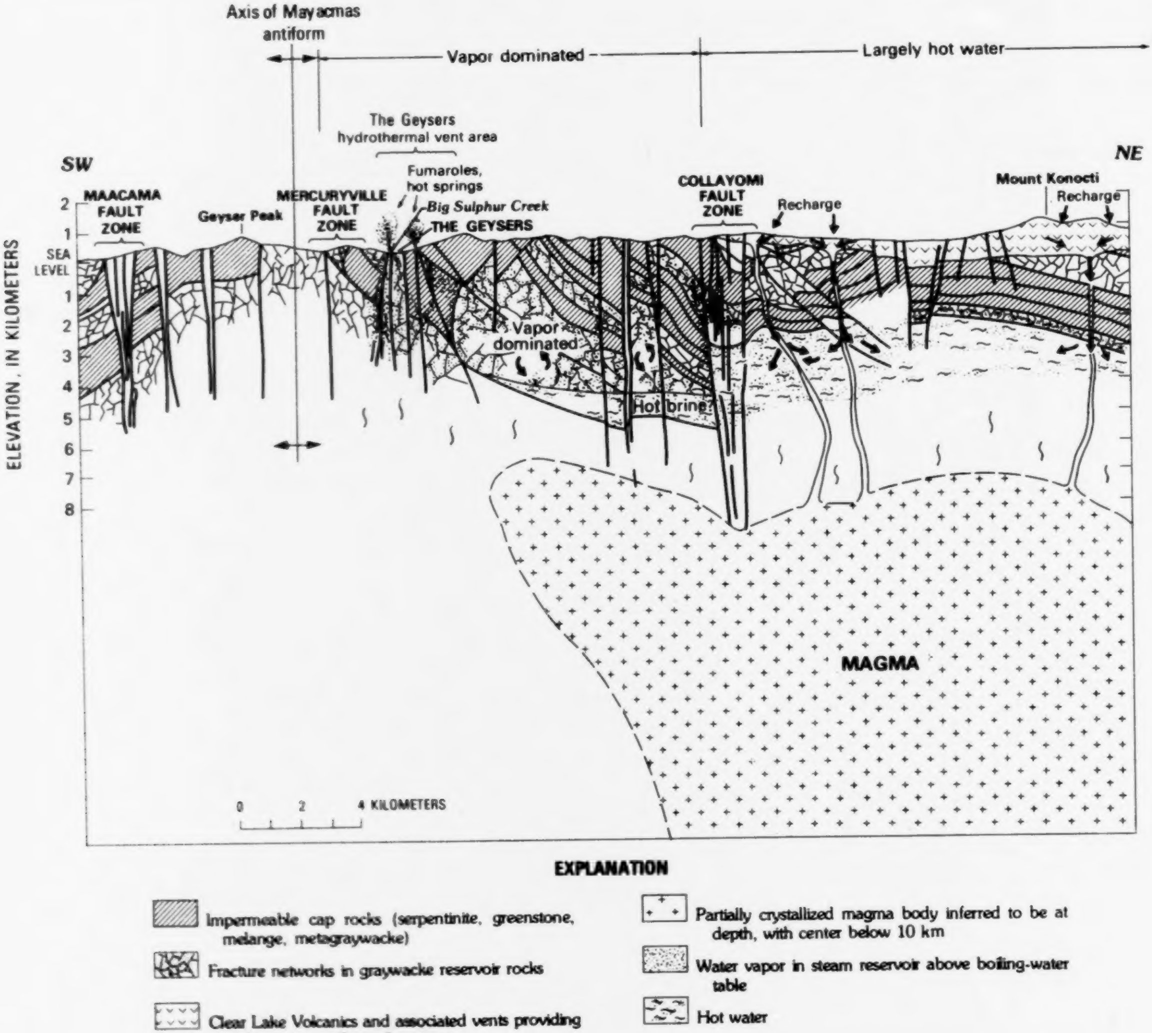
Axis of Mayacmas antiform
Vapor dominated
Largely hot water
?
The Geysers hydrothermal vent area
Fumaroles, hot springs
Big Sulphur Creek
THE GEYSERS
SW
NE
MAACAMA FAULT ZONE
Geyser Peak
MERCURYVILLE FAULT ZONE
COLLAYOMI FAULT ZONE
Recharge
Mount Konocti
Recharge
Vapor dominated
Hot brine?
MAGMA
ELEVATION, IN KILOMETERS
2
1
SEA LEVEL
1
2
3
4
5
6
7
8
0
2
4 KILOMETERS
EXPLANATION
Impermeable cap rocks (serpentinite, greenstone, melange, metagraywacke)
Fracture networks in graywacke reservoir rocks
Clear Lake Volcanics and associated vents providing recharge to geothermal systems
Partially crystallized magma body inferred to be at depth, with center below 10 km
Water vapor in steam reservoir above boiling-water table
Hot water

FIGURE 6.—Structural model of the Geysers geothermal system. Modified after McLaughlin (1977b).

southwest side of the gravity anomaly within the confines of closure on the gravity low (fig. 1).

The northeast-dipping Mercuryville fault zone also appears to have considerable local influence on the southwest boundary of the steam reservoir. Near The Geysers Resort, there is a marked decrease in the number of successful steam wells drilled near the fault zone, and intense hydrothermal alteration is not present southwest of the fault zone. In addition, the fault zone coincides approximately with closure on the southwest side of the regional gravity low. Extensive hydrothermal alteration along the trend of the Mercuryville fault zone suggests that in the past it was a major thermal vent area for the Geysers hydrothermal system, perhaps when there was a larger volume of water in the reservoir or heat supply to the system was greater. The hydrothermal reservoir may since have boiled down and shrunk down-structure and northeastward along the Mercuryville fault zone to where it now vents along steeply dipping faults in Big Sulphur Creek (fig. 6).

The Geysers steam field appears to be limited on the northeast by the Collayomi fault zone, according to the interpretation of thermal-water chemistry by Goff, Donnelly, Thompson, and Hearn (1977); they suggest that hot-water resources are present northeast of the Collayomi fault zone. Although reservoir rocks for the hot-water system are poorly known owing to their thick volcanic cover and a lack of deep drill hole data, they probably include both Franciscan rocks and marine strata of the Great Valley sequence. The hot-water system in this area has not yet been successfully developed, but it might include local vapor-dominated areas (Goff and others, 1977). The existence of a deep vapor-dominated system separated by impermeable rocks from the overlying hot-water system has been suggested as a remote exploration possibility by some geothermal companies. Regional structure probably accounts at least in part for the change in character of geothermal resources northeast of the Collayomi fault zone. Much of this area to the northeast is underlain by a thick folded and imbricated section of Great Valley sequence and ophiolitic rocks in the upper plate of the Coast Range thrust. This cover of Great Valley sequence rocks and ophiolite is on the downthrown side of the Collayomi fault zone and probably has acted as an impermeable cap to thermal fluid in the underlying Franciscan reservoir rocks (McLaughlin, 1977b). Goff, Donnelly, Thompson, and Hearn (1977) further suggest that numerous lava vents beneath the Clear Lake Volcanics provide conduits for recharge to deep structural levels. Although an extensive volcanic cover is present to the northeast, the uplifted Mayacmas Mountains southwest of the Collayomi fault zone largely expose only Franciscan rocks. In this uplifted area, maintenance of a hot-water system is inhibited because little if any recharge occurs, and several of the fractures and fault zones that are significant reservoir structures at depth are also conduits for leakage of the reservoir at the surface in the hydrothermal areas.

STRUCTURE OF THE STEAM RESERVOIR

The most difficult structural features to delineate in the Geysers-Clear Lake region are those that control the local distribution of steam within the production area. Such structural control is best confirmed through interpretation of closely spaced drill holes in conjunction with the surface geology. Development of the Geysers steam field has not yet reached a stage where local structural features are known in detail. However, assuming that the reservoir will decline, as has the Larderello steam field in central Italy, more thorough evaluations of local structural features at The Geysers may soon be necessary to determine the more productive areas.

The steam reservoir is, in most instances, within interconnected fracture networks in intact slabs of graywacke in the intermediate and possibly the lower Franciscan structural units (figs. 5 and 6). These reservoir rocks, along with intercalated melanges, greenstone, semischistose metagraywacke, and serpentinite that act as the cap rocks, compose a stack of northeast- to southeast-dipping imbricate thrust sheets (McLaughlin, 1977b). Heat is convected in water and steam in the fracture networks of the reservoir rocks to the southwest and southeast, up-structure toward the Geysers steam field.

Of primary importance to the production of steam from the reservoir rocks is distribution, continuity, and density of the open fracture networks, as rocks in the steam reservoir are otherwise impermeable. Through-going fracture networks are statistically most abundant in the least reconstituted graywackes, although a few producing steam wells tap Franciscan greenstone.

It is apparent from the surface geology that within graywacke units there are very large lenses of more or less unfractured sandstone surrounded by more penetratively fractured and sheared sandstone. This characteristic strongly implies the presence in the subsurface of unproductive, unfractured regions within reservoir rocks. Thus boudinage and brittle shear fracture, in combination with original lenticularity of Franciscan sandstone units, may be of great significance in determining distribution of the open fracture networks. Discontinuous communication of reservoir rock fractures in the Geysers steam field was described by Lipman, Strobel, and Gulati (1978) in

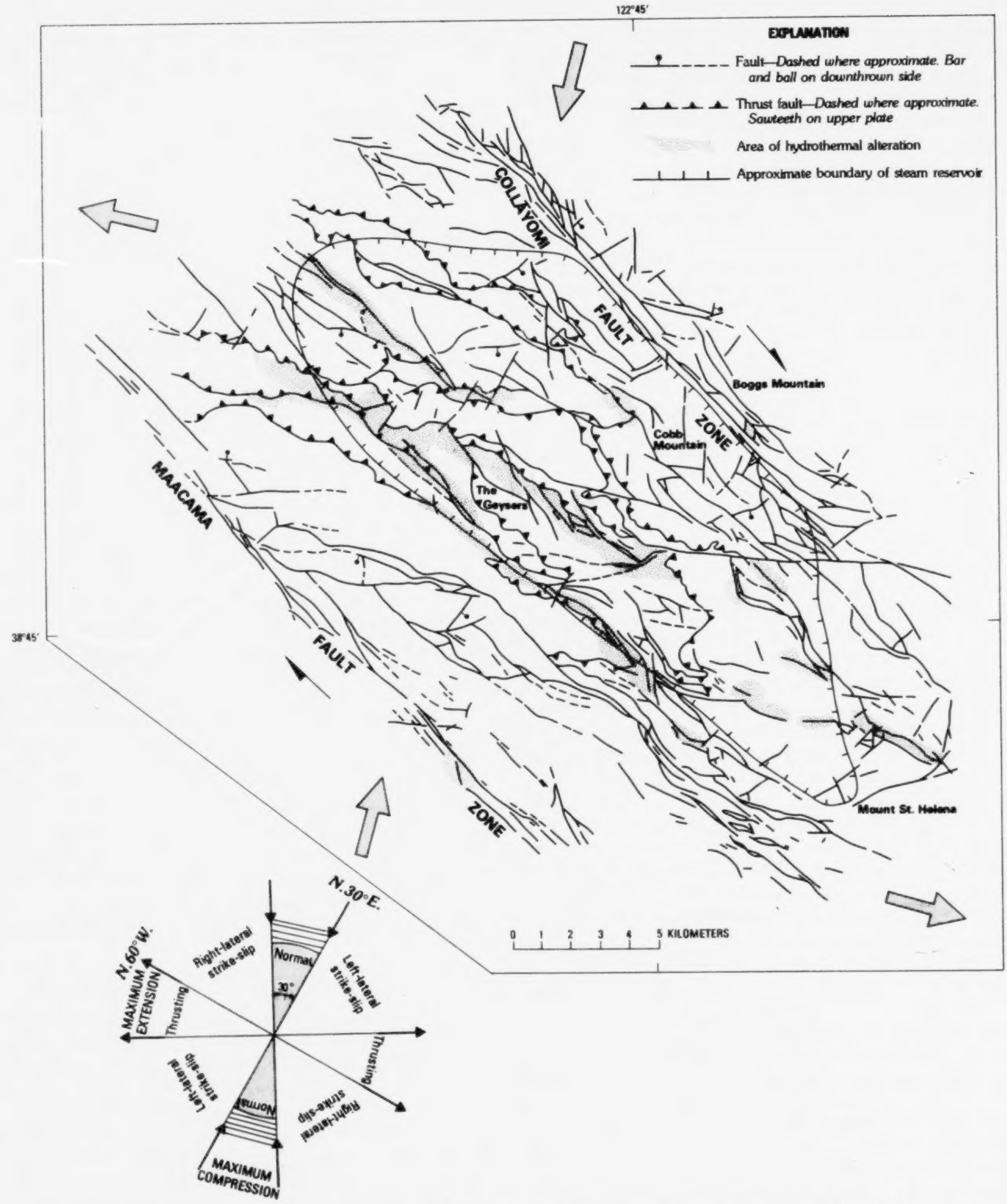
122°45'
38°45'
EXPLANATION
Fault—Dashed where approximate. Bar and ball on downthrown side
Thrust fault—Dashed where approximate. Sawteeth on upper plate
Area of hydrothermal alteration
Approximate boundary of steam reservoir
COLLAYOMI FAULT ZONE
MAACAMA FAULT ZONE
Boggs Mountain
Cobb Mountain
The Geysers
Mount St. Helena
0 1 2 3 4 5 KILOMETERS
N.30°E.
N.60°W.
MAXIMUM EXTENSION
MAXIMUM COMPRESSION
Normal
30°
Right-lateral strike-slip
Left-lateral strike-slip
Thrusting
Thrusting
Left-lateral strike-slip
Right-lateral strike-slip
Normal

FIGURE 7.—Faulting over the Geysers steam reservoir. *A*, Black arrows show dominant right-lateral sense of faulting along Maacama and Collayomi fault zones. Large white arrows show approximate vectors of regional compression and extension. *B*, Principal horizontal vectors of stress field for the Geysers area, suggested by Bufe and others (this volume), and predicted displacements for vertical faults of various orientations.

their evaluation of reservoir performance in the Sulphur Bank and Happy Jack areas. Early steam wells drilled in these areas tapped shallow reservoir fractures at depths above 640 m that had static pressures much lower than the prevailing pressures in a separate, more extensive fracture system 183 m deeper. This discovery led to the early recognition of two discrete steam reservoirs at different structural levels. More recent studies of reservoir drainage by Lipman and his colleagues have demonstrated that while these fractured areas are separated locally by pendants of impermeable unfractured rock, the shallow fracture network is connected with the deeper more regional fracture zone elsewhere in the area.

INFLUENCE OF REGIONAL STRESS ON RESERVOIR STRUCTURE

The large number of shallow earthquakes associated with the Geysers steam field indicates that the region is tectonically active and that stress is locally relieved along zones of weakness in rocks of the steam reservoir. The steam reservoir occupies a more or less rigid uplifted block between two major strike-slip fault zones (fig. 7*A*). This uplifted block is broken by numerous faults, fractures, and joints formed before and during development of the San Andreas shear system.

McLaughlin and Stanley (1976) stated that the steeply dipping northwest-trending strike-slip and normal faults along which fumaroles and hot springs vent near The Geysers Resort may be major channels from the steam reservoir. They further suggested that the hydrothermal lubrication of these fault zones (fig. 7) promotes the release of regional stress and localization of shallow earthquakes.

Recent seismic studies (Bufe and others, this volume) and investigations of vertical and horizontal surface changes over the area of steam production (Lofgren, this volume) suggest that much seismic activity at The Geysers may also be due to fluid withdrawal and reservoir subsidence, probably along pre-existing faults in the area of steam production.

Earthquake first-motion studies by Bufe and others (this volume) indicate that the vectors of maximum regional compression in the Geysers area range from about N. 30° E. to more northerly orientations compatible with the right-lateral offsets observed on northwest-trending faults of the San Andreas system. An approximate north-south maximum compression vector (fig. 7*A*) agrees with the observed sense of offset on most of the major Quaternary faults in the Geysers area. The 30° of eastward scatter in the vectors of compression may be due wholly or in part to local factors such as (1) variable amounts of strain accumulated within the Geysers-Clear Lake region, (2) the release of strain along fault segments of variable lengths and orientations, or (3) the effect of steam reservoir subsidence on the distribution of regional stress.

Optimum horizontal extension predicted from the earthquake studies is perpendicular to the vectors of principal compression (fig. 7*B*). Fractures oriented north to N. 30° E. are therefore highly favorable geothermal targets, since their orientation parallel to the vector of maximum regional compression should produce optimum northwest-southeast extension. Fractures oriented somewhat outside that range should exhibit lesser components of extension in addition to strike-slip and thrust faulting (fig. 7*B*).

INSIGHTS INTO RESERVOIR STRUCTURE FROM SURFACE GEOLOGY

Wells producing high volumes of steam in the Larderello area of central Italy are known to be associated with the crests of northwest-plunging horsts (Cataldi and others, 1963, 1978). Detailed well production records, necessary to demonstrate such a relation at The Geysers, are generally unavailable, but upwarps and other structural highs could be of considerable importance to reservoir permeability in the subsurface of the Geysers steam field. In the axial regions of structural highs, significant vertical extension can occur along gently dipping or subhorizontal bedding planes, joints, fractures, and thrust faults. These open subhorizontal features may be particularly significant where intersected by favorably oriented vertical fractures (fig. 8).

I have mapped structural highs over the Geysers steam reservoir (McLaughlin, 1978) and a horstlike structure in the Castle Rock Springs area of the steam field (McLaughlin and Stanley, 1976). Numerous producing wells are associated with the latter structural high, possibly due to localization of favorably oriented open-fracture networks (fig. 9).

The axial regions of folds similarly should be impor-

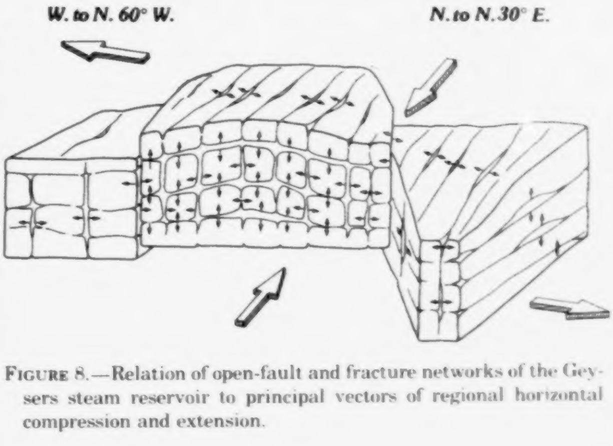

FIGURE 8.—Relation of open-fault and fracture networks of the Geysers steam reservoir to principal vectors of regional horizontal compression and extension.

tant in producing permeability in the subsurface. Folded Franciscan rocks of differing competency and permeability are present near The Geysers Resort, where interbedded graywacke, chert, greenstone, and melange are major constituents of the Franciscan assemblage (fig. 10). These rocks form a slab of relatively intact strata tightly folded into southeast-plunging anticlines and synclines. These rocks are overthrust by a thick sheet of serpentinite which acts as a cap rock (fig. 10). In the subsurface, the chert, greenstone, and melange are local impermeable barriers to hydrothermal circulation, and the graywacke composes the permeable reservoir rocks. Hinge areas of the southeast-plunging folds (fig. 10) should be the loci of tensional fractures and faults which probably provide important open fracture networks to the graywacke beds in the subsurface where they project beneath the serpentinite cap rock.

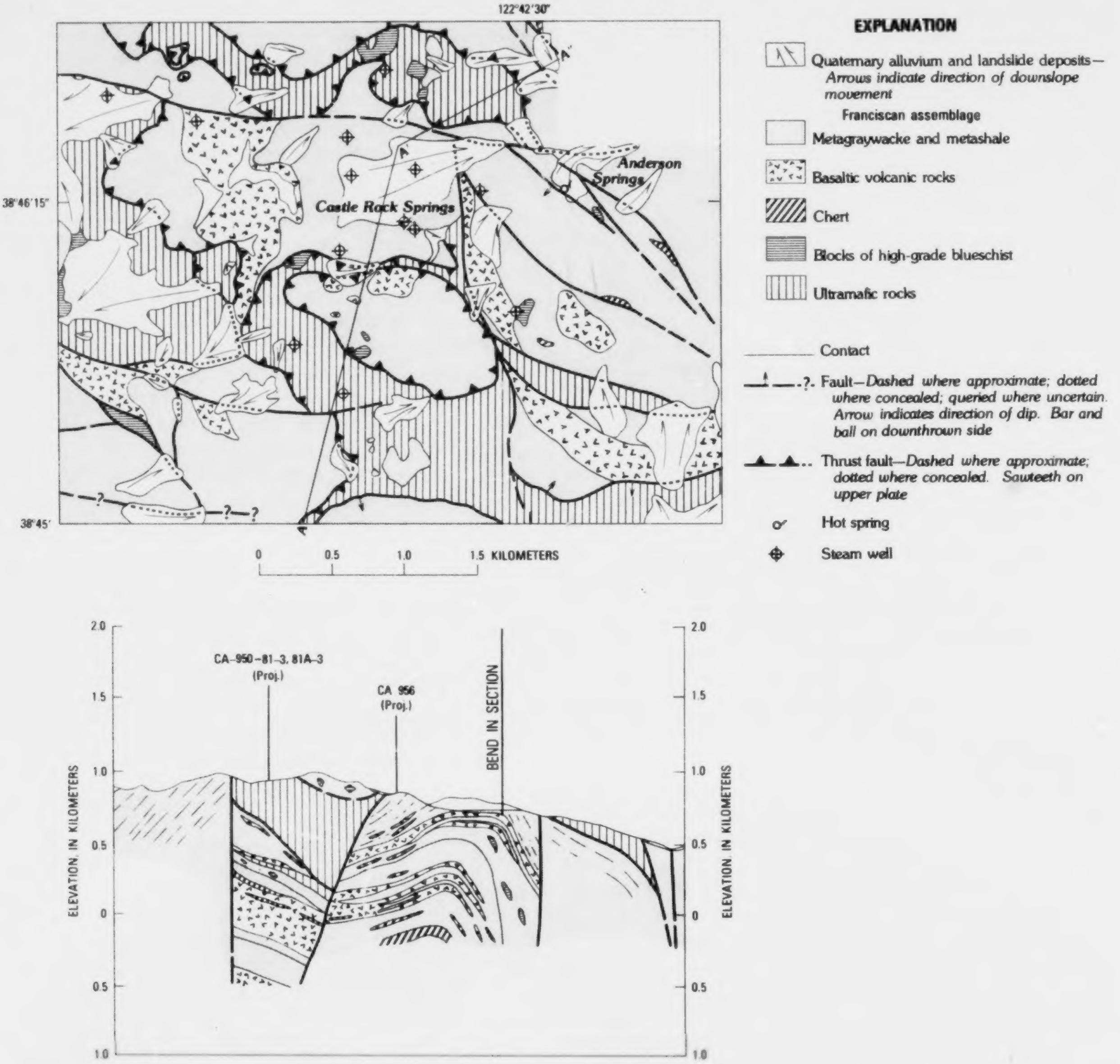
122°42'30"
38°46'15"
38°45'
A'
A
Anderson Springs
Castle Rock Springs
?
0 0.5 1.0 1.5 KILOMETERS
EXPLANATION
Quaternary alluvium and landslide deposits—Arrows indicate direction of downslope movement
Franciscan assemblage
Metagraywacke and metashale
Basaltic volcanic rocks
Chert
Blocks of high-grade blueschist
Ultramafic rocks
Contact
Fault—Dashed where approximate; dotted where concealed; queried where uncertain. Arrow indicates direction of dip. Bar and ball on downthrown side
Thrust fault—Dashed where approximate; dotted where concealed. Sawteeth on upper plate
Hot spring
Steam well
CA-950-81-3, 81A-3 (Proj.)
CA 956 (Proj.)
BEND IN SECTION
ELEVATION, IN KILOMETERS
2.0
1.5
1.0
0.5
0
0.5
1.0

FIGURE 9.—Complex structural high associated with Castle Rock Springs area of the Geysers steam field. Modified after McLaughlin and Stanley (1976).

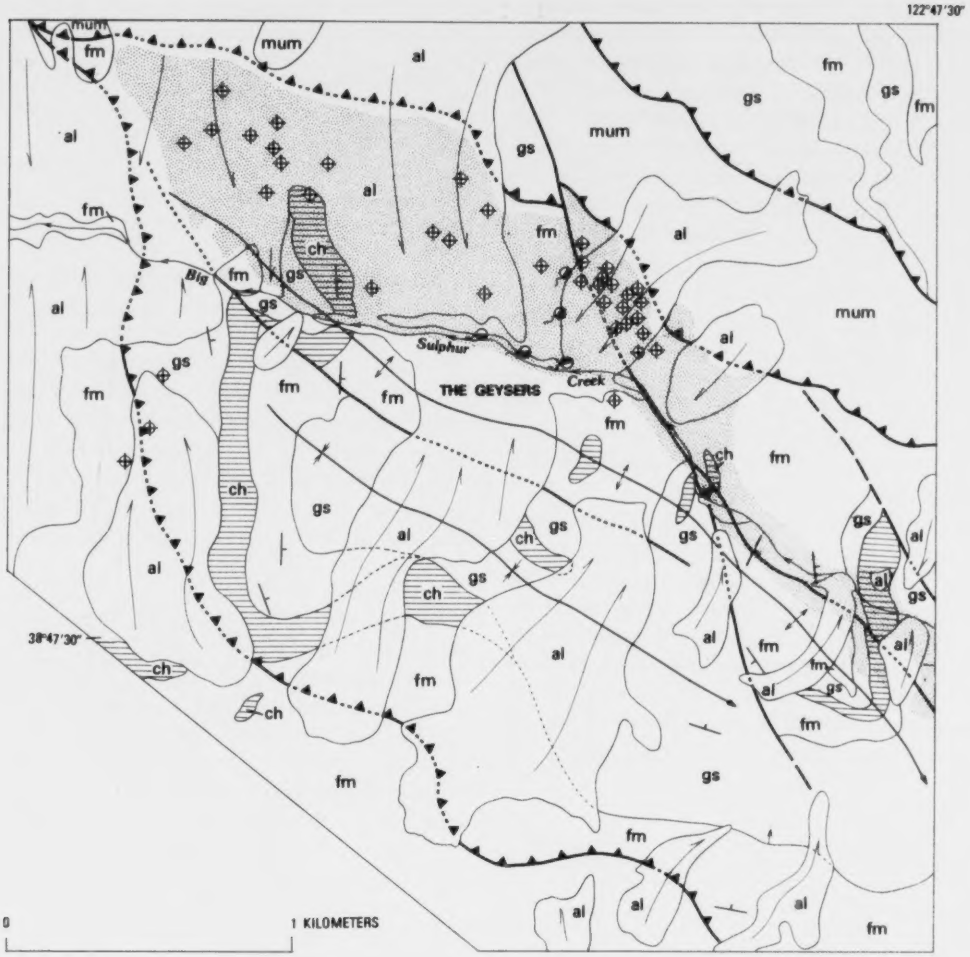

EXPLANATION

al	Alluvial deposits, including landslides
	Franciscan assemblage
fm	Melange, undivided
gs	Greenstone
ch	Chert
mum	Actinolitic serpentinite
...	Contact—*Showing dip where known. Dotted where concealed*
...	High-angle fault—*Dashed where approximate; dotted where concealed. Bar and ball on downthrown side*
▲.▲.▲.	Thrust fault—*Dashed where approximate; dotted where concealed. Sawteeth on upper plate*
	Anticline—*Showing crestline and direction of plunge*
	Syncline—*Showing troughline and direction of plunge*
⊥	Strike and dip of beds
	Hydrothermal alteration
⊕	Steam well
~●	Hot spring or fumarole area

FIGURE 10.—Geology of the Geysers area, illustrating folds in Franciscan chert and extensive hydrothermal activity along Big Sulphur Creek.

All fault-bounded uplifts do not necessarily contribute to the permeability of the Geysers steam reservoir. Figure 11 illustrates that downward-pinching uplifts formed through horizontal compression are likely to develop fracture networks that close with depth. These compressional features may be less desirable exploration targets than the downward-opening horstlike features resulting from extension, since extensional uplifts are more likely to contain fractures that open with depth. Shell Oil Company has extensively explored a diapirlike uplift in the southeast part of the Geysers steam field (fig. 12) and drilled three exploration wells. High temperature gradients were reported in these wells (Fehlberg, 1975), but no commercially significant open fracture networks were found. The failure of these wells to reach appreciable open fractures may be related to the diapiric compressional uplift over which the wells were sited.

Horizontal extension is also important along warps or irregularities in the trend of steeply dipping strike-slip faults (fig. 8). No specific examples of such a feature are known within the Geysers steam field, but significant extension is indicated southwest of the Geysers along the Maacama strike-slip fault zone, where late Tertiary fluvial and lacustrine sedimentary rocks are deposited in elongate fault-bounded depressions that formed contemporaneously with sedimentation. (see fig. 5).

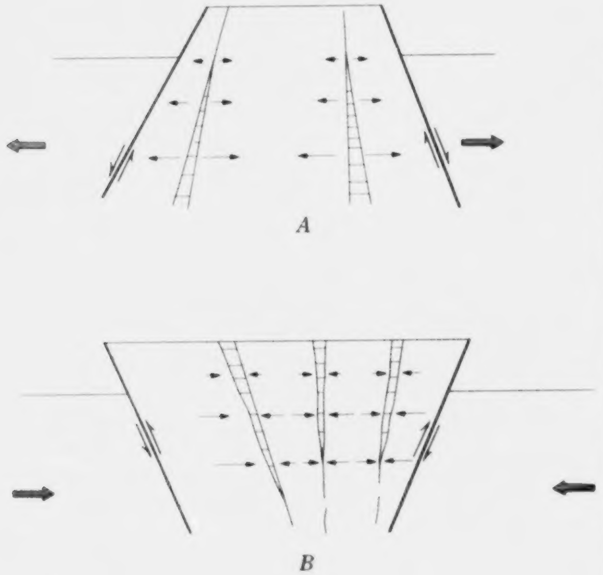

FIGURE 11.—Hypothetical relation of open fractures to structural highs. *A*, Downward-opening structural high produced by horizontal extension. *B*, Downward-pinching structural high produced by horizontal compression.

RESERVOIR RECHARGE

White, Muffler, and Truesdell (1971) showed that steam in the Geysers hydrothermal system is derived for the most part from meteoric water. They further hypothesized that vapor-dominated hydrothermal systems such as The Geysers may begin as hot-water systems and ultimately boil down to the vapor-dominated state. They argued that in such a system, the reservoir rocks must have a low recharge rate, and hydrothermal leakage in the form of hot springs and fumaroles (and presently, steam wells) must exceed recharge in order for the vapor state to be maintained. Some natural recharge is necessary in their model, however, to ensure that the system does not completely boil off. Vapor-dominated hydrothermal systems do not maintain a perfect balance between reservoir leakage and recharge; thereby they eventually do get drowned or boil off. However, the time framework for this is unknown.

Natural recharge to the Geysers system is constrained by the low permeability of the Franciscan reservoir rocks. However, since the steam reservoir is underpressured with respect to surrounding water-dominated parts of the system (White and others, 1971), meteoric water is readily absorbed, provided that conduits into the reservoir are present.

Induced recharge of the reservoir may be demonstrated by the numerous re-injection wells in the Geysers steam field. These wells recycle approximately 25 percent of the steam condensate collected from the cooling towers of the geothermal power plants. This reinjected condensate represents only a small proportion of the total volume of fluid mined from the system since a much larger volume is lost through evaporation. However, it is not known whether these reinjected fluids circulate into deep levels of the steam reservoir.

Specific areas of natural recharge in the Geysers region are subject to speculation. Goff, Donnelly, Thompson, and Hearn (1977) suggested that late Tertiary and Quaternary volcanic vents are major sources of reservoir recharge. Within the Geysers steam field, Cobb Mountain, a funnel-shaped volcanic dome composed of a rhyolite flow and two dacite flows of early Pleistocene age, may be a major source of this recharge. The silicic rocks of Cobb Mountain have a high porosity and are capable of absorbing large volumes of water during the rainy season. At least three vents beneath Cobb Mountain could allow meteoric water to percolate deep into the Franciscan basement. Other volcanic vents present within and adjacent to the vapor-dominated part of the steam field include vents beneath small volumes of olivine basalt at Caldwell Pines, a small rhyolite dome southeast of

Castle Rock Springs (Pine Mountain), and possibly the vents beneath small dacite and rhyolite intrusions (Pilot Knob) adjacent to Mount St. Helena. In the region northeast of the Collayomi fault zone, extensive Quaternary volcanic flows and domes are underlain by numerous vents, and thus significantly larger volumes of water may recharge this part of the hydrothermal system (Goff and others, 1977). This larger potential recharge area may be significant in limiting the extent of the vapor-dominated geothermal system.

At least some recharge to the reservoir probably takes place along segments of steeply dipping extensional faults. Some additional downward percolation may occur along the Mercuryville and Collayomi fault zones, especially where the faults transect or coincide with major drainages or where large volumes of water are trapped along extensional warps or along contacts between different rock units.

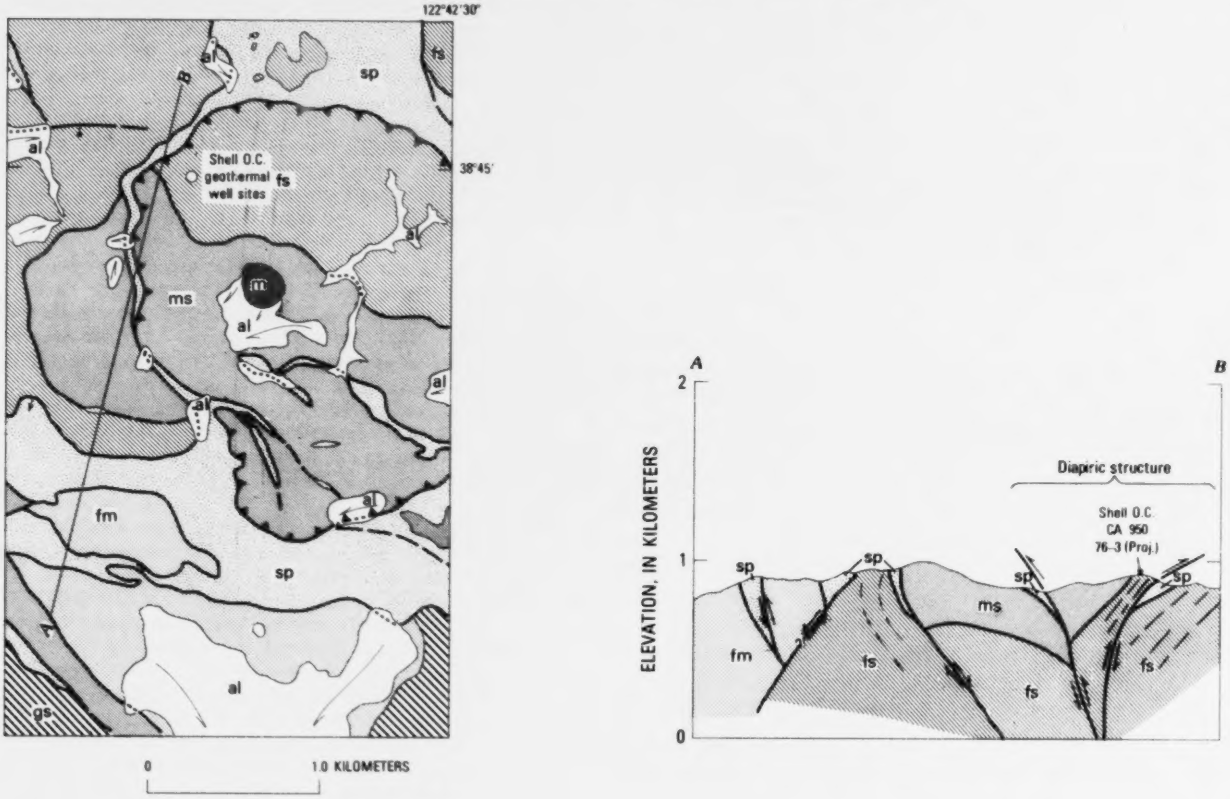

EXPLANATION

al Surficial deposits—*Arrows show direction of movement of unconsolidated material*

sp Serpentinite

Franciscan assemblage

fm Melange, undivided

fs Graywacke

ms Lawsonitic metagraywacke

m High-grade blueschist

gs Greenstone

Contact

Fault—*Dashed where approximate; dotted where concealed; queried where uncertain. Bar and ball on downthrown side; on map, arrow on fault indicates direction of dip; in cross section, arrows indicate relative direction of movement*

Thrust fault—*Dotted where concealed. Sawteeth on upper plate*

FIGURE 12.—A diapiric structure associated with unproductive exploratory wells in the Geysers steam field.

CONCLUSIONS

Major vapor-dominated geothermal systems such as the one in the Geysers-Clear Lake area are rare, and its presence perhaps is due to the complex tectonics of the northern Coast Ranges.

The structural stacking of permeable and impermeable rocks in the Geysers steam reservoir and the penetrative shear deformation characteristic of Franciscan melanges and broken formations are thought to be the consequence of deformation associated with the formation of melanges and subduction. The pattern of distribution and orientation of fracture networks within the steam reservoir are largely controlled by this early episode of penetrative deformation that preceded propagation of the San Andreas fault system.

Considerable evidence indicates that extension associated with the San Andreas fault system provided deep zones of weakness along which magma was emplaced into the crust beneath the Geysers-Clear Lake area. Late Tertiary and Quaternary volcanism apparently closely followed the termination of subduction and initiation of strike-slip faulting. Furthermore, several of the present depositional basins in the northern Coast Ranges, including Clear Lake basin, appear to be the result of east-southeast extension within the broad zone of right-lateral shear created since passage of the Mendocino triple junction and initiation of the San Andreas fault system.

The present pattern of regional stress may be the principal factor determining which fracture networks control permeability in the steam reservoir. First-motion studies of earthquakes predict that maximum horizontal extension should occur along north- to northeast-oriented vertical fractures. Significant vertical extension may occur along upwarps in subhorizontal fractures and partings. Permeability provided by vertical extension may be particularly significant along the axes of anticlinal or horstlike structures, especially where subhorizontal fractures are intersected by the north- to northeast-oriented vertical fractures. Local bends or warps in northwest-oriented strike-slip faults may also produce significant horizontal extension.

Several specific structures described in this paper are of unproven importance to steam production at The Geysers. However, depletion of the Geysers steam reservoir is increasing as a result of exploration and development activity. Geothermal developers may soon find it necessary to consider the economic advantages of preferential exploitation of specific structures in the older more depleted areas of the steam field.

REFERENCES CITED

Alvarez, Walter, Kent, D. V., Premoli-Silva, Isabella, Schweikert, R. A., and Larson, R. L., 1979, Franciscan limestone deposited at 17° south paleolatitude: Geological Society of America, 75th Cordilleran Section, Annual Meeting, Abstracts with Programs, p. 66.

Atwater, Tanya, 1970, Implications of plate tectonics for the Cenozoic tectonic evolution of western North America: Geological Society of America Bulletin, v. 81, p. 3513–3536.

Atwater, Tanya, and Molnar, Peter, 1973, Relative motion of the Pacific and North American plates deduced from sea floor spreading in the Atlantic, Indian, and south Pacific Oceans, *in* Kovach, R. L., and Nur, Amos, eds., Proceedings of the conference on tectonic problems of the San Andreas fault system: Stanford Univ., Publications in the Geological Sciences, v. 13, p. 136–148.

Bailey, E. H., Blake, M. C., Jr., and Jones, D. L., 1970, On-land Mesozoic oceanic crust in California Coast Ranges: U.S. Geological Survey Professional Paper 700–C, p. C70–C81.

Bailey, E. H., Irwin, W. P., and Jones, D. L., 1964, Franciscan and related rocks and their significance in the geology of western California: California Division of Mines and Geology Bulletin 183, 177 p.

Berkland, J. O., Raymond, L. A., Kramer, J. C., Moores, E. M., and O'Day, Michael, 1972, What is Franciscan?: American Association of Petrol. Geologists Bulletin, v. 56, no. 12, p. 2295–2302.

Beutner, E. C., 1977, Evidence and implications of a Late Cretaceous-Paleogene island arc and marginal basin along the California coast: Geological Society of America, Cordilleran Section, Annual Meeting, 73d, Abstracts with Programs, p. 389.

Blake, M. C., Jr., Campbell, R. H., Dibblee, T. W., Jr., Howell, D. G., Nilsen, T. H., Normark, W. R., Vedder, J. C., and Silver, E. A., 1978, Neogene basin formation in relation to plate-tectonic evolution of San Andreas fault system, California: American Association of Petroleum Geologists Bulletin, v. 62, p. 344–372.

Blake, M. C., Jr., Irwin, W. P., and Coleman, R. G., 1967, Upside-down metamorphic zonation, blueschist facies, along a regional thrust in California and Oregon: U.S. Geological Survey Professional Paper 575–C, p. C1–C9.

Blake, M. C., Jr., and Jones, D. L., 1974, Origin of Franciscan melanges in northern California: Society of Economic Paleontologists and Mineralogists Special Publication 19, p. 345–357.

Blake, M. C., Jr., and Jones, D. L., 1978, Allochthonous terranes in northern California?—A reinterpretation, *in* Mesozoic paleogeography of the western United States: Society of Economic Paleontologists and Mineralogists, Pacific Section, Pacific Coast Paleogeography symposium, 2d, April 1978, Proceedings, p. 397–400.

Cataldi, R., Lazzarotto, Antonio, Muffler, L. J. P., Squarci, Paolo, and Stefani, G. C., 1978, Assessment of geothermal potential of central and southern Tuscany, *in* Proceedings of the Larderello workshop on geothermal resource assessment and reservoir engineering, Sept. 12–16, 1977, Pisa, Italy: Geothermics, v. 7, no. 2–4, p. 91–131.

Cataldi, R., Stefani, G. C., and Tongiorgi, Marco, 1963, Geology of Larderello Region (Tuscany): Contribution to the study of the geothermal basins, *in* Tongiorgi, Marco, ed., Nuclear geology on geothermal areas: Pisa, Consiglio Nazionale delle Ricerche, Laboratorio di Geologia Nucleare, p. 235–261.

Coleman, R. G., and Lanphere, M. A., 1971, Distribution and age of high-grade blueschists, associated eclogites, and amphibolites from Oregon and California: Geological Society of America Bulletin, v. 82, p. 2397–2412.

Coleman, R. G., and Lee, D. E., 1963, Glaucophane-bearing metamorphic rocks of the Cazadero area, California: Journal of Petrology, v. 4, p. 260–261.

Crowell, J. C., 1974a, Sedimentation along the San Andreas fault, *in* Modern and ancient geosynclinal sedimentation: Society of Economic Paleontologists and Mineralogists Special Publication 19, p. 292–303.

——— 1974b, Origin of late Cenozoic basins in southern California, *in* Tectonics and sedimentation: Society of Economic Paleontologists and Mineralogists Special Publication 22, p. 190–203.

Dickinson, W. R., 1970, Clastic sedimentary sequences deposited in shelf, slope, and trough settings between magmatic arcs and associated trenches: Pacific Geology, v. 3, p. 15–30.

Dickinson, W. R., and Snyder, W. S., 1979, Geometry of triple junctions related to the San Andreas transform: Journal of Geophysical Research, v. 84, p. 561–572.

Donnelly, J. M., 1977, Geochronology of the Clear Lake volcanic field: Berkeley, University of California, Ph. D. thesis, 48 p.

Eaton, J. P., 1963, Crustal structure between Eureka, Nevada, and San Francisco, California, from seismic-refraction measurements: Journal of Geophysical Research, v. 68, no. 20, p. 5789–5806.

Ernst, W. G., 1970, Tectonic contact between the Franciscan melange and the Great Valley sequence—Crustal expression of a late Mesozoic Benioff zone: Journal of Geophysical Research, v. 75, p. 886–902.

——— 1971, Do mineral parageneses reflect unusually high-pressure conditions of Franciscan metamorphism?: American Journal of Science, v. 270, p. 81–108.

Fehlberg, E. L., 1975, Shell's activity in The Geysers area: Stanford, California, Stanford University, Proceedings of workshop on geothermal reservoir engineering, Rept. 5GP–TR–20, 7 p.

Goff, F. E., Donnelly, J. M., Thompson, J. M., and Hearn, B. C., Jr., 1977, Geothermal prospecting in The Geysers-Clear Lake area, northern California: Geology, v. 5, no. 8, p. 509–515.

Hamilton, Warren, 1969, Mesozoic California and the underflow of Pacific mantle: Geological Society of America Bulletin, v. 80, no. 12, p. 2909–2429.

Herd, D. G., 1979, Neotectonic framework of Coastal California and its implications to microzonation of the San Francisco Bay region, *in* Brabb, E. E., ed., Progress on seismic zonation in the San Francisco Bay region: U.S. Geological Survey Circular 807, p. 3–10.

Ingersoll, R. V., Rich, E. I., and Dickinson, W. R., 1977, Field trip guide to the Great Valley sequence: Geological Society of America, Cordilleran Section, Annual Meeting, 73d, April 1977, 72 p.

Jones, D. L., Blake, M. C., Jr., Bailey, E. H., and McLaughlin, R. J., 1978, Distribution and character of upper Mesozoic subduction complexes along the west coast of North America: Tectonophysics, v. 47, p. 207–222.

Jones, D. L., Silberling, N. J., and Hillhouse, John, 1977, Wrangellia—A displaced terrane in northwestern North America: Canadian Journal of Earth Science, v. 14, p. 2565–2577.

Lanphere, M. A., Blake, M. C., Jr., and Irwin, W. P., 1978, Early Cretaceous metamorphic age of the South Fork Mountain Schist in the northern Coast Ranges of California [abs.]: American Journal of Science, v. 278, p. 798–815.

Lipman, S. C., Strobel, C. J., and Gulati, M. S., 1978, Reservoir performance of the Geysers field, *in* Proceedings of the Larderello workshop on geothermal resource assessment and reservoir engineering, Sept. 12–16, 1977, Pisa, Italy: Geothermics, v. 7, p. 209–219.

Mankinen, E. A., 1972, Paleomagnetism and potassium-argon ages of the Sonoma Volcanics, California: Geological Society of America Bulletin, v. 83, p. 2063–2072.

McLaughlin, R. J., 1975, Structure of Franciscan rocks in the central Mayacmas Mountains, Sonoma and Lake Counties, California [abs.]: Geological Society of America Cordilleran Section, Annual Meeting, 71st, Proceedings, p. 345–346.

——— 1977a, Late Mesozoic-Quaternary plate tectonics and The Geysers-Clear Lake geothermal anomaly, northern Coast Ranges, California: Geological Society of America Abstracts with Programs, v. 9, no. 4, p. 464.

——— 1977b, The Franciscan assemblage and Great Valley sequence in The Geyser-Clear Lake region of northern California: Geological Society of America, Cordilleran Section, Field trip guide, Apr. 1977, p. 3–24.

——— 1978, Preliminary geologic map and structural sections of the central Mayacmas Mountains and the Geysers steam field, Sonoma, Lake, and Mendocino Counties, California: U.S. Geological Survey Open-File Map 78–389, scale 1:24,000.

McLaughlin, R. J., and Pessagno, E. A., Jr., 1978, Significance of age relations above and below Upper Jurassic ophiolite in The Geysers-Clear Lake region, California: U.S. Geological Survey Journal of Research, v. 6, p. 715–726.

McLaughlin, R. J., and Stanley, W. D., 1976, Pre-Tertiary geology and structural control of geothermal resources, the Geysers steam field, California: United Nations symposium on development and use of geothermal resources, 2d, 20–29 May, 1975, Proceedings, v. 1, p. 475–486.

Morgan, W. J., 1972, Plate motions and deep mantle convection: Geological Society of America Memoir 132, 22 p.

Ogle, B. A., 1953, Geology of Eel River Valley area, Humboldt County, California: California Division of Mines and Geology Bulletin 164, 128 p.

Platt, J. P., 1975, Metamorphic and deformational processes in the Franciscan Complex, California: Some insights from the Catalina Schist terrane: Geological Society of America Bulletin, v. 86, p. 1337–1347.

Seiders, V. M., Pessagno, E. A., Jr., and Harris, A. G., 1979, Radiolarians and conodonts from pebbles in the Franciscan assemblage and the Great Valley sequence of the California Coast Ranges: Geology, v. 7, p. 37–40.

Sims, J. D., and Rymer, M. J., 1975, Preliminary description and interpretation of cores and radiographs from Clear Lake, Lake County, California: Core 7: U.S. Geological Survey Open-File Report 75–144, 21 p.

Suppe, J., and Armstrong, R. L., 1972, Potassium-argon dating of Franciscan metamorphic rocks: American Journal of Science, v. 272, p. 217–233.

White, D. E., Muffler, L. J. P., and Truesdell, A. H., 1971, Vapor-dominated hydrothermal systems compared with hot water systems: Economic Geology, v. 66, p. 75–97.

THE CLEAR LAKE VOLCANICS: TECTONIC SETTING AND MAGMA SOURCES

By B. Carter Hearn, Jr., Julie M. Donnelly-Nolan, and Fraser E. Goff

ABSTRACT

The Clear Lake Volcanics may be the latest surface manifestation of a mantle hot spot that has left a track of Tertiary and Quaternary volcanic centers in the California Coast Ranges. These centers are progressively older to the south and are anomalously close to the former position of the subduction zone between the North American and Farallon crustal plates. Although initiation of volcanism may be correlated with cessation of subduction, problems of geometry and heat transfer probably preclude magma genesis from the newly detached slab of oceanic crust.

One or more predecessors of an inferred shallow magma chamber have been located beneath the central part of the field since about 0.6 m.y. ago, and perhaps since 1.1 m.y. ago. The current chamber is the ultimate source of heat for the vapor-dominated geothermal system at The Geysers and the inferred hot-water geothermal system beneath the volcanic field. Geophysical studies locate the magma chamber in Franciscan rocks and underlying crustal rocks of oceanic and possible continental affinity. Strontium isotopes, major and trace elements, and seismic velocities indicate that basaltic magmas have been generated from several mantle sources which probably consist of pyroxenite, peridotite, and eclogite. The many lavas, which as a group show a complete range of composition from basalt to rhyolite, are the products of fractional crystallization, wallrock assimilation, and magma mixing which have affected the primary melts from the mantle. The effect of assimilated Franciscan rocks is obscure, but incorporation of ophiolitic ultramafic rocks may show as elevated MgO content and variable Cr content. Rhyolite lavas of each age group show similar levels of incompatible trace elements, considerably less than the strong enrichments in major ash flows (Bishop Tuff, Bandelier Tuff). The lower abundances may result from regional differences of sources or may suggest that, as a result of the active tectonic setting, the Clear Lake magma system has leaked frequently enough to prevent the buildup of volatiles necessary for a voluminous ash-flow eruption. The most recent volcanic activity is northeast of the main volcanic field and has associated thermal fluids, possibly above a new focus of deep heating. In that area, expected future volcanic activity will probably be mafic in composition and will form phreatomagmatic craters, cinder cones, or flows. However, the large magma chamber suggests that a catastrophic, silicic ash-flow eruption, with attendant caldera collapse, is also possible.

Numerous faults of northwest to north-northwest trend are related to right-lateral stress of the San Andreas system. The possibly active northwest-trending Collayomi and north-northwest-trending Konocti Bay fault zones break the Clear Lake Volcanics and show geomorphic evidence of late Pleistocene strike-slip, normal, and thrust movements. Part of the Collayomi fault zone showed ground breakage in the 1906 San Francisco earthquake. Fault directions and displacements are those expected by analogy with clay-cake modelling of right-lateral systems. Two north-south alinements of mafic vents, 0.35–0.5 m.y. and 0.01–0.2 m.y. old, fit the expected orientation of tension fractures, whereas vents for dacites from 0.35–0.5 m.y. and for basaltic lavas from 1.3–2.0 m.y. tend to be alined northwest or north-northwest. At depth in Franciscan rocks, faults probably have produced fracture permeability which is important in the localization and accessibility of geothermal fluids.

INTRODUCTION

The Clear Lake volcanic field (figs. 13 and 14) and the late Pliocene and early Pleistocene Sutter Buttes (Williams and Curtis, 1977) are the only Quaternary volcanic fields that lie west of the southern projection of the Cascade trend of Quaternary volcanism. However, the Clear Lake volcanic field is the youngest and most northerly of several volcanic fields (Sonoma, Tolay, Berkeley Hills, Quien Sabe, Neenach-Pinnacles) that generally increase in age southward and have erupted in similar geologic settings: in the structurally complex terrane of Franciscan assemblage, Great Valley sequence, and ophiolites close to the San Andreas fault system. This geographic progression of age also holds within the Clear Lake volcanic field, where isotopic ages and the eruptive sequence show a general decrease in age northward from 2 m.y. in the south to about 10,000 years in the north (Donnelly-Nolan and others, this volume). Although any volcanic system young enough to produce surface thermal anomalies may be of geothermal significance, silicic systems tend to develop high-level magma chambers and show the greatest geothermal potential at economically accessible depths (Smith and Shaw, 1975).

A shallow magma chamber, defined by geophysical evidence, underlies the Clear Lake volcanic field. Heat from that chamber, its wallrocks, and conjectural newly developing magma systems is producing the geothermal resources of the Geysers-Clear Lake area. In this paper we examine data on the structural setting of the Clear Lake volcanic field, its volcanic rocks, depth of generation of magma, location of magma chambers, and the possible processes that have modified deep-source magmas to produce the erupted lavas.

Many geoscientists have added to our comprehension of the problems of Clear Lake geology and volcanology by stimulating discussions in the field. We are grateful to residents of the area for access to their properties and succor during the long hot summers. Republic Geothermal Inc., Aminoil USA, Magma Energy Inc., Dow Chemical Co., Getty Oil Co., Pacific Energy Corp., Union Oil Co., Shell Oil Co., E.B. Towne, Geothermal Resources International Corp., and E.V. Ciancanelli provided geologic information or subsurface samples to further the geothermal knowledge of the Geysers-Clear Lake area.

STRUCTURE

The Clear Lake Volcanics provides structural markers that record the stress field during the past 2 million years in the Geysers-Clear Lake area. Faults, particularly those of northwest and north-northwest trend, provide major avenues for movement of thermal fluids to the surface (Goff and others, 1976, 1977). Many of the numerous faults have produced fracture porosity at depth, which is important for geothermal production in the Geysers steam field (McLaughlin, 1975, 1977a) and which will be important in exploration and development to the north in the inferred hot-water field (Goff and others, 1976, 1977; Goff and Donnelly, 1977; Donnelly, Goff, Thompson, and Hearn, 1976). Repeated faulting during the development of one or more magma chambers may explain the abundance of separate vents and flows within the Clear Lake volcanic field.

The volcanic field lies within the San Andreas fault system although the main fault zone is 60 km to the west. The San Andreas system is increasingly recognized as affecting a wide zone beyond the main fault by accumulation of strain or creep on numerous subsidiary fault zones (Thatcher, 1975, 1977). The two main fault zones in the Clear Lake volcanic field (figs. 14 and 15) are the Collayomi fault zone of northwest trend (Donnelly, McLaughlin, Goff, and Hearn, 1976) and the Konocti Bay fault zone of north-northwest trend (Goff and others, 1976).

Both fault zones are part of the San Andreas system and when more detailed mapping is available to the southeast, both zones may extend as far as or into the

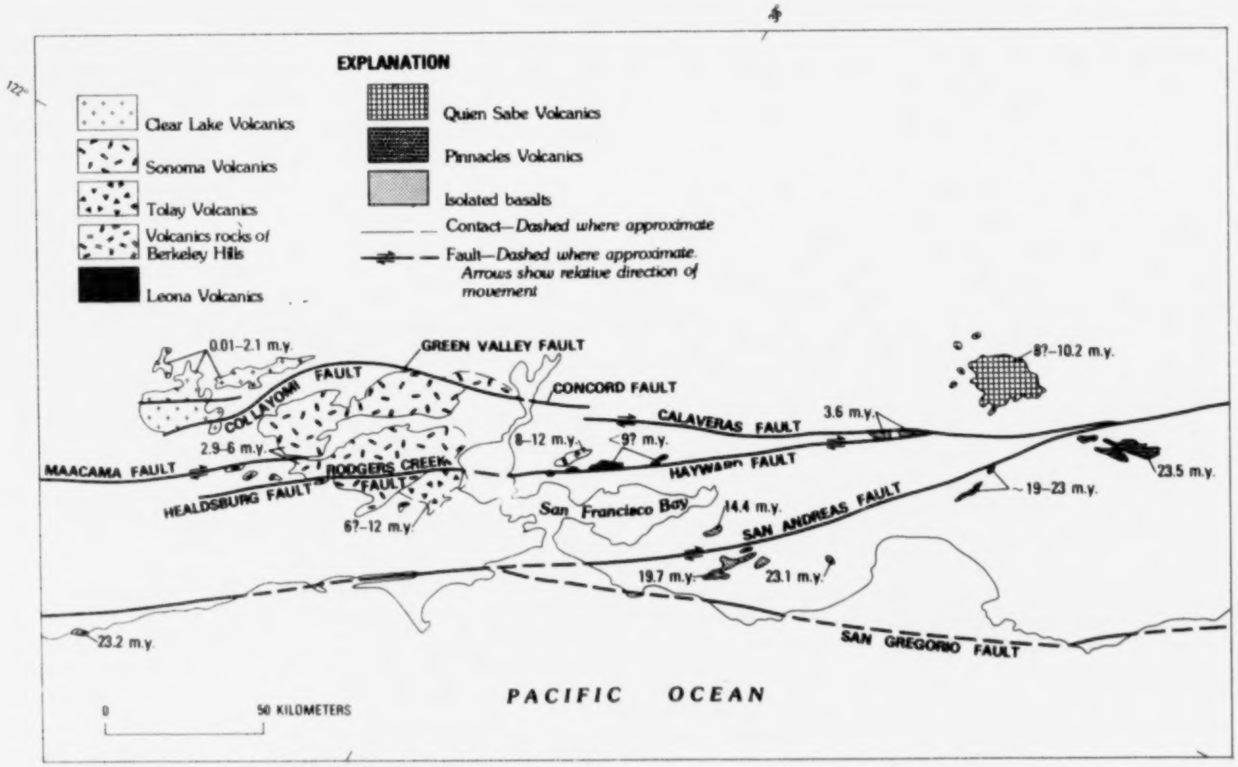
122°
EXPLANATION
Clear Lake Volcanics
Sonoma Volcanics
Tolay Volcanics
Volcanics rocks of Berkeley Hills
Leona Volcanics
Quien Sabe Volcanics
Pinnacles Volcanics
Isolated basalts
Contact—Dashed where approximate
Fault—Dashed where approximate. Arrows show relative direction of movement
0.01–2.1 m.y.
GREEN VALLEY FAULT
COLLAYOMI FAULT
CONCORD FAULT
CALAVERAS FAULT
3.6 m.y.
8?–10.2 m.y.
2.9–6 m.y.
8–12 m.y.
<9? m.y.
MAACAMA FAULT
RODGERS CREEK FAULT
HAYWARD FAULT
23.5 m.y.
HEALDSBURG FAULT
~19–23 m.y.
San Francisco Bay
14.4 m.y.
SAN ANDREAS FAULT
6?–12 m.y.
19.7 m.y.
23.1 m.y.
23.2 m.y.
SAN GREGORIO FAULT
PACIFIC OCEAN
0
50 KILOMETERS

FIGURE 13.—Ages of volcanic rocks, central Coast Ranges, California, from Allen (1946), Donnelly-Nolan, Hearn, Curtis, and Drake (this volume), Evernden, Savage, Curtis, and James (1964), Morse and Bailey (1935), Prowell (1974), Mankinen (1972), Radbruch and Case (1967), Turner (1970) and Turner, Curtis, Berry, and Jack (1970). Ages are by potassium-argon and by correlation with formations dated by faunal assemblages.

active Green Valley fault zone (Frizzell and Brown, 1976). Both show evidence of late Pleistocene movement: valleys, ridges, and other geomorphic features and Pleistocene volcanic rocks are offset. As further evidence of Pleistocene movement, serpentinite is squeezed up between volcanic units as young as 1.1 m.y. (Hearn and others, 1975b; Donnelly, McLaughlin, Goff, and Hearn, 1976; Donnelly, Hearn, and Goff, 1977). Felt earthquakes reported by residents near each zone and earthquake epicenters close to the Konocti Bay fault zone (Bufe and others, 1976; this volume) suggest that the zones are active. Southeast of Kelseyville, ground breakage for a distance of about 1.6 km in the 1906 San Francisco earthquake (Lawson, 1908, p. 188) corresponds in location and approximate direction with the southeastern part of the Big Valley fault (Lake County Flood Control and Water Conservation District, 1967), which is an offshoot of the Collayomi fault zone. Thus the southeastern part of the Big Valley fault is active. Within both the Collayomi and Konocti Bay zones, most faults show normal displacement. Along one fault in the Collayomi zone, right-lateral offset of volcanic rocks 0.5–0.6 m.y. old indicates an average movement of about 1 mm/yr over the past 0.5 m.y. Thrust or reverse faults in the Collayomi zone near Glenbrook in NE¼ sec. 29, T. 12 N., R. 8 W. (Donnelly and others, 1977, p. 37) and in the Konocti Bay zone along Soda Bay Road on the east edge of Ely Flat in the SW. cor. sec. 27, T. 13 N., R. 8 W. (Hearn and others, 1975b, 1976a) are shallow subsidiary structures which are consistent with and to be expected in a strike-slip fault system. Changes in horizontal distance across the Clear Lake volcanic field and to the southwest are consistent with active right-lateral deformation (Lofgren, this volume).

Faults of northwest and north-northwest trend are dominant within the Clear Lake volcanic field, and many of these faults are part of the Collayomi or Konocti Bay fault zones. These directions are also typical in fault zones to the southwest (McLaughlin, 1975, 1978) and northeast of the Clear Lake volcanic field. Faults of northeast trend are rather common, but those of east-west trend are less abundant. The overall pattern of faulting (fig. 15) fits a system of deformation related to a right-lateral northwest-southeast strike-slip couple by analogy to deformation of clay-cake models (Cloos, 1955; Wilcox and others, 1973). Expected directions of synthetic and antithetic shear faults would be at about 15° (north-northwest) and about 80° (northeast) respectively from the main couple, and maximum potential for tension fracture opening would be at about 45° (north-south) from the main couple. In the Clear Lake field, north-northwest-trending faults should show right-lateral strike-slip, and some do show it. By analogy to models, northeast-trending faults should show left-lateral strike-slip, but their lateral displacements could be small because of rotation effects (Wilcox and others, 1973). Some northeast-trending faults do locally show offsets which could be in part left-lateral strike-slip, but the apparent major displacement is normal slip.

The direction of maximum tension significantly corresponds to two north-south-trending zones of upward penetration and eruption of mafic magma: the zone of vents of 0.55 m.y. and younger basaltic andesite that extends across Mount Konocti, and the zone of young mafic cinder cones that extends from Roundtop Mountain on the south to Round Mountain in High Valley on the north. Some basaltic lavas that erupted in these two zones have "primitive" compositions characteristic of deep-source magma that has had minimal interaction with wallrocks or other melts on the way up. The ascent of deep-source magma may have been facilitated by tension fractures. Similarly, tension may have helped to create the space for shallow magma chambers. Other directions of vent alinements are northwest for the 0.55–0.35 m.y. dacites, and northwest to north-northwest for the early basalts; both are parallel to dominant regional fault directions that could have provided access for magma to the surface.

Also, by analogy with clay-cake models, faults along a major fault zone that follows a discontinuity at depth would be expected to be initially arranged in echelon, each segment trending 15° from the zone, and to later form an anastomosing group of active and inactive faults as new faults continue to develop (Rogers, 1973; Wilcox and others, 1973). With continued deformation, the antithetic northeast faults would be rotated clockwise, eventually far enough that new faults would form at about 80° from the main couple. In the Clear Lake Volcanics, deformation has probably been insufficient for detectable rotations except for small blocks within fault zones. Rotations should be more apparent in older units, but they have not been detected in paleomagnetic directions (Mankinen and others, this volume).

The Clear Lake topographic basin is delineated in part by faults of north, north-northwest, and west trend (Sims and Rymer, 1974, 1976). Formation of the Clear Lake basin and the earlier, geographically separate basin of deposition of the Cache Formation to the east (Anderson, 1936; Hodges, 1966; Rymer, 1978; 1981) could be related to subsidence between strike-slip faults by the mechanism outlined by Crowell (1974). The likely causative strike-slip faults would lie on the northeast side of Clear Lake and farther northeast within the Wilson Valley fault zone, but strike-

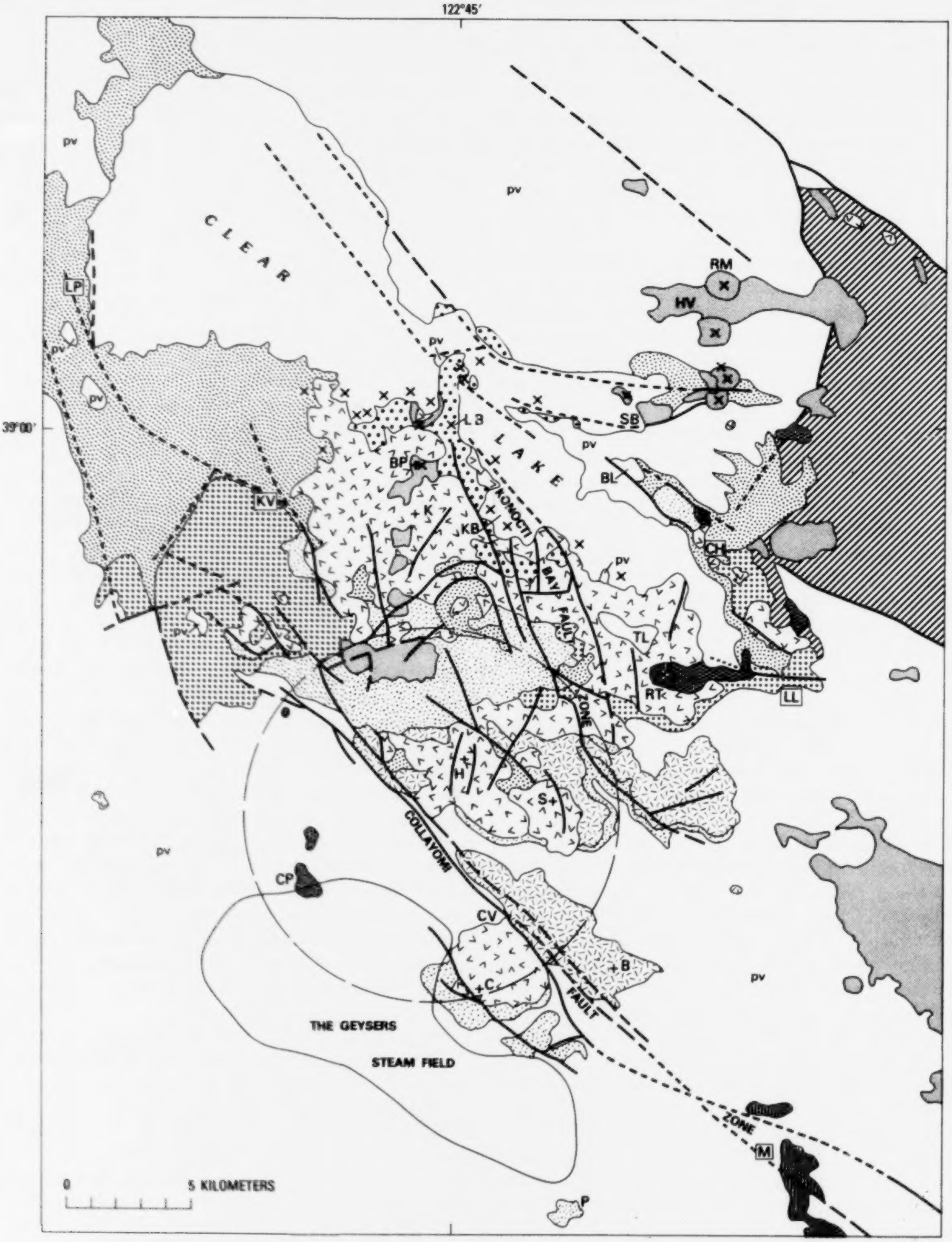
122°45'
39°00'
pv
CLEAR
LAKE
LP
RM
HV
SB
LB
BP
K
KV
KB
KONOCTI
BAY
FAULT
ZONE
BL
CH
TL
RT
LL
H
S
COLLAYOMI
FAULT
CV
B
C
CP
THE GEYSERS
STEAM FIELD
ZONE
M
P
0
5 KILOMETERS

slip displacement has not been proved. Although the outline and depth of the lake have changed in the past 50,000 years, the lake basin has been collecting sediment for at least the past 0.6 m.y. as sedimentation kept pace with subsidence (Sims, 1976; Donnelly, 1977). South of Kelseyville, northward tilting of lake and fluvial deposits (Kelseyville Formation, Rymer, 1978; 1981; equivalent to basin deposits of Kelseyville, Hearn and others, 1975b, 1976a), and the presence of deeper water and steeper slopes along the northeastern shores of Clear Lake suggest that northward or northeastward tilting of the lake basin has continued to recent time.

The overall structural pattern of the San Andreas fault system is overprinted by more local features related to volcanism. The large circular basin southeast of Mount Konocti, 1.6 km in diameter, may be related to collapse after eruptions of biotite rhyolite or dacite. The arc-like outcrop band of the rhyolite of Thurston Creek suggests a possible ring-fracture distribution of vents 0.6 m.y. ago. The abundance of related rhyolitic pumice in the basal part of the Kelseyville Formation (Rymer, 1981) suggests that eruption of the rhyolite could have produced or closed the basin, but evidence of large-scale caldera collapse is lacking. There is no known northern, eastern, or western counterpart to the arc, nor are there any age-equivalent volcanic units along the projection of the arc in those directions. The semicircular shape of the northern shore of Clear Lake suggests partial control by circular collapse, but the pattern could be a fortuitous result of deltaic sedimentation and linear north- to northwest-trending fault segments along the borders of the topographic basin. No young volcanic rocks are known to be exposed around the northern part of the lake, and the northern extent of the Clear Lake Volcanics beneath the lake bottom sediments has not been determined.

The active tectonics of this region will be documented by the monitoring of changes in elevations, horizontal distances, and lake level (Lofgren, 1973; this volume). Recently established close-spaced stations have potential for determining the displacement rate on individual faults.

EXPLANATION

░ Lake beds and alluvial deposits (*mostly Holocene*)

⁘ Synvolcanic clastic deposits, L and K members of the Cache Formation of Rymer (this volume) (*Pleistocene*)

▨ B member of Cache Formation of Rymer (this volume) (*Pleistocene and Pliocene*)

pv Prevolcanic rocks (*lower Tertiary, Cretaceous, Jurassic, and pre-Jurassic*)

CLEAR LAKE VOLCANICS

⁘ Young pyroclastic deposits

■ Basalt

□ Basaltic andesite

░ Andesite

△ Dacite

░ Rhyolite

——— Contact—*Numerous contacts omitted for clarity; some between flows of different age and (or) magnetic polarity shown within a single rock type*

— — - Fault—*Long dashed where inferred; short dashed where concealed*

× Vent—*Less than 0.2 m.y. old; older vents not shown*

— — Dashed circle is vertical projection of spherical magma chamber modeled by Isherwood (1976 and this volume) for gravity data

FIGURE 14.—Generalized geologic map of Clear Lake volcanic field showing geophysically inferred outline of present magma chamber. Lake and alluvial deposits are shown only near Clear Lake. Distribution of the Cache Formation is modified from Brice (1953), Rymer (1978; 1981) and mapping by the authors. Volcanic units in explanation are not chronologic in sequence. Lateral extent of cinder cones shown where associated with flows. Geology in part modified from Brice (1953), California Department of Water Resources (1962), Lake County Flood Control and Water Conservation District (1967), McNitt (1968a, b, c), and Sims and Rymer (1976). Abbreviation of geographic names (+ denotes locations of peaks): B-Boggs Mountain, C-Cobb Mountain, H-Mount Hannah, HV-High Valley, K-Mount Konocti, S-Seigler Mountain, BP-Buckingham Peak, KB-Konocti Bay, CP-Caldwell Pines, CV-Cobb Valley, SB-Sulphur Bank, BL-Borax Lake, LB-Little Borax Lake, TL-Thurston Lake, CH-Clearlake Highlands, KV-Kelseyville, LL-Lower Lake, LP-Lakeport, M-Middletown, P-Pine Mountain, RM-Round Mountain, RT-Roundtop Mountain.

OCCURRENCE AND LITHOLOGY OF THE CLEAR LAKE VOLCANICS

Eruptive rocks of the Clear Lake Volcanics range in composition from basalt to rhyolite and occur in four age groups: 0.01–0.1 m.y., 0.30–0.65 m.y., 0.8–1.1 m.y. and 1.3–2.1 m.y. (fig. 16) (Donnelly-Nolan and others, this volume). Basalt, basaltic andesite, and andesite occur as flows, cinder cones, and maar deposits. Dacite occurs primarily as rubbly to massive domes and thick flows, in accord with its higher viscosity. Rhyolite occurs as domes, as large flows, and as fragmental pumiceous deposits of tuff to agglomerate, which have been deposited by air-fall, or less commonly by mudflow. In contrast to the abundant dacitic to rhyolitic ash flows of the Sonoma Volcanics, ash flows are absent in the Clear Lake Volcanics.

The rock names used in this paper are based mainly on chemical composition, but those for unanalyzed volcanic units are based on hand-lens mineralogy, petrography, and flow characteristics. In general, basalt contains less than 54 percent SiO_2, basaltic andesite 54–58 percent SiO_2, andesite 58–62 percent SiO_2, dacite 62–71 percent SiO_2, and rhyolite greater than 71 percent SiO_2; considered on a water-free basis, the respective SiO_2 contents are less than 55, 55–59, 59–63.5, 63.5–72, and greater than 72 percent. The term dacite includes rhyodacite, which cannot be distinguished petrographically from dacite in the Clear Lake field.

Petrographic data are given by Anderson (1936) and Brice (1953). All the basalts and most of the basaltic andesites contain olivine phenocrysts (1–10 percent); plagioclase phenocrysts, generally less than 2 mm in size, are present in a few flows and tephra deposits of basalt and basaltic andesite. The groundmass in these rocks consists of clinopyroxene, olivine, and plagioclase.

Andesites typically contain phenocrysts of plagioclase, orthopyroxene, and clinopyroxene, and rarely

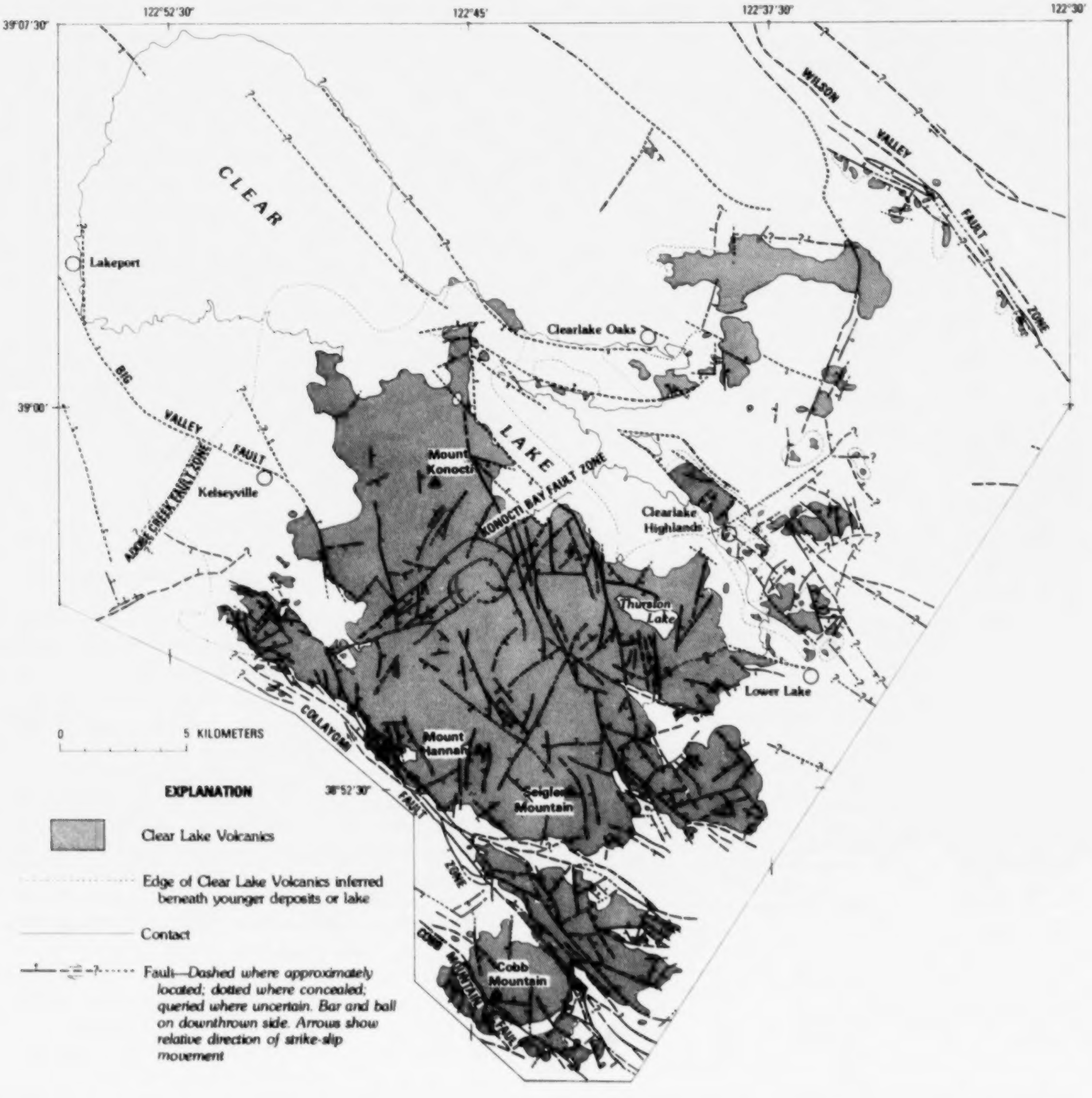
122°52'30"
122°45'
122°37'30"
122°30'
39°07'30"
39°00'
38°52'30"
CLEAR
LAKE
Lakeport
Clearlake Oaks
Kelseyville
Mount Konocti
Clearlake Highlands
Thurston Lake
Lower Lake
Mount Hannah
Seigler Mountain
Cobb Mountain
WILSON VALLEY FAULT ZONE
BIG VALLEY FAULT
ADOBE CREEK FAULT ZONE
KONOCTI BAY FAULT ZONE
COLLAYOMI FAULT ZONE
COBB MOUNTAIN FAULT
0
5 KILOMETERS
EXPLANATION
Clear Lake Volcanics
Edge of Clear Lake Volcanics inferred beneath younger deposits or lake
Contact
Fault—Dashed where approximately located; dotted where concealed; queried where uncertain. Bar and ball on downthrown side. Arrows show relative direction of strike-slip movement

FIGURE 15.—Fault map of the Clear Lake Volcanics and vicinity, compiled from Hearn, Donnelly, and Goff (1976a), Sims and Rymer (1976), Lake County Flood Control and Water Conservation District (1967), McNitt, (1968b), Brice (1953), Swe and Dickinson (1970), Jennings and Strand (1960), and the authors' mapping and photoreconnaissance.

olivine, hornblende, or obvious ilmenite. Amounts of pyroxene and plagioclase phenocrysts vary widely from one andesite unit to another.

The many varieties of dacite range from strongly porphyritic to weakly porphyritic, and all contain phenocrysts of plagioclase, clinopyroxene, orthopyroxene, and quartz. Most varieties contain small amounts of biotite, and many varieties contain both biotite and hornblende. Only a few contain olivine. Strongly porphyritic dacites contain sanidine phenocrysts and are mainly of more silicic, rhyodacitic composition. Most, but not all, of the weakly porphyritic dacites are less silicic. Strongly porphyritic dacites contain a range of sizes of feldspar phenocrysts (as much as 3 cm in some) and contain several compositions of feldspar and pyroxene phenocrysts in the same rock (Anderson, 1936; Brice, 1953; Donnelly, 1977). Such variations in phenocryst compositions have been cited as evidence of a hybrid origin (Anderson, 1936; Brice, 1953; Eichelberger, 1975). A few weakly porphyritic dacites have widespread glassy chilled facies on the top, base, and edges of flows.

Rhyolites are of two types, biotite-bearing and nearly biotite-free. Biotite rhyolites are commonly perlitic in glassy facies and typically crystal-rich (15–30 percent total of quartz, plagioclase, and sanidine phenocrysts; 0.5–5 percent biotite phenocrysts). Biotite rhyolites have quartz and feldspar phenocrysts of uniform size (2–5 mm) and lack the large size and multiple compositions of feldspar seen in the strongly porphyritic dacites. Rhyolites lacking biotite or containing less than 0.5 percent biotite are typically crystal-poor (less than 3 percent phenocrysts) and have widespread obsidian facies. Of the biotite-poor rhyolites, only the rhyolite of Bonanza Springs formed widespread pyroclastic deposits. Several of the biotite rhyolites occur mainly as pumiceous pyroclastic deposits although none are as extensive as the rhyolite of Bonanza Springs.

Two types of lithic inclusions and large quartz grains of problematical origin occur in the Clear Lake Volcanics. Type 1 inclusions have diabasic to granular texture and have larger grains and more mafic composition than their host; they are common in some dacites and most biotite rhyolites. Type 2 inclusions are schistose to granular metamorphic rocks; they are common in the andesite of Perini Hill, are less common in the andesites of Seigler Canyon, Boggs Mountain, and Grouse Springs, and are quite rare in basaltic andesites and basalts. Clear, irregular to rounded quartz grains, commonly 1–10 mm in size and rarely as large as 5 cm, occur in more than half the basaltic andesites, are abundant in the andesite of Perini Hill, and are less abundant in the andesites of Seigler Canyon, Split Top Ridge, Boggs Mountain, and Grouse Springs.

Type 1 inclusions (1 on fig. 17) have a relatively narrow position within the basaltic to andesitic range of compositions and are probably cognate with the Clear Lake Volcanics because they are not found as exposed country rocks. Type 1 inclusions are possibly (1) derivatives of their host flow that crystallized at hypabyssal depths, (2) recrystallized inclusions of earlier volcanic rocks, or (3) blobs of more mafic magma which were partly chilled upon injection into the more silic, cooler part of a magma chamber as proposed by Eichelberger and others (1976).

Type 2 inclusions are silicic to aluminous in composition and commonly contain garnet, cordierite, and spinel. Such inclusions could have been derived from (1) Franciscan or Great Valley shaly or silty rocks, or (2) rocks beneath the Franciscan assemblage. The schistose metamorphic fabric suggests regional rather than contact metamorphism and may indicate that a sialic basement of regional metamorphic rocks lies beneath part of the Clear Lake volcanic field. Such a sialic basement would be anomalous in or beneath the Franciscan, which is commonly assumed to be underlain by oceanic crust (Eaton, 1966; Warren, 1968; Bailey and others, 1970), although seismic data do not preclude the presence of continental crust.

Brice (1953) linked the origin of quartz grains in the andesite of Perini Hill and in some flows of basaltic andesite to disintegration of quartz-rich type 2 inclusions, a conclusion with which we concur for andesite of Perini Hill. Other proposed origins for quartz inclusions in basaltic and andesitic rocks are (1) rapid transport and chilling of a basaltic melt in which quartz phenocrysts are stable at 25 kilobars or higher pressures (Nicholls and others, 1971), (2) recrystallization of chert inclusions, or (3) phenocrysts surviving from silicic magma which mixed with basalt.

PRESENT AND PAST MAGMA CHAMBERS

The presence of a magma chamber (fig. 13) beneath the Clear Lake volcanic field is indicated by geophysical evidence. Gravity surveys (Chapman, 1966; Isherwood and Chapman, 1975) show a circular 25-mGal gravity low about 20 km in diameter, centered over Mount Hannah in the south-central part of the volcanic field (Isherwood, this volume). The gravity anomaly and aeromagnetic data (U.S. Geological Survey, 1973) have been interpreted as expressions of a spherical to cylindrical magma chamber about 14 km in diameter whose top is within 7 km of the surface (Chapman, 1966, 1975; Isherwood, this volume). In addition, teleseismic P-waves arriving within the area of the gravity low show delays of 0.5–1.5 seconds that are consistent with the presence of a subsurface mass containing a large proportion of melt and having a horizontal extent roughly equivalent to the size of the source of the gravity anomaly and a vertical extent to 30 km depth (Iyer and others, this volume). Seismic hypocenters are no deeper than 6 km in the area of the gravity low (Bufe and others, 1976; this volume). Electrical resistivity surveys may be sensing some shallow indirect effects (hot fluids, high salinity) of a magma chamber (Stanley and others, 1973). Although resistivity could be sensing the presence of magma at depths greater than 5 km (Stanley and others, 1973), such data are ambiguous and could be explained by other models without magma at 5–7 km depth (Isherwood,

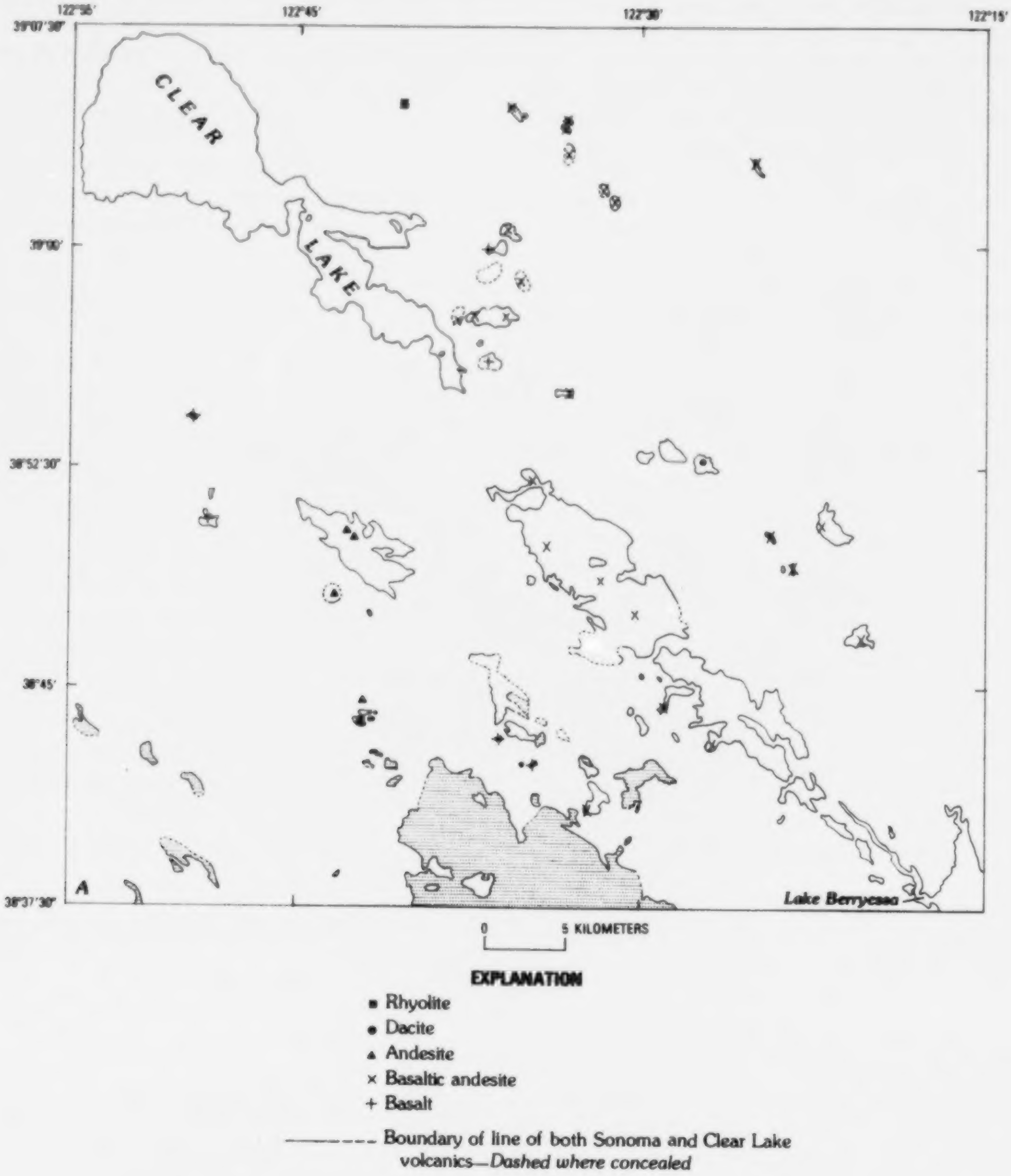
122°55'
122°45'
122°30'
122°15'
39°07'30"
39°00'
38°52'30"
38°45'
38°37'30"
CLEAR
LAKE
A
Lake Berryessa
0
5 KILOMETERS
EXPLANATION
■ Rhyolite
● Dacite
▲ Andesite
× Basaltic andesite
+ Basalt
Boundary of line of both Sonoma and Clear Lake volcanics—Dashed where concealed

FIGURE 16.—Present distribution of young volcanic rocks in Clear Lake area. *A*, Sonoma Volcanics (patterned) (2.9 m.y. and older) and age group 4 (1.3–2.1 m.y.). *B*, Age group 3 (0.8–1.1 m.y.). *C*, Age group 2 (0.30–0.65 m.y.). *D*, Age group 1 (0.01–0.1 m.y.). Vents shown only for Clear Lake Volcanics. Compiled from Hearn, Donnelly, and Goff (1976a), McLaughlin (1978), Fox, Sims, Bartow, and Helley (1973), Koenig (1963), and California Department of Water Resources (1962).

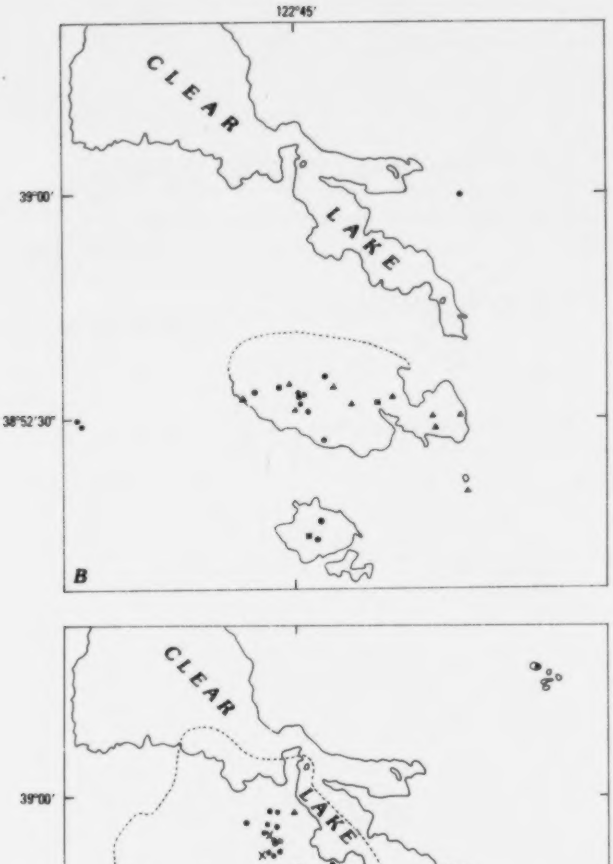

FIGURE 16.—Continued.

this volume). The presence of one or more magma chambers is suggested by the large volume of silicic relative to mafic volcanic rocks (Smith and Shaw, 1975).

Smith and Shaw (1975) estimated a considerably larger magma chamber for the Clear Lake system on the basis of the distribution of vents, regardless of composition, and of the diameter of the −35-mGal gravity contour of Chapman (1966). The vertical extent of the magma chamber could be greater than that inferred by Isherwood (1975) and Chapman (1975) if there is a substantial body of higher density mafic magma beneath the silicic magma. The mafic part could show little or no expression in the gravity data or, if denser than its surroundings, could cancel out part of the gravity low that is due to overlying silicic melt and hot rock. A deeper, more mafic root of the magma chamber is likely, and its detection may depend on seismic surveys to delineate the region of shear-wave attenuation or *P*-wave delays. The lack of volcanic rocks younger than 1 m.y. in the Geysers steam field conflicts with an inferred shallow lateral extension of the magma chamber (Isherwood, 1975; McLaughlin, 1977a) based on gravity data.

The inferred magma chamber may have an overlying shadow zone (Smith and Shaw, 1975), an area of dacite and rhyolite in which no mafic vents occur, presumably because ascending dense mafic magma could not penetrate the lower density silicic magma in the upper part of the shallow magma chamber. However, the evidence is ambiguous as none of the most recent volcanic rocks occur above the inferred magma chamber. In the most recent eruptive period, 0.1 m.y. to 10,000 years ago, igneous activity shifted from the geophysically inferred magma chamber to the area near the southeastern arms of Clear Lake and northeast of the lake (fig. 16*D*). Most of the lavas and tephra were basalt, basaltic andesite, or andesite, rocks that suggest a new cycle of deep-source magma generation, heating of the crust, and possible development of other magma chambers. Judging from the fractionated composition and the large negative europium anomaly of the rhyolite of Borax Lake, at 0.09 m.y., it is the only eruptive unit in the youngest age group that may have evolved in a magma chamber. Whether the Borax Lake flow was fed laterally from the inferred main magma chamber or derived from its own subjacent chamber is unknown. Existing geophysical data are insufficient to determine whether one or more small magma chambers are present near Borax Lake or farther northeast of Clear Lake.

Evidence of a major magma chamber for age group 4 rocks (1.3–2.1 m.y.) (fig. 16*A*) is nonexistent. Basalts and basaltic andesites erupted from widely dispersed

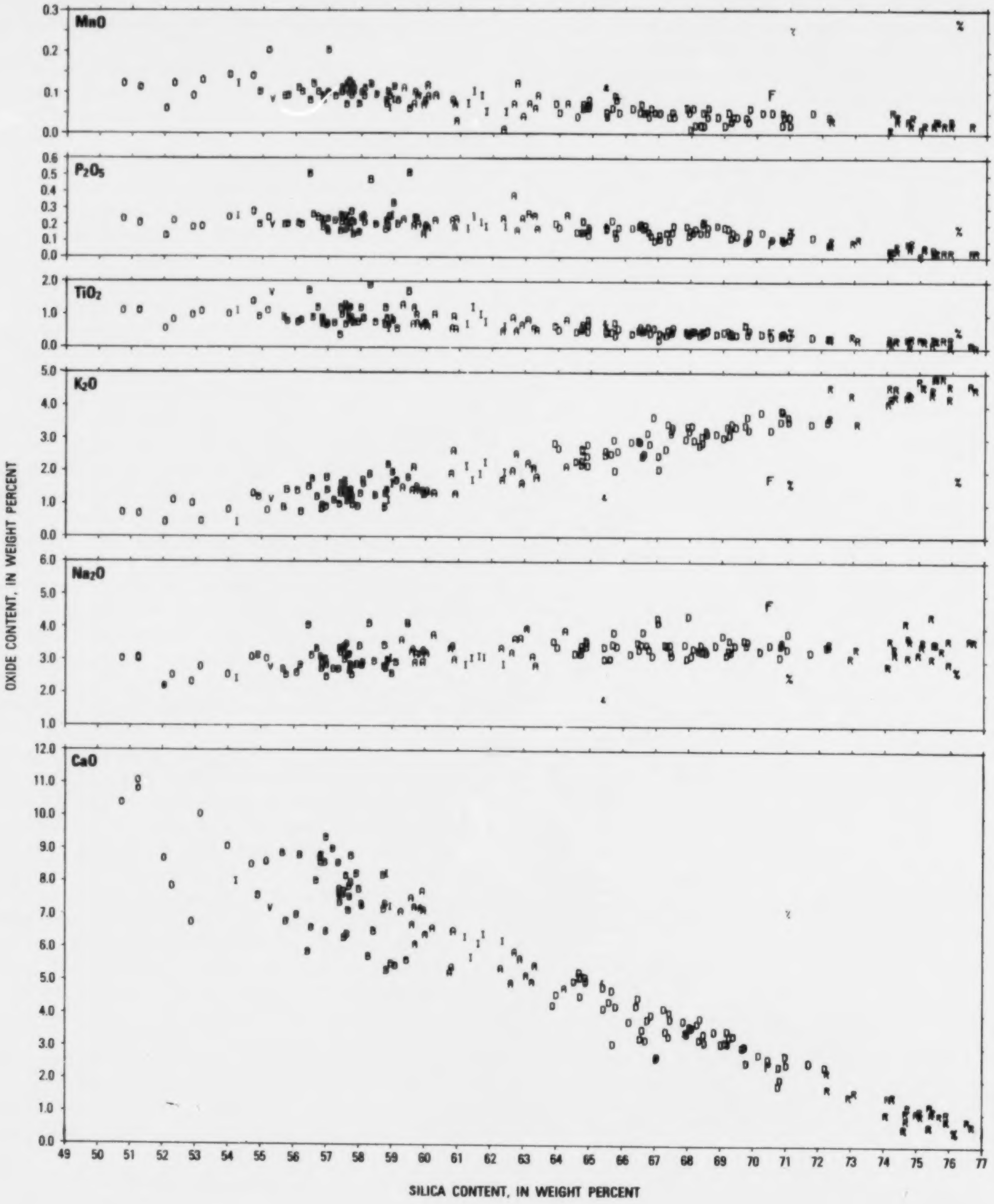
MnO
0.0
0.1
0.2
0.3
P_2O_5
0.0
0.1
0.2
0.3
0.4
0.5
0.6
TiO_2
0.0
1.0
2.0
K_2O
0.0
1.0
2.0
3.0
4.0
5.0
Na_2O
1.0
2.0
3.0
4.0
5.0
6.0
CaO
0.0
1.0
2.0
3.0
4.0
5.0
6.0
7.0
8.0
9.0
10.0
11.0
12.0
OXIDE CONTENT, IN WEIGHT PERCENT
49
50
51
52
53
54
55
56
57
58
59
60
61
62
63
64
65
66
67
68
69
70
71
72
73
74
75
76
77
SILICA CONTENT, IN WEIGHT PERCENT

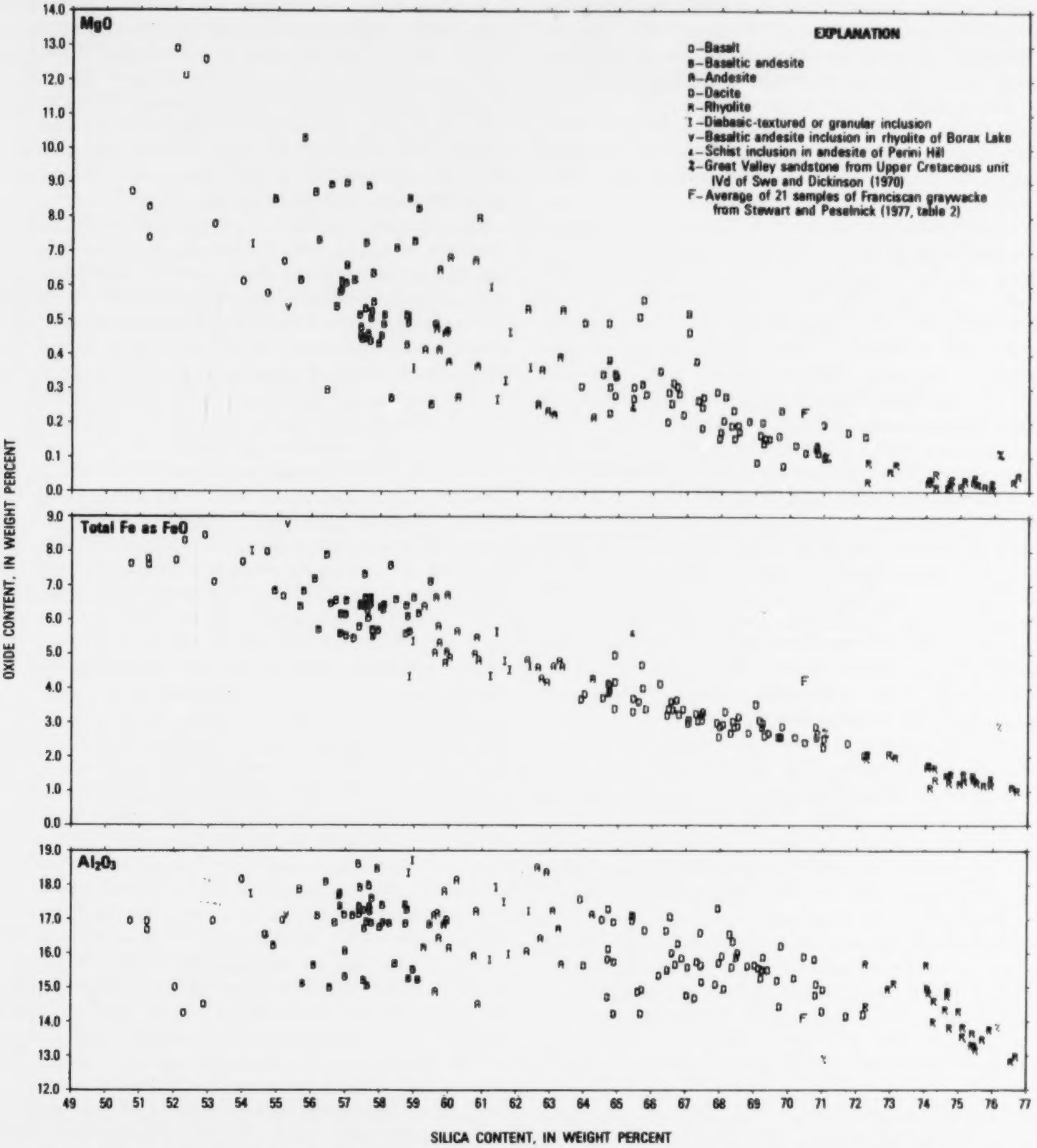

FIGURE 17.—Variation of major elements with silica for Clear Lake Volcanics, three samples of rhyolite from the Sonoma Volcanics, and samples of wallrocks. Analyses have CO_2 and equivalent CaO removed as calcite and are normalized to 100 percent dry weight, except for average Franciscan graywacke and additional point (% symbol) for Great Valley sandstone plotted with CO_2 removed as CO_2. Sources of data: Anderson (1936), Carmichael (1967), and unpublished analyses by U.S. Geological Survey, mainly by rapid rock analysis methods.

vents but were concentrated in a northwest-trending zone of deep magma access possibly controlled by the regional right-lateral stress system. Andesitic eruptive activity was focused in the Boggs Mountain area. The 1 km^3 of andesitic to rhyolitic volcanic rocks at Pine Mountain are probably cogenetic and could have been derived from a small magma chamber, which would be totally cooled by now but may contribute to a local gravity low (Isherwood, 1976, fig. 4).

A logical model of magma chamber evolution is that the current inferred chamber has evolved from one or more predecessors. Such early chambers may date back at least to the eruption of the 5-km^3 rhyolite of Alder Creek about 1.12 m.y. ago, during group 3 volcanism (1.1–0.8 m.y.), and may have been initiated by deep injection of basaltic magma 1.3–1.6 m.y. ago. The 1.02-m.y. rhyolite of Bonanza Springs and most of the andesites and dacites of group 3 age were vented in an elongate east-west 7-by-14-km area, the west part of which is directly above the current magma chamber. This series of eruptions culminated in the Mount Hannah edifice of several dacite bodies erupted within less than 5,000 years, possibly within 100 years (Mankinen and others, this volume; Donnelly-Nolan and others, this volume). The rhyolite of Alder Creek (1.12 m.y.) erupted earlier at Cobb Mountain either from the same chamber or from a satellitic chamber to the south. Down-faulting of part of that rhyolite has been interpreted as the result of possible collapse above a local magma chamber (Goff and McLaughlin, 1976).

Nearly all silicic eruptions of group 2 (0.30–0.65 m.y.) age occurred to the north of the group 3 eruptions (fig. 16*B*, 16*C*). Several dacite flows and a rhyolite flow of about 0.6 m.y. age indicate that a magma chamber or chambers were in existence by that time. Locations of group 2 silicic vents do not support a simple pattern of arcuate distribution above a single magma chamber. The 4-km^3 rhyolite of Thurston Creek, an early group 2 flow, erupted from vents along a 13-km northward-concave arc and may have initiated formation of part of the Clear Lake basin. If the arc is an expression of a ring-fracture zone, it has no northern counterpart and has no simple relation to the dacite vents of similar age or to the current inferred magma chamber.

Dacites of 0.5–0.6 m.y. age, slightly older or younger than the rhyolite of Thurston Creek, erupted from widely distributed vents as much as 19 km apart (at the west end of the rhyolite arc, and 1–5 km north, 8 km east, and 5 km south of the arc). Their pattern suggests that (1) the magma chamber was much larger than the present one, or (2) several magma reservoirs existed, or (3) magma migrated significantly in a lateral direction.

Dacites of 0.5–0.35 m.y. age vented in a west-northwest-trending zone 5 by 20 km which lies mainly to the north of the 0.5–0.6 m.y. pattern. These eruptions culminated at the northwest end of the zone in the voluminous edifice of Mount Konocti. This elongate zone of dacite vents suggests that shallow ascent of magma was controlled by regional northwest-trending structures rather than by arcuate structures generated by a subjacent magma chamber.

The apparent shadow zone for group 2 rocks permits the correlation of a 0.65–0.35-m.y. magma chamber and the present chamber (figs. 14, 16*C*), but the shadow zone is not well defined. The group 2 chamber is limited on the west by the 7-km-long, north-trending zone of basaltic andesite vents which runs from the basaltic andesite of McIntire Creek (about 0.55 m.y.) to the mafic vents (about 0.35 m.y.) high on Mount Konocti. To the east the chamber is limited only by a concealed basaltic vent (Donnelly, 1977) inferred to have been in the vicinity of the southeastern arm of Clear Lake and to have contributed mafic tuff to the Lower Lake Formation (Rymer, 1978, 1981; equivalent to basin deposits of Wildcat Canyon, Hearn and others, 1976a). The chamber is not limited to the north or south by any known group 2 mafic rocks. The western limit suggests that the dacites in the Kelsey Creek-Mount Olive area were erupted from a separate magma chamber, or that if they were fed laterally from the main chamber, the connecting conduit had crystallized by about 0.55 m.y. ago.

Mount Konocti contains the largest volume of dacite in the volcanic field (Donnelly-Nolan and others, this volume) and must have been fed from a sizable magma chamber, but the interleaved mafic units show that Mount Konocti was beyond the northern limit of the chamber at that time and thus was probably fed laterally from the main chamber. Where such extensive lateral migration of magma has occurred, the limits of a shadow zone are indistinct. Mount Konocti is beyond the northern limit of the present chamber.

Calculations for conductive cooling indicate that a spherical magma chamber 14 km in diameter (1,430 km^3) would have cooled to less than 650°C and completely crystallized in about 0.5 m.y. (Smith and Shaw, 1975). The calculations imply that if the current magma chamber has been present for the past 0.6 m.y. it was originally much larger, or that it has been resupplied with magma and heat several times. Either seems more likely than the alternative that several magma chambers have developed and cooled in nearly the same space.

In the regional strike-slip tectonic regime of the Clear Lake area, a simple arcuate distribution of silicic vents and a central shadow zone, more typical of stable areas, may not develop, because the deep and shallow ascent of magma may be dominated by regional structures and frequent fracturing. However, a shallow magma chamber and its hot aureole would be expected to transmit the regional strike-slip stresses poorly or not at all, and could cause a tectonic "shadow zone" of fewer faults above the magma chamber. In the Clear Lake volcanic field, a tectonic shadow zone is doubtful. Although faults may be somewhat less numerous above the northeastern half of the geophysically inferred magma chamber (figs. 14 and 15) than farther northeast, the Collayomi fault zone crosses the vertically projected position of the magma chamber. More significant is the lack of any seismic events at depths greater than 6 km in the area of the inferred magma chamber (Bufe and others, this volume).

Although regional stresses and local uplift can contribute to creation of the space occupied by magma at depth, some of that space is probably developed by stoping, partial melting and assimilation of wallrocks; these processes could have significant effects on the temperature and chemical variation of the magma. For the inferred position of the present magma chamber, extending from about 7–21 km depth (Isherwood, 1976; this volume), or to 30 km depth (Iyer and others, this volume), such wallrocks would be of the Franciscan assemblage to a depth of 13–15 km, and at greater depth would be the 6.8–7.2 km/s crust beneath the Franciscan. These assumed wallrock depths are based on seismic profiles to the west (Warren, this volume) and in the San Francisco Bay area (Warren, 1968) and on experimental determination of seismic velocities of Franciscan clastic and metaclastic rocks (Stewart and Peselnick, 1977). If lower crustal rocks are a major influence on the Clear Lake magmas, then the predominance of silicic lava compositions could indicate that part of the lower crust is sialic and of continental origin, because predominance of silicic lavas is atypical of areas underlain by oceanic crust.

In summary, a magma chamber in the Franciscan and underlying crust is indicated by geophysical data. Geologic data suggest that a magma chamber has been present in that location since about 0.6 m.y. ago. An earlier chamber (0.8–1.1 m.y.) may have evolved into the present chamber, but it could have been centered farther south.

CHEMISTRY

Major-element compositions for the entire age span of the Clear Lake Volcanics vary continuously from basalt to rhyolite with no gap in the dacite range (fig. 17). However, within each of the four age groups the range is not complete. Group 4, the oldest, lacks rocks with 61–67 percent SiO_2. Group 3 contains no basalt or basaltic andesite. In group 2, the range 60 to 63 percent SiO_2 is represented only by type 1 diabasic-textured inclusions. Group 1 lacks dacite other than the hybrid members of the basalt-dacite-rhyolite series at Borax Lake (Anderson, 1936; Bowman and others, 1973). In basalts and basaltic andesites, the considerable scatter in SiO_2, TiO_2, and other oxides may be indicative of generation from several deep sources. The basalts and basaltic andesites as groups are not obviously related by olivine fractionation from a single parental basalt. On SiO_2 variation diagrams (fig. 17) for all the Clear Lake Volcanics, K_2O, CaO, and total FeO show a linear variation with SiO_2 with little scatter, whereas Al_2O_3 and MgO show more scatter. Na_2O shows a linear trend that changes by only about 1.5 percent across the entire SiO_2 range.

Analyses are plotted (fig. 17) for three rock types which could have been assimilated: a sandstone (rhyolitic SiO_2 content) from the Great Valley sequence (Upper Cretaceous, unit IVd of Swe and Dickinson, 1970), an average Franciscan graywacke (rhyolitic SiO_2 content, Stewart and Peselnick, 1977, table 2), and a type 2 inclusion, quartz-biotite-garnet-pyroxene schist (dacitic SiO_2 content), from the andesite of Perini Hill. All three types plot within several oxide trends for the Clear Lake Volcanics on SiO_2 variation diagrams. However, compared to volcanic rocks of equivalent SiO_2 content, the schist is significantly higher in total FeO, the sandstone is significantly higher in CaO (in part due to carbonate cement, CO_2 4.8 percent) and MnO, and both are lower in Na_2O. The graywacke is higher in total FeO and in Na_2O and is lower in K_2O. Thus none of the three rocks can be an end-member for simple one-stage assimilation to account for the compositional variation of the Clear Lake Volcanics. Analytical data for various Franciscan rock types are needed to test assimilation models.

On an alkali-iron-magnesia (AFM) diagram (fig. 18), samples from the Clear Lake Volcanics show a diffuse trend across the central part of the diagram like that of lavas from the Cascade Range, but they tend to be lower in FeO and higher in MgO than average Cascade lavas (Anderson, 1936; Carmichael, 1964), possibly owing to interaction with ultramafic rocks and serpentinite at shallow depth. The AFM trend converges toward rhyolite from the widely scattered basalts and basaltic andesites, which have a wide range of FeO/MgO ratios. The scatter of basalts and basaltic andesites indicates the likelihood of several parental mafic magmas. Although a few contemporaneous basalts or basaltic andesites appear to be related by iron enrichment, there is no single fractionation trend among the mafic rocks.

Trace elements in the Clear Lake Volcanics show rather systematic variation relative to SiO_2, total Fe, differentiation index, and other measures of major-element variation, similar to relations in other basalt-andesite-dacite-rhyolite magma systems. Bowman, Asaro, and Perlman (1973) have shown closely linear trace-element variations in the dacite-rhyolite series near Borax Lake that indicate some mixing process of basalt and rhyolite. The basalt end-member of the series apparently was not found by Bowman, Asaro, and Perlman (1973), but the basalt of Arrowhead Road (Hearn and others, 1976a), adjacent to the rhyolite and dacite, is that end-member according to our analytical data for major and trace elements.

In each period of volcanism, five minor elements (Rb, Cs, Ta, Hf, and Th) and total rare-earth elements tend to increase with increasing SiO_2 and K_2O and reach about the same maximum values in rhyolites of each period. The maximum values are considerably below the extreme enrichment shown by some large ash-flow sheets such as the Bandelier Tuff (Smith and Bailey, 1966) and Bishop Tuff (Hildreth, 1977) in continental settings. The lower values for Clear Lake rhyolites may be in part a result of regional differences between continental and continental-border settings. The uniform values suggest that when the Clear Lake magmatic system lost its silicic fraction to the surface, these elements had reached a particular amount of enrichment in the upper part of the magma chamber. Approximately the same values are found for two bodies of rhyolite in the Sonoma Volcanics (Napa Glass Mountain, and an erosional remnant of welded ash-flow tuff northwest of Mount St. Helena).

Trace elements of basaltic affinity (Cr, Co, Zn, and Sc) show systematic decreases from basic to silicic rocks in the series and have more scattered values in the basalts and more uniform low values in the rhyolites. Of these elements, Cr varies in concentration in rocks of similar SiO_2 content through the whole series. Cobalt values, typically 1/4 to 1/20 of chromium, in part follow the high variability of Cr, but in a few rocks Co is nearly equal to Cr. Variability of these elements may indicate the addition of Cr and Co from the ultramafic rocks and serpentinite beneath parts of the Clear Lake Volcanics. Alternatively, some of their variability in intermediate rocks could reflect the Cr and Co content of parental basaltic melts, particularly if magma mixing has occurred. Cr and Co values range from 25 to 1,050 ppm and 24 to 56 ppm respectively in the basalts, suggesting (1) variability in deep sources of the basalts, (2) interaction with more shallow ultramafic rocks, or (3) varying amounts of preeruption separation of chrome spinel.

The total concentration of REE's (rare-earth elements) varies from a minimum of about 35 ppm in the most primitive basalt (of Caldwell Pines) to a range of about 110–180 ppm in rhyolites. Anomalously high total REE's are found in several units of the Clear Lake Volcanics peripheral to the main volcanic field: basal-

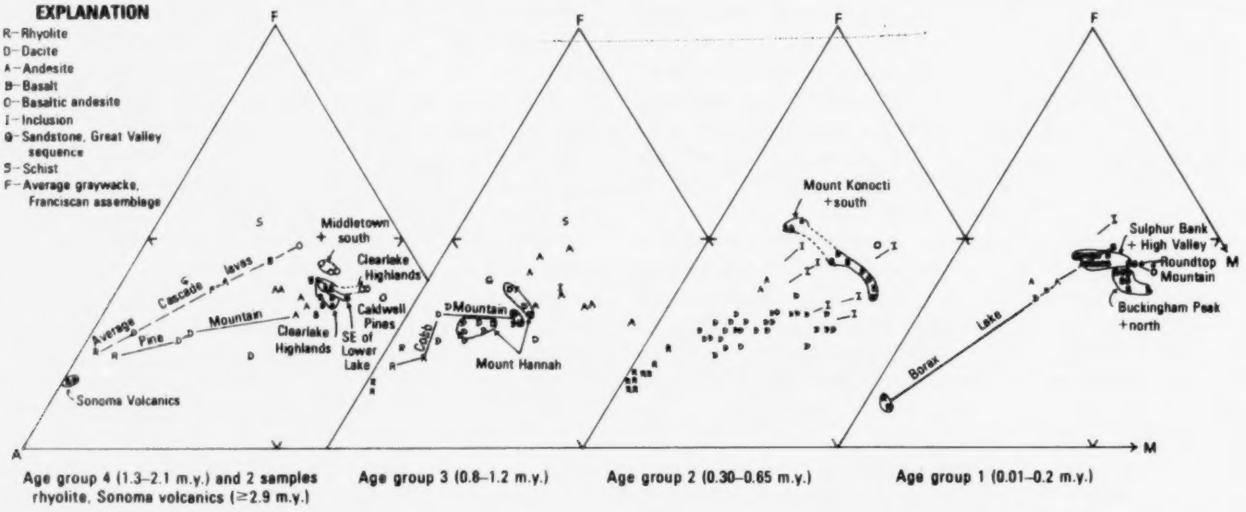

Age group 4 (1.3–2.1 m.y.) and 2 samples rhyolite, Sonoma volcanics (≥2.9 m.y.)

Age group 3 (0.8–1.2 m.y.)

Age group 2 (0.30–0.65 m.y.)

Age group 1 (0.01–0.2 m.y.)

FIGURE 18.—AFM diagrams for Clear Lake Volcanics and other rocks. $A = Na_2O + K_2O$, $M = MgO$, $F =$ total Fe as $FeO + MnO + TiO_2$. Lines join samples from units close in space and time. Outlined areas enclose samples from specific geographic areas. Lines from inclusion symbols point toward host rock. Dashed line shows trend of average composition of rhyolite, dacite, andesite, basaltic andesite, and basalt in the Cascade Range (Carmichael, 1964, table 8).

tic andesite of Table Mountain (338 ppm), and two of the northernmost early basalts (98 and 109 ppm).

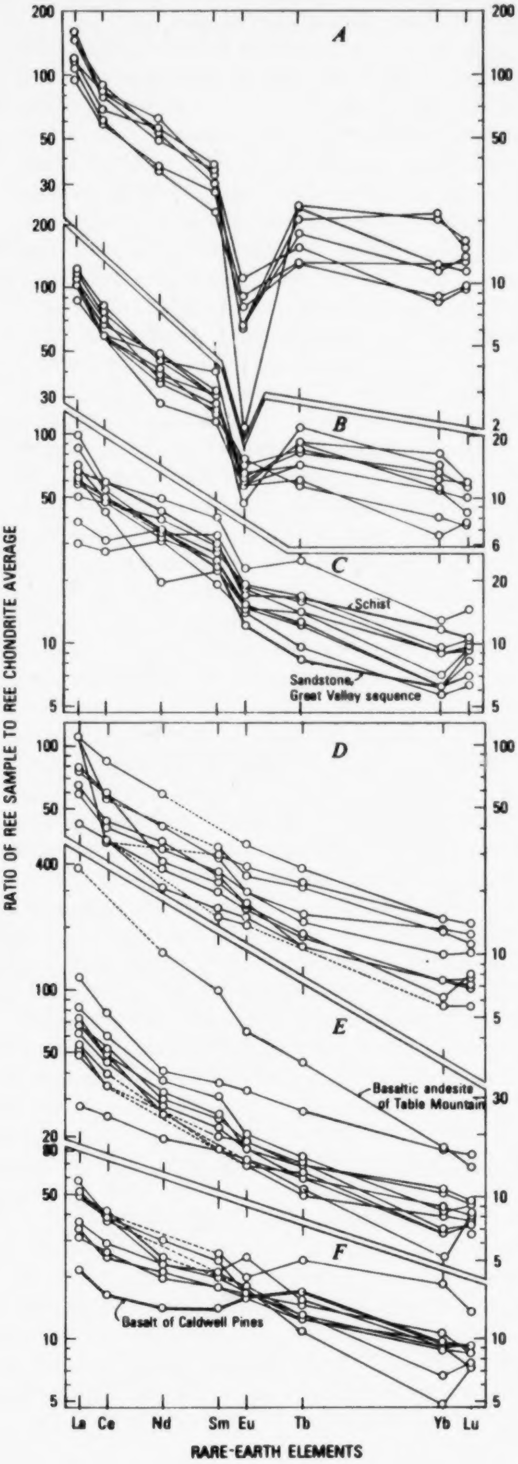

Within the main volcanic field, anomalously high REE contents occur in several units that do not otherwise show evidence of strong fractionation. For instance, the basaltic andesite of Buckingham Peak contains high REE's (70–80 ppm) although its Sr^{87}/Sr^{86} ratio (Futa and others, this volume) is quite low. These high REE contents may be due to a small degree of partial melting of upper mantle rocks in the deep source area.

The REE patterns relative to chondritic REE concentrations show enrichment in light REE's relative to heavy REE's for nearly all samples of the Clear Lake Volcanics analyzed (fig. 19). Light-REE enrichment is generally less in basalts and greater in dacites and rhyolites. Patterns for andesites, dacites, and rhyolites are slightly concave upward. The lowest enrichment in light REE's is shown by the basalt of Caldwell Pines, which also has the lowest potassium and total REE contents. No basalt shows a pattern of depleted light REE's and flat heavy REE's as shown by oceanic ridge tholeiites. REE patterns of two basalt units of the Medicine Lake Highlands area in northeastern California (Philpotts and others, 1971) are similar to the patterns of oceanic ridge tholeiites. The light-REE enrichment of the Clear Lake basalts is not compatible with their generation from partial or complete melting of subducted ocean-ridge tholeiitic basalts or associated oceanic crust; the Clear Lake basalts more probably came from a relatively unfractionated source. Although light-REE enrichment could be compatible with generation from subducted light-REE-enriched basalt from some oceanic islands, or associated light-REE-enriched oceanic crust, such material is volumetrically small in the oceans and in subducted oceanic slabs.

Enrichment in light REE's has been ascribed to generation from a garnet-bearing source rock (Philpotts and others, 1971), but a clinopyroxene-rich source rock could also contribute to that enrichment (Leeman, 1976). Calculated REE patterns (Zielinski and Lipman, 1976) for 40–50 percent partial melting of a trace-element-enriched source rock containing both garnet and clinopyroxene (such as eclogite or mafic granulite) are similar to REE patterns of Clear Lake basalts and basaltic andesites. The Clear Lake REE patterns also are similar to the calculated REE pat-

FIGURE 19.—Representative chondrite-normalized rare-earth element (REE) patterns of Clear Lake Volcanics, inclusions, and Great Valley sandstone. *A*, Rhyolites. *B*, Dacites. *C*, Diabase-textured and granular inclusions, schist inclusion in andesite of Perini Hill, and sandstone of Great Valley sequence from unit IVd of Swe and Dickinson (1970). *D*, Andesites. *E*, Basaltic andesites. *F*, Basalts. Neutron-activation analyses by P. A. Baedecker, L. J. Schwarz, and J. J. Rowe, U.S. Geological Survey.

terns for partial melting of garnet peridotite shown by Leeman (1976).

Positive europium (Eu) anomalies are interpreted to indicate addition of plagioclase to the melt or selective fusion of plagioclase in the area of magma generation, whereas negative Eu anomalies typically indicate loss of plagioclase from the melt or that plagioclase is residual in the area of generation. However, for the Bishop Tuff, an ash flow in the Long Valley area, California, Hildreth (1977) has shown that the rhyolitic upper part of the magma chamber contained significant gradients in Eu content, Ce/Yb ratio, and other trace elements, which were unrelated to partial melting or crystal fractionation. Thus, in silicic melts at shallow depths, other processes such as thermogravitational diffusion (Hildreth, 1977) may be producing Eu anomalies and changes in slope of chrondrite-normalized REE patterns.

The absence of Eu anomalies in most basalts and basaltic andesites in the Clear Lake Volcanics suggests that plagioclase has not been fractionated between the source and the surface. The absence of Eu anomalies also suggests that (1) the source area lacked plagioclase, or (2) plagioclase in the source area was completely melted when basalt was generated. The light-REE enrichment and absence of Eu anomalies in Clear Lake basalts do not uniquely characterize the possible phase assemblages in the source area. These REE characteristics are qualitatively compatible with garnet peridotite, eclogite, pyroxenite, plagioclase peridotite, gabbroic granulite, or gabbro: upper mantle or lower crustal rocks. More quantitative modelling may narrow the range of possible source rocks. Although plagioclase may be stable to depths of about 60 km for gabbroic compositions and to about 35 km for peridotite compositions, the 8.0 km/s compressional wave velocity below about 22 km (Warren, 1968) suggests that plagioclase is sparse or absent at depths of basalt generation beneath the Coast Ranges.

One porphyritic plagioclase basalt has a small positive Eu anomaly (Eu/Eu* = 1.3), indicative of plagioclase enrichment. Andesites have either no Eu anomaly or small positive or negative Eu anomalies. Nearly all dacites shows moderate negative Eu anomalies (Eu/Eu* = 0.5); these negative anomalies could result from loss of plagioclase phenocrysts, or from mixing of an Eu-depleted rhyolite with basalt or andesite, or from both processes. Although the present abundance of plagioclase phenocrysts in many dacites may support mixing, prior settling of plagioclase in the magma chamber also could have produced the low Eu. All samples of rhyolite show moderate to strong negative Eu anomalies, ranging from Eu/Eu* of about 0.4 to the strongest, 0.06, for rhyolite of Borax Lake. These rhyolites are likely to be products of extensive fractional crystallization and possibly some thermogravitational diffusion, as shown by Hildreth (1977).

Diabasic-textured inclusions are enriched in light REE's and have REE patterns that parallel those of their host rhyolites and dacites but have lower REE content in accord with their basaltic andesitic and andesitic compositions. Chondrite-normalized REE patterns of six out of seven inclusions show small negative Eu anomalies (Eu/Eu* = 0.60 to 0.83). Thus the diabasic inclusions are unlike most Clear Lake andesites and basaltic andesites which have no Eu anomalies or have less pronounced negative Eu anomalies than the inclusions. In that sense, the inclusions do not appear to be simply chilled blobs of basaltic magma, but they are likely related to high-level magmas by fractional crystallization involving plagioclase.

REE data are sparse for Great Valley, Franciscan, or other rocks at depth which could have been assimilated by the Clear Lake magmas. No data are available for Franciscan graywacke or greenstone. REE's in a serpentinized periodotite (Frey and others, 1971) are too low to have a recognizable effect. A sandstone of the Great Valley sequence (rhyolitic SiO_2 content) and a type 2 inclusion, quartz-rich schist (dacitic SiO_2 content), are enriched in light REE's. The schist has a slight negative Eu anomaly, much less pronounced than the dacites or rhyolites of equivalent REE content. The sandstone shows no Eu anomaly and rather low REE concentrations, about equivalent to those in basaltic andesites. In a general way, the REE patterns permit the assimilation of schist but in detail may not fit a one-stage process. For instance, basalt or basaltic andesite plus schist could produce dacite, but magmatic plagioclase separation is needed to explain the observed Eu anomalies of dacites; an alternative explanation, that plagioclase was left in the schist during partial melting, is not likely. Assimilation of the sandstone by mafic melts to make dacite would not give the higher REE contents of dacite. Assimilation of sandstone by rhyolite could lower the REE content of the resultant rhyolite.

PLATE-TECTONIC SIGNIFICANCE

The relation of the Clear Lake Volcanics to plate tectonics is not clear. In comparison to the Cascade chain of volcanoes, the Clear Lake Volcanics and earlier eruptive centers are anomalously close to the inferred position of the offshore subduction zone that was the boundary between the North American and Farallon plates before migration of the Mendocino triple junction changed the boundary to a strike-slip transform fault (Atwater, 1970). In timing and geographic position, these eruptive centers do not fit the usual model of melting related to active subduction of oceanic crust, but instead there is an apparent correlation between initiation of volcanism and the cessation of subduction.

Volcanism in the northern Coast Ranges has followed the northward passage of the Mendocino triple junction and attendant initiation of San Andreas transform faulting, which could have provided paths for ascent of deep magma (McLaughlin, this volume). A quiescent period of about 0.5–1 m.y. between the Sonoma Volcanics (Mankinen, 1972) and the Clear Lake Volcanics is postulated to be the time required for conduits to develop and for magma to reach the surface from the detached subducted slab or from a mantle diapir (McLaughlin, 1977b). However, three questions are unresolved. (1) If magma is already present, it should not take 0.5–1 m.y. to reach the surface in a region which has newly-developed steep faults and numerous earlier faults in part related to probable strike-slip components of subduction. Instead of lying on the main San Andreas fault zone, most of the older volcanic centers are east of the main fault, and more recent centers for Sonoma and Clear Lake volcanism aline northward or northeastward from the main fault. (2) Calculations of Toksöz, Minear, and Julian (1971) indicate that 0.5–1 m.y. is too short a time to reach melting temperatures in a subducted oceanic slab at typical depths within 100 km of the subduction zone. (3) Once started, why does volcanism cease after 3 to 5 million years?

We favor a model involving a mantle heat source, or hot spot, which is fixed beneath the North American plate so that the path of volcanism could be an indication of the apparent amount and direction of motion of the North American plate or a separate sliver of that plate. The apparent path of volcanism has some superimposed clockwise rotation due to right-lateral motion on faults within the San Andreas system (Hearn and others, 1975a, 1976b). However, in contrast to the west-southwest or westerly directions of movement of the North American plate deduced from the Yellowstone and Raton, New Mexico, hot spots (Suppe and others, 1975) or the Mid-Atlantic Ridge spreading, the Clear Lake hot spot implies a southward movement of this part of the North American plate. Alternatively, the northward progression of volcanism could imply that the hot spot is moving approximately parallel to the Pacific plate and somehow is tied to that plate.

In the hot-spot model, volcanism in a new location would begin when magma from the deep hot spot reached the surface, would become more silicic as shallow magma chambers developed with accompanying assimilation and crystal fractionation, and would cease after movement of the overlying plate shut off the source of deep magma and the shallow magma chambers crystallized. Episodic plate motion could be a factor. Pressure release during initiation or intensification of transform faulting may have accelerated deep partial melting processes and facilitated the ascent of deep-source magmas.

Although there is no evidence that such a heat source is the onshore projection of an oceanic spreading ridge, as proposed by Marshak and Karig (1977) to explain volcanism anomalously close to plate boundaries, a heat source could be related to a detached segment of the East Pacific rise overridden by the North American plate. Evidence for a projected position of such a segment could lie within the near-shore area of magnetic anomalies (Mason and Raff, 1961) immediately south of the Mendocino fracture zone, where age assignment of individual anomalies has not been made (Atwater and Menard, 1970). If the Clear Lake Volcanics and earlier volcanic centers are related to a hot spot formerly on the East Pacific rise, its track could be shown by offshore seamounts or their buried expression as shallow-depth magnetic anomalies near the shore.

Low Sr isotopic ratios (0.70316–0.70356, Futa and others, this volume) for the basalts at Clear Lake favor a mantle source. REE data favor a trace-element-enriched source that is too high in total REE's and too enriched in light REE's to be subducted ocean-floor basalt, its higher pressure derivatives, or its subjacent oceanic crust. Although the REE data do not uniquely define the lithology of the source, seismic velocities suggest that rock types such as peridotite, pyroxenite, and eclogite are more likely than plagioclase-bearing rock types of lower density. Eclogitic rocks are likely major components of the deeper parts of subducted oceanic crust of the Farallon plate, but their depleted light REE's and geometric and heat-transfer considerations probably preclude recently subducted oceanic crust as a source for the volcanic rocks. Thus a garnet-clinopyroxene-bearing source would have to be related to earlier subduction of another type of crust or to other processes of mantle evolution.

FUTURE VOLCANIC ACTIVITY

The complex eruptive history over the past 2 million years and the 10,000-year age of the youngest eruption indicate that the Clear Lake magmatic system is not extinct and that future eruptions are likely. Such a long period of multiple volcanic events and the large volume ($\sim$1,400 km^3) of the inferred magma chamber suggest that the Clear Lake system could be in a precaldera early evolutionary stage preliminary to major ash-flow eruptions and large-scale caldera collapse, as shown by other silicic magma systems such as Long Valley, California; Valles, New Mexico; and Yellowstone, Wyoming. Voluminous eruptions (10–200 km^3) of that type would be major volcanic hazards (Mullineaux, 1976) for the whole Clear Lake basin, and, if large enough, could spill over into adjacent drainage basins of the Eel, Russian, and Sacramento Rivers and Napa Valley. In addition, air-fall ash would affect a large area of several thousand square kilometers. Rhyolites of the Clear Lake Volcanics do not show the same trace-element enrichment shown by ash flows of some other major silicic systems, but they may never reach those enrichments because of regional source differences. Also, comparison with trace elements for precaldera rhyolites of other major silicic systems could have predictive significance but data are unavailable. Relative movement of the heat source at depth may preclude a duration of heating sufficient to generate the volume of volatile-rich silicic melt necessary for a large ash-flow eruption. Also, in this tectonic setting, faults of the active right-lateral stress system may tap the magma chamber or chambers often enough to prevent the buildup of volatiles necessary for a voluminous ash-flow eruption. The absence of eruptions since 0.35 m.y. ago above the present geophysically inferred magma chamber is puzzling, but it may indicate that that magma chamber is no longer being resupplied with deep-source magma and is quiescent and cooling. If the chamber were tapped again, eruptions would be silicic flows with accompanying minor pyroclastic activity, and would be vented along faults within about 10 km of Mount Hannah or farther northeast.

The Clear Lake Volcanics and Sonoma Volcanics are similar in that both are complex sequences that have an overall range from basalt to rhyolite, and larger volume of silicic than mafic rocks. However, the scarcity of pyroclastic eruptions in the Clear Lake field contrasts markedly with the Sonoma Volcanics, which contains numerous dacitic to rhyolitic ash flows (Fox and others, 1973). Sonoma ash flows are small in comparison with those in major silicic systems. Because the Sonoma Volcanics lies within the strike-slip tectonic regime, its complexity and lack of large-volume ash flows may be related to frequent tapping of the magma chambers or sources, although other factors such as chemical composition, volatile content, and depth of magma sources may have been important also.

Although future eruptions are likely in the Clear Lake field, prediction of the timing is difficult because activity has been episodic in the past. From extrapolated dates and numbers of ash beds beneath Clear Lake (Sims, 1976; Sim and Rymer, 1975), the apparent lack of eruptions in the past 10,000 years is a geologically brief lull in activity after frequent eruptions (about 34, or averaging one every 1,800 years) in the previous 60,000 years. The average interval between eruptions for the past 130,000 years has been about 2,500 years (Sims, 1976). For the period 0.35–0.65 m.y. ago, about 60 volcanic units were erupted (Hearn and others, 1976a; Donnelly, 1977), for an average interval of 5,000 years, or less if mapped units were produced by more than one eruption. Episodes of volcanic activity have typically continued for at least 0.3 m.y., so that the youngest episode which began about 0.1 m.y. ago could be in an early stage and thus could continue for another 0.2 m.y.

To the northeast of the geophysically inferred magma chamber, future eruptions would probably be mafic, similar to the youngest cinder cones and flows, although the 90,000-year-old rhyolite of Borax Lake shows that silicic eruptions are a possibility, particularly if there is a small magma chamber northeast of Clear Lake. Eruptions are likely to be located close to, beneath, or northeast of Clear Lake, especially around the east arm of the lake, near High Valley and Chalk Mountain, which are the areas of the youngest past eruptions and are above the apparent current focus of heating. A more distant area for possible future volcanism is the Wilbur Springs quicksilver district that contains a basaltic andesite dike of Pleistocene age, many thermal springs, mercury deposits, and extensive hydrothermal alteration within a small area. Eruptions near the lake are likely to be phreatomagmatic and would pose ash-fall and wave hazards to the lake shore and ash-fall hazards to areas within a few kilometers of the vent. Eruptions away from the lake would produce cinder cones and flows and would be hazardous within a few kilometers of the vents.

GEOTHERMAL SIGNIFICANCE

The magma chamber inferred beneath the central part of the Clear Lake Volcanics is clearly the ultimate source of heat for the Geysers steam field and for the extensive hot-water system or systems that are inferred to underlie most of the Clear Lake volcanic field (Donnelly, Goff, Thompson, and Hearn, 1976; Goff and Donnelly, 1977; Goff and others, 1977). Geothermal potential beneath the main volcanic field is promising. Within the main volcanic field, published geophysical data are not detailed enough to determine the extent of localized geothermal systems. Published geophysical data are inadequate to determine whether small satellitic magma chambers are present at depth. The young volcanic activity and thermal anomalies around the east arm of Clear Lake, and east-northeast of Clear Lake as far east as the Wilbur Springs area, indicate geothermal potential, but the distribution of thermal springs shows the zone to be narrow and possibly not continuous. The boundary between thermal influence of the main magma chamber and current heating to the northeast is indistinct. In the northeast area, acquisition of geological, geophysical (Harrington and Verosub, this volume), and geochemical (Goff and Donnelly, 1977) data has only begun. Existing data are probably insufficient to determine subsurface structure or the presence or absence of small magma chambers.

CONCLUSIONS

The volcanic rocks of the Clear Lake area are the eruptive products of mantle-source heating, crustal-level fractionation and assimilation of the Great Valley, Franciscan, and underlying crustal rocks. Pyroxenite, peridotite, and eclogite are likely rock types in the deep source area. Volcanism may be a result of a mantle hot spot which has generated a series of Tertiary and Quaternary volcanic centers as the North American plate moved relatively southward across it. A geophysically inferred large (1,400 km^3 or greater) magma chamber beneath the Clear Lake volcanic field has existed since about 1.1 m.y. ago, or perhaps earlier, and it is the shallow-level source of geothermal heat in the Geysers-Clear Lake area. Tapping of the magma chamber and eruption of deeper magmas have been controlled in part by the stress field of the San Andreas fault system, which includes several active fault zones across and near the Clear Lake Volcanics. Future eruptions are likely to produce mafic flows and cinder cones, but possibly could produce catastrophic silicic ash-flows with accompanying caldera collapse.

REFERENCES CITED

Allen, J. E., 1946, Geology of the San Juan Bautista quadrangle, California: California Division of Mines and Geology Bulletin 133, 112 p.

Anderson, C. A., 1936, Volcanic history of the Clear Lake area, California: Geological Society of America Bulletin, v. 47, no. 3, p. 629–664.

Atwater, Tanya, 1970, Implications of plate tectonics for the Cenozoic tectonic evolution of western North America: Geological Society of America Bulletin, v. 81, no. 12, p. 3513–3536.

Atwater, Tanya, and Menard, H. W., 1970, Magnetic lineations in the northeast Pacific: Earth and Planetary Science Letters, v. 7, p. 445–450.

Bailey, E. H., Blake, M. C., Jr., and Jones, D. L., 1970, On-land Mesozoic oceanic crust in the California Coast Ranges: U.S. Geological Survey Professional Paper 700–C, p. C70–C81.

Bowman, H. R., Asaro, Frank, and Perlman, I., 1973, On the uniformity of composition in obsidians and evidence for magmatic mixing: Journal of Geology, v. 81, no. 3, p. 312–327.

Brice, J. C., 1953, Geology of Lower Lake quadrangle, California: California Division of Mines Bulletin 166, 72 p.

Bufe, C. G., Pfluke, J. H., Lester, F. W., and Marks, S. M., 1976, Map showing preliminary hypocenters of earthquakes in the Healdsburg (1:100,000) quadrangle, Lake Berryessa to Clear Lake, California, January 1969–June 1976: U.S. Geological Survey Open-File Report 76–802.

California Department of Water Resources, 1962, Reconnaissance report on upper Putah Creek basin investigation: California Department of Water Resources Bulletin 99, 254 p.

Carmichael, I. S. E., 1964, The petrology of Thingmuli, a Tertiary volcano in eastern Iceland: Journal of Petrology, v. 5, no. 3, p. 435–460.

——— 1967, The iron-titanium oxides of salic volcanic rocks and their associated ferromagnesian silicates: Contributions to Mineralogy and Petrology, v. 14, p. 36–64.

Chapman, R. H., 1966, Gravity map of Geysers area: California Division of Mines and Geology Mineral Information Service, v. 19, no. 9, p. 148–149.

——— 1975, Geophysical study of the Clear Lake region, California: California Division of Mines and Geology Special Report 116, 23 p.

Cloos, Ernst, 1955, Experimental analysis of fracture patterns: Geological Society of America Bulletin, v. 66, no. 3, p. 241–256.

Crowell, J. C., 1974, Origin of late Cenozoic basins in southern California, *in* Dickinson, W. R., ed., Tectonics and sedimentation: Society of Economic Paleontologists and Mineralogists Special Publication 22, p. 190–204.

Donnelly, J. M., 1977, Geochronology and evolution of the Clear Lake volcanic field: Berkeley, University of California, Ph. D. thesis, 48 p.

Donnelly, J. M., Goff, F. E., Thompson, J. M., and Hearn, B. C., Jr., 1976, Implications of thermal water chemistry in The Geysers-Clear Lake area, *in* Tucker, F. L., and Anderson, M. D., eds., Geothermal environmental seminar-76, Lake County, California: Lakeport, Calif., Shearer Graphic Arts, p. 99–103.

Donnelly, J. M., Hearn, B. C., Jr., and Goff, F. E., 1977, The Clear Lake Volcanics, California: Geology and field trip guide, *in* Field trip guide to The Geysers-Clear Lake area: Cordilleran Section, Geological Society of America, p. 25–56.

Donnelly, J. M., McLaughlin, R. J., Goff, F. E., and Hearn, B. C., Jr., 1976, Active faulting in The Geysers-Clear Lake area, northern California [abs.]: Geological Society of America Abstracts with Programs, v. 8, no. 3, p. 369–370.

Eaton, J. P., 1966, Crustal structure in northern and central California from seismic evidence, *in* Bailey, E. H., ed., Geology of northern California: California Division of Mines and Geology Bulletin 190, p. 419–426.

Eichelberger, J. C., 1975, Origin of andesite and dacite: Evidence of mixing at Glass Mountain in California and at other circum-Pacific volcanoes: Geological Society of America Bulletin, v. 86, no. 10, p. 1381–1391.

Eichelberger, J. C., Gooley, Ronald, Nitsan, Uzi, and Rice, A. R., 1976, A mixing model for andesitic volcanism [abs.]: EOS (American Geophysical Union Transactions), v. 57, no. 12, p. 1024.

Evernden, J. F., Savage, D. E., Curtis, G. H., and James, G. T., 1964, Potassium-argon dates and the Cenozoic mammalian chronology of North America: American Journal of Science, v. 262, p. 145–198.

Fox, K. F., Jr., Sims, J. D., Bartow, J. A., and Helley, E. J., 1973, Preliminary geologic map of eastern Sonoma County and western Napa County, California: U.S. Geological Survey Miscellaneous Field Studies Map MF–483.

Frey, F. A., Haskin, L. A., and Haskin, M. A., 1971, Rare-earth abundances in some ultramafic rocks: Journal of Geophysical Research, v. 76, no. 8, p. 2057–2069.

Frizzell, V. A., Jr., and Brown, R. D., Jr., 1976, Map showing recently active breaks along the Green Valley fault, Napa and Solano Counties, California: U.S. Geological Survey Miscellaneous Field Studies Map MF–743.

Goff, F. E., and Donnelly, J. M., 1977, Applications of thermal water chemistry in The Geysers-Clear Lake geothermal area, California [abs.]: Geological Society of America Abstracts with Programs, v. 9, no. 7, p. 992.

Goff, F. E., Donnelly, J. M., Thompson, J. M., and Hearn, B. C., Jr., 1976, The Konocti Bay fault zone, California: Potential area for geothermal exploration [abs.]: Geological Society of America Abstracts with Programs, v. 8, no. 3, p. 375–376.

——— 1977, Geothermal prospecting in The Geysers-Clear Lake area, northern California: Geology, v. 5, no. 8, p. 509–515.

Goff, F. E., and McLaughlin, R. J., 1976, Geology of the Cobb Mountain-Ford Flat geothermal area, Lake County, California: U.S. Geological Survey Open-File Report 76–221.

Hearn, B. C., Jr., Donnelly, J. M., and Goff, F. E., 1975a, Geology and geochronology of the Clear Lake volcanic field, Lake County, California: U.S. Geological Survey Open-File Report 75–296, 18 p.

——— 1975b, Preliminary geologic map of the Clear Lake volcanic field, Lake County, California: U.S. Geological Survey Open-File Report 75–391.

——— 1976a, Preliminary geologic map and cross-section of the Clear Lake volcanic field, Lake County, California: U.S. Geological Survey Open-File Report 76–751.

——— 1976b, Geology and geochronology of the Clear Lake Volcanics, California: United Nations Symposium on the Development and Use of Geothermal Resources, 2d, San Francisco, 1975, Proceedings, v. 1., p. 423–428.

Hildreth, E. W., 1977, The magma chamber of the Bishop Tuff: Gradients in temperature, pressure, and composition: Berkeley, University of California, Ph. D. thesis, 328 p.

Hodges, C. A. 1966, Geomorphic history of Clear Lake, California: Stanford, Calif., Stanford University, Ph. D. thesis, 210 p.

Isherwood, W. F., 1975, Gravity and magnetic studies of The Geysers-Clear Lake geothermal region, California, U.S.A.: U.S. Geological Survey Open-File Report 75–368, 37 p.

——— 1976, Gravity and magnetic studies of The Geysers-Clear Lake region, California: United Nations Symposium on the Development and Use of Geothermal Resources, 2d, San Francisco, 1975, Proceedings, v. 2, p. 1065–1073.

Isherwood, W. F., and Chapman, R. H., 1975, Principal facts for gravity stations in The Geysers-Clear Lake region, California: U.S. Geological Survey Open-File Report 75–107.

Jennings, C. W., and Strand, R. G., 1960, Ukiah sheet, geologic map of California: California Division of Mines and Geology, scale 1:250,000.

Koenig, J. B., 1963, Santa Rosa sheet, geologic map of California: California Division of Mines and Geology, scale 1:250,000.

Lake County Flood Control and Water Conservation District, 1967, Big Valley ground-water recharge investigation, 63 p.

Lawson, A. C., 1908, The California earthquake of April 18, 1906: Report of the State Earthquake Investigation Commission: Carnegie Institution of Washington Pub. 87, v. 1 and atlas, 451 p.

Leeman, W. P., 1976, Petrogenesis of McKinney (Snake River) olivine tholeiite in light of rare earth and Cr/Ni distributions: Geological Society of America Bulletin, v. 87, no. 11, p. 1582–1586.

Lofgren, B. E., 1973, Monitoring ground movement in geothermal areas, *in* Hydraulic engineering and the environment: American Society of Civil Engineers, Hydraulic Division Specialty Conference, Bozeman, Montana, August 15–17, 1973, Proceedings, p. 437–447.

——— 1978, Monitoring crustal deformation in The Geysers-Clear Lake geothermal area, California: U.S. Geological Survey Open-File Report 78–597, 19 p.

Mankinen, E. A., 1972, Paleomagnetism and potassium-argon ages of the Sonoma Volcanics, California: Geological Society of America Bulletin, v. 83, p. 2063–2072.

Marshak, R. S., and Karig, D. E., 1977, Triple junctions as a cause for anomalously near-trench igneous activity between the trench and volcanic arc: Geology, v. 5, no. 4, p. 233–236.

Mason, R. G., and Raff, A. D., 1961, Magnetic survey off the west coast of North America, 32° N. latitude to 42° N latitude: Geological Society of America Bulletin, v. 72, no. 8, p. 1259–1265.

McLaughlin, R. J., 1975, Preliminary compilation of in-progress geologic mapping in The Geysers geothermal area, California: U.S. Geological Survey Open-File Report 75–198.

——— 1977a, The Franciscan assemblage and Great Valley sequence in The Geysers-Clear Lake region of northern California, *in* Field trip guide to the Geysers-Clear Lake area: Cordilleran Section, Geological Society of America, p. 3–24.

——— 1977b, Late Mesozoic-Quaternary plate tectonics and The Geysers-Clear Lake geothermal anomaly, northern Coast Ranges, California [abs.]: Geological Society of America Abstracts with Programs, v. 9, no. 4, p. 464.

——— 1978, Preliminary geologic map and structural sections of the central Mayacmas Mountains and The Geysers steam field, Sonoma, Lake, and Mendocino Counties, California: U.S. Geological Survey Open-File Report 78–389.

McNitt, J. R., 1968a, Geologic map of the Kelseyville quadrangle, Sonoma, Lake and Mendocino Counties, California: California Division of Mines and Geology Map Sheet 9.

——— 1968b, Geologic map of the Lakeport quadrangle, Lake County, California: California Division of Mines and Geology Map Sheet 10.

——— 1968c, Geology of the Clearlake Oaks 15-minute quadrangle, Lake County, California: California Division of Mines and Geology Open-File Release 68–12.

Morse, R. R., and Bailey, T. L., 1935, Geological observations in the Petaluma district, California: Geological Society of America Bulletin, v. 46, p. 1437–1456.

Mullineaux, D. R., 1976, Preliminary overview map of volcanic hazards in the 48 conterminous United States: U.S. Geological Survey Miscellaneous Field Studies Map MF–786, scale 1:7,500,000.

Nicholls, James, Carmichael, I. S. E., and Stormer, J. C., Jr., 1971, Silica activity and P_{total} in igneous rocks: Contributions to Mineralogy and Petrology, v. 33, no. 1, p. 1–20.

Philpotts, J. A., Martin, Wayne, and Schnetzler, C. C., 1971, Geochemical aspects of some Japanese lavas: Earth and Planetary Science Letters, v. 12, no. 1, p. 89–96.

Prowell, D. C., 1974, Geology of selected Tertiary volcanics in the central Coast Range mountains of California and their bearing on the Calaveras and Hayward fault problems: Santa Cruz, University of California, Ph. D. thesis, 182 p.

Radbruch, D. H., and Case, J. E., 1967, Preliminary geologic map and engineering geologic information, Oakland and vicinity, California: U.S. Geological Survey open-file map, scale 1:24,000.

Rogers, T. H., 1973, Fault trace geometry within the San Andreas and Calaveras fault zones—A clue to the evolution of some transcurrent fault zones, *in* Kovach, R. L., and Nur, Amos, eds., Proceedings of conference on tectonic problems of the San Andreas fault system: Stanford University Publications in the

Geological Sciences, v. 13, p. 251–259.

Rymer, M. J., 1978, Stratigraphy of the Cache Formation (Pliocene and Pleistocene) in Clear Lake basin, Lake County, California: U.S. Geological Survey Open-File Report 78–924, 102 p.

——— 1981, Stratigraphic revision of the Cache Formation (Pliocene and Pleistocene), Lake County, California: U.S. Geological Survey Bulletin 1502–C [in press].

Sims, J. D., 1976, Paleolimnology of Clear Lake, California, U.S.A., *in* Horie, Shoji, ed., Paleolimnology of Lake Biwa and the Japanese Pleistocene; v. 4, p. 658–702.

Sims, J. D., and Rymer, M. J., 1974, Gaseous springs in Clear Lake, California, and the structural control of the lake basin [abs.]: Geological Society of America Abstracts with Programs, v. 6, no. 3, p. 254.

——— 1975, Preliminary description and interpretation of cores and radiographs from Clear Lake, Lake County, California: Core 4: U.S. Geological Survey Open-File Report 75–666, 19 p.

——— 1976, Map of gaseous springs and associated faults in Clear Lake, California: U.S. Geological Survey Miscellaneous Field Investigations Map MF-721, scale 1:48,000.

Smith, R. L., and Bailey, R. A., 1966, The Bandelier Tuff: A study of ash-flow eruption cycles from zones magma chambers: Bulletin Volcanologique, v. 29, no. 1, p. 83–104.

Smith, R. L., and Shaw, H. R., 1975, Igneous-related geothermal systems, *in* White, D. E., and Williams, D. L., eds., Assessment of geothermal resources of the United States—1975: U.S. Geological Survey Circular 726, p. 58–83.

Stanley, W. D., Jackson, D. B., and Hearn, B. C., Jr., 1973, Preliminary results of geoelectrical investigations near Clear Lake, California: U.S. Geological Survey open-file report, 20 p.

Stewart, Roger, and Peselnick, Louis, 1977, Velocity of compressional waves in dry Franciscan rocks to 8 kbar and 300°C: Journal of Geophysical Research, v. 82, no. 14, p. 2027–2039.

Suppe, John, Powell, Christine, and Berry, Robert, 1975, Regional topography, seismicity, Quaternary volcanism, and the present-day tectonics of the western United States: American Journal of Science, v. 275–A, p. 397–436.

Swe, Win, and Dickinson, W. R., 1970, Sedimentation and thrusting of Late Mesozoic rocks in the Coast Ranges near Clear Lake, California: Geological Society of American Bulletin, v. 81, no. 1, p. 165–189.

Thatcher, Wayne, 1975, Strain accumulation on the northern San Andreas fault zone since 1906: Journal of Geophysical Research, v. 80, no. 35, p. 4873–4880.

——— 1977, Secular deformation and the earthquake cycle on the San Andreas fault [abs.]: EOS (American Geophysical Union Transactions), v. 58, no. 12, p. 1227.

Toksöz, M. N., Minear, J. W., and Julian, B. P., 1971, Temperature field and geophysical effects of a downgoing slab: Journal of Geophysical Research, v. 76, no. 5, p. 1113–1138.

Turner, D. L., 1970, Potassium-argon dating of Pacific Coast Miocene foraminiferal stages, *in* Bandy, O. L., ed., Radiometric dating and paleontologic zonation: Geological Society of America Special Paper 124, p. 91–129.

Turner, D. L., Curtis, G. H., Berry, F. A. F., and Jack, R. N., 1970, Age relationship between the Pinnacles and Parkfield felsites and felsite clasts in the Temblor Range, California—Implications for San Andreas fault displacement [abs.]: Geological Society of America Abstracts with Programs, v. 2, p. 154–155.

U.S. Geological Survey, 1973, Aeromagnetic map of the Clear Lake area, Lake, Sonoma, Napa, and Mendocino Counties, California: U.S. Geological Survey open-file map, scale 1:62,500.

Warren, D. H., 1968, Transcontinental geophysical survey (35°–39°N): Seismic refraction profiles of the crust and upper mantle from 112°W longitude to the coast of California: U.S. Geological Survey Miscellaneous Geologic Investigations Map I–532–D.

Wilcox, R. E., Harding, T. P., and Seely, D. R., 1973, Basic wrench tectonics: American Association of Petroleum Geologists Bulletin, v. 57, no. 1, p. 74–96.

Williams, Howel, and Curtis, G. H., 1977, The Sutter Buttes of California: A study of Plio-Pleistocene volcanism: University of California Publications in Geological Sciences, v. 116, 56 p.

Zielinski, R. A., and Lipman, P. W., 1976, Trace-element variations at Summer Coon volcano, San Juan Mountains, Colorado, and the origin of continental-interior andesite: Geological Society of America Bulletin, v. 87, no. 10, 1477–1485.

GEOCHRONOLOGY AND EVOLUTION OF THE CLEAR LAKE VOLCANICS

By Julie M. Donnelly-Nolan, B. Carter Hearn, Jr.,
Garniss H. Curtis, and Robert E. Drake

ABSTRACT

The Clear Lake Volcanics covers approximately 400 km^2 in the northern California Coast Ranges. Seventy-three potassium-argon ages established the age range of the lavas as from 2.1 m.y. to 10,000 yr B.P. The K-Ar ages were especially important for isolated units and sequences and have been essential to understanding the evolution of the magmatic system in time and space. In a general way, the Clear Lake Volcanics is younger to the north, as are other Tertiary volcanic rocks along the length of the California Coast Ranges.

The dates strongly suggest the existence of three time breaks in the volcanic sequence, and possibly a fourth. Each break covered a period of about 0.2 m.y. in which no known volcanic eruptions took place. The earliest and most recent periods of volcanism were dominated by basaltic eruptions. The greatest volume of lava was erupted during the period from 0.6 to 0.3 m.y. ago, when about 35 cubic kilometers of dacite built Mount Konocti, which represents more than a third of the total volume of the volcanic field.

The time-volume pattern of evolution provides some constraints on when future volcanic activity might be expected, but questions remain as to the generation and source materials of the magmatic liquids.

Mapping of the volcanic rocks has revealed an abundance of faults, some of which may be currently active. Hundreds of meters of tilting has been recorded by volcanic units. Thus, the volcanic rocks have been structural markers for determining the rates and kinds of synvolcanic and postvolcanic tectonic activity in this structurally complex region where the volcanic field overlies older thrust sheets of the Franciscan assemblage and the Great Valley sequence.

The K-Ar dates and magnetic polarities of the volcanic units agree well with previously published geomagnetic-reversal time scales. Together, the dates and the magnetic polarities have identified at least nine units representing the Jaramillo normal-magnetic-polarity event. Although many units erupted near the Jaramillo, no eruptions occurred within 0.1 m.y. on either side of the 0.7-m.y.-old Matuyama-Brunhes magnetic-polarity reversal.

Almost no usable dates were obtained from basalts and basaltic andesites less than half a million years old because of their low radiogenic argon content. Whole-rock dates from andesites were good provided that fusion times were long enough to release all of the radiogenic argon. Sanidine dates on crystal-rich dacites and rhyolites were generally excellent, with small analytical uncertainties. Where dacites and rhyolites were crystal-poor, glassy whole-rock samples produced good results.

INTRODUCTION AND PREVIOUS WORK

The Clear Lake volcanic field covers approximately 400 km^2, overlies the Franciscan assemblage, the Great Valley sequence, and the Martinez (Paleocene) and Tejon (Eocene) Formations, and is in part interbedded with the Cache, Lower Lake, and Kelseyville Formations, collectively of Pliocene and Pleistocene age (Rymer, 1981). Much of the northern part of the volcanic field was mapped in reconnaissance by Anderson (1936). Brice (1953) and McNitt (1968a, b, c) mapped quadrangles that include portions of the volcanic field along with the pre-Quaternary rocks. Studies of the Great Valley sequence in the area (Swe and Dickinson, 1970) and the Franciscan assemblage (Yates and Hilpert, 1946; McLaughlin, 1974 and 1975; McLaughlin and Stanley, 1976) predate this work.

The largest power-producing steam field in the world, The Geysers, lies adjacent to the Clear Lake volcanic field and within a 25-milligal negative gravity anomaly centered over the volcanic field (Isherwood, this volume). The gravity anomaly is thought to reflect the presence of a silicic magma chamber about 8 km in diameter whose top lies about 6 km below the surface (Isherwood, this volume). This postulated magma chamber is interpreted to be the heat source for the Geysers steam field and for the numerous warm springs in the area.

The Clear Lake Volcanics lies north of the Sonoma Volcanics, of Pliocene age (youngest published date, 2.9 ±0.2 m.y.; Mankinen, 1972), and has been thought by previous workers to be Pliocene or Pleistocene in age (Anderson, 1936). Accepting the Pliocene-Pleistocene boundary to be at 1.6 m.y. (Haq and others, 1977), the present study shows that the lower part of the Clear Lake Volcanics is Pliocene, but most of it is Pleistocene. No young volcanic rocks are found to the north in the California Coast Ranges. The nearest Quaternary volcanic centers are at the Sutter Buttes, about 80 km east-northeast, and Lassen Volcanic National Park, about 190 km northeast of Clear Lake.

Acknowledgments.—J. Hampel, University of California at Berkeley, performed nearly all the potassium analyses reported here and provided advice on techniques of mineral separation. C. Wahrhaftig provided comments and suggestions and the locations of three K-Ar samples (Nos. 1, 2, and 3) which he collected in 1961. M. Alexander, U.S. Geological Survey, contributed a substantial number of the sanidine separates.

PROCEDURES

Seventy-three potassium-argon ages were determined on 43 rock units of the Clear Lake Volcanics (fig. 20). Seventy of the argon extractions were performed in the K-Ar laboratory in the Department of Geology and Geophysics at the University of California, Berkeley. Three of the argon extractions were done in the geochronology laboratories at the U.S. Geological Survey in Menlo Park. All the argon determinations were done by standard techniques of isotope dilution (Dalrymple and Lanphere, 1969) with Reynolds-type mass spectrometers.

All samples were crushed and sieved to size fractions between 10 and 100 mesh. All samples except biotite separates were treated with a 5-percent HF solution to etch the surface of the grains and reduce the amount of air argon (Evernden and Curtis, 1965). Samples were treated for 30 seconds to 1 minute (whole-rock samples) or 10–15 minutes (sanidine separates), then rinsed with distilled water. In addition, whole-rock basalt and basaltic andesite samples were treated with 50-percent HCl for ½ hour to remove carbonates and sulfides. Samples weighing from 2 to 18 g were fused by induction heating for half an hour or more. Beginning with No. 27 (see table 1), all extractions were performed in unlined bottles, a procedure that resulted in lower air argon corrections. Potassium analyses were performed by flame photometry. Results are listed in table 1 at the end of this chapter.

Magnetic polarities were determined (Hearn and others, 1976a) by collecting oriented samples in the field and using a flux-gate magnetometer to determine directions of magnetization of the samples. Units whose magnetic polarities were checked in the laboratory are indicated on table 1. At least three samples were collected and run for each polarity given.

GOALS OF THE AGE-DATING PROJECT

Potassium-argon ages were determined to establish (1) the total age range of volcanism near Clear Lake, (2) the eruptive timing of various rock types in mapped sequences to define the evolution of the magmatic system, and (3) the ages of volcanic units that are geographically separate (fig. 20). The first task has been largely accomplished. For the second, the dating together with the mapping has defined times during which no eruptions took place (fig. 21). For the third, the sanidine and whole-rock ages greater than 0.5 m.y. have been important.

K-Ar dating of the youngest lavas (less than 0.3 m.y.) has been largely ineffective, yielding results with high atmospheric corrections (greater than 97 percent air argon) and thus a large analytical error. The only analytically precise date on young lava was obtained from the one rhyolite (No. 5, table 1). Almost all the other young volcanic rocks are mafic in composition and generally fine grained; they are commonly pyroclastic (representing, for example, maar eruptions and cinder cones) and vesicular in texture, making K-Ar dating even more difficult. Several dates on these young volcanic rocks were attempted (for example, Hearn and others, 1975), but none provided results that were accurate enough to be useful.

By contrast, the sanidine dates (25 are reported here) and whole-rock dates greater than 0.5 m.y. yielded results that are analytically precise and consistent with mapped stratigraphy and with magnetic polarity determinations. Wherever possible, sanidine was dated, but it was only found in rhyolite and dacite. Only one biotite date is reported here. Biotite samples were found to contain relatively high atmospheric argon contents for material of this age and produced results with a large analytical error. Most sanidine samples, however, yielded enough radiogenic argon for precise dates even at less than 0.5 m.y. (see No. 21). This mineral was found to be relatively resistant to alteration, especially oxidation, weathering, and hydrothermal alteration (see No. 27 and No. 48). Surface etching of sanidine grains by dilute HF proved to be highly effective in reducing atmospheric argon corrections (Evernden and Curtis, 1965).

Basalt and basaltic andesite gave imprecise whole-rock dates; only one sample, No. 43, yielded more than 16 percent radiogenic argon. Whole-rock andesite gave more precise dates; only one sample, No. 30, yielded less than 13 percent radiogenic argon. We found that some andesites required fusion times longer than the standard one-half hour to release all the argon from the sample. The data show that fusion times of 45 minutes or more may be necessary to expel all the argon from some andesite samples. For other samples the ages remained essentially unchanged with longer fusion times (Nos. 14 and 15).

Dacites were dated as whole-rock samples if no sanidine was present, and black glassy samples were preferred. Radiogenic argon content ranged from 4.7 to 29.1 percent. Whole-rock rhyolite samples (obsidians) produced either excellent results or contained nearly 100 percent atmospheric argon; four samples were in the latter category and are not reported here. Physical appearance (selection of black, nonvesicular samples) was not a sufficient criterion to determine which obsidian samples would yield good results and which would not.

RESULTS

Potassium-argon ages on the Clear Lake Volcanics range from 2.06 to 0.09 m.y. The youngest mapped lavas have not been dated by the potassium-argon method and the southeastward extension of the early basaltic lavas has not been mapped, but the Clear Lake Volcanics is thought to be entirely younger than the Sonoma Volcanics (youngest published age, 2.9 ± 0.2 m.y., Mankinen, 1972).

The dating has identified several time breaks in the eruptive sequence which were not determined by field observation and mapping. The most pronounced gap (fig. 21) occurred between about 0.8 and 0.6 m.y. ago. Other breaks occurred about 0.3–0.1 m.y. and 1.3–1.1 m.y. ago. A gap may exist at 1.9–1.7 m.y., although it

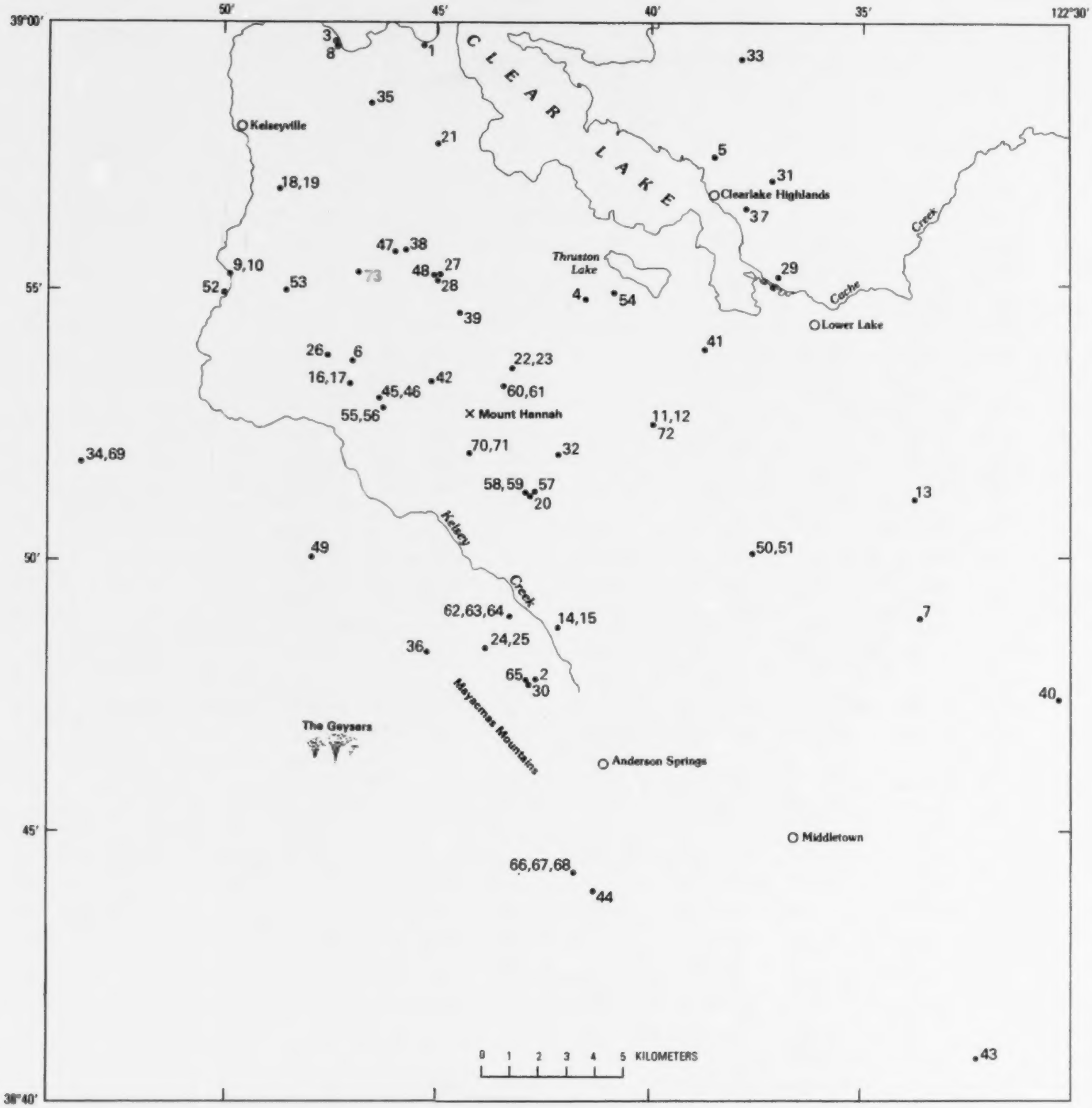
39°00'
50'
45'
40'
35'
122°30'
55'
50'
45'
38°40'
CLEAR LAKE
Kelseyville
Clearlake Highlands
Thruston Lake
Lower Lake
Cache Creek
Mount Hannah
Kelsey Creek
Mayacmas Mountains
The Geysers
Anderson Springs
Middletown
3
8
1
33
35
21
5
31
18,19
37
47
38
48
27
28
73
9,10
52
53
29
4
54
39
41
26
6
22,23
16,17
42
45,46
60,61
55,56
11,12
72
34,69
70,71
32
58,59
57
20
13
49
50,51
62,63,64
14,15
7
36
24,25
65
2
30
40
66,67,68
44
43
0 1 2 3 4 5 KILOMETERS

FIGURE 20.—Locations of samples for potassium-argon dating (see table 1).

TABLE 1.—*K-Ar dates and analytical data, Clear Lake Volcanics*

[For explanation of unit symbols see map explanation of Hearn, B. C., Jr, Donnelly, J. M., and Goff, F. E., 1976a. K_2O analyses (except samples 4–6) by J. Hampel. Ages and errors (1σ) calculated by method of Dalrymple and Lanphere (1969), using the following constants: $\lambda_\epsilon = 0.581 \times 10^{-10} yr^{-1}$, $\lambda_\beta = 4.962 \times 10^{-10} yr^{-1}$, and $^{40}K/K = 1.67 \times 10^{-4}$ atom percent. Magnetic polarity: N, normal; R, reversed; U, unique. Samples 33 and 53, polarity determined in field using portable magnetometer; samples 1–3, 8 and 35 checked in laboratory by Allan Cox, 1962; samples 31, 43, 47, and 49 checked by W. F. Isherwood, 1975; all others (including samples 3, 8, and 35) checked by E. A. Mankinen and C. S. Gromme, 1973–77]

Map No. (fig. 1)	Sample No.	Rock type	Sample location		Material dated	K_2O (weight percent)	Radiogenic ^{40}Ar		Age (10^6 years)	Magnetic polarity	Replicate dates and other comments	Unit symbol
			Latitude N.	Longitude W.			Moles/g ($\times 10^{-12}$)	Percent				
1	1815[1]	Dacite	39° 0.25′	122° 45.80′	Sanidine	10.820	5.385	25.0	0.35±0.02	N/		dh
2	1838[1]	Rhyolite	38° 48.10′	122° 43.00′	do.	10.450	16.467	45.0	1.11±0.02	U′	Nos. 36, 65, same unit, different sample, float block.	ra
3	1839[1]	Dacite	39° 0.35′	122° 48.00′	do.	10.079	6.307	8.0	0.43±0.05	N	No. 8	dsb
4	USGS 1[2]	Rhyolite (obsidian)	38° 55.30′	122° 41.80′	Whole rock	[3]4.74	3.268	32.7	0.479±0.015	N	Nos. 6, 26; same unit, different samples.	r
5	USGS 2[2]	do.	38° 58.10′	122° 38.70′	do.	[3]4.72	.618	9.1	0.091±0.013	N		rb
6	USGS 3[2]	do.	38° 54.15′	122° 47.55′	do.	[3]4.69	3.176	40.9	0.551±0.016	N	Nos. 4, 26; same unit, different samples.	r
7	2658	Basaltic andesite	38° 49.30′	122° 33.70′	do.	1.624	3.144	4.7	1.34±0.29	R		be′
8	2668	Dacite	39° 0.35′	122° 48.00′	Sanidine	[4]10.674	4.008	6.9	0.26±0.04	N	No. 3; same unit, different sample.	dsb
9	2669	do.	38° 55.90′	122° 50.55′	do.	[4]11.272	8.534	14.6	0.53±0.03	N		dkc
10	2669R	do.	38° 55.90′	122° 50.55′	do.	[4]11.272	9.398	61.2	0.58±0.02	N		dkc
11	2703R2	Andesite	38° 52.90′	112° 40.30′	Whole rock	[4]1.609	2.426	29.5	1.05±0.03	N	No. 12	asc
12	2703R3	do.	38° 52.90′	122° 40.30′	do.	[4]1.609	2.439	25.6	1.05±0.04	N	No. 11	asc
13	2704	Basaltic andesite	38° 53.10′	122° 33.80′	do.	[4]1.362	2.608	2.5	1.33±0.53	R		be′
14	2705	Andesite	38° 49.10′	122° 42.45	do.	[4]1.400	2.936	25.1	1.46±0.06	R	No. 15	abm
15	2705R	do.	38° 49.10′	122° 42.45′	do.	[4]1.400	3.038	35.4	1.51±0.04	R	No. 14, fused longer than ½ hour.	abm
16	2716R2	do.	38° 53.80′	122° 47.60′	do.	[4]1.389	1.670	16.6	0.84±0.05	R	No. 17	aps
17	2716R3	do.	38° 53.80′	122° 47.60′	do.	[4]1.389	1.717	20.1	0.86±0.04	R	No. 16	aps
18	2723	Rhyolite	38° 57.50′	122° 49.35′	Sanidine	10.604	7.206	11.7	0.47±0.04		No. 19	rcc
19	2723R	do.	38° 57.50′	122° 49.35′	do.	9.787	7.617	25.5	0.54±0.02		No. 18	rcc
20	2844	Rhyolite (obsidian)	38° 51.60′	122° 43.20′	Whole rock	4.551	6.707	27.6	1.02±0.04	R		rbp
21	2866	Dacite	38° 58.40′	122° 45.45′	Sanidine	10.488	5.224	47.1	0.35±0.02			dwp
22	2867	do.	38° 54.05′	122° 43.60′	Whole rock	[5]3.438	4.549	26.9	0.92±0.03		No. 23	dd
23	2867R	do.	38° 54.05′	122° 43.60′	do.	[5]3.438	4.529	29.1	0.92±0.03		No. 22	dd
24	2868	do.	38° 48.70′	122° 44.30′	Sanidine	[4]11.056	16.936	62.6	1.06±0.02	R	No. 25	dc
25	2868R	do.	38° 48.70′	122° 44.30′	do.	[4]11.056	16.731	69.5	1.05±0.02	R	No. 24	dc
26	2890	Rhyolite (obsidian)	38° 54.15′	122° 48.20′	Whole rock	4.740	4.339	18.9	0.64±0.03	N	No. 4, 6; same unit, different samples.	r
27	2911[6]	Dacite	38° 55.80′	122° 45.40′	Sanidine	9.211	7.933	44.2	0.60±0.02		No. 48; No. 27 hydrothermally altered.	dsm
28	2922[6]	Rhyolite (obsidian)	38° 55.70′	122° 45.50′	Whole rock	4.736	3.828	38.0	0.56±0.02			rp
29	2961	Dacite	38° 55.80′	122° 37.10′	do.	3.440	1.991	9.3	0.40±0.04			dcc
30	2968	Andesite	38° 48.00′	122° 43.15′	do.	1.286	3.164	7.9	1.71±0.21			aff
31	2969	Basaltic andesite	38° 57.70′	122° 37.25′	do.	1.548	3.698	16.0	1.66±0.10	R		be′
32	2972	Dacite	38° 52.40′	122° 42.50′	Sanidine	11.220	9.840	55.3	0.61±0.02	N		ds
33	2973	do.	38° 59.90′	122° 38.00′	Biotite	7.449	12.756	5.0	1.2±0.3	R	Poor spectrogram	dr
34	2974	do.	38° 52.30′	122° 54.10′	Sanidine	11.208	13.941	51.0	0.86±0.02	N	No. 69 is same sample, treated again with HF.	dtv
35	2975	do.	38° 59.15′	122° 47.10′	do.	11.245	6.606	6.7	0.41±0.06	N		dsb
36	2976	Rhyolite	38° 48.60′	122° 45.60′	do.	10.499	17.376	79.9	1.15±0.02	U	No. 2, 65; same unit, different samples.	ra
37	2978	Dacite	38° 57.20′	122° 37.95′	Whole rock	2.818	2.112	8.9	0.52±0.06			dhi
38	2980	Rhyolite	38° 56.35	122° 46.25′	Sanidine	11.216	8.741	72.3	0.54±0.02			rps
39	2982	Rhyolite	38° 55.10′	122° 44.95′	Sanidine	10.363	7.506	39.2	0.50±0.02			rrp
40	2983	Basaltic andesite	38° 47.70′	122° 30.25′	Whole rock	1.793	3.742	12.4	1.45±0.12			be′
41	2984	Dacite	38° 54.45′	122° 38.95	do.	2.596	1.7818	13.8	0.48±0.03			dpl
42	2985	Andesite	38° 53.80′	122° 45.60′	do.	1.515	2.184	21.2	1.00±0.05	R		ag
43	2986	Basaltic andesite	38° 40.80′	122° 30.25′	do.	1.205	3.393	31.0	1.96±0.06	R		be′
44	2987	Rhyolite	38° 44.05′	122° 41.70′	Sanidine	11.197	33.190	84.4	2.06±0.02		Float block	rpm
45	2988	Dacite	38° 53.45	122° 46.85′	Whole rock	2.746	3.887	10.4	0.98±0.09	R	No. 46	db
46	2988R	do.	38° 53.45′	122° 46.85′	do.	2.746	3.892	11.1	0.98±0.09	R	No. 45	db
47	2989	Basaltic andesite	38° 56.40′	122° 46.55′	do.	1.056	0.671	5.2	0.44±0.08	N		bl
48	2990	Dacite	38° 55.80′	122° 45.60′	Sanidine	11.798	9.742	42.8	0.57±0.02		No. 27; No. 48 relatively unaltered.	dsm
49	2991R3	Basalt	38° 50.50	122° 48.55′	Whole rock	[7].472	1.130	13.2	1.66±0.12	R		bc
50	2992	Andesite	38° 50.50	122° 37.80′	do.	1.440	1.938	17.0	0.93±0.05	R	No. 51	ac
51	2992R	do.	38° 50.50	122° 37.80′	do.	1.440	1.907	20.8	0.92±0.05	R	No. 50	ac
52	2993	Rhyolite	38° 55.50′	122° 50.70′	Sanidine	11.667	10.036	30.2	0.60±0.02			rm
53	2994	Dacite	38° 55.55	122° 49.20′	do.	10.561	8.909	51.7	0.59±0.02	N		dch
54	2996	do.	38° 55.50′	122° 41.15′	Whole rock	2.568	1.619	20.1	0.44±0.03			dv
55	2998	Andesite	38° 53.25′	122° 46.85′	do.	2.535	3.024	28.7	0.83±0.03	U	No. 56; see also from same unit Nos. 57, 60, 61.	ast
56	2998R	do.	38° 53.25′	122° 46.85′	do.	2.535	3.148	31.4	0.86±0.03	U	No. 55; see also Nos. 57, 60, 61; No. 56 fused >1/2 hour.	ast
57	2999	do.	38° 51.65	122° 43.10′	do.	2.679	3.378	43.7	0.88±0.02	U	See also from same unit Nos. 55, 56, 60, 61.	ast
58	3000	Dacite	38° 51.70′	122° 43.40′	do.	3.513	4.531	23.8	0.90±0.04	U	No. 59	dl
59	3000R	do.	38° 51.70′	122° 43.30′	do.	3.513	4.530	26.4	0.90±0.03	U	No. 58	dl
60	3001	Andesite	38° 53.70′	122° 43.80′	do.	3.155	3.698	13.4	0.81±0.06	U	No. 61; see also Nos. 55, 56, 57.	ast
61	3001R	do.	38° 53.70	122° 43.80′	do.	3.155	3.991	15.6	0.88±0.06	U	No. 60; see also Nos. 55, 56, 57; No. 61 fused >1/2 hour.	ast

TABLE 1.—*K-Ar dates and analytical data, Clear Lake Volcanics*—Continued

Map No. (fig. 1)	Sample No.	Rock type	Sample location		Material dated	K_2O (weight percent)	Radiogenic ^{40}Ar		Age (10^6 years)	Magnetic polarity	Replicate dates and other comments	Unit symbol
			Latitude N.	Longitude W.			Moles/g ($\times 10^{-12}$)	Percent				
62	3153	Dacite	38° 49.20′	122° 43.90′	do.	[3]2.590	3.953	20.1	1.06±0.03	R	Nos. 63, 64	dcv
63	3153R	do.	38° 49.20′	122° 43.90′	do.	[3]2.590	4.041	26.9	1.08±0.03	R	Nos. 62, 64	dcv
64	3153R2	do.	38° 49.20′	122° 43.90′	do.	[3]2.590	4.114	48.7	1.10±0.02	R	Nos. 62, 63	dcv
65	3154	Rhyolite	38° 48.10′	122° 43.20′	Sanidine	[1]11.024	17.640	64.1	1.11±0.02		Nos. 2, 36; same unit, different samples.	ra
66	3155	Andesite	38° 44.45′	122° 42.15′	Whole rock	[3]1.942	5.534	5.9	1.98±0.35		Nos. 67, 68	ahm
67	3155R	do.	38° 44.45′	122° 42.15′	do.	[3]1.942	6.279	7.9	2.24±0.29		Nos. 66, 68	ahm
68	3155R2	do.	38° 44.45′	122° 42.15′	do.	[3]1.942	5.395	5.8	1.93±0.33		Nos. 66, 67	ahm
69	3185	Dacite	38° 52.30′	122° 54.10′	Sanidine	11.992	14.054	72.6	0.82±0.02	N	No. 34, same sample, but No. 69 treated again with HF.	dtv
70	3197	do.	38° 52.45′	122° 44.70′	Whole rock	[3]2.818	3.605	26.6	0.89±0.03	U	No. 71	dhf
71	3197R	do.	38° 52.45′	122° 44.70′	do.	[3]2.818	3.721	15.0	0.92±0.04	U	No. 70	dhf
72	3202	Andesite	38° 52.90′	122° 40.30′	do.	[3]2.015	2.787	35.6	0.97±0.03	N	Nos. 11, 12, same unit, different samples.	asc
73	3204	Dacite	38° 55.90′	122° 47.45′	Sanidine	10.594	8.093	63.5	0.53±0.02			do

[1] C. A. Wahrhaftig and G. H. Curtis (unpub. data, 1963).
[2] Berry and others (1976).
[3] Indicates replicate analysis; the difference between measurements in all cases (except samples 4-6 and 49) is less than 1.1 percent and averages 0.3 percent.
[4] B. C. Hearn, Jr., J. M. Donnelly, and F. E. Goff (unpub. data, 1975).
[5] G. H. Curtis and R. E. Drake (unpub. data, 1975).
[6] 3 percent different from K_2O value on another sample from same location.

may disappear with future mapping and dating of early basalts.

The gap in eruptive activity between 0.8 and 0.6 m.y. was followed by two small dacite eruptions and then by extrusion of a voluminous sparsely porphyritic rhyolite flow. The rhyolite was followed by a sequence of basaltic rocks and crystal-rich rhyolite with dacite interspersed. At about 0.45 m.y., dacite became the dominant eruptive phase, with minor interbedded basalt.

It is interesting that the oldest dated lava is a rhyolite, and it appears that each phase of Clear Lake volcanism began with one or more silicic eruptions. The earliest rhyolite, at Pine Mountain, was followed by large volumes of basaltic and andesitic lava. The next time break, at 1.3–1.1 m.y., ended with the eruption of the rhyolite of Alder Creek, the dacite of Cobb Mountain, and the rhyolitic tuff of Bonanza Springs. These silicic eruptions were followed by eruption of numerous flows of andesite and dacite.

The K-Ar dating was useful in establishing stratigraphic order in cases where little or no overlap of units could be discovered in the field. Where the dates can be checked by stratigraphy, results are good, as in the case of the sequence at the Loch Lomond church (Nos. 20, 22, 57, 58, 32) and the sequence at Kelsey Creek Gorge (Nos. 26, 47, 53, 10, 9). Certain sequences and units presented their own challenges to unravelling their true ages. We discuss these individual problems below, beginning with the oldest dated rocks.

INDIVIDUAL DATING PROBLEMS

Pine Mountain area.—The oldest dated unit in the Clear Lake volcanic field is the rhyolite of Pine Mountain, which was dated at 2.06 ± 0.02 m.y. (No. 44) on sanidine. Hydrothermal alteration of the rhyolite outcrops made magnetic polarity determinations impossible. The hydrothermal alteration is thought to be associated with emplacement of mercury at the nearby Helen mine. Most of the andesite of the Helen mine has also been hydrothermally altered, probably by ore-forming fluids. Mercury was deposited within small andesite intrusions and in adjacent silica-carbonate rock (hydrothermally altered serpentinite), both of which are located along a prominent fault (Yates and Hilpert, 1946). Dating of unaltered samples of the andesite gives three ages (No. 66, 67, 68); the average of the three ages is 2.05 m.y. This is a maximum age for the mercury deposition. No hydrothermal activity such as thermal springs or fumaroles exists in the area today, although a successful steam well was drilled just 2 km to the north.

Early basalt other than Caldwell Pines.—Five K-Ar dates have been run on widely separated early basalt flows other than the Caldwell Pines basalt. This group of basalt and quartz-bearing basaltic andesite flows yields ages ranging from 1.33 to 1.96 m.y., and all the rocks are magnetically reversed. These rocks occur as erosional remnants covering some 100 km² in an elongate area east and southeast of Clear Lake, extending as far as Lake Berryessa, some 40 km away. The lava flow at Table Mountain, 6 km southeast of Middletown, near the southern limit of the Clear Lake volcanic field, is 1.96±0.06 m.y. old (No. 43). Farther north, on Spruce Grove Road, dates on two adjacent flows are 1.34±0.29 m.y. (No. 7) and 1.33±0.53 m.y. (No. 13). To the east, at Hell's Half Acre, one flow is 1.45±0.12 m.y. old (No. 40). Farther to the north, near the east end of Clear Lake, the basaltic andesite at Schoolteacher Hill is 1.66±0.10 m.y. old (No. 31). Where magnetic polarities are known (all but No. 40), they are consistent with the dates. It appears that there was no pattern to the distribution in space and time of these older basaltic rocks. No basaltic rocks in this age range have been found under the main Clear Lake volcanic field.

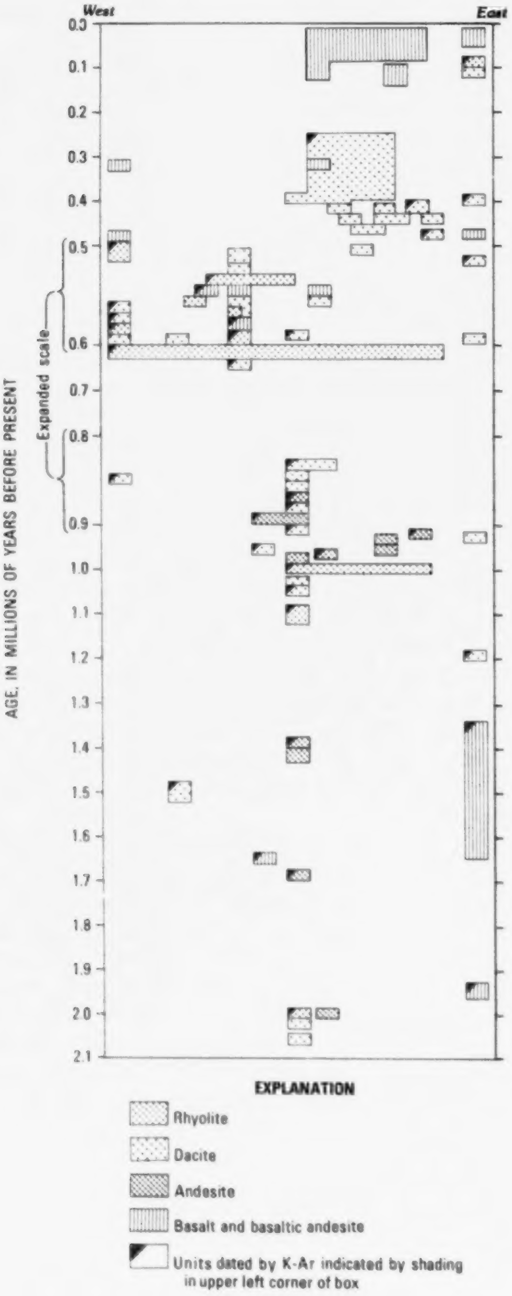

FIGURE 21.—Generalized stratigraphic sequence of lavas and their age relations in the Clear Lake volcanic field. Size of box not directly related to volume of unit; units where boxes extend part way across chart occur in more than one stratigraphic sequence. For more detailed chart see Hearn, Donnelly, and Goff (1976a).

Caldwell Pines.—The remnants of basalt of Caldwell Pines sit directly on Franciscan bedrock within the northern part of the explored Geysers steam field. It is one of the few true basalts of the Clear Lake volcanic field in that it contains no quartz and it has 50.2 weight percent silica. Because of its composition, its position adjacent to the producing steam field, and its lack of stratigraphic age control, this unit was an important one for K-Ar dating. Treatment of the sample (No. 49, 1.66±0.12 m.y.) with dilute HF for 30 seconds to 1 minute and the use of an unlined bottle for the extraction combined to produce an acceptable result with an analytical error of 7 percent. This age is geologically reasonable and is consistent with the reversed paleomagnetic direction.

Cobb Mountain sequence.—The silicic flows of Cobb Mountain have recorded a short normal-polarity event which precedes the Jaramillo (Mankinen and others, 1978). Dates of 1.11±0.02 m.y. (No. 2), 1.15±0.02 m.y. (No. 36), and 1.11±0.02 m.y. (No. 65) were obtained on sanidine from samples of the rhyolite of Alder Creek.

Some of the rhyolite's pumiceous carapace was stripped off before eruption of the dacite of Cobb Mountain, for which sanidine gives ages of 1.06±0.02 m.y. (No. 24) and 1.05±0.02 m.y. (No. 25). The dacite of Cobb Valley is the youngest, least silicic, and least voluminous of the Cobb Mountain silicic flows. Three whole-rock dates give ages of 1.06±0.03 m.y. (No. 62), 1.08±0.03 m.y. (No. 63), and 1.10±0.02 m.y. (No. 64), which suggests that the silicic lavas of Cobb Mountain erupted within a very short period of time.

The oldest and least voluminous lava on Cobb Mountain is the andesite of Ford Flat, 1.71±0.21 m.y. old (No. 30), which makes up small patches of mudflow deposits on the southeastern side of the mountain, beneath the rhyolite of Alder Creek.

Rhyolite of Bonanza Springs and andesites of Childer's Peak and Perini Hill.—The air-fall rhyolite tuff of Bonanza Springs, the largest single pyroclastic unit in the volcanic field, is also one of the most widespread units. Its age is important because of its position at the base of the southern edge of the central volcanic field. A K-Ar date of 1.02±0.04 m.y. (No. 20) was obtained on a clast of obsidian from the tuff.

No paleomagnetic measurements have been made on this unit, partly due to its friable nature, but it clearly underlies 0.92±0.03-m.y.-old dacite (No. 22 and 23). A 35-m-thick section of the tuff underlies the andesite of Perini Hill. The andesite has not been dated owing to the abundance of inclusions it contains and the consequent probability that it would yield too old an age, but its normal magnetic polarity and the thickness of easily erodable rhyolitic tuff preserved under it suggest that it erupted during the Jaramillo normal-polarity event. A similar thickness of tuff also underlies the andesite of Childer's Peak, an erosional remnant some 4 km southeast of Perini Hill. The andesite of Childer's Peak yielded whole-rock dates of 0.93±0.05 m.y. (No. 50) and 0.92±0.05 m.y. (No. 51); these dates do not agree with the andesite's magnetic polarity and are probably too young. The dates agree with each other but both have relatively large errors, and the reversed magnetic polarity of the andesite strongly suggests that it should be older than 0.97 m.y., the older boundary of the Jaramillo. This unit may be another of the Clear Lake andesites which have not yielded all of their radiogenic argon (see below).

Andesites of Seigler Canyon and Split Top Ridge.—These two andesites, petrographically very similar, were mapped as the same unit until K-Ar dating suggested and chemical analyses confirmed that they were separate flows. They can only be distinguished with difficulty in the field. The andesite of Seigler Canyon initially yielded ages which were too old (1.05±0.03 m.y. and 1.05±0.04 m.y., No. 11. and No. 12), since it overlies the rhyolite of Bonanza Springs, dated at 1.02±0.04 m.y. (No. 20). The ages of the two units easily fall within the limits of uncertainty on the dates, but the andesite has normal magnetic polarity which suggests that it was probably erupted during the Jaramillo magnetic event, which began about 0.97 m.y. ago according to evidence from other rocks at Clear Lake and elsewhere around the world. The explanation for the discrepancy may lie in the mineralogy of the andesite of Seigler Canyon. It contains occasional grains of cordierite, and according to Seidemann (1976), cordierite can contain excess argon and thus can cause a K-Ar date to be too old. Another sample of the andesite of Seigler Canyon yielded an age of 0.97±0.03 m.y. (No. 72).

The andesite of Split Top Ridge yielded ages that were consistently too young. Fusion times longer than the standard one-half hour have produced older ages in each case, thus partly solving the problem. A sample from the type locality on Split Top Ridge east of Mount Hannah was dated at 0.81±0.06 m.y. (No. 60) but, on longer fusion, at 0.88±0.06 m.y. (No. 61). A sample 5 km to the west on the other side of Mount Hannah was 0.83±0.03 m.y. (No. 55) but, with longer fusion, 0.86±0.03 m.y. old (No. 56). The only locality with good stratigraphic control, 3 km southeast of Mount Hannah at Loch Lomond, was 0.88±0.02 m.y. old (No. 57), where the andesite is overlain by a dacite which yielded replicate ages of 0.90±0.04 m.y. (No. 58) and 0.90±0.03 m.y. (No. 59). Since the andesite of Split Top Ridge overlies another dacite flow with replicate ages of 0.92±0.03 m.y. (No. 22 and 23), its age is probably about 0.91 m.y.

Andesite of Poison Smith Spring.—The andesite of Poison Smith Spring was dated at 0.84±0.05 m.y. (No. 16) and 0.86±0.04 m.y. (No. 17). However, it underlies the dacite of Harrington Flat with ages of 0.89 and 0.92 m.y. While the ages of the units overlap within the precision estimates, the andesite ages do appear to be too young, and samples from this unit may need a longer fusion time to release all of their radiogenic argon.

Dacites of Diener Drive and Boggs Lake.—These two glassy, phenocryst-poor dacites are very similar in appearance, although the dacite of Boggs Lake is slightly more crystal-rich. The dacite of Boggs Lake is exposed west of Mount Hannah in an area covering less than a square kilometer. It is the oldest lava in its sequence, and replicate dates of 0.98±0.09 m.y. (No. 45 and 46) are consistent with its stratigraphic position.

The dacite of Diener Drive is exposed over an area of almost 10 km^2 and is found as a thin layer in the sequence at Loch Lomond, 4 km south of its area of extensive outcrop. This dacite was apparently very fluid and is glassy over much of its areal extent, despite its age of 0.92±0.03 m.y. (Nos. 22 and 23). It was erupted during the Jaramillo magnetic event.

Chalk Mountain.—Near the north edge of the Cache Formation is the hypersthene dacite flow and intrusion of Chalk Mountain (sec. 12, T. 14 N., R. 7 W.), which derives its name from its conspicuous white color due to present-day hydrothermal alteration. It was this appearance that convinced Anderson (1936) that Chalk Mountain was the youngest unit in the Clear Lake Volcanics. Its normal magnetic polarity tends to support Anderson's conclusion. However, Stony Top, 2 km to the southeast of Chalk Mountain, is a remnant of the same dacite flow, and two small patches of the same distinctive dacite occur between the two peaks. It is apparent that this dacite, which discordantly overlies the Cache Formation and Franciscan assemblage, once covered a much larger area. The extent of erosion suggests a much greater age than Anderson proposed, probably Jaramillo or early Brunhes.

Recent mapping indicates that the current hydrothermal alteration in the area occurs along and near to parallel northwest-trending fault zones, and that areas of fumarolic activity are found in the Cache Formation and Franciscan assemblage as well as at Chalk Mountain. Mineral springs around the base of Chalk Mountain are thermal, but only slightly so (about 20°C), and the current thermal phenomena are unrelated to the emplacement of the dacite. A single attempt at dating the dacite produced less than 1 percent radiogenic argon and is not reported here.

Dacite of Tyler Valley.—The dacite of Tyler Valley is another isolated unit, some 8 km southwest of the main part of the Clear Lake volcanic field and 8 km west-northwest of Caldwell Pines. The dacite forms an eroded, irregular intrusive body; it yielded two sanidine ages of 0.86±0.02 m.y. (No. 34) and 0.82±0.02 m.y. (No. 69). These dates appear to disagree with the unit's normal magnetic polarity although other dates of this age and polarity are reported by Hirooka and Kawai (1967) and Watkins (1968).

Mount Hannah.—The age of Mount Hannah, the composite dacite dome which lies at the center of the 25-milligal negative gravity anomaly associated with the Clear Lake volcanic field, has been difficult to ascertain. The mountain, which rises more than 400 m over its surroundings, has a symmetrical appearance and was thought by Garrison (1972) to be the youngest volcanic landform in the Clear Lake volcanic field and by Brice (1953) to be younger than Mount Konocti.

Attempts to date a partially devitrified sample of the medium-grained dacite of Mount Hannah, the mountain's youngest unit, yielded large atmospheric argon corrections and thus no reliable age. The most voluminous unit on Mount Hannah, a coarse-grained dacite flow, is also typically devitrified. Neither dacite contains sanidine, biotite is rare, and plagioclase is usually altered. However, both dacites overlie the andesite of Glenview, 1.00±0.05 m.y. old (No. 42), and the dacite of Harrington Flat, which yielded ages of 0.89±0.03 m.y. (No. 70) and 0.92±0.04 m.y. (No. 71).

Determinations of magnetic polarity were initially weak or indeterminate, despite repeated attempts to measure them, but laboratory tests (Mankinen and others, this volume) indicate intermediate directions for most of the units on Mount Hannah and suggest a very brief time span near the end of the Jaramillo magnetic event for their eruption. Interpretation of aeromagnetic data by Isherwood (1976) indicates that Mount Hannah has mixed or weak magnetic polarity.

Rhyolite of Thurston Creek.—This unit of rhyolite and rhyolitic obsidian forms an arcuate belt in the center of the Clear Lake volcanic field. It is 11 km long and varies from 1 to 5 km in width. Most exposures display obsidian and minor pumice breccia. Erosion has exposed the stony rhyolite core in only a few major drainages (Cole Creek, Thurston Creek, McIntire Creek) and locally along faults. No mappable physical or mineralogical differences can be found throughout its extent, although Bowman, Asaro, and Perlman (1973) found some slight chemical differences. Potassium-argon ages on whole-rock obsidian samples range from 0.479±0.015 m.y. (No. 4) near the east edge to 0.551±0.016 m.y. (No. 6) and 0.64±0.03 m.y. (No. 26) in the western part of the unit. An obsidian clast from a rhyolite pyroclastic unit which underlies the north-central part of the rhyolite flow and is thought to be its immediate precursor at Sulphur Mound mine is 0.56±0.02 m.y. old (No. 28).

It is probable that the rhyolite of Thurston Creek was erupted from several vents and it may not have just one age. However, because the samples from the western part of the flow were collected within a kilometer of each other, at least some of the apparent age variation may be analytical. All of these whole-rock obsidian dates, however, have small analytical errors.

At Mount Olive, the same rhyolite overlies dacite dated at 0.53±0.02 m.y. (No. 73). At Sulphur Mound mine, the rhyolite of Thurston Creek is underlain by the dacite of Sulphur Mound mine, which yielded two sanidine ages of 0.60±0.02 m.y. (No. 27) and 0.57±0.02 m.y. (No. 48). To the northwest of the mine, the obsidian is overlain by crystal-rich biotite rhyolite pumice with an age of 0.54±0.02 m.y. (No. 38). These bracketing ages suggest that, at Sulphur Mound mine, the true age of the obsidian flow is 0.55 m.y., where it overlies rhyolite pyroclastic rock 0.56±0.02 m.y. old (No. 28).

To complicate matters, the westernmost end of the obsidian flow is cut by a dikelike body of the dacite of Camel's Hump, which yielded a sanidine date of 0.59±0.02 m.y. (No. 53). This dacite overlies and intrudes the biotite rhyolite of Milky Creek, dated from sanidine at 0.60±0.02 m.y. (No. 52), a unit which is in fault contact with rhyolite of Thurston Creek and contains inclusions of it. Both the rhyolite of Milky Creek and dacite of Camel's Hump are overlain by the dacite of Kelsey Creek Gorge, dated from sanidine at 0.53±0.03 m.y. (No. 9) and 0.58±0.02 m.y. (No. 10). This sequence of ages agrees with field relations. It is possible, therefore, that at its west end, the rhyolite of Thurston Creek is older than 0.59 m.y., and the 0.64 m.y. date near this end of the flow may be close to the real age.

Mount Konocti and adjacent dacite field.—Mount Konocti is a composite dacite dome 1,000 m high with minor interbedded basalt. All flows are apparently less than 0.5 m.y. old, because at its southwestern edge, dacite overlies the rhyolite of Cole Creek, which was dated from sanidine at 0.47±0.04 m.y. (No. 18) and 0.54±0.02 m.y. (No. 19). Five K-Ar dates exist for dacite from Mount Konocti. The oldest and youngest dates are on two samples collected less than 0.2 km apart from the same flow. The ages, 0.43±0.05 m.y. (No. 3) and 0.26±0.04 m.y. (No. 8), were determined in the same laboratory, but the first date was run more than 10 years before the second. Both samples produced less than 10 percent radiogenic argon, unusually low for sanidine separates. A third date on the same unit gave an age of 0.41±0.06 m.y. (No. 35), also with less than 10 percent radiogenic argon. It is possible that an average of the three dates (0.37 m.y.) represents more closely the true age of the flow, but there is no independent stratigraphic evidence to limit the age.

Another unit low on the north side of the mountain yielded an age of 0.35±0.02 m.y. (No. 1), as did the uppermost dacite flow on the mountain's highest peak (No. 21). Overall, the evidence suggests that at least 35 cubic kilometers of dacite built the mountain in a relatively short magmatic episode between 0.4 and 0.3 m.y. ago.

Extending more than 15 km to the southeast from Mount Konocti is a field of dacite flows covering nearly as much area as the mountain itself, but only built 100–200 m above Clear Lake rather than the 1000 m of Mount Konocti. Dates obtained on flows about 8 km southeast of Mount Konocti were 0.48±0.03 m.y. (No. 41) for the oldest dacite in the sequence near Thurston Lake and 0.44±0.03 m.y. (No. 54) for the youngest dacite in the same sequence. These ages suggest that this field was erupted in the 0.1 m.y. previous to the building of Mount Konocti.

Clearlake Highlands area.—Located at the southeast end of Clear Lake, this area encompasses some of the oldest and youngest lavas in the Clear Lake volcanic field. The oldest lavas here are basalt and basaltic andesite, such as the lava forming Schoolteacher Hill and Quackenbush Mountain, which yielded a date of 1.66±0.10 m.y. (No. 31). Lakebeds that include basaltic maar deposits overlie the dacite of Clearlake Highlands, dated at 0.52±0.06 m.y. (No. 37). These lakebeds underlie the dacite of Cache Creek, which has been dated at 0.40±0.04 m.y. (No. 29); therefore, there must have been a basaltic eruption between about 0.4 and 0.5 m.y. ago in or near the southeast end of Clear Lake.

The lake deposits are transgressive into similar deposits that extend continuously west from Lower Lake some 6 km into the central volcanic field. Rymer (1981) includes them in the Lower Lake Formation. They occur as high as 270 m above the present level of Clear Lake, where they underlie the dacite of Pinkeye Lake, dated at 0.48±0.03 m.y. (No. 41). Near Lower Lake, this series of fossiliferous lakebeds, basaltic maar deposits, and obsidian-bearing gravels dips toward Clear Lake at angles up to 40°. It is apparent that relative uplift of 270 m or more to the south has taken place since these deposits were laid down about half a million years ago. Uplift to the east of Clearlake Highlands has been of a similar magnitude since the basaltic andesite at Schoolteacher Hill was erupted some million and a half years ago. In both cases, relative movements have tended to maintain the area in and near Clear Lake as a structural basin.

Clear Lake, which is mostly less than 10 m deep, continues to exist for tectonic reasons, since any reasonable estimate of sedimentation rate, such as 1 mm/yr (Sims and Rymer, 1975), would fill the lake basin in 10,000 years. A core taken from the bottom of the upper arm of Clear Lake (Sims and Rymer, 1975) went through over 115 m of rather uniform sediment without hitting bedrock. The palynology of that core indicates that it records 130,000 years of sedimentation (Sims and others, this volume). Faults along the north and northeast side of the lake appear to control the structure of the basin (Sims and Rymer, 1976), so that the lake floor has been going down at a rate approximately equal to the rate of sedimentation. Lake deposits in Big Valley to the west of Mount Konocti also suggest that Clear Lake existed there half a million years ago.

Cache Creek, the present outlet of Clear Lake, follows a tortuous course east, north, and then east again across upturned beds of the Great Valley sequence at the west edge of the Sacramento Valley. It is apparent that tectonics has played a significant role in the development of this drainage, and it can be argued that Clear Lake did not always empty down Cache Creek as it does today. Davis (1933) believed that this eastern outlet of Clear Lake was blocked by a lava flow at Redbank Gorge, and the lake was forced to drain west through Blue Lakes into the Russian River. Then, according to Davis, a few centuries ago a landslide blocked the western outlet, forcing the lake to rise and overtop the lava dam across Cache Creek. While it is highly probable that Clear Lake, at least the upper part of it, did drain to the west for some large part of the lake's history (Hodges, 1966), evidence for a major lava dam across Cache Creek is absent. No lava at all crops out at Redbank Gorge where the red color results from limonite in half-million-year-old lake deposits. The eastern barrier, if it ever existed, must have been tectonic.

Some of the early basaltic lavas in the Clearlake Highlands area are interbedded in the upper part of the Pliocene and Pleistocene Cache Formation, which consists dominantly of fluvial sand and gravel. One such body of basaltic andesite at Quackenbush Mountain, dated at 1.66±0.10 m.y. (No. 31), has had its cover of gravel largely eroded away, but a sprinkling of chert remains. Deposition of the Cache apparently continued until at least 1.6 m.y. ago, but when it terminated is unknown. At Chalk Mountain, where the dacite flow lies discordantly on the tilted Cache Formation, deposition of the Cache ended in early Brunhes time or earlier. The Cache covers about 150 km^2, and, according to Brice (1953), reaches a maximum thickness of 2,100 m. An even greater thickness is suggested by more recent work (Rymer, 1978). The present extensive area of Cache Formation deposits has since been uplifted and is being rapidly eroded by Cache Creek and its tributaries.

The youngest lavas in the Clearlake Highlands area includes the youngest rhyolite in the volcanic field. The rhyolite of Borax Lake, 0.091±0.013 m.y. old (No. 5), overlies a dacite flow which also appears to be very young. Both overlie eroded remnants of basaltic cinder cones whose ages are unknown.

Basaltic rocks less than half a million years old.—The most recent period of volcanism, although minor in total volume (fig. 22), is dominated by basalt and basaltic andesite which include the youngest flows in the Clear Lake volcanic field. No lava of this type is known to have erupted between about 1.3 m.y. and 0.5 m.y. ago. On the west side of the volcanic field at least seven mafic vents line up on a nearly straight north-south trend, some 8 km long. On the east side of the central volcanic field, eight basaltic vents (all appearing to be less than 0.1 m.y. old) occur along 15 km on a trend N. 10° E. No fault or other surface manifestation is directly associated with either of these trends.

Not all young basaltic vents follow these trends, however. Many young maar volcanoes, probably between 0.01 and 0.1 m.y. old (Sims and Rymer, 1975), erupted along the lakeshore north and east of Mount Konocti and farther southeast along the southeast shore of Clear Lake. And at least one very young vent lies 3 km west of the N. 10° E. trend, where a cinder cone forms the southeast end of Rattlesnake Island, just northwest of Sulphur Bank mine.

Samples from two of the youngest basaltic vents produced only 0.2 and 0.1 percent radiogenic argon, attesting to their youth, but giving no real information on their age other than what had already been gained by simple observation. One of these young basaltic andesites was found to be less than 44,500 ± 800 years old (Minze Stuiver, written communication, 1975) by carbon-14 dating of a stump found in sediment under the lava at Sulphur Bank mine.

Dating of one of the older of these young basaltic rocks proved to be similarly frustrating. The basaltic andesite of Lower Lake Road underlies a 0.54-m.y.-old rhyolite flow (No. 38) but yielded an age of 0.44 ± 0.08 m.y. (No. 47), with 5.2 percent radiogenic argon. The ages overlap within their analytical uncertainties, but K-Ar dates on basaltic rocks less than 1 m.y. old are apparently the least informative in the Clear Lake volcanic field. If no other material in this age range were available for dating, basaltic lavas could give only general age information, with 20 to 200 percent analytical uncertainty.

MAGNETIC POLARITIES

Several units were found to have significance for the geomagnetic-polarity time scale. At least nine units ranging in age from about 0.89 to 0.92 m.y. represent the Jaramillo normal-polarity event. Some of those units have unique polarities, suggesting that they erupted at the end of the Jaramillo event (Mankinen and others, this volume). Another unit with a unique magnetic polarity, the 1.1-m.y.-old rhyolite of Alder Creek on Cobb Mountain, identifies a separate magnetic event earlier than the Jaramillo (Mankinen and others, 1978). In spite of the overall abundance of eruptions, none took place for nearly 0.1 m.y. before or after the Matuyama-Brunhes reversal, which occurred about 0.7 m.y. ago.

SPATIAL EVOLUTION OF THE VOLCANIC FIELD

Evolution of the volcanic field has apparently not been random in space. In general, volcanic rocks in the field become progressively younger to the north. No lavas less than 0.5 m.y. old have been found south of the extensive half-million-year-old sparsely porphyritic obsidian flow, the rhyolite of Thurston Creek. Early volcanic activity was geographically more randomly distributed. A large field of basaltic rocks, which are dominantly quartz-bearing, formed to the east of the main volcanic field and are found as far north as the most recent activity. These basaltic lavas still cover an area of about 100 km^2, which may represent only about half of their original extent. The eruption of the quartz-free basalt of Caldwell Pines, one of the few true basalts of the Clear Lake Volcanics, was contemporaneous with these early basaltic rocks but about 16 km to the west. If any early basaltic lava underlies the main part of the present volcanic field, it has not been found.

Activity within the last 0.1 m.y. has been concentrated to the north and east of Mount Konocti, and any future eruptions would be expected in the same area, or about 20 km east of Clear Lake in the Wilbur Springs quicksilver district, where there is anomalous thermal activity (see Harrington and Verosub, this volume).

LAVA TYPES AND VOLUMES

Original volumes of lava types are difficult to estimate because the earliest lavas are the most eroded, but the total erupted volume was probably about 100 cubic kilometers. Twice as much silicic lava (rhyolite and dacite) erupted as mafic lava (basalt, basaltic andesite, and andesite). Of the silicic lava, dacite (most of which is represented by Mount Konocti) greatly exceeds rhyolite in volume and is thus the most abundant rock type in the Clear Lake Volcanics. Of the mafic lava, true basalt represents only a small fraction of the total, but together with basaltic andesite dominates over andesite. Estimates of existing volumes of rock through time yield the graph in figure 22. A bar graph showing estimated total volumes of rock types is given in figure 23.

Basalt, which is quartz-free and contains less than 53 percent SiO_2, is the rarest of Clear Lake lava types, amounting to less than 2 cubic kilometers in volume. Quartz-bearing basaltic andesite is common. This rock contains both forsteritic olivine and clear, irregular quartz fragments up to an inch or more across. The quartz, if an inclusion, is the only inclusion in many of the flows. Similar quartz-bearing basaltic lavas are reported in other volcanic fields such as the Jemez Mountains, New Mexico (Iddings, 1890), the Coso Mountains, California (Duffield and Bacon, 1976), and Lassen Volcanic National Park, California (Diller, 1891). The wide distribution and abundance of these lavas suggest that the quartz may have crystallized from the lava which contains it. Nicholls, Carmichael, and Stormer (1971) suggested that quartz can crystallize from a basaltic liquid at pressures equal to about 25 kilobars. It is also possible that the quartz is derived from quartz-rich metasedimentary inclusions, such as those found in the andesite of Perini Hill.

COMPARISON WITH THE SONOMA VOLCANICS

By contrast, the Sonoma Volcanics immediately to the south contains little or no quartz, regardless of composition (K. F. Fox, Jr., written commun., 1977). Also, according to Fox, the northern part of the Sonoma Volcanics, which ranges in age from 2.9 to about 6 m.y., consists largely of pyroclastic rocks including large volumes of welded tuff. The Clear Lake Volcanics includes only rare pyroclastic units, perhaps 5 percent of the total volume, none of which are welded tuffs. It appears, therefore, that differences in style of eruption and chemical composition, as well as age and distance, separate Clear Lake and Sonoma volcanism into distinct magmatic episodes.

FAULTING

Faults disrupt nearly all units of the Clear Lake Volcanics (Hearn and others, 1976a). Most of the faults are short (less than a kilometer), show little offset, and are predominantly normal faults with dip-slip movements. Dominant trends are northwesterly (following the regional trend), northerly, and northeasterly. Northwest- and north-trending faults dominate over and appear to cut northeast-trending faults. Two of the most important fault zones through the volcanic field are the Collayomi and Konocti Bay fault zones, at least 18 and

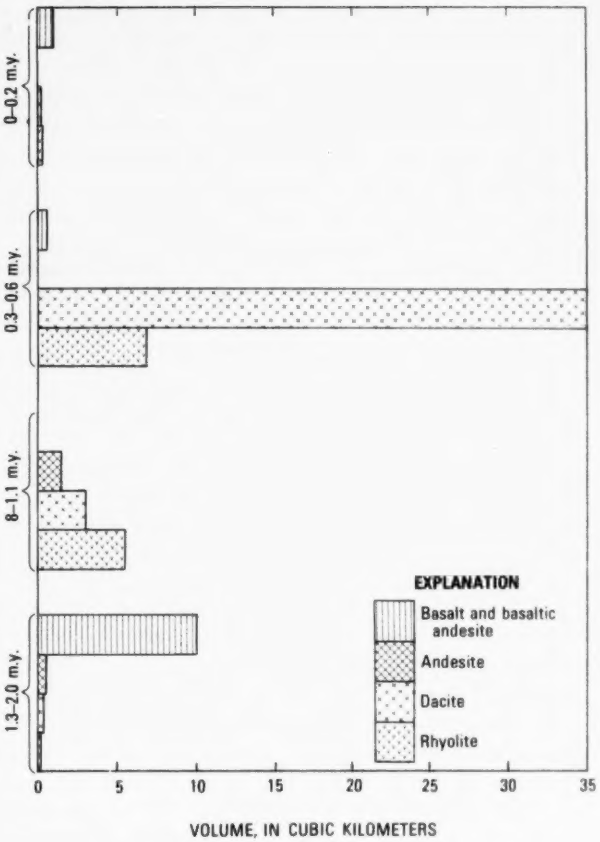

FIGURE 22.—Volumes of lava erupted during four different periods of volcanism. Volumes estimated from field observation (Hearn and others, 1976a and unpub. data).

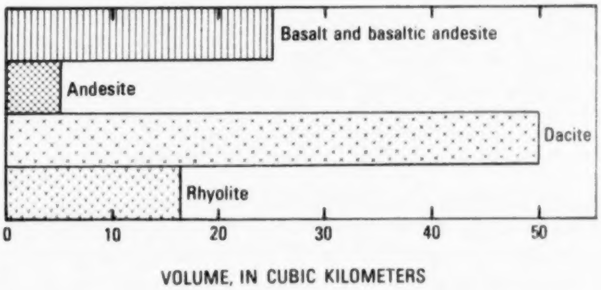

FIGURE 23.—Total erupted volumes of lava. Existing volumes of each rock type (from fig. 22) plus estimated volumes for amounts eroded since deposition.

21 km long, respectively. Both show right-lateral as well as vertical movements, and it is possible that both are still active (Hearn and others, this volume). These two faults are related to the San Andreas system, as are probably others to the northeast of Clear Lake. It is possible that many of the northeast-trending faults are produced by crustal adjustments to right-lateral fault couples. Many of the small faults have probably resulted from crustal adjustments following extrusion of magma. One example is found on the south side of Cobb Mountain where detailed mapping (Goff and McLaughlin, 1976) has shown that downfaulting of rhyolite blocks by about 250 m occurred soon after extrusion of the rhyolite of Alder Creek (about 1.1 m.y.) but before emplacement of the overlying dacite of Cobb Mountain (about 1.05 m.y.).

Faulting accounts for movements of less than a kilometer laterally and no more than 300 m vertically. Some faulting may have controlled the site of volcanic eruptions, for example, in the dacite which dammed the north and east sides of Thurston Lake. Some eruptions took place along linear trends for which there is no other obvious surface expression, such as the remarkable alinements of cinder cones previously mentioned.

Faults also act as avenues of movement for thermal fluids, including ore-forming fluids, as at the Sulphur Bank mercury mine (Everhart, 1946). Major faults also tend to be loci of slivers and masses of serpentinite, and they act as water barriers. One fault zone, the Collayomi, acts as the northeastern boundary of the vapor-dominated system of the Geysers steam field (Goff and others, 1977).

There is nothing to indicate that faulting is presently any more or less active than during earlier stages in the evolution of the volcanic field. The Geysers-Clear Lake area, particularly the steam field, is one of the most seismically active in northern California. Most earthquakes in the area are shallow (generally less than 8 km deep) and small (magnitude 4 or less) (Bufe and others, this volume). The heaviest shaking in historic time was felt during the 1906 San Francisco earthquake, when local ground breakage was reported (Lawson and others, 1908, p. 188-190).

SPECULATIONS ON MAGMATIC EVOLUTION: GENESIS AND FUTURE

Evolution of the magmatic system has not been random. Despite the complex sequence of nearly a hundred volcanic units, the Clear Lake volcanic field displays a discernible pattern of evolution in time and space. The general trend of increasingly younger volcanism to the north in the California Coast Ranges is repeated in the Clear Lake volcanic field. Early basaltic volcanism is scattered over the whole Clear Lake area, but rhyolitic volcanism is successively younger to the north. The generalized correlation chart (fig. 21) and the graph of volumes of preserved lava erupted during the different episodes of volcanism (fig. 22) show distinct episodes of activity separated by time breaks, each episode having its own pattern of magma types.

The most recent eruption in the Clear Lake volcanic field was about 10,000 years ago (Sims and Rymer, 1975). There is every reason to expect future eruptions. Since activity has been intermittent in the past, however, there is no way to predict exactly when the next eruption might occur. Figure 21 suggests that episodes of volcanic activity can be expected to continue for at least 0.3 m.y. On that basis, the present period of activity which began about 0.1 m.y. ago is in its early stage, and numerous eruptions can be expected in the next 0.2 m.y. The most recent eruptions have been basaltic in composition, and it is likely that the next lava will also be basaltic.

The virtual lack of pyroclastic eruptions and the complete absence of welded tuffs during the past 2 m.y. might suggest that no large pyroclastic eruptions are to be expected. The Sonoma Volcanics is dominantly pyroclastic and contains many welded tuffs, but the ash flows are small in volume and extent compared to ash flows in large silicic caldera complexes (such as Yellowstone, Wyoming). The complexity of the Sonoma Volcanics suggests frequent small eruptions through time. Hearn, Donnelly, and Goff (1976b) suggested that frequent tapping of the magma chamber by movement along right-lateral strike-slip faults may have caused the abundance of small volcanic units in the Clear Lake volcanic field. Since the Sonoma Volcanics lies in the same region of strike-slip faulting parallel to the San Andreas fault zone, the abundance of small Sonoma eruptions may be explained by the same mechanism. But the contrast in composition, especially the near-absence of explosive eruptions in the Clear Lake volcanic field and the lack of quartz in the Sonoma Volcanics, must result from differences in chemical composition, volatile content, or depth of the magmatic sources.

Whereas the Sonoma Volcanics never reached a stage of voluminous ash-flow eruption and large-scale caldera collapse, Clear Lake volcanism has not ceased, and such a catastrophic eruption must be considered a possibility. The inferred silicic magma chamber currently underlying the Clear Lake volcanic field, as modeled by Isherwood (this volume), contains approximately 1,300 km^3 of magma. According to the model of Smith and Shaw (1975), such a magma chamber could be expected to erupt 10 percent of its volume. An eruption of this magnitude would indeed be catastrophic since it would produce more lava than during the entire 2 m.y. history of the volcanic field. However, such an eruption is a remote possibility although future small eruptions seem likely.

The evolution of magmatic activity in space suggests that future eruptions would be expected in the areas north and east of Mount Konocti, especially around the eastern arm of Clear Lake and to the northeast near High Valley and Chalk Mountain. Another possible area for future volcanism is the Wilbur Springs quicksilver district, about 16 km east of Clear Lake, where a definite thermal anomaly is present along with early basalt of the Clear Lake Volcanics. Future detailed gravity and seismic studies might locate small magma bodies in these areas.

Mapping and dating of the Clear Lake Volcanics have delineated the evolution of the magmatic system in time and space, producing order out of apparent chaos. Analysis of the pattern of evolution (figs. 21 and 22) has resulted in some constraints on when volcanic activity might be expected, where it might occur, and what composition of lava might be expected. Questions remain as to the cause of the volcanic activity and the source of the magmatic liquids.

Hearn, Donnelly-Nolan, and Goff (this volume) suggest that the Sonoma and Clear Lake Volcanics may both be related to the same hot spot or thermal anomaly in the mantle. Movement of the North American plate to the southeast over such a hot spot would produce the trend of increasing age of volcanism to the south in the Coast Ranges. McLaughlin (1977) suggested that Clear Lake volcanism followed soon after passage of the Mendocino triple junction and cessation of subduction in the area about 3 m.y. ago. Magma then rose to shallower levels in the crust where faulting established conduits to the surface.

We suggest here that volcanism may be related to propagation of the San Andreas fault and its branches. Volcanic centers in the Coast Ranges lie astride the San Andreas (Pinnacles and Neenach Volcanic Formations) or to the east, adjacent to one or more of its branches (Quien Sabe Volcanics, volcanic rocks of the Berkeley Hills, Sonoma, and Clear Lake Volcanics). It may be that propagation of these faults produces zones of weakness or tears deep in the crust which lower the pressure in the upper mantle and allow partial melting. The basaltic magma thus created invades the crust, producing a thermal anomaly which melts crustal rocks, dominantly Franciscan graywacke, shale, and greenstone. The first melting fraction of these rocks would be a silicic melt which might rise to the surface or might branch into isolated reservoirs where differentiation would take place before eruption (for example, the Cobb Mountain sequence of rhyolite, followed by a smaller rhyodacite eruption, followed by a still smaller dacite). The episodic nature of Clear Lake volcanism suggests that there have been several periods when basaltic intrusions from the upper mantle have penetrated into the crust.

CONCLUSIONS

Potassium-argon dating, magnetic polarity determinations, and detailed geologic mapping have deciphered a complex sequence of nearly 100 volcanic units erupted during the last two million years in the Clear Lake volcanic field, California. The volcanic field is generally younger to the north, and there were significant periods of time during which no eruptions took place. Future eruptions in the area are probable, and likely sites for this activity have been identified.

Procedures for the K-Ar dating followed established practice, but some innovations substantially improved the measured percentages of radiogenic argon. Unlined extraction bottles, brief HF treatments of whole-rock samples, and longer-than-standard fusions of some andesite samples made significant improvements in the analytical results.

REFERENCES CITED

Anderson, C. A., 1936, Volcanic history of the Clear Lake area, California: Geological Society of America Bulletin, v. 47, no. 3, p. 629–664.

Berry, A. L., Dalrymple, G. B., Lanphere, M. A., and Von Essen, J. C., 1976, Summary of miscellaneous potassium-argon age measurements, U.S. Geological Survey, Menlo Park, California, for the years 1972–74: U.S. Geological Survey Circular 727, 13p.

Bowman, H. R., Asaro, Frank, and Perlman, I., 1973, On the uniformity of composition in obsidians and evidence for magmatic mixing: Journal of Geology, v. 81, no. 3, p. 312–317.

Brice, J. C., 1953, Geology of Lower Lake quadrangle, California: California Division of Mines Bulletin 16, 72 p.

Dalrymple, G. B., and Lanphere, M. A., 1969, Potassium argon dating: San Francisco, W. H. Freeman, 258 p.

Davis, W. M., 1933, The lakes of California: California Journal of Mines and Geology, v. 29, p. 175–236.

Diller, J. S., 1891, A late volcanic eruption in northern California and its peculiar lava: U.S. Geological Survey Bulletin 79, 33 p.

Duffield, W. A., and Bacon, C. R., 1976, Preliminary geologic map of the Coso rhyolite domes and adjacent areas, Inyo County, California: U.S. Geological Survey Open-File Report 76–238, scale 1:50,000.

Everhart, D. L., 1946, Quicksilver deposits at the Sulphur Bank mine, Lake County, California: California Journal of Mines and Geology, v. 42, p. 125–153.

Evernden, J. F., and Curtis, G. H., 1965, Potassium-argon dating of late Cenozoic rocks in East Africa and Italy: Current Anthropology, v. 6, p. 343–385.

Garrison, L.E., 1972, Geothermal steam in The Geysers-Clear Lake region, California: Geological Society of America Bulletin, v. 83, no. 5, p. 1449–68.

Goff, F. E., Donnelly, J. M., Thompson, J. M., and Hearn, B. C., Jr., 1977, Geothermal prospecting in The Geysers-Clear Lake area, northern California: Geology, v. 5, p. 509–515.

Goff, F. E., and McLaughlin, R. J., 1976, Geology of the Cobb Mountain-Ford Flat geothermal area, Lake County, California: U.S. Geological Survey Open-File Report 76–221, scale 1:24,000.

Haq, B. U., Berggren, W. A., and Van Couvering, J. A., 1977, Corrected age of the Pliocene/Pleistocene boundary: Nature, v. 269, no. 5628, p. 483–488.

Hearn, B. C., Jr., Donnelly, J. M., and Goff, F. E., 1975, Preliminary geologic map of the Clear Lake volcanic field, Lake County, California: U.S. Geological Survey Open-File Report 75–391, scale 1:24,000.

——— 1976a, Preliminary geologic map and cross-section of the Clear Lake volcanic field, Lake County, California: U.S. Geol. Survey Open-File Report 76–751, scale 1:24,000.

——— 1976b, Geology and geochronology of the Clear Lake Volcanics, California: Second United Nations Symposium on the Development and Use of Geothermal Resources, San Francisco, 1975, Proceedings, v. 1, p. 423–428.

Hirooka, Kimio, and Kawai, Naoto, 1967, Results of age determinations of some late Cenozoic rocks in southwestern Japan: Annual Progress Report Paleogeophysics Research Group in Japan, Osaka, p. 69–73.

Hodges, C. A., 1966, Geomorphic history of Clear Lake, California: Stanford, Calif., Stanford University, Ph.D. thesis, 210 p.

Iddings, J. P., 1890, On a group of volcanic rocks from the Tewan Mountains, New Mexico, and on the occurrence of primary quartz in certain basalts: U.S. Geological Survey Bulletin 66, 34 p.

Isherwood, W. F., 1975, Gravity and magnetic studies of The Geysers-Clear Lake geothermal region, California, U. S. A.: U.S. Geological Survey Open-File Report 75–368, 37 p.

——— 1976, Gravity and magnetic studies of The Geysers-Clear Lake geothermal region, California: Second United Nations Symposium on the Development and Use of Geothermal Resources, San Francisco, 1975, Proceedings, v. 2, p. 1065–1073.

Lawson, A. C., 1908, The California earthquake of April 18, 1906; Report of the State Earthquake Investigation Commission: Carnegie Institution of Washington, Publication No. 87, v. 1 and atlas, 451 p. (reprinted 1969).

Mankinen, E. A., 1972, Paleomagnetism and potassium-argon ages of the Sonoma Volcanics, California: Geological Society of America Bulletin, v. 83, no. 7, p. 2063–2072.

Mankinen, E. A., Donnelly, J. M., and Gromme, C. S., 1978, Geomagnetic polarity event recorded at 1.1 m.y. B.P. on Cobb Mountain, Clear Lake volcanic field, California: Geology, v. 6, p. 653–656.

McLaughlin, R. J., 1974, Preliminary geologic map of The Geysers steam field and vicinity, Sonoma County, California: U.S. Geological Survey Open-File Report 74–238, scale 1:24,000.

——— 1975, Preliminary compilation of in-progress geologic mapping in The Geysers geothermal area, California: U.S. Geological Survey Open-File Report 75–198, scale 1:24,000.

——— 1977, Late Mesozoic-Quaternary plate tectonics and The Geysers-Clear Lake geothermal anomaly, northern Coast Ranges, California: Geological Society of America Abstracts with Programs, v. 9, no. 4, p. 464.

McLaughlin, R. J., and Stanley, W. D., 1976, Pre-Tertiary geology and structural control of geothermal resources, The Geysers steam field, California: Second United Nations Symposium on the Development and Use of Geothermal Resources, San Francisco, 1975, Proceedings, v. 1, p. 475–486.

McNitt, J. R., 1968a, Geologic map of the Kelseyville quadrangle, Sonoma, Lake, and Mendocino Counties, California: California Division of Mines and Geology Map Sheet 9.

——— 1968b, Geologic map of the Lakeport quadrangle, Lake County, California: California Divisions of Mines and Geology Map Sheet 10.

——— 1968c, Geology of the Clearlake Oaks 15-minute quadrangle, Lake County, California: California Division of Mines and Geology Open-File Release 68–12, scale 1:62,500.

Nicholls, James, Carmichael, I. S. E., and Stormer, J. C., Jr., 1971, Silica activity and P_{total} in igneous rocks: Contributions to Mineralogy and Petrology, v. 33, p. 1–20.

Rymer, M. J., 1978, Stratigraphy of the Cache Formation (Pliocene and Pleistocene) in Clear Lake basin, Lake County, California: U. S. Geological Survey Open-File Report 78–924, 102 p., map in pocket, scale 1:24,000.

Rymer, M. J., 1981, Stratigraphic revision of the Cache Formation (Pliocene and Pleistocene), Lake County, California: U.S. Geological Survey Bulletin 1502–C (in press).

Seidemann, D. E., 1976, An ^{40}Ar/^{39}Ar age spectrum for a cordierite-bearing rock; Isolating the effects of excess radiogenic ^{40}Ar: Earth and Planetary Science Letters, v. 33, p. 268–272.

Sims, J. D., and Rymer, M. J., 1975, Preliminary description and interpretation of cores and radiographs from Clear Lake, Lake County, California: Core 4: U.S. Geological Survey Open-File Report 75–666, 19 p.

——— 1976, Map of gaseous springs and associated faults in Clear Lake, California: U.S. Geological Survey Miscellaneous Field Studies Map MF–721, scale 1:48,000.

Smith, R. L., and Shaw, H. R., 1975, Igneous-related geothermal systems, *in* White, D. E., and Williams, D. L., eds., Assessment of geothermal resources of the United States—1975: U.S. Geological Survey Circular 726, p. 58–83.

Swe, Win, and Dickinson, W. R., 1970, Sedimentation and thrusting of Late Mesozoic rocks in the Coast Ranges near Clear Lake, California: Geological Society of America Bulletin, v. 81, no. 1, p. 165–189.

Watkins, N. D., 1968, Short period geomagnetic polarity events in deep-sea sedimentary cores: Earth and Planetary Science Letters, v. 4, p. 341–349.

Yates, R. G., and Hilpert, L. S., 1946, Quicksilver deposits of the eastern Mayacmas district, Lake and Napa Counties, California: California Division of Mines Report 42, p. 231–286.

STRONTIUM ISOTOPES IN THE CLEAR LAKE VOLCANICS

By Kiyoto Futa, Carl E. Hedge, B. C. Hearn, Jr.
and Julie M. Donnelly-Nolan

ABSTRACT

The complex array of ^{87}Sr/^{86}Sr values, when combined with Rb, Sr, and rare-earth concentration data, provides insight into the processes of magma genesis and evolution of the Clear Lake Volcanics. Some of the oldest and some of the youngest basalts and basaltic andesites are quite primitive, both in terms of ^{87}Sr/^{86}Sr ratios (0.7032) and Rb and Sr concentrations. These rocks are almost certainly mantle derived. The other basaltic andesites, which have higher ^{87}Sr/^{86}Sr ratios and less primitive geochemical characteristics than the more primitive basalts, were derived from a different source. Rhyolites tend to have high ^{87}Sr/^{86}Sr ratios (0.7040–0.7055), and other evidence is indicative of fractional crystallization of feldspar. Overall, the ^{87}Sr/^{86}Sr ratio increases with decreasing Sr content and increasing SiO_2 content. In many of the rhyolites and dacites the feldspar phenocrysts are more or less out of equilibrium with their host lavas in terms of both ^{87}Sr/^{86}Sr ratios and Sr concentrations.

The data suggest that numerous magmas were generated from at least two different sources. These magmas then probably fractionally crystallized in crustal-level magma chambers, interacted extensively with their wallrocks, and in some cases mixed with other magma batches.

INTRODUCTION

About 100 km^3 of lava was erupted in the Clear Lake volcanic field from the onset of volcanism about 2.0 m.y. ago until about 10,000 years ago. Geologic mapping (Hearn and others, 1976) has distinguished nearly 100 volcanic units within the Clear Lake field, and these probably represent 100–200 separate eruptions. The compositions of the lavas range from basalt to rhyolite. True basalt is rare, but basaltic andesite is second in volume only to dacite.

Extensive K-Ar dating (Donnelly-Nolan and others, this volume) has revealed that the volcanism was not continuous. Three significant time breaks have been demonstrated in the volcanic sequence and another has been suggested. The volcanic rocks are generally younger to the north. The earliest and latest periods of volcanism were dominated by basaltic lavas, and the intermediate period was dominated by dacite and rhyolite.

We have determined initial ^{87}Sr/^{86}Sr ratios on 27 lava samples that range widely in composition and age, six feldspar phenocryst separates, and four xenolith inclusions. The data are variable but consistent with the complex geologic pattern of eruptions.

Evidence for a number of magma chambers occurs in different places in the Clear Lake region. Geophysical evidence suggests that a magma chamber (Isherwood, this volume) underlies the central part of the volcanic field at a depth of 6–14 km. In the past other magma chambers may have existed to the south of the present chamber; the previous chambers would have been generated from different source rocks at depth. Numerous young vents to the northeast suggest that heating of another source region at depth is occurring, with the potential for the development of a new magma chamber. The combination of northward migration of volcanism and the presence of relatively shallow magma chambers allows several mechanisms to produce the ^{87}Sr/^{86}Sr ratios of the surface rocks. Possible explanations for the variety of ^{87}Sr/^{86}Sr values are (1) generation of magmas from different source regions, (2) variable amounts of assimilation of wallrocks, and (3) mixing of magmas. Wallrocks at shallow depth are either part of the Great Valley sequence, including ophiolite, or part of the Franciscan assemblage; wallrocks at greater depth are Franciscan, and beneath them are presumably oceanic crust and upper mantle. Oxygen isotopic ratios (Taylor, 1968) and Pb isotopic ratios (Doe and Delevaux, 1973) also suggest that crustal contamination has played a significant role in the genesis of this region and that the evolution of these lavas was quite complex.

DATA

^{87}Sr/^{86}Sr ratios and Rb and Sr concentrations are given in table 2, and sample locations are shown in figure 24. In table 2 the samples are arranged in the general order of increasing age. We have subdivided the samples into four age groups that are recognized from the K-Ar dating. Group I is from 0 to 0.2 m.y. old, group II from 0.3 to 0.6, group III from 0.8 to 1.1, and group IV from 1.3 to 2.1 m.y. old.

The youngest sample studied, a basaltic andesite (sample 1), has a high Rb content (49.2 ppm) and a high ^{87}Sr/^{86}Sr ratio (0.70402) compared with a slightly older basaltic andesite (sample 2). This relatively primitive lava has a low Rb content (14.4 ppm) and one of the lowest ^{87}Sr/^{86}Sr ratios (0.70319) found in the Clear

Lake field. Samples 3, 4, and 5, which are rhyolite, dacite, and basalt respectively, are closely associated in space and time and are probably genetically related. The rhyolite and dacite are part of a series which shows remarkably linear variation in major and trace elements (Bowman and others, 1973); this relation extends to the olivine basalt (sample 5) (Hearn and others, this volume). These three samples exhibit a pattern that is common in the Clear Lake Volcanics: the siliceous lavas generally have higher ^{87}Sr/^{86}Sr ratios than associated more mafic lavas. The basalt of this trio (sample 5) has a low ^{87}Sr/^{86}Sr of 0.70317, while the rhyolite (sample 3) has one of the highest in this study (0.70544).

Within group II (0.3–0.6 m.y.), sample 7 is one of the several dacites from Mount Konocti, which represents the most voluminous lava type in the Clear Lake volcanic field. It has a remarkably low ^{87}Sr/^{86}Sr ratio (0.70351) for a siliceous rock.

Sample 8, quartz-bearing basaltic andesite, has a rather high ^{87}Sr/^{86}Sr ratio for a mafic lava (0.70392). This ratio suggests that the quartz crystals might be xenocrysts rather than phenocrysts.

The other samples of age group II are all rhyolites and dacites. The ^{87}Sr/^{86}Sr ratios of these rocks range from 0.70367, for dacite sample 12, to 0.70501 for rhyolite sample 11.

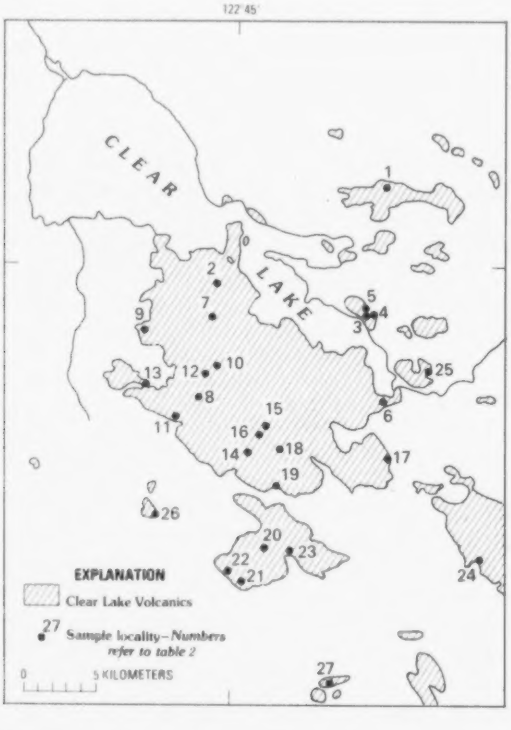

FIGURE 24.—Sample localities in the Clear Lake Volcanics, Calif.

Age group III (0.8–1.1 m.y.) contains no basaltic rocks. The most mafic lava of this group, an ilmenite andesite (no. 18), has a high ^{87}Sr/^{86}Sr of 0.70463, although two other andesites have ^{87}Sr/^{86}Sr of 0.70391 and 0.70402. Dacites and rhyolites have ^{87}Sr/^{86}Sr ratios from 0.70366 to 0.70511, much like those of group II but slightly higher. Within group III, samples 20, 21, and 22 are close in age and location at Cobb Mountain, but they show increasing ^{87}Sr/^{86}Sr with decreasing silica, opposite to the more typical relation.

Group IV (1.3–2.1 m.y.) is dominated by more mafic lavas. Three samples have high ^{87}Sr/^{86}Sr ratios compared to mafic rocks of the younger groups, but sample 26 has one of the lowest ratios, 0.70316.

Only one sample older than 2 m.y. was studied, a rhyolite (sample 27) having a high ^{87}Sr/^{86}Sr ratio, 0.70512.

In addition to the whole-rock samples, feldspar phenocrysts from six samples were studied. Three of the six feldspars are markedly different in their ^{87}Sr/^{86}Sr ratios from the rocks in which they are found. These nonequilibrium phenocrysts are strong evidence of some sort of assimilation or mixing process, and their importance will be discussed in detail later.

Four inclusions were studied as possible representatives of the rocks at depth. The two diabases and the one leucogabbro (nos. 28, 29, and 31) are coarser grained but similar in composition to the mafic and intermediate rocks erupted at the surface. They are therefore presumably related to the Clear Lake Volcanics. The quartz-feldspar-garnet-mica schist inclusion (no. 30) may be a Franciscan or Great Valley sedimentary rock that was contact-metamorphosed at depth, or it may be derived from previously unrecognized regionally metamorphosed pelitic rocks at depth. In either case, it is important because it is a sample of quartzofeldspathic material that occurs at depth. Its ^{87}Sr/^{86}Sr (0.70638) is distinctly higher than all the volcanic rocks. Therefore it could not be the direct source of any of them, but it could have played a role in raising ^{87}Sr/^{86}Sr ratios of magmas through assimilation processes.

When initial ^{87}Sr/^{86}Sr ratios are plotted against the sample age (fig. 25), there are no clear simple trends, but several aspects are significant. The lowest ^{87}Sr/^{86}Sr ratios are found in some of the oldest (no. 26) and youngest (nos. 2 and 5) samples. These are mafic rocks from time periods when mafic lava was abundant. Geographically they are some of the most southwesterly and northeasterly samples. Age group IV (1.3–2.1 m.y.) rocks except sample 26, while being fairly mafic, have higher ^{87}Sr/^{86}Sr ratios than basalt of the youngest group. Rocks of groups II and III are centrally located in both time and space. In these periods, siliceous volcanism dominated, and no really low ^{87}Sr/^{86}Sr ratios were found among these samples.

DISCUSSION

In interpreting the data we have accepted certain well-established principles: (1) any fractional crystallization step will result in an increase in the Rb content of the remaining liquid, (2) during fractional crystallization, Sr concentrations may increase or decrease slightly when going from basalt to andesite depending on the relative proportions of plagioclase and mafic minerals, and the Sr concentration will decrease when going from andesite to dacite to rhyolite, (3) ^{87}Sr/^{86}Sr does not change through fractional crystallization, and (4) ^{87}Sr/^{86}Sr will almost certainly increase through assimilation processes.

The first two guidelines are the result of the well-documented behavior of Rb and Sr during the crystallization of common igneous minerals (Arth, 1976). The concept that assimilation of crustal Sr will increase the ^{87}Sr/^{86}Sr ratio of the magmas is based on the premise that the crust is vertically zoned in ^{87}Sr/^{86}Sr (Zartman

TABLE 2.—*Rubidium and strontium concentrations and ^{87}Sr/^{86}Sr, Clear Lake Volcanics*

[Rb and Sr concentrations determined by isotope dilution. ^{87}Sr/^{86}Sr corrected for any growth of radiogenic ^{87}Sr since eruption. Eimer and Amend standard value is 0.70800. Precision is $2\sigma \pm 0.00008$]

Sample No.	Sample description	Rb (ppm)	Sr (ppm)	^{87}Sr/^{86}Sr
	Age group I (0–0.2 m.y.)			
1	Basaltic andesite of High Valley at Round Mountain	49.2	389	0.70402
2	Basaltic andesite of Buckingham Peak	14.4	464	.70319
3	Rhyolite of Borax Lake	211	20.8	.70544
4	Dacite of Clear Lake Park	123	114	.70359
5	Olivine basalt of Arrowhead Road	49.8	220	.70317
6	Basalt of Roundtop Mountain	10.6	476	.70356
	Age group II (0.3–0.6 m.y.)			
7	Dacite of Mount Konocti	94.4	366	.70351
7	Sanidine phenocrysts		284	.70476
8	Basaltic andesite of McIntire Creek	55.7	316	.70392
9	Rhyolite of Cole Creek	139	255	.70414
9	Plagioclase phenocrysts		169	.70469
10	Rhyolite southwest of Sugarloaf	185	80.8	.70463
10	Sanidine phenocrysts		230	.70464
11	Rhyolite of Thurston Creek	206	69.0	.70501
12	Dacite of Sulfur Mound Mine	126	293	.70367
12	Sanidine phenocrysts		263	.70469
13	Dacite of Camel's Hump	141	203	.70454
	Age group III (0.8–1.1 m.y.)			
14	Dacite of Mount Hannah	117	294	.70425
15	Andesite of Split Top Ridge	81.6	455	.70391
16	Dacite of Diener Drive	104	318	.70366
17	Andesite of Pirini Hill	50.0	587	.70402
18	Ilmenite andesite of Salmina Flat	58.5	487	.70463
19	Rhyolite of Bonanza Springs	149	94.9	.70495
20	Dacite of Cobb Valley	85.8	375	.70511
21	Dacite of Cobb Mountain	134	260	.70437
22	Rhyolite of Alder Creek	188	116	.70407
22	Sanidine phenocrysts		236	.70427
	Age group IV (1.3–2.1 m.y.)			
23	Andesite of Boggs Mountain	32.7	687	.70390
24	Basaltic andesite at Hidden Valley Lake	42.6	473	.70453
25	Basaltic andesite, 26th St.	33.6	349	.70438
26	Olivine basalt of Caldwell Pines	11.7	379	.70316
27	Rhyolite of Pine Mountain	148	84.9	.70512
27	Sanidine phenocrysts		223	.70463
	Inclusions			
28	Diabase in 13	86.2	594	.70328
29	Diabase in 7	36.3	509	.70378
30	Quartz-plagiocase garnet-mica schist in 14	32.8	221	.70638
31	Leucogabbro	8.9	322	.70451

and Wasserburg, 1969) and on the observed values for Franciscan and Great Valley rocks (Peterman and others, 1967) as well as the metasedimentary xenolith (no. 30, table 2).

The Rb and Sr concentrations plotted in figure 26 define a broad field in which Rb increases as Sr decreases. Such a trend is normal for igneous rocks. The trend is so broad, however, as to preclude all of the samples being related by any single mechanism such as fractional crystallization from one parent magma. For example, a basalt such as no. 5 could not possibly have been parental to andesites such as nos. 17 and 23. Samples from age group I tend to be distinctly lower in Rb and Sr than most samples from groups II and III. The Rb and Sr concentrations seem to require at least two different magma types.

Rubidium concentrations and ^{87}Sr/^{86}Sr ratios are positively correlated such that both are highest in rhyolite, lowest in basalt, and intermediate in dacite and andesite (fig. 27). The basalt samples with the lowest ^{87}Sr/^{86}Sr ratios, nos. 5 and 26, are chemically the most primitive (Hearn and others, this volume).

Plotting the Sr concentrations against the ^{87}Sr/^{86}Sr ratios (fig. 28) demonstrates that fractional crystallization of only two magma stems cannot entirely explain the data as the most mafic lavas alone have a range of ^{87}Sr/^{86}Sr from 0.70316 to 0.70453. Fractional crystallization alone could not account either for the variability in Rb and Sr concentrations or for the range in ^{87}Sr/^{86}Sr ratios. Assimilation of various amounts of radiogenic crustal Sr could explain the variable ^{87}Sr/^{86}Sr ratios of the basaltic rocks but would not be consistent with other petrochemical principles. For such a range, large amounts of assimilation (in excess of 50 percent) of material like that of the schist sample 30 or the Franciscan or the Great Valley sediments (Peterman and others, 1967) would be required. Simple thermal balance requires that extensive fractional crystallization must accompany the incorporation of so much material into the magma. Combined large-scale assimilation and fractional crystallization would have produced andesite or dacite rather than another basalt or basal-

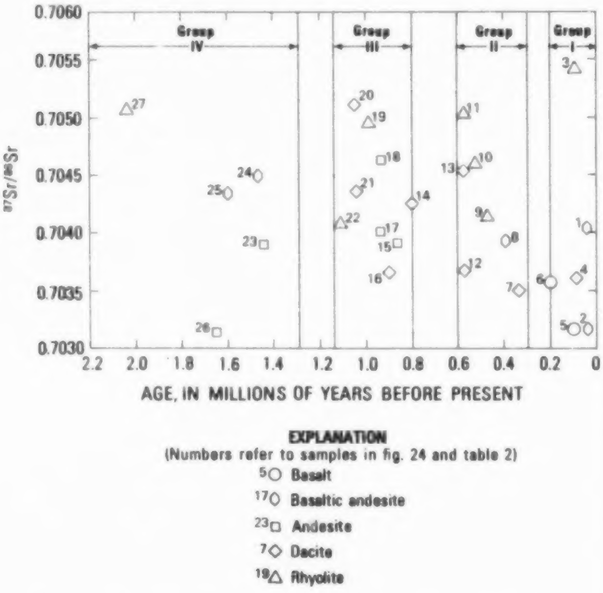

FIGURE 25.—^{87}Sr/^{86}Sr ratios versus K-Ar ages. Groups I–IV are separated according to age (see table 1).

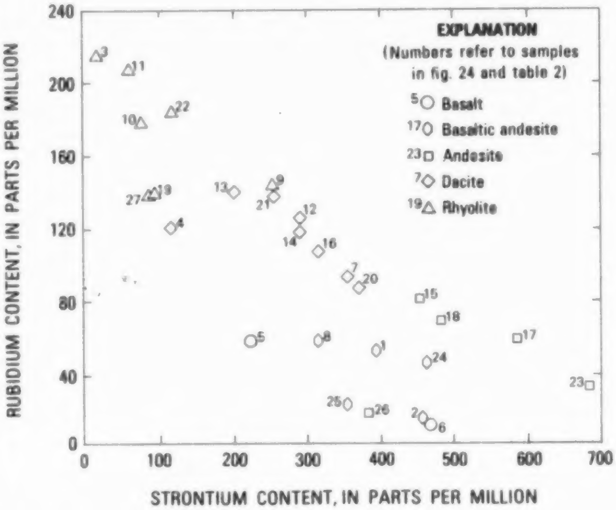

FIGURE 26.—Rubidium versus strontium concentrations.

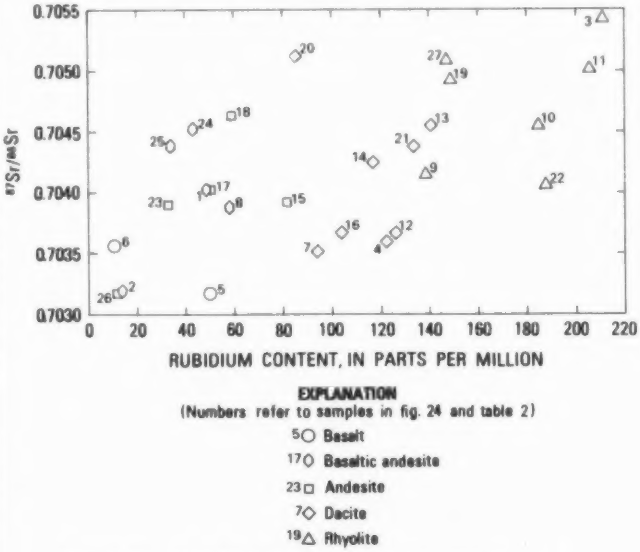

FIGURE 27.—^{87}Sr/^{86}Sr ratios versus Rb concentrations.

tic andesite. Therefore we must conclude that the majority of the range in ^{87}Sr/^{86}Sr of the more mafic lavas is a primary feature and that these magmas were derived from diverse source materials having a considerable range of ^{87}Sr/^{86}Sr ratios.

At the other end of the spectrum, the rhyolites are definitely the result of fractional crystallization and are not themselves primary melts. This conclusion is required by their low Sr concentrations (Noble and others, 1969) and their negative Eu anomalies (Hearn and others, this volume), which are both the result of feldspar removal. The fact that the rhyolites tend to have higher ^{87}Sr/^{86}Sr ratios than the other rock types, combined with the conclusion that they are the result of fractional crystallization, indicates that assimilation of wallrock Sr accompanied the fractional crystallization.

Five of the six feldspar samples (table 2) are out of chemical and isotopic equilibrium with their rhyolitic and dacitic host rocks. Feldspars of these compositions (sodic plagioclase and sanidine) have crystal/liquid distribution coefficients for Sr in the range of 2.5 to 4.0 (see Arth, 1976 for a review of distribution coefficients). Therefore feldspar crystallized in equilibrium with melt should have about three times the Sr content of the volcanic rock and the same ^{87}Sr/^{86}Sr ratio. The feldspar from sample 10 is in equilibrium both chemically and isotopically with respect to Sr. Those from 22 and 27 are close to equilibrium, but the phenocrysts from 7, 9, and 12 are severely out of equilibrium, both in Sr content and ^{87}Sr/^{86}Sr ratio. Noble and Hedge (1969) postulated from similar data from southwest Nevada that the eruptions tapped zoned magma chambers which were in the process of undergoing fractional crystallization and were simultaneously incorporating radiogenic Sr from their wallrocks. Because no known source of highly radiogenic Sr (such as Precambrian sialic crust) is known to exist beneath the Clear Lake volcanic field, such a mechanism is probably not adequate to explain the more severe causes of disequilibrium observed here. Another way of interpreting the disequilibrium feldspars is that they are the result of magma mixing. The interpretation fits both the Sr data and the petrographic observations (Hearn and others, this volume) so well that we accept it as an integral part of the Clear Lake magma-genesis processes.

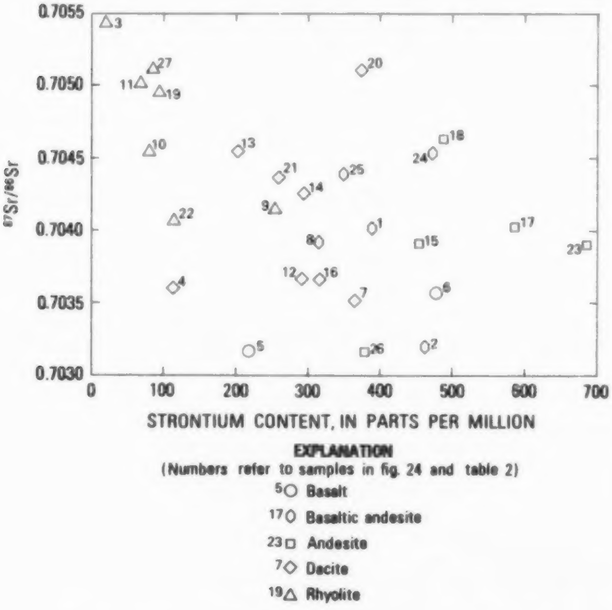

FIGURE 28.—^{87}Sr/^{86}Sr ratios versus Sr concentrations.

We have now established that (1) the sources of the various mafic magmas (and presumably the more siliceous magmas) were of variable ^{87}Sr/^{86}Sr, (2) the rhyolites are the result of fractional crystallization, (3) the more siliceous magmas incorporated various amounts of crustal Sr, and (4) mixing of magmas was a factor in generation of some lavas. Combining these four observations with the guidelines concerning Rb and Sr behavior, outlined earlier, we propose the following genesis of the various rocks listed in table 2.

Basaltic andesite 1 could have been derived from a basalt like 6 if a significant amount of crustal Sr were added in the process. Basaltic andesite 2 is very primitive, in terms of its Rb content and ^{87}Sr/^{86}Sr ratio, and cannot be derived from any sample that we studied by fractional crystallization.

The rhyolite-dacite-basalt trio (3, 4, and 5), closely associated in time and space, plot by themselves on several diagrams (particularly figs. 26 and 28) and are almost certainly a genetic series in which significant amounts of crustal Sr have been incorporated and from which plagioclase has been removed. Bowman, Asaro, and Perlman (1973) used these rocks as examples of mixed magmas. The Sr data would be compatible with a mixing origin for the dacite, but only if we allow that the rhyolite we studied was somewhat more fractionated than the rhyolite magma involved in the mixing.

Within group II, dacite 7 has the lowest ^{87}Sr/^{86}Sr ratio, and by addition of crustal Sr and removal of plagioclase it could be parental to dacites 12 and 13 and rhyolites 9, 10, and 11. This group of samples includes several samples with feldspar in disequilibrium, however, and we must therefore consider magma mixing as an alternative process. Samples 7 and 12 contain feldspars that are well out of equilibrium, and these rocks could be the results of mixing of magmas like 10 or 11 with a mafic magma similar to sample 2 but having a slightly higher ^{87}Sr/^{86}Sr ratio. The basaltic andesite 8 has no apparent relation to other rocks.

None of the studied basalts could have given rise to the group III andesites 15 and 17, but an andesite like 23 (from group IV) could be parental to 15 and 17. The dacite of Cobb Valley (sample 20) is difficult to interpret because of its high ^{87}Sr/^{86}Sr ratio and high Sr content. Perhaps it fractionated from a magma like 18 or 24 and simultaneously incorporated Sr from material that was high in ^{87}Sr/^{86}Sr. Sample 20 is closely associated in time and space with dacite 21 and rhyolite 22. Rhyolite 22 has a low ^{87}Sr/^{86}Sr and must have been derived from an andesite more like 17. It is plausible that the dacite 21 is the result of mixing of magmas 20 and 22.

The group IV samples include three basalts and one andesite, none of which appear to be related.

If we ignore the age groupings, we can see that larger groups of samples with similar ^{87}Sr/^{86}Sr ratios and Rb and Sr characteristics form geographically coherent patterns. For example, there is a group of samples with high ^{87}Sr/^{86}Sr ratios and high Sr correlations to the other samples, nos. 18, 20, and 24 (shown on fig. 28), that are all located in the southeastern part of the field. Another group of samples that are internally similar, having lower ^{87}Sr/^{86}Sr ratios relative to Rb and Sr contents, would include nos. 7, 9, 10, 11, 12, 16, and 22. Intermediate both geographically and in terms of ^{87}Sr/^{86}Sr would be nos. 14, 15, 17, 19, 21, and 23. The samples with the lowest ^{87}Sr/^{86}Sr ratios (2, 5 and 26) are geographically peripheral to the second lowest group. It appears that the Rb, Sr, and ^{87}Sr/^{86}Sr characteristics may be partially controlled by the geology at depth. That is, certain isotopic and chemical characteristics tend to occur in certain areas, and the subjacent regions at depth may have produced similar magmas at more than one time.

CONCLUSIONS

Variations in ^{87}Sr/^{86}Sr ratios in the Clear Lake Volcanics indicate that as volcanism moved with time, different regions within the upper mantle or lower crust were melted to produce the lavas. The oldest basalt studied has a very low ^{87}Sr/^{86}Sr ratio and was almost certainly derived from the upper mantle. However, as volcanism moved northward the most mafic lavas had higher ^{87}Sr/^{86}Sr ratios and were less primitive chemically. These must have melted from a different source material from the oldest and youngest basalt, possibly partly or totally within the lower crust. The other lavas that erupted during these intermediate time periods show geographic variations in ^{87}Sr/^{86}Sr that probably reflect variations within the source rocks. The most recent mafic lavas were erupted on the northeast side of the volcanic field, and their low ^{87}Sr/^{86}Sr ratios show them to be mantle derived.

The more siliceous lavas formed from the more mafic lavas by a combination of fractional crystallization and assimilation processes within crustal-level magma chambers. Periodic injection of mafic lava into magma chambers that had become relatively siliceous produced mixed magmas having nonequilibrium phenocryst assemblages.

The widely varying ^{87}Sr/^{86}Sr ratios are the result of melting of different source rocks, fractional crystallization and assimilation in shallow magma chambers, and mixing of magmas—a complex picture which fits the complexity of the volcanic sequence.

REFERENCES CITED

Arth, J. G., 1976, Behavior of trace elements during magmatic processes—a summary of theoretical models and their application: U.S. Geological Survey Journal of Research, v. 4, p. 41–47.

Bowman, H. R., Asaro, Frank, and Perlman, I., 1973, On the uniformity of composition in obsidians and evidence for magmatic mixing: Journal of Geology, v. 81, p. 312–327.

Doe, B. R., and Delevaux, M. H., 1973, Variations in lead-isotopic compositions in Mesozoic granitic rocks of California: A preliminary investigation: Geological Society of American Bulletin, v. 84, p. 3513–3526.

Hearn, B. C., Jr., Donnelly, J. M., and Goff, F. E., 1976, Preliminary geologic map and cross section of the Clear Lake volcanic field, Lake County, California: U.S. Geological Survey Open-File Report 76–751, scale 1:24,000.

Noble, D. C., and Hedge, C. E., 1969, ^{87}Sr/^{86}Sr variations within individual ash-flow sheets: U.S. Geological Survey Professional Paper 650–C, p. C133–C139.

Noble, D. C., Haffty, Joseph, and Hedge, C. E., 1969, Strontium and magnesium contents of some natural peralkaline silicic glasses and their petrogenetic significance: American Journal of Science, v. 267, p. 598–608.

Peterman, Z. E., Hedge, C. E., Coleman, R. G., and Snavely, P. D., Jr., 1967, ^{87}Sr/^{86}Sr ratios in some eugeosynclinal sedimentary rocks and their bearing on the origin of granitic magmas in orogenic belts: Earth and Planetary Science Letters, v. 2, p. 433–439.

Taylor, H. P., Jr., 1968, The oxygen isotope geochemistry of igneous rocks: Contributions to Mineralogy and Petrology, v. 19, p. 1–71.

Zartman, R. E., and Wasserburg, G. J., 1969, The isotopic composition of lead in potassium feldspars from some 1.0-b.y.-old North American igneous rocks: Geochimica et Cosmochimica Acta, v. 33, p. 901–942.

PALEOMAGNETISM OF THE CLEAR LAKE VOLCANICS AND NEW LIMITS ON THE AGE OF THE JARAMILLO NORMAL-POLARITY EVENT

By E. A. Mankinen, J. M. Donnelly-Nolan, C. S. Grommé, and B. C. Hearn, Jr.

ABSTRACT

Paleomagnetic studies and potassium-argon age determinations on rocks from the Clear Lake volcanic field, California, have provided additional information on the limits of the Jaramillo normal-polarity event. Several flows record part of the polarity transition at the end of the event. Reversed-polarity flows that provide a limit to the older boundary of this event have also been found. Detailed K-Ar dating of these flows, when combined with data from other localities, shows that the Jaramillo event lasted from 0.97–0.90 m.y. ago, an age that is in excellent agreement with estimates made from deep-sea sediment cores and mid-oceanic magnetic anomalies. VGP (virtual geomagnetic pole) positions calculated from intermediate-polarity lavas from Clear Lake fall very close to the published VGP path for the Matuyama-Brunhes polarity transition recorded in sediments from Lake Tecopa, California. Recurrence of similar VGP positions during at least three polarity reversals over a time span of 500,000 years suggests that transitional VGP paths may be controlled by some long-term regional features.

INTRODUCTION

Magnetic polarities of many of the volcanic units of the Clear Lake Volcanics were determined using a fluxgate magnetometer as an aid to the geologic mapping of the area. The polarity and magnetic stability of some of these units were later verified in the laboratory. These early magnetic measurements, along with potassium-argon age determinations (Hearn and others, 1976; Donnelly, 1977), formed the basis for additional paleomagnetic sampling. This later detailed sampling concentrated on the silicic volcanic units on Cobb Mountain, which document a brief polarity event (Mankinen and others, 1978), and on several dacite and andesite flows that were erupted near the time of the Jaramillo normal-polarity event. The majority of these flows are located in the vicinity of Mount Hannah near the center of the volcanic field.

Acknowledgments.—We thank Republic Geothermal Inc. for providing the drill-hole sample of the rhyolite of Bonanza Springs. We also thank Allan Cox and W. F. Isherwood for the use of previously unpublished data.

METHODS

Three to nine oriented cores were collected from each of 14 rock units within the Clear Lake volcanic field at the localities shown in figure 29. AF (alternating field) demagnetization was performed on one or more samples from each locality. Samples with anomalous components of magnetization were magnetically cleaned at a peak alternating field chosen on the basis of behavior during partial demagnetization (the stable end-point method). Thermal demagnetization on selected samples was done in vacuum with ambient fields of less than 100 gammas. Strong-field thermomagnetic curves were also obtained in vacuum with applied fields between 3,000 and 6,000 Oe. Weak-field susceptibilities were measured at 1,000 Hz with a commercial bridge.

Directions of remanent magnetization, after magnetic cleaning if needed, are listed in table 3. Also included in this table are the data for oriented hand samples from an additional eight units with reliable ages. Oriented hand samples from these units were measured in the field using a portable fluxgate magnetometer (Hearn and others, 1976), and cores from at least one hand sample from each locality were checked in the laboratory for polarity and magnetic stability. These data meet the requirements of magnetic category III B (Cox and others, 1966) and are considered reliable for defining the polarity time scale. The data listed in table 3 supersede preliminary polarity determinations for the same units given by Hearn, Donnelly, and Goff (1976) and Donnelly (1977).

Potassium-argon ages for the units studied have been calculated using the K-Ar constants based on the ^{40}K activity of Beckinsale and Gale (1969) and the potassium abundance measurements of Garner and others (1975); these constants were recommended for adoption by the IUGS Subcommission on Geochronology (Steiger and Jäger, 1977). Analytical data for these determinations may be found in Berry, Dalrymple, Lanphere, and Von Essen (1976), Donnelly (1977), and elsewhere in this volume (Donnelly-Nolan and others, this volume). Ages for units from other localities cited in this report have been recalculated using the recommended constants and are given in the compilation by Mankinen and Dalrymple (1979).

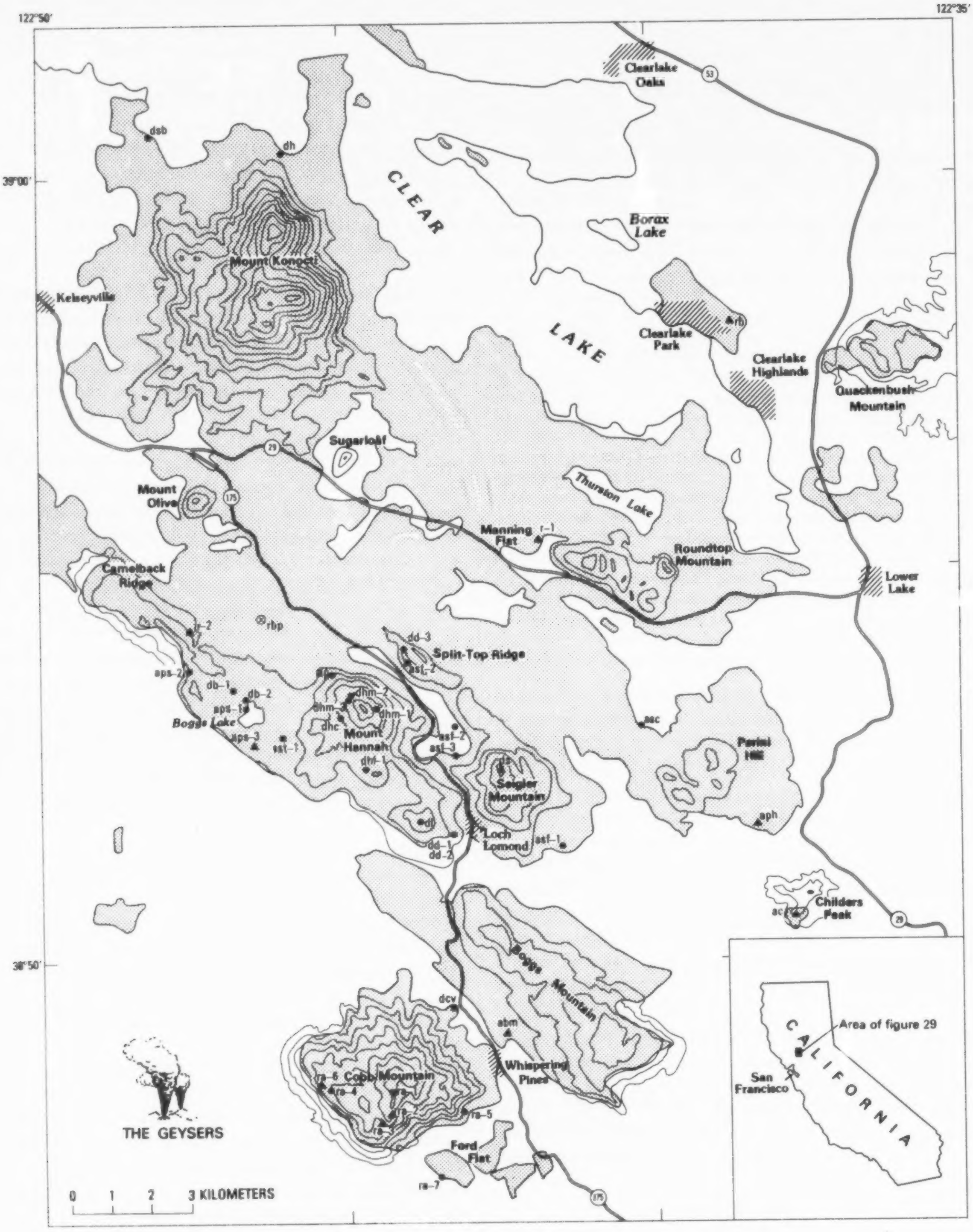
122°50′
122°35′
39°00′
38°50′
Clearlake Oaks
53
CLEAR
LAKE
Borax Lake
dsb
dh
Mount Konocti
Kelseyville
Clearlake Park
rb
Clearlake Highlands
Quackenbush Mountain
Sugarloaf
29
Mount Olive
175
Thurston Lake
Manning Flat
r–1
Roundtop Mountain
Lower Lake
Camelback Ridge
r–2
rbp
dd–3
Split-Top Ridge
ast–2
aps–2
db–1
db–2
aps–1
Boggs Lake
aps–3
ast–1
dhm–2
dhm–3
dhm–1
dhc
Mount Hannah
dhf–1
asf–2
ast–3
ds
Seigler Mountain
asc
Perini Hill
aph
ddl
dd–1
dd–2
Loch Lomond
asf–1
Childers Peak
ac
29
Boggs Mountain
dcv
abm
Whispering Pines
ra–6
ra–4
Cobb Mountain
ra–5
ra–7
Ford Flat
175
THE GEYSERS
0 1 2 3 KILOMETERS
Area of figure 29
CALIFORNIA
San Francisco

FIGURE 29.—Clear Lake area, California, showing prominent topographic features and sample localities. Contours depict physiographic features but do not show actual elevations. Stippled pattern shows areal extent of Clear Lake Volcanics.

TABLE 3.—*Paleomagnetic results and K-Ar ages*

[Location of samples shown in figure 29. K-Ar ages determined using the following constants: $\lambda_\epsilon = 0.581\times10^{-10}$ yr^{-1}; $\lambda_\beta = 4.962\times10^{-10}$ yr^{-1}; $^{40}K/K_{total} = 1.167\times10^{-4}$ mol/mol. N, number of samples; H, peak demagnetizing field (in oersteds); NRM, natural remanent magnetization; inclination is positive downward, declination is east of north. J, geometric mean intensity after magnetic cleaning ($\times10^{-3}$ emu/cm^3); K, Fisher's (1953) precision parameter; α_{95}, 95-percent confidence oval about average direction. VGP, virtual geomagnetic pole. n.d., not determined]

Sample locality	K-Ar age (m.y.)	N	H	Incl.	Decl.	J	K	α_{95}	VGP	
									Lat (°N.)	Long (°E.)
rb	[1]0.091±0.013	2	NRM	+58	342	2.68	n.d.	n.d.	+76	153
dh[2]	.35±0.02	3	NRM	+56.7	011.5	13.3	338	6.7	+80.8	334.7
dsb[2]	.34±0.10	5	NRM	+57.4	003.2	12.6	118	7.1	+87.3	347.7
r-1	[1]479±0.015	1	NRM	+60	023	14.6	n.d.	n.d.	+73	313
r-2	[1].551±0.016	1	NRM	+35	341	13.9	n.d.	n.d.	+64	103
ds	.61±0.02	1	NRM	+69	351	27.4	n.d.	n.d.	+76	214
dtv	.84±0.03	1	NRM	+51	013	20.4	n.d.	n.d.	+77	358
dhm-1	n.d.	5	400	+11.9	069.8	.89	249	4.9	+19.4	335.4
dhm-2	n.d.	9	400	-30.6	072.3	.35	103	5.1	+02.8	351.1
dhm-3	n.d.	5	300	-40.6	097.2	.26	279	4.6	-19.7	341.7
dhc	n.d.	7	400	-02.9	077.4	1.50	144	5.1	+08.9	336.4
dhf	.90±0.02	8	400	-18.5	069.5	.76	103	5.5	+09.5	347.8
aps-1	[3].90±0.03	3	800	-41.0	130.7	.89	167	9.6	-45.7	321.9
aps-2	[3].90±0.03	4	800	-40.2	132.8	.55	148	7.6	-47.0	319.6
aps-3	[3].90±0.03	1	700	-41	132	.05	n.d.	n.d.	-47	321
aps(avg)	[3].90±0.03	7	800	-40.5	131.9	.68	182	4.5	-46.4	320.6
dl	.90±0.03	5	300	-08.8	077.3	.37	14	21.4	+07.0	338.7
ast-1	[3].91±0.04	8	300	-12.1	084.3	2.58	57	7.4	+00.6	355.6
ast-2	[3].91±0.04	5	500	-56.7	092.7	.19	56	10.4	-24.2	356.6
dd-1	.92±0.02	4				Indeterminate				
dd-2	.92±0.02	4				Indeterminate				
dd-3	.92±0.02	4				Indeterminate				
ac[4]	.92±0.02	2	200	+25	167	.38	n.d.	n.d.	-37	253
aph	n.d.	2	NRM	+56	319	2.30	n.d.	n.d.	+58	156
asc[4]	.97±0.03	8	NRM	+56.4	296.6	2.11	906	1.9	+41.0	166.1
db-1	.98±0.06	8	400	-42.2	156.3	1.88	29	10.5	-65.3	298.3
db-2	.98±0.06	4	200	-25.4	125.1	2.53	817	3.2	-35.4	315.1
asf-1	n.d.	8	NRM	-65.0	162.6	3.06	148	4.6	-75.0	005.4
asf-2	n.d.	4	NRM	-53.2	165.7	7.95	451	4.3	-77.4	307.4
asf-3	n.d.	4	500	-50.3	199.9	6.42	46	13.8	-72.0	166.9
ag	1.00±0.05	5	400	-42.2	203.4	6.13	194	5.5	-65.5	176.5
ra-7	[5]1.12±0.02	9	300	+14.7	094.3	2.13	91	5.4	+01.3	318.7
abm	1.49±0.04	1	NRM	-64	231	12.6	n.d.	n.d.	-52	120

[1] Berry, Dalrymple, Lanphere, and Von Essen (1976).
[2] Allan Cox (unpub. data, 1962).
[3] Age determined from stratigraphic relations; see text.
[4] Flow not reliable for defining polarity time scale because of possible errors in age determinations.
[5] Mankinen, Donnelly, and Gromme (1978).

EXPLANATION

Sample locality—*Letters refer to map unit* (see table 3)

ra-1 ● Oriented-core locality
aps-3 ▲ Hand-sample locality
rbp ⊗ Drill-hole locality

Map Unit

rb	Rhyolite of Borax Lake
dh	Dacite of Horseshoe Bay
dsb	Dacite of Soda Bay
r	Rhyolite of Thurston Creek
ds	Dacite of Siegler Mountain
dhc	Coarse-grained dacite of Mount Hannah
dhm	Medium-grained dacite of Mount Hannah
dhf	Dacite of Harrington Flat
aps	Andesite of Poison Smith Spring
dl	Dacite of Loch Lomond
ast	Andesite of Split-Top Ridge
dd	Dacite of Diener Drive
ac	Andesite of Childers Peak
aph	Andesite of Perini Hill
asc	Andesite of Siegler Canyon
db	Dacite of Boggs Lake
asf	Andesite of Salmina Flat
ag	Andesite of Glenview
rbp	Rhyolite tuff of Bonanza Springs
dcv	Dacite of Cobb Valley
ra	Rhyolite of Alder Creek
abm	Andesite of Boggs Mountain
▨	Clear Lake Volcanics

OLDER LAVAS OF THE MOUNT HANNAH AREA

The oldest units exposed near Mount Hannah are the rhyolite tuff of Bonanza Springs, the andesite of Glenview, the andesite of Salmina Flat, and the dacite of Boggs Lake (fig. 29). The andesite of Childers Peak may also belong in this time interval, as will be discussed later. The stratigraphic relations of these and other units related to the Jaramillo normal-polarity event are shown schematically in figure 30. AF demagnetization shows that the andesites of Glenview and Salmina Flat and the dacite of Boggs Lake are stably magnetized and all are of reversed polarity (fig. 31). The andesite of Salmina Flat was sampled in three localities, one southeast of Seigler Mountain (locality asf-1) and two small isolated outcrops in Salmina Flat about 3.5 km to the northwest (localities asf-2 and asf-3). The remanence direction for locality asf-2 is similar to that determined for locality asf-1, but the direction at locality asf-3 is different and shows considerable dispersion. Four large separate blocks were sampled at this locality, and all have apparently been slightly rotated with respect to each other. Eight oriented cores were collected from the dacite of Boggs

Lake at locality db–1. Four additional cores were collected from locality db–2 at Boggs Lake because oriented hand samples from this locality indicated an unusual direction of magnetization for this unit (Hearn and others, 1976). Samples at db–1 were collected from the glassy top of this flow over a lateral distance of about 90 m, and its remanence direction was found to be reversed. The unusual direction at locality db–2 was confirmed and apparently results from tilting of the outcrop.

OLDER BOUNDARY OF THE JARAMILLO EVENT

The stratigraphic position of the andesite of Salmina Flat in the Mount Hannah area sequence clearly places this unit in the reversed-polarity interval immediately preceding the Jaramillo event. Although no reliable age has been obtained for this andesite because of large atmospheric argon contents (97 percent), it overlies the air-fall rhyolite tuff of Bonanza Springs, which is dated at 1.02 ± 0.04 m.y. A rhyolite flow within this tuff, at a depth of 595 m in a drill hole 3 km northwest of Mount Hannah, has reversed polarity (inclination, −56°), as do the andesite of Glenview (1.00 m.y.) and the dacite of Boggs Lake (0.98 m.y.). The reversed interval represented by these units, together with three normal-polarity lavas with ages of 0.96 m.y. reported from France (Cantagrel and Prévot, 1971) and from Lanzarote and Tenerife in the Canary Islands (Abdel-Monem and others, 1971, 1972), show that the Jaramillo event must have begun about 0.97 m.y. ago.

The andesite of Siegler Canyon, which has intermediate polarity, yielded an age of 0.97 ± 0.03 m.y., consistent with our suggestion that the Jaramillo event began about 0.97 m.y. ago. Previous dating of this unit yielded ages of 1.03 and 1.04 m.y. (Hearn and others, 1976; Donnelly, 1977), inconsistent with its magnetic polarity and its stratigraphic position overlying the rhyolite of Bonanza Springs (1.02 m.y.). While normal-polarity lavas with similar ages (1.03–1.07 m.y.) have been reported from Réunion Island (Chamalaun and McDougall, 1966; McDougall and Chamalaun, 1966), southern Argentina (Fleck and others, 1972), and the Canary Islands (Abdel-Monem and others, 1972), this particular andesite occasionally contains grains of cordierite, which could account for an anomalously old age because cordierite commonly contains excess argon (Damon and Kulp, 1958; Seidemann, 1976). Some of these older normal-polarity lavas from other localities may have formed during the Cobb Mountain normal-polarity event (Mankinen and others, 1978) rather than during the Jaramillo event.

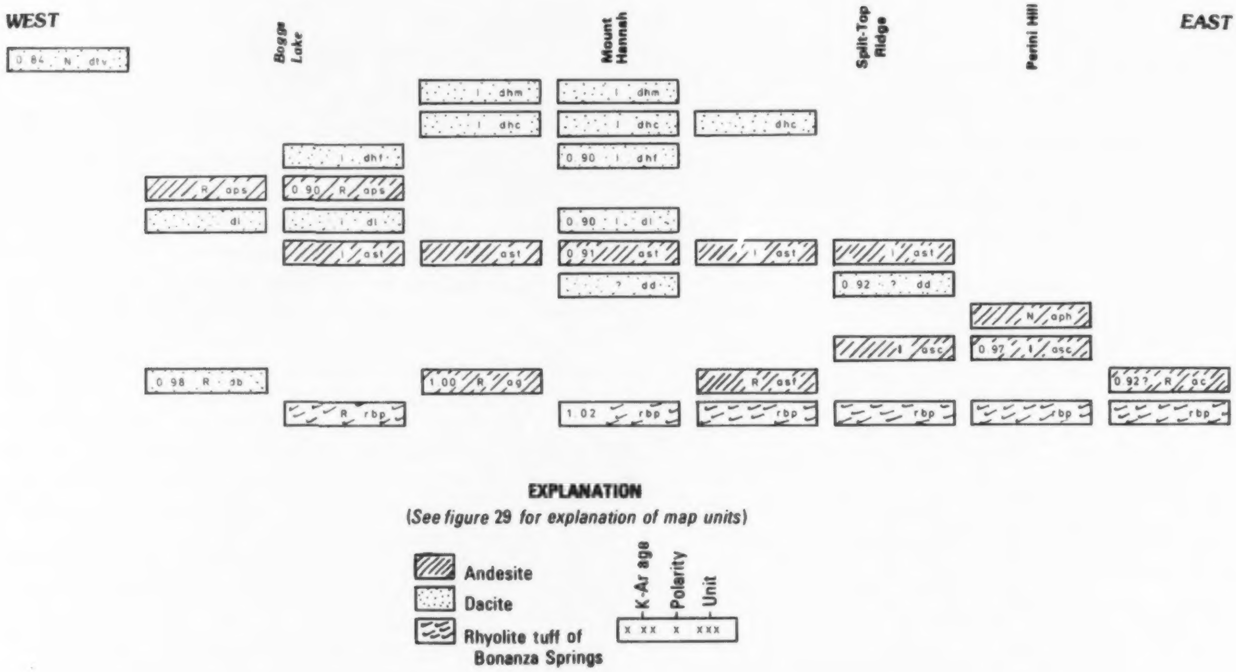
WEST
Boggs Lake
Mount Hannah
Split-Top Ridge
Perini Hill
EAST
0 84 N dlv
I dhm
I dhm
I dhc
I dhc
dhc
I dhf
0 90 I dhf
R aps
0 90 R aps
dl
I dl
0 90 I dl
I ast
ast
0 91 ast
I ast
I ast
? dd
0 92 ? dd
N aph
I asc
0 97 I asc
0 98 R db
1 00 R ag
R ast
0 92 ? R ac
R rbp
1 02 rbp
rbp
rbp
rbp
rbp
EXPLANATION
(See figure 29 for explanation of map units)
Andesite
Dacite
Rhyolite tuff of Bonanza Springs
K-Ar age
Polarity
Unit
x xx x xxx

FIGURE 30.—Stratigraphic relations, K-Ar ages, and magnetic polarity of units related to Jaramillo normal-polarity event. Each column indicates known stratigraphic relations from west to east across south-central part of Clear Lake volcanic field. Polarities: N, normal; R, reversed; I, intermediate; ?, uncertain.

The somewhat low VGP latitude (41° N.) determined for the andesite of Siegler Canyon may indicate that it was erupted during the polarity transition at the beginning of the Jaramillo event, and this interpretation is supported by the more northerly VGP position (58° N.) for the overlying andesite of Perini Hill. The andesite of Perini Hill has not been dated because it contains an abundance of metasedimentary rock inclusions.

YOUNGER LAVAS OF THE MOUNT HANNAH AREA

Potassium-argon ages from the younger andesites and dacites near Mount Hannah show that at least five flows were erupted about 0.91 m.y. ago. Most of these younger units have distinctive directions of remanent magnetization that are nearly horizontal toward the east and northeast (table 3 and fig. 32). The intermediate polarity of these units suggests that they were erupted during a geomagnetic-field excursion or during a polarity transition. In this case, the age of the lavas suggests that they record the polarity transition at the end of the Jaramillo normal-polarity event.

Andesite of Split-Top Ridge.—The andesite of Split-Top Ridge sampled near Boggs Lake (locality ast–1) was found to be very stable in direction during both AF and thermal demagnetization. Samples from Split-Top Ridge locality ast–2, approximately 3 km to the northeast, show considerable scatter in direction of natural remanent magnetization along with initial rapid decreases in intensity during AF demagnetization. These characteristics are typical of magnetic changes due to lightning strikes. Magnetic cleaning at 600 Oe produced a consistent grouping for five of the eight samples collected. After magnetic cleaning, the direction at locality ast–2 is about 30° to 40° different from the direction determined for locality ast–1. This result suggests that either some anomalous components were not completely removed from these samples or, because locality ast–2 is bounded by faults, that the difference in direction is due to tectonic rotation down to the west. However, the outcrop at locality ast–2 is very well exposed, and no evidence for this amount of rotation is apparent. Strong-field thermomagnetic curves show that whereas the magnetic mineral in

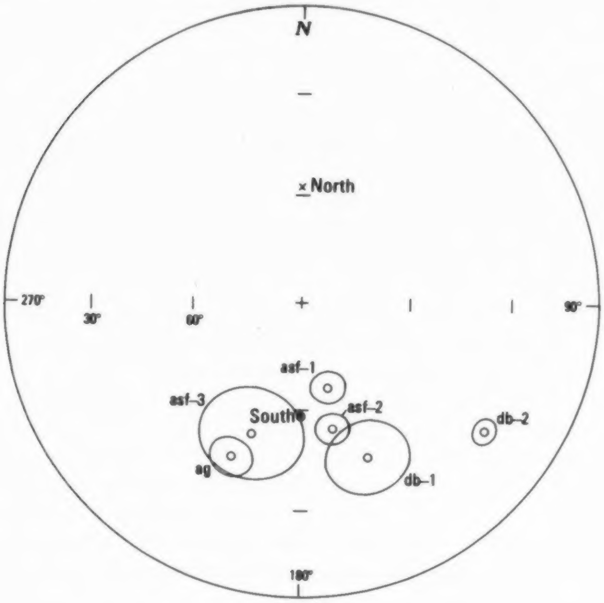

EXPLANATION

○ Direction on upper hemisphere of equal-area projection

× ● Axial dipole field direction

ag ⬭ 95-percent confidence limit about average direction—*Letters refer to sample localities in figure 29 table 3*

FIGURE 31.—Average remanent magnetization directions for older lavas of Mount Hannah area. Localities on figure 29.

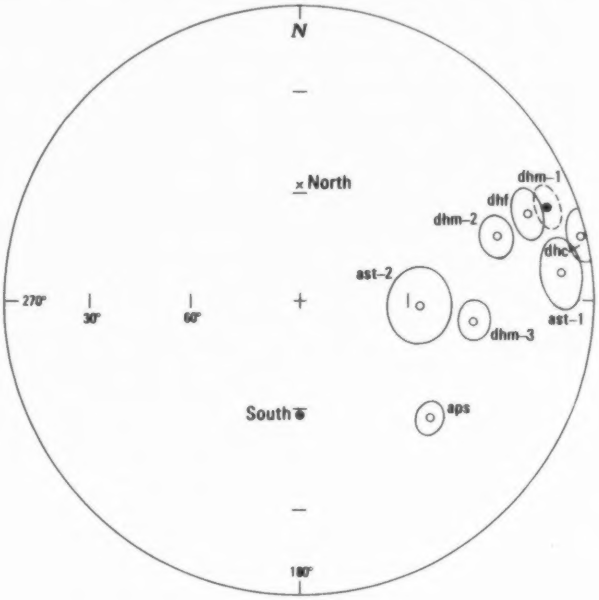

EXPLANATION

● Direction on lower hemisphere of equal-area projection

○ Direction on upper hemisphere of equal-area projection

× ● Axial dipole field direction

aps ⬭ 95-percent confidence limit about average direction—*Dashed where lower hemisphere. Letters refer to sample localities in figure 29 and table 3*

FIGURE 32.—Average remanent magnetization directions for younger lavas of Mount Hannah area. Localities on figure 29.

samples from locality ast–1 is either magnetite or Ti-poor titanomagnetite, the samples from locality ast–2 may contain a different magnetic phase. While the stratigraphic relations at both localities are unambiguous, the differences in magnetization direction together with the difference in magnetic mineralogy may also indicate that two separate andesitic lavas were erupted within a short period of time. Some differences in trace elements between the two localities are suggestive of two eruptions.

Dacites of Loch Lomond and Diener Drive.—The dacite of Loch Lomond and the dacite of Diener Drive, which respectively overlie and underlie the andesite of Split-Top Ridge, proved to be magnetically unstable. Directions of natural remanent magnetization of samples from the dacite of Loch Lomond were quite scattered, but AF demagnetization at 300 Oe did produce some consistency in direction. While the confidence limits about the mean direction for this unit are quite large, it is also of intermediate polarity and not very different from the underlying andesite of Split-Top Ridge. The dacite of Diener Drive was sampled at two outcrops near Loch Lomond, localities dd–1 and dd–2, and at a third outcrop on Split-Top Ridge, locality dd–3. All samples were weakly magnetized and completely unstable to AF demagnetization. Little consistency in direction within a particular outcrop was found, and none between the different outcrops, so the original remanence of this unit remains indeterminate. Why these units are such poor recorders of the Earth's field is not known. Strong-field thermomagnetic curves show that some samples in both dacites contain titanomaghemite and others may have a secondary component. One possibility is that, in these particular flows, the original titanomagnetite has been oxidized to such a high degree as to render it magnetically unstable. A lower magnetic stability together with the presence of a strong secondary component may have completely masked the primary remanence in the case of the dacite of Diener Drive.

Andesite of Poison Smith Spring and dacites of Harrington Flat and Mount Hannah.—Overlying the andesite of Split-Top Ridge and the dacite of Loch Lomond is the reversely magnetized andesite of Poison Smith Spring. Consistent directions were obtained from oriented cores taken from localities aps–1 and aps–2 within this unit and from oriented hand samples at locality aps–3. This andesite is directly overlain by the dacite of Harrington Flat, which records a return to an intermediate polarity (fig. 33).

The youngest units in this sequence are the coarse- and medium-grained dacites of Mount Hannah, which overlie the dacite of Harrington Flat. All outcrops of these units are also of intermediate polarity (dhm and dhc, table 3), and their directions are quite similar to that determined for the dacite of Harrington Flat. Small differences in direction between the localities sampled for these three units suggest that this part of Mount Hannah was built up by a number of small eruptions separated by short intervals of time. However, beginning with the dacite of Harrington Flat, eruptions may have occurred almost continuously and these units may have originally recorded the same field direction. This possibility must be considered because the distribution of sampling sites (around the summit of Mount Hannah) is such that continued uplift of the summit region after the units cooled below their Curie temperature could produce at least some of the differences in direction.

YOUNGER BOUNDARY OF THE JARAMILLO EVENT

Good replicate ages have been obtained from three of

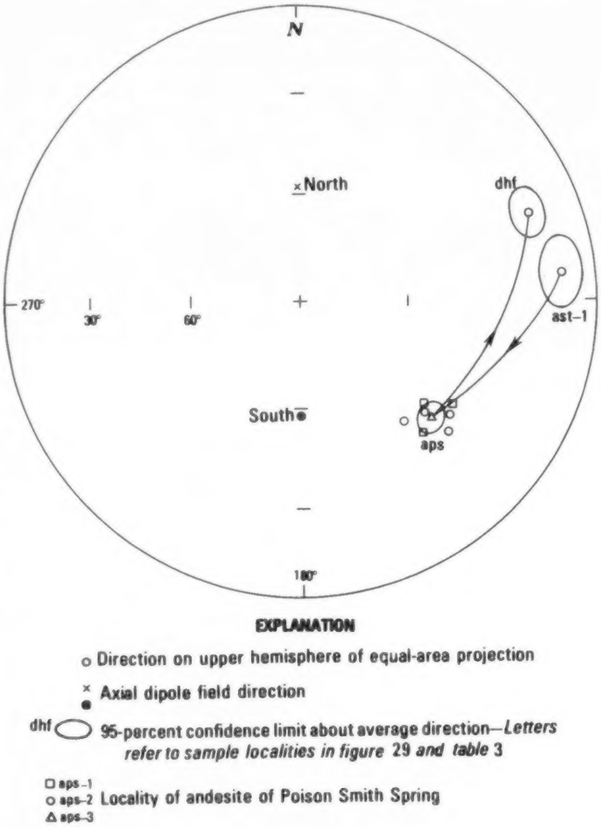

FIGURE 33.—Average remanent magnetization directions showing sequence of eruption (arrows) for andesite of Split-Top Ridge (ast), andesite of Poison Smith Spring (aps), and dacite of Harrington Flat (dhf). Localities on figure 29.

the dacites in the Mount Hannah sequence. The ages for the dacite of Diener Drive (0.92 ±0.02 m.y.), the dacite of Loch Lomond (0.90 ± 0.02 m.y.), and the dacite of Harrington Flat (0.90 ± 0.02 m.y.) are very similar and indistinguishable at the 95-percent confidence level. The andesite of Split-Top Ridge proved to be difficult to date; it is one of the andesites shown by Donnelly (1977) to be unusually retentive of argon during fusion in the argon extraction procedure. By using longer-than-standard fusion times, the apparent age of one sample increased from 0.81 m.y. to 0.88 m.y. and that of another from 0.83 m.y. to 0.86 m.y. However, this procedure has only partially solved the problem because the stratigraphic position of this andesite between two well-dated flows (the dacites of Diener Drive and Loch Lomond) shows that its age is 0.91 ± 0.04 m.y. The andesite of Poison Smith Spring has yielded ages ranging from 0.66 m.y. to 0.86 m.y., showing either that some argon loss has occurred or that not all of the radiogenic argon was released during extraction. The stratigraphic position of this unit, however, shows that its age is 0.90 ± 0.03 m.y. No reliable determinations have been obtained from either the medium- or coarse-grained dacites, which are the youngest units on Mount Hannah. Both dacites are typically devitrified, neither contains sanidine, and the plagioclase is usually altered. However, the paleomagnetic results strongly suggest that neither unit is likely to be significantly younger than the underlying dacite of Harrington Flat.

While reversely polarized rocks younger than the Jaramillo event have not been found in the Clear Lake Volcanics, eight such units with ages ranging from 0.81 to 0.90 m.y. have been reported from other localities (Mankinen and Dalrymple, 1979). These data, together with an intermediate direction reported for a unit from New Mexico of the same age as the Mount Hannah intermediate-direction units (Doell and Dalrymple, 1966; Doell and others, 1968), suggest that the Mount Hannah lavas were erupted during the transition from normal to reversed polarity at the end of the Jaramillo normal-polarity event. The sequence of intermediate-polarity lavas (andesite of Split-Top Ridge and dacite of Loch Lomond) followed by a reversed-polarity lava (andesite of Poison Smith Spring), which in turn is followed by more intermediate-polarity lavas (dacites of Harrington Flat and Mount Hannah), represents a brief polarity fluctuation associated with a true reversal boundary such as have been found for other polarity transitions (Watkins, 1969; Dunn and others, 1971). This type of geomagnetic field behavior has been recorded at both boundaries of the Jaramillo event in deep-sea sediment cores V21–156 (Opdyke and Foster, 1970) and RC14–14 (Opdyke and others, 1973). It has also been detected at the younger Jaramillo boundary in deep-sea sediment cores KH70–2–5, KH73–4–7, and KH73–4–8 (Kawai and others, 1973, 1977). The best estimate for the end of the Jaramillo event is 0.90 m.y.; this estimate is based on ages determined for the intermediate-polarity units from Clear Lake and New Mexico.

TIME SPANNED BY ERUPTIONS

The K-Ar ages and paleomagnetic directions reported here show that much of Mount Hannah was formed quite rapidly during a polarity transition. The actual time spanned by these eruptions is beyond the resolution of K-Ar dating, but an estimate can be made using information that is known about the time required for reversals of the Earth's field. Cox and Dalrymple (1967), using a probability model with the then-available polarity-radiometric data, estimated the average time of a polarity transition to be 4,600 years. After more data became available along with revisions to the polarity time scale, McElhinny (1973) obtained an estimate of 2,000 years, using the same model. From a study of deep-sea cores, Ninkovich, Opdyke, Heezen, and Foster (1966) estimated that reversals of direction occur within an interval of about 1,000 years. While there are many difficulties in the different methods of estimating transition times, these and other estimates that have been made are at least in general agreement and attest to the rapidity of the reversal process.

Particularly relevant to the Clear Lake Volcanics is the observation by Steinhauser and Vincenz (1973) that in 23 polarity transitions studied, very few VGP positions were located in low latitudes. Steinhauser and Vincenz (1973) suggest that some reversals are characterized by a rotation of the dipole axis and that the small number of equatorial VGP's could be due to accelerated motion of the dipole axis as it approached the equator. A similar conclusion was reached by Opdyke, Kent, and Lowrie (1973), who noted that the motion of the VGP through the equatorial latitudes apparently occurred during only a few hundred years. Finally, Watkins (1969) estimated that the polarity fluctuation near the end of the polarity transition recorded on Steens Mountain, Oregon, lasted less than 1,000 years and may have been as short as 150 years. Because only a small part of the polarity transition is recorded on Mount Hannah, and because most of the transitional VGP's are located in low latitudes, most of these lavas, beginning with the andesite of Split-Top Ridge (or possibly the dacite of Diener Drive) were probably erupted during an interval of not more than a few hundred years or possibly as short as a few tens of years.

CHILDERS PEAK AND TYLER VALLEY

AF demagnetization of samples from two separate, oriented hand specimens from the andesite of Childers Peak (locality ac) shows this flow to have a shallow magnetic inclination. However, Hearn, Donnelly, and Goff (1976) suggested that this flow might be tilted down to the south. Correcting for this rotation gives the flow a more typical reversed magnetization direction. The likelihood of tilting indicates that the flow is probably of reversed rather than intermediate polarity, although its age (0.92 ± 0.02 m.y.) seems somewhat inconsistent with a reversed polarity. The uncertainty in the age does not preclude the possibility that the flow was erupted just after the Jaramillo event, but the geologic evidence suggests that the andesite preceded the Jaramillo event. The andesite of Childers Peak overlies 35 m of the easily eroded 1.02-m.y.-old rhyolite tuff of Bonanza Springs. No similar thickness of tuff, so far from its vent area, underlies Jaramillo or younger lavas. It is likely that this is another andesite which did not yield all of its radiogenic argon, so 0.92 m.y. should be considered a minimum age.

The normally magnetized dacite of Tyler Valley, approximately 14 km southwest of Mount Hannah (locality dtv, table 3), is an intrusive body with a mean age of 0.84 ± 0.03 m.y.; this age is significantly younger than the Jaramillo event. This age is very close to the 0.85 ± 0.03 m.y. age determined for a normal-polarity lava from Japan (Hirooka and Kawai, 1967) and would tend to support the suggestion by Watkins (1968) that a brief polarity event occurred at about 0.83 m.y. Watkins' suggestion is based on the study of some marine sedimentary cores. However, additional evidence for this proposed event has not been found in the many deep-sea cores that have been studied with the possible exception of a single normal-polarity specimen between the Matuyama-Brunhes boundary and the Jaramillo event in sediment core RC11-171 (Opdyke and Foster, 1970). While the dacite of Tyler Valley yields an analytically good age on a mineral of proven reliability (sanidine), it is an isolated outcrop and no independent stratigraphic evidence confirms its age. For these reasons, the possibility of a brief polarity event at about this time must remain speculative.

COBB MOUNTAIN

The oldest units from which oriented cores were obtained are from Cobb Mountain near the southwest edge of the volcanic field and immediately adjacent to the Geysers geothermal area. Details of the paleomagnetic studies and K-Ar age determinations for these rocks have been published elsewhere (Mankinen and others, 1978). In summary, the oldest unit, the rhyolite of Alder Creek, has an intermediate direction of magnetization that is 80°–100° different from a reversed axial dipole field direction. The overlying dacite of Cobb Mountain is reversely magnetized. The third and youngest of the silicic units forming Cobb Mountain, the dacite of Cobb Valley, is also reversely magnetized but with a direction about 40° different from a reversed axial dipole. Potassium-argon age determinations show that all three units are significantly older than the Jaramillo event, and the intermediate direction of the rhyolite of Alder Creek is interpreted to represent the beginning of a brief normal-polarity event. The shallow reversed direction of the dacite of Cobb Valley probably represents a subsequent excursion. This new event, the Cobb Mountain normal-polarity event (Mankinen and others, 1978), probably lasted about 0.01 m.y. or less, and the best estimate of its age is 1.12 ± 0.02 m.y.

In addition to the localities already reported, oriented cores were also obtained from 10–15 m above the base of one of the large intact rhyolite masses exposed at locality ra–7 in the Ford Flat area. The Ford Flat area has been interpreted to be either a large landslide complex (Brice, 1953; Yates and Hilpert, 1946) or a series of fault blocks down-dropped along northeast-trending normal faults (Goff and McLaughlin, 1976). The magnetization direction determined for this block is shown in figure 34 along with the directions determined for localities ra–1 to ra–3 near the top of the same unit on Cobb Mountain and for localities ra–4 to ra–6 near its base. The close agreement in direction of all the localities clearly favors the fault-block interpretation of Goff and McLaughlin (1976) because the directions show no evidence of rotation, which would be expected if the blocks were emplaced by landsliding. Our results also show that this block must have originated from quite high in the rhyolite flow because its direction matches that of samples taken from near the top of the mountain. It should be emphasized that a minimum of 20°–30° of rotation about both vertical and horizontal axes would be required for an original lower-part direction to coincide with the upper-part direction, which would be extremely unlikely. Because this particular block contains only the upper part of the rhyolite flow, the vertical displacement could be as much as 500–600 m. Goff and McLaughlin (1976) estimated a minimum of 200–260 m of displacement for these blocks.

MISCELLANEOUS LAVAS

Several units that have not yet been discussed (fig. 29; table 3) have yielded reliable K-Ar ages, and their magnetic polarity and stability were verified by AF demagnetization experiments. These units are reported here because they are reliable for defining the polarity time scale. The andesite of Boggs Mountain sampled north of Whispering Pines (loc. abm) is 1.49 m.y. old; it erupted during an early episode of Clear Lake volcanism. Its reversed magnetic polarity places it near the middle of the Matuyama reversed-polarity epoch. The remainder of the units studied were found to have normal polarity and were erupted during the Brunhes normal-polarity epoch. After the eruption of the dacites of Mount Hannah and Tyler Valley, a gap in eruptive activity intervened until about 0.6 m.y. ago (Donnelly, 1977), when the dacite of Seigler Mountain (loc. ds), the voluminous rhyolite of Thurston Creek, and other dacites near the center of the volcanic field were erupted. Oriented hand samples from two sites in the rhyolite of Thurston Creek were collected north of Manning Flat (loc. r–1) and on Camelback Ridge (loc. r–2). Oriented cores were obtained by Allan Cox (unpub. data, 1962) from two of the dacite units forming Mount Konocti: the dacite of Horseshoe Bay (loc. dh), and the dacite of Soda Bay (loc. dsb). Oriented hand samples were obtained from the youngest rhyolite in the Clear Lake field, the rhyolite of Borax Lake (loc. rb).

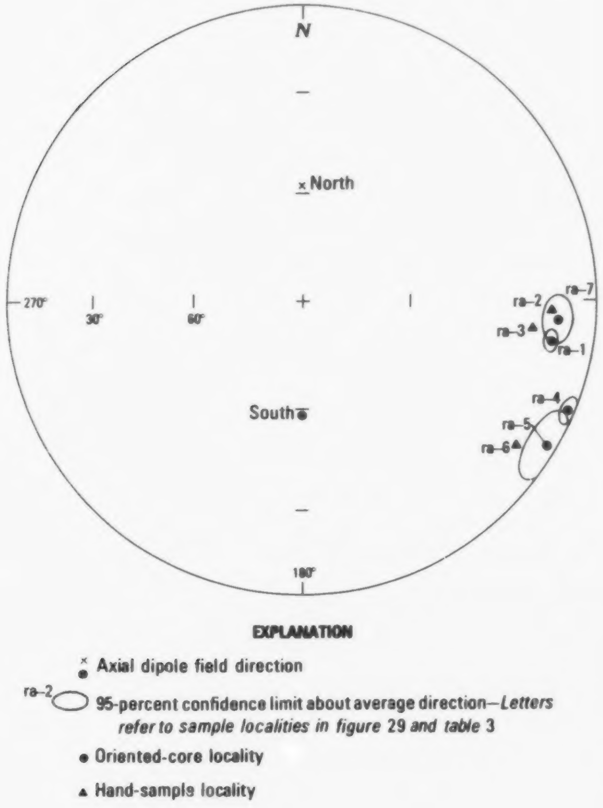

FIGURE 34.—Average remanent magnetization directions for localities sampled in rhyolite of Alder Creek (fig. 29). Directions on lower hemisphere of equal-area projection.

RELIABILITY OF MAGNETIC DIRECTIONS

Strong-field thermomagnetic measurements and thermal demagnetization were performed on samples from selected lavas of the Clear Lake area. Four types of strong-field thermomagnetic curves have been found, and these are shown in figure 35. Type 1 curves, such as aps–1 in figure 35, show a gradual decrease on magnetization during heating, becoming quite steep just before the Curie temperature is reached. Curie temperatures of type 1 curves range from 544° to 568°C (average 559°C) in the Clear Lake lavas. Heating and cooling curves are nearly identical when the experiments are performed in vacuum. This type of curve is typical of magnetite or Ti-poor titanomagnetite. Type 2 heating curves (dl, fig. 35) show a saddle or kink between 300° and 400°C, either a plateau or rise in magnetization at about 400°C, followed by a rapid decrease to a Curie temperature which is usually between 500° and 550°C. Heating and cooling curves differ; the magnetization upon cooling may be many times stronger than before heating. This type of behavior is characteristic of cation-deficient titanomagnetite (titanomaghemite); the cation deficiency results from low-temperature oxidation during weathering. The hump at 400°C occurs as the titanomaghemite spontaneously inverts into its various breakdown products, including magnetite. Type 3 heating curves (fig. 35) are similar in appearance to type 2 curves except that the saddle occurs above 400°C, the hump at 500°C, and the Curie temperature is commonly between 550° and 600°C. The type 3 cooling curve is either considerably below the heating curve (ast–2, fig. 35) or else the cooling curve crosses the heating curve at the saddle with the final magnetization only slightly stronger than before heating (dd–3, fig. 35). It is not certain whether the magnetic material producing type 3 curves is also a titanomaghemite but one which is more highly oxidized or had a lower initial Ti content than samples producing type 2 curves, or whether a second magnetic phase is present. The type 4 heating curve (db–1, fig. 35) was only found in one sample from the dacite of Boggs Lake at locality db–1. The magnetic material in this case has an original Curie temperature about 480°C and chemically alters during heating, resulting in nonidentical heating and cooling curves. Samples from locality db–1 are from the very glassy margin of this flow, and a sample from the crystallized part of the same flow at locality db–2 shows a typical type 1 thermomagnetic curve. The difference between the two localities may mean that the interior of the flow at locality db–2 cooled at a normal rate allowing high-temperature oxidation of titanomagnetite to occur, resulting in a Ti-poor titanomagnetite containing ilmenite lamellae. The glassy part of the flow sampled at db–1 may have cooled much too rapidly for this oxidation to occur, resulting in a titanomagnetite with a higher Ti content than at locality db–2 and, therefore, a lower Curie temperature.

Thermal demagnetizations of NRM in samples from the dacites of Boggs Lake (locality db–2), Harrington Flat, Mount Hannah (localities dhc and dhm–1), and the andesites of Poison Smith Spring (localities aps–1 and aps–2) and Split-Top Ridge (locality ast–1) all show similar results. The stable directions indicated by these measurements confirm the directions obtained by AF demagnetization. Samples from these localities give type 1 thermomagnetic curves and show a steady decrease in magnetization during thermal demagnetization, with temperatures above 500°C necessary to remove two-thirds of the original intensity. All samples have maximum blocking temperatures which are within a few degrees of their Curie temperatures determined from the strong-field thermomagnetic curves. After heating past their Curie temperatures, all samples accurately acquired the direction of a magnetic field applied during cooling. Both the thermal demagnetization and strong-field thermomagnetic measurements show that the magnetization of these units is carried by a single magnetic phase (magnetite or Ti-poor titanomagnetite), which rules out the possibility that the intermediate-polarity units could have directions that are mineralogically controlled.

Samples containing maghemite, those having type 2 thermomagnetic curves, were variable in behavior during both AF and thermal demagnetization. A sample from the dacite of Cobb Valley (dcv, fig. 35) showed thermal demagnetization behavior similar to samples having type 1 curves; heating to 525°C was necessary to remove two-thirds of the original magnetization. This sample was also very stable during AF demag-

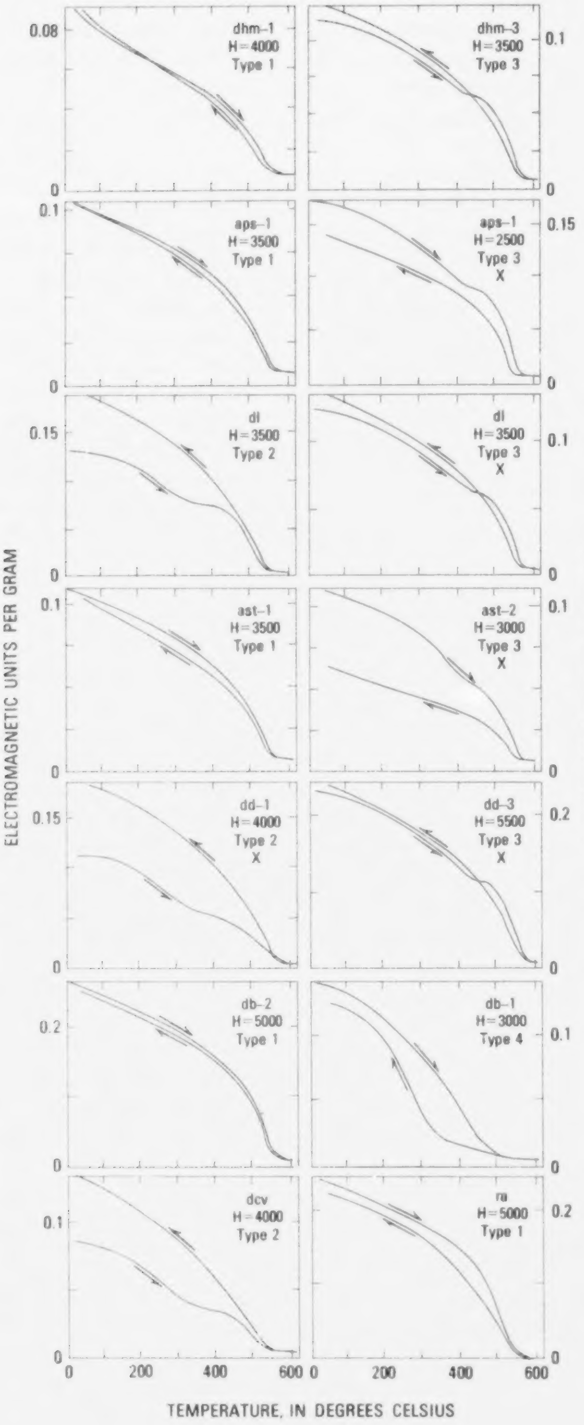

FIGURE 35.—Four types of strong-field thermomagnetic curves. Heating and cooling curves indicated by arrows. All runs in vacuum using applied fields, H (in Oe). X, denotes sample in which anomalous components of magnetization could not be removed. *A*, Variation of strong-field induced magnetization with temperature for samples from medium-grained dacite of Mount Hannah (dhm), andesite of Poison Smith Spring (aps), and dacite of Loch Lomond (dl). ***B***, Variation of strong-field induced magnetization with temperature for samples from the andesite of Split-Top Ridge (ast) and dacite of Diener Drive (dd). ***C***, Variation of strong-field induced magnetization with temperature for samples from the dacite of Boggs Lake (db), dacite of Cobb Valley (dcv), and rhyolite of Alder Creek (ra).

netization and had an MDF (median demagnetizing field) of 450 Oe. The type 2 sample from the dacite of Loch Lomond (dl, fig. 35), however, had a much more rapid loss of magnetization during heating with two-thirds of its original intensity removed by 300°C. Also, the MDF for this sample was only 90 Oe, and both experiments show that the magnetic stability of this flow is fairly low. Because the same direction is obtained by both demagnetization methods, that direction is probably the true remanence direction for the dacite of Loch Lomond as previously mentioned.

Some samples showing type 3 thermomagnetic curves proved to be difficult to interpret. Type 1 and type 3 samples from the medium-grained dacite of Mount Hannah (dhm–1 and –3, fig. 35) behaved the same with either thermal or AF demagnetization, and the results from all localities are quite good. The direction for the andesite of Poison Smith Spring (sample aps–1, fig. 35) is well defined by samples from three separate outcrops (fig. 33). The type 1 samples gave good results whereas the direction of the type 3 sample would approach only within 40° of the main group with either demagnetization method. For the dacite of Loch Lomond (dl, fig. 35), the type 2 sample gave a reliable direction, but the remanent magnetization in the type 3 sample only began to move toward the reliable mean direction with AF demagnetization and did not move with heating. Because of the variability in behavior of type 3 samples, the possibility that the primary remanence direction was not obtained for the andesite of Split-Top Ridge at locality ast–2 (fig. 35) must be considered. One specimen from this locality behaved similarly to the type 3 sample from the dacite of Loch Lomond, but others from the same locality produced a consistent grouping with both demagnetization methods. However, it is possible that this direction does contain a secondary component that was not completely removed, as was demonstrated for the type 3 sample from the andesite of Poison Smith Spring. Neither type 2 or type 3 samples of the dacite of Diener Drive (dd–1 and –3, fig. 35) gave results that appeared to be reliable. However, the type 2 samples (dd–1, fig. 35) may have another phase present as there appears to be an inflection in the heating curve at about 525°C as well as a higher Curie temperature of 580°C. The type 4 sample from the dacite of Boggs Lake (db–1, fig. 35) gave reliable results with both thermal and AF demagnetization.

Except for the dacite of Diener Drive and, possibly, locality ast–2 for the andesite of Split-Top Ridge, the reliability of the magnetization directions for the intermediate-polarity lavas of the Mount Hannah area has been demonstrated by AF and thermal stability measurements. No geologic evidence has been found to suggest that these lavas have been rotated extensively. Furthermore, it is very unlikely that all the units with intermediate directions could have been rotated in similar directions. A secondary magnetization acquired during a single episode when the Earth's field was of intermediate polarity is also ruled out. Such a remagnetization process would have to be extremely selective in order to bypass the andesite of Poison Smith Spring and the dacites of Cobb Mountain and Cobb Valley. All the geologic and paleomagnetic evidence, therefore, indicates that these units have accurately recorded the Earth's magnetic field that was present at the time the units cooled.

SUSCEPTIBILITIES AND Q RATIOS

Susceptibilities of samples from many units of the Clear Lake Volcanics have been measured and are grouped by rock type in table 4 and figure 36 along with NRM (natural remanent magnetization) intensities and Koenigsberger (Q) ratios. Most of the samples measured were collected during the course of the present study or were obtained from oriented hand samples collected for laboratory stability measurement (Hearn and others, 1976). Data for the basalts were obtained from samples collected by Allan Cox (unpub. data, 1962), from Mankinen (1972), and from measurements made by W. F. Isherwood (written commun., 1977), which were included in the averages reported by Isherwood (1976).

Similar mean values of susceptibility were found for most rocks, with the exception of a somewhat lower value for the andesites. However, individual andesite

TABLE 4.—*Magnetic properties of Clear Lake volcanic rocks*

[N, number of samples; J, geometric mean NRM intensity ($\times 10^{-4}$ emu cm^{-3}); K, geometric mean susceptibility ($\times 10^{-4}$); Q, geometric mean on site of remanent to induced magnetization (Koenigsberger ratio)]

Rock type	N	J	Range of s.d. of J	K	Range of s.d. of K	Q	Range of s.d of Q
Intermediate-direction dacite and rhyolite	64	2.79	5.84–1.33	1.99	3.96–0.99	2.8	5.6–1.4
Normal dacite and rhyolite	50	9.67	25.6–3.66	1.66	2.93–0.94	11.2	21.8–1.8
All dacite and rhyolite	114	—	—	1.84	3.50–0.96	—	
Basalt[1]	50	13.2	57.3–3.04	2.27	5.74–0.90	11.2	38.3–3.3
Andesite	54	3.69	9.98–1.36	.96	2.11–0.44	7.4	18.0–3.0
Basalt and andesite	104	6.81	27.5–1.69	1.46	3.78–0.56	9.0	26.6–3.1

[1] Includes measurements by W. F. Isherwood (written commun., 1977).

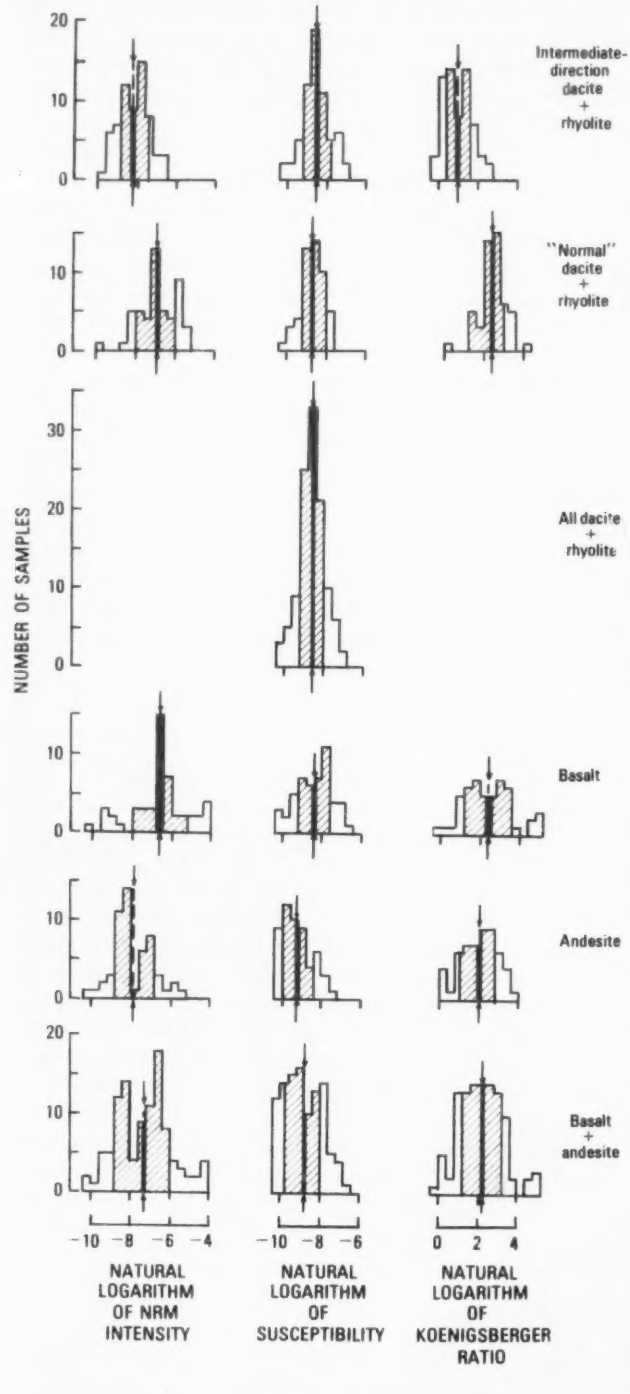

FIGURE 36.—Histograms showing NRM intensity, susceptibility, and Koenigsberger ratio for rock types of Clear Lake Volcanics. Arrow, geometric mean; ruled area, range of standard deviation; solid area, range of standard error of mean.

and basalt flows can be quite variable, so this difference may be more apparent than real. It may also be that more samples are necessary to obtain an accurate average for this group because the measurements available do not approximate a log-normal distribution (fig. 36). If basalt and andesite are considered together, the range of one standard deviation about the mean of this group completely encloses the range for rhyolite and dacite, although the susceptibilities of the latter group are concentrated over a much narrower range. Differences in the standard error range of the rhyolite-dacite (1.95 to 1.73 × 10^{-4}) and basalt-andesite (1.60 to 1.33 × 10^{-4}) groups may indicate that there is a small, but real, susceptibility difference between the two groups.

The Koenigsberger ratios (Q) are also very similar for all rock types, but Q values are distinctly low for the intermediate-polarity dacites and rhyolites of Mount Hannah and Cobb Mountain. Because the susceptibilities of all rhyolites and dacites were the same, these lower Q values are entirely due to the lower NRM intensities of these samples. Analysis of local magnetic highs and lows in the aeromagnetic survey of the Clear Lake area led Isherwood (1976) to suggest that Mount Hannah might be weakly magnetized or have mixed polarity. The large volume of rock having a low intensity of magnetization and an intermediate polarity could account for the lack of a magnetic anomaly directly associated with Mount Hannah. The rhyolite of Alder Creek on Cobb Mountain is also of intermediate polarity and weakly magnetized, but, in this case, the mountain is capped by strongly magnetic reversed-polarity rocks and may be reversely magnetized at depth. Cobb Mountain therefore appears to be reversely magnetized on the aeromagnetic map (Isherwood, 1976). The weaker original magnetization of the intermediate-polarity lavas is probably due to eruption of the rocks during polarity transitions when the strength of the earth's main dipole field was greatly diminished.

DISCUSSION

Paleomagnetic studies and potassium-argon age determinations in the Clear Lake Volcanics have resulted in well-defined limits for the boundaries of the Jaramillo normal-polarity event (this paper) and have established the existence of a brief polarity event 1.12 m.y. ago (Mankinen and others, 1978). The paleomagnetic and K-Ar results reported here along with previously published data have shown that the Jaramillo event lasted from 0.97–0.90 m.y. ago (fig. 37). This duration is in very good agreement with es-

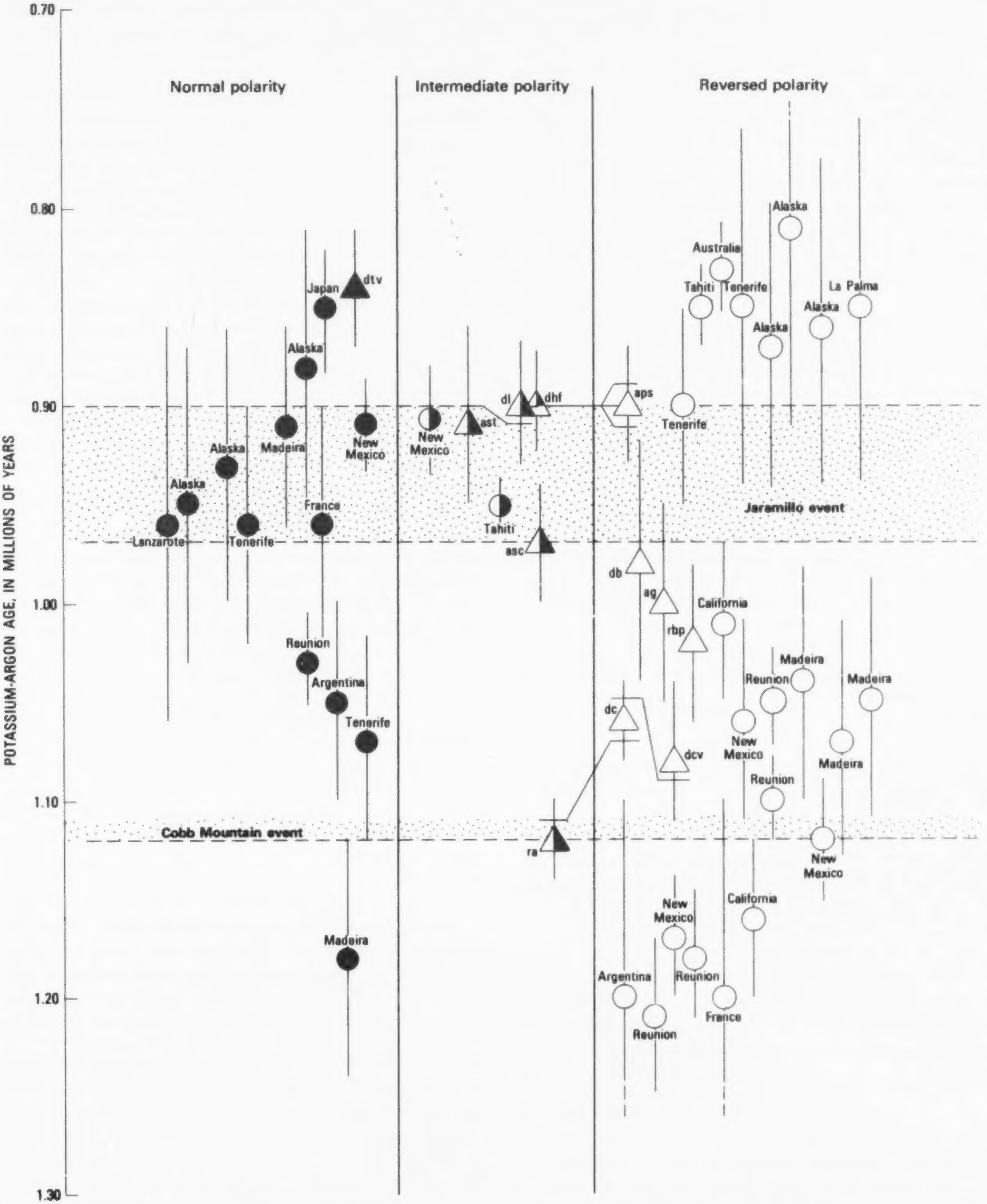

FIGURE 37.—Polarity and K-Ar ages of Clear Lake Volcanics (triangles) and data (circles) compiled by Mankinen and Dalrymple (1979) for the period between 0.8 to 1.2 m.y. ago. Open symbols, reversed polarity; mixed symbols, intermediate polarity; closed symbols, normal polarity. Vertical bars, estimated precision of K-Ar ages; horizontal bars, superposition of Clear Lake lavas. Stippled pattern, Cobb Mountain and Jaramillo normal-polarity events. Letters refer to map units (see fig. 29).

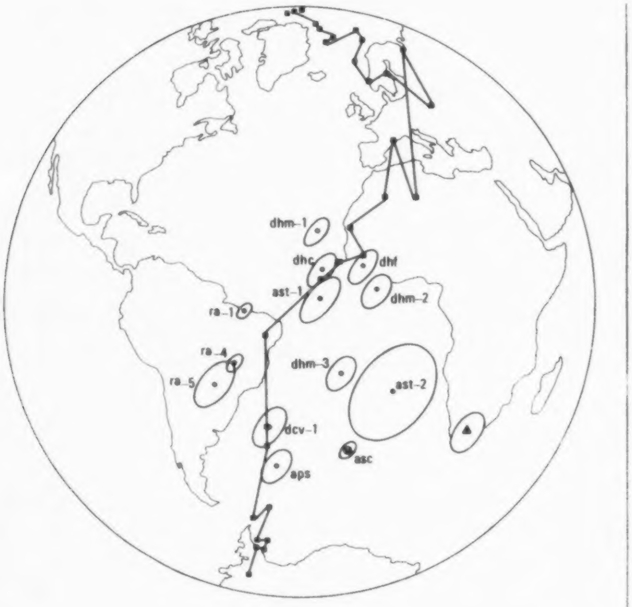

EXPLANATION

- ra-5● VGP position for transitional lavas from Clear Lake—*Letter symbols refer to map units in figure* 29 *and table* 3
- aps◯ 95-percent confidence limit about average direction
- ● Virtual south pole
- ▲ Upper Jaramillo VGP from New Mexico (Doell and others, 1968)
- •—• Brunhes-Matuyama polarity transition from Lake Tecopa, Calif. (Hillhouse and Cox, 1976)

FIGURE 38.—VGP positions for transitional lavas from Clear Lake and Brunhes-Matuyama polarity transition from Lake Tecopa, Calif.

timates obtained from deep-sea sedimentary cores (Opdyke, 1969) and midoceanic magnetic anomalies (Cox, 1969; LaBrecque and others, 1977).

Another interesting result from both of these studies is that many of the units sampled had intermediate directions of magnetization, all apparently erupted during polarity transitions. This by itself is not unreasonable given the episodic nature of volcanic eruptions and the high frequency of eruption during particular episodes. These intermediate-polarity units were all formed during an active period of volcanism at Clear Lake from 1.1 m.y.–0.8 m.y. ago when approximately 11 km^3 of lava was erupted (Donnelly, 1977). Perhaps more surprising is the fact that most of the VGP positions calculated for these intermediate-polarity lavas (as well as for those with shallow reversed directions) are very similar and fall between longitudes 300°–360°, and are similar to those obtained by Hillhouse and Cox (1976) for the Matuyama-Brunhes polarity transition recorded in sediments from Lake Tecopa, Calif. (fig. 38). It should be emphasized that all intermediate and shallow VGP positions within the Clear Lake Volcanics fall in this fairly narrow longitudinal sector except for the andesite of Childers Peak, which has probably been rotated and the andesite of Seigler Canyon, which was probably erupted at the beginning of the Jaramillo event. It can be seen that the virtual *south* pole position for the andesite of Seigler Canyon falls into the same longitudes as the other intermediate and low latitude VGP's shown in figure 10. Opdyke, Kent, and Lowrie (1973) show that the VGP paths for the upper and lower boundaries of the Jaramillo event are, indeed, nearly 180° apart.

This remarkable coincidence of intermediate VGP positions for at least three different polarity transitions might seem to support the various models which indicate that the transitional magnetic field is dipolar in nature. However, if the transitional field was dipolar, pole paths for different sites around the world recording the same transition should coincide. Hillhouse and Cox (1976) have shown that the transitional path for the Matuyama-Brunhes boundary as recorded in sediments from Lake Tecopa and from the Boso Peninsula in central Japan (Niitsuma, 1971) are completely different and, therefore, the ambient field could not have been dipolar during this transition.

Recently, Hoffman (1977) noted that transitional VGP paths are strongly dependent on site location—they are often centered about the meridian passing through the site or its antipode. This behavior is very apparent in the records of 15 Miocene and younger transitions from various sites in the northern hemisphere. Hoffman and Fuller (1978) show that the data from these transitions not only are nonrandomly distributed, but they are most often in the hemisphere centered about the site meridian. The data from Clear Lake are similar to these, showing VGP directions between 60° and 120° from the site longitude. Both octupole (Hoffman, 1977) and quadrupole (Dodson and others, 1978) models of the transitional field have been proposed to explain this type of behavior. In these axisymmetric models, the transitional field is a consequence of the reversal process beginning preferentially either in one hemisphere (quadrupole) or in different latitudes (octupole) within the core and then spreading to the remaining regions. Both models predict VGP paths that follow meridians through the sampling locality or through a point antipodal to the site. However, this condition is rarely met, and both models must invoke the presence of some nonaxisymmetrical field components, as those authors have pointed out. The model currently being developed by Hoffman (1978) has a reversal propagating both azimuthally and latitudinally from a localized region in the core;

this model may provide some of these required nonaxisymmetric components.

Many of the published studies on both sedimentary and igneous rocks have reported very low intensities of magnetization during a transition; thus, these studies suggest that the Earth's field does, in fact, decay during a polarity reversal. As Opdyke, Kent, and Lowrie (1973) noted, the large looping VGP excursions that are prominent in some records rarely extend into equatorial latitudes; this fact shows that the nondipole field must at some point also decay or be stationary. If both the dipole and drifting nondipole fields decay during a polarity reversal, the restriction of low-latitude VGP's to narrow sectors of longitude, as shown in figure 38 over successive transitions, suggests that some of the observed transitional VGP paths may be controlled by some long-lived geomagnetic feature that is regional in extent. If this is the case, such a feature must be able to influence transitional VGP's from the western United States over a distance of at least 650 km between Clear Lake and Lake Tecopa. The VGP from the younger Jaramillo boundary in New Mexico (Doell and others, 1968) does not coincide with the Clear Lake VGP positions, but the difference may or may not be significant. VGP paths and transitional poles determined for Miocene volcanic rocks from Oregon and Nevada (Heinrichs, 1967; Watkins, 1969; Larson and others, 1971) are also different from the Clear Lake and Lake Tecopa VGP's, but age differences as well as distance are both much greater.

An indication of what such a regional feature might be comes from the work of Yukutake and Tachinaka (1969). They refined the original analysis of Bullard, Freedman, Gellman, and Nixon (1950) and found that the historic geomagnetic record allows the nondipole field to be divided into two parts, a drifting part describable by a few low-order spherical harmonics, and a standing (or very slowly varying) part that has a more complicated description. Yukutake and Tachinaka further concluded that the drifting and standing nondipole fields do not interact with each other, hence they may have separate origins within the fluid core of the Earth. To make use of this analysis of the historic field, we may suppose that during a reversal the drifting part of the nondipole field decays and grows with the dipole field, and that the standing part of the nondipole field does not decay but persists in strength and configuration over times spanning several reversals. In interpreting the Matuyama-Brunhes transition at Lake Tecopa, Hillhouse and Cox (1976) used this hypothesis and concluded that it is a useful model but that the standing nondipole field was different for different reversals. The present evidence seems to indicate that the standing field persists for somewhat longer times.

Data from Clear Lake and Lake Tecopa show that similar transitional directions can recur over a period of 0.4 m.y., but it is difficult to determine if the cause of these similar directions persisted over a much longer period of time. Three shallow VGP positions were reported from the Sonoma Volcanics immediately south of the Clear Lake field (Mankinen, 1972). Unit S25 of early Gauss age has a virtual *south* pole position at 33° S., 314° E. and the VGP for unit S15 of late Gilbert age is located at 47° S., 321° E.; both directions are very close to those reported here. However, the 12-m.y.-old andesite flow, S1, has a very different VGP position at 27° S., 97° E. These data suggest that the features controlling transitional directions in western North America could have persisted over a period of about 4 m.y. but appear to have lasted for less than 11 m.y. Dodson and others (1978) showed that the VGP paths for the 17-m.y.-old Tatoosh (northwestern Washington) and 8-m.y.-old Laurel Hill (western Oregon) intrusions remained remarkably similar for a period of about 10 m.y. Similar VGP paths seen for the 15-m.y. Steens Mountain (southeastern Oregon) and Santa Rosa Range (northern Nevada) transition show the areal extent of that earlier nondipole feature.

Thus, although the exact nature of the Earth's geomagnetic field during polarity transitions is still poorly understood, further studies should take into account the possibility of persistent nondipole features originating in the fluid core and controlling VGP paths on a regional scale for times on the order of 10^6 years.

REFERENCES CITED

Abdel-Monem, A. A., Watkins, N. D., and Gast, P. W., 1971, Potassium-argon ages, volcanic stratigraphy, and geomagnetic history of the Canary Islands—Lanzarote, Fuerteventura, Gran Canaria, and La Gomera: American Journal of Science, v. 271, p. 490–521.

——— 1972, Potassium-argon ages, volcanic stratigraphy, and geomagnetic history of the Canary Islands—Tenerife, La Palma, and Hierro: American Journal of Science, v. 272, p. 805–825.

Beckinsale, R. D., and Gale, N. H., 1969, A reappraisal of the decay constants and branching ratio of ^{40}K: Earth and Planetary Science Letters, v. 6, p. 289–294.

Berry, A. L., Dalrymple, G. B., Lanphere, M. A., and Von Essen, J. C., 1976, Summary of miscellaneous potassium-argon age measurements, U.S. Geological Survey, Menlo Park, California, for the years 1972–74: U.S. Geological Survey Circular 727, 13 p.

Brice, J. C., 1953, Geology of the Lower Lake quadrangle, California: California Division of Mines and Geology Bulletin 16, 72 p.

Bullard, E. C., Freedman, C., Gellman, H., and Nixon, J., 1950, The westward drift of the earth's magnetic field: Philosophical Transactions of the Royal Society of London, Series A, v. 243, p. 67–92.

Cantagrel, J. M., and Prevot, Michel, 1971, Paleomagnetisme et age potassium-argon des basaltes du Deves aux environs de Saint-Arcons-d'Allier (Massif Central, France): Comptes Rendus Hebdomadaires des Seances de l'Academie des Sciences, Paris, v. 273B, p. 261–264.

Chamalaun, F. H., and McDougall, Ian, 1966, Dating geomagnetic polarity epochs in Reunion: Nature, v. 210, p. 1212–1214.

Cox, Allan, 1969, Geomagnetic reversals: Science, v. 163, p. 237–245.

Cox, Allan, and Dalrymple, G. B., 1967, Statistical analysis of geomagnetic reversal data and the precision of potassium-argon dating: Journal of Geophysical Research, v. 72, p. 2603–2614.

Cox, Allan, Hopkins, D. M., and Dalrymple, G. B., 1966, Geomagnetic polarity epochs—Pribilof Islands, Alaska: Geological Society of America Bulletin, v. 77, p. 883–910.

Damon, P. E., and Kulp, J. L., 1958, Excess helium and argon in beryl and other minerals: American Mineralogist, v. 43, p. 433–459.

Dodson, R. E., Dunn, J. R., Fuller, M. D., Williams, I., Ito, Haruaki, Schmidt, V. A., and Wu, Y. M., 1978, Paleomagnetic record of a late Tertiary field reversal: Geophysical Journal of the Royal Astronomical Society, v. 53, p. 373–412.

Doell, R. R., and Dalrymple, G. B., 1966, Geomagnetic polarity epochs—A new polarity event and the age of the Brunhes-Matuyama boundary: Science, v. 152, p. 1060–1061.

Doell, R. R., Dalrymple, G. B., Smith, R. L., and Bailey, R. A., 1968, Paleomagnetism, potassium-argon ages, and geology of rhyolites and associated rocks of the Valles Caldera, New Mexico: Geological Society of America Memoir 116, p. 211–248.

Donnelly, J. M., 1977, Geochronology and evolution of the Clear Lake volcanic field: Berkeley, University of California, Ph. D. thesis, 48 p.

Dunn, J. R., Fuller, M. D., Ito, Haruaki, and Schmidt, V. A., 1971, Paleomagnetic study of a reversal of the earth's magnetic field: Science, v. 172, p. 840–845.

Fisher, R. A., 1953, Dispersion on a sphere: Proceedings of the Royal Society [London], ser. A, v. 217, p. 295–305.

Fleck, R. J., Mercer, J. H., Nairn, A. E. M., and Peterson, D. N., 1972, Chronology of late Pliocene and early Pleistocene glacial and magnetic events in southern Argentina: Earth and Planetary Science Letters, v. 16, p. 15–22.

Garner, E. L., Murphy, T. J., Gramlich, J. W., Paulsen, P. J., and Barnes, I. L., 1975, Absolute isotopic abundance ratios and the atomic weight of a reference sample of potassium: Journal of Research National Bureau of Standards, v. 79A, p. 713–725.

Goff, F. E., and McLaughlin, R. J., 1976, Geology of the Cobb Mountain-Ford Flat geothermal area, Lake County, California: U.S. Geological Survey Open-File Report 76–221, scale 1:24,000, 1 sheet.

Hearn, B. C., Jr., Donnelly, J. M., and Goff, F. E., 1976, Preliminary geologic map and cross-section of the Clear Lake volcanic field, Lake County, California: U.S. Geological Survey Open-File Report 76–751, scale 1:24,000, 3 sheets.

Heinrichs, D. F., 1967, Paleomagnetism of the Plio-Pleistocene Lousetown Formation, Virginia City, Nevada: Journal of Geophysical Research, v. 72, p. 3277–3294.

Hillhouse, J. W., and Cox, Allan, 1976, Brunhes-Matuyama polarity transition: Earth and Planetary Science Letters, v. 29, p. 51–64.

Hirooka, Kimio, and Kawai, Naoto, 1967, Results of age determinations of some late Cenozoic rocks in southwestern Japan: Annual Progress Report Paleogeophysics Research Japan, Osaka, p. 69–73.

Hoffman, K. A., 1977, Polarity transition records and the geomagnetic dynamo: Science, v. 196, p. 1329–1332.

——— 1978, A model of the reversal dynamo: Transactions of the American Geophysical Union, v. 59, p. 1055.

Hoffman, K. A., and Fuller, M. D., 1978, Transitional field configurations and geomagnetic reversal: Nature, v. 273, p. 715–718.

Isherwood, W. F., 1976, Gravity and magnetic studies of The Geysers-Clear Lake geothermal region, California: Second United Nations Symposium on the Development and Use of Geothermal Resources, San Francisco, 1975, Proceedings, v. 2, p. 1064–1073.

Kawai, Naoto, Nakajima, Tadashi, Hirooka, Kimio, and Kobayashi, Kunio, 1973, The transition of field at the Brunhes and Jaramillo boundaries in the Matuyama geomagnetic epoch: Proceedings of the Japan Academy, v. 49, p. 820–824.

Kawai, Naoto, Sato, Takahiro, Sueishi, T., and Kobayashi, Kunio, 1977, Paleomagnetic study of deep-sea sediments from the Melanesia Basin: Journal of Geomagnetism and Geoelectricity, v. 29, p. 211–223.

LaBrecque, J. L., Kent, D. V., and Cande, S. C., 1977, Revised magnetic polarity time scale for Late Cretaceous and Cenozoic time: Geology, v. 5, p. 330–335.

Larson, E. E., Watson, D. E., and Jennings, William, 1971, Regional comparison of a Miocene geomagnetic transition in Oregon and Nevada: Earth and Planetary Science Letters, v. 11, p. 391–400.

Mankinen, E. A., 1972, Paleomagnetism and potassium-argon ages of the Sonoma Volcanics, California: Geological Society of America Bulletin, v. 83, p. 2063–2072.

Mankinen, E. A., and Dalrymple, G. B., 1979, Revised geomagnetic polarity time scale for the interval 0 to 5 m.y. B.P.: Journal of Geophysical Research, v. 84, p. 615–626.

Mankinen, E. E., Donnelly, J. M., and Grommé, C. S., 1978, Geomagnetic polarity event recorded at 1.1 m.y. B.P. on Cobb Mountain, Clear Lake volcanic field, California: Geology, v. 6, p. 653–656.

McDougall, Ian, and Chamalaun, F. H., 1966, Geomagnetic polarity scale of time: Nature, v. 212, p. 1415–1418.

McElhinny, M. W., 1973, Paleomagnetism and plate tectonics: Cambridge, Cambridge University Press, 358 p.

Niitsuma, Nobuaki, 1971, Detailed study of sediments recording the Matuyama-Brunhes geomagnetic reversal: Tohoku University Science Reports (Geology), v. 43, p. 1–39.

Ninkovich, Dragoslav, Opdyke, N. D., Heezen, B. C., and Foster, J. H., 1966, Paleomagnetic stratigraphy, rates of deposition and tephrachronology in north Pacific deep-sea sediments: Earth and Planetary Science Letters, v. 1, p. 476–492.

Opdyke, N. D., 1969, The Jaramillo event as detected in oceanic cores: *in* Runcorn, S. K., ed., The application of modern physics to earth and planetary interiors: New York, John Wiley, p. 549–552.

Opdyke, N. D., and Foster, J. H., 1970, Paleomagnetism of cores from the north Pacific: Geological Society of America Memoir 126, p. 83–119.

Opdyke, N. D., Kent, D. V., and Lowrie, William, 1973, Details of magnetic polarity transitions recorded in a high deposition rate deep-sea core: Earth and Planetary Science Letters, v. 20, p. 315–324.

Seidemann, D. E., 1976, An ^{40}Ar/^{39}Ar age spectrum for a cordierite-bearing rock—Isolating the effects of excess radiogenic ^{40}Ar: Earth and Planetary Science Letters, v. 33, p. 268–272.

Steiger, R. H., and Jäger, Emilie, 1977, Subcommission on geochronology: Convention on the use of decay constants in geo- and cosmochronology: Earth and Planetary Science Letters, v. 36, p. 359–362.

Steinhauser, Peter, and Vincenz, S. A., 1973, Equatorial paleopoles and behavior of the dipole field during polarity transitions: Earth and Planetary Science Letters, v. 19, p. 113–119.

Watkins, N. D., 1968, Short period geomagnetic polarity events in deep-sea sedimentary cores: Earth and Planetary Science Letters, v. 4, p. 341–349.

——— 1969, Non-dipole behavior during an Upper Miocene geomagnetic polarity transition in Oregon: Geophysical Journal of the Royal Astronomical Society, v. 17, p. 121–149.

Yates, R. G., and Hilpert, L. S., 1946, Quicksilver deposits of the eastern Mayacmas district, Lake and Napa Counties, California: California Division of Mines Report 42, p. 231–286.

Yukutake, Takesi, and Tachinaka, H., 1969, Separation of the earth's magnetic field into the drifting and the standing parts: University of Tokyo, Bulletin of the Earthquake Research Institute, v. 47, p. 65–97.

GEOPHYSICAL OVERVIEW OF THE GEYSERS

By William F. Isherwood

ABSTRACT

Geophysical evidence in and near The Geysers can support inferences about (1) the heat source, (2) the reservoir structure, (3) geologic structure not related to the geothermal reservoir, and (4) current changes taking place in the region. Gravity studies provided the first geophysical indication of a magma chamber in the middle crust beneath the Clear Lake Volcanics. Subsequent results of interpretation of magnetic data, teleseismic *P*-wave delay data, and heat-flow data appear to substantiate this model of the geothermal heat source.

Without accurate knowledge of the physical properties of the reservoir, correlation of geophysical anomalies with the limits of potential geothermal production is largly empirical, based on the downhole information available. The Geysers steam zone appears to correlate with a residual gravity low and possibly with an anomaly of pseudogravity derived from aeromagnetic data. If there is a productive hot-water zone, it may be delineated by an electrical resistivity low and shallow temperature gradients.

Geophysical data can help in estimating the thickness of surface volcanic rocks, the location of feeder vent areas, the location of the Great Valley sequence beneath the volcanic field, and the size of the ultramafic body along the Collayomi fault zone.

Temporal changes include subsidence and horizontal movements, reservoir depletion, and associated changes in the stress field. These can be monitored by accurate geodetic measurements and by microearthquake activity. Changes are related to both regional tectonics and fluid withdrawal. Decreasing gravity detected between 1974 and 1977 probably results from the lack of recharge to the reservoir. Interpretation suggests that the dominant mechanism of depletion involves flashing of liquid water in the reservoir in response to production.

INTRODUCTION

The coincidence of active hydrothermal alteration, steam at shallow depths, and Quaternary volcanic rocks led many early geologists to speculate on the presence of an underlying magma body as the source of heat for the Geysers geothermal system. Rodger Chapman (1966) first gave this idea geophysical credence by publishing a gravity map showing a major negative Bouguer anomaly centered near Mount Hannah and suggesting that the anomaly could be due to low-density molten rock. Subsequent research includes analyses of more refined gravity data, aeromagnetic and ground magnetic surveys, heat-flow measurements, microearthquake surveys, studies of teleseismic P-wave delays and local seismic reflection and refraction, determining electrical resistivities by a variety of methods, and miscellaneous investigations by remote sensing. Each of these techniques contributes to our present ideas about the heat source and its relation to the structure of the region.

Most geophysical studies at The Geysers have concentrated on determining the nature of the heat source, its location, and its size. Gravity studies, the first geophysical indicator to help answer these questions, remain a major source of information.

GRAVITY AND MAGNETICS

A recent map of residual gravity (fig. 39) shows the salient features of the gravity field (discussed in considerable detail by Chapman, 1975, and Isherwood, 1975). The major feature of the field is a nearly circular gravity low divided into two parts. The deepest part—referred to as the Mount Hannah low—lies northeast of the producing steam field and appears to coincide with the volcanic edifice of Mount Hannah. The other minimum—called the production low—coincides with the producing steam field. Part of the overall gravity low must be the result of shallow density contrasts related to the thickness of near-surface volcanic rocks and the reservoir structure, but the major low probably reflects the low-density upper silicic differentiate of a magma chamber centered between about 6 and 14 km depth (Isherwood, 1976). (The term "magma chamber" is used here to suggest an intruded igneous body including a considerable volume of partial melt.)

Magnetic anomalies are difficult to interpret in regions with highly magnetic surface rocks such as volcanic flows and serpentinite. The most obvious topographic and other near-surface effects can be subdued, however, by the filtering provided by analytic upward continuation of the digitalized magnetic field. The 3-km continuation illustrated in figure 2 shows a major magnetic high along the Collayomi fault zone. The high indicates that the serpentinite seen at the surface along the zone may extend to a depth of several kilometers.

Poisson's relation between the gravitational and magnetic fields due to an arbitrary homogeneous mass distribution can be used to calculate what has been termed a pseudogravity map from aeromagnetic data. Cordell and Taylor (1971) described the use of pseudogravity maps for combined analysis of gravity

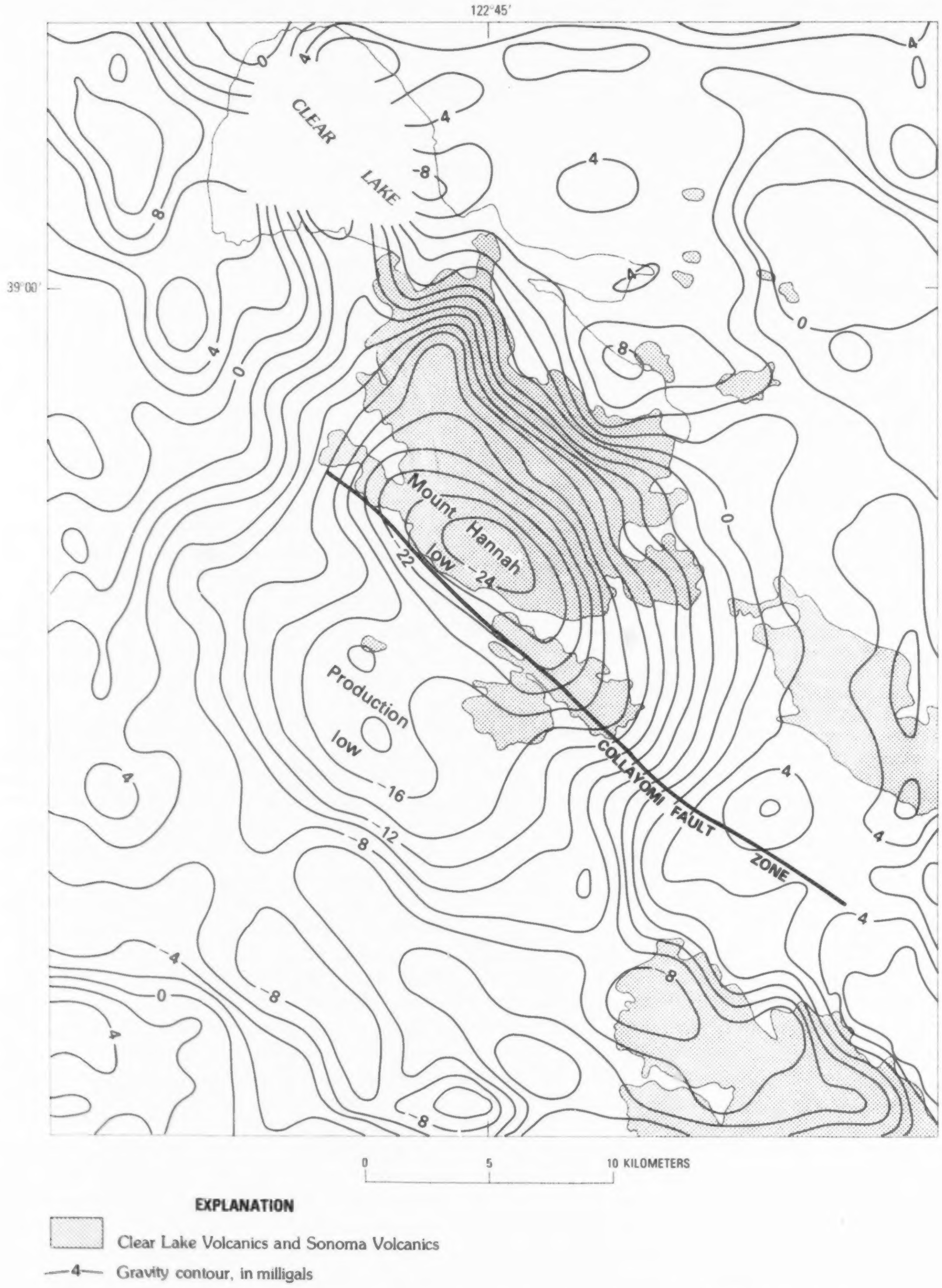
122°45′
39°00′
CLEAR LAKE
Mount Hannah low
Production low
COLLAYOMI FAULT ZONE
4
0
-4
-8
-12
-16
-22
-24
0 5 10 KILOMETERS
EXPLANATION
Clear Lake Volcanics and Sonoma Volcanics
—4— Gravity contour, in milligals

FIGURE 39.—The Geysers area, Calif., showing residual gravity based on reduction densities of 2.67 g/cm^3. Contour interval, 2 mGal. From Isherwood (1975).

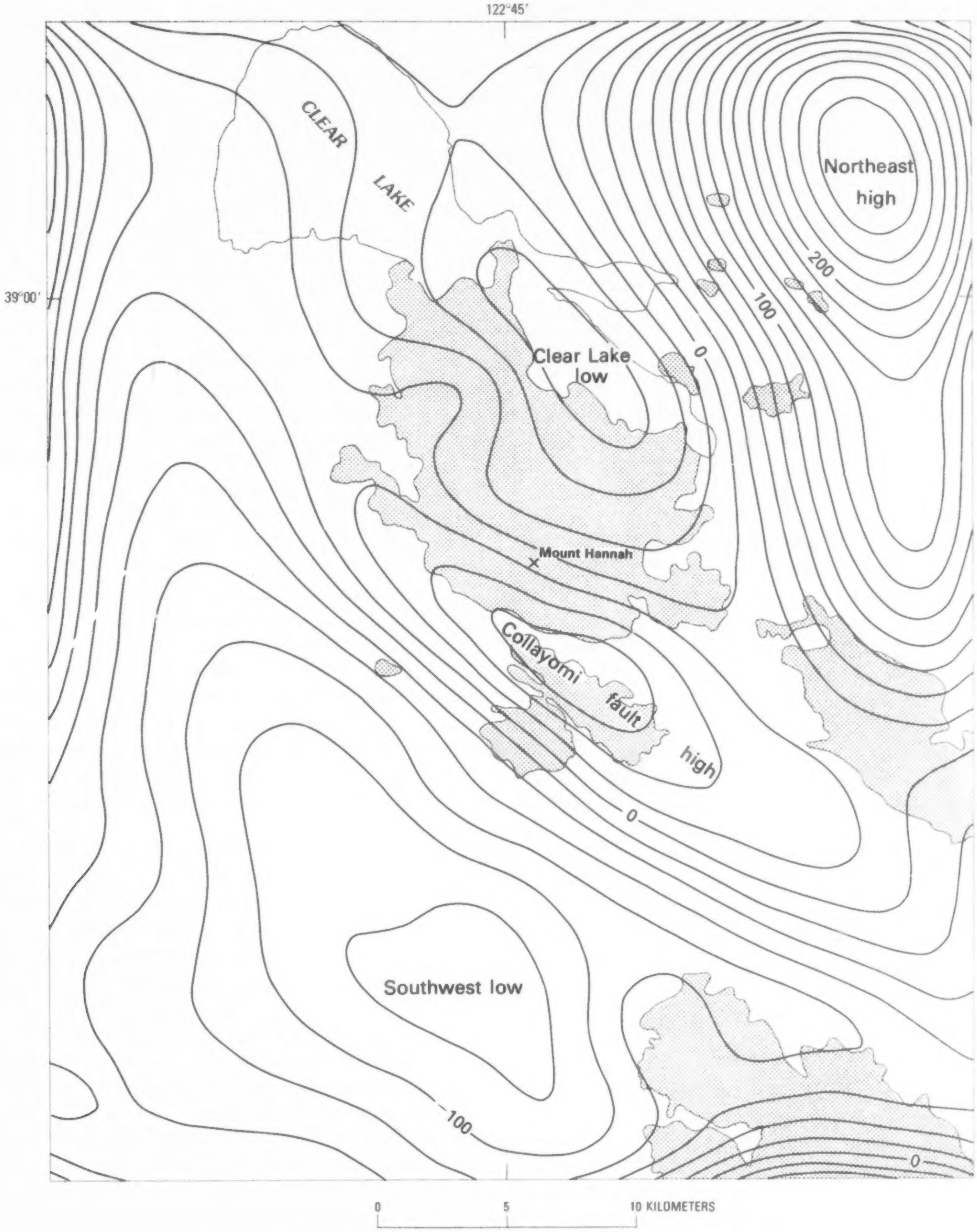
122°45'
39°00'
CLEAR LAKE
Northeast high
200
100
0
Clear Lake low
Mount Hannah
Collayomi fault
high
0
Southwest low
100
0
0
5
10 KILOMETERS

EXPLANATION

▨ Clear Lake Volcanics and Sonoma Volcanics

—100— Magnetic contour, in gammas

FIGURE 40.—The Geysers area showing digitized magnetic field continued upward 3 km. Contour interval, 20 gammas. From Isherwood (1975).

and magnetic fields. In the case of The Geysers, the pseudogravity field, calculated with any given density and magnetization contrast (fig. 41), looks quite unlike the gravity field. These maps demonstrate that no simple anomalous body produces the features of both the gravitational and magnetic fields, although correlation between the gravity and magnetic fields may be greater after compensation for the effects of near-surface volcanic rocks. A pseudogravity anomaly corresponds roughly to the presently producing steam field and terminates abruptly on the northeast along the Collayomi fault zone. This boundary could reflect destruction of magnetite by alteration within the hydrothermal system, which is bounded by less permeable (and highly magnetic) serpentinite along the fault zone.

The combined analysis of gravity and magnetic fields provides the following evidence for a deep magma chamber: (1) The negative gravity anomaly extends farther to the southwest than could be explained merely by the low densities of the Clear Lake Volcanics and the Great Valley sequence, located primarily northeast of the Collayomi fault zone. (2) The spatial wavelength of the nearly circular gravity anomaly corresponds to an equivalent sphere centered at about 13.5 km depth. (3) No magnetic anomaly corresponds to the major gravity low nor can any magnetic sources deeper than about 6.5 km be identified. This lack of correspondence is consistent with the body of anomalous density being above the Curie temperature (probably greater than 500°C for expected compositions). (4) Rocks within 2 or 3 km of the surface have been reached by numerous steam wells without finding any low-density mass. Thus to account for the large mass deficiency indicated by the gravity anomaly, the density contrast between the low-density body and the surrounding rocks must be large. The only likely material that can give a large enough contrast of density compared with that of typical rocks of the Franciscan assemblage is partially molten silicic rock, or magma.

SEISMIC STUDIES

Seismic studies provide data that constrain the limits of models of the Geysers geothermal system. The teleseismic *P*-wave delay technique provides an independent test of the magma-chamber hypothesis. The travel times of seismic waves from earthquakes reflect changes in the velocity of material through which they pass. Velocity generally decreases with temperature and decreases sharply in melted rock (Murase and McBirney, 1973). Comparing observed seismic traveltimes with theoretical traveltimes over an array of recording stations allows mapping of regions of low-velocity material. Initial measurements (Steeples and Iyer, 1976) suggested that seismic body waves indeed showed delayed arrivals in a region roughly corresponding to the gravity low. More detailed studies (Iyer and others, this volume, fig. 54*A*) show the location of the observed delays more accurately. A refraction study by Majer and McEvilly (1977) shows that this low-velocity material is not in the upper 3 km. Consequently, Iyer and others (this volume) attribute the delays to a magma chamber centered between Mount Hannah and The Geysers that extends in depth from 4 km to below 30 km.

Theory also predicts attenuation of seismic body waves by rock materials with any degree of partial melt. Recording earthquake signals at an array of stations throughout a region can detect seismic attenuation on a relative basis. Young and Ward (this volune) mapped a region of high attenuation coinciding roughly with the gravity low at The Geysers, which they too attribute to underlying magma.

The occurrence of microearthquakes in the vicinity of The Geysers has been known for some time (Lange and Westphal, 1969; Hamilton and Muffler, 1972). Continuous monitoring since 1975 (Bufe and others, this volume) has recorded substantial shallow seismicity, much of it induced, in the geothermal region. Brace and Byerlee (1970) demonstrated the lack of stick-slip (earthquake-producing) faulting at high temperatures. The absence of earthquake hypocenters deeper than about 5 km in the region of the gravity low (Marks and others, 1978; this volume) is consistent with the hypothesis of elevated temperature associated with a magma body at depth.

Denlinger (1979) has shown that recent microearthquakes are concentrated in the portion of the reservoir undergoing fluid depletion and strain. This pattern of seismicity (and geodetic changes, described below) suggests that some seismic activity is caused by release of regional tectonic stress triggered by production of steam. Most fault-plane solutions for local seismic events suggest extensional motion along short faults trending more northerly than the geologically well defined Maacama, Mercuryville, or Collayomi fault zones (Bufe and others, this volume).

Active seismic techniques have the potential to shed light upon the structure of the geothermal reservoir. Standard oil-field interpretations of reflection and refraction seismic sections are of marginal use in many geothermal areas because of the complex metamorphic and volcanic terranes involved. At The Geysers, present production comes primarily from fractures in the Franciscan graywacke. Denlinger and Kovach (this volume), from a relatively shallow penetration Vibroseis survey, recognized reflecting horizons within the Fran-

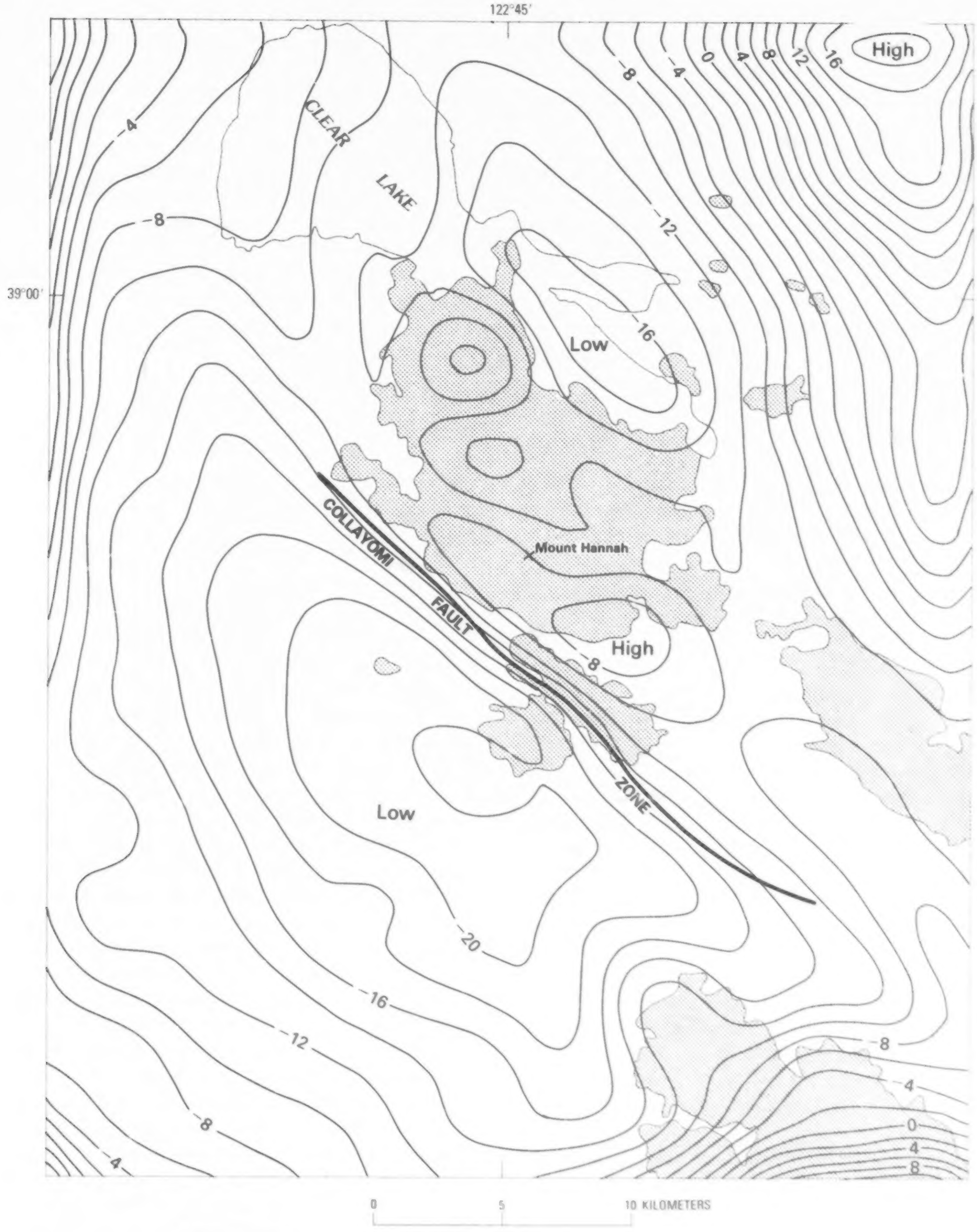
122°45'
39°00'
CLEAR LAKE
High
Low
Mount Hannah
High
Low
COLLAYOMI FAULT ZONE
-4
-8
-8
-4
0
4
8
12
16
-12
-16
-8
-20
-16
-12
-8
-4
-8
-4
0
4
8
0
5
10 KILOMETERS

EXPLANATION

▨ Clear Lake Volcanics and Sonoma Volcanics

—8— Pseudogravity contour, in milligals

FIGURE 41.—The Geysers area showing pseudogravity derived from filtered aeromagnetic data (5-km cutoff); density contrast, 0.15 g/cm^3; magnetization contrast, 0.003 cgs units. Contour interval, 2 mGal. From Isherwood (1975).

ciscan complex southeast of The Geysers which may be shear zones. The equipment used severely limited resolution, but their results raise the possibility that some fracture zones may be mappable from the surface.

ELECTRICAL METHODS

Electrical resistivity and magnetotelluric methods have been employed by Stanley, Jackson, and Hearn (1973) in this region. They used resistivity measurements combining total-field "bipole-dipole" mapping and VES (vertical electrical sounding) techniques to construct a composite apparent-resistivity map (fig. 42). Since bipole-to-dipole separations varied, they could not quantify the depth of the features related to these apparent resistivities. However, ignoring higher values close to the source bipoles made it possible to relate mapped apparent resistivities to units beneath the surface volcanic rocks. The vertical electrical soundings were also used to determine resistivity as a function of depth. Both methods show low resistivity values near Mount Hannah. The large apparent-resistivity low (fig. 42) corresponds roughly to the lowest part of the Mount Hannah gravity low, with steep gradients near the Collayomi fault zone. Relatively high resistivities, from 25 to over 1,000 ohm-meters, characterize the surface volcanic rocks. Interpretation of a less resistant unit beneath indicates a thin volcanic sequence. Thicknesses of volcanic rocks determined from soundings range from 50 m to 1,100 m. Depths to "resistive basement" underlying the low resistivity unit were interpreted for two VES profiles at 1.5 km and 2.6 km, and from one dipole sounding at 5 km. Minimum depths to resistive basement were determined elsewhere. The model published by Stanley, Jackson, and Hearn (1973) shows the volcanic field to be underlain by shale of the Great Valley sequence, with low (2-3 ohm-meter) resistivities, attributed largely to hot pore fluids. The authors extended this underlying unit to over 4.5 km depth beneath the Mount Hannah anomaly and considered the same unit to be the source of the gravity anomaly as well. W. D. Stanley (oral commun., 1975) modified his 1973 interpretation to include a deep body—possibly magma—beneath the Geysers-Clear Lake area.

No unambiguous interpretation can be made from these data, as shown by the dual interpretation given in the report of Stanley, Jackson, and Hearn (1973). Moreover, their interpretation assumes horizontal layering in a region with demonstrated lateral variation in rock types. For instance, one VES site indicates electrical basement of high resistivity at an apparent depth of 2.6 km, but the station lies within 1 km of steeply dipping serpentinite along the Collayomi fault zone.

Other than the correspondence between near-surface high resistivities and surface volcanic rocks, correlation between resistivity units and rock units remains ambiguous. Physical properties of some Franciscan rock types resemble rocks in the Great Valley sequence more than they do other Franciscan rocks. Inaccurate lithologic identification from mud logs and inaccuracies of induction logs (especially at high resistivities) prevent well data from providing the distinctions necessary for interpretation of resistivity soundings. In particular, discrimination between the Great Valley sequence and the Franciscan assemblage in the subsurface is unclear at present on the basis of surface resistivity measurements.

Identifying the major rock units is not the only problem. Distinguishing between lithologies within rock units on the basis of observed electrical resistivity is also difficult. For example, serpentinite is electrically resistive under surface conditions, but becomes a good electrical conductor at temperatures of 500°C (Parkhomenko and others, 1973). Although temperatures within the penetration range of these resistivity soundings are not expected to be this high, alteration of serpentine combined with slightly elevated temperature may similarly decrease resistivity. The available electric logs from wells do not clearly establish whether large serpentinite bodies at depth have high or low resistivities. Although the lowest resistivities in two holes northeast of Mount Hannah correlate with shaly units, resistivity lows appear to correlate with greenstone in another nearby hole (R. J. McLaughlin, oral commun., 1976). Furthermore, if the resistivity of the dominantly graywacke-greenstone unit is as low as 6-8 ohm-meters with pore fluids at 100°C, one might expect to detect resistivities low enough to be indistinguishable from those of the more shaly units at temperatures exceeding 200°C. Interpretations of resistivity are further complicated if pore fluids are in the gas phase.

The composition of the high-resistivity electrical basement that underlies the low-resistivity unit is similarly unclear. This "resistive basement" may reflect (1) lateral resistivity contrasts above any true geologic basement, (2) solidified intrusive rocks surrounding a magma chamber, or (3) unrelated intrusive or volcanic rocks. The nature of a magma chamber also affects the conductivity of the rock in it. Molten rock itself is probably conductive (Zablocki, 1978), but a realistic magma chamber is probably not a simple pool of liquid rock. A magma chamber heated by numerous injections from below will more likely contain regions of partial melt and may include crystallized portions, which could

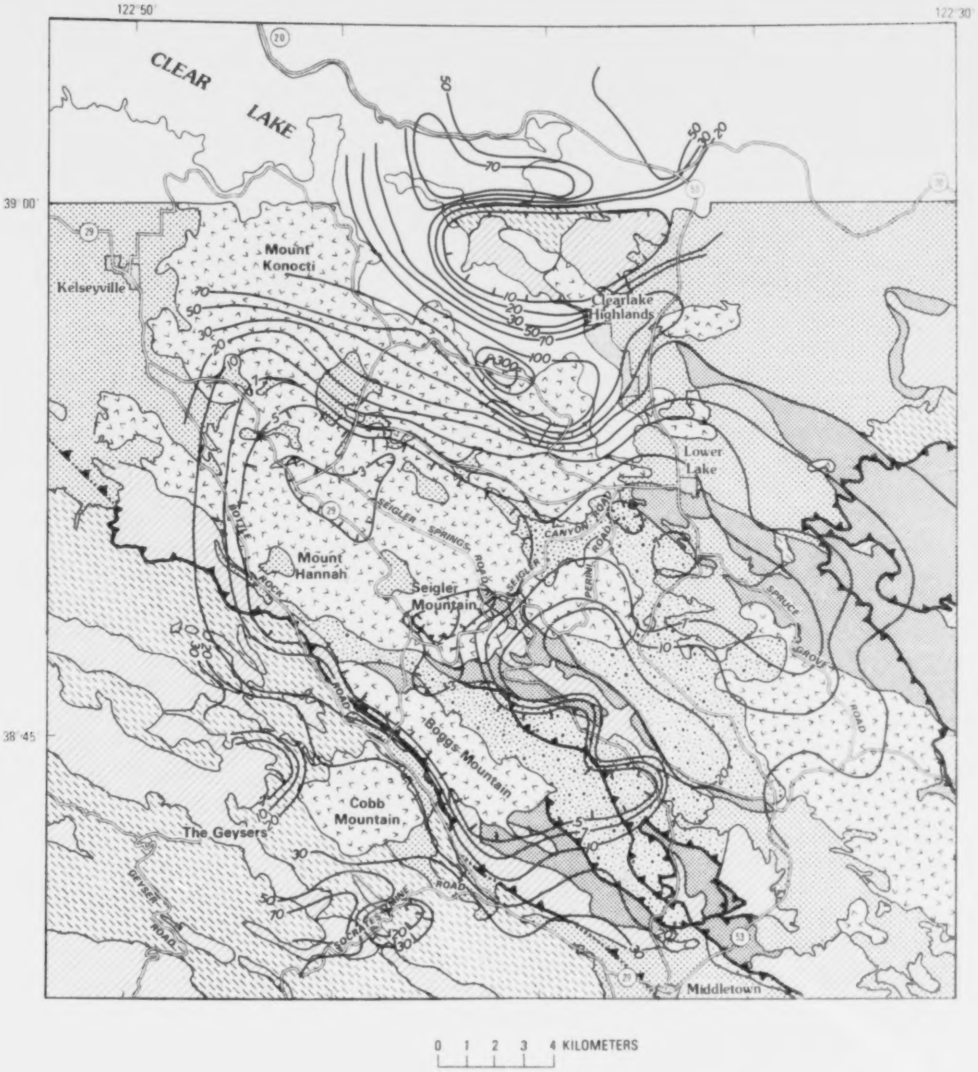
122°50'
122°30'
39°00'
38°45'
CLEAR LAKE
Mount Konocti
Kelseyville
Clearlake Highlands
Lower Lake
Mount Hannah
Seigler Mountain
Boggs Mountain
Cobb Mountain
The Geysers
Middletown
SEIGLER SPRINGS ROAD
CANYON ROAD
PERINI ROAD
SPRUCE GROVE ROAD
BOTTLE ROCK ROAD
GEYSERS ROAD
SOCRATES MINE ROAD
20
29
53
175
10
20
30
50
70
100
300
5
0 1 2 3 4 KILOMETERS

EXPLANATION

▨ Clear Lake Volcanics

▨ Sedimentary rocks

▨ Mafic intrusive rocks

▨ Great Valley sequence (upper part)

▨ Great Valley sequence (lower part)

▨ Franciscan assemblage

——— Contact

▲▲.▲. Thrust fault—*Sawteeth on upper plate. Dotted where inferred*

—— ⊥⊥ Resistivity contour, in ohm-meters—*Hachures indicate low areas*

FIGURE 42.—Generalized geologic map showing apparent resistivity near Clear Lake (from Stanley and others, 1973).

be quite resistive electrically. Likewise, high resistivities may arise from nearby rocks with vapor-filled pores rather than liquid-filled pores. Vapor-filled pores are generally accepted for vapor-dominated geothermal systems (White and others, 1971). Although vapor-dominated systems are generally believed to be highly resistive, appropriate experiments in rock physics have not yet been carried out. Resistivity highs have not been found at the Lardarello steam field in Italy, one of the classic vapor-dominated fields.

I generally find the interpretations of Stanley, Jackson, and Hearn (1973) to be compatible with other gravity and magnetic results. Their conclusions may be modified, however, by discarding their proposed one-to-one correlation between the sources of the electrical and gravity anomalies. The bipole-dipole map may largely indicate the location of especially conductive shaly rocks of the Great Valley sequence beneath the volcanic rocks. However, at great depth and high temperature, these Great Valley sequence rocks do not seem distinguishable either by conductance or by density from typical Franciscan rocks, especially where they are significantly altered hydrothermally and their fractures are liquid filled. The serpentinite body along the Collayomi fault zone would be a resistive region, at least in the near surface, and may be detected laterally by some of the VES, and possibly by the deep dipole soundings. Other resistive basement may be the chilled portion of a batholith, magma chamber complex, or a surrounding vapor-dominated region. Recent magnetotelluric recordings indicate that no large conducting mass is present within about 7 km of the surface beneath the recording stations (W. D. Stanley, oral commun., 1975), although coverage to date is sparse.

Nevertheless, the electrical data are helpful in interpreting the near-surface stratigraphy and may indicate the extent of a possible hot-water reservoir. Near-surface rock units may account for part of the gravity anomaly northeast of the Collayomi fault zone. However, the near-surface source bodies associated with the electrical anomalies appear incapable of accounting for the total mass deficiency calculated from the gravity anomalies or the lateral extent of the gravity gradients.

HEAT FLOW

Heat-flow measurements are difficult to interpret in regions of known hydrothermal convection owing to the complicated combinations of heat transfer processes that take place. Consequently, few heat-flow interpretations are available for the Geysers region.

At the Geysers, convection may be limited to the reservoir itself, with thermally conductive regions above and below. For two drill holes within the Geysers steam field, away from active steam fumaroles, Urban, Diment, Sass, and Jamieson (1976) found the interval between the surface and the steam reservoir to be mainly conductive. In this zone above the fractured reservoir, heat flow was determined in the two holes at 7.5 and 9.3 hfu. Assuming equilibrium, the heat flux would be the same beneath the reservoir to the depth of the heat source. Given similar thermal conductivities and steady-state conduction, similar temperature gradients would extend from the base of the convecting zone to the heat source.

None of the deep (up to 3.4 km) holes has penetrated the region beneath the essentially isothermal region of the steam zone. The deep temperature measurements within this isothermal region provide one set of boundary conditions, limiting the nearness to the surface of injected magma. Jamieson (1976) attempted to model the heat source for a region on the southwest flank of the gravity anomaly. He interpreted the heat flow to be consistent with hot (over 700°C) intrusive rocks at a depth of about 8 km over a wide area, with regional heat flow from this heat source to the surface primarily by conduction. Superimposed on the regional heat flux, Jamieson found high temperature gradients in the producing area. These gradients reflect elevated near-surface temperatures due to convective transfer of heat from depth by local steam and hot-water systems along high-angle fractures.

GEODESY

Geodetic studies underway at The Geysers fall in two general categories: (1) resurveys of precise control networks, beginning in 1972-73, to determine changes in both vertical and horizontal movements of the ground, and (2) accurate measurements in observed gravity to determine changes with time. The data from these two methods complement one another, and both apparently reflect changes related to the withdrawal of fluid from the reservoir. Their combined interpretation yields insight into the mechanical and recharge characteristics of the geothermal system.

In resurveys of precise geodetic control networks from 1972 to 1978, Lofgren (this volume) found significant crustal deformation at The Geysers, occurring primarily as (1) regional right-lateral horizontal movement along northwest-trending fault systems, (2) vertical and horizontal compression of the region of present steam production, and (3) a local tectonic tilt downward to the northwest. Of these, at least the vertical and horizontal compression relates directly to production from the geothermal system. All these movements are superimposed on a background of slope instability, which affects the reliability of some individual reference points in interpreting tectonic deformations and subsidence.

Subsidence is commonly associated with removal of liquid from subsurface reservoir rocks at near hydrostatic pressure, where the hydraulic forces may locally bear some of the lithostatic load. Within the steam reservoir at The Geysers, pore pressures are much less than hydrostatic, and changes in pore pressure from steam production are only 1-5 percent of the lithostatic load (Denlinger, 1979). Despite the low initial formation pressure and relative competency of the rocks, some measured subsidence and horizontal motion appear related to production from the geothermal reservoir, although some apparent subsidence reflects landsliding. The maximum subsidence of 13 cm in 4½ years occurred in the area of most concentrated steam withdrawals (Lofgren, this volume). Subsidence correlates strongly with the region of decreased reservoir pressure reported by Lipman, Strobel, and Gulati (1977), and with sites of decreased gravity. Horizontal ground movements of up to 2.0 cm/yr were measured around the perimeter of the steam production area. As predicted by the generalized modeling of Safai and Pinder (1977), movement was generally inward toward the center of production (fig. 43).

Precision gravity measurements provide collaborating information regarding depletion mechanisms of the geothermal reservoir (Isherwood, 1977). A change in the observed gravity at a particular location in a geothermal field can be interpreted in terms of change in elevation and fluid movement in nearby reservoir rocks, other factors being either corrected for or held constant. Modern portable gravity meters can reliably measure differences in gravitational acceleration of between 5 and 10 μGal (1 $\mu\text{Gal} = 10^{-8}\ \text{m/s}^2$). Because of dependence on baselines established with older equipment, changes in gravity measured to date are probably accurate to only about 30 μGal.

A 5-10-μGal decrease in gravity can be caused either by several centimeters increase in elevation or by the draining of liquid water from a layer about 1 m thick from an infinite aquifer with 20-percent porosity. Repeated measurements of gravity provide the potential for detecting mass loss (depletion) from geothermal reservoirs. This net depletion can be used for determining the extent of recharge, for detecting areas of drainage, and for testing various reservoir models, provided that gravity data are corrected for elevation changes measured independently and production data are available to establish the mass produced.

Areas of gravity decreases shown in figure 44 (with respect to a reference station outside the producing field) closely match areas of production and areas of reservoir pressure decline shown by Lipman, Strobel, and Gulati (1977). Thirty-six of the gravity stations coincide with remeasured elevation points. Figures 45*A* and 45*B* show the correlation between subsidence and gravity decrease. The resultant correlation coefficient of +0.72 is particularly significant, inasmuch as changes of gravity caused by landslides or block tectonic elevation changes would produce a correlation coefficient of −1.

The gravity measurements for The Geysers clearly show that a net mass loss has occurred in the reservoir region. The most likely mechanism is the replacement of hot liquid water (density, 0.8 g/cm^3 at 240°C) in the pore space by water vapor (density, 0.02 g/cm^3 at 240°C) as fluids were removed from the reservoir by producing wells. Alternative mechanisms of mass loss—removal of steam, thermal contraction, or compaction of rock — are unlikely or inadequate to explain observed changes (Isherwood, 1977).

Gauss's potential theorem can be used to determine the total change of mass (in this case the net fluid loss) that corresponds to a gravity change without assuming a shape or depth of the source. Preliminary calculations of the mass balance at The Geysers by Gauss's theorem show the loss of mass to be roughly the same as the calculated mass of steam produced during the same time (estimated at 8×10^{10} kg over 2½ years). Because of the limited areal coverage and duration of the study, this estimate, which suggests no significant recharge, could be in error by as much as 20 percent.

If the shape of the depleted zone is assumed to be that of a vertical cylinder with a constant density change and using the mass of the net produced fluid as a maximum loss, the gravity effect at the surface can be calculated for various combinations of cylinder radius and depth. Using the maximum observed gravity decreases of 120±30 μGal, it is possible to rule out a model of steam being derived solely from a boiling water table deeper than about 2,500 m (Isherwood, 1977). Some contribution from this depth is not precluded, but the major loss of mass must be shallower, probably near the 1-2-km completion depth of most wells.

This conclusion tends to substantiate the model of Truesdell and White (1973); they propose that liquid water throughout the reservoir flashes to steam as a direct result of pressure decrease caused by withdrawal of steam. This water was probably distributed either in zones of gradationally higher liquid saturation or in small perched water tables.

In March 1979, a stationary cryogenic gravitymeter was installed at The Geysers by personnel with the University of California, San Diego. This meter is now continuously recording gravity changes. Long-term drift rates are not yet established, but the initial one-month record segment indicates a gravity decrease consistent with the repeat measurements described above (J. J. Olson, oral commun., 1979). Preliminary results from recording cryogenic gravity meters have shown significant variations in gravity to be caused by variations in near-surface water saturation due to rainfall. Seasonal effects may also be significant. These potential errors to the interpretation of discrete measurements probably do not alter the basic conclusions from the repeat gravity studies to date.

Reliable projections of reservoir life at The Geysers can be calculated only when we have a longer period of observations and when our interpretation techniques are refined. Gravity changes reflect changes that happened between measurements, and these changes, in conjunction with other reservoir data, can eventually allow projections of reservoir behavior which will lead to informed management of geothermal reservoirs.

CONTEMPORARY DYNAMICS

The concept of a silicic magma chamber in the middle crust at The Geysers is consistent with what is known of the occurrence of batholiths. Geologists have found that batholiths commonly occur near continental margins along which subduction has taken place. The batholiths are generally silicic because (1) silicic

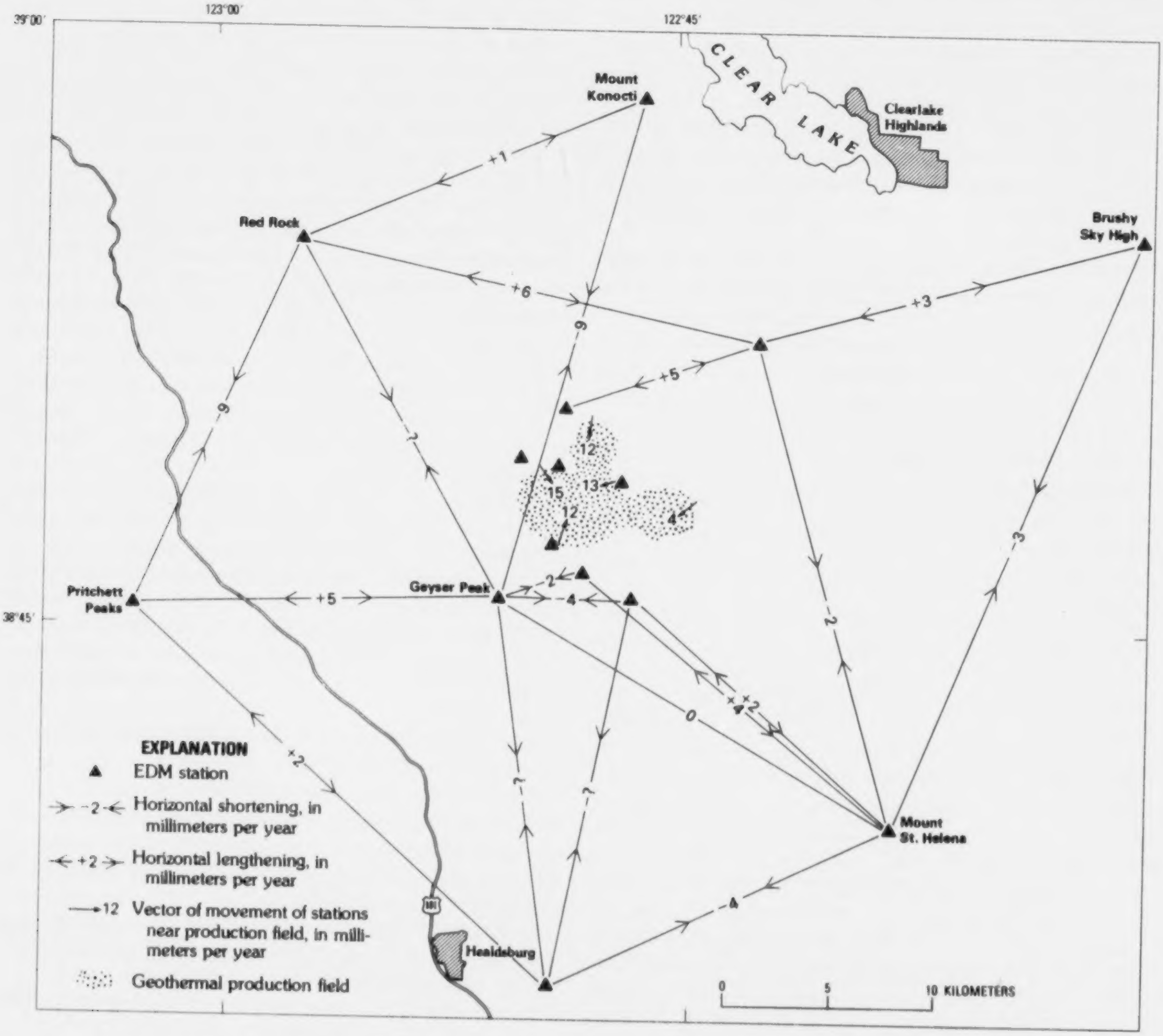
39°00'
123°00'
122°45'
38°45'
CLEAR LAKE
Clearlake Highlands
Mount Konocti
Red Rock
Brushy Sky High
Pritchett Peaks
Geyser Peak
Mount St. Helena
Healdsburg
101
+1
+6
+3
+5
-6
-6
-7
+5
12
15
13
12
4
-2
-4
-2
-3
0
+4
+2
+2
-7
-7
-4
EXPLANATION
▲ EDM station
→ -2 ← Horizontal shortening, in millimeters per year
← +2 → Horizontal lengthening, in millimeters per year
—→12 Vector of movement of stations near production field, in millimeters per year
Geothermal production field
0 5 10 KILOMETERS

FIGURE 43.—Generalized horizontal ground movement in the Geysers-Clear Lake area, 1972-77 (from Lofgren, 1978).

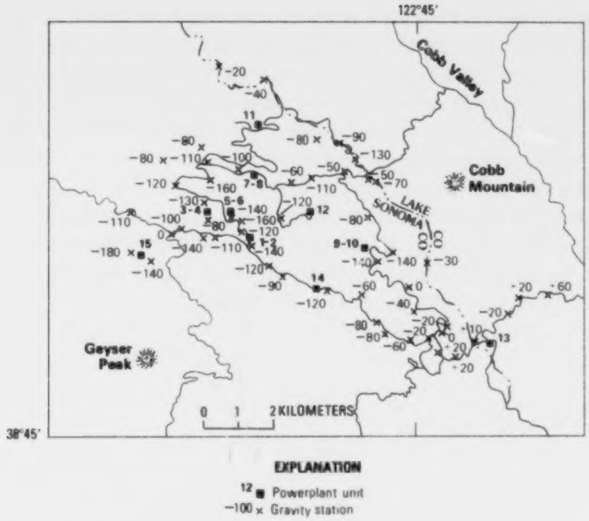
122°45′
38°45′
Cobb Valley
Cobb Mountain
Geyser Peak
LAKE SONOMA CO
0 1 2 KILOMETERS
-20
-40
11
-80
-90
-130
-80
-110
-100
-120
-160
7-8
-60
-50
50
-70
-110
-130
3-4
5-6
-140
-160
-120
12
-80
-110
-100
0
80
-120
1-2
-140
-140
-110
9-10
15
-180
-140
-30
-120
-90
14
-120
-60
0
-40
+20
+60
-20
-80
-80
-60
-20
-20
0
+10
13
+20
+20
EXPLANATION
12 Powerplant unit
-100 Gravity station

FIGURE 44.—Gravity changes, in microgals, between July 1974 and February 1977 in the Geysers geothermal area. From Isherwood (1977).

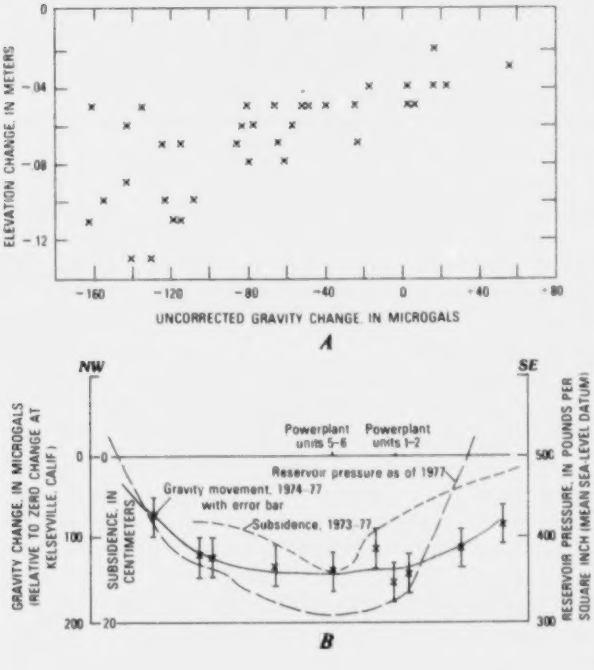

FIGURE 45.—Correlation between subsidence, gravity decrease, and pressure decline at The Geysers. Pressure data from Lipman, Strobel, and Gulati (1977); subsidence data from Lofgren (this volume). *A*, Relation between gravity change (July 1974 to February 1977) and elevation change (late 1973 to late 1975). *B*, Relation of gravity change to subsidence and reservoir pressure decline along a northeast-southwest line through the producing steam field.

magma is relatively more viscous than basaltic magma (because of its low viscosity, basalt does not form large pools in the crust but instead flows to the surface), (2) magma in the continental lithosphere assimilates sialic continental material, and (3) large masses of mafic rocks do not have the buoyancy to rise to the Earth's surface by isostasy. Structural and metamorphic associations, as well as geochemical evidence, suggest that final equilibration of many granite batholiths occurred at mid-crustal depths (Bateman and Eaton, 1967).

Many andesitic volcanoes form over active Benioff zones. Some characteristics of the Sonoma Volcanics and Clear Lake Volcanics can be interpreted as deriving from subducted materials with later modification in the crust (Donnelly and Hearn, 1978). However, no active Benioff zone occurs beneath the Sonoma or Clear Lake Volcanics. Furthermore, the line of volcanoes interpreted to derive from earlier subduction, the Cascades, lies much farther to the east (fig. 46).

The pattern and history of volcanism parallel the migration of the Mendocino triple junction past the Clear Lake area about three million years ago and suggest a causal relationship. One model to explain this relationship considers the oceanic crust of the Farallon plate being subducted beneath the North American

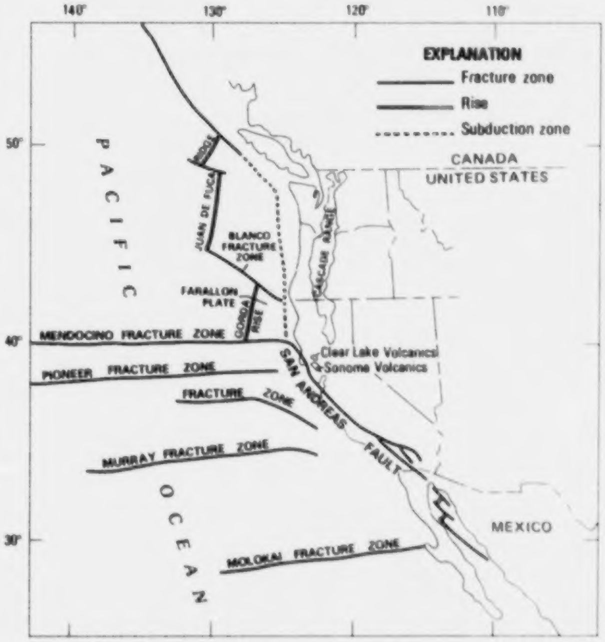
140°
130°
120°
110°
50°
40°
30°
EXPLANATION
Fracture zone
Rise
Subduction zone
CANADA
UNITED STATES
PACIFIC
OCEAN
RIDGE
JUAN DE FUCA
BLANCO FRACTURE ZONE
CASCADE RANGE
FARALLON PLATE
GORDA RISE
MENDOCINO FRACTURE ZONE
Clear Lake Volcanics
Sonoma Volcanics
PIONEER FRACTURE ZONE
FRACTURE ZONE
SAN ANDREAS FAULT
MURRAY FRACTURE ZONE
MOLOKAI FRACTURE ZONE
MEXICO

FIGURE 46.—Generalized volcanism and plate tectonics of western United States, showing relation of Sonoma Volcanics and Clear Lake Volcanics to Cascade Range.

plate (Moore, 1970). As the Farallon plate was being subducted, North America was sliding southeastward relative to the Pacific plate (Atwater, 1970). As the triple junction migrated northward, the southern part of the subducting slab was decoupled from the new crust originating at the Gorda Rise by attachment to the North American plate. Without a supply of material from behind to force it farther eastward, this partially subducted, decoupled slab sank vertically by gravitational forces alone, rather than continuing the combined sinking and eastward motion of the still intact Farallon plate to the north (see fig. 47). When subducted ocean crust sinks to depths below about 100 km, the edges begin to melt (Turcotte and Schubert, 1973); the melting results in convective transfer of heat to the rock mass above, and the consequent magma rise could eventually produce volcanoes at the surface. Thus, the Sonoma Volcanics and Clear Lake Volcanics could result from the sinking and melting of Farallon plate material which was decoupled by the passage of the Mendocino triple junction (Isherwood, 1975). With the cessation of Farallon plate subduction, further northward migration of this volcanic trend may be limited.

It is overly simplistic to say that the heat source for any geothermal system is a body of magma, or to think of an active magma chamber as a single bubble of molten rock which has suddenly become emplaced in the middle to upper crust. The initial melt deep in the Earth would not be silicic magma but mafic ocean crust or primary mantle melt which becomes buoyant upon melting. Heat would be transferred upward as rocks undergo stoping and anatexis, and as the melt undergoes fractional crystallization with multiple pulses of heat from below supplied by convecting magma. Much material would solidify as the heat pulses work their way upward, and the final level of any magma mass would be related to its density contrast with the enclosing rocks (isostasy) and the available energy for melting of the surrounding rocks.

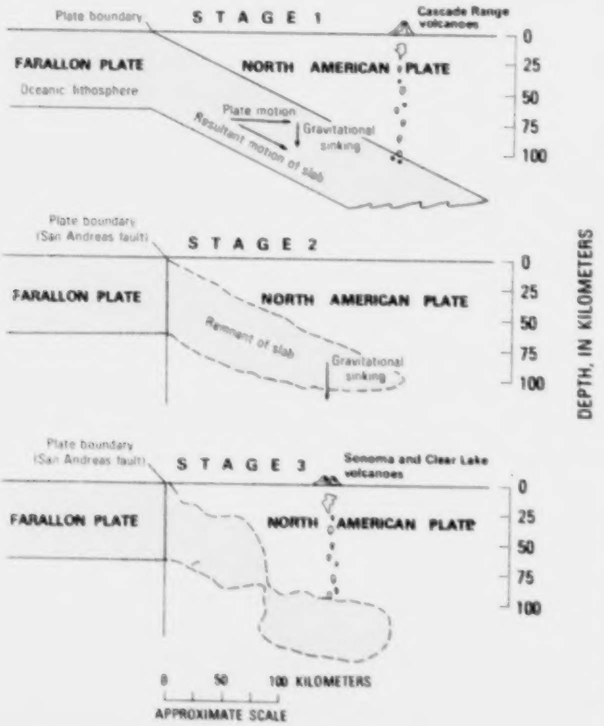
Plate boundary
STAGE 1
Cascade Range volcanoes
FARALLON PLATE
Oceanic lithosphere
NORTH AMERICAN PLATE
Plate motion
Resultant motion of slab
Gravitational sinking
0
25
50
75
100
Plate boundary (San Andreas fault)
STAGE 2
FARALLON PLATE
NORTH AMERICAN PLATE
Remnant of slab
Gravitational sinking
0
25
50
75
100
DEPTH, IN KILOMETERS
Plate boundary (San Andreas fault)
STAGE 3
Sonoma and Clear Lake volcanoes
FARALLON PLATE
NORTH AMERICAN PLATE
0
25
50
75
100
0 50 100 KILOMETERS
APPROXIMATE SCALE

FIGURE 47.—Proposed evolution of the Clear Lake Volcanics from severed limb of subducting Farallon plate.

Calculations by Lachenbruch, Sass, Munroe, and Moses (1976) for Long Valley, California illustrate that a single magmatic event in the middle crust cannot sustain volcanic eruptions for even one million years. Volcanic eruptions have occurred in the Geysers-Clear Lake region for more than two million years. Therefore, the Geysers-Clear Lake magma chamber is probably composite, containing some fully solidified and some partly molten rock from recent heat injection. Smith and Shaw (1975) point out that basaltic magma is unlikely to pass through a body of molten silicic rock; therefore, the basaltic eruptions of less than 100,000 years ago adjacent to Mount Konocti may indicate that the underlying portion of the silicic complex is now solidified. No basaltic eruptions more recent than about 500,000 years have been recognized in the southern or southwestern parts of the Clear Lake volcanic field under the gravity low. The geophysical data suggest that the present magma chamber is south of the most recent eruptive activity. This is compatible with the pattern of shifting volcanic centers seen in the past (Donnelly, 1977), despite the overall northward migration of volcanism.

Plate-tectonic theory suggests that volcanic activity along the Cascades is decreasing as subduction motion converts to strike-slip motion along the continental margin. This transition is taking place as the motions of plates gradually change relative to one another. With cessation of spreading at the Gorda Rise and possibly at the Juan de Fuca Ridge, the geometry of the plate margins must change. Consequently, the current plate boundary in northern California can be described as a soft plate margin. Strike-slip motion is not concentrated entirely along the San Andreas fault but is distributed over a wide zone which appears to include the Geysers area. Donnelly (1977) attributed the triggering of local volcanism to pressure decreases accompanying the propagation of fault branches of this transform shear system. However, seismological studies indicate that the concentration of earthquake strain release is tens of kilometers southwest of the volcanism. Hearn, Donnelly, and Goff (1976) considered the strike-slip faulting as superimposed deformation which may prevent the normal volcanic evolution shown by other volcanic systems. They suggested that, if the geometry of the magma chamber continually changes and its roof is fracturing as a result of regional stresses, a progressive accumulation of gas-rich silicic differentiate, necessary for voluminous ash-flow eruptions, may not occur. The existence of the negative gravity anomaly at The Geysers indicates that dynamic forces are still active in the region.

REFERENCES CITED

Atwater, Tanya, 1970, Implications of plate tectonics for the Cenozoic evolution of western North America: Geological Society of America Bulletin, v. 81, no. 12, p. 3513-3536.

Bateman, P. C., and Eaton, J. P., 1967, Sierra Nevada batholith: Science, v. 158, p. 1407-1417.

Brace, W. F., and Byerlee, J. D., 1970, California earthquakes: Why only shallow focus?: Science, v. 168, p. 1573-1575.

Chapman, R. H., 1966, Gravity map of The Geysers area, California: California Division of Mines and Geology Mineral Information Service, v. 19, p. 148-149.

—— 1975, Geophysical study of the Clear Lake region, California: California Division of Mines and Geology Special Report 116, 23 p.

Cordell, Lindrith, and Taylor, P. T., 1971, Investigaton of magnetization and density of a North Atlantic seamount using Poisson's theorem: Geophysics, v. 36, p. 919-937.

Denlinger, R. P., 1979, Geophysical constraints of The Geysers geothermal system, northern California: Stanford, Calif., Stanford University, Ph. D. thesis, 85 p.

Donnelly, J. M., 1977, Geochronology and evolution of the Clear Lake volcanic field: Berkeley, University of California, Ph. D. thesis, 23 p.

Donnelly, J. M., and Hearn, B. C., Jr., 1978, Geochronology and evolution of the Clear Lake Volcanics, northern California: Geological Society of America Abstracts with Programs, v. 10, p. 103.

Hamilton, R. M., and Muffler, L. J. P., 1972, Microearthquakes at The Geysers geothermal area, California: Journal of Geophysical Research, v. 77, p. 2081-2086.

Hearn, B. C., Jr., Donnelly, J. M., and Goff, F. E., 1976, Geology and geochronology of the Clear Lake Volcanics, California: U.N. Symposium on Development and Use of Geothermal Resources, 2d, San Francisco, 1975, Proceedings, v. 1, p. 423-428.

Isherwood, W. F., 1975, Gravity and magnetic studies of The Geysers-Clear Lake geothermal region, California: Boulder, University of Colorado, Ph. D. thesis, 109 p.

—— 1976, Gravity and magnetic studies of The Geysers-Clear Lake geothermal region, California: U.N. Symposium on Development and Use of Geothermal Resources, 2d, San Francisco, 1975, Proceedings, v. 2, p. 1065-1073.

—— 1977, Geothermal reservoir interpretations from changes in gravity: Geothermal Reservoir Engineering Workshop, 3d, Stanford, Calif., 1977, Proceedings, p. 18-23.

Jamieson, I. M., 1976, Heat flow in a geothermally active area: The Geysers, California: Riverside, University of California, Ph. D. thesis, 143 p.

Lachenbruch, A. H., Sass, J. H., Munroe, R. J., and Moses, T. H., Jr., 1976, Geothermal setting and simple heat conduction models for the Long Valley Caldera: Journal of Geophysical Research, v. 81, p. 769-784.

Lange, A. L., and Westphal, W. H., 1969, Microearthquakes near The Geysers, Sonoma County, California: Journal of Geophysical Research, v. 74, p. 4377-4378.

Lipman, S. C., Strobel, C. J., and Gulati, M. S., 1977, Reservoir performance of The Geysers field: Ente Nazionale per l'Energia Elettrica—Research and Development Administration Workshop, Lardello, Italy, 1977, Proceedings, p. 233-255.

Lofgren, B. E., 1978, Monitoring crustal deformation in The Geysers-Clear Lake geothermal area, California: U.S. Geological Survey Open-File Report 78-597, 19 p.

Majer, E. L., and McEvilly, T. V., 1977, Seismological investigations at the Geysers geothermal field: Berkeley, University of California, Lawrence Berkeley Laboratory Report LBL-7023, 71 p.

Marks, S. M., Ludwin, R. S., Louie, K. B., and Bufe, C. G., 1978, Seismic monitoring at The Geysers geothermal field, California: U.S. Geological Survey Open-File Report 78-798, 26 p.

Moore, G. W., 1970, Sea floor spreading at the junction between Gorda Rise and Mendocino Ridge: Geological Society of America Bulletin, v. 81, no. 9, p. 2817-2824.

Murase, Tadashi, and McBirney, A. R., 1973, Properties of some common igneous rocks and their melts at high temperatures: Geological Society of America Bulletin, v. 84, no. 11, p. 3563-3592.

Parkhomenko, E. I., Belikov, B. P., and Dvorzhak, E., 1973, Influence of serpentinization upon the elastic and electrical properties of rocks: Izvestia, Earth Physics, no. 8, p. 101-108.

Safai, N. M., and Pinder, G. F. 1977, Simulation of saturated-unsaturated deformable porous media: Geothermal Reservoir Engineering Workshop, 3d, Stanford, Calif., 1977, Proceedings, p. 188-191.

Smith, R. L., and Shaw, H. R., 1975, Igneous-related geothermal systems, *in* Assessment of geothermal resources of the United States—1975: U.S. Geological Survey Circular 726, p. 58-83.

Stanley, W. D., Jackson, D. B., and Hearn, B. C., Jr., 1973, Preliminary results of geoelectrical investigations near Clear Lake, California: U.S. Geological Survey open-file report, 20 p.

Steeples, D. W., and Iyer, H. M., 1976, Teleseismic P-wave delays in geothermal exploration: U.N. Symposium on the Development and Use of Geothermal Resources, 2d, San Francisco, 1975, Proceedings, v. 2, p. 1199-1206.

Truesdell, A. H., and White, D. E., 1973, Production of superheated steam from vapor-dominated geothermal reservoirs: Geothermics, v. 2, p. 154-173.

Turcotte, D. L., and Schubert, Gerald, 1973, Frictional heating of the descending lithosphere: Journal of Geophysical Research, v. 78, p. 5876-5886.

Urban, T. C., Diment, W. H., Sass, J.H., and Jamieson, I. M., 1976, Heat flow at The Geysers, California: U.N. Symposium on Development and Use of Geothermal Resources, 2d, San Francisco, 1975, Proceedings, v. 2, p. 1241-1245.

White, D. E., Muffler, L. J. P., and Truesdell, A. H., 1971, Vapor-dominated hydrothermal systems compared with hot water systems: Economic Geology, v. 66, p. 75-97.

Zablocki, C. J., 1978, Application of the VLF induction method for studying some volcanic processes of Kilauea Volcano, Hawaii: Journal of Volcanology and Geothermal Research, v. 3, p. 155-195.

LARGE TELESEISMIC P-WAVE DELAYS IN THE GEYSERS-CLEAR LAKE GEOTHERMAL AREA

By H. M. Iyer, David H. Oppenheimer, Tim Hitchcock,
Jeffrey N. Roloff, and John M. Coakley

ABSTRACT

It has long been postulated that the Clear Lake volcanic field is underlain by a magma chamber. In order to see if a magma chamber is present and, if so, to delineate its shape and physical properties, teleseisms recorded by 26 telemetered and 12 portable seismic stations were examined. Severe signal-shape changes and large teleseismic delays were observed at stations located on the volcanic field centered at Mount Hannah and at the geothermal production zone at The Geysers. For teleseisms in the southwest azimuth, the average delays were 1.5 seconds at Mount Hannah, 0.9 s at Siegler Mountain, and 1.0 s at Black Oaks in the steam production zone. For events in the other azimuths, the delays were less by as much as 0.5 s though still considered quite significant. The spatial distribution outlines a broad region of 0.5-s delay centered at Mount Hannah and extending into the production zone to the southwest, with large delays exceeding 1 s near The Geysers and at Mount Hannah. Results of a seismic-refraction survey in the region show that the delays cannot be attributed to anomalous velocities associated with the complex geologic structure near the surface, and hence a deep low-velocity body in the upper crust is required to explain their presence. A simple modeling technique involving computation of the length of anomalous ray paths is used to determine the size of the low-velocity body. The results show that a plausible model is one in which the low-velocity body about 10 km thick with compressional velocity lower than normal by 15 percent extends under the young Clear Lake volcanic field and the steam-production zone. The body also has a deep core underlying Mount Hannah and part of the production zone in which the velocity decrease is about 25 percent. We believe that this low-velocity body is composed of partially molten rock under the volcanic zone and fractured steam-filled rock with or without an underlying magmatic body under the production area.

INTRODUCTION

It has long been postulated that a reduction in *P*- and *S*-wave velocities and strong *S*-wave attenuation can be expected in regions of Cenozoic volcanism, but few actual data were available to substantiate these claims. Kubota and Berg (1967) and Matumoto (1971) used the observed strong attenuation of *S* waves from nearby earthquakes to postulate the presence of several magma pockets under the Mount Katmai volcano region, Alaska. Only during the last few years have teleseismic *P* waves been used to probe the structure of the crust and upper mantle under volcanic areas. Iyer (1975) found teleseismic delays in excess of 1.4 s in Yellowstone National Park, Wyo., and he interpreted them in terms of a deep crustal and upper-mantle magma chamber. Subsequent work has shown that the magma body, which extends to depths of 150-250 km, has a horizontal extent almost as large as the Yellowstone caldera at the surface but increases with depth (Iyer, 1979). Steeples and Iyer (1976a, 1976b) found nearly 0.5 s relative teleseismic delays in Long Valley, Calif., another potential geothermal area with surface volcanic and thermal expressions. The spatial pattern of the delays and their magnitude are thought to be caused by a magma body approximately 10 km in diameter beneath the central part of the caldera. The compressional-wave velocity inside the body was estimated to be 10-15 percent less than in the surrounding rock. In another active geothermal region, the Imperial Valley, Calif., preliminary study of teleseisms gave inconclusive results (Steeples and Iyer, 1976a). Recently, however, Savino and others (1977), using a technique of combined inversion of teleseismic and gravity data, showed that in the Imperial Valley, the crust under the geothermal areas outlined by high heat flow is thinner than elsewhere. Teleseismic delays of about 0.2 s, observed in another geothermal area in the Coso Range of southern California, have been shown to be caused by a low-velocity body at a depth of 10 km beneath the area where recent rhyolitic volcanism, high heat flow, and hydrothermal activity are present (Reasenberg and others, 1980).

Steeples and Iyer (1976a) first presented preliminary observations of large delays in the vicinity of the Geysers geothermal area. In this paper and a summary paper (Iyer and others, 1979), we present evidence that large teleseismic delays are indeed present in the volcanic field and in the geothermal production zone of the Geysers-Clear Lake region. We show that the probable cause of the delays is a body of low-velocity material in the upper crust.

The Geysers is one of the very few dry-steam systems known in the world. It is located southwest of the Clear Lake volcanic field (fig. 48), which ranges in age from 10,000 years to 2 m.y. (Donnelly-Nolan and others, this volume). A strong gravity low with amplitude of ap-

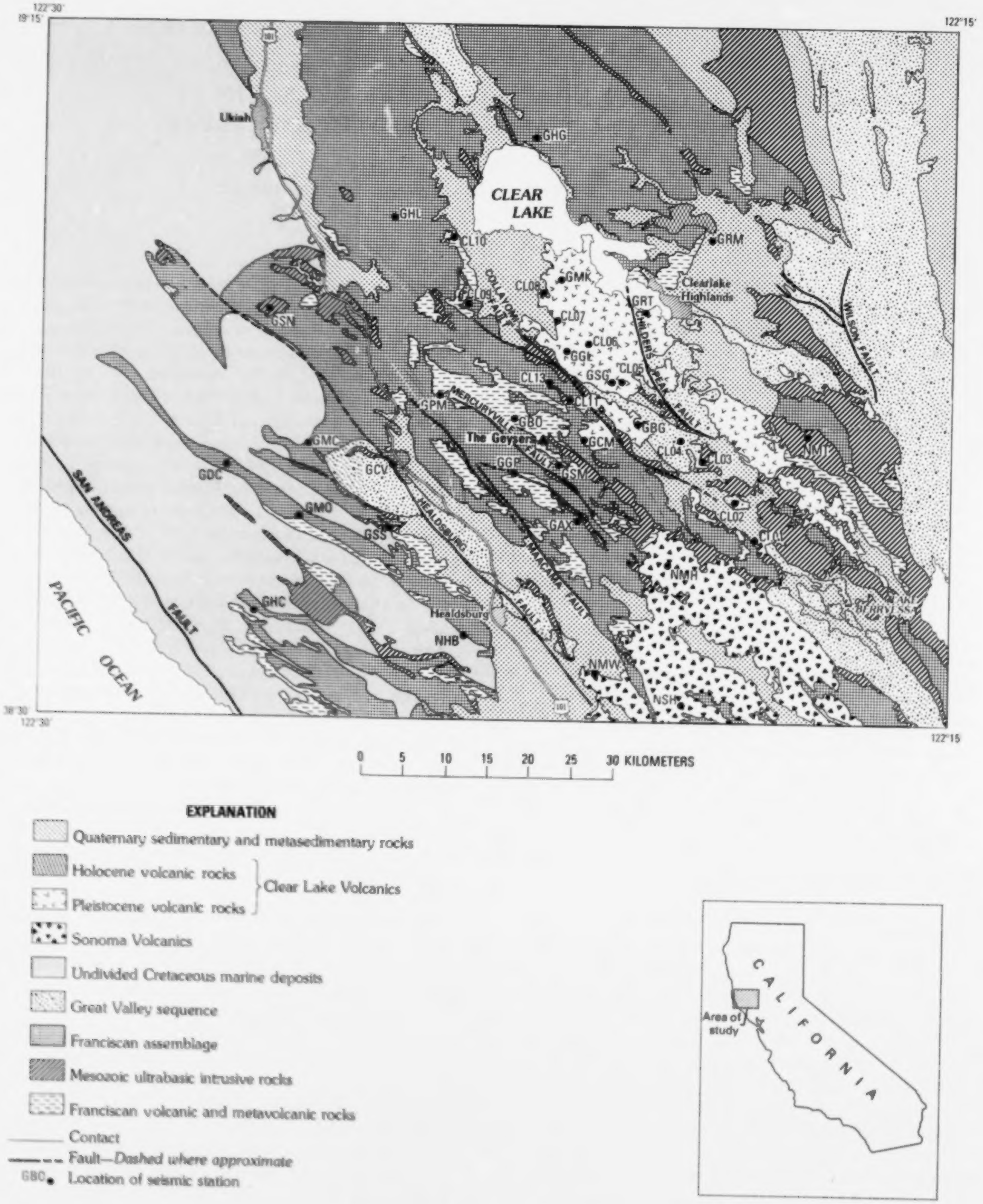
122°30'
39°15'
122°15'
38°30'
122°30'
122°15'
101
Ukiah
GHG
CLEAR
LAKE
GHL
CL10
GRM
GMK
CL08
Clearlake
Highlands
CL09
GRT
GSN
COLLAYOMI FAULT
CL07
CL06
GGL
WILSON FAULT
CL05
GSG
CL13
CL11
GPM
MERCURYVILLE FAULT
GBO
GBG
The Geysers
GMC
GCM
CL04
CL03
NMT
GDC
GCV
GGP
GSM
SAN ANDREAS FAULT
GMO
CL02
HEALDSBURG FAULT
GAX
GSS
CL01
MAACAMA FAULT
NMH
GHC
Healdsburg
NHB
PACIFIC OCEAN
NMW
NSH
101
0 5 10 15 20 25 30 KILOMETERS
EXPLANATION
Quaternary sedimentary and metasedimentary rocks
Holocene volcanic rocks
Pleistocene volcanic rocks
Clear Lake Volcanics
Sonoma Volcanics
Undivided Cretaceous marine deposits
Great Valley sequence
Franciscan assemblage
Mesozoic ultrabasic intrusive rocks
Franciscan volcanic and metavolcanic rocks
Contact
Fault—Dashed where approximate
GBC Location of seismic station
CALIFORNIA
Area of study

FIGURE 48.—Generalized geologic map of the Geysers-Clear Lake area.

proximately −25 mGal in the region (fig. 49) has been interpreted as reflecting the presence of a shallow magma chamber (Isherwood, this volume). Goff, Donnelly, Thompson, and Hearn (1977), analyzing the geochemistry of thermal waters and available geophysical data, postulated a dual hydrothermal system for the Geysers-Clear Lake region, composed of a hot-water system located under the volcanic zone between Clear Lake and the Collayomi fault zone and a vapor-dominated system southwest of Clear Lake under The Geysers (fig. 50; Goff and others, 1977, fig. 5). These studies suggest that the teleseismic residual (*P* delay) technique would be useful in the Geysers-Clear Lake area to delineate the magmatic heat source in the volcanic zone and the steam reservoir under the production zone.

DATA ANALYSIS AND RESULTS

The U.S. Geological Survey has been monitoring the seismicity of the Geysers-Clear Lake region since May 1975, using part of the extensive telemetered seismic network in northern California. In this study we analyzed teleseisms recorded during 1976 and 1977 by 26 stations of this network located between Santa Rosa and Clear Lake (figs. 49, 50). The region south of Clear Lake, the area of study, includes the locations of current geothermal steam production, recent volcanic flows, and the gravity anomaly cited above. In addition to the permanent network, a northwesterly profile of 12 closely spaced portable seismic stations passing through the center of the Mount Hannah gravity anomaly was in operation during July to September 1976. Information regarding the temporary and permanent stations is given in table 5.

READING OF TELESEISMS

Severe signal-shape changes were observed at stations GMK (Mount Konocti), GGL (Glen View), GSG (Siegler Mountain), and GBO (Black Oaks), in comparison to other recording stations. Stations GMK, GGL, and GSG are located on the Clear Lake Volcanics, and GBO is located on the steam-production zone (figs. 48, 50). These changes in signal shape made it difficult to pick the onset of teleseisms recorded by the network; hence, it was necessary to reject a large number of events. Our present study is, therefore, based on only a small fraction of recorded events for which the *P*-wave arrival times could be read with a reasonable degree of confidence. Figure 51 shows two typical teleseisms recorded by the telemetered network. The event originating near the Bonin Islands shows a drastic signal shape change at GGL and less severe, though noticeable, changes at GBO and GMK. The northern Chile events shows strong alternation of signal at GMK. Where extreme variation in signal shapes resulted in ambiguous picks, those stations were rejected for that event. Stations CL05, CL06, and CL07 of the portable network also showed very severe signal-shape changes, and, hence, few readings from these stations were used in this study. Young and Ward (this volume) examined in

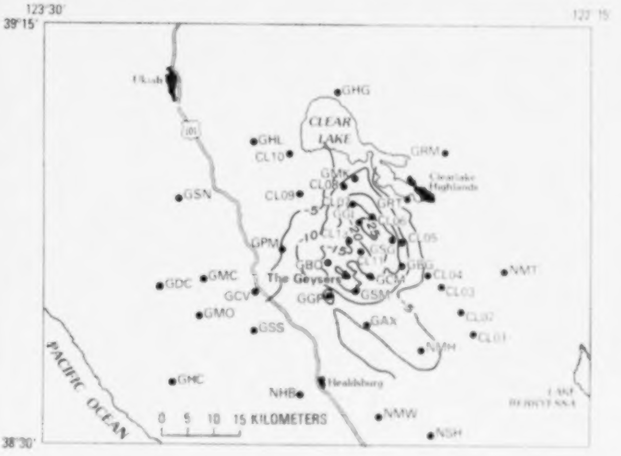
123°30'
122°15'
39°15'
38°30'
Ukiah
GHG
CLEAR LAKE
GHL
CL10
GRM
Clearlake Highlands
GSN
CL09
GMK
CL08
GRT
-5
GPM
-10
CL05
GBO
The Geysers
HBG
CL04
NMT
GDC
GMC
GCV
GGP
GSM
CL03
GMO
CL02
GSS
GAX
CL01
NMH
PACIFIC OCEAN
GHC
NHB
Healdsburg
LAKE BERRYESSA
0 5 10 15 KILOMETERS
NMW
NSH

EXPLANATION

—-5— Residual Bouger gravity in 5-mGal contours

GMO Location of seismic station

FIGURE 49.—Residual gravity map of the Geysers-Clear Lake region (after Isherwood, 1976).

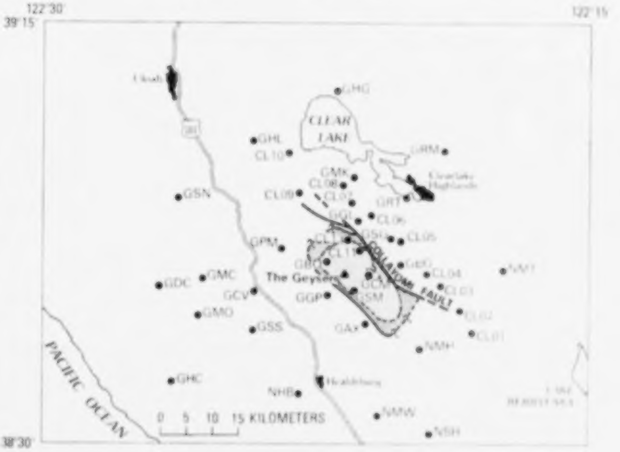
122°30'
122°15'
39°15'
38°30'
Ukiah
GHG
CLEAR LAKE
GHL
CL10
GRM
GMK
CL08
Clearlake Highlands
GSN
CL09
CL07
GRT
GGL
CL06
GSG
CL05
GPM
GBO
HBG
CL04
NMT
The Geysers
COLLAYOMI FAULT
GDC
GMC
GCV
GCM
CL03
GGP
GSM
GMO
CL02
GSS
GAX
CL01
NMH
PACIFIC OCEAN
GHC
NHB
Healdsburg
LAKE BERRYESSA
0 5 10 15 KILOMETERS
NMW
NSH

EXPLANATION

▨ Vapor-dominated area

☐ Approximate steam-production area

GMO● Location of seismic station

FIGURE 50.—Inferred approximate outlines of vapor-dominated and steam-production areas in the Geysers-Clear Lake region.

TABLE 5.—*Geographic information and periods of operation of the seismic stations located south of Clear Lake*

Station		Latitude		Longitude		Elevation	Period of operation
Name	Symbol	(Deg)	(Min)	(Deg)	(Min)	(m)	
Clear Lake	CL01	38	41.74	122	30.67	524	7/4/76-7/22/76, 8/14/76-9/9/76
	CL02	38	44.07	122	32.38	323	7/3/76-7/22/76, 8/14/76-9/9/76
	CL03	38	46.79	122	35.30	330	7/3/76-7/22/76, 8/14/76-9/9/76
	CL04	38	48.30	122	36.95	347	7/3/76-7/22/76, 8/15/76-9/9/76
	CL05	38	52.26	122	42.33	1049	7/4/76-7/22/76, 8/15/76-9/10/76
	CL06	38	54.67	122	42.33	756	7/4/76-7/22/76, 8/16/76-9/9/76
	CL07	38	55.70	122	47.33	622	7/5/76-7/22/76, 8/16/76-9/9/76
	CL08	38	57.90	122	48.71	494	7/4/76-7/22/76, 8/15/76-9/9/76
	CL09	38	56.68	122	54.75	543	7/5/76-7/22/76, 8/15/76-9/9/76
	CL10	39	0.70	122	55.75	463	7/7/76-7/22/76, 8/16/76-9/9/76
	CL11	38	50.84	122	47.15	805	8/19/76-9/5/76
	CL13	38	51.95	122	48.30	786	8/21/76-9/4/76
Alexander Valley	GAX	38	42.65	122	45.30	379	permanent
Boggs Mountain	GBG	38	48.84	122	40.76	1125	permanent
Black Oaks	GBO	38	49.46	122	50.57	879	permanent
Cobb Mountain	GOM	38	48.35	122	45.31	1286	permanent
Cloverdale	GCV	38	46.14	123	0.89	150	permanent
Dry Creek	GDC	38	46.03	123	14.31	772	permanent
Glenview	GGL	38	53.80	122	46.58	893	permanent
Geyser Peak	GGP	38	45.88	122	50.65	1054	permanent
House Creek	GHC	38	36.36	123	11.81	518	permanent
Hogback Ridge	GHG	39	7.70	122	49.47	903	permanent
Highland Springs	GHL	39	2.43	123	1.12	956	permanent
McLaughlin Ranch	GMC	38	47.56	123	7.08	426	permanent
Mount Konocti	GMK	38	58.17	122	47.22	906	permanent
Moffitt Ranch	GMO	38	42.61	123	8.59	802	permanent
Pine Mountain	GPM	38	50.85	122	56.72	783	permanent
Round Mountain	GRM	39	1.23	122	35.06	469	permanent
Round Top Mountain	GRT	38	56.32	122	40.18	619	permanent
Seigler Mountain	GSG	38	52.00	122	42.60	1080	permanent
Socrates Mine	GSM	38	46.16	122	46.88	1017	permanent
Snow Mountain	GSN	38	56.43	123	11.50	870	permanent
Skaggs Springs	GSS	38	42.12	123	0.81	282	permanent
Healdsburg	NHB	38	35.36	122	54.54	165	permanent
Mount St. Helena	NMH	38	40.22	122	38.03	1200	permanent
Middletown	NMT	38	48.34	122	26.76	422	permanent
Mark West Springs	NMW	38	33.03	122	43.37	134	permanent
Saint Helena Road	NSH	38	31.20	122	36.43	328	permanent

detail the signal shape changes and attenuation in the Geysers-Clear Lake area using our data from the portable network.

An Eclipse computer was used to analyze the teleseisms recorded by the permanent network. Data telemetered into Menlo Park, Calif. were multiplexed with IRIGE time code from a digital chronometer and WWVB radio time code and recorded on magnetic tape. The computer was used to search the time code, demultiplex and digitize the signals, and display the data on a cathode-ray tube for interactive manipulation. A digitizing rate of 100 samples per second was used for all events in this study. An interactive picking algorithm allows the user to scale and time-shift individual traces for visual correlation and to determine the consistency of phases by lining up the waveform of all traces (figs. 52). Typically, two picks were made per event, and they were chosen within the first two cycles of the teleseism. The precision of the picks by this method is ±0.1 s.

As the ½-inch tapes from the portable stations could not be manipulated by the Eclipse system, playbacks of teleseisms were manually picked for first breaks using a criterion similar to that of the permanent stations. Correct picks for stations CL05, CL06, CL07, CL11, and CL13 were quite difficult to make. Again, ambiguous picks were rejected in the analysis.

COMPUTATION OF RESIDUALS

The traveltime from the source of the earthquake to the recording station is calculated by subtracting from the arrival time the earthquake origin time reported in the U.S. Geological Survey's *Preliminary Determination of Epicenters* (PDE). The theoretical traveltime is calculated from the standard Herrin traveltime tables using the epicentral distance and depth of the event (Herrin, 1968). From the epicenter location, also reported in the PDE, and the station coordinates, the distance and azimuth of the epicenter from the station are computed. Traveltime residuals are then obtained by subtracting from the observed traveltime the theoretical traveltime. Accordingly, a negative residual indicates an arrival earlier than predicted, and a positive residual (delay) indicates an arrival later than that predicted. Such raw residuals contain the contributions from structures in the crust and upper mantle under the recording station, effects associated with differences in station elevations, contributions due to errors in earthquake location (approximately ±25 km), origin-time errors, and the effects due to earth structure under the earthquake source and along the propa-

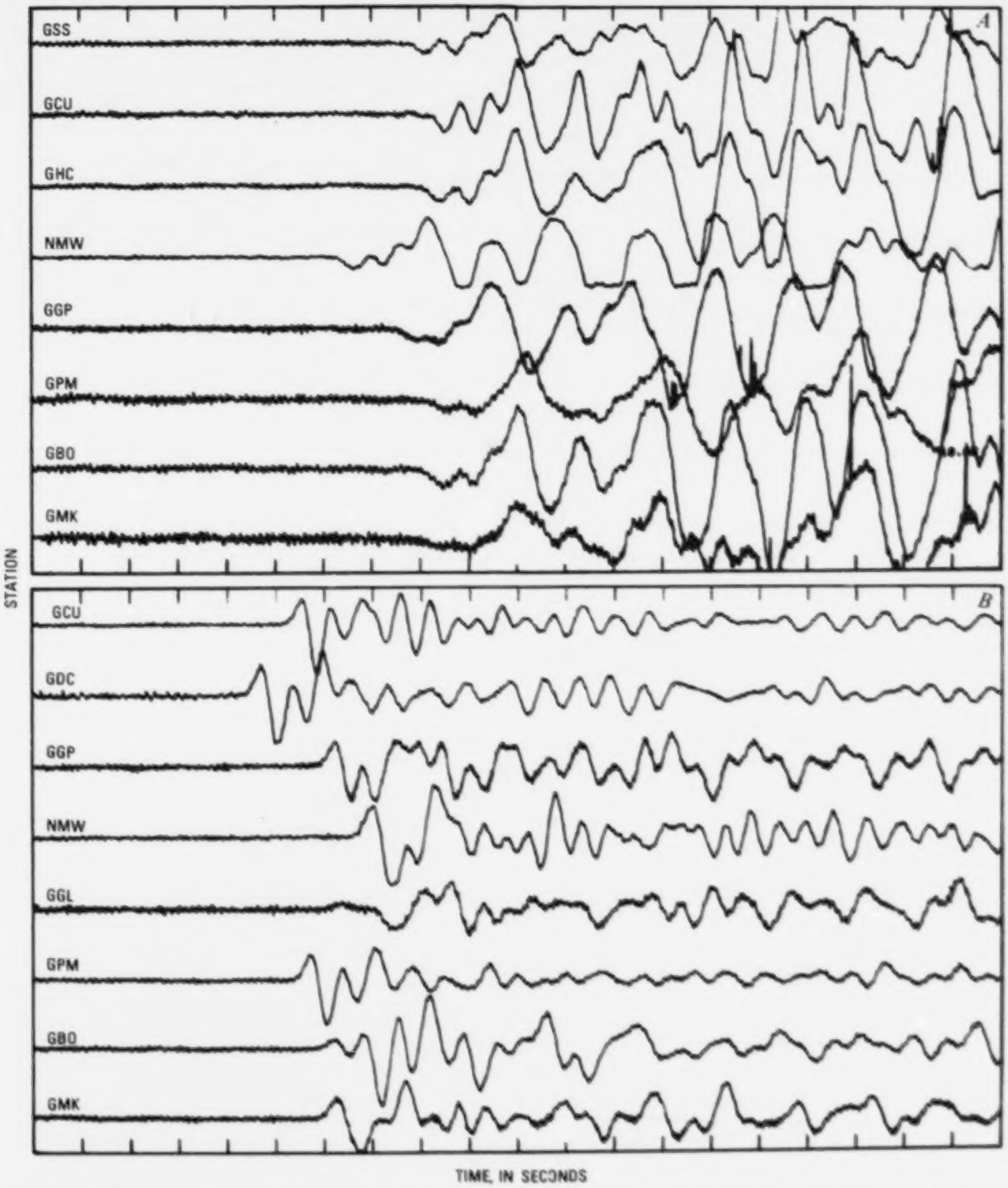

FIGURE 51.—Two teleseisms recorded by telemetered network in the Geysers-Clear Lake region. Only eight stations per event are shown. *A*, Northern Chile, November 30, 1976. *B*, Bonin Islands, December 12, 1976. Note change in signal shape at stations GGL, GBO, and GMK.

gation path of the waves. Together, these effects and resulting errors could be, on an average, as high as ±0.5 second. In addition to these errors, the timing of anything other than first arrivals adds a component to the

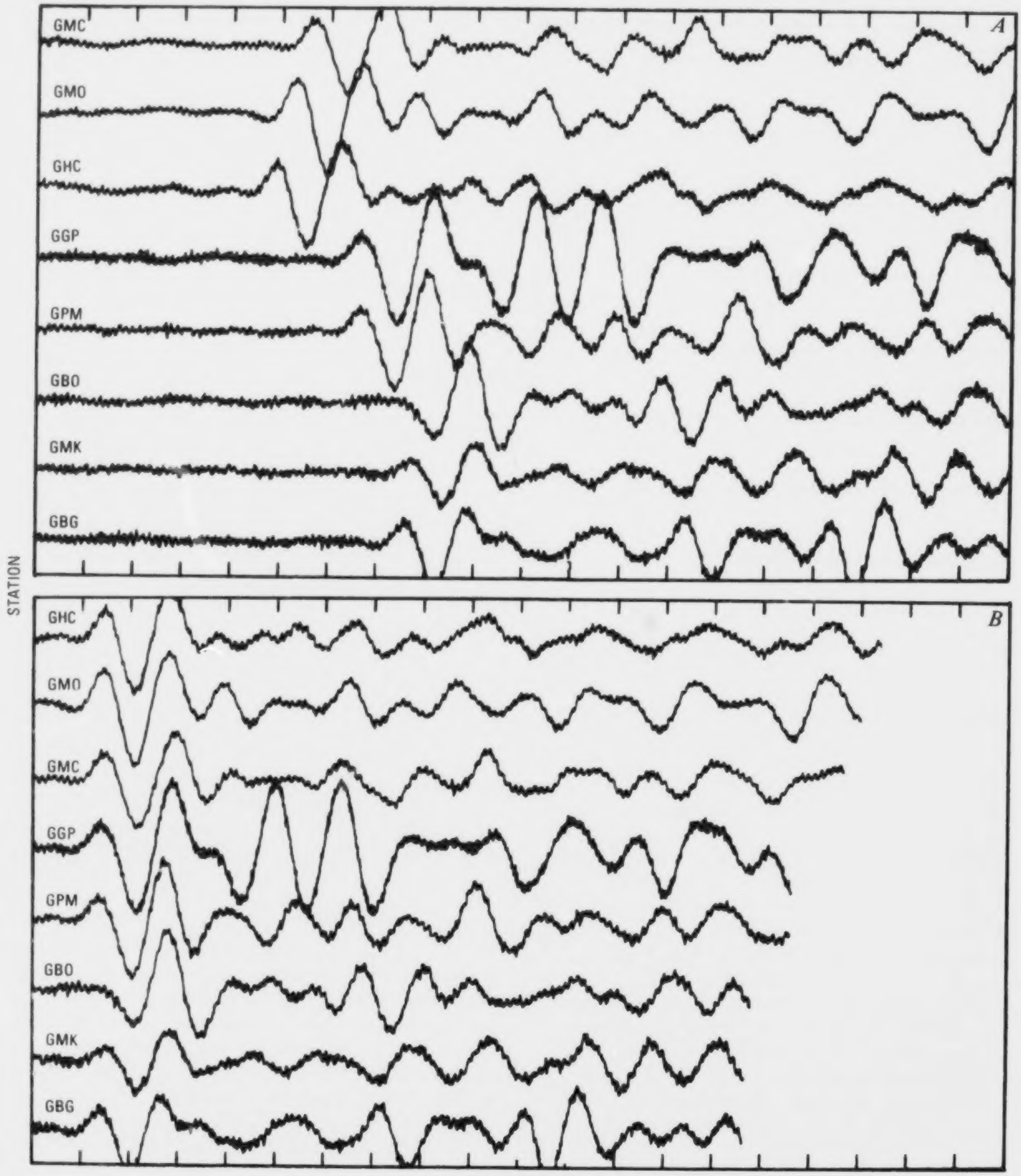

FIGURE 52.—Computer display of a teleseism from Norfolk Island, October 17, 1977, recorded by eight stations of the Geysers-Clear Lake seismic network. *A*, Arranged according to actual arrival times. *B*, Traces shifted by computer to pick time of first break. Note absence of a sharp first break at station GBO.

residuals which is constant for all the stations, neglecting any distortion in signal shape across the seismic array. To correct for these effects, it is common practice to use relative residuals, calculated for each event by subtracting from all raw residuals the raw residual at a reference station. The reference station is normally located well outside the area under investigation. Stations NMW (Mark West Springs) and CL02 were established as the reference stations for the permanent and temporary networks, respectively.

DISTRIBUTION OF TELESEISMS

The 48 teleseisms analyzed in this study were recorded by both the temporary and permanent networks (table 6). They originate mainly in the northwest, southeast, and southwest azimuths. Normally, the events along the soutneast and northwest azimuths have a good distance distribution ranging from 40 to 90 degrees (1 degree = 111 km). These events provide a reverse profile along the northwest-southeast direction and enable the study of crustal and upper mantle structure. The events in the southwest azimuth occur in a narrow distance range of 70° to 90°. Occasionally, events are recorded from other azimuths (for example, Soviet nuclear events occur to the north). The angle measured from the vertical at which the seismic rays reach the surface ranges from 16° to 26° for distances 40° to 90°. An optimum use of the total possible distribution of events in distance and azimuth was not achieved because in this study only selected events of superior quality were analyzed. A more detailed study, including a three-dimensional mathematical inversion of teleseismic residual data, has been completed.

SPATIAL DISTRIBUTION OF RELATIVE RESIDUALS

The relative residuals with respect to stations NMW and CL02 have been averaged for each of the three main aziumuth groups (table 7). The unaveraged residuals for events along the three prime azimuths as a function of distance at stations GGL, GSG, GMK, and GBO are shown in figures 53*A*, *B*, *C*, and *D*, respectively. The data have been corrected for elevation differences by assuming a normal surface velocity of 6.0 km/s along the ray path. Results for events from the southwest azimuth exhibit the largest relative residuals (relative residuals hereafter will be called residuals or delays). For this azimuth the residuals in seconds are shown near station locations in figure 7*A*. Delays greater than 0.5 s coincide with a region that exhibits a gravity low defined by values less than −15 mGal (fig. 49). The delay field is dominated by large values of 1.5 s at stations GGL and CL06, 0.9 s at station GSG in the vicinity of GGL, and 1.1 s at GBO in the steam-production area. The few readings available at stations CL11 and CL13 indicate that the large delays at GBO and GGL represent two separate maxima within the general 0.5-s delay field. Note that the gravity low also exhibits dual minima (fig. 49); Isherwood (this volume) describes the −25 mGal low near the southwest edge of the Quaternary volcanic field as the "Mount Hannah low" and the secondary −15 mGal low in the region of steam production as the "production low." The correspondence between the teleseismic delays and gravity lows suggests that both reflect the presence of the same bodies composed of material of relatively low compressional velocity and density. A broad, low-velocity zone underlies not only the region of Cenozoic volcanism bounded by Mount Konocti, Mount Hannah, and Cobb Mountain, but also the Mesozoic Franciscan complex to the west. Superimposed on this low-velocity zone are the very low velocities under Mount Hannah and under the steam production zone. Note the extremely small relative delays at all the stations to the west and south of the 0.2-s contour; these small values, which are within the noise level of our data, indicate that the crustal structure to the south and west of the anomalous region is fairly homogenous. This homogeneity over a large area confirms the appropriateness of the choice of reference stations NMW and CL02. Also, note that the small delays at stations GGP (Geyser Peak), GSM (Socrates mine), GPM (Pine Mountain), and GCV (Cloverdale) constrain the possible extent of the production zone anomaly to a narrow zone a few kilometers southwest of GBO. In the absence of data in this region, the contours are drawn such that the larger delays lie within the extent of the production low. There is also considerable uncertainty in the definition of the low-velocity zone northeast of the main anomaly. Stations GRT (Round Top Mountain) amd GRM (Round Mountain) both show about 0.3 s delay. It is not clear whether these delays are associated with the main anomalies or are due to station effects. Similarly, GHG to the north and NMT to the south show about 0.25 s delays. Because of these uncertainties, the 0.2-s contour is left open on the northeast.

Figure 54*B* depicts the spatial distribution of average delays for events from the northwest azimuth. Details of the data are given in table 7 and figures 6*A*-*D*. Figures 53*A*, 53*D*, 54*A*, and 54*B* demonstrate that delays for the northwest azimuth in comparison with the southwest azimuth are lower by about 0.7 s at GGL and 0.5 s at GBO. GSG has roughly the same delay of about 0.9 s for both azimuths, and the residual anomaly is now centered at this station. Note that the dual peaks in delay contours seen for the southwest events do not appear at this azimuth, although the magnitude of the average delay field (0.5 s) and the spatial extent are quite similar for both data sets. As previously noted,

TABLE 6.—*List of teleseisms*

Event location	Date	Origin time (G.m.t.)			Depth (km)	Lat N.		Long W.		Distance/azimuth to GCL (degrees)	Numbers of stations recording
		H	M	S		Deg	Min	Deg	Min		
Kermadec Islands	1/24/76	21:	48:	25.9	78	−28	38.10	177	35.60	84.5/226.2	19
Fiji Islands	2/03/76	12:	27:	30.1	477	−25	8.20	−179	41.60	83.4/230.3	24
Colombia	5/19/76	4:	7:	15.8	157	4	27.80	75	47.00	54.6/116.6	22
Kermadec Islands	6/29/76	18:	30:	9.1	48	−33	49.00	177	50.00	88.5/223.1	24
*Kamchatka	7/10/76	11:	37:	12.8	387	47	24.00	−145	42.00	63.8/310.8	8
*Panama	7/11/76	16:	54:	31.8	22	7	18.00	78	30.00	50.5/116.6	5
*Panama	7/11/76	20:	41:	47.5	3	7	24.00	78	6.00	50.7/116.2	9
*Panama	7/17/76	2:	5:	22.0	25	5	48.00	82	42.00	48.7/122.0	7
*New Britain	7/17/76	21:	6:	32.1	53	−4	12.00	−152	48.00	88.4/263.4	5
*Kermadec Islands	7/20/76	22:	51:	43.1	370	−31	12.00	180	0.00	87.7/226.3	6
*Kuril Islands	7/22/76	6:	57:	22.1	79	46	12.00	−151	30.00	60.9/307.5	8
*Fiji Islands	8/15/76	18:	43:	45.0	509	−25	7.80	−179	42.00	83.4/230.5	3
*Aleutians	8/16/76	5:	11:	38.9	65	51	30.00	178	24.00	40.5/307.1	5
*Kamchatka	8/16/76	12:	28:	32.4	50	51	55.20	−158	25.80	54.5/311.6	5
*China	8/16/76	14:	6:	45.9	16	32	48.00	−104	12.00	96.6/321.9	4
*Chile	8/20/76	6:	54:	11.3	81	−20	24.00	70	0.00	76.7/130.1	6
*Alaska	8/22/76	2:	1:	47.4	144	60	12.00	153	18.00	28.9/328.1	6
*New Hebrides	8/22/76	21:	9:	41.9	31	−14	0.00	−170	54.00	81.2/244.3	10
*China	8/23/76	3:	30:	7.6	33	32	30.00	−104	12.00	96.9/321.7	10
*Chile	8/24/76	21:	26:	12.2	8	−25	18.00	70	42.00	80.1/133.7	8
*Aleutians	8/28/76	2:	30:	9.2	145	52	36.00	175	18.00	38.5/308.8	10
*Kermadec Islands	8/31/76	9:	6:	50.4	55	−30	6.00	178	6.00	85.8/225.8	9
*Kermadec Islands	8/31/76	13:	22:	10.9	51	−28	18.00	176	36.00	83.6/225.9	10
*New Hebrides	9/01/76	13:	25:	29.8	75	−20	24.00	−169	24.00	86.7/240.6	10
*Guatemala	9/02/76	10:	20:	25.9	81	13	18.00	90	0.00	38.3/122.4	7
*Solomon Islands	9/04/76	11:	41:	59.7	83	−10	12.00	−161	6.00	85.9/253.6	8
Kuril Islands	9/22/76	0:	16:	8.2	64	44	52.80	−149	13.50	62.6/306.9	24
Fiji Islands	11/25/76	14:	6:	35.4	442	−19	29.90	177	42.30	77.6/232.2	23
Chile	11/30/76	0:	40:	57.8	88	−20	31.20	68	55.10	77.7/129.2	22
Kazakh SSR	12/07/76	4:	56:	57.4	1	49	53.00	−78	54.30	89.5/346.2	19
Bonin Islands	12/12/76	1:	8:	50.1	491	28	2.60	−139	34.50	78.4/296.6	20
Ryukyu Islands	12/14/76	16:	6:	44.4	41	28	17.60	−130	41.90	84.3/301.8	24
Argentina	2/04/77	7:	46:	33.8	549	−24	41.30	63	21.70	84.2/128.1	22
Honshu, Japan	2/18/77	20:	51:	29.8	42	33	4.30	−140	49.00	74.5/300.0	24
Korea	3/09/77	14:	27:	53.6	528	41	36.40	−130	52.70	75.6/312.0	22
Kuril Islands	3/19/77	10:	56:	25.1	70	44	12.00	−148	11.80	63.6/306.6	16
Peru	4/09/77	4:	4:	12.5	564	−10	0.90	71	10.90	68.3/123.8	24
Honshu, Japan	4/20/77	20:	4:	29.4	493	30	35.90	−137	29.00	78.3/299.8	24
Solomon Islands	4/21/77	4:	24:	9.6	33	−9	57.90	−160	43.90	85.9/253.8	21
Fiji Islands	6/17/77	2:	29:	9.8	690	−19	52.60	179	5.90	78.7/233.0	21
Tonga Islands	6/22/77	12:	8:	28.3	33	−23	11.40	175	55.20	79.3/228.5	17
Fiji Islands	7/06/77	11:	28:	31.5	594	−21	4.10	178	34.40	79.3/231.8	21
Rat Islands	9/04/77	15:	40:	57.4	33	51	24.00	−178	25.80	42.2/307.0	18
Rat Islands	9/04/77	23:	20:	44.3	33	51	24.60	−178	21.60	42.2/307.1	21
Peru	10/08/77	3:	3:	38.3	100	−10	37.20	73	39.00	67.2/126.3	18
Fiji Islands	10/10/77	11:	53:	56.3	33	−25	39.60	174	46.80	80.6/226.1	21
Tonga Islands	10/14/77	4:	55:	33.8	33	−15	44.40	173	19.20	72.0/231.4	22
Norfolk Islands	10/17/77	17:	26:	40.3	33	−27	52.80	−172	52.80	89.6/232.9	22

*Teleseisms recorded by the temporary seismic network.

TABLE 7.—*Mean relative residuals and their standard deviations for three azimuth groups*

Station	Azimuth		Distance		Number of events	Relative residual (s)	Standard deviation (s)
	Range	Deg.	Range	Deg.			
CL01	116.2	133.7	48.7	80.0	5	0.13	0.05
	225.8	263.4	81.2	88.5	8	0.12	0.08
	307.2	328.1	28.9	96.9	8	0.12	0.05
CL02	116.2	133.7	38.3	80.1	6	0.00	0.00
	225.8	263.4	81.2	88.4	8	0.00	[1]0.00
	307.1	328.1	28.9	96.9	8	0.00	[2]0.00
CL03	116.2	133.7	38.4	80.1	5	0.08	0.07
	225.7	263.4	81.2	88.4	8	0.01	[1]0.11
	307.1	328.1	28.8	96.8	7	0.10	[2]0.03
CL04	116.1	133.7	38.5	80.2	5	0.04	0.12
	225.7	263.4	81.2	88.4	7	0.15	[1]0.11
	307.1	328.1	28.8	96.8	8	0.35	[2]0.05

TABLE 7.—*Mean relative residuals and their standard deviations for three azimuth groups*—Continued

Station	Azimuth		Distance		Number of events	Relative residual (s)	Standard deviation (s)
	Range	Deg.	Range	Deg.			
CL05	116.1	122.4	38.5	50.9	3	0.19	0.12
	225.8	263.3	81.2	88.3	3	0.68	[3]0.41
	307.0	328.0	28.7	96.7	8	1.06	[2]0.31
CL06	116.1	122.4	38.6	50.9	3	0.83	[3]0.47
	225.8	244.1	81.2	86.6	3	1.46	[1]0.23
	307.4	321.6	60.7	96.6	3	1.53	[2]0.13
CL07	116.1	133.6	38.6	80.3	4	0.44	0.06
	225.6	253.4	83.6	86.6	4	0.35	[1]0.14
	308.6	310.7	38.2	63.6	2	0.16	[2]0.03
CL08	116.1	122.4	38.6	51.0	3	0.23	0.09
	225.6	253.4	83.6	86.6	4	0.24	[1]0.07
	308.5	321.5	38.2	96.6	3	0.24	[2]0.16
CL09	121.7	133.5	49.1	80.4	3	0.12	0.09
	225.5	253.3	81.1	87.7	6	− 0.01	[1]0.13
	307.3	321.5	38.2	96.5	3	− 0.28	[2]0.07
CL10	121.7	133.5	49.1	80.5	3	− 0.13	0.11
	225.5	244.0	81.1	87.7	4	− 0.12	[1]0.11
	307.3	328.0	28.5	63.4	4	− 0.19	0.06
CL11	240.5	253.4	81.1	86.6	3	0.47	[1]0.13
	308.6	321.5	38.3	96.7	2	0.55	0.20
CL13	129.9	133.6	76.9	80.3	2	0.63	0.12
	225.6	244.1	81.1	86.5	3	0.46	[1]0.14
	321.5	....	96.6	....	1	0.69	...
GAX	116.5	129.2	54.4	84.0	5	− 0.15	0.03
	223.1	253.8	71.9	89.4	11	− 0.01	0.07
	296.6	312.1	42.3	84.4	7	0.05	0.10
GBG	116.6	129.3	54.5	84.1	5	− 0.01	0.06
	226.2	253.9	72.0	89.5	10	0.41	0.10
	299.9	312.1	42.3	84.4	7	0.56	0.12
GBO	116.5	129.2	54.6	84.2	5	0.30	0.04
	223.0	253.8	71.9	89.4	11	1.07	0.31
	296.6	312.0	42.2	84.3	9	0.66	0.21
GCM	116.6	129.2	54.6	84.1	4	− 0.20	0.11
	223.1	253.1	72.0	89.5	11	0.38	0.09
	296.6	312.0	42.3	84.4	9	0.58	0.10
GCV	116.3	129.0	54.7	84.2	5	0.17	0.06
	222.9	232.8	71.8	89.3	8	0.17	0.04
	296.5	307.2	42.1	84.2	7	0.10	0.15
GDC	116.1	128.9	54.9	84.4	5	0.07	0.08
	222.8	253.5	71.6	88.2	9	0.06	0.08
	296.4	311.8	42.0	84.1	9	0.01	0.10
GGL	116.6	129.2	54.6	84.2	5	0.63	0.07
	223.1	233.0	72.0	88.5	6	1.50	0.21
	299.8	312.0	74.5	84.2	4	0.67	0.29
GGP	116.4	129.1	54.6	84.1	4	− 0.07	0.08
	223.0	253.8	71.9	89.4	11	− 0.01	0.07
	296.6	312.1	42.3	84.4	7	0.05	0.10
GHC	116.0	128.9	54.8	84.3	5	− 0.02	0.05
	222.8	253.6	71.6	89.1	11	− 0.05	0.06
	296.4	311.9	42.1	84.2	9	− 0.05	0.11
GHG	123.9	129.2	68.5	84.3	3	0.18	0.10
	226.2	232.2	77.7	88.7	4	0.26	0.08
	296.5	311.9	42.1	84.2	6	0.26	0.15
GHL	116.5	129.1	54.9	84.4	5	− 0.01	0.02
	222.9	253.6	71.9	89.5	11	0.08	0.06
	296.4	311.9	42.0	84.1	9	0.00	0.07

TABLE 7.—*Mean relative residuals and their standard deviations for three azimuth groups*—Continued

Station	Azimuth		Distance		Number of events	Relative residual (s)	Standard deviation (s)
	Range	Deg.	Range	Deg.			
GMC	116.2	128.9	54.8	84.3	5	0.07	0.05
	222.8	253.6	71.7	89.3	11	−0.03	0.05
	296.4	311.9	42.1	84.1	9	−0.09	0.10
GMK	123.9	129.2	68.4	84.2	3	0.00	0.14
	223.0	253.8	72.0	89.6	11	0.41	0.15
	296.6	312.0	42.2	84.3	9	0.41	0.08
GMO	116.2	128.9	54.8	84.3	5	−0.17	0.04
	222.8	253.8	71.7	89.2	11	−0.14	0.06
	296.4	311.9	42.1	84.2	9	−0.19	0.09
GPM	116.4	129.1	54.6	84.2	4	0.02	0.06
	223.0	253.8	71.9	89.4	10	0.20	0.07
	296.6	312.0	42.2	84.3	9	0.15	0.07
GRM	116.8	129.4	54.5	84.1	5	−0.04	0.09
	223.3	253.9	72.2	89.7	6	0.35	0.08
	296.7	312.1	62.7	84.4	6	0.45	0.18
GRT	116.7	129.3	54.6	84.1	5	−0.26	0.08
	223.1	253.9	72.1	89.6	11	0.33	0.09
	299.8	312.1	42.3	84.4	6	0.32	0.14
GSG	123.9	126.3	67.1	68.3	2	−0.01	0.07
	231.5	253.9	72.0	89.6	4	0.92	0.10
	299.8	312.0	42.3	78.4	4	0.99	0.10
GSM	116.5	129.2	54.6	77.6	3	−0.18	0.04
	223.1	253.8	77.5	88.4	6	0.12	0.15
	296.6	306.9	62.7	84.4	6	0.40	0.11
GSN	123.5	128.9	67.5	84.5	4	0.17	0.05
	222.8	253.5	71.8	89.3	11	0.14	0.07
	299.6	311.8	41.9	84.0	8	0.06	0.10
GSS	116.3	129.0	54.7	84.2	5	0.00	0.03
	222.9	253.7	71.7	89.3	10	−0.09	0.07
	296.5	311.9	42.4	84.3	9	−0.04	0.10
NHB	116.3	129.1	54.6	77.6	2	−0.04	0.07
	223.0	233.0	71.7	89.3	8	−0.06	0.06
	296.6	307.4	42.3	84.4	6	−0.07	0.09
NMH	116.6	128.2	54.4	83.9	3	−0.18	0.04
	223.1	233.1	78.7	89.5	6	0.08	0.17
	299.9	307.0	62.9	78.5	4	0.09	0.03
NMT	116.8	124.1	54.3	68.1	2	−0.25	0.07
	223.3	233.1	77.7	89.7	5	0.21	0.08
	296.8	307.0	62.9	84.6	5	0.41	0.06
NMW	116.4	129.2	54.4	83.9	5	0.00	0.00
	223.1	253.9	71.8	89.4	5	0.00	0.00
	296.7	312.1	42.5	84.5	9	0.00	0.00
NSH	116.5	129.3	54.3	83.8	5	−0.13	0.08
	223.2	253.9	71.9	89.4	11	−0.04	0.04
	296.8	312.1	42.5	84.6	9	−0.02	0.06

Adjustment of +0.08 seconds necessary to account for differences in reference station locations for southwest events.

Adjustment of +0.02 seconds necessary to account for differences in reference station locations for northwest events.

Value rejected in depth computation.

the boundaries of the delay field are constrained on all sides except northeast of the main anomaly. The delays at GHG, GMK, GRT, GRM, and NMT are approximately 0.4 s outlining a broad region northeast of Clear Lake.

As mentioned earlier, the data from the northwest and southeast azimuths, when analyzed together, provide reverse profile information. Reversal in azimuths allows one to determine whether the observed anomalies are associated with surface features or with a deeper structure, such as a magma body. In this context a comparison between the northwest delay pattern (fig. 54*B*) and the southeast pattern (fig. 54*C*) demonstrates that delays greater than 0.5 s occur over a much narrower zone for events arriving from the southeast as opposed to the northwest. Several stations to the south and southeast of GGL, which showed large northwest delays (for example GSG, GCM, and GBG) show very small southeast delays. A clear change in the pattern of delays is observed as the source direction is reversed; the change most apparent south of the main anomaly. Figure 55, a profile of the northwest and southeast delays along a northwest line passing through GGL, clearly demonstrates this effect; the largest delays occur at different locations as the azimuth of travel of the seismic waves is reversed. For the southeast azimuth the largest delay, 0.6 s, occurs at GGL, whereas for the northwest azimuth the largest delay, 1 s, occurs at GSG. Note also that the two delay profiles are different in appearance; the southeast profile has a much narrower peak than the northwest profile. The peak of the Bouguer gravity profile (fig. 55) coincides with the peak for delays from the southeast. Because of the complex delay patterns, interpretation of the Geysers-Clear Lake data in terms of a simple body at depth will be more complicated than in the case of Long Valley (Steeples and Iyer, 1976b).

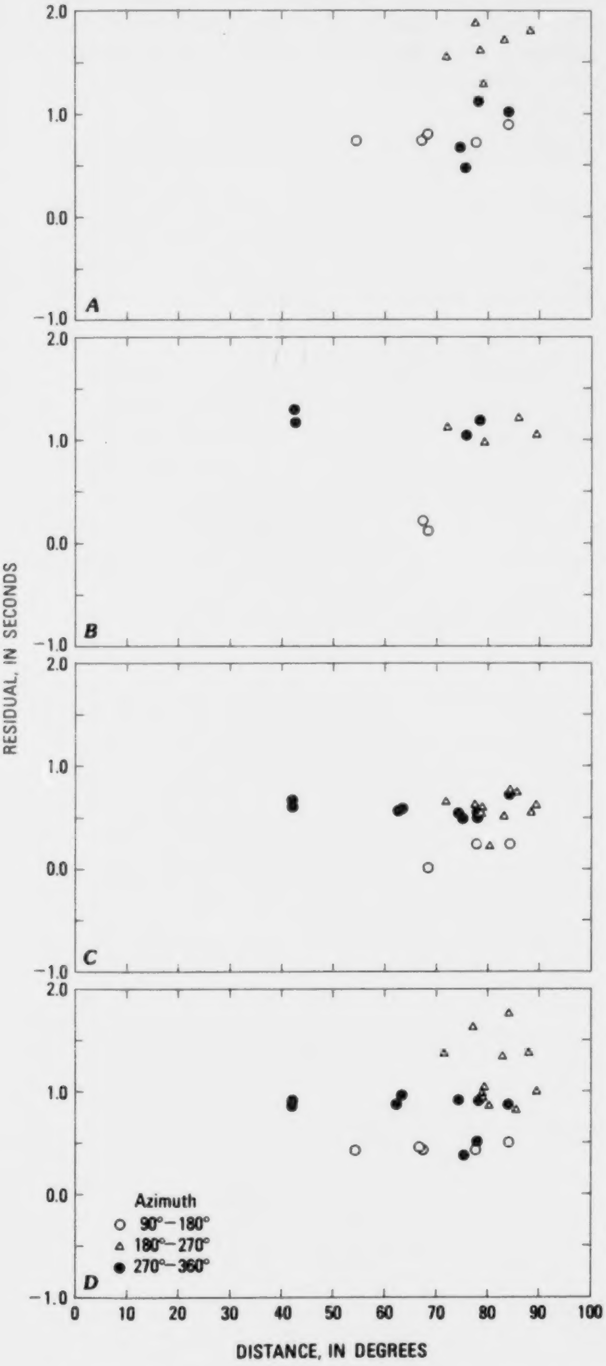

FIGURE 53.—Variation of relative residuals as a function of distance and azimuth at stations in the Geysers-Clear Lake area. *A*, GGL. *B*, GSG. *C*, GMK. *D*, GBO.

DISCUSSION

The large teleseismic delays in the Geysers-Clear Lake region can be broadly divided into three components: (1) the general delay field of 0.5 s amplitude centered at Mount Hannah and extending into the steam production zone to the southwest, (2) the large delays of 1 s and greater observed in the vicinity of Mount Hannah, and (3) the large delay at station GBO in the steam production zone. It is not difficult to interpret these observations in terms of a crustal magma chamber under Mount Hannah and a magma chamber overlain by a dry-steam reservoir under the production zone. In fact, the recent volcanism in the Geysers-Clear Lake region, the availability of thermal energy, and the presence of gravity lows are all indications of the presence of a magmatic heat source. The presence of a magma chamber at depth under Mount Hannah was first suggested by Chapman (1966) to explain the large gravity low in the region. Isherwood (1976), analyzing recent gravity and aeromagnetic data, modeled a magma chamber 10-15 km in diameter with its center at a depth of 15 km under Mount Hannah and estimated the magma to be above the Curie temperature (550°C). If it is assumed that there is a velocity decrease of 15 percent inside a magma body of 15 km diameter, a maximum delay of about 0.5 s can be expected over the body. Such a velocity contrast appears reasonable, based on observations at Long Valley (Steeples and Iyer, 1976a, b) and Yellowstone (Iyer and Stewart, 1977; Iyer, 1979), for a crustal magma chamber. However, in order to explain the large delays in excess of 1 s at GBO (over the production zone) and at GGL and surroundings, it is necessary to postulate an unusually large velocity contrast within a body of realistic size or an unusually large body with reasonable contrast. Iyer (1979) found that a body approximately 150-250 km deep with a velocity contrast of 5-15 percent was required to explain the 1.5-s delay observed inside the Yellowstone caldera. The spatial distribution of delays for various azimuths in the Geysers-Clear Lake area excludes the deep-body hypothesis and suggests that unusually large velocity contrasts are necessary to explain the large delays.

Magma alone need not be the causative mechanism for low seismic velocities. Theoretical and laboratory results suggest that a large compressional velocity decrease can occur in rock containing an abundance of dry cracks (Birch, 1960; Walsh, 1965). Thus, a dry-steam system, such as that postulated under the production zone, may also be at least partly responsible for the observed delays in that region. A tentative interpretation of the delay field in the Geysers-Clear Lake area, therefore, is that it reflects the presence of a magmatic body in which the seismic velocity decreases by about 15 percent regionally but which has greater velocity decrease under Mount Hannah (because of a higher degree of partial melting than in the surrounding rock) and in the production zone (because of the presence of a dry-steam system over the partially molten rock). However, before pursuing this line of interpretation, it is necessary to examine the effect of local geologic structure on the delays.

EFFECT OF LOCAL GEOLOGIC STRUCTURE

Seismic wave velocities are a function of local geologic structure near the seismic recording stations. The anomalous stations GGL and GSG are located on the Clear Lake Volcanics, a complex sequence of volcanic rocks overlying an unknown thickness of rocks of the Great Valley sequence and ophiolite on a Franciscan basement complex. Station GBO, showing a maximum delay of 1.0 s for the southwest azimuth, is located over the Franciscan metavolcanic rocks in a region of complex geology (McLaughlin, this volume) and is within the steam production zone (Goff and others, 1977). However, we shall show that results based on seismic-refraction surveys indicate that the

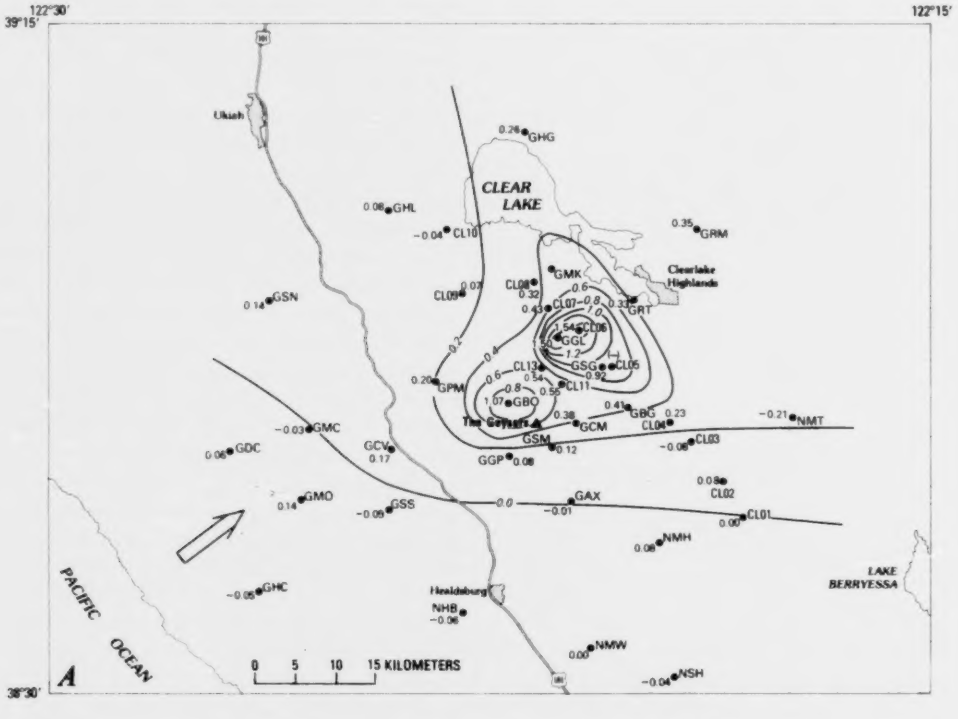
122°30'
39°15'
122°15'
38°30'
Ukiah
CLEAR LAKE
Clearlake Highlands
The Geysers
Healdsburg
PACIFIC OCEAN
LAKE BERRYESSA
0.26 GHG
0.08 GHL
-0.04 CL10
0.35 GRM
0.14 GSN
CL09 0.07
CL08 0.32
GMK
0.43 CL07
0.33 GRT
1.54 CL06
GGL
CL13
0.54
GSG
CL05
0.92
CL11
0.55
0.20 GPM
1.07 GBO
0.38 GCM
0.41 GBG
0.23 CL04
-0.21 NMT
GSM 0.12
-0.06 CL03
GGP 0.08
-0.03 GMC
0.06 GDC
GCV 0.17
0.08 CL02
0.14 GMO
-0.08 GSS
GAX -0.01
0.00 CL01
0.08 NMH
-0.06 GHC
NHB -0.06
0.00 NMW
-0.04 NSH
0.0
0.2
0.4
0.6
0.8
1.0
1.2
A
0 5 10 15 KILOMETERS

FIGURE 54.—Relative residual contour maps. *A*, Southwest events. To adjust for differences due to reference station locations, 0.08 has been added to all temporary-station residuals. *B*, Northwest events. To adjust for differences due to reference station locations, 0.20 has been added to all temporary-station residuals. *C*, Southeast events.

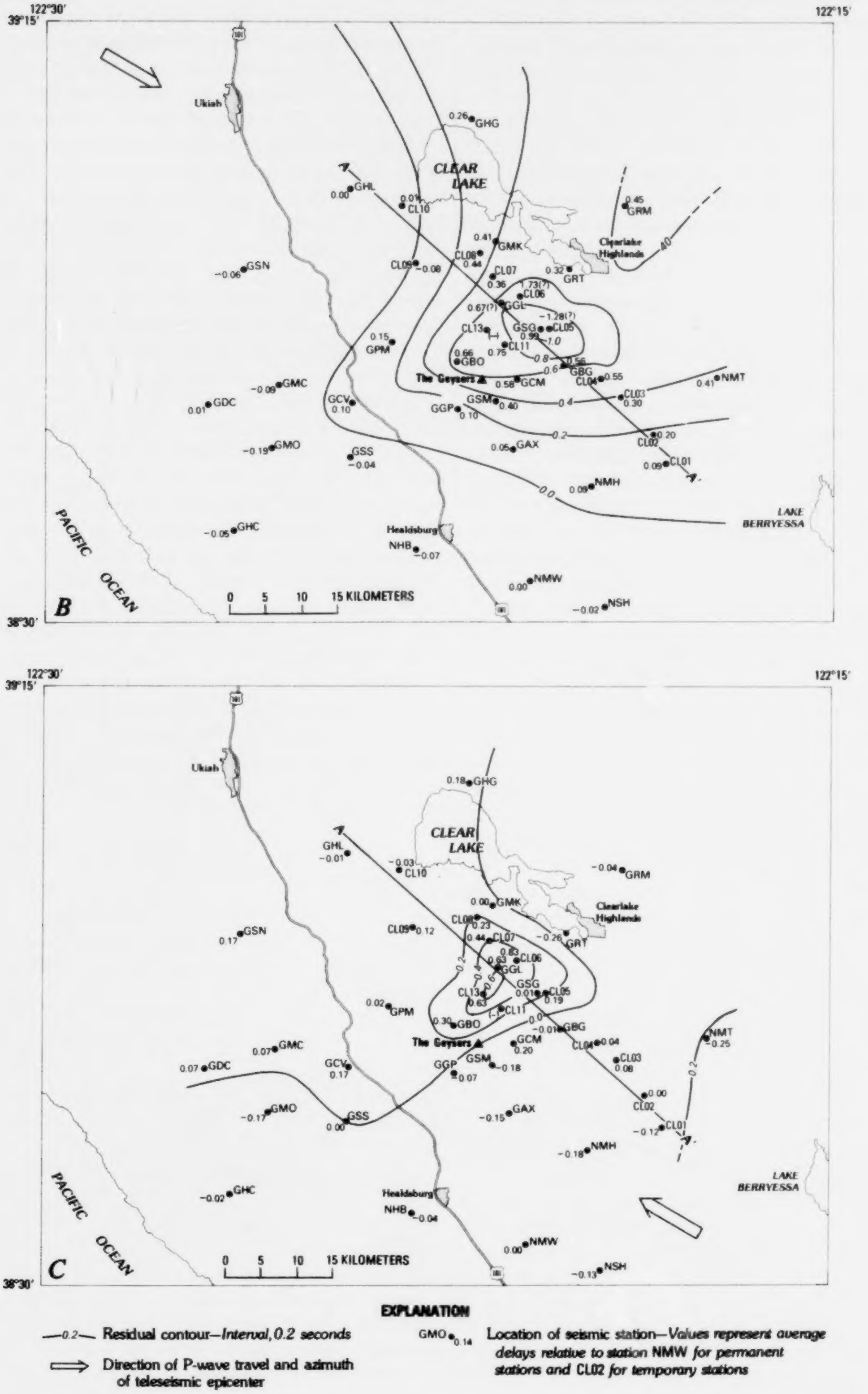
122°30'
122°15'
39°15'
38°30'
B
C
Ukiah
CLEAR LAKE
Clearlake Highlands
The Geysers
Healdsburg
LAKE BERRYESSA
PACIFIC OCEAN
0 5 10 15 KILOMETERS
A
A'
GHG
GHL
CL10
GSN
CL09
GMK
CL08
CL07
CL06
GGL
CL13
GSG
CL05
CL11
GBO
GBG
CL04
GCM
GPM
GMC
GDC
GCV
GSM
GGP
CL03
CL02
CL01
GAX
GMO
GSS
NMH
NMT
GRM
GRT
GHC
NHB
NMW
NSH
0.0
0.2
0.4
0.6
0.8
1.0
0.40
-0.2

EXPLANATION

—0.2— Residual contour—*Interval, 0.2 seconds*

⟹ Direction of P-wave travel and azimuth of teleseismic epicenter

GMO ● 0.14 Location of seismic station—*Values represent average delays relative to station NMW for permanent stations and CL02 for temporary stations* delays associated with the top 5 km under these stations are only on the order of a few tenths of a second.

During September 1976 the U.S. Geological Survey fired five shots in the Geysers-Clear Lake area to study the regional crustal structure. In an attempt to evolve velocity and attenuation models for the Geysers steam production zone, Majer and McEvilly (1979) analyzed data from two of the shots (Skaggs Springs and The Geysers) recorded by the U.S. Geological Survey telemetered network and an array of 13 closely spaced portable stations. Using data from a selected group of U.S. Geological Survey stations which are not located on the young volcanic rocks, they found best-fitting regional velocities of 4.49 and 4.98 km/s, respectively, for the top two layers in the upper 3 km of the crust. Station GMK showed the largest refraction delays, 0.2 to 0.45 s, with respect to this model. Stations GBO, GGL, and GSG, which show large teleseismic delays, were delayed by only 0.1 s for the shots, and were similar to teleseismically nonanomalous stations GPM and GGP. Thus, it appears that the contribution to the delays due to structure in the top 2-3 km of the crust at these stations is quite small. Using data from the closely spaced array of portable stations oriented in a northeasterly direction perpendicular to the regional geologic trends with the center of the array located about 2.5 km GBO, Majer and McEvilly postulated a model for the top 3 km of the crust in its vicinity. This model shows a thin layer of high-velocity, high-*Q* (low attenuation) material underlain by a low-velocity zone of unknown thickness. The important finding from our point of view is that the top few kilometers of the crust contributed only about ±0.1 s to the anomalous delay observed at station GBO in the production zone and at stations GGL and GSG in the volcanic zone.

Warren (this volume), in an attempt to estimate the seismic velocity in the top few kilometers of the volcanic zone, also analyzed the data from the Skaggs Springs explosion recorded by the group of northeasterly stations including the anomalous stations GGL, GSG, and GBO (Warren's stations GLV, SGM, and BKO). He fitted the data to a crustal model in which the top 3.7 km is made up of two layers with velocities 4.2 and 5.2 km/s, respectively. These velocities are somewhat different from those of Majer and McEvilly. However, Warren found more significant differences in the refraction residuals; the delays at stations GGL and GSG are 0.3-0.4 s (see fig. 97 of his paper). According to Warren's model, GBO does not show any delays. We are unable to explain the discrepancy between the results of Majer and McEvilly (1979) and Warren (this volume). The same data set was used to construct both models, though Warren did not use all the data. The results of Majer and McEvilly suggest that the large teleseismic delays cannot be attributed to local geology. However, Warren's results indicate that even with appropriate correction the largest teleseismic delay at GGL will still exceed 1.0 s, but the delay at GSG will be reduced to about 0.6 s.

The residual at station GMK, based on the refraction model of Majer and McEvilly, is on the same order as the teleseismic delays for the northwest and southwest azimuths (0.4 s). GMK is located on Mount Konocti, which is near the region of youngest silicic eruptions in

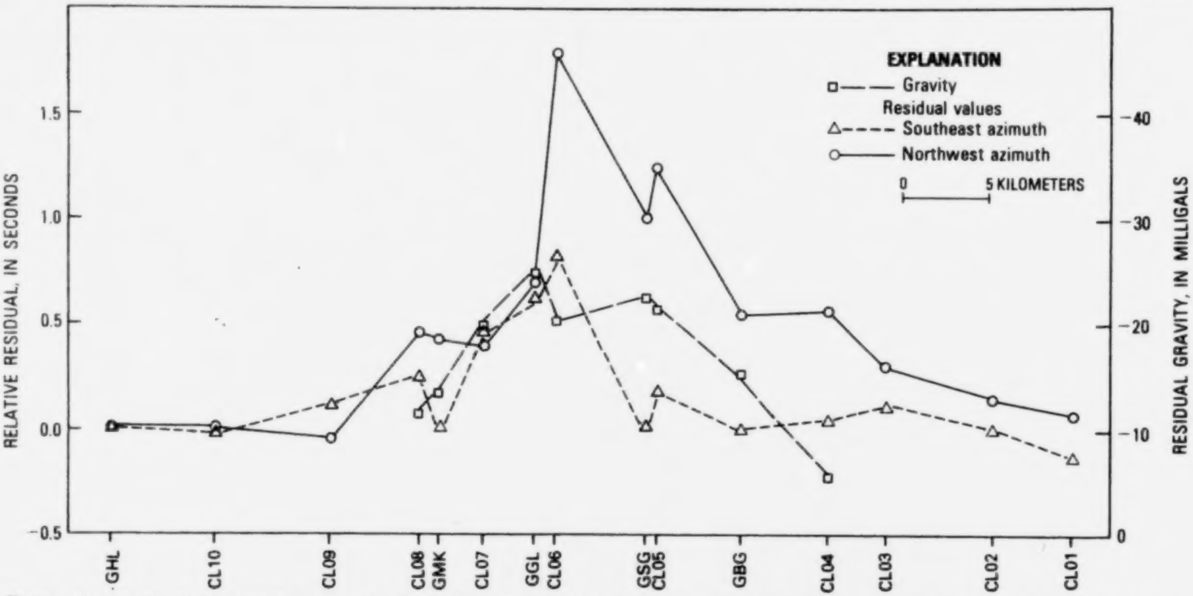

FIGURE 55.—Profile of northwest and southeast residual values and gravity along a southeast-northwest line *AA'* (see fig. 54*C*) from CL01 to GHL. Points are extrapolated to values at line *AA'*, not projected.

the Clear Lake volcanic field (Donnelly-Nolan and others, this volume). Two drill holes near Mount Konocti reached a depth of about 1.5 km but did not locate the lower boundary of the Clear Lake Volcanics. The consistency between the magnitudes of delays obtained by refraction and teleseismic surveys indicates that the teleseismic delays at GMK may be due to purely surface effects of the volcanic rocks. The results at GBO, GGL, and GSG show that even with extreme corrections, large delays must still be explained by deeper phenomena. The effect of deeper rocks, such as those of the Great Valley sequence and ophiolite, is difficult to evaluate and may contribute to the large delays observed at GGL and GSG through some fortuitous combination of effects. However, a body 25 km thick in which the velocity is 25 percent less than that of the surrounding material is required to produce a relative delay of 1.0 s. It is quite unlikely that such thick, low-velocity material overlies the Franciscan basement under the Clear Lake Volcanics.

Further evidence that complex surface geology is not a critical factor in interpreting the Geysers-Clear Lake teleseismic delays is provided by the results of a reflection survey conducted by Denlinger and Kovach (this volume) in the Castle Rock Springs area, about 5 km to the southeast of the present production area. This region is under intensive investigation for geothermal potential. Their detailed velocity model for the top 1 km of the crust does not show any strong low-velocity features and is likely to contribute only less than 0.1 s delay. Station GSM is located in this general region and does not show any large delays.

DEEP DELAY SOURCES

The previous discussion indicates that even after applying corrections for surface geology to the teleseismic delays, it is still necessary to interpret a regional delay field of 0.5 s extending over part of the Clear Lake volcanic field and the steam production field including large delays of 1 s at GGL, GBO, and GSG.

We have made the following assumptions regarding the interpretation of the anomaly: (1) the relative delay observed at a station is caused by the seismic ray traversing obliquely through a low-velocity body; (2) the velocity decrease inside the body relative to the surrounding rock is constant throughout the body by a specified amount; (3) the top of the low-velocity body is flat and at a depth of 4 km. (This value is close to the maximum depth of the seismogenic zone under the Geysers-Clear Lake region (Bufe and others, this volume). If the low-velocity body is magmatic, it will be unable to sustain earthquake strains.

The anomalous ray path inside the body is calculated at each station from residuals at various azimuths according to the equation

$$L = -VR\,(1 + 1/k),$$

where L is the distance the wave travels in the anomalous body, V is the velocity for a normal ray path, R is the average relative residual (positive for delays), and k is the fraction by which velocity inside the body deviates from normal; k is positive for higher-than-normal velocities and negative for lower-than-normal velocities. Having calculated L, the average angle of ray emergence at the surface, and the average event azimuth, it is possible to calculate the position of a three-dimensional surface of a body at depth.

The results of this modeling are shown in figures 56*A* and *B*, corresponding to a 15- and 25-percent velocity decrease. The contours indicate depths to the bottom of the low-velocity body. (As defined earlier, the top of the body is flat and constrained to a depth of 4 km.) For a 15-percent velocity decrease, there is considerable scatter in the values due to computed depths arising from large and small residuals at different stations being projected adjacent to each other. However, in spite of the discrepancies, we can define approximately a low-velocity body about 10 km deep and extending over a broad triangular region from the northeast shore of Clear Lake area including the steam production zone and part of the Clear Lake volcanic field. The 20-km contour approximately defines the deepest section of the body with considerable uncertainty in the northeast boundary.

As mentioned above, previous work suggests that a 15-percent velocity decrease may be appropriate for low-velocity bodies in geothermal areas. However, as shown in figure 56*B*, *P*-wave delays in the Geysers-Clear Lake region can also be modeled assuming a 25-percent velocity decrease. The 10-km contour outlines a smaller area than that within the similar contour line for the 15 percent model but still encompasses the steam production zone and the volcanic field. This model also reveals core regions near The Geysers and Mount Hannah where the low-velocity body may be 20 km or deeper. No serious contradictions in depth values were found for this model, thus a 25-percent decrease in velocity may be more appropriate, particularly for the central part of the anomalous body.

In figure 57 we show a consolidated model by combining both the 15- and 25-percent contrast models of figures 56*A* and *B*. In the following discussion, we shall concentrate on the hypothesis that the low-velocity body under Mount Hannah is of volcanic origin and that the body under the Geysers steam-production zone

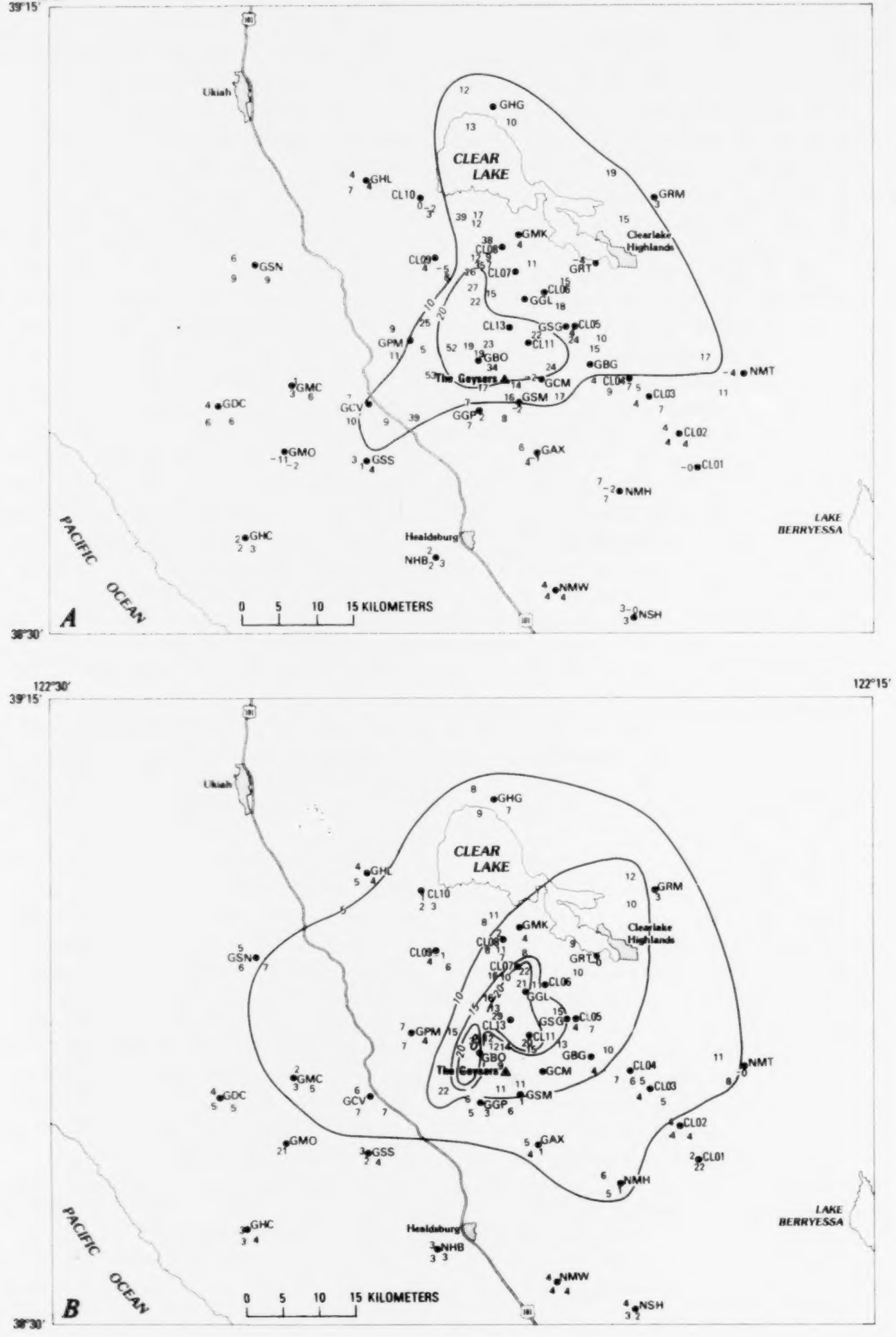
122°30′
122°15′
39°15′
38°30′
Ukiah
CLEAR LAKE
Clearlake Highlands
The Geysers
Healdsburg
PACIFIC OCEAN
LAKE BERRYESSA
GHG
GHL
CL10
GRM
GMK
CL08
CL09
GRT
CL07
GSN
CL06
GGL
CL13
GSG
CL05
CL11
GPM
GBO
GBG
GCM
CL04
NMT
GMC
CL03
GDC
GCV
GSM
GGP
CL02
GMO
GSS
GAX
CL01
NMH
GHC
NHB
NMW
NSH
0 5 10 15 KILOMETERS
A
B

is associated with the steam reservoir with or without an underlying magmatic body.

MAGMA CHAMBER UNDER MOUNT HANNAH

The presence of a magma chamber under Mount Hannah was first proposed by Chapman (1966); later Isherwood (1976), analyzing recent gravity and aeromagnetic data, modeled a magma chamber with its center at a depth of 15 km under Mount Hannah. Using geologic and geochronological data, Hearn and others (this volume) show that the central part of the Clear Lake volcanic field underlain by the postulated magma chamber is younger than 0.5 m.y. The geophysically inferred magma chamber, however, does not correspond to the youngest rocks of the Clear Lake Volcanics which lie to the northeast (Hearn and others, this volume). A strong resistivity anomaly (Stanley and Jackson, 1973), centered slightly to the northwest of Mount Hannah, may also be due to indirect effects of the magma chamber. Young and Ward (this volume) analyzed the spectra of teleseisms recorded by our portable seismec array in the Geysers-Clear Lake area and found a broad low-*Q* zone over the Clear Lake Volcanics and the production zone. They postulate that the low *Q* is associated with a zone of partial melting or magma chamber underlying the Geysers-Clear Lake area.

In spite of our modeling limitations and difficulty in assigning appropriate velocity contrasts, no serious differences exist between Isherwood's gravity model and our model. However, Isherwood's model, based on an expected mass deficiency, does not specify the extent of melting inside the magmatic body. In our model, a decrease in compressional velocity of 25-30 percent is required. A *P*-wave velocity decreases greater than 10 percent, though possibly caused by several factors, is best attributed to partial melting, particularly when observed in young volcanic areas. The interpretation of *P*-wave delays in terms of partially molten bodies has been discussed in detail in the analysis of Long Valley data by Steeples (1975) and Steeples and Iyer (1976b), and for Yellowstone by Iyer and Stewart (1977). In the Geysers-Clear Lake region, we believe that the most plausible explanation of the observed delays in the Mount Hannah area is the presence of partially molten rock in the crust. Whereas the increase of temperature alone is sufficient to cause a slow decrease in the velocity of compressional waves, a dramatic decrease in velocity occurs at the onset of partial melting (Mizutani and Kanamori, 1964; Spetzler and Anderson, 1968; Murase and McBirney, 1973). *P*-wave velocity data alone are not sufficient to determine the degree of partial melting. The accepted model for partially molten rock is one in which the main body of the solid has a large number of fluid-filled cracks. The extent of velocity decease depends not only on the number of cracks but also on their shape. Measurement of other seismologic variables such as shear-wave velocities and compressional and shear-wave attenuation are necessary in estimating the degree of partial melt in a magmatic system. A joint interpretation of our results together with the attenuation data of Young and Ward (this volume) may provide further constraints in estimating the composition of the magma body under the Geysers-Clear Lake area.

LOW-VELOCITY BODY ASSOCIATED WITH THE DRY-STEAM RESERVOIR

Goff, Donnelly, Thompson, and Hearn (1977) modeled the Geysers-Clear Lake geothermal region as a dry-steam system under The Geysers between the Mecuryville and Collayomi fault zones and an extensive hot-water system to the northeast (see fig. 5 of their paper and figs. 48 and 50 of this paper). Nur and Simmons (1969) showed that the presence of dry fractures, as would be found in the dry-steam system, lowers the compressional velocity of a medium. Hence, a significant velocity decrease can be expected in a vapor-dominated field such as The Geysers in contrast to a water-dominated field. However, it is again difficult to make an estimate of the expected velocity decrease and to interpret that estimate in terms of production-zone size. Our models show that a 25-percent velocity decrease requires depths of 25-30 km. However, note that this value is derived solely from the southwest delays at station GBO. The delays for other azimuths indicate about half that depth. Our modeling has incorporated the azimuthal dependence of the residuals, which results in the width of the anomalous low-velocity zone being restricted along the northwesterly direction.

The strong azimuthal dependence of the observed delays at GBO may also be attributed to material which has an anisotropic velocity distribution beneath the production zone. It is not unreasonable to expect velocity anisotropy in fractured rock. Walsh (1965) found that anisotropy can be due to the effect of cracks on the compressibility of rocks; the maximum velocity decrease occurs along a plane perpendicular to the crack orientation. In a study of the seismicity of the Geysers-Clear Lake area, Bufe and others (this vol-

FIGURE 56.—Calculated depth to bottom of anomalous body required to account for observed delays. Top of body is considerd flat and assumed to be at a depth of 4 km. Numbers near station locations indicate depth in km (+) or above (−) top of body. Normal seismic velocity outside body is 6 km/s. *A*. 15-percent velocity decrease. Contour interval, 10 km. *B*. 26-percent velocity decrease. Contour interval, 5 km.

ume) estimate the axis of maximum compression to be N. 30° E., which indicates that cracks should form at an angle of 45° to the axis of minimum compression and are thus oriented N. 15° W. Therefore, maximum velocity decrease should occur approximately along a southwesterly direction, as observed.

It is not possible to determine from seismic data alone whether part of the delays observed in the production zone is due to the extension of the Mount Hannah magma chamber underneath a fractured steam-filled reservoir. Isherwood's magma chamber extends (see fig. 17 of his 1976 paper) under the steam production zone. In the absence of any definitive evidence and since no estimates as to the size of the steam reservoir are available, we will not speculate on the relative sizes of the steam reservoir and magma body under the geothermal production zone.

A conceptual model for the subsurface structure of the Geysers-Clear Lake region is shown in three cross-sectional diagrams along *AA'* (northwest through the volcanic zone), *BB'* (northwest through the production zone), and *CC"* (northeast through the production zone and volcanic zone) in figures 58*A*, *B*, and *C*. The models are primarily constructed from teleseismic data, but other geologic and geophysical information is also used for completeness.

CONCLUSIONS

A plausible interpretation of the large teleseismic delays observed in the Geysers-Clear Lake region is that they are due to the presence of a low-velocity body in the crust. The body, with an average thickness of about 10 km, extends over a large area to the south of Clear Lake including the steam-production zone at The Geysers. The average compressional velocity inside the body is less than normal by about 15 percent. In a core region under Mount Hannah and part of the steam-production zone, the volocity decrease exceeds 25 percent. We interpret the low-velocity body to be composed of partially molten rock under the volcanic zone and fractured rock, responsible for the dry-steam reservoir, under the production zone. Because it is not possible to distinguish between partially molten rock and dry fractures from teleseismic residuals alone, it is

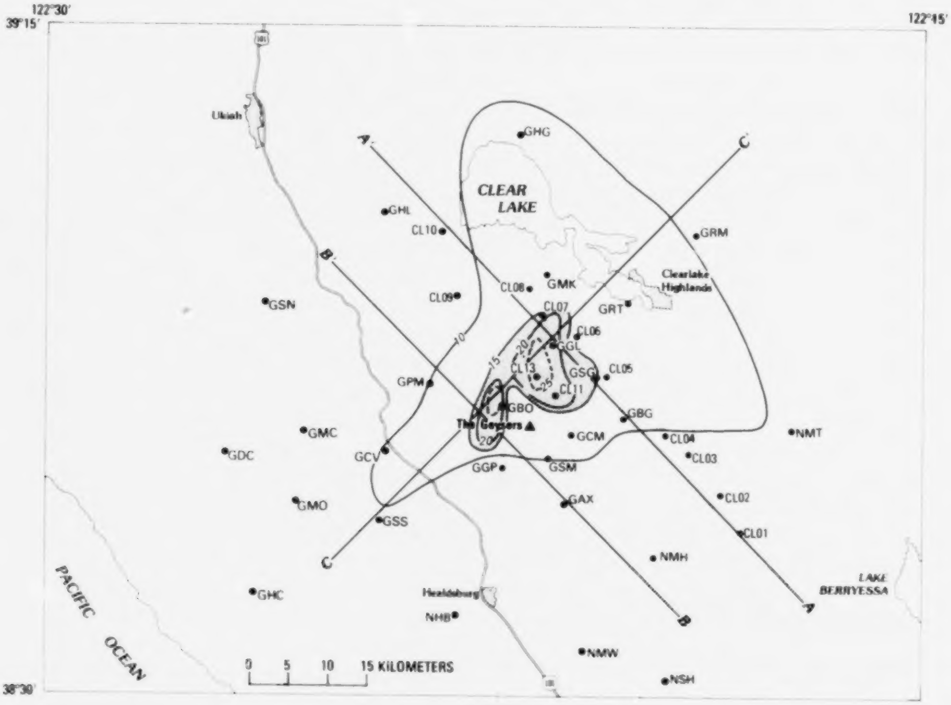
122°30'
39°15'
122°15'
38°30'
101
Ukiah
A
A'
B
B'
C
C'
CLEAR
LAKE
GHG
GHL
CL10
GRM
CL08
GMK
Clearlake
Highlands
GSN
CL09
CL07
GRT
CL06
10
15
20
GGL
CL13
25
GSG
CL05
GPM
CL11
GBO
The Geysers
GBG
GMC
GCM
CL04
NMT
GDC
GCV
20
CL03
GGP
GSM
GMO
GAX
CL02
GSS
CL01
NMH
PACIFIC
OCEAN
LAKE
BERRYESSA
GHC
Healdsburg
NHB
NMW
NSH
0
5
10
15 KILOMETERS

FIGURE 57.—Composite of figure 56 indicating depth to bottom surface of body responsible for observed delays. Velocity decrease with respect to normal is 25 percent within shaded "core" area, and 15 percent outside core and within 10-km contour. Contour interval, 5 km. Profile lines indicate position of cross sections shown in figure 58.

not possible to determine whether a magmatic intrusion is present under the dry steam reservoir. Our results are in basic agreement with Isherwood's (1976) analysis of gravity and magnetic data which also indicate the presence of a magma chamber under the Geysers-Clear Lake area. If the high degree of partial melting indicated by our results is valid. it would appear that the Clear Lake volcanic system is by no means extinct.

REFERENCES CITED

Birch, A. F., 1960, The velocity of compressional waves in rocks to 10 kilobars, part 1: Journal of Geophysical Research, v. 65, p. 1083-1102.

Chapman, R. H., 1966, Gravity map of Geysers area: California Division of Mines and Geology Mineral Information Service, v. 19, p. 148-149.

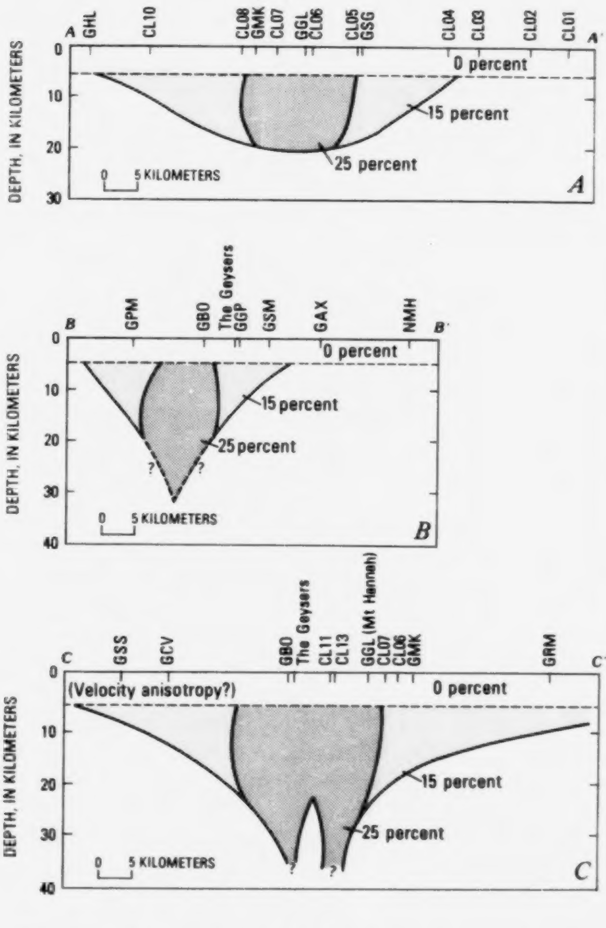

FIGURE 58.—Conceptual model of subsurface structure and percent decrease in velocity in the Geysers-Clear Lake region. *A*, Northwest cross section along *AA'* of figure 57 passing through volcanic zone. *B*, Northwest cross section along *BB'* of figure 57 passing through production zone. *C*, Northeast cross section along *CC'* of figure 57 passing through production and volcanic zones.

Goff, F. E., Donnelly, J. M., Thompson, J. M., and Hearn, B. C., Jr., 1977, Geothermal prospecting in The Geysers-Clear Lake area, northern California: Geology, v. 5, p. 509-515.

Hearn, B.C., Jr., Donnelly, J. M., and Goff, F. E., 1976, Preliminary geologic map and cross-section of the Clear Lake volcanic field, Lake County, California: U.S Geological Survey Open-File Report 76-751, scale 1:24,000, 2 sheets.

Herrin, Eugene, 1968, Seismological tables for P: Seismological Society of America Bulletin, v. 58, p. 1193-1241.

Isherwood, W. F., 1976, Gravity and magnetic studies of The Geysers-Clear Lake geothermal region, California: United Nations Symposium on the Development and Use of Geothermal Resources, 2d, San Francisco, 1975, Proceedings, v. 2, p. 1065-1073.

Iyer, H. M., 1975, Anomalous delays of teleseismic P waves in Yellowstone National Park: Nature, v. 253, p. 425-427.

—— 1979, Deep structure under Yellowstone National Park, U.S.A.: A continental "hot spot": Tectonophysics, v. 56, p. 165-197.

Iyer, H. M., Oppenheimer, D. H., and Hitchcock, Tim, 1979, Abnormal P-wave delays in The Geysers-Clear Lake geothermal area, California: Science,v. 204, p. 495-497.

Iyer, H. M., and Stewart, R. M., 1977, Teleseismic technique to locate magma in the crust and upper mantle, *in* Dick, H. J. B., ed., Magma genesis, Proceedings of the American Geophysical Union Chapman Conference of Partial Melting in the Earth's Upper Mantle, 1977: Oregon Department of Geology and Mineral Industries, p. 281-299.

Koenig, J. B., compiler, 1963, Santa Rosa sheet *of* Geologic map of California: California Division of Mines and Geology, scale 1:250,000.

Kubota, Susumu, and Berg, Edward, 1967, Evidence for magma in the Katmai volcanic range: Bulletin Volcanologique, v. 31, p. 175-214.

Majer, E., and McEvilly, T. V., 1979, Seismological investigations at The Geysers geothermal field: Geophysics, v. 44, p. 246-269.

Matumoto, Tosimatu, 1971, Seismic body waves observed in the vicinity of Mount Katmai, Alaska, and evidence for the existence of molten chambers: Geological Society of America Bulletin, v. 82, p. 2905-2920.

McLaughlin, R. J., 1978, Preliminary geologic map and structural sections of the central Mayacmas Mountains and the Geysers steam field, Sonoma, Lake, and Mendocino Counties, California: U.S. Geological Survey Open-File Report 78-389, scale 1:24,000, 2 sheets.

Mizutani, Hitoshi, and Kanamori, Hiroo, 1964, Variation of elastic wave velocity and attenuative property near the melting temperature: Journal of Physics of the Earth, v. 12, p. 43-49.

Murase, Tsutomu, and McBirney, A. R., 1973, Properties of some common igneous rocks and their melts at high temperatures: Geological Society of America Bulletin, v. 84, p. 3563-3592.

Nur, Amos, and Simmons, Gene, 1969, The effect of saturation on velocity in low porosity rocks: Earth and Planetary Science Letters, v. 7, p. 183-193.

Reasenberg, P. A., Ellsworth, W. L., and Walter, A. W., 1980, Teleseismic evidence for a low-velocity body under the Coso geothermal area: Journal of Geophysical Research, v. 85, p. 2471-2483.

Savino, J. M., Rodi, W. L., Goff, R. C., Jordan, T. H., Alexander, H., and Lambert, D. G., 1977, Inversion of combined geophysical data for determination of structure beneath the Imperial Valley geothermal region: Systems, Science and Software (Co.) Report SSS-R-78-3412 to U.S. Energy Research and Development Administration, 82 p.

Spetzler, H. A., and Anderson, D. L., 1968, The effect of temperature and partial melting on velocity and attenuation in a simple binary system: Journal of Geophysical Research, v. 73, p. 6051-6060.

Stanley, W. D., and Jackson, D. B., 1973, Geoelectric investigations near Clear Lake, California: U.S. Geological Survey open-file report, 20 p.

Steeples, D. W., 1975, Teleseismic P-delays in geothermal exploration with application to Long Valley, California: Stanford, Calif., Stanford University, Ph. D. thesis, 228, p.

Steeples, D. W., and Iyer, H. M., 1976a, Teleseismic *P*-wave delays in geothermal exploration: United Nations Symposium on the Development and Use of Geothermal Resources, 2nd, San Francisco, 1975, Proceedings, v. 2, p. 1199-1205.

——1976, Low-velocity zone under Long Valley as determined from teleseismic events: Journal of Geophysical Research, v. 81, p. 849-860.

Walsh, J. B., 1965, The effect of cracks on the compressibility of rock: Journal of Geophysical Research, v. 70, p. 381-389.

SEISMIC-REFLECTION INVESTIGATIONS AT CASTLE ROCK SPRINGS IN THE GEYSERS GEOTHERMAL AREA

By ROGER P. DENLINGER and ROBERT L. KOVACH

ABSTRACT

Seismic-reflection profiling verifies the presence of an anticlinal trap in the vicinity of the Castle Rock Springs steam field. Strong reflection amplitudes recorded near the crest of the anticline correlate in depth with an observed fracture zone in a nearby well, and strong reflections within the core of the anticline may also be due to the fracture zones from which steam is produced in this area. Southwest of the anticline, a band of seismic energy may indicate the contact between fractured graywacke reservoir rock and its mafic caprock. The seismic sections also indicate southeast and northeast extensions of the cap which could not be inferred on the basis of previous information.

A strong deep reflection which we believe represented a tectonic boundary in the Fransiscan assemblage was recorded below 4 km. This boundary dips northeastward toward a possible heat source and occurs at depths between the heat source and the steam system.

INTRODUCTION

The Geysers steam field produces more power than any other steam field in the world. Although many studies have been conducted in the field, little detailed information has been obtained that indicates the spatial distribution of the steam-filled fracture zones. The principal means of exploring in this area at present is by explorational drilling with air until good steam zones are located.

The Castle Rock Springs steam system is near the periphery of the major steam field at The Geysers (figs. 59 and 60), as indicated by explorational drilling and the residual gravity field analyzed by Denlinger (1979). McLaughlin (1978) described the regional structure of The Geysers and vicinity in terms of a southeast-plunging antiform. The major part of the area studied here occupies the northeast flank of this antiform, whose axis is close to the Mercuryville fault zone. In describing the local structure of the steam fields and the pattern of steam occurrences, McLaughlin and Stanley (1975) noted (1) the occurrence of impermeable mafic rocks overlying steam-producing graywacke, suggesting that the mafic rocks act as a caprock, and (2) the existence of anticlinal warps in the predominantly eastward dipping metagraywacke and shale section, which may serve as structural traps in a convecting geothermal system.

The Castle Rock Springs steam field is an example of an anticlinal warp within the geologic section. McLaughlin and Stanley (1975) hypothesized that fracturing induced by folding in the crest of these anticlinal warps increases the rocks' permeability. Thus such anticlinal structures could act as structural traps, concentrating upward-convecting geothermal fluid.

According to this model, some of the fracture zones would be expected to be nearly horizontal near the crest of the anticline. This raises the possibility that the fractures may be mapped by seismic-reflection profiling, given sufficient lateral continuity in both the fracture zones and the subsurface velocity structure.

In the spring of 1976, we conducted a seismic-reflection survey over two profiles in the Castle Rock Springs area. The data obtained represent the first reflection survey undertaken in Franciscan geology, and we hope that the success of this project will prompt further seismic-reflection work in the Geysers area.

This research was supported by the U.S. Geological Survey under contract number 14-08-0001-15329. Special thanks are due to Western Geophysical Company and the survey manager, Stewart Mitchell, for conducting the survey in difficult terrain. Ron Chambers, Ted Clee, and Chang-sheng Wu of Western's Research Division were most helpful with the data processing. We also thank Aminoil and Shell Oil Companies for permission to enter their leaseholdings in the Castle Rock Springs area.

DATA ACQUISITION AND PROCESSING

Two lines were laid out along gravel roads in the Castle Rock Springs area (figs. 60 and 61). The survey was carried out by Western Geophysical, using standard field procedures. Four Vibroseis trucks spaced 3 m apart were used as a source, with a 16-s downsweep applied four times from each truck. The lines were laid out split spread, 12 fold, with a 33-m group interval and a cable length of 880 m (Sheriff, 1973). It was determined at the site that a 58- to 12-Hz downsweep gave the best signal-to-noise ratio. Data were recorded in floating-point form 250 times a second.

Processing was standard except for Western Geophysical automatic statics routine (Wiggins and others, 1976). Velocity spectra (Taner and Koehler,

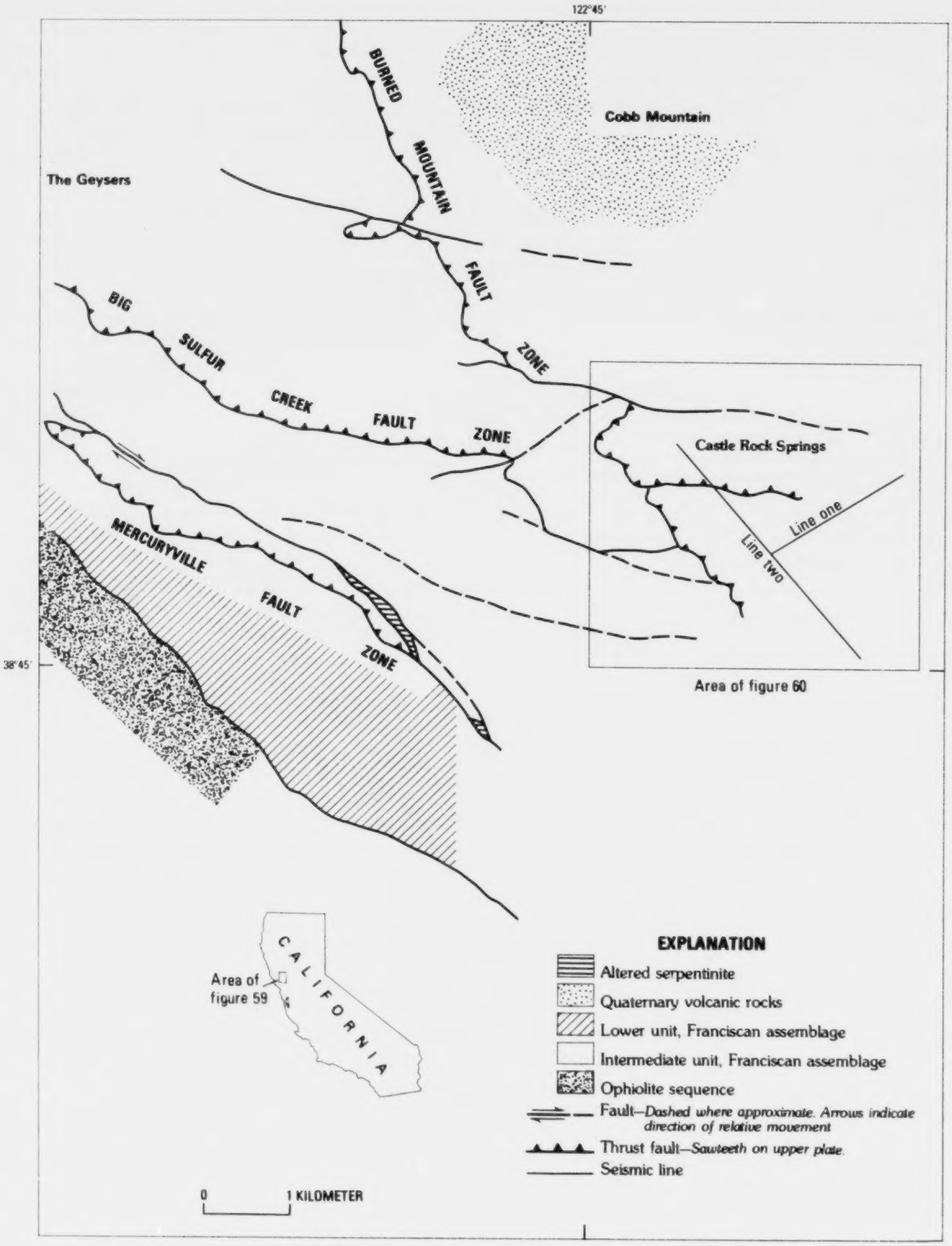
122°45'
38°45'
Cobb Mountain
The Geysers
BURNED MOUNTAIN FAULT ZONE
BIG SULFUR CREEK FAULT ZONE
MERCURYVILLE FAULT ZONE
Castle Rock Springs
Line one
Line two
Area of figure 60
CALIFORNIA
Area of figure 59
EXPLANATION
Altered serpentinite
Quaternary volcanic rocks
Lower unit, Franciscan assemblage
Intermediate unit, Franciscan assemblage
Ophiolite sequence
Fault—Dashed where approximate. Arrows indicate direction of relative movement
Thrust fault—Sawteeth on upper plate
Seismic line
0 1 KILOMETER

FIGURE 59.—Regional geology and structure of the Geysers-Castle Rock Springs geothermal area, modified from McLaughlin (1978).

1969) were used to pick preliminary velocities before statics determination. To reduce the possibility of introducing artificial coherence, the static time shifts were limited to one-half the dominant period of the data (20 ms). After static corrections were determined, they were applied to the original cross-correlated data and the velocity spectra, correlating the spectra with events observed on the records. Both floating-point (relative amplitude) and fixed-point (normalized amplitude) sections for lines one and two were produced. These are shown for comparison in figures 62 and 65.

The sections are unmigrated. The wavelengths observed range from 100 to 300 m, and 10 points per wavelength are needed to migrate effectively. Because the station spacing used was 33 m, all but the longest wavelengths are spatially undersampled for migration processing.

INTERPRETATION

The velocity time curves that produce the most coherent sum of the data may be used to calculate an interval velocity structure for the lines (Dix, 1955). Assuming that plane interfaces separate regions of constant velocity, we used Dix's formula to calculate the velocity structure shown in figures 64 and 67. The interval velocity so obtained forms the basis for our interpretation of the seismic sections. In addition, we had lithologic logs for wells C5 (courtesy of Shell Oil Co.). Our velocities are in good agreement with the sonic log data for well C5, at the intersection of lines one and two.

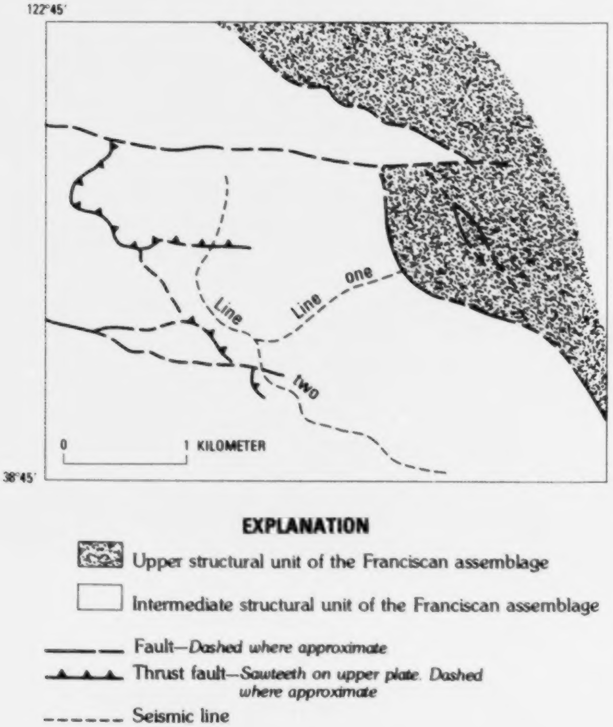
122°45'
38°45'
Line one
Line two
0
1 KILOMETER
EXPLANATION
Upper structural unit of the Franciscan assemblage
Intermediate structural unit of the Franciscan assemblage
Fault—Dashed where approximate
Thrust fault—Sawteeth on upper plate. Dashed where approximate
Seismic line

FIGURE 60.—Regional geology and structure of study area, modified from McLaughlin (1978).

The velocity structure found along line two is roughly consistent with the geologic structure shown in figure 63. Since the predominant wavelengths were averaged over distances of 100 m, much of the lithologic detail cannot be seen. Strong reflections are also needed to pick velocities out of the noise during processing, and thus the strongest reflections control where the velocity horizons are placed.

A better correlation may be made between the reflection sections (figs. 62 and 65) and the respective geologic sections. The anticlinal structure beneath shotpoints 139 to 104 is evident as well as the gently dipping layered structure to the southeast. Reflected energy from the southeast flanks of the anticline can be seen below 1 second on section two. A thick fracture zone near the crest of the anticline in a nearby well correlates in depth with a strong reflection evident on seismic section two just below 0.3 seconds near shotpoints 127-104. Other high-amplitude reflections associated with the anticline seen in section two may also indicate the presence of fracture zones; their presence would substantiate the anticlinal trap hypothesis of McLaughlin and Stanley (1975). Many reflections are highlighted within the anticlinal structure. Velocity information is lacking below 1.0 seconds (fig. 64) due to a lack of strong continuous events below this level. Thus the depths of events visible below this level cannot be determined.

Southeast of the anticline, the velocity and seismic sections (figs. 62 and 64) both verify the gently dipping layered structure McLaughlin (1978) determined on the basis of surface geology and well data. The bottom of the 2.38-km/s layer is interpreted on the basis of depth to be the base of the serpentinite. The melange section above greenstone shown in the geologic section is interpreted to be the 4.07- and 4.36-km/s layers. The contact between greenstone and graywacke (McLaughlin, 1978) could not be extended on the basis of available data. On the reflection section, however, a band of seismic energy at 1.1 seconds may indicate the extension of this contact and possible fracturing associated with this tectonic boundary. Based on the velocity above it, the depth of this boundary is about 1.7 km; this is the depth that producing steam zones begin to occur (from well information along the profile). It is possible here that the greenstone acts as an impermeable mafic cap for the fractured graywacke, and the graywacke, in turn, acts as the reservoir. The existence of a mafic or ultramafic cap over fractured graywacke fits the pattern of steam occurrences in other areas of the Geysers steam field (McLaughlin and Stanley, 1975).

Line one meets line two at the marked intersection on both the reflection and geologic sections. The velocities found for both sections are consistent with the sonic log for well C5, near the line intersection. The velocities and reflected events match between the lines, thus line one indicates how the geology near the intersection changes northeast of line two. Both the melange units and the seismic energy band just below 1.1 seconds on line two dip gently to the northeast. Much deeper, at about 2.1 seconds, a much stronger reflection dips toward the northeast. Assuming an average velocity of 4.23 km/s below the last reflector, this reflector is at least 3.1 km deep. Given the observed increase of velocity with depth, 4 km may be more likely. This reflector may indicate a major tectonic boundary in the Franciscan assemblage, and seismic energy reflected from it may be enhanced by increased fracturing along the boundary or by the presence of imbricate layers due to shearing. It occurs at a depth between the heat source (Isherwood, 1976) and the steam system observed in the wells. Thus if permeable, such a boundary could act as a conduit for convection of the geothermal fluid from the heat source into the geothermal system.

CONCLUSIONS

We have shown that seismic-reflection techniques applied to the steam system at Castle Rock Springs may be useful in detecting fracture systems within the

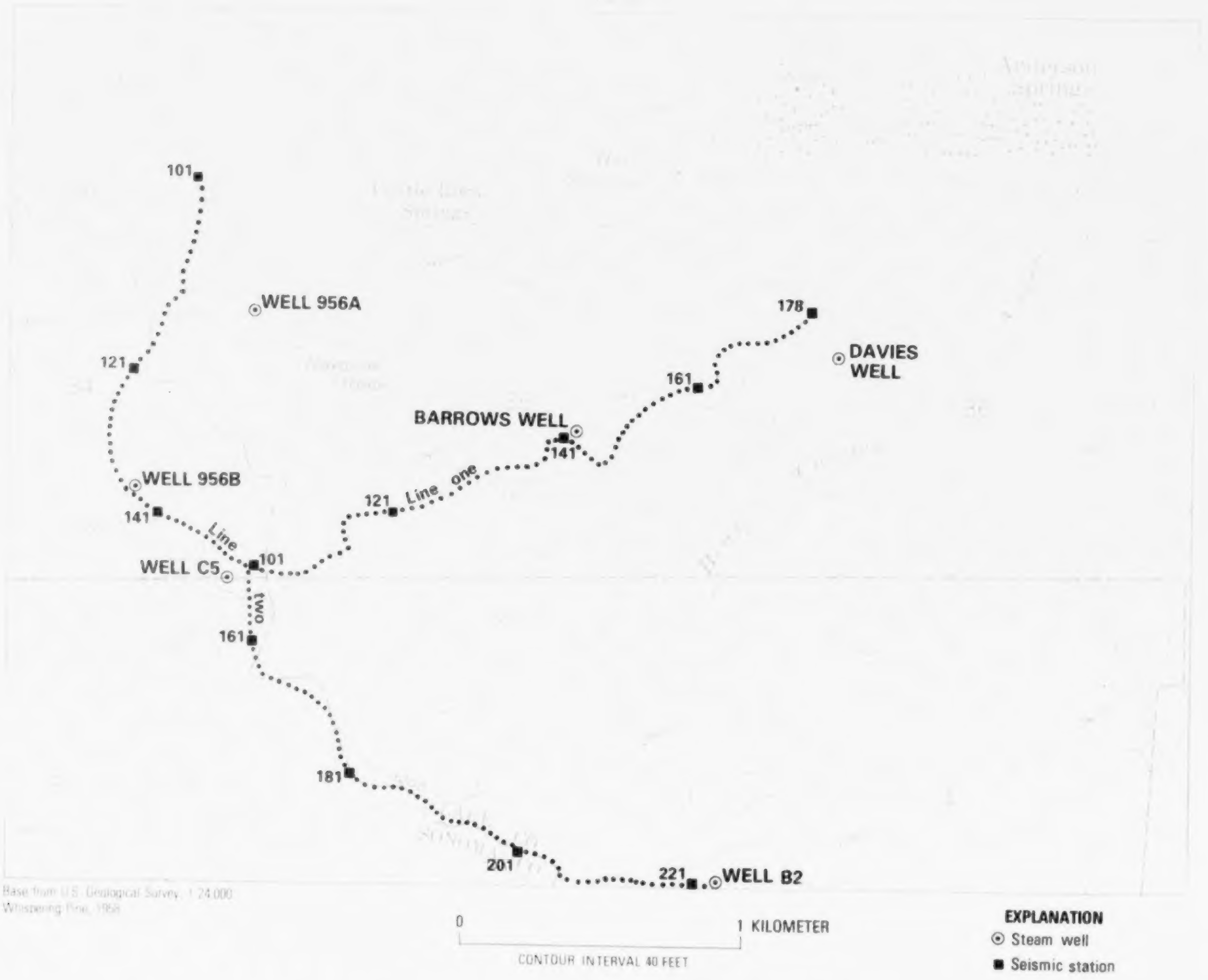
101
WELL 956A
121
WELL 956B
141
Line
WELL C5
101
two
161
181
201
221
WELL B2
121
Line one
BARROWS WELL
141
161
178
DAVIES WELL
0
1 KILOMETER
CONTOUR INTERVAL 40 FEET
EXPLANATION
⊙ Steam well
■ Seismic station

Base from U.S. Geological Survey, 1:24,000
Whispering Pine, 1958

FIGURE 61.—Location of seismic stations and producing steam wells in study area.

steam reservoir and deep geologic structure beneath the reservoir. This survey was an experiment to determine whether or not standard reflection techniques, if modified with state-of-the-art processing schemes, would be useful in geothermal prospecting. Basically we succeeded in obtaining interpretable data in a difficult area, but significant improvement in survey design and processing can be made from what we learned from this project.

In designing this survey, a line length of 1.6 km (1 mile) was chosen as a compromise. If long line lengths are used, good control on velocity is obtained by convolving the records with some best-fit hyperbola, as the tail of the hyperbola which best fits a single velocity to a reflector is then well defined. In areas of strong lateral variations in velocity, however, the traveltime-offset curve deviates significantly from a hyperbola. Thus, short lines are needed to improve the signal-to-noise ratio during the sum/convolution of the records with a best-fit hyperbola (an approximation). The price to be paid, with short lines, is decreased resolution in velocity and hence depth to a reflecting horizon.

Because we wanted to maximize our signal-to-noise ratio at depths between 1 and 3 km, we chose short lines, knowing that we would lose our depth resolution in doing so. A better, more expensive compromise would have been to run the survey 48-fold on lines two to three times longer than we used. The best method (and necessary if seismic-reflection methods are to become a useful tool in geothermal exploration) is to obtain good velocity control from outside sources such as refraction profiles or microearthquakes. Once velocity is known, it is possible to construct the actual curve (instead of some assumed hyperbola) along which the common midpoint data should be summed, and this will produce a dramatic improvement in the signal-to-noise ratio. In this way, seismic-reflection methods will provide the most detailed information on the structure of geothermal systems.

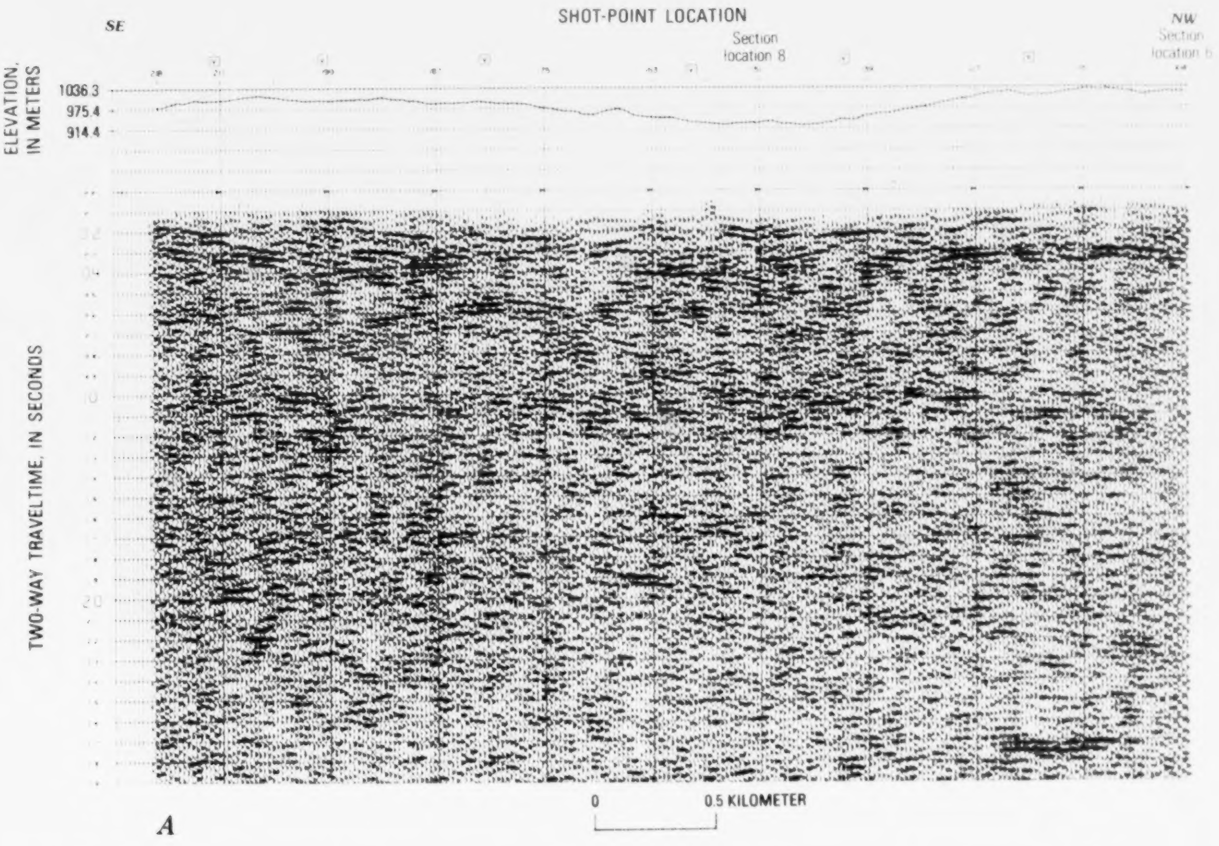

FIGURE 62.—Stacked seismic section along line two showing reflection profile and two-way traveltime. V's mark position of velocity analyses. Southwest end of line one intersects at section location 8. *A*, Amplitudes normalized to near-surface rms amplitude. *B*, Structures accentuated for comparison with geologic section of figure 63. *C*, Relative amplitudes preserved.

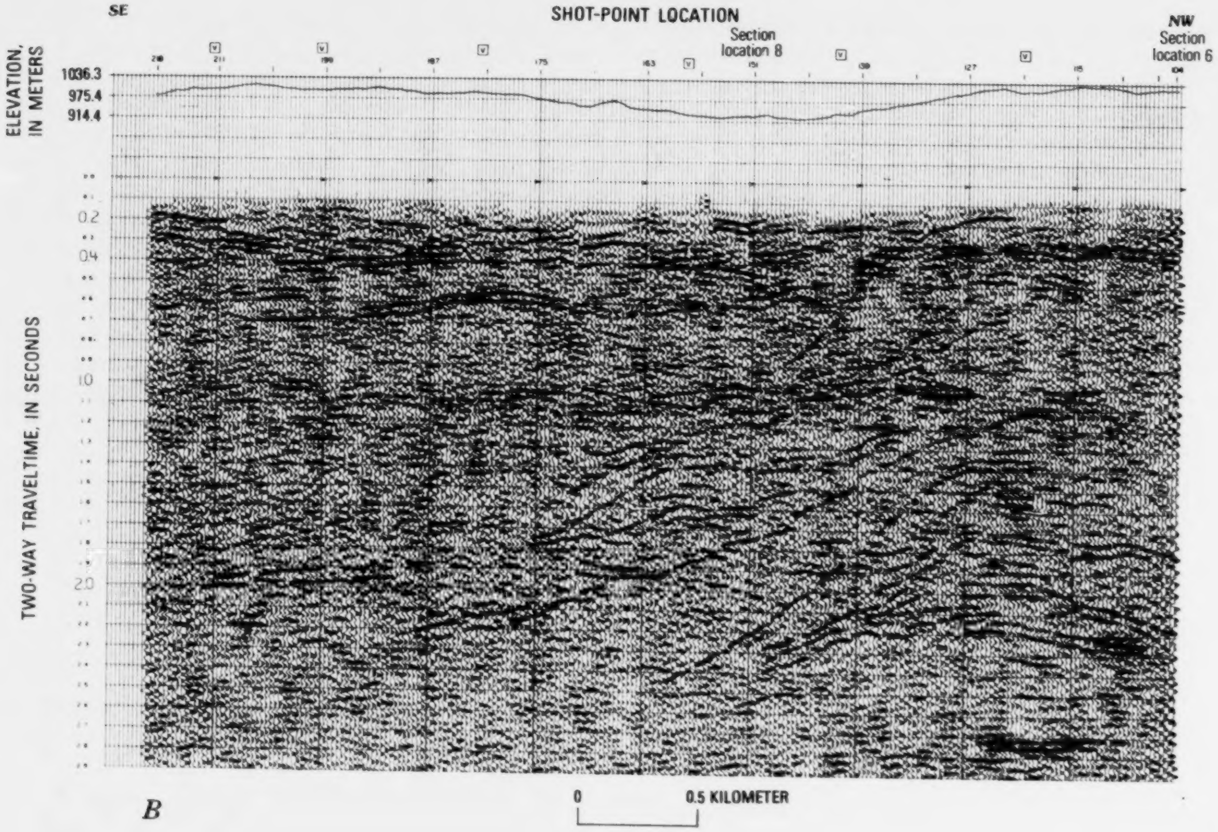

FIGURE 62.—Continued.

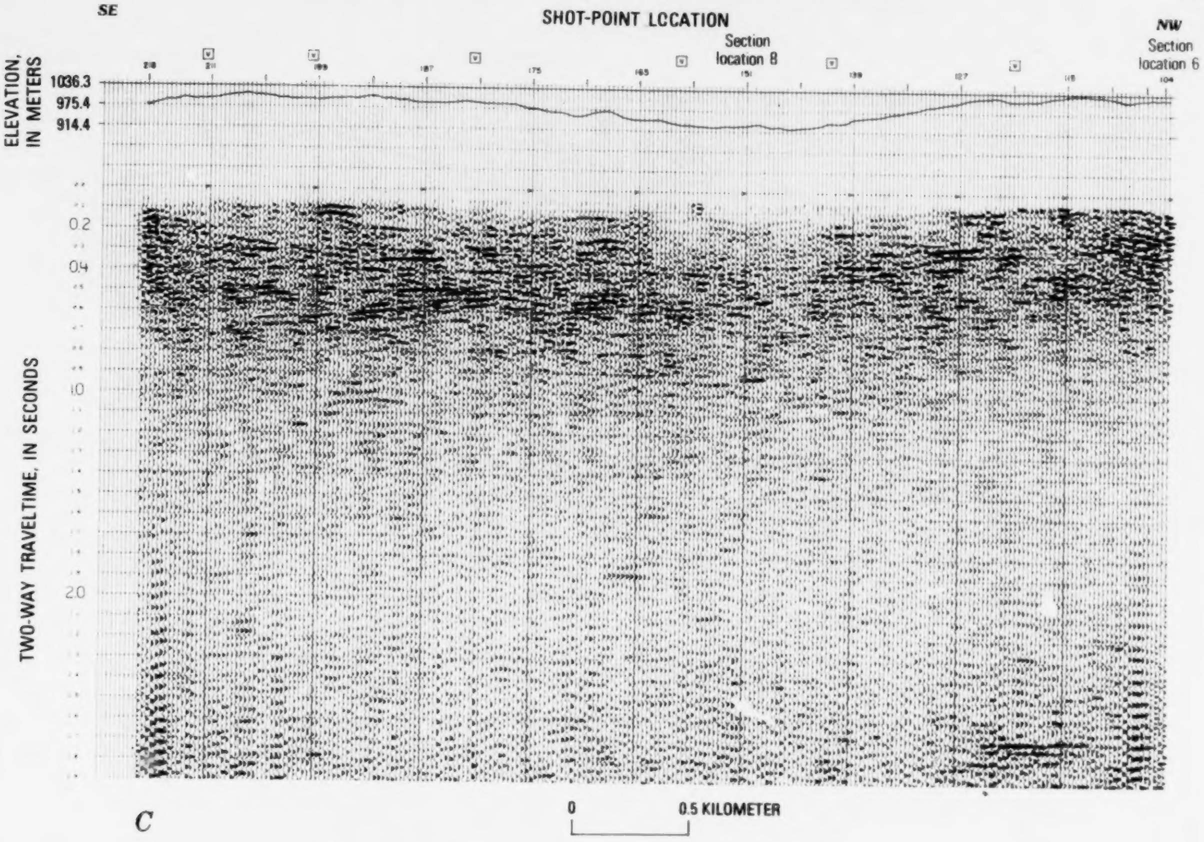

FIGURE 62.—Continued.

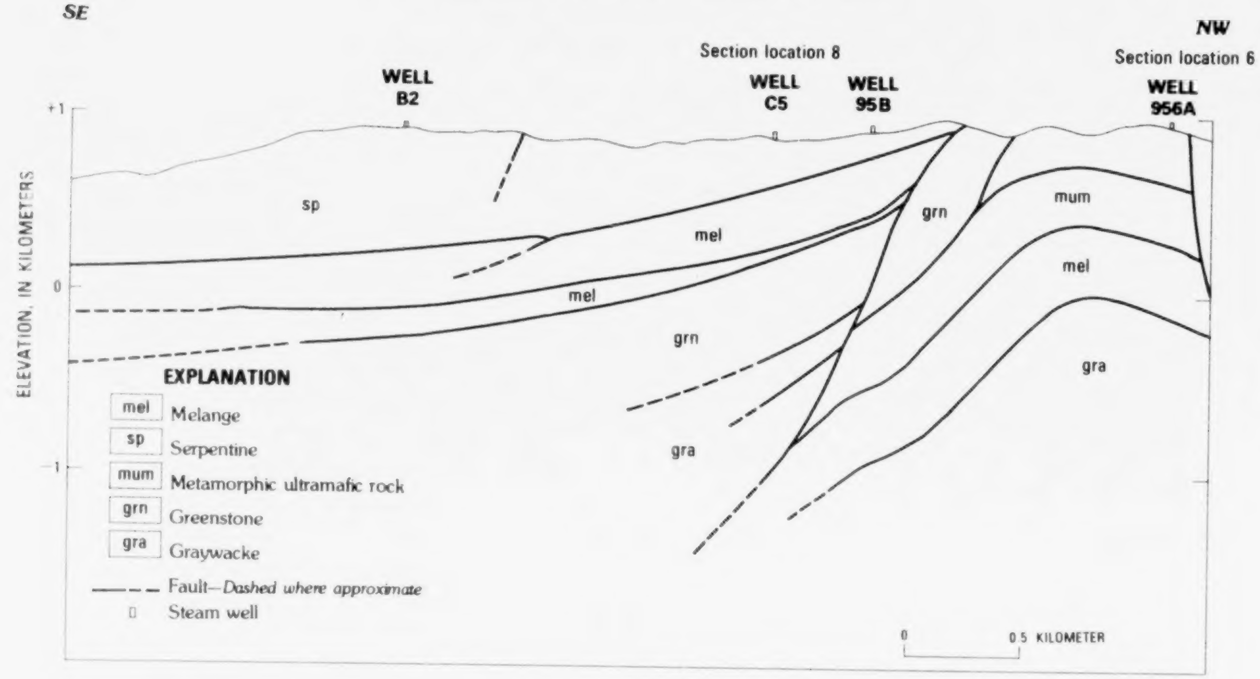
SE
NW
Section location 8
Section location 6
WELL B2
WELL C5
WELL 95B
WELL 956A
ELEVATION, IN KILOMETERS
+1
0
−1
sp
mel
mel
grn
grn
mum
mel
gra
gra
EXPLANATION
mel Melange
sp Serpentine
mum Metamorphic ultramafic rock
grn Greenstone
gra Graywacke
Fault—Dashed where approximate
Steam well
0
0.5 KILOMETER

FIGURE 63.—Geological section along reflection line two.

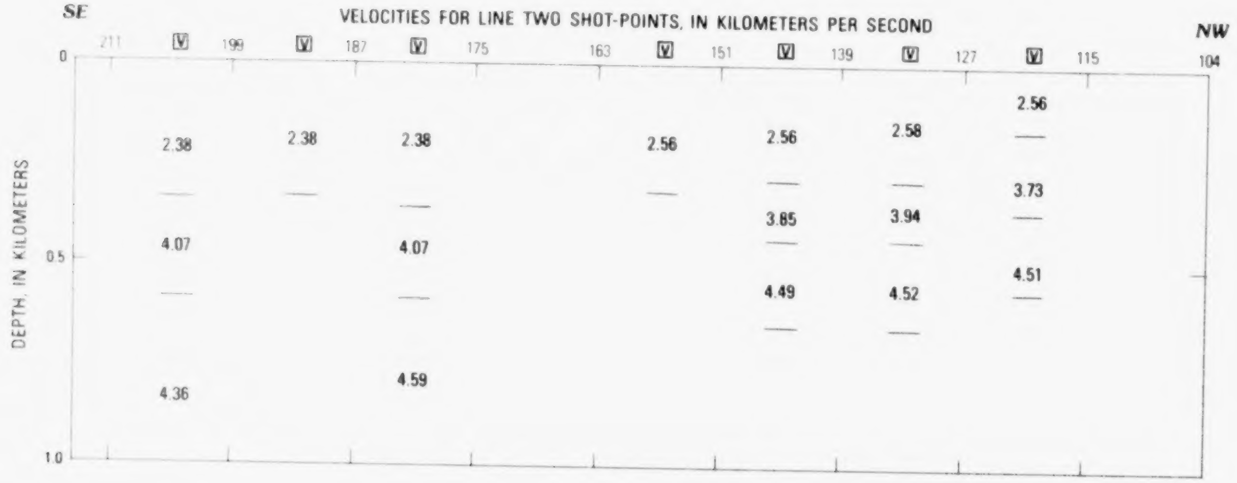

FIGURE 64.—Interval velocity section calculated for seismic line two. V's mark position of velocity analyses.

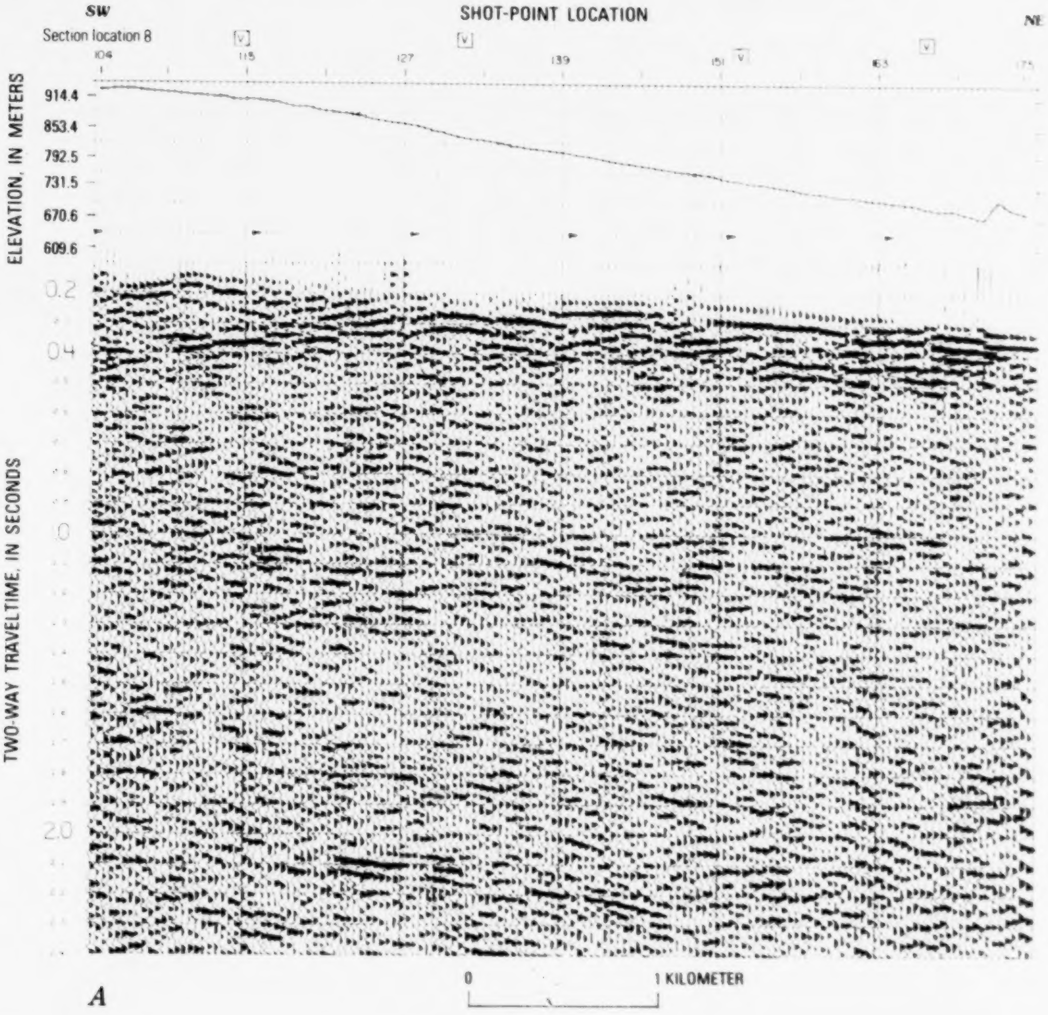

FIGURE 65.—Stacked seismic section along line one showing reflection profile and two-way traveltime. V's mark the position of velocity analyses. Intersection of line two is at section location 8. Deep reflector near 2.1 seconds dipping northeast may represent a major tectonic boundary in the Franciscan assemblage. *A*. Amplitudes normalized to near-surface rms amplitude. *B*. Structures accentuated for comparison with geologic section of figure 66. *C*. Relative amplitudes preserved.

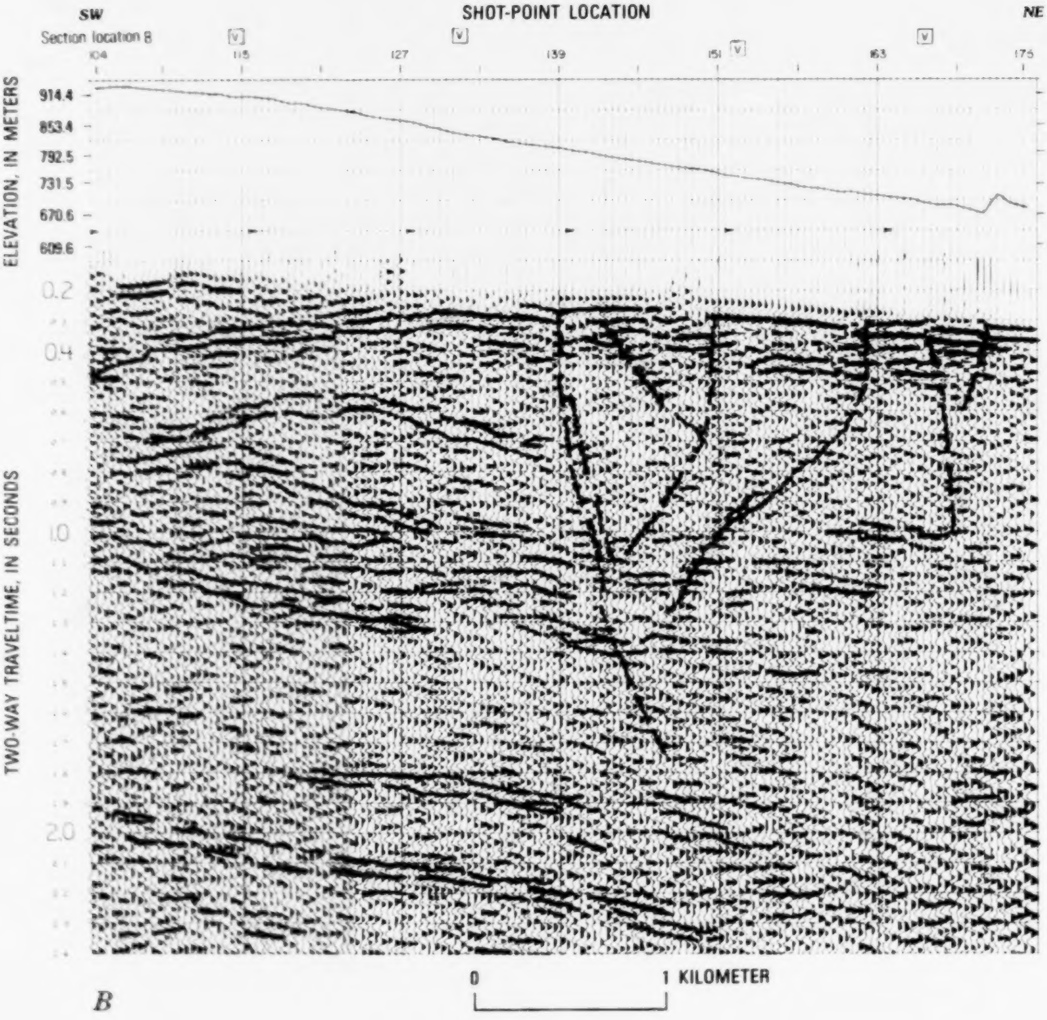

FIGURE 65.—Continued.

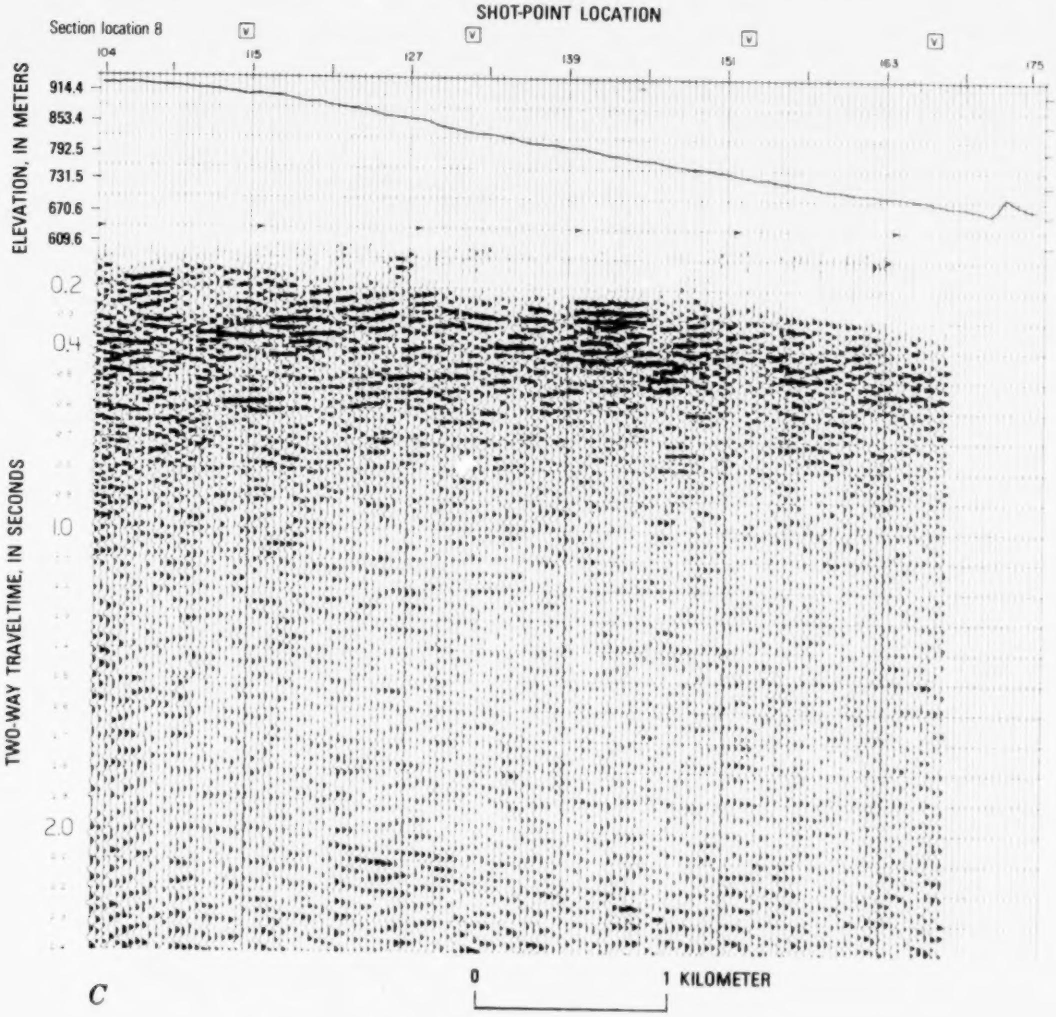

FIGURE 65.—Continued.

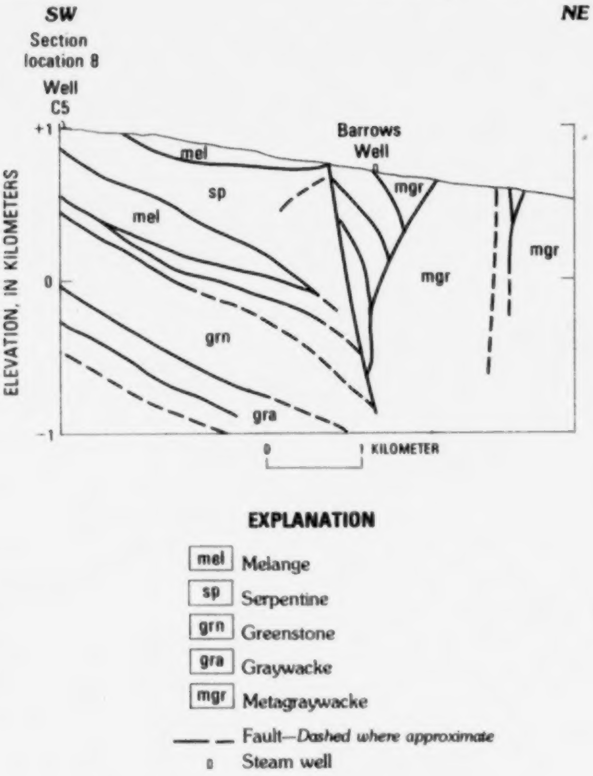
SW
NE
Section location 8
Well C5
Barrows Well
+1
0
−1
ELEVATION, IN KILOMETERS
mel
sp
mel
grn
gra
mgr
mgr
mgr
0
1 KILOMETER
EXPLANATION
mel Melange
sp Serpentine
grn Greenstone
gra Graywacke
mgr Metagraywacke
Fault—Dashed where approximate
Steam well

FIGURE 66.—Geologic section along reflection line one (from McLaughlin, 1978).

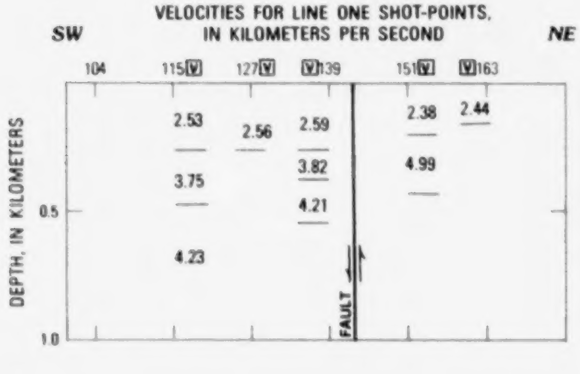

FIGURE 67.—Interval velocity section calculated for seismic line one. Major fault near shotpoint 139 is a tectonic boundary evident from reflection data, surface geology, and lithologic data at Borrows well (see fig. 61).

REFERENCES CITED

Denlinger, R. F., 1979, Geophysics of The Geysers geothermal system, northern California: Stanford, Calif., Stanford University, Ph. D. thesis, 82 p.

Dix, C. H., 1955, Seismic velocities from surface measurements: Geophysics, v. 20, no. 1, p. 68-86.

Isherwood, W. F., 1976, Gravity and magnetic studies of the Geysers-Clear Lake region, California: United Nations Symposium on the Development and Use of Geothermal Resources, 2d, San Francisco, 1975, Proceedings, v. 2, p. 1965-1073.

McLaughlin, R. J., 1978, Preliminary geologic map and structural sections of the central Mayacmas Mountains and The Geysers Steam Field, Sonoma, Lake, and Mendocino Counties, California: U.S. Geological Survey Open-File Report 78-389, scale 1:24,000.

McLaughlin, R. J., and Stanley, W. D., 1975, Pre-Tertiary geology and structural control of geothermal resources, the Geysers steam field, California: U.N. Symposium on Development and Use of Geothermal Resources, 2d, San Francisco, Calif., 1975, Proceedings, p. 475.

Sheriff, R. E., 1973, Encyclopedic dictionary of exploration geophysics: Tulsa, Oklahoma, Society of Economic Geologists, 266 p.

Taner, M. T., and Koehler, Fulton, 1969, Velocity spectra-digital computer derivation and applications of velocity functions: Geophysics, v. 34, no. 5, p. 859-881.

Wiggins, R. A., Larner, K. A., and Wisecup, R. D., 1967, Residual static analysis as a general linear inverse problem: Geophysics, v. 41, no. 5, p. 922-938.

SEISMICITY OF THE GEYSERS-CLEAR LAKE REGION

By C. G. Bufe, S. M. Marks, F. W. Lester, R. S. Ludwin,
and M. C. Stickney

ABSTRACT

Microearthquake activity in the Geysers-Clear Lake region has been monitored continuously since 1975. The seismogenic zone across the geothermal area and gravity low is relatively shallow; earthquake focal depths are generally less than 5 km. The absence of deeper earthquakes is consistent with the hypothesis of elevated temperatures associated with a magma body at depth. The present average tectonic-stress orientation, deduced from *P*-wave first motions, indicates maximum compression at N. 20° E. and minimum compression at N. 70° W. over most of the region. This stress orientation is rotated approximately 20° clockwise from that producing maximum right-lateral shear on faults subparallel to the San Andreas fault, possibly accounting for the diffuse pattern of epicenters in the region. Most fault-plane solutions suggest right-lateral strike-slip motion on short, possibly echelon faults trending more northerly than the geologically well defined Maacama and Collayomi fault systems. Most of the earthquakes in the geothermal region occur in two clusters at The Geysers. Earthquakes in the steam-production area and in the surrounding region are characterized by an unusually large number of small earthquakes (high *b* values). The present seismicity at The Geysers is essentially continuous, in contrast to the episodic nature of earthquake activity in the surrounding region. The spatial distribution of earthquakes with regard to the producing steam field and the continuous nature of earthquake activity strongly suggest that much of The Geysers' seismicity is induced. In late September 1977, the deep pattern of faulting at The Geysers changed from predominantly strike-slip to predominantly normal faulting, indicating a decrease in northeasterly tectonic compression.

INTRODUCTION

The Geysers-Clear Lake region lies 50-80 km northeast of the San Andreas fault in the broad zone of transform faulting along the west boundary of the North American plate (fig. 68). A pronounced gravity low extends from The Geysers to the vicinity of Clear Lake (Isherwood, this volume). Large local delays in teleseismic P waves (Iyer and others, this volume) and, as we shall demonstrate, the shallowness of the seismogenic zone lend credence to the hypothesis that a zone of elevated temperatures and partial melting underlies the region of the gravity low at shallow (5-7 km) depths. Regional structures are bounded or cut by a series of northwest-trending faults, some with major Quaternary right-lateral strike-slip displacement (Herd, 1978, McLaughlin, this volume, Hearn and others, this volume). The seismically active Maacama fault system passes along the southwest edge of the gravity low and is outside the area of recent volcanic and geothermal activity.

REGIONAL SEISMICITY

The segment of the San Andreas fault southwest of the Geysers-Clear Lake region last ruptured in the great earthquake of 1906. Since then the region has experienced only minor earthquakes as elastic strain

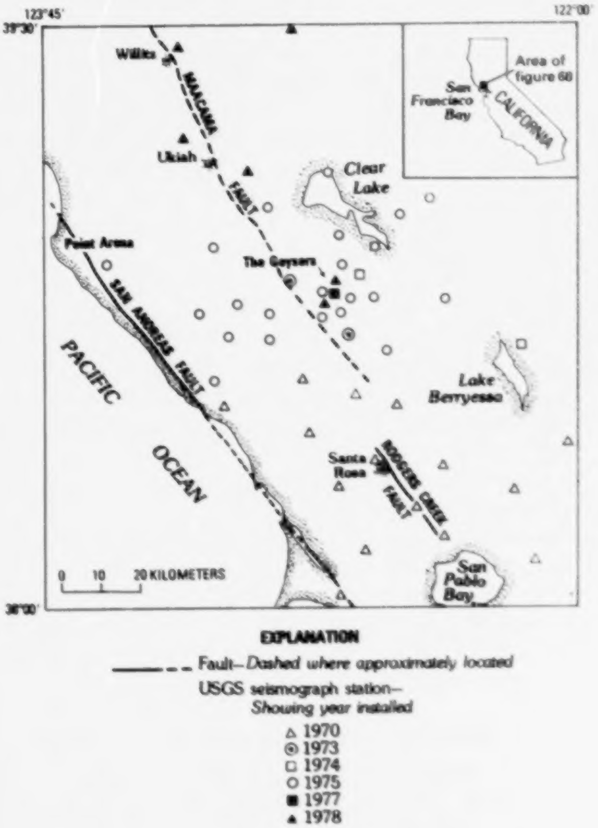
123°45'
122°00'
39°30'
38°00'
Willits
MAACAMA FAULT
Ukiah
Clear Lake
Point Arena
The Geysers
SAN ANDREAS FAULT
PACIFIC OCEAN
Lake Berryessa
Santa Rosa
RODGERS CREEK FAULT
San Pablo Bay
0 10 20 KILOMETERS
Area of figure 68
San Francisco Bay
CALIFORNIA
EXPLANATION
Fault—Dashed where approximately located
USGS seismograph station—Showing year installed
△ 1970
⊙ 1973
□ 1974
○ 1975
■ 1977
▲ 1978

FIGURE 68.—Evolution of the U. S. Geological Survey seismographic network north of San Francisco Bay, Calif.

slowly accumulates. Between 1911 and 1969, only one earthquake larger than magnitude 5 (June 1962, magnitude 5.2) occurred in the region of figure 68, near the town of Ukiah; it was located by the sparse seismographic network of the University of California at Berkeley (Bolt and Miller, 1975).

In October 1969, two earthquakes (magnitudes 5.6 and 5.7) occurred along the Rodgers Creek fault at Santa Rosa, 40 km south of The Geysers. After these earthquakes, the U.S. Geological Survey's dense central California network of seismographs was extended northward into the Santa Rosa area. The evolution of that network north of San Francisco Bay is shown in figure 68. Data-analysis procedures are described by Lester, Kirkman, and Meagher (1976). Preliminary epicenters of earthquakes located by the network are shown in figure 69; most of the earthquakes shown were located in 1975-78 after the network had expanded north to Clear Lake. The Geysers, which is marked by the largest cluster of earthquakes, lies along a 100-km-long lineament (dashed line in fig. 69) that is well developed on ERTS imagery and extends from the north end of Lake Berryessa toward Point Arena. Surface faulting and seismicity patterns appear to be disrupted at the lineament. A gap in the rather diffuse pattern of earthquakes southeast of The Geysers corresponds to the northern part of the Sonoma Volcanics, whose basement apparently behaves as a stable tectonic unit. Also evident at the bottom of figure 69 is a seismicity gap southeast of Santa Rosa along the Rodgers Creek fault.

With the exception of The Geysers, the largest concentrations of earthquakes in the area of figure 69 occur along the Green Valley, Rodgers Creek, and Maacama faults. The Maacama system was very active in 1977-78. The Ukiah earthquake sequence of March 1978 (main-shock magnitude, 4.4) was preceded on the southeast (south of The Geysers) by the Alexander Valley swarm of September 1977 and on the northwest by the Willits sequence (main-shock magnitude, 4.9) of November 1977. These earthquake clusters span a distance of 100 km along the Maacama fault zone. This zone provides a backdrop of tectonic earthquake activity against which the seismicity of the Geysers-Clear Lake geothermal region can be evaluated.

SEISMICITY OF THE GEOTHERMAL AREA

An epicentral map (July 1, 1975 - September 30, 1977) and hypocentral cross section spanning the geothermal area, as outlined by the gravity low, are shown in figure 70. Only those events with adequate depth control (standard error, ±2 km) are plotted in the section. Most events shown are contained in a catalog and map by Marks and Bufe (1978).

Based on the location error for an explosion fired at The Geysers, earthquake location accuracy is estimated to be a few hundred meters in epicenter and about 1 km in depth. Standard errors of most solutions indicate a location precision of 500 m or better. Section *A-A'* (fig. 70*B*) extends from south to north across the Maacama fault at Alexander Valley, through The Geysers and under Mount Konocti. Note that the seismogenic zone at The Geysers and northward across the gravity low is unusually shallow. This dearth of earthquake activity below 5 km is highly unusual in central California. The range of focal depths of earthquakes along the San Andreas system is normally 2-12 km, and deeper (12-20 km) earthquakes occur in a few regions. Yet the lithospheric plates in relative motion across the San Andreas system are believed to be much thicker. Brace and Byerlee (1970) have suggested that the decrease in earthquake activity below 10 km may be due to elevated temperatures which prevent the rock from responding as an elastic solid to long-term increases in shear stress. This explanation may apply to the Geysers-Clear Lake region, with elevated temperatures occurring at much shallower depths.

Elevated temperature at very shallow (5 km) depth is consistent with the presence of a molten or partially molten magmatic body beneath the area. Similar conclusions have been reached from consideration of the gravity data (Isherwood, this volume) and P-wave delays (Iyer and others, this volume). Aside from the concentrated earthquake activity at The Geysers, most of the seismicity in the geothermal region has occurred southeast of Mount Konocti along the north flank of the gravity low near the areas of most recent volcanism.

THE GEYSERS

The Geysers steam field lies adjacent to the Clear Lake Volcanics in fractured graywacke of the Franciscan assemblage, which is overthrust by ophiolite, sandstone, and shale of the Great Valley sequence. The Franciscan and Great Valley terrane of the steam field was recently mapped by McLaughlin (1978). Two main clusters of microearthquakes can be recognized at The Geysers in figure 71. These clusters, shown on the map and east-west cross section in figure 71, are spatially correlated with two independent pressure sinks resulting from steam production described by Lipman, Strobel, and Gulati (1978). From earthquake records of the U.C. Berkeley station at Calistoga in the early 1960's and three weeks of data from an eight-station portable network operated at The Geysers by the U.S. Geological Survey (Hamilton and Muffler, 1972), Marks, Ludwin, Louie, and Bufe (1978) concluded that the present level of seismicity at The Geysers is higher than the preproduction level. Thus it appears that the withdrawal of steam and injection of condensate are inducing many of the earthquakes that occur on a daily basis at The Geysers. It is also likely that some of the earthquakes at The Geysers are triggered by natural tectonic processes. These probably occur as infrequent swarms of short duration, like the 13 small earthquakes that occurred at Rabbit Valley, 5 km north of The Geysers, on August 22-31, 1975, or the

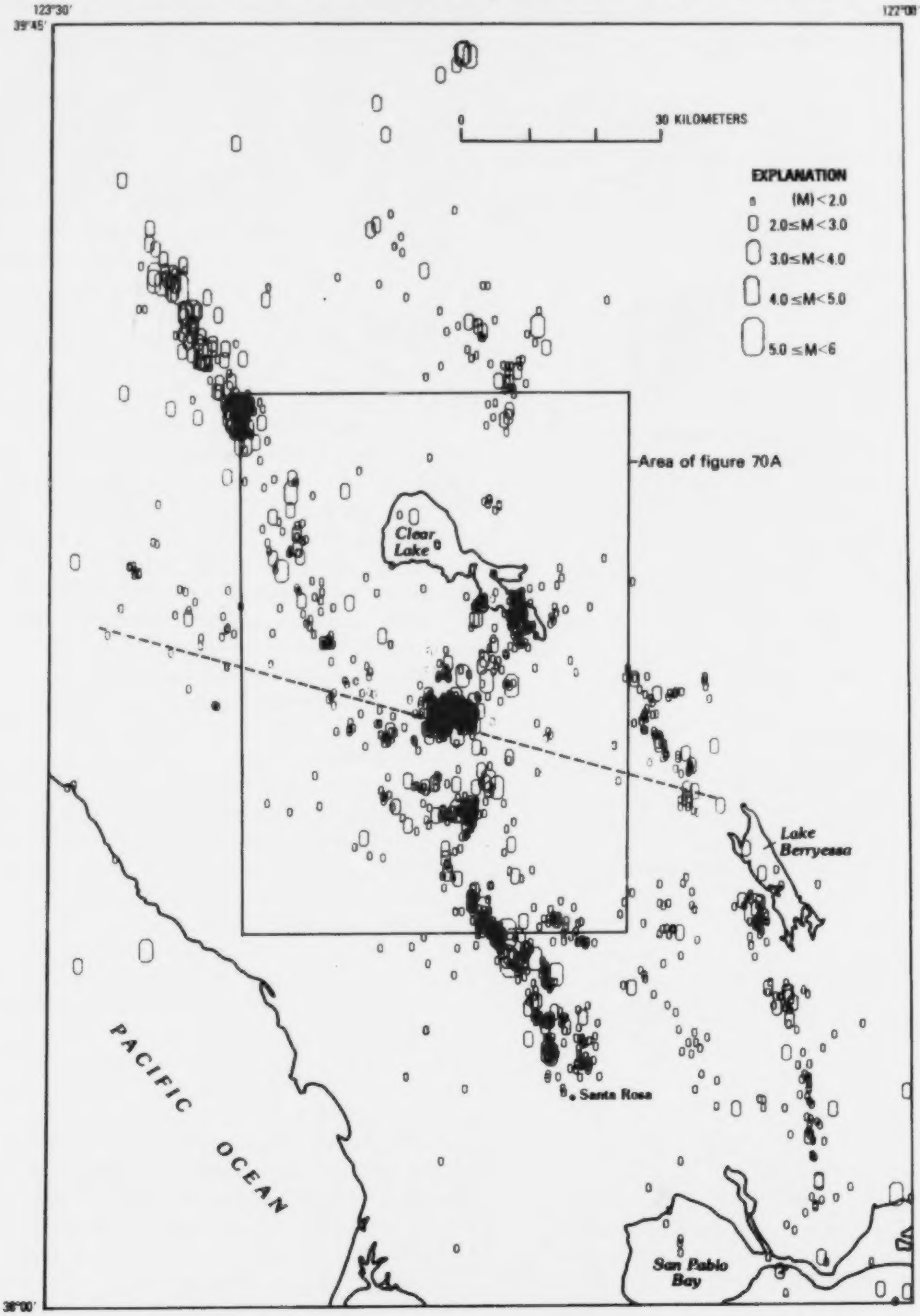
123°30'
122°00'
39°45'
38°00'
0
30 KILOMETERS
EXPLANATION
(M)<2.0
2.0≤M<3.0
3.0≤M<4.0
4.0≤M<5.0
5.0≤M<6
Area of figure 70A
Clear Lake
Lake Berryessa
PACIFIC OCEAN
Santa Rosa
San Pablo Bay

FIGURE 69.—Preliminary epicenters of earthquakes north of San Francisco Bay, 1969-78. Dashed line indicates 100-km-long lineament from ERTS imagery.

19 events on the south flank of Mount Konocti (fig. 70, section *A-A′*), which occurred between September 29 and October 1, 1975.

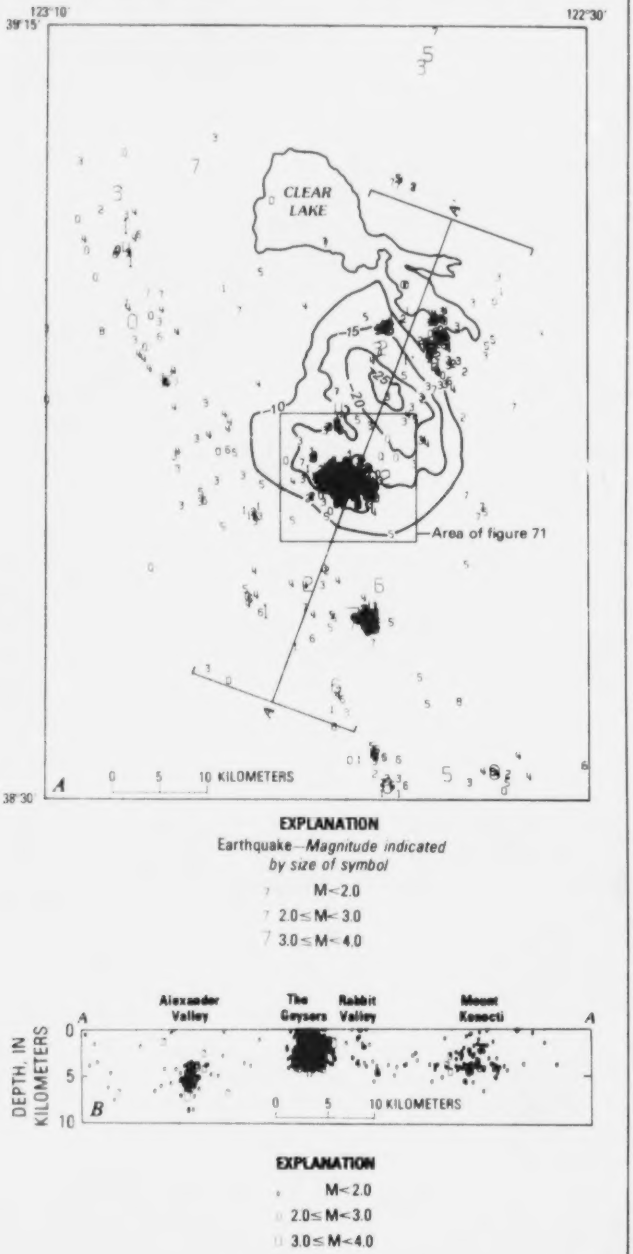

FIGURE 70.—Earthquakes in the Geysers-Clear Lake area and geothermal region. See figure 69 for location. *A*, Location of earthquake epicenters, June 1975-September 1977. Gravity contours, in milligals, are from Isherwood (1976). Numbers indicate focal depths, truncated to integer. *B*, Section *A-A′* is a projection of hypocenters within 9 km of a line *A-A′* onto a vertical plane passing through *A-A′*.

Although distributed much more uniformly in time than earthquakes elsewhere, the earthquakes at The Geysers show similar source characteristics (Peppin and Bufe, 1980), and the same magnitude distribution ($b = 1.2$) as those in the surrounding region.

FAULT-PLANE SOLUTIONS

Representative focal mechanisms of earthquakes in the Geysers-Clear Lake region are shown in figure 72, superimposed on a preliminary, unpublished fault map by B. C. Hearn and R. J. McLaughlin. It is evident from the fault map that the region is characterized by numerous short faults with many different orientations. The dominant mode of faulting at the present time, as indicated by the focal-plane solutions, is strike slip. This is true of earthquakes in the geothermal region as well as those along the Maacama fault system to the south and west. The earthquakes for which focal-plane solutions are shown in figure 72 are described in table 8. The orientation of regional tectonic stress consistent with these focal-plane solutions is maximum compression at N. 20° E. and minimum compression at N. 70° W. Open fractures thus are most likely to be oriented north-northeasterly. This stress orientation is rotated clockwise approximately 20° from that producing maximum right-lateral shear on faults subparallel to the San Andreas; an apparent clockwise stress rotation east of the San Andreas fault can be traced southward as far as Hollister, opposite the south end of the 1906 rupture. This pattern appears also to be representative of earthquakes as far north as the south shore of Clear Lake. Included in figure 72 are fault-plane solutions for the largest events in the August 1975 swarm, which occurred along the Konocti Bay fault zone south of Mount Konocti, and for events in 1976 near Thurston Lake. Both areas are of interest from the standpoint of geothermal exploration.

Fault-plane solutions at The Geysers are somewhat more complicated and show significant temporal variation. Because of instabilities resulting from fluid withdrawal and injection or perhaps inherent in a steam reservoir, The Geysers may be more sensitive to tectonic-stress changes than the surrounding region. Before late September 1977, the dominant mode of faulting was strike slip (Marks and others, 1978; Majer and McEvilly, 1979). From late September 1977 to May 1978 the dominant mechanism was normal faulting. The change in stress orientation (fig. 73) followed a magnitude 3.7 strike-slip event on September 22, 1978, the largest earthquake to be located at The Geysers to date. The change can be explained as a reduction in northeasterly compression such that the vertical (lithostatic) compression, which was the intermediate stress, became the principal compression. This interpretation is supported by the observation that most of the very shallow (less than 2 km depth) earthquakes at The Geysers continued to be caused by strike-slip or thrust movement. The majority of deeper (2-4 km) earthquakes had focal mechanisms indicating normal faulting. The reduction (at least 500 bars, or 50 percent) in northeasterly compression may be a local response to the September 22 earthquake, since strike-slip faulting continues to predominate (fig. 73*B*) along the Maacama fault to the south. However, these strike-slip mechanisms at Alexander Valley show a subtle counterclockwise stress reorientation at about the time of the change in earthquake mechanisms at The Geysers. Regional stress changes may also be inferred from the greatly increased earthquake activity in the surrounding region that began 10 km south of The Geysers with the swarm at Alexander Valley in September 1977. In addition to the earthquakes along the Maacama system at Ukiah and Willits, a sequence of earthquakes occurred near the San Andreas fault at Fort Ross, an area normally quiet (Stickney, 1979).

CONCLUSIONS

The reduced thickness of the seismogenic zone above the heat source for the Geysers-Clear Lake geothermal region implies that this is a zone of relative weakness within the North American plate. Faulting within this zone is complex, and the pattern of earthquakes is diffuse in space and episodic in time. Earthquake activity at the Geysers geothermal development is, on the other hand, highly concentrated and nearly continuous, reflecting local instability and stress concentrations at shallow depths. This result is consistent with surface deformation (Lofgren, this volume) of 2 cm/yr of horizontal convergence and 3 cm/yr of subsidence over the geothermal reservoir, and Isherwood's (this volume) temporal changes in gravity in the same area.

Withdrawal of large quantities of steam for power production from the already underpressured reservoir and massive injection of relatively cool condensate combine to progressively weaken the reservoir rock. Because of this continuing instability, The Geysers may be a tectonic barometer sensitive to small changes in regional stress.

REFERENCES CITED

Bolt, B. A., and Miller, R. D., 1975, Catalogue of earthquakes in northern California and adjoining areas, 1 January 1910-31 December 1972: Berkeley, University of California, Bulletin of the Seismographic Stations, 567 p.

Brace, W. F., and Byerlee, J. D., 1970, California earthquakes: Why only shallow focus?: Science, v. 168, p. 1573-1575.

Hamilton, R. M., and Muffler, L. J. P., 1972, Microearthquakes at The Geysers geothermal area, California: Journal of Geophysical Research, v. 77, p. 2081-2086.

Herd, D. G., 1978, Intracontinental plate boundary east of Cape Mendocino, California: Geology, v. 6, p. 721-725.

Isherwood, W. F., 1976, Gravity and magnetic studies of The Geysers-Clear Lake region, California: United Nations Symposium on the Development and Use of Geothermal Resources, 2nd, San Francisco, 1975, Proceedings, v. 2, p. 1065-1073.

Lester, F. W., Kirkman, S. L., and Meagher, K. L., 1976, Catalog of earthquakes along the San Andreas fault system in central California, October-December, 1973: U.S. Geological Survey Open-File Report 76-732, 37 p.

Lipman, S. C., Strobel, C. J., and Gulati, M. S., 1978, Reservoir performance of The Geysers field: Geothermics, v. 7, p. 209-219.

Majer, E., and McEvilly, T. V., 1979, Seismological investigations at The Geysers geothermal field: Geophysics, v. 44, p. 246-269.

Marks, S. M., and Bufe, C. G., 1978, Preliminary hypocenters of earthquakes in the Healdsburg (1:100,000) quadrangle, Lake Berryessa to Clear Lake, California, October 1969-December 1976: U.S. Geological Survey Open-File Report 78-953, 33 p.

Marks, S. M., Ludwin, R. S., Louie, K. B., and Bufe, C. G., 1978, Seismic monitoring at the Geysers geothermal field, California: U.S. Geological Survey Open-File Report 78-798, 26 p.

Mc Laughlin, R. J., 1978, Preliminary geologic map and structural sections of the central Mayacmas Mountains and the Geysers steam field, Sonoma, Lake, and Mendocino Counties, California: U.S. Geological Survey Open-File Report 78-389, 2 pls.

Peppin, W. A., and Bufe, C. G., 1980, Induced(?) versus natural earthquakes: Search for a seismic discriminant: Seismological Society of America Bulletin, v. 70, p. 269-281.

Stickney, M. C., 1979, The Fort Ross earthquake sequence, March-April, 1978: Seismological Society of America Bulletin, v. 69, p. 1841-1849.

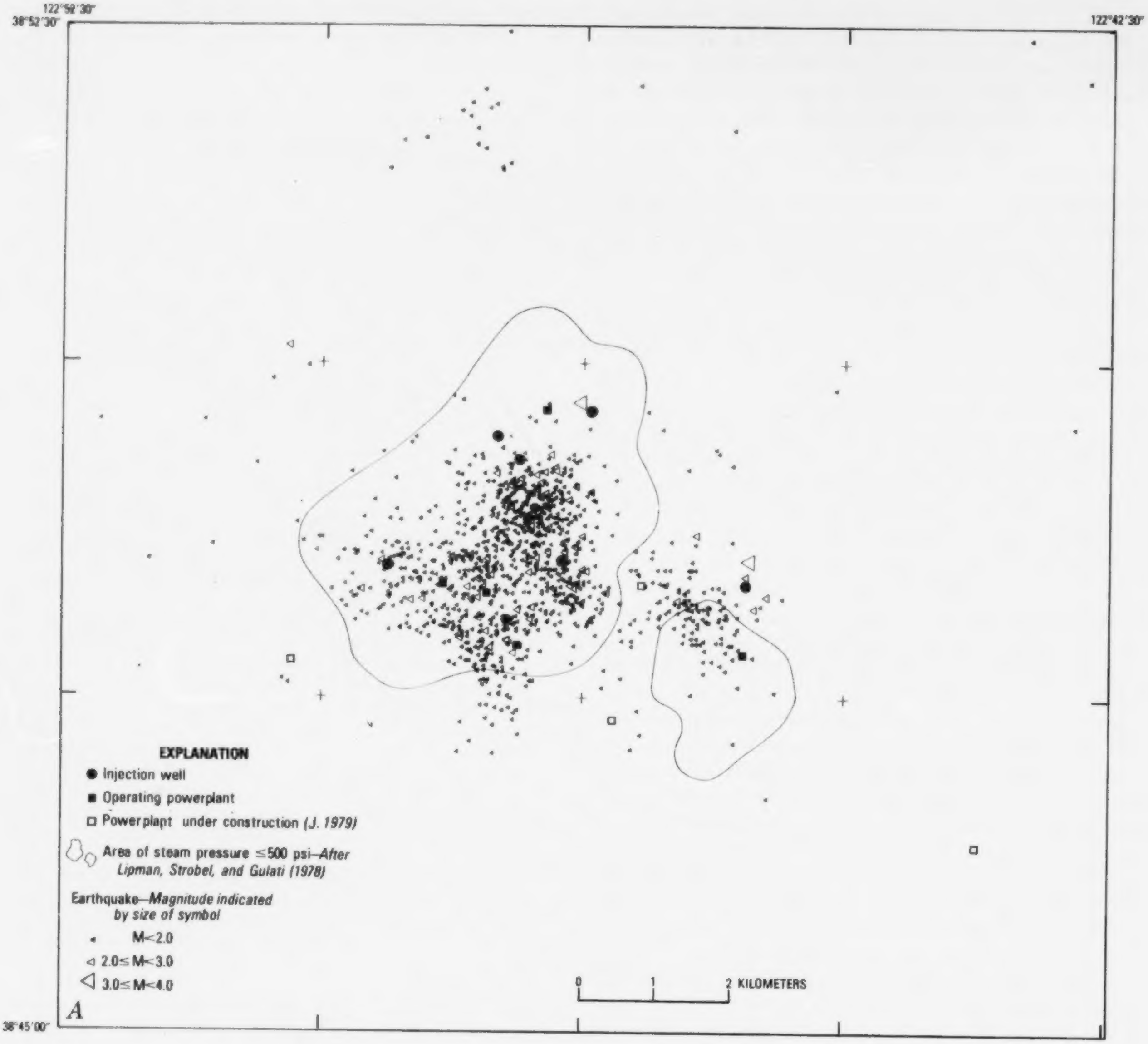
122°52'30"
38°52'30"
122°42'30"
38°45'00"
EXPLANATION
● Injection well
■ Operating powerplant
□ Powerplant under construction (J. 1979)
Area of steam pressure ≤500 psi—After Lipman, Strobel, and Gulati (1978)
Earthquake—Magnitude indicated by size of symbol
M<2.0
◁ 2.0≤M<3.0
◁ 3.0≤M<4.0
0
1
2 KILOMETERS
A

FIGURE 71.—Two main clusters of microearthquakes recognized at The Geysers. See figure 70*A* for location. *A*, Preliminary hypocenters of earthquakes, June 1975 - September 1977. *B*, Events between lat 38°46' N. and lat 38°51' N. are projected onto an east-west vertical plane in section. Modified from plate 1 (1:24,000) of Marks, Ludwin, Louie, and Bufe (1978), with improved coordinates for injection wells.

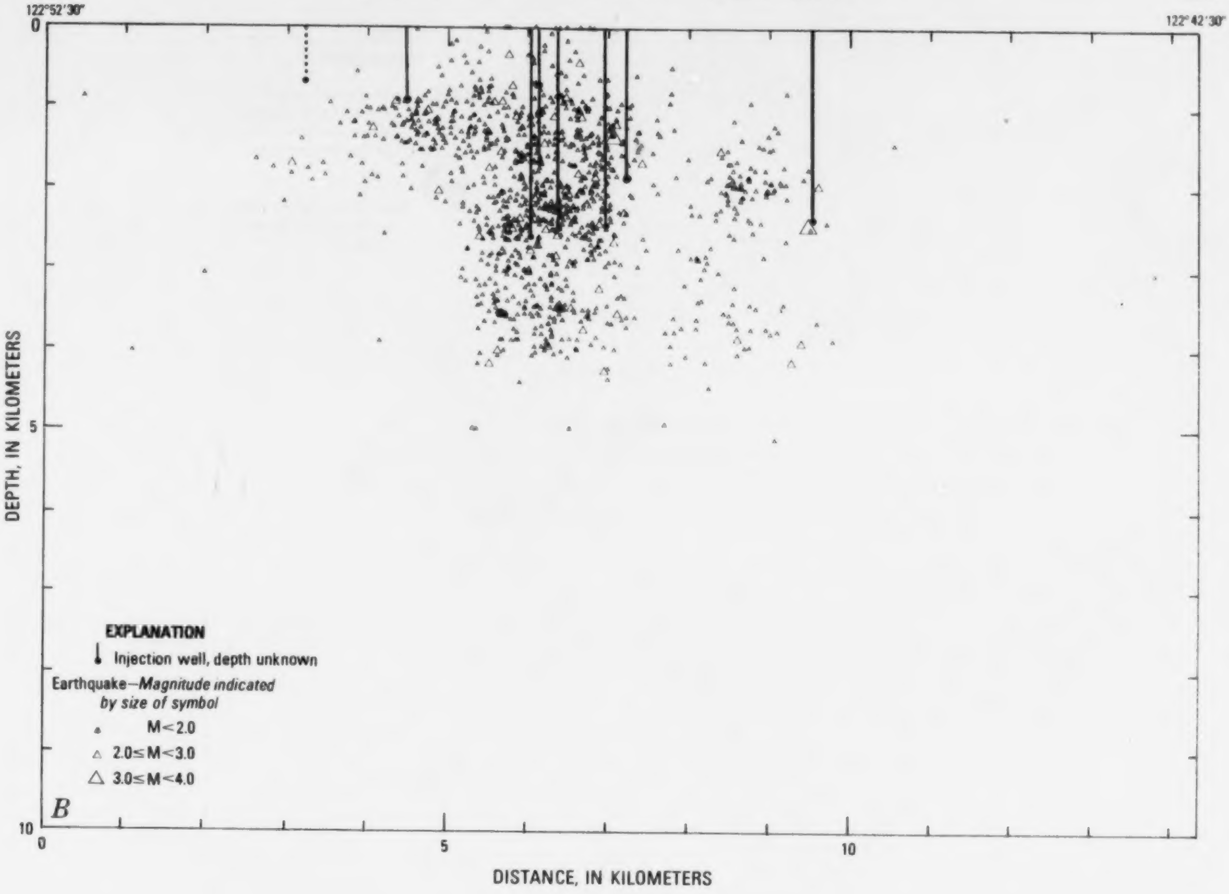

FIGURE 71.—Continued.

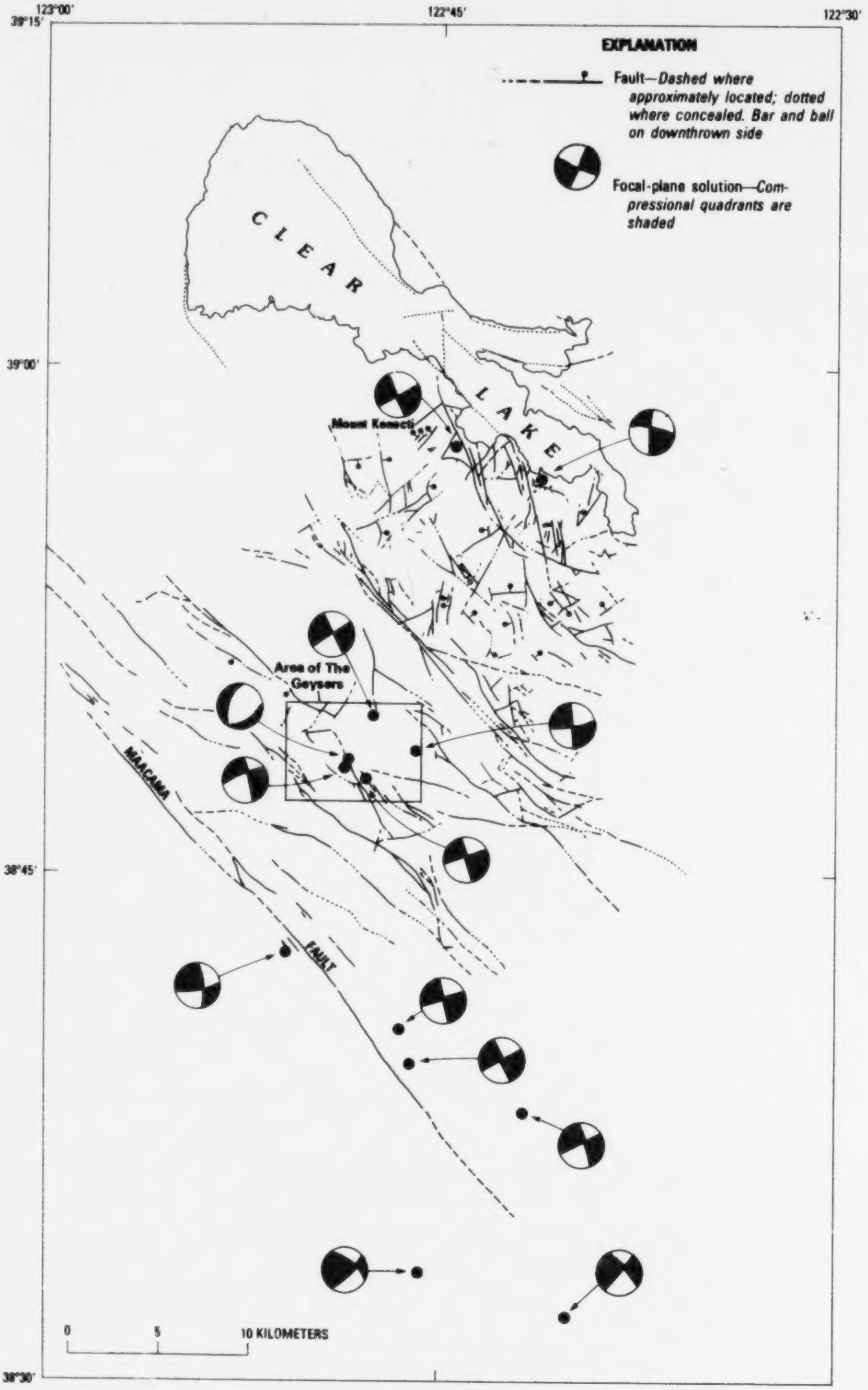
123°00'
122°45'
122°30'
39°15'
39°00'
38°45'
38°30'
EXPLANATION
Fault—Dashed where approximately located; dotted where concealed. Bar and ball on downthrown side
Focal-plane solution—Compressional quadrants are shaded
CLEAR
LAKE
Mount Konocti
Area of The Geysers
MAACAMA
FAULT
0
5
10 KILOMETERS

FIGURE 72.—Representative focal-plane solutions (lower hemisphere) for earthquakes in the Geysers-Clear Lake region. Preliminary faults from R. J. McLaughlin and B. C. Hearn (unpub. data, 1978). Each earthquake and solution are described in table 8.

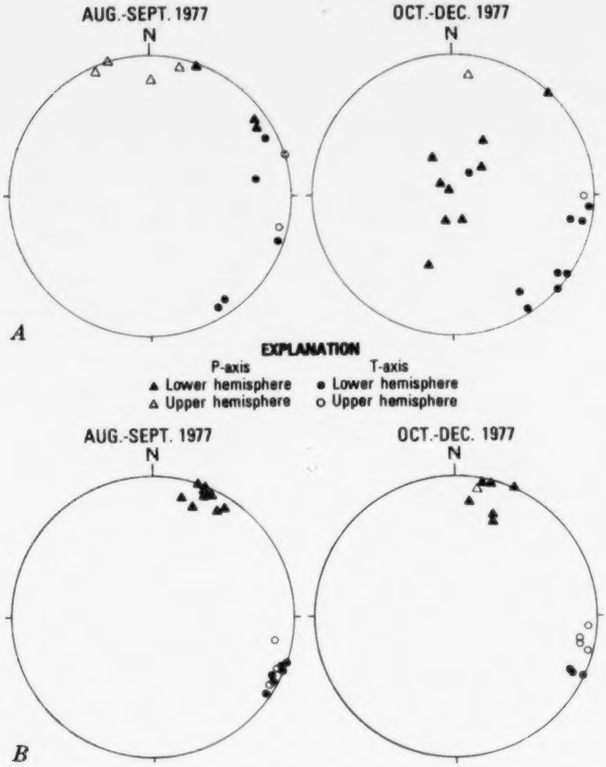

FIGURE 73.—Temporal changes in stress orientation from focal-plane solutions in the Geysers region. *A*, Inferred maximum (P) and minimum (T) principal stress orientations from earthquakes in or near steam-production zone at The Geysers preceding and following the September 22, 1978, earthquake ($M = 3.7$). September 22 earthquake was strike-slip. *B*, Inferred stress orientations from earthquake along Maacama fault at Alexander Valley, 10 km south of The Geysers, during same time periods as in *A*.

TABLE 8.—*Description of earthquakes shown on figure 72*

Date	Time	Latitude		Longitude		Depth	Magnitude	Principal stresses			
								Maximum		Minimum	
Yr/Mo/Da	(G.m.t.)	Deg.	Min.	Deg.	Min.	(km)		(Azi.	Dip)	(Azi.	Dip)
75/05/27	1711	38	47.71	322	47.82	3.30	1.92	28°	00°	298°	00°
75/06/03	1447	38	37.78	122	41.70	5.99	2.54	202	16	296	16
75/09/29	1708	38	57.45	122	44.71	3.98	2.00	24	00	114	00
75/02/25	0125	38	42.54	122	50.75	2.14	2.24	217	20	307	16
76/03/31	0706	38	32.93	122	45.57	6.21	1.24	174	10	270	30
76/08/16	2248	38	56.91	122	40.95	2.37	2.53	184	10	275	02
76/12/22	0042	38	49.64	122	47.45	1.01	3.07	194	02	285	06
76/12/23	0123	38	48.02	122	48.53	2.39	2.90	209	20	116	08
77/02/24	2240	38	31.79	122	40.04	5.99	2.09	176	12	268	12
77/09/08	0028	38	39.97	122	46.15	4.99	3.12	22	00	292	00
77/09/11	2346	38	40.28	122	46.09	4.86	3.24	32	06	302	06
77/09/22	2048	38	48.45	122	46.02	3.21	3.27	37	08	307	06
77/10/07	0201	38	48.29	122	48.45	2.73	2.05	47	67	305	03

MONITORING CRUSTAL DEFORMATION IN THE GEYSERS-CLEAR LAKE REGION

By BEN E. LOFGREN

ABSTRACT

Geodetic surveys from 1973 to 1977 reveal significant crustal deformation in the Geysers-Clear Lake region. Resurveys of precise control networks are measuring both vertical and horizontal ground movement, mostly in the area of geothermal fluid withdrawal. Preliminary evidence suggests right-lateral horizontal movement on northwest-trending fault systems and vertical and horizontal compression of the deep geothermal reservoir system. A direct correlation is suggested between ground-surface deformation and subsurface pressure changes in the reservoir system. Although surface changes appear too small to be of environmental concern in the Geysers-Clear Lake region, they indicate significant hydrodynamic changes in the reservoir.

Two types of vertical changes at The Geysers are indicated in the 1973-77 data: a regional subsidence between the Collayomi and Mercuryville fault zones and local subsidence directly related to the area of principal steam production. Maximum subsidence of 13 cm in $4\frac{1}{2}$ years occurred in the area of most concentrated steam withdrawals and where fluid-pressure declines were near maximum. Subsidence rates throughout the production area from 1973 to 1975 were about half the 1975-77 rates, in apparent correlation with pressure changes measured in the reservoir system. Horizontal ground movement as great as 2.0 cm per year, generally inward toward the center of production, was measured around the perimeter of the steam production area.

INTRODUCTION

Significant crustal deformation frequently accompanies the withdrawal of large volumes of fluids from subsurface reservoirs. Induced hydraulic stresses cause rocks to deform, either along well-defined zones of weakness or as a regional compression of the stressed reservoir system. Although the stress changes are generated in the reservoir system at depth, some of the effects are transmitted to the land surface and can be measured by precise field surveys. Interpretation of measured surface changes can yield insight not only on the nature of the continuing subsurface deformation, but also on the mechanical and recharge characteristics of the reservoir system.

In order to monitor the surface effects of geothermal production at The Geysers, geodetic networks of precise vertical and horizontal control were established by the U.S. Geological Survey and the National Geodetic Survey in the Geysers-Clear Lake region in 1972-73. Many researchers had theorized that because fluid pressures were relatively low in the producing geothermal reservoir, changes caused by continued steam production would be minimal. Subsequent resurveys of the geodetic networks, however, documented significant crustal movement in the period 1972-77. Although the period of recorded change is short, some movement apparently is occuring along major fault zones of the region. More significant, however, are vertical and horizontal surface deformations over the producing part of the geothermal reservoir system in apparent direct response to fluid withdrawals. The surface changes are small and of no environmental importance, but the rates and areal pattern of movements and their correlation with observed fluid pressure and gravity changes suggest a continuing deformation of the reservoir system heretofore not considered.

The Geysers-Clear Lake geothermal region is characterized by rugged topography, unstable terrain, a complex system of active and inactive faults, and highly folded, fractured, and sheared rocks of the Franciscan assemblage of Late Jurassic and Cretaceous age. The principal landforms and fault systems of the region trend generally northwest and suggest active tectonic processes. Whatever deformation results from geothermal production, therefore, is superimposed on a background of slope instability, local and regional tectonism, and waning volcanism.

LAYOUT OF GEODETIC NETWORKS

Within the area of geothermal production, the following types of land-surface deformation might be induced (Lofgren, 1973) either directly or indirectly by fluid withdrawals:

1. Vertical and horizontal compression or expansion of the reservoir system due to induced fluid pressure gradients and hydraulic stresses. Expected changes would be subsidence in areas of fluid extraction and uplift in areas of fluid injection.
2. Vertical and horizontal movement caused by the thermal expansion or compression of subsurface rocks. Thermal effects would be complex, dependent on movement of fluids in re-

sponse to production, recharge, and changes in permeability. Conceivably, reservoir rocks could be cooling due to recharge while the overburden is heating in the areas of steam production wells.

3. Increased landsliding or mass wasting due to induced seismicity or induced slope instability.
4. Local natural tectonic faulting or folding triggered by local hydraulic stresses or by induced seismicity.

In the Geysers-Clear Lake region (fig. 74), northwest-trending faults (Hearn and others, this volume) dominate the structure of the region. Tectonic movement has occurred along the faults within the past 500,000 years and probably continues today. The Maacama fault zone is active (McLaughlin, 1975), the Collayomi fault zone contains at least one active fault (Hearn and others, 1976), and continuing seismic activity (Bufe and others, 1976) suggests that the Konocti Bay fault zone could be active. There is no evidence that the Mercuryville fault zone is active. Also shown in figure 74 is the boundary of the geothermal steam field (Donnelly, Goff, Thompson, and Hearn, 1976).

Circles of 1.6-km radius (fig. 74) have been drawn around each of the producing powerplants to approximate the respective areas of geothermal fluid withdrawal (Reed and Campbell, 1975, p. 1405). These circles overlap in the area of powerplants 1 to 8 and 11 (see fig. 76 for locations); a separate area of production surrounds powerplants 9-10. Also shown in figure 74 is Reed and Campbell's (1975, fig. 2) delineated geothermal resource area, modified to include the Borax Lake area, which was used to define the area of potential geothermal production in designing the vertical- and horizontal-control networks. All first-order leveling in this area is by the National Geodetic Survey or the Geological Survey.

VERTICAL CONTROL

A network of precise vertical control was established in the geothermal production area in mid-1973. It consists of a loop of first-order leveling through the production area (fig. 74) and a line extending northeastward to bench mark Y626 near Lower Lake. This net was resurveyed in the fall of 1975, and an additional tieline was surveyed southwestward from the loop to benchmark D106 (fig.74) near Lytton (north of Healdsburg). Then in the late fall of 1977, with financial assistance from the U.S. Department of Energy, all of the 1975 net (solid lines, fig. 74) was resurveyed, and continuing into spring of 1978, the net was further expanded (all dashed lines, fig. 74). All the above surveys were of first-order accuracy, with closure errors less than 1 mm times the square root of the loop distance in kilometers.

In a region as tectonically active as The Geysers, absolute stability of any area is unlikely. Relative movement within the region, however, is of principal concern in detecting both natural or induced surface changes. Thus, all surveys in this investigation have been referenced to bench marks outside the region potentially affected by geothermal steam production. Bench mark Y626, near the town of Lower Lake, was assumed to be stable and its elevation, established in 1942, was held fixed for the 1973, 1975, and 1977 surveys. This bench mark is east of the principal fault zones, and outside the edge of probable geothermal development. In the more localized interpretative analysis of changes within the loop through the production area (figs. 76 and 77) bench mark R1243 was assumed to be stable. Actually, bench mark R1243 subsided 5.56 cm with respect to stable Y626 from 1973 to 1977.

HORIZONTAL CONTROL

Two types of surveys are included in the horizontal control net (fig. 75): (1) long-distance regional control lines (solid lines) surveyed with highly precise long-distance electonic distance-measuring(EDM)equipment with precision better than 3 mm per 10 km of line length, and (2) local control lines surveyed with medium-range EDM equiment (dashed lines) with a precision of better than 3 mm per 1 km of line length. For changes occurring in a relatively narrow zone, the accuracy of highly precise equipment spanning long distances is about the same as the less precise equipment spanning shorter distances.

Layout of the horizontal network began with several dozen lines surveyed in 1972 and progressively expanded through 1977. As of December 1977, the extensive network array (fig. 75) was being monitored. Many of the lines were surveyed three or four times, others only once. Collectively, these lines provide baseline references for measuring both the magnitude and the rate of horizontal ground movement in the region

As shown in figure 75, the network of horizontal control is concentrated in the area of geothermal production. The net is designed to monitor horizontal ground movement throughout the region, with special emphasis on areas of suspected movement areas of active steam production and principal fault zones.

MEASURED GROUND MOVEMENT

Although measured rates of ground movement are small and the length of records is short, significant crustal changes have occurred both in the area of geothermal production and in the surrounding region.

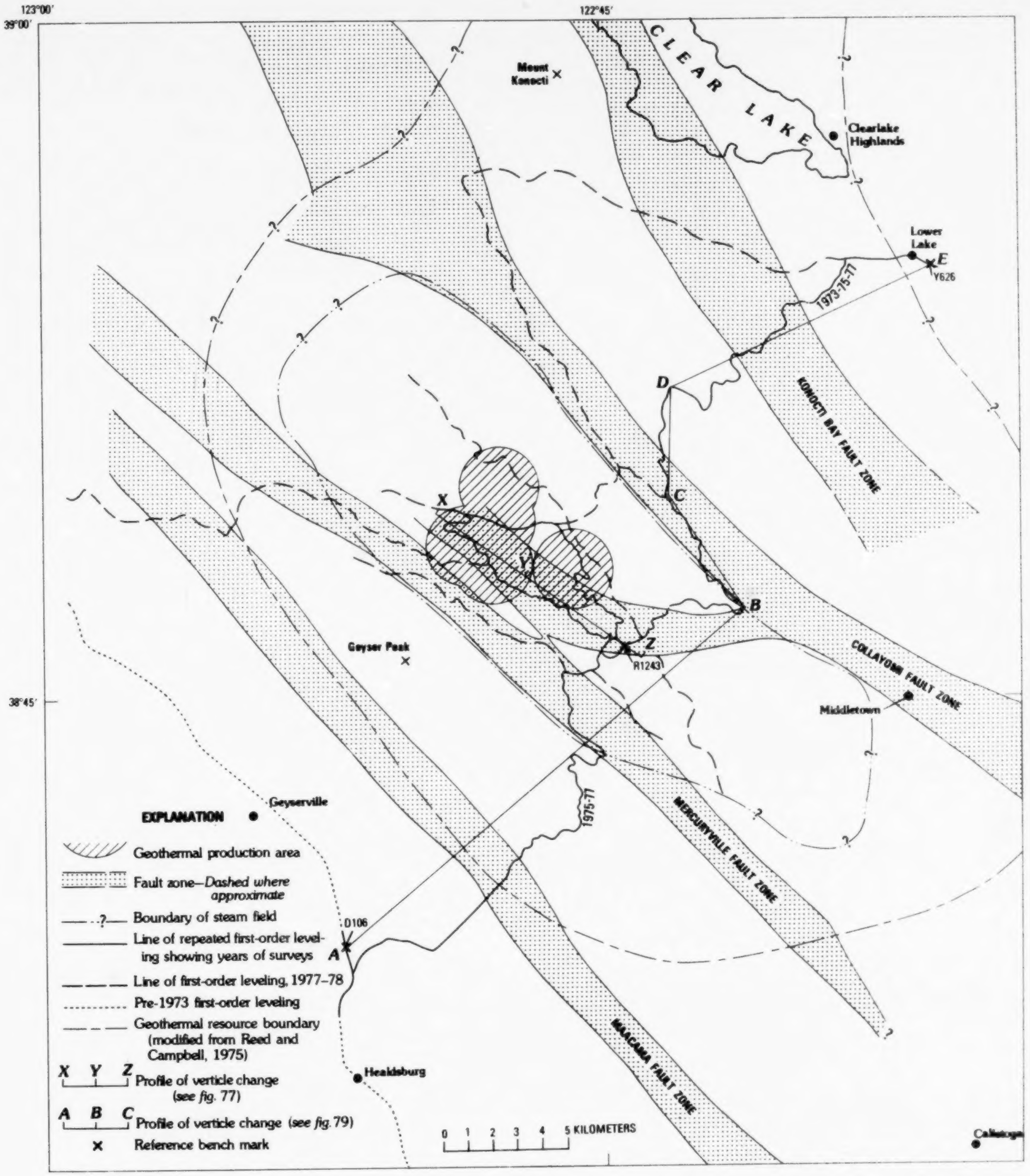
123°00′
122°45′
39°00′
38°45′
Mount Konocti
CLEAR LAKE
Clearlake Highlands
Lower Lake
E
Y626
1973-75-77
D
C
KONOCTI BAY FAULT ZONE
X
Y
B
Z
R1243
Geyser Peak
COLLAYOMI FAULT ZONE
Middletown
MERCURYVILLE FAULT ZONE
Geyserville
1975-77
D106
A
Healdsburg
MAACAMA FAULT ZONE
Calistoga
0 1 2 3 4 5 KILOMETERS
EXPLANATION
Geothermal production area
Fault zone—*Dashed where approximate*
Boundary of steam field
Line of repeated first-order leveling showing years of surveys
Line of first-order leveling, 1977–78
Pre-1973 first-order leveling
Geothermal resource boundary (modified from Reed and Campbell, 1975)
X Y Z Profile of verticle change (see *fig.* 77)
A B C Profile of verticle change (see *fig.* 79)
Reference bench mark

FIGURE 74.—Regional setting of the Geysers geothermal production area and network of first-order leveling in the Geysers-Clear Lake area.

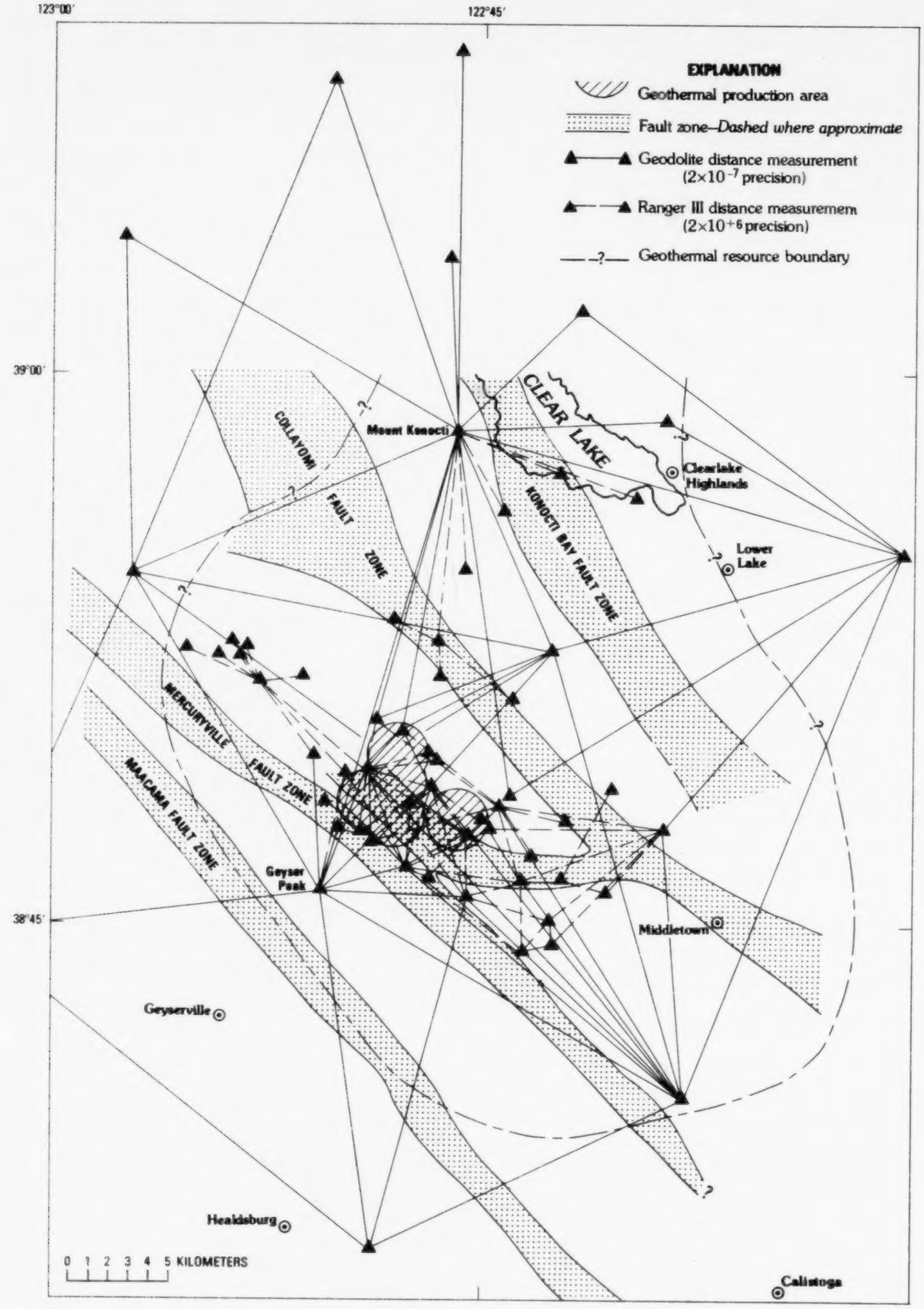
123°00′
122°45′
39°00′
38°45′
EXPLANATION
Geothermal production area
Fault zone–*Dashed where approximate*
Geodolite distance measurement (2×10^{-7} precision)
Ranger III distance measuremem ($2\times10^{+6}$ precision)
—?— Geothermal resource boundary
CLEAR LAKE
COLLAYOMI FAULT ZONE
KONOCTI BAY FAULT ZONE
MERCURYVILLE FAULT ZONE
MAACAMA FAULT ZONE
Mount Konocti
Clearlake Highlands
Lower Lake
Geyser Peak
Middletown
Geyserville
Healdsburg
Calistoga
?
0 1 2 3 4 5 KILOMETERS

FIGURE 75.—Network of precise horizontal control in the Geysers-Lake geothermal area in relation to areas of present and potential geothermal production and major fault systems.

From these measured changes, tentative conclusions can be drawn. The reliability and predictive capability of the observed trends, however, will increase substantially as the length of record increases.

VERTICAL CHANGES

Vertical changes at each bench mark for 1973-75, 1975-77, and 1973-77 (fig. 76) were calculated relative to bench mark R1243 (at the south end of the loop), which was assumed to be stable during the 4½-year period. Bench mark R1243 was arbitrarily selected because it is outside the area of steam production, is common to control lines of figures 77 and 79, and appears as stable as any mark of the region. (It subsided 5.56 cm with respect to the network datum Y626.)

Vertical changes during 1973-75 and 1975-77 along profile X-Y-Z (fig. 77) suggest two types of ground movement: (1) a tectonic local tilt, apparently downward toward the northwest, for about 3.5 km and (2) substantial subsidence in areas of steam production for powerplants 1-8 and 11. Maximum subsidence rates occurred where the circles of influence of powerplants 1-2, 3-4, 5-6, and 7-8 overlap, and decreased from about 4.0 cm per year (bench mark W1244 at powerplants 5-6) in 1973-75 to 2.0 cm per year in 1975-77. The more or less uniform uplift from 1975 to 1977 (fig. 4) southeast to the area of fluid withdrawal may be real—possibly due in part to thermal expansion of the overburden in areas of new drilling—or may be computational—resulting from holding bench mark R1243 stable. Vertical changes in the vicinity of power-

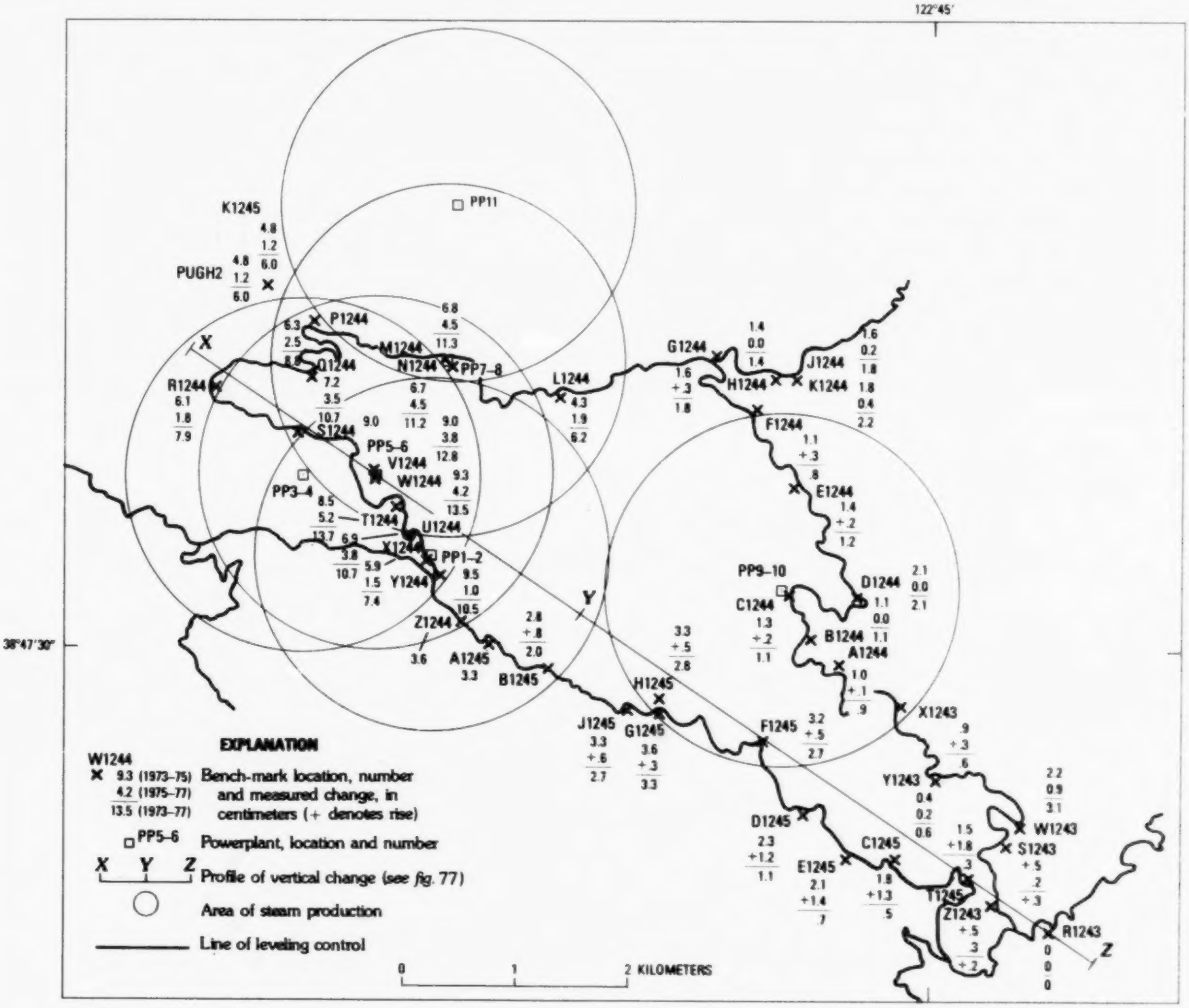
122°45'
38°47'30"
K1245 4.8 1.2 6.0
PUGH2 4.8 1.2 6.0
PP11
P1244 6.3 2.5 8.8
M1244 6.8 4.5 11.3
N1244
PP7–8
X
R1244 6.1 1.8 7.9
Q1244 7.2 3.5 10.7
S1244 9.0
6.7 4.5 11.2
9.0 3.8 12.8
L1244 4.3 1.9 6.2
PP5–6
V1244
W1244 9.3 4.2 13.5
PP3–4
T1244 8.5 5.2 13.7
U1244
X1244 6.9 3.8 10.7
Y1244 5.9 1.5 7.4
PP1–2 9.5 1.0 10.5
Z1244 3.6
A1245 3.3
B1245 2.8 +.8 2.0
Y
G1244 1.6 +.3 1.8
1.4 0.0 1.4
H1244
J1244 1.6 0.2 1.8
K1244 1.8 0.4 2.2
F1244 1.1 +.3 .8
E1244 1.4 +.2 1.2
PP9–10
D1244 2.1 0.0 2.1
C1244 1.3 +.2 1.1
B1244 1.1 0.0 1.1
A1244 1.0 +.1 .9
3.3 +.5 2.8
H1245
J1245 3.3 +.6 2.7
G1245 3.6 +.3 3.3
F1245 3.2 +.5 2.7
X1243 .9 +.3 .6
Y1243 0.4 0.2 0.6
W1243 2.2 0.9 3.1
S1243 +.5 .2 +.3
D1245 2.3 +1.2 1.1
E1245 2.1 +1.4 .7
C1245 1.8 +1.3 .5
T1245 1.5 +1.8 .3
Z1243 +.5 .3 +.2
R1243 0 0 0
Z
EXPLANATION
W1244
9.3 (1973–75)
4.2 (1975–77)
13.5 (1973–77)
Bench-mark location, number and measured change, in centimeters (+ denotes rise)
PP5–6 Powerplant, location and number
X Y Z Profile of vertical change (see fig. 77)
Area of steam production
Line of leveling control
0 1 2 KILOMETERS

FIGURE 76.—Measured vertical changes in the Geysers area, 1973-77, relative to bench mark R1243.

plants 9-10 are minimal (fig. 76), even though large-scale steam production began in 1972.

Reservoir pressure changes in the principal steam reservoir system at The Geysers (Lipman and others, 1977) correlate with the crustal changes reported above. Both the areal extent and magnitude of reported pressure changes in the vicinity of powerplants 1-8 closely agree with measured subsidence (fig. 78) and suggest a direct casual relationship between them. Also, the marked change in subsidence rates between the 1973-75 and the 1975-77 periods agrees in time and magnitude with stepped pressure drops caused by periodic increases in steam production (Lipman and others, 1977, fig. 9). These data suggest that declines in deep reservoir pressure and rates of subsidence are greatest soon after new sources of steam are put on line, and diminish as recharge gradients reach a steady state. In the vicinity of powerplants 9-10, even though steam withdrawals had produced a sizable cone of pressure decline by 1977 (Lipman and others, 1977, fig. 8), most of the pressure change and thus most of the net fluid extractions were considerably west of the line of control bench marks through the area.

In the area of maximum subsidence, reservoir pressures had declined about 126 m of hydraulic head (180 psia) from 1969 to 1977, or about 15.7 m per year, due to steam extractions (fig. 78). Also, 13.7 cm of subsidence, largely due to reservoir compaction, occurred from 1973 to 1977 for an average rate of 3.4 cm per year. Thus 1 cm of subsidence (reservoir compaction) occurred for each 4.6 m of hydraulic head decline, or equivalently, 2.2 mm of subsidence occurred for each meter of head decline. Although neither the length of record nor the accuracy of data (reservoir compaction and pressure change) in this computation are adequate to predict long-term trends, this type of correlation is effective in defining the relations of stress and strain related to fluid production and the compressibility characteristics of subsurface reservoir systems (Lofgren and Klausing, 1969; Poland and others, 1975).

A profile of vertical changes was drawn along a line of bench marks (ABCDE, fig. 74) across the Mayacmas Mountains (fig. 79). 1975 bench-mark elevations (precise first-order leveling along the entire route) are used as the horizontal base of reference in the profile, and 1973 and 1977 differences in elevations are shown. The locations of all bench marks are projected at right angles to the line of profile, and all elevation changes are calculated by holding the elevation of bench mark Y626, east of Lower Lake, stable during the 4½-year period. The elevation of the terrain along the line of bench marks is also shown in figure 79.

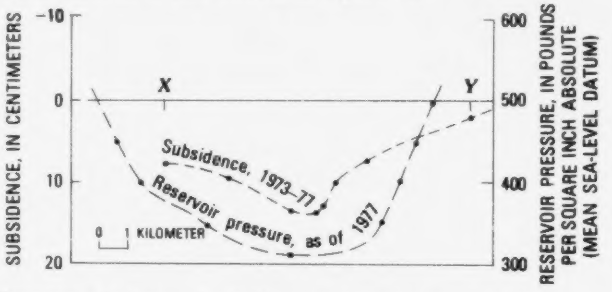

FIGURE 78.—Relation of subsidence to reservoir pressure along line X-Y. Pressure curve from Lipman, Strobel, and Gulati (1977, fig. 2).

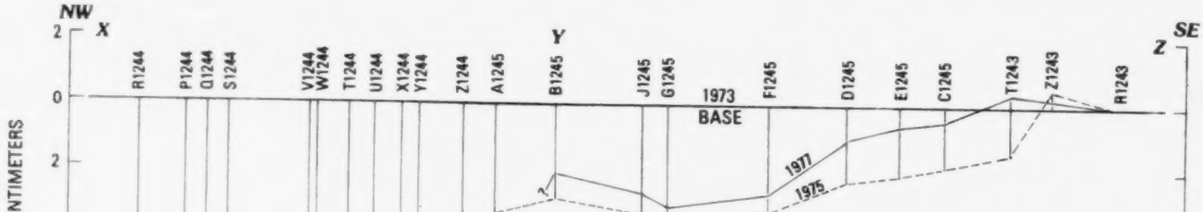

FIGURE 77.—Profiles of vertical changes through the geothermal production area, 1973-77.

Although there was considerable instability indicated in the leveling data from Lower Lake to Cobb (reaches E-D and D-C in figs. 74 and 79), there were no accumulative changes in the 1973-77 data that suggested regional deformation. Elevation differences in this eastern part of the line indicated local changes due to frost action, bench-mark instability, or possibly to movement along numerous faults. From Cobb to Anderson Springs (reach C-B), apparent tilt is to the south or southeast and occurs mainly within or close to the Collayomi fault zone. In the eastern half of reach B-A, apparent tilting is down to the northeast. Regional subsidence is indicated during both the 1973-75 and the 1975-77 periods. Although some of this change may be due to bench-mark instability, there is strong evidence that the mountainous region between the Collayomi fault zone and the Mercuryville fault zone — the region overlying the dry steam part of the geothermal reservoir system — may be subsiding as much as 2 cm per year. Because this profile is 4 km or more distant from the present areas of steam production, it is highly pertinent to problems of reservoir depletion and ownership of subsurface fluids. Field data suggest that bench mark R1243 — the assumed stable reference mark of figure 77 — subsided 5.56 cm with respect to bench mark Y626 from 1973 to 1977.

HORIZONTAL CHANGES

Two types of horizontal ground movement were anticipated during the layout of the control net: slow right-lateral tectonic creep, principally along major fault zones, and radial inward horizontal compression of the geothermal production area. Control lines (fig. 75) were laid out to accommodate the monitoring of both processes. The survey data indicate that both types of movement occur in the Geysers-Clear Lake region. Because many of the control lines had only one or two sets of measurements, the generalized rates of movement summarized in figures 80 and 81 are based on the measured changes along about 30 lines with sufficient record to indicate trends.

Two types of horizontal changes are presented in figure 80: (1) average rates of horizontal shortening or lengthening of long lines spanning the major fault zones outside the geothermal production area, and (2) generalized movement vectors suggesting the direction and rate of local compression in the production area. All rates are based on more than one set of measured changes. Measured rates of change on all except three lines of figure 80 suggest right-lateral movement on the principal fault zones. The exceptions are the −2, −4, and −4 lines that cross the Mercuryville fault zone. Rates of change shown are 9 mm per year or less, but in each instance the lines register only a component of the actual movement along the various fault zones. North and west of the steam-production areas, calculated rates of movement along northwest-trending fault planes, resolved from the data of figure 80, exceed 1.2 cm per year during the 5-year period. Repeated measurements along three other lines (fig. 80) spanning the Mercuryville and Maacama fault zones were not consistent—all showed regional shortening but erratic

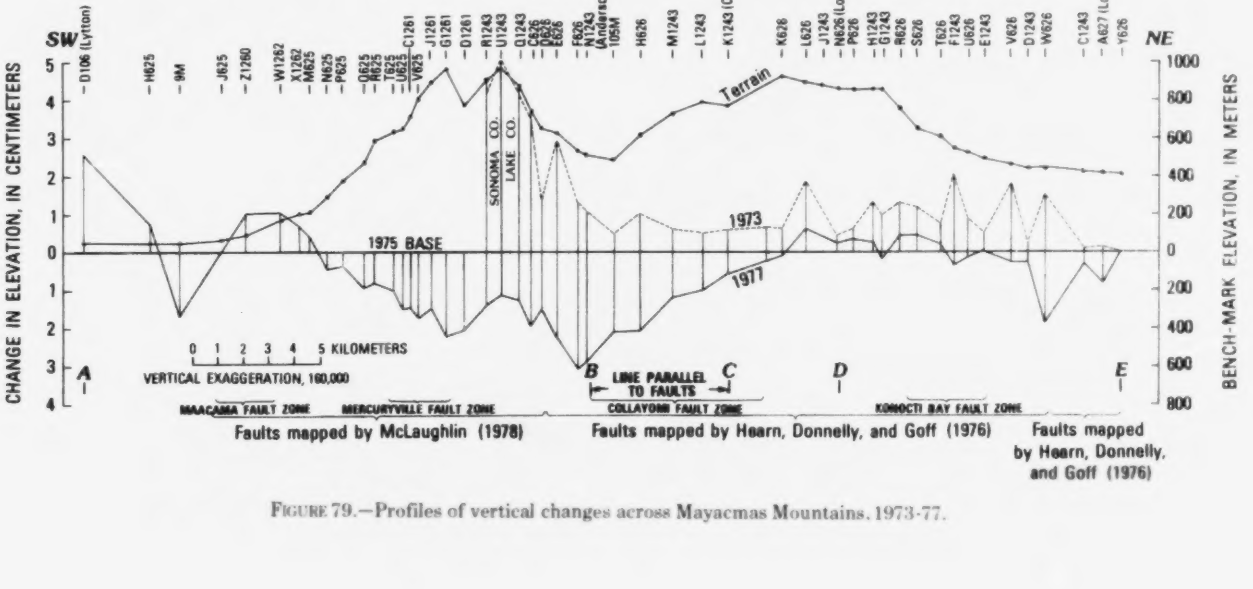

FIGURE 79.—Profiles of vertical changes across Mayacmas Mountains, 1973-77.

rates. These rates are considered questionable pending future surveys.

A few lines of the control net are alined directly across the steam-production area but would include at least a component of right-lateral tectonic change that might occur in the Big Sulphur Creek fault zone. The generalized local vectors of horizontal movement on the production area (fig. 80) resolved from measured changes along local control lines after removing the regional tectonic changes. These vectors denote calculat-

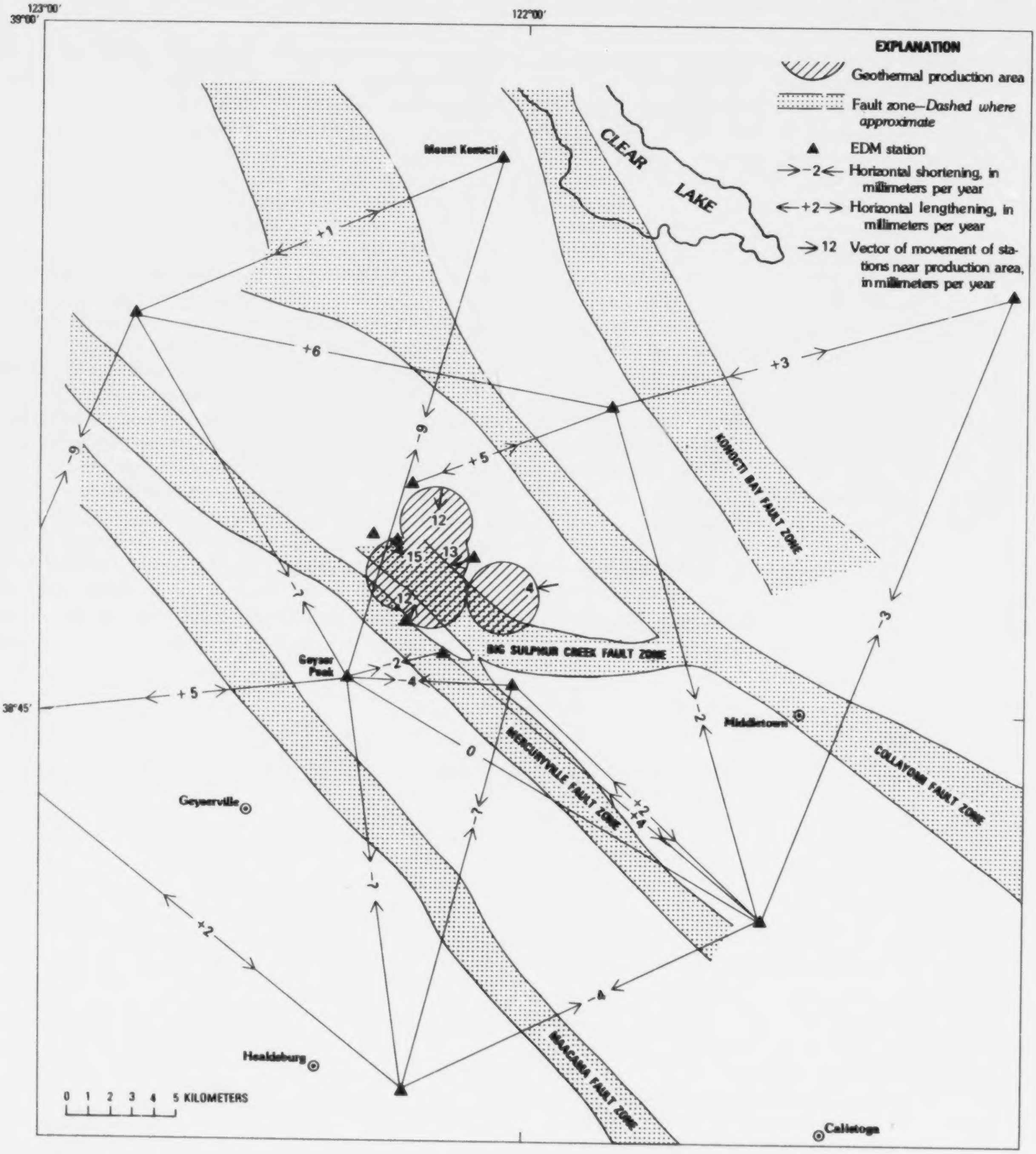
123°00′
39°00′
122°00′
38°45′
EXPLANATION
Geothermal production area
Fault zone—Dashed where approximate
EDM station
→−2← Horizontal shortening, in millimeters per year
←+2→ Horizontal lengthening, in millimeters per year
→12 Vector of movement of stations near production area, in millimeters per year
CLEAR LAKE
Mount Konocti
KONOCTI BAY FAULT ZONE
BIG SULPHUR CREEK FAULT ZONE
MERCURYVILLE FAULT ZONE
COLLAYOMI FAULT ZONE
MAACAMA FAULT ZONE
Geyser Peak
Middletown
Geyserville
Healdsburg
Calistoga
+1
+6
+3
−6
+5
−6
12
15
13
4
17
−7
−2
−4
+5
0
−2
+2
+4
−7
−7
−3
+2
−4
0 1 2 3 4 5 KILOMETERS

FIGURE 80.—Generalized horizontal ground movement in the Geysers-Clear Lake area, 1972-77, in millimeters per year.

ed rates of relative movement within the production area and are not changes in lengths of survey lines. The horizontal movements in the production area, in all instances toward the center of fluid withdrawal, range from about 15 millimeters per year in areas of heaviest fluid production to about 4 millimeters per year in the peripheral area.

Of particular significance are the abrupt changes in rate of movement, and sometimes reversals in direction of ground movement, in areas of new steam production (fig. 81). Survey lines spanning the well field supplying steam to powerplant 11 (upper two graphs) showed marked changes in rate soon after steam production began in 1975. Lines crossing the older producing areas (lower two graphs) show twice as much horizontal compression and many more uniform changes. As with vertical compression of the geothermal reservoir system, surface measurements to date suggest that the horizontal compression of the deep reservoir system is directly related to fluid-pressure changes—changing rapidly soon after the effects of new steam production are felt, and gradually establishing more or less steady rates of compression as the rate of pressure decline stabilizes.

CONCLUSIONS

Two types of surface ground movement are occurring in the Geysers-Clear Lake area: (1) regional tectonism of natural origin, with right-lateral creep along the

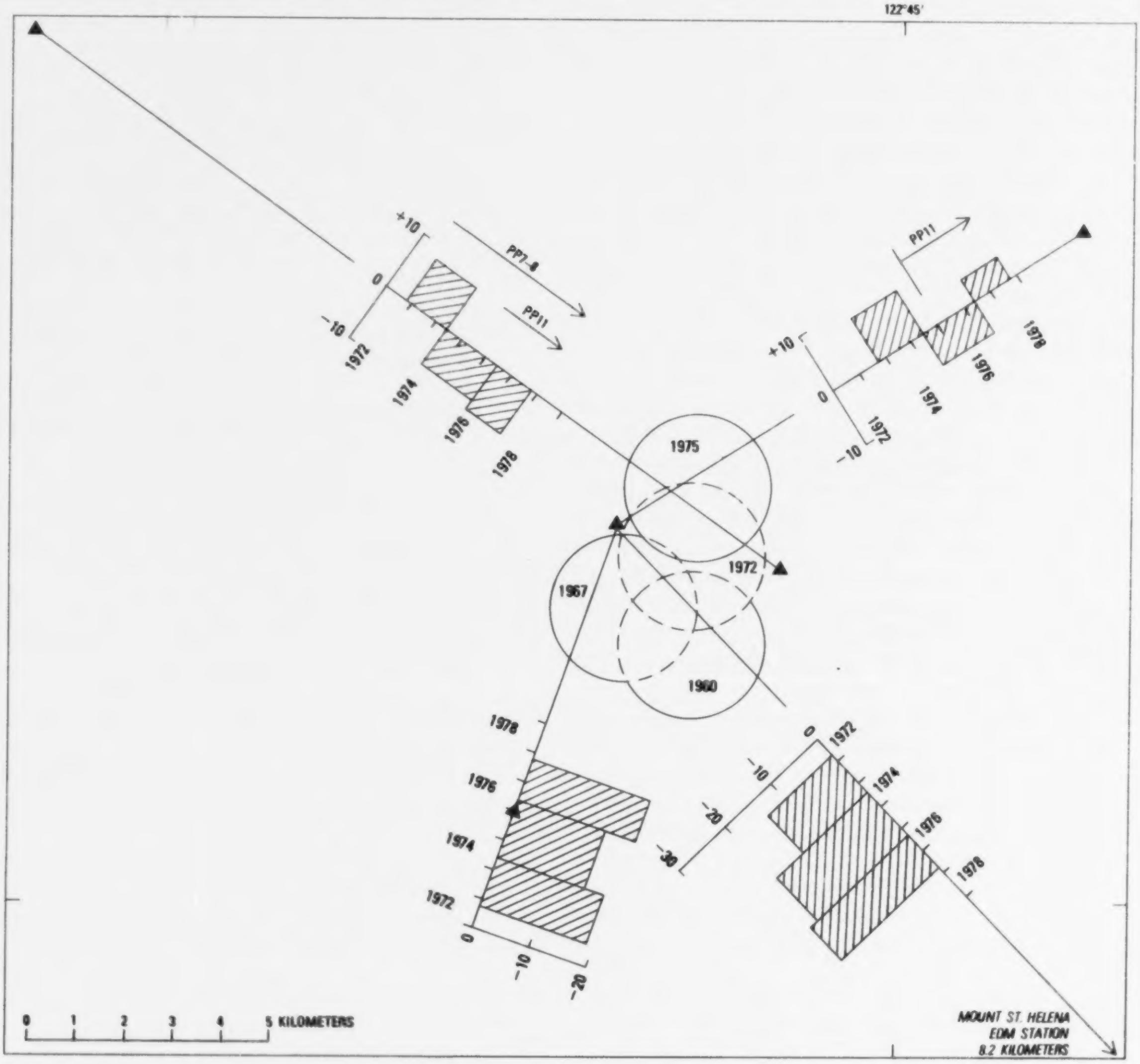
122°45'
38°45'
+10
0
−10
1972
1974
1976
1978
PP7-8
PP11
PP11
+10
0
−10
1972
1974
1976
1978
1975
1972
1967
1960
1978
1976
1974
1972
0
−10
−20
0
1972
−10
−20
−30
1974
1976
1978
0 1 2 3 4 5 KILOMETERS
MOUNT ST. HELENA
EDM STATION
8.2 KILOMETERS

FIGURE 81.—Changing rates of ground movement on lines spanning the geothermal production area (circles with rates of first production). Rates are in millimeters per year; lengthening (+) above line, shortening (−) below line. ▲, EDM station.

principal fault zones and regional subsidence between the Collayomi and Mercuryville fault zones, and (2) local subsidence and horizontal compression related to steam production. Regional changes are at rates of a few millimeters per year; local movements are at rates of a few centimeters per year. Measured surface effects over comparatively short periods suggest that the deep geothermal reservoir is being compressed both vertically and horizontally as fluid pressures within it are drawn down by production.

Of particular interest, and quite unexpected in view of similar studies in other areas, are the abrupt changes in rate of both vertical and horizontal surface deformation in areas of new production. Surface changes suggest that both the vertical and the horizontal compression of the geothermal reservoir are most rapid soon after new or increased steam production. Within months after the inception of steam production or after an increase in rate of production, deformation rates tend to stabilize. These changes are most noticeable on horizontal lines spanning the production area for powerplant 11 (fig. 81), which began production several years after monitoring networks were established.

Because the depth of production wells and the areal distribution of powerplant are on the same order of magnitude, the vertical and horizontal dimensions of the geothermal reservoir system affected by fluid withdrawals for that power plant are about the same. It is expected, therefore, that the rates of vertical and horizontal surface deformation for a given stress change would also be of the same general order of magnitude for reservoir systems at shallow depth. Because the measured rates of horizontal and vertical deformation over the steam-production area are about the same, it appears that both the horizontal and vertical stresses induced by steam production, and the rock compressibilities of the reservoir system, are about the same in the horizontal and vertical directions.

Interpretation of the regional tectonic strain rates may be complicated by the possibly episodic nature of local strain over geologically short periods. Longer periods of monitoring and more detailed nets should make it possible in the future to assign movement to specific fault zones and to assign increments of tilting to specific fault blocks. Such data will be important in assessing the seismic risks in the region.

REFERENCES CITED

Bufe, C. G., Pfluke, J. H., Lester, F. W., and Marks, S. M., 1976, Map showing preliminary hypocenters of earthquakes in the Healdsburg (1:100,000) quadrangle, Lake Berryessa to Clear Lake, California, January 1969-June 1976: U.S. Geological Survey Open-File Report 76-802, scale 1:100,000.

Donnelly, J. M., Goff, F. E., Thompson, J. M., and Hearn, B. C., Jr., 1976, Implications of thermal water chemistry in the Geysers-Clear Lake area: Lake County Geothermal Environmental Seminar, Oct. 28, 1976, Proceedings.

Hearn, B. C., Jr., Donnelly, J. M., and Goff, F. E., 1976, Preliminary geologic map and cross-section of the Clear Lake volcanic field, Lake County, California: U.S. Geological Survey Open-File Report 76-751.

Lipman, S. C., Strobel, C. J., and Gulati, M. S., 1977, Reservoir performance of The Geysers field: Ente Nazionale per l'Energia Elettrica-Energy Research and Development Administration Workshop, Larderello, Italy, 1977, Proceedings, p. 233-255.

Lofgren, B. E., 1973, Monitoring ground movement in geothermal areas: American Society of Civil Engineers Annual Hydraulics Division Specialty Conference, 21st, Bozeman, Mont., 1973, Proceedings, p. 437-447.

Lofgren, B. E., and Klausing, R. L., 1969, Land subsidence due to ground-water withdrawal, Tulare-Wasco area, California: U.S. Geological Survey Professional Paper 437-B, 103 p.

McLaughlin, R. J., 1975, Preliminary compilation of in-progress geologic mapping in the Geysers geothermal area, California: U.S. Geological Survey Open-File Report 75-198, scale 1:24,000.

—— 1978, Preliminary geologic map and structural sections of the central Mayacmas Mountains and the Geysers steam field, Sonoma, Lake, and Mendocino Counties, California: U.S. Geological Survey Open-File Report 78-389.

Poland, J. F., Lofgren, B. E., Ireland, R. L., and Pugh, R. G., 1975, Land subsidence in the San Joaquin Valley as of 1972: U.S. Geological Survey Professional Paper 437-H, 78 p.

Reed, M. J., and Campbell, G. E., 1975, Environmental impact of development in the Geysers geothermal field, USA: United Nations Symposium on the Development and Use of Geothermal Resources, 2d, San Francisco, 1975, Proceedings, p. 1399-1410.

Swe, Win, and Dickinson, W. R., 1970, Sedimentation and thrusting of late Mesozoic rocks in the Coast Ranges near Clear Lake, California: Geological Society of America Bulletin, v. 81, no. 1, p. 165-187.

ATTENUATION OF TELESEISMIC *P* WAVES IN THE GEYSERS-CLEAR LAKE REGION

By Chi Yuh Young and Ronald W. Ward

ABSTRACT

During July and September 1976, the U.S. Geological Survey deployed 14 portable short-period seismographs along a line trending roughly northwest-southeast between Clear Lake and The Geysers to study traveltime delays of teleseismic *P* waves associated with magma or partially molten zones beneath the geothermal system. The *P* waves of 22 teleseismic events, suitable for attenuation analysis, were recorded by 13 seismographs. The events were digitized and spectrally analyzed using both periodograms and the maximum entropy method (MEM). Seismograms exhibited both a significant drop in amplitude and waveform broadening.

The location and extent of the zones of high attenuation were qualitatively inferred from the power-density spectra of the seismograms. The reduced spectral ratio technique was applied to determine the differential attenuation factor δt^* quantitatively, assuming that the quality factor *Q* is independent of frequency. The maximum differential attenuation is about 0.3 s, which roughly corresponds to a 5-km-thick zone with *Q* equal to 25 embedded in a high-*Q* medium. The lateral variation of δt^* was used to infer the *Q* structure in the frequency range 0.25–2.5 Hz, assuming that the teleseismic wave propagating to each station is identical when it enters the bottom of the crust-upper mantle model. A shallow zone of high attenuation extends from the Geysers steam field an undetermined distance toward the northeast and is 15 km wide. The zone of high attenuation deepens to the northwest between stations CL07 and CL08 and toward the southeast near station CL05. The thickest part is probably located beneath station CL06 or Mount Hannah and possibly station CL12, where the zone is very close to the surface. This anomaly extends southwestward toward the Geysers steam field, which is associated with the vapor-dominated hydrothermal reservoir inferred from other geophysical surveys.

INTRODUCTION

This study uses the lateral variation of power-density spectra of *P* waves observed across a geothermal system. The degree of attenuation of *P* waves depends critically upon the physical state and thermal regime within the Earth. The surface observations are then related to a quantitative model of the quality factor, *Q*. Studies of *P*-wave attenuation can be a useful tool to constrain the geologic crustal structure beneath The Geysers, the site of the world's largest producer of geothermal electricity.

Three mechanisms proposed for seismic attenuation are partial melting, grain-boundary relaxation, and "high temperature internal friction background" (Jackson and Anderson, 1970). Each of these mechanisms depends on temperature. The degree of seismic attenuation reflects the thermal state of the medium and the extent of partial melting (Walsh, 1968, 1969). In the vapor-dominated porous medium that typifies the Geysers geothermal system, the coupling between fluid-flow waves and seismic body waves in the zone of liquid-vapor mixture will affect the velocity and increase the attenuation of the seismic waves. Compressional or *P* waves are the only ones affected by this mechanism (White, 1975).

The volcanic sequences of the area (fig. 82) range in age from 2.1 m.y. to 10,000 years (Donnelly-Nolan and others, this volume). Changes in magma composition from basalt or andesite through dacite to rhyolite reflect a silicic differentiation process. Other detailed studies show that the Geysers-Clear Lake region is a structurally controlled geothermal resource area (McLaughlin, this volume). The Geysers steam reservoirs are related to the northwest-southeast-trending faults dipping steeply northeast which control the structural traps. A magma chamber beneath the Clear Lake volcanic field is also suggested as the heat source of the geothermal system (Isherwood, this volume).

Geophysical studies conducted in the Geysers-Clear Lake area include microearthquake surveys, gravity and magnetic surveys, seismic-reflection profiles, seismic refraction, and teleseismic *P*-wave traveltime delays. These investigations are detailed in other chapters of this volume as well as elsewhere (Iyer and others, 1979; Majer and McEvilly, 1979). The gravity and magnetic studies have aided in determining the deep geologic structure, and the microearthquake studies have aided in mapping the active faults. The studies also suggest that the gravity, the *P*-wave traveltime delays, and the electrical source of the geophysical anomalies could be a magma chamber or partially molten zone at shallow depth beneath the geothermal area.

If a magma chamber or partially molten zone does exist, it may or may not produce observable attenuation of seismic waves as they pass through the anomalous zone. For instance, in Yellowstone National Park

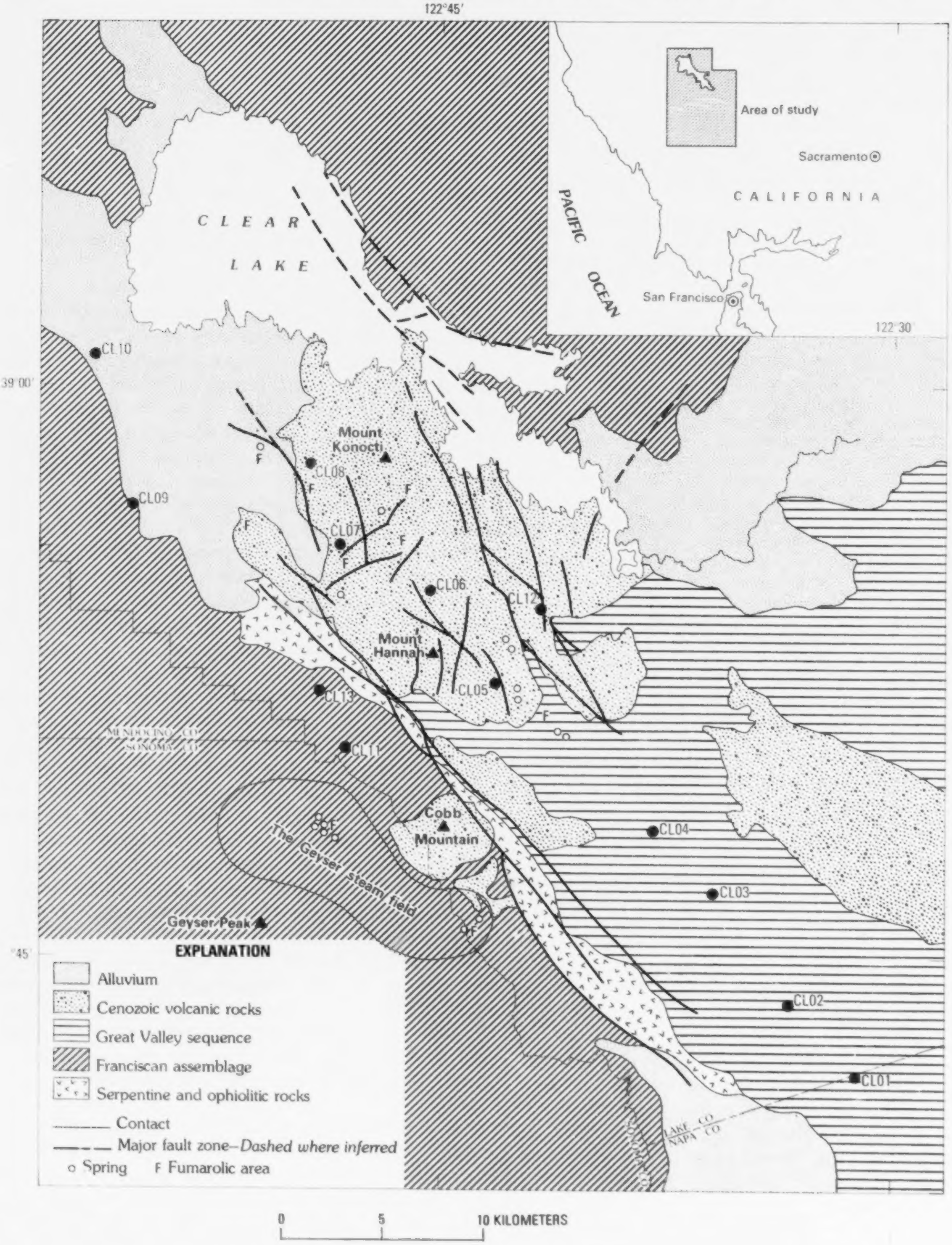
122°45'
122°30'
39°00'
°45'
CLEAR LAKE
Mount Konocti
Mount Hannah
Cobb Mountain
Geyser Peak
The Geyser steam field
CL01
CL02
CL03
CL04
CL05
CL06
CL07
CL08
CL09
CL10
CL11
CL12
CL13
F
MENDOCINO CO
SONOMA CO
LAKE CO
NAPA CO
Area of study
Sacramento
CALIFORNIA
PACIFIC OCEAN
San Francisco
EXPLANATION
Alluvium
Cenozoic volcanic rocks
Great Valley sequence
Franciscan assemblage
Serpentine and ophiolitic rocks
Contact
Major fault zone—Dashed where inferred
Spring
F Fumarolic area
0
5
10 KILOMETERS

FIGURE 82.—Generalized geologic and structural map of the Geysers-Clear Lake area (modified from Hearn, 1976), showing location of seismic array.

a large magma chamber was inferred from the *P*-wave traveltime residuals (Iyer, 1975) and yet the seismograms do not exhibit significant waveform broadening, one indication of seismic attenuation, but there is considerable amplitude variation (12–20 dB) across the array. Using a spectral data analysis technique, such as the reduced spectral ratio method (Teng, 1968; Solomon, 1973), we have attempted to delineate the extent and size and possibly estimate the fraction of melt within the magma chamber at The Geysers. In applying this technique, we assume that the effect of seismic attenuation dominates the spectrum of the seismogram compared to other medium effects such as crustal reverberation.

Acknowledgements.—We thank H. M. Iyer, Craig Weaver, Tim Hitchcock, and Alan Walter of the U.S. Geological Survey in Menlo Park, Calif., for helpful discussions, assistance in digitizing data, and providing computer programs to read the data at the North Texas Regional Computer Center in Dallas. This research was supported by National Science Foundation (Research Applied to National Needs) Grant AER75-23619 during the data acquisition, and by U.S. Department of the Interior, Geological Survey Grant 1408-0001-G-426 during the data analysis, interpretation, and preparation of the study.

DATA

During July 1976, and again from mid-August through the first week of September 1976, short-period vertical or three-component portable seismographs were deployed by the U.S. Geological Survey for a total of 42 days and operated at 14 stations along a northwest-southeast line in the Geysers-Clear Lake region (fig. 82). (One station, CL14, produced no satisfactory data and has been excluded from the study.) The seismograms are used for the study of the teleseismic *P*-wave traveltime delays (Iyer and others, 1979; Iyer and others, this volume) as well as the attenuation study.

The seismograms for a total of 22 events (table 9) were found to have large enough signal-to-noise ratio (S/N) for attenuation analysis and were selected for digitization at 100 samples per second. Most of the events arrived from three narrow ranges of azimuths: northwest, southeast, and southwest. The *P*-wave seismograms of various events exhibit significant amplitude variation across the array and a frequency shift to longer periods correlating with the amplitude decrease above the center of the array (fig. 83).

The events recorded characteristically had emergent waveforms, possibly due to heterogeneity of the crust and upper mantle beneath the geothermal area. In this region, the seismograms are usually accompanied by a high noise level, which severely contaminates some *P*-wave signals. These factors made the selection of a time window for the spectral analysis very difficult and introduced large uncertainties into amplitude spectra of the waves. In general, a time window less than 5 s was chosen, and the power-density spectrum was computed using both periodogram analysis (Blackman and Tukey, 1958) and Burg's maximum entropy method (MEM) (J. P. Burg, unpub. data, 1967; Ulrych and Bishop, 1975). By picking the proper length of the prediction error filter, the MEM generally gives a smoother spectrum than the periodograms analysis. The spectrum obtained by the MEM was used in this study.

MEASUREMENT OF DIFFERENTIAL ATTENUATION

BACKGROUND

The effect of seismic attenuation can be observed qualitatively from the seismograms; however, the quantitative measurements of the attenuation factors are more useful for inferring important physical properties of the geothermal area. The observation of a distant earthquake across a rather small area allows us to make certain simplifying assumptions, as illustrated in figure 84. The *P* wave entering the upper mantle beneath the geothermal area is approximately planar with constant amplitude over the area. It propagates through the geothermal system and is recorded by seismographs on the surface. There is obvious lateral variation in the amplitude, frequency content, and coda duration of the waveform. To extract this information from the body-wave signals, we can apply the technique of body-wave equalization (Ben-Menahem and others, 1965), which has been used in different forms to study attenuation (Teng, 1968; Solomon and Toksöz, 1970; Ward and Toksöz, 1971; Solomon, 1972, 1973).

We can write the observed amplitude spectrum of a body wave as

$$A(f,\theta,\phi) = A_0(f,\theta,\phi)\, A_m(f)\, A_c(f)\, A_i(f), \qquad (1)$$

where $A_0(f,\theta,\phi)$ is the source function, which depends on the frequency f and the propagation direction (θ,ϕ). In general, A_0 includes the source time function, the radiation pattern, and the finiteness effect due to the dynamics of rupture; A_m is the mantle transfer function, which includes geometric spreading and attenuation effects; A_c is the crustal transfer function for source and receiver, containing the effect of differential attenuation as well as reverberation and amplitude ef-

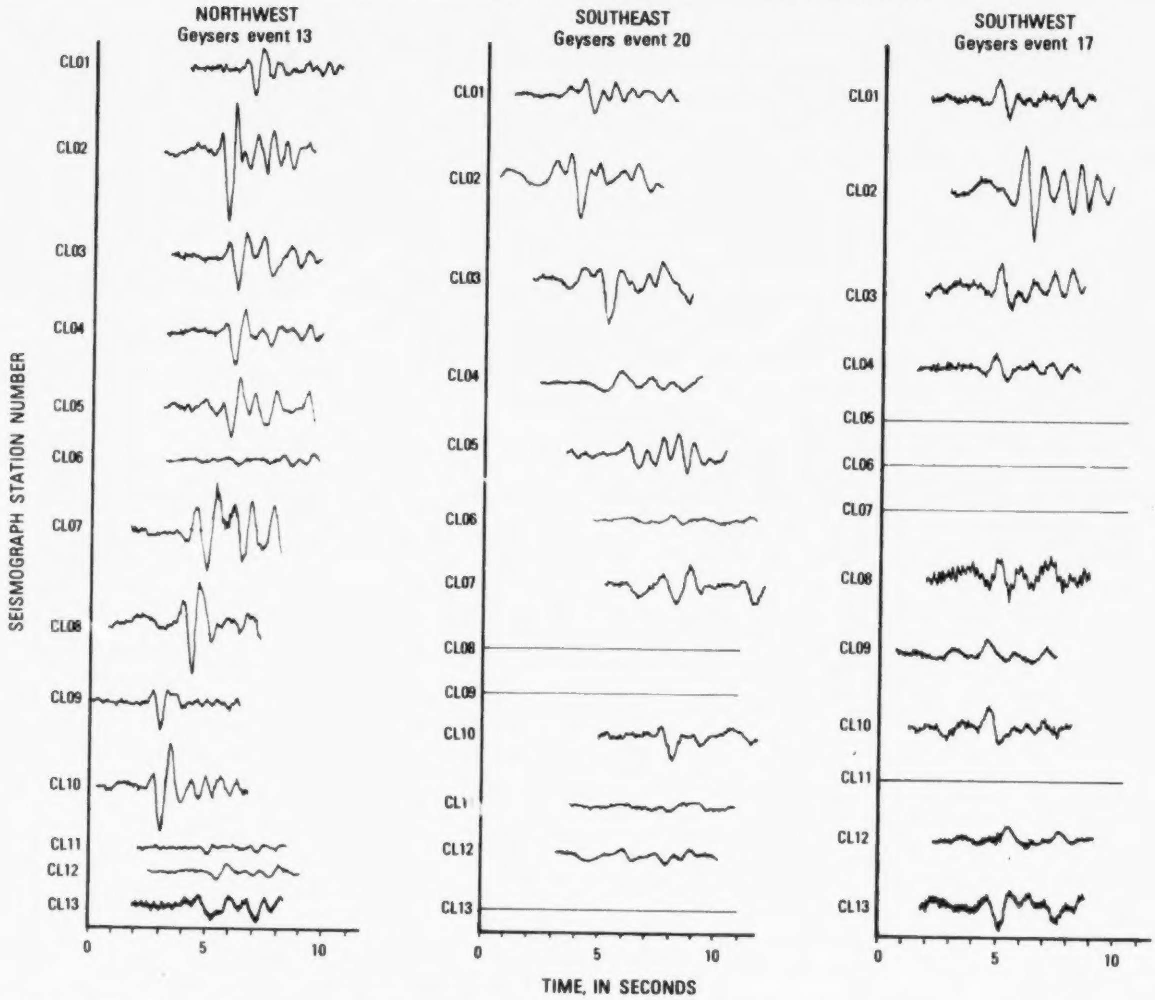
NORTHWEST
Geysers event 13

SOUTHEAST
Geysers event 20

SOUTHWEST
Geysers event 17

FIGURE 83.—Sample *P* wave seismograms recorded by the Geysers-Clear Lake vertical-component array for three events from different azimuths (see table 9).

TABLE 9.—*List of teleseismic events used in this study*

Event	Date	Time (G.m.t)	Lat N.	Long E.	Region	M	Depth (km)	Distance	
1	8-15-76	18:43:45.0	−25.129°	−179.699°	Fiji	5.4	509	83.344°	229.9°
2	8-16-76	12:28:32.4	51.918°	158.431°	Kamchatka	5.3	50	54.158°	311.678°
3	8-16-76	14:06:45.9	32.753°	104.157°	Szechwan	6.1	16	93.792°	318.572°
4	8-16-76	16:11:07.3	6.262°	124.023°	Philippines	6.4	33	103.831°	290.041°
5	8-17-76	04:19:27.3	7.249°	122.939°	Philippines	6.2	22	103.948°	291.540°
6	8-20-76	03:56:00.6	45.048°	149.781°	Kuril Is.	5.5	47	61.046°	306.880°
7	8-20-76	06:54:11.3	−20.412°	−69.993°	N. Chile	5.6	81	77.020°	130.200°
8	8-22-76	02:01:47.4	60.220°	−153.304°	Alaska	5.5	144	28.714°	328.105°
9	8-22-76	21:09:41.9	−14.047°	170.939°	New Hebrides	5.7	31	81.434°	244.110°
10	8-23-76	03:30:07.7	32.492°	104.181°	China	6.2	33	96.483°	321.809°
11	8-24-76	21:26:12.2	−25.326°	−70.694°	Chile	5.6	8	80.440°	133.859°
12	8-26-76	14:30:00.2	37.125°	−116.082°	Nevada Test Site	5.3	0	5.398°	106.805°
13	8-28-76	02:30:09.2	52.597°	−175.343°	Aleutians	5.1	145	38.318°	308.732°
14	8-28-76	02:56:57.5	49.969°	79.001°	E. Kazakhstan	5.8	0	89.155°	346.322°
15	8-28-76	21:50:37.8	−10.669°	−78.189°	Peru	5.1	59	64.488°	130.398°
16	8-30-76	08:37:54.8	1.099°	147.530°	Caroline Is.	5.8	53	89.291°	270.275°
17	8-31-76	09:06:50.4	−30.099°	−178.114°	Kermadec Is.	5.4	55	86.193°	225.642°
18	8-31-76	13:22:10.9	−28.290°	−176.633°	Kermadec Is.	5.5	51	83.976°	225.803°
19	9-01-76	13:25:29.8	−20.414°	169.364°	New Hebrides	5.7	75	86.921°	240.529°
20	9-02-76	10:20:25.9	13.259°	−89.989°	Guatemala	5.0	81	38.507°	122.673°
21	9-04-76	11:54:20.0	−10.247°	161.094°	Solomon Is.	5.6	83	86.025°	253.459°
22	9-09-76	09:27:45.2	77.828°	7.770°	Svalbard	5.2	5	59.526°	10.747°

fects due to lateral velocity changes; and A_I is the instrumental transfer function, which is considered to be identical for all the stations used in this study.

As mentioned, the aperture of the seismometer array is much smaller than the epicentral distances for the teleseisms used in this study, and it can be assumed that the frequency-dependent source radiation pattern and the effects on the seismic waves of propagation through the mantle for a particular event are not functions of the particular coordinates. Therefore, the spectral ratio of A_0 and the spectral ratio of A_m may be considered independent of frequency. The spectral ratio R_{ij} for a given body wave recorded at two stations i and j from a single earthquake is obtained from

$$R_{ij}(f) = a_{ij}\frac{A_{c_i}(f)}{A_{c_j}(f)}, \tag{2}$$

where a_{ij} contains the ratio of A_m, A_0 and A_I. This ratio is independent of frequency, and a_{ij} will be treated as a constant. $A_c(f)$ is the crustal transfer function beneath the receiver and may be factored into three parts:

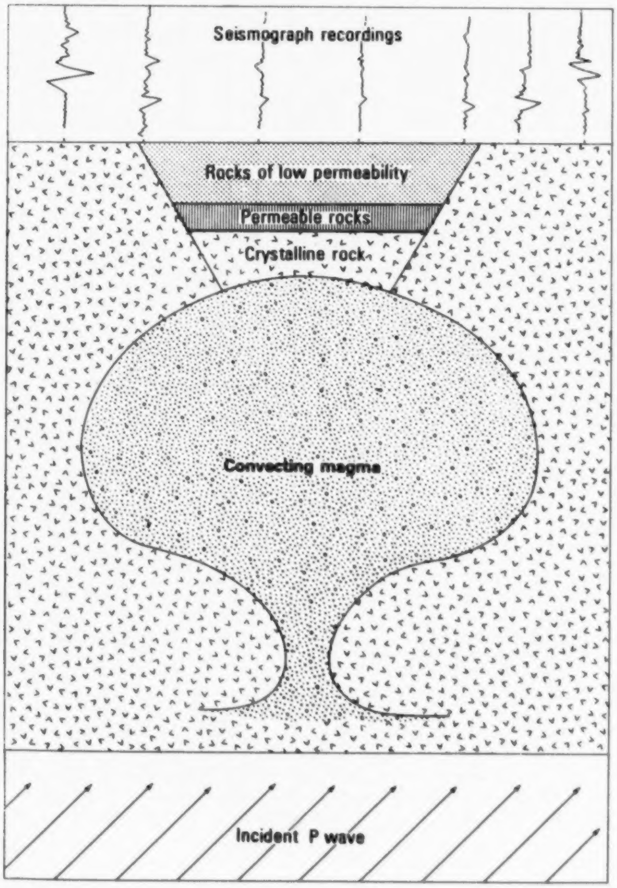

FIGURE 84.—Teleseismic *P* wave incident beneath a model geothermal system, showing variations in seismograph recordings on surface.

$$A_c(f) = G\exp(-ft^*)\exp(-f\delta t^*) \tag{3}$$

where G represents a constant amplitude factor, t^* is a regional attenuation factor which will be assumed to be the same for all stations, and δt^*, called the differential attenuation factor, is the local effect and can be written as

$$\begin{aligned}\delta t^* &= \pi\int \delta Q^{-1}v^{-1}(s)ds \\ &= \pi\int \delta Q^{-1}dt,\end{aligned} \tag{4}$$

where Q is the quality factor, v is the velocity, and dt is the traveltime for the wave passing through the travel path ds. Substituting equation 3 into equation 2 gives

$$R_{ij}(f) = C_{ij}\exp\{-f(\delta t^*_i - \delta t^*_j)\}, \tag{5}$$

where C_{ij} is independent of frequency and is equal to $a_{ij}G_i/G_j$. For convenience of calculation we assume that the δt^* for the reference station j is equal to zero. Taking the logarithm of both sides of equation 5 we get

$$\ln R_{ij} = \ln C_{ij} - f\delta t^*_i . \tag{6}$$

Both C_{ij} and δt^*_i are assumed to be independent of frequency. Using a least-squares error criterion, a straight line is fitted to the spectral ratio versus frequency within a frequency band in which the signal-to-noise ratio is at least 6 dB (typically 0.25–2.5 Hz). The negative of the slope of the straight line is equal to the estimated differential attenuation, δt^*_i. The power-density spectra and spectral ratios for a typical event are illustrated in figure 85.

DIFFERENTIAL ATTENUATION

Q is the quality factor, which measures the anelasticity of a solid. Q^{-1} is a dimensionless parameter, indicating the fraction of the energy dissipated per cycle by a seismic wave; that is, a seismic wave loses $1/Q$ of its energy by anelastic loss for each wavelength it propagates. Partial melting, grain-boundary relaxation, internal friction, and other mechanisms attenuate seismic waves. Each mechanism has a different dependence on frequency. Several mechanisms acting simultaneously may lead to a weaker dependence on frequency than is predicted for the individual mechanisms (Jackson and Anderson, 1970). In the present study, the spectral ratio is determined in a narrow frequency band (approximately 0.25–2.5 Hz) so that Q^{-1} in that band can be considered to be approximately independent of frequency.

The relation between the differential attenuation δt^* and the quality factor Q is expressed in equation (4). Assume a constant velocity of 6 km/s; then, a δt^* equal to 0.1 s for a station, a high seismic attenuation, could be produced by a 10-km-thick zone with a Q of 50, or a 5-km-thick zone with a Q of 25 embedded in a medium with infinite Q. The maximum individual δt^* observed across the Geysers-Clear Lake array is about 0.3 s.

The most important factor which affects the estimation of δt^* is the quality of the P waveform. Many P waveforms recorded in the Geysers-Clear Lake region are emergent, noisy, and exhibit interfering phases (fig. 83); this situation may be caused by the complexity of the local geology. Since δt^* according to equation 4 is integrated along the ray path, we can expect to see δt^* vary with the changes of epicentral distance and azimuth. This variation, which is caused by lateral changes of Q, may indicate the depth of the anomaly beneath the station.

The variation in the frequency content of the P-wave seismograms is documented by noting the frequency of the peak in the power-density spectrum at each station for the events from the three primary azimuths: northwest, southwest, and southeast (fig. 86). The events from the southwest exhibit an average dominant frequency of 0.80 Hz at most stations. The events from this azimuth may be lower frequency. P-wave teleseisms arriving from the northwest and southeast

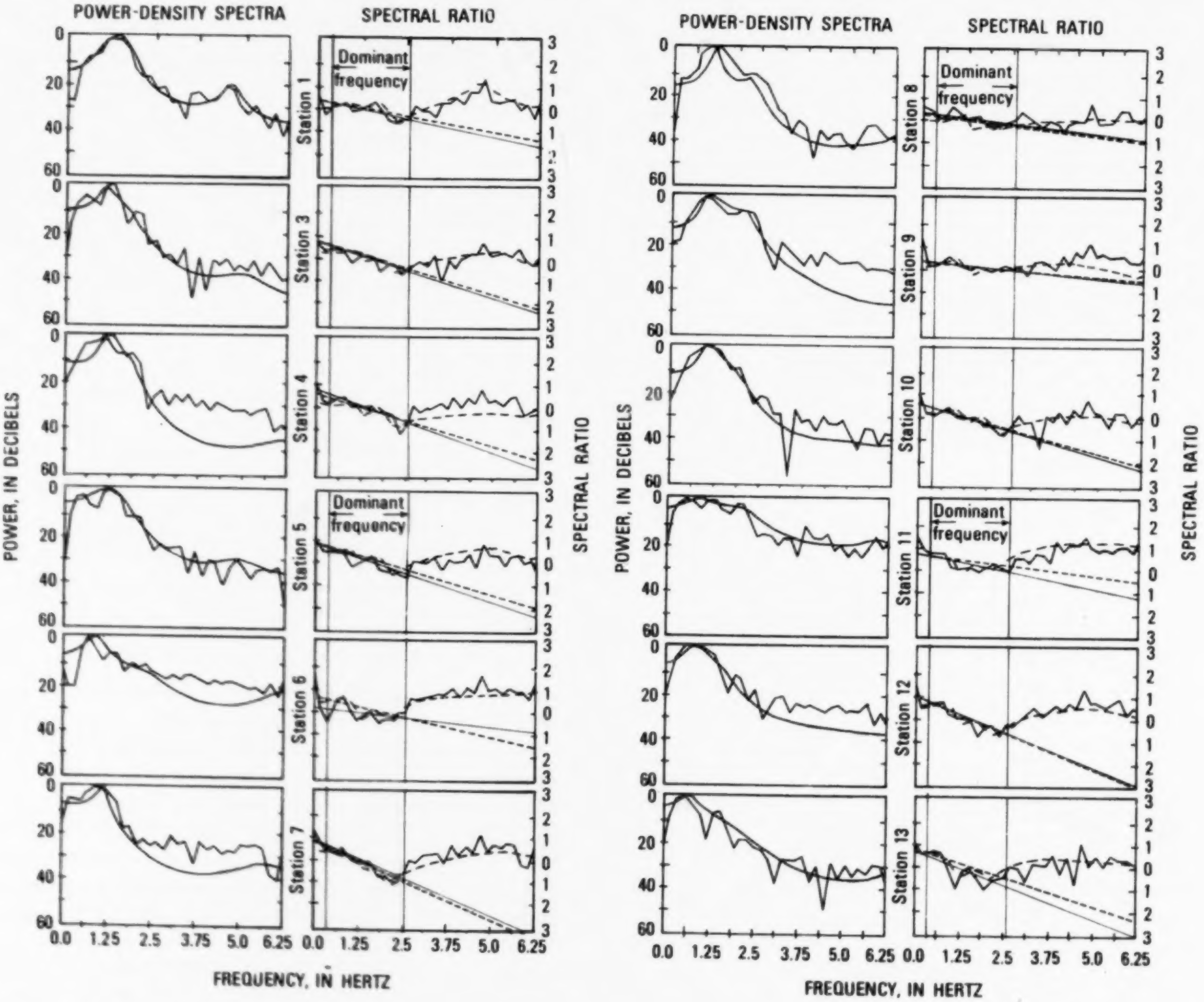

FIGURE 85.—Power-density spectra (left) and spectral ratios from the Geysers-Clear Lake array for event 13. Smooth lines of power-density spectra and broken lines of spectral ratios are computed using maximum entropy method (MEM); others are computed from periodograms. Linear least-squares error fit is shown for spectral ratio. Short-dashed line is fitted to MEM spectral ratio.

exhibit greater variation in dominant frequency. For events from the northwest, stations CL01 through CL04 have average dominant frequencies greater than 1.2 Hz. For events from the southeast, stations CL01 and CL05 have the highest dominant frequencies. Stations CL07 and CL13 are the lowest. This method of analysis is qualitative. However, it seems to indicate the presence of an attenuation anomaly between stations CL05 and CL09. The δt^* analysis will permit a more quantitative interpretation of the Q structure.

In this study, we chose station CL02 as the reference station. Presumably it lies outside the region of the geothermal anomaly (fig. 82), and the attenuation of seismic waves recorded by this station is unaffected by the geothermal system. Station CL01 is located farther away from the Clear Lake volcanic field (fig. 82), but it did not record as many events well. The δt^* obtained for station CL01 is very small and shows no pronounced attenuation. This justifies the above assumptions that the reference station selected is unaffected by the geothermal system and also shows the stability of the spectral ratio technique applied in the study. The assumption that crustal reverberation effects can be neglected is supported by these data.

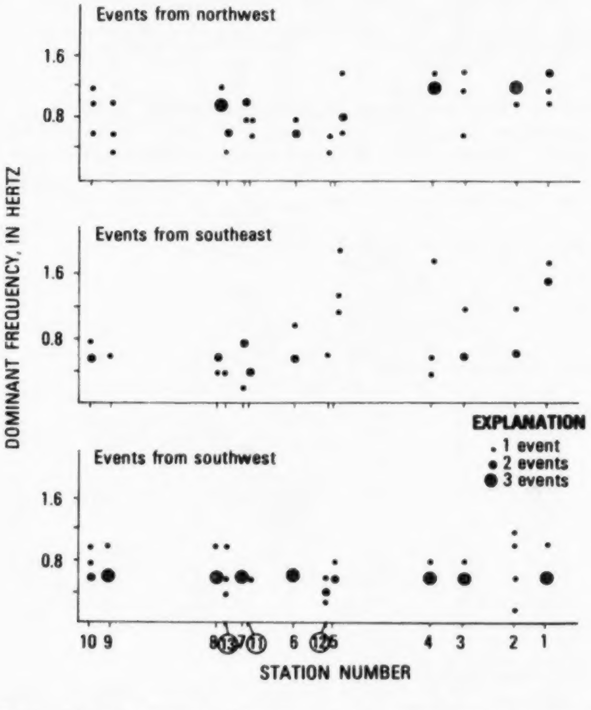

FIGURE 86.—Dominant frequencies of *P* waves studied along a northwest-southeast line. Lower frequency correlates with higher attenuation of seismic waves. Stations CL11, CL12, and CL13 are projected onto line.

The δt^* are calculated in this manner for each station and for each of the 22 events listed in table 9. The events whose ray paths pass too close to the core-mantle boundary are eliminated from the interpretation. Those events from azimuths other than the three primary azimuths are also eliminated, leaving the 13 events in table 10. The variation of δt^* with azimuth and distance for each station is plotted in figure 87. These data contain all the information needed by a generalized inversion algorithm to compute a detailed quantitative two-dimensional Q model in a future study.

The δt^* calculated for several stations (CL03, CL04, CL06, CL10, and CL12 in fig. 87) are constant regardless of the change of epicentral distance or azimuth. Beneath these stations the observed attenuation anomaly must be shallow, and no lateral variation in attenuation can be inferred for the deeper part of the crust and upper mantle.

The δt^* data are independent of epicentral distance, within the resolution of the present data, but usually

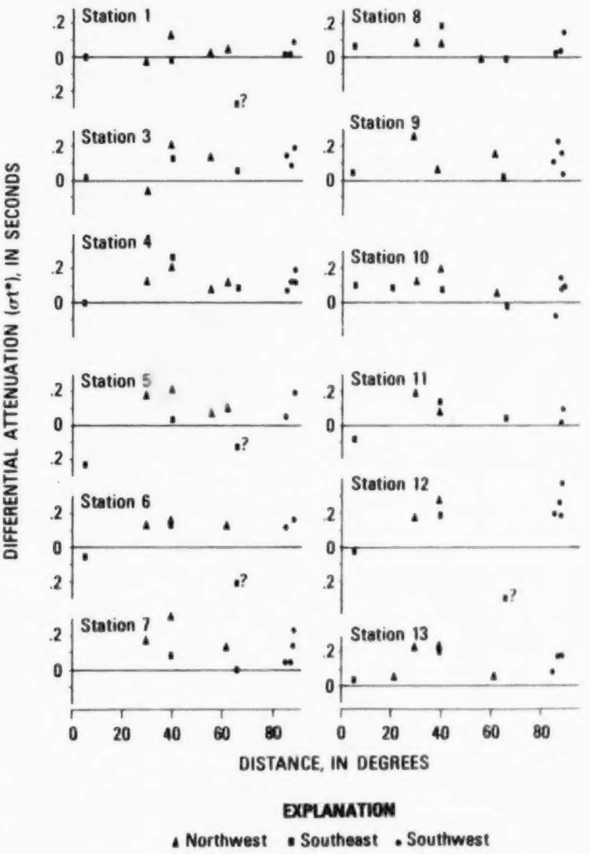

FIGURE 87.—Differential attenuation for each station as a function of distance and azimuth.

vary with azimuth. The values of δt^* were averaged for events from a given azimuth. The events were separated into three groups based on azimuth—northwest, southwest, and southeast.

A contour map of δt^* was drawn from the average δt^* values of table 10 (fig. 88). A two-dimensional grid of values at equal increments, which have been contoured, was calculated from the five nearest data values (Davis, 1973, chap. 6). Each data value among the five nearest neighbors is weighted by the inverse distance from the station to the grid point. This contouring algorithm has been shown to produce small mean error, though the root-measure-square error at a given control point may be larger than in other schemes (Harbaugh and others, 1977).

In figure 88*A* the observed δt^* is contoured for events to the southwest. These rays arrive perpendicular to the strike of the seismometer array, and this plot resembles refraction fan shooting. Low seismic attenuation is observed at station CL01. The geothermal system appears to be bounded on the southeast by the 90-ms contour. High attenuation occurs in a zone extending from The Geysers to the northeast. Three local areas exhibit high seismic attenuation, two near stations CL03 and CL13 and a large area around station CL12 east-northeast of Mount Hannah. Regional high attenuation ($\delta t^* > 90$ ms) occurs in an area east of a line through Mount Konocti and station CL13.

Figure 88*B* shows seismic attenuation of events to the southeast. Attenuation with $\delta t^* > 90$ ms occurs over most of the map area except for a low-attenuation area observed to the southeast. Local high-attenuation anomalies are associated with station CL03 and with CL12 as for events from the southwest. Another zone of high attenuation includes stations CL08 and CL13 from Mount Konocti.

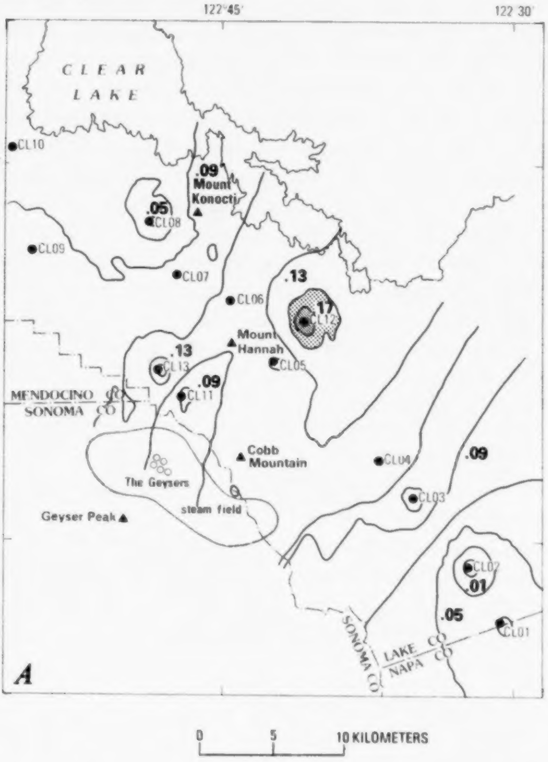

FIGURE 88.—Two-dimensional contoured surface fitted to averaged δt^*. Contour interval, 0.02 s. *A*, δt^* data for seismic waves from the southwest. *B*, δt^* data from southeast. *C*, δt^* data from the northwest. δt^* is assumed zero at reference station, CL02. Solid area has maximum value of δt^*.

TABLE 10.—*List of differential attenuation δt^*, in milliseconds, for each station*

[Using station CL02 as a reference, numbers with queries were omitted from the average]

Event no.	Azimuth	Station											
		CL01	CL03	CL04	CL05	CL06	CL07	CL08	CL09	CL10	CL11	CL12	CL13
		Differential Attenuation for each Station (in ms)											
2	NW	-17	139	75	68	----	----	-22	----	----	----	----	----
6	NW	41	----	118	112	138	135	10	148	30	----	----	49?
8	NW	-12	-59	114	184	124	165	83	----	114	181	182	229
9	SW	25	129	114	128	----	----	18	131	36	-95?	87	----
12	SE	8	15?	3?	-222?	-50?	----	61	54	104	-91?	-21?	33?
13	NW	129?	208	201	205	156	312	87	66	201	----	273	223
14	NW	37	-4?	174	60	106?	142	104	41	54	40	-11?	185
15	SE	-282?	53	82	-124?	-205?	-6?	1?	25	-23?	41	----	----
17	SW	15	84	120	----	----	40	41	230?	134	----	253	164
18	SW	6	146	77	41	116	44	38	103	-78	----	194	63?
19	SW	85	184	198	183	169	237	153	41	91	97	374?	174
20	SE	-28	133	261	33	142	79	181	----	77	128	180	209
21	SW	----	133	109	110	103	138	-45	164	64	64	180	----
		Average Differential Attenuation of Primary Azimuths (in ms)											
	SW	35	138	126	111	129	114	42	103	96	81	209	169
	SE	-28	133	261	33	142	79	181	----	77	128	180	209
	NW	4	174	127	142	139	204	50	107	115	130	227	226
		Average Differential Attenuation of All Events for All Stations											
		17	141	147	113	135	133	46	99	91	102	210	197

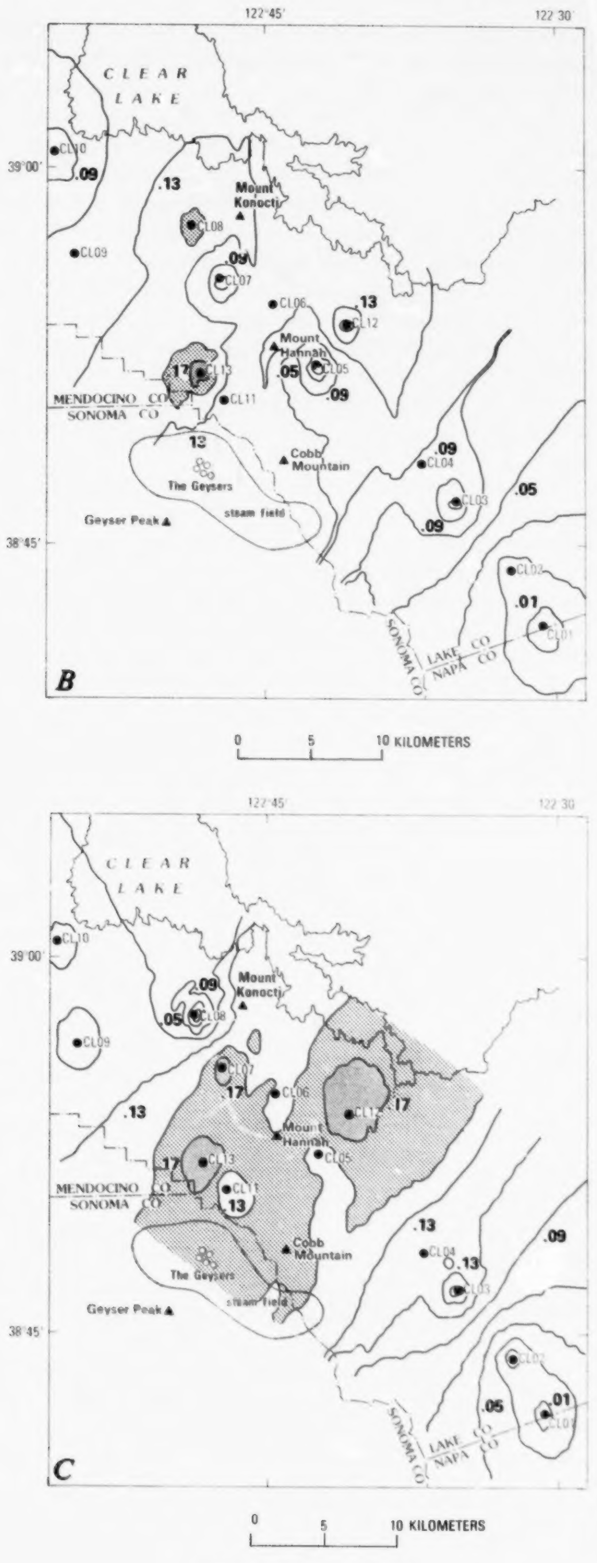

FIGURE 88.—Continued

The seismograms of teleseismic P waves from the northwest (fig. 88*C*) show the highest attenuation. The southeast station, CL01, shows negligible attenuation as it did for events from other azimuths. High local attenuation is evident at stations CL03, CL13, and CL12, as it is for the other events, indicating a very shallow attenuation anomaly that is strongest at stations CL13 and CL12. The high-attenuation anomaly for events from the northwest lies south and east of Mount Konocti, with the highest attenuation anomaly occurring near station CL12.

Q STRUCTURE

Partial melting in the crust or upper mantle produces a Q value less than 50 for shear waves and correspondingly a Q less than 125 for P waves (Solomon, 1972). Measurement of this Q can serve as evidence for the existence of a partially molten magma chamber or to map a liquid-vapor steam reservoir beneath a geothermal area. In order to obtain a preliminary simplified Q model from the δt^* data presented in the previous section, the following assumptions are made:

1. At each station a simplified two-layer Q model is used. Q in the upper layer is 50, and beneath is a half-space with infinite Q. The thickness of the layer will vary as δt^* varies from station to station. This model will give a preliminary estimate of the lateral distribution of the high-attenuation zone. Any layer may be replaced by a thinner layer with lower Q value.
2. All the rays are assumed to be vertically incident from the bottom of the model, since the ray paths are incident within 20° of the vertical and there is no apparent variation of δt^* with epicentral distance. A cross section of the Q structure will be determined along a northwest-southeast-trending line.
3. The velocity is assumed constant within the upper layer, so that the integration can be carried out easily. The simplified Q model of the Geysers-Clear Lake region is shown in figure 89 as the thickness of the upper layer with $Q=50$. The thickness of the low-Q layer is plotted for the average of the events from each of three azimuths and the average for all events.

Several stations, such as stations CL03, CL09, CL11, CL12, and CL13, exhibit little azimuthal variation of the thickness of the low-Q layer. The implication is that a zone of high attenuation lies immediately beneath the station. The interpretation of the differential attenuation observations must consider the effect of the near-surface geology before confirming the thickness of the low-Q zone in figure 89. The near-surface local geology, such as unconsolidated alluvial deposits, produces higher seismic attenuation than consolidated Cenozoic volcanic rocks, the Great Valley sequence, or the Franciscan assemblage. Station CL03 is situated on thick alluvial deposits. Station CL12 observes the highest differential attenuation of 0.3 s. Although it sits on thick young pyroclastic deposits, it is doubtful that the near-surface lithology accounts for all the attenuation. Alternative convincing explanations exist for the attenuation observed at stations CL11 and CL13.

The assumption that seismic waves are vertically incident from the bottom of the Q model may not be valid if the Q model varies with azimuth (see stations CL05, CL07, and CL08 in figs. 88 and 89). This azimuthal variation will aid in estimating the depth of the low-Q zone. The low Q values inferred for stations CL06, CL11, CL12, and CL13 define a shallow high-attenuation zone stretching from stations CL13 to CL06 to CL12 (fig. 88). This zone exhibits high attenuation independent of the azimuth of the events.

If the ray comes from the southeast (fig. 88*B*) at a distance of 40° to station CL05, the angle of incidence is about 20° from vertical. A thin low-Q layer for station CL05 is indicated for waves from the southeast. A thick low-Q zone is indicated for station CL05 for waves from the northwest at a distance of 40° (fig. 88*C*). The east boundary of the low-Q region follows the contour for δt^* of 0.11 where it trends southwest-northeast and passes to the northwest of station CL05 (fig. 88*B*). The zone of high attenuation must lie at some depth to the northwest of station CL05.

The results obtained for stations CL07 and CL08 are similar to station CL05. We combine the interpretation for each station and postulate that a small low-Q zone (which is possibly elongate and connected to the zone around station CL13) is at a depth of about 8 km between stations CL07 and CL08. A narrow zone of high attenuation appears to dip from station CL13 toward Mount Konocti between stations CL07 and CL08. The low-Q zone is less than 4 km wide, which is the distance between stations CL07 and CL08. When seismic waves arrive from the southwest (almost vertical incidence), neither station CL07 nor CL08 detects a zone of high attenuation.

A broad attenuation anomaly exists beneath Mount Hannah, centered at station CL06 and bounded by station CL05 and CL08. The northeast boundary of the anomaly cannot be determined by this study because of insufficient data, but it must include station CL12. The attenuation anomaly correlates with the teleseismic *P*-wave traveltime anomaly (Iyer and others, this volume). Isherwood (1975) identified a broad negative gravity anomaly centered beneath Mount Hannah, which he attributed to a magma chamber at a depth of 10 km (fig. 90). The present study suggests a shallower seismic attenuation anomaly trending southwest-northeast which may be produced by a magma

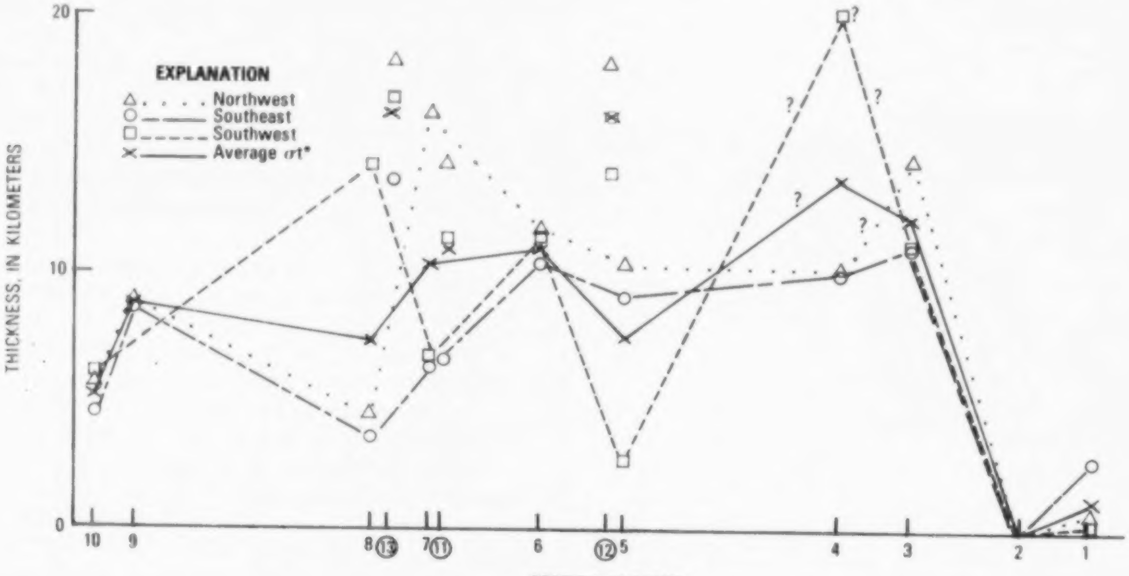

FIGURE 89.—Simplified Q model for the Geysers-Clear Lake area, showing thickness of a layer with $Q = 50$. Lines are for average δt^*. Stations CL11, CL12, and CL13 are projected onto abscissa but not connected to lines. Higher seismic-wave attenuation has thicker low-Q layer.

chamber. The exact depth of this magma chamber may be determined from the attenuation data for these station locations, using a generalized inversion of the data.

A consistent thick layer of low Q is obtained for stations CL11 and CL13, independent of azimuth. No gravitational anomalies with closed contours were found in this area. A buried magma chamber may not exist here. We prefer the interpretation that the region beneath stations CL11 and CL13 is capped by impermeable rocks of the Franciscan assemblage that act as a conduit for vapor-dominated hydrothermal activity towarf the southeast and the Geysers steam field (Isherwood, 1975; Goff and others, 1977).

DISCUSSION AND CONCLUSIONS

The small variation and small values of the differential attenuation factor δt^* for station CL01 suggest that the local geology of station CL01 is similar to that of the reference station CL02. Both stations are located outside the area affected by the geothermal system. The consistency of this result gave us confidence in applying the spectral ratio technique to study the seismic-wave attenuation beneath a geothermal system. By carefully picking the correct P-phases recorded by each station, the errors in obtaining δt^* can be reduced to a minimum.

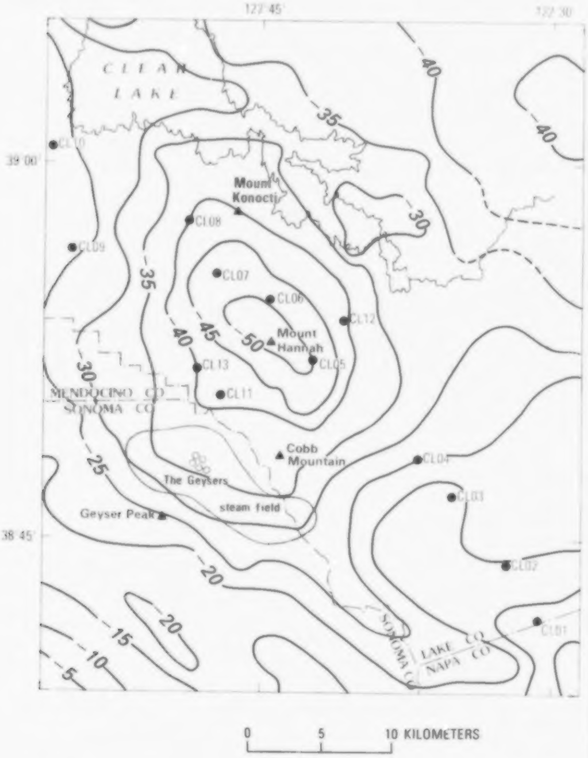

FIGURE 90.—Bouguer gravity map of study area (after Isherwood, 1975). Contour interval, 5 mGal; dashed where data are incomplete.

A broad low-Q zone is found beneath The Geysers and the Clear Lake area. This anomaly is bounded to the southeast by a southwest-northeast trend at station CL05, where there is a sharp decrease in the thickness of the low-Q layer, which appears to be buried at depth. The center of the shallow high-attenuation zone extends from station CL06, beneath Mount Hannah to station CL12. This low-Q zone may be the same source of the gravity low and positive teleseismic P-wave traveltime delays found in that region, though the shape of the attenuation anomaly is different. The value of Q is low enough to indicate a partial melting zone or a magma chamber associated with the Geysers-Clear Lake geothermal area. The top of the low-Q zone is very close to the surface, as no significant variation in δt^* is observed for stations in this area with the changes of epicentral distances or azimuths. A very shallow zone of high attenuation beneath station CL05 cannot be explained. A low-resistivity zone (5–10 ohm meters) is found by Stanley, Jackson, and Hearn (1973) at the same place, but the gravity studies by Isherwood (1975) did not detect this anomaly. The attenuation source must be very shallow and localized, though it probably is associated to some extent with the large anomaly extending beneath Mount Hannah. Another small low-Q zone is at a depth of approximately 8 km between stations CL07 and CL08. The width of this high-attenuation zone is probably less than 4 km, as inferred from the small δt^* obtained for the waves from the southwest, incident almost vertically to these two stations. This result did not correlate with other geophysical evidence, but this low-Q zone may coincide with a contact between the Franciscan assemblage and Great Valley sequence in the bedrock beneath these two stations. Moderate to small attenuation of the seismic P waves is observed at stations CL09 and CL10, and these two stations are probably not located above any magma chamber or partially molten zone directly related to The Geysers. Station CL08 is at the northwest boundary of the low-Q zone. At the surface, station CL08 is also located close to the northwest edge of the Cenozoic volcanic rocks. The source of attenuation of the seismic waves observed at station CL09 and CL10 is probably related to the thick Cenozoic unconsolidated or weakly consolidated alluvial deposits.

The values of δt^* calculated for the waves from the southwest to stations CL11 and CL13 are smaller than those for the other two azimuths. The results suggest that the low-Q zone may not continue all the way across the Collayomi fault zone to become the thermal source driving the Geysers steam field. Instead, fracture zones act as channels directing the hydrothermal activity from the main heat source (the main low-Q zone) toward the producing steam field.

The low-Q region determined in this study has a width about 15 km measured on a line trending northwest-southeast. The thickest part of the high-attenuation zone is probably located beneath station CL06 or Mount Hannah and possibly beneath station CL12, where the tops of these anomalies are very close to the surface. The high-attenuation zone extends southwest toward the Geysers steam field. This attenuation anomaly is postulated to be associated with the vapor-dominated hydrothermal reservoirs, which is consistent with other geophysical surveys. The northeast boundary of the thermal source cannot be defined in this study.

REFERENCES CITED

Ben-Menahem, Ari, Smith, S. W., and Teng, T. L., 1965, Procedure for source studies from spectrums of long-period seismic body waves: Seismological Society of America Bulletin, v. 55, p. 203–235.

Blackman, R. B., and Turkey, J. W., 1958, The measurement of power spectra: New York, Dover, 190 p.

Davis, J. C., 1973, Statistics and data analysis in geology: New York, John Wiley, 550 p.

Goff, F. E., Donnelly, J. M., Thompson, J. M., and Hearn, B. C., Jr., 1977, Geothermal prospecting in The Geysers-Clear Lake area, northern California: Geology, v. 5, p. 509–515.

Harbaugh, J. W., Doveton, J. H., and Davis, J. C., Probability methods in oil exploration: New York, John Wiley, 269 p.

Hearn, B. C., Jr., 1976, Preliminary geologic map and cross-section of the Clear Lake volcanic field, Lake County, California: U.S. Geol. Survey Open-File Report 76–751.

Isherwood, W. F., 1975, Gravity and magnetic studies of The Geysers-Clear Lake region, California: U.N. Symposium on the Development and Use of Geothermal Resources, 2d, San Francisco, 1975, Proceedings, v. 2, p. 1065–1073.

Iyer, H. M., 1975, Anomalous delays of teleseismic P waves in Yellowstone National Park: Nature, v. 253, p. 425–427.

Iyer, H. M., Oppenheimer, D. H., and Hitchcock, Tim, 1979, Abnormal P-wave delays in The Geysers-Clear Lake geothermal area, California: Science, v. 204, p. 495–497.

Jackson, D. D., and Anderson, D. L., 1970, Physical mechanisms of seismic-wave attenuation: Reviews of Geophysics and Space Physics, v. 8, p. 1–63.

Majer, E. L., and McEvilly, T. V., 1979, Seismological investigating at The Geysers geothermal field: Geophysics, v. 44, p. 246–269.

Stanley, W. D., Jackson, D. B., and Hearn, B. C., 1973, Preliminary results of geolectrical investigations near Clear Lake, California: U.S. Geological Survey open-file report, 20 p.

Solomon, S. C., 1972, Seismic-wave attenuation and partial melting in the upper mantle of North America: Journal of Geophysical Research, v. 77, p. 1483–1502.

———1973, Shear wave attenuation and melting beneath the mid-Atlantic ridge: Journal of Geophysical Research, v. 78, p. 6044–6059.

Solomon, S. C., and Toksöz, M. N., 1970, Lateral variation of attenuation of P and S waves beneath the United States: Seismological Society of America Bulletin, v. 60, p. 819–838.

Teng, T. L., 1968, Attenuation of body waves and the Q structure of the mantle: Journal of Geophysical Research, v. 73, p. 2195–2208.

Ulrych, T. J., and Bishop, T. N., 1975, Maximum entropy spectral analysis and autoregressive decomposition: Reviews of Geophysics and Space Physics, v. 13, p. 183–200.

Walsh, J. B., 1968, Attenuation in partially melted material: Journal of Geophysical Research, v. 73, p. 2209–2216.

———1969, New analysis of attenuation in partially melted rock: Journal of Geophysical Research, v. 74, p. 4333–4337.

Ward, R. W., and Toksöz, M. N., 1971, Causes of regional variation of magnitudes: Seismological Society of America Bulletin, v. 61, p. 649–670.

White, J. E., 1975, Computed seismic speeds and attenuation in rocks with partial gas saturation: Geophysics, v. 40, p. 224–232.

A DETAILED GRAVITY SURVEY OF THE WILBUR SPRINGS AREA, CALIFORNIA

By JOHN M. HARRINGTON and KENNETH L. VEROSUB

ABSTRACT

Quicksilver deposits, hot springs, and exploratory geothermal drilling demonstrate the existence of a thermal anomaly in the Wilbur Springs area, 18 km east of Clear Lake. In addition, the trend of volcanic activity in the Geysers-Clear Lake region indicates that Wilbur Springs may be the site of future activity. In an attempt to determine the source of the thermal anomaly, a detailed gravity survey was conducted in an area corresponding to the Wilbur Springs SW.7½-minute quadrangle. Complete Bouguer anomalies were computed based on reduction densities of 2.67 g/cm^3 and 2.50 g/cm^3. After removal of a regional gradient, two features of significance emerged from the data. The first is a gravity high apparently associated with the presence of mafic or ultramafic material. The other is a gravity low that can be interpreted as a manifestation of a very shallow geothermal reservoir located in the southeast part of the study area. Additional geophysical studies are needed to delineate the actual nature of this reservoir and to evaluate its geothermal potential.

INTRODUCTION

The spatial and temporal distribution of volcanic activity associated with the Clear Lake volcanic field suggests that the trend of future volcanic eruptions will be to the north and east of the present field (Donnelly-Nolan and others, this volume). One possible center for such activity is the vicinity of Wilbur Springs, an area of abundant hot springs and quicksilver deposits located approximately 18 km east of Clear Lake (fig. 91). Preliminary geothermal exploration in the mid-1960's confirmed the existence of a pronounced thermal anomaly in the Wilbur Springs area. A series of shallow holes drilled to a maximum depth of 100 m indicated thermal gradients as high as 0.3°C/m, and two deep holes drilled to depths of 400 m (Magma Power Co.) and 1,200 m (Cordero Mining Co.) reached maximum bottom temperatures of 120°C and 140°C, respectively (D. E. White, written communication, 1977). At the same time an extensive study of the geology and geochemistry of the area (Moisseeff, 1966) demonstrated that the occurrence of cinnabar is closely related to the location of the hot springs and that the quicksilver deposits had resulted from hydrothermal alteration that was contemporaneous with recent volcanic activity near Clear Lake. All these observations imply the presence of a heat source at depth in the Wilbur Springs area. The existence of such a source is also consistent with the results of a regional gravity study of the Clear Lake-Geysers area in which there was some suggestion of a small negative anomaly near Wilbur Springs (Chapman, 1975; Isherwood, 1976). With these factors in mind, we undertook in the summer of 1977 a detailed gravity survey of the Wilbur Springs area in an attempt to determine the nature of the source of the thermal anomaly.

Acknowledgments.—We are indebted to R. H. Chapman for his invaluable advice, assistance, and encouragement throughout this work. Useful conversations with J. M. Donnelly-Nolan, R. J. McLaughlin, W. F. Isherwood, and Quinton Aune are also acknowledged.

GEOLOGIC SETTING

The area surveyed is essentially coincident with the Wilbur Springs SW. 7½-minute quadrangle. It is an area of moderately rugged relief, ranging in elevation from 400 m in the valleys to 1,200 m at the highest peak, Cold Spring Mountain. A major geologic feature is a band of serpentine that trends north-northwest through the center of the area (fig. 92). To the east of the serpentine are little-deformed sedimentary rocks of the Great Valley sequence, consisting of Upper Jurassic and Lower Cretaceous sandstone, siltstone, and conglomerate that dip homoclinally eastward under the Sacramento Valley. The serpentinite band itself is believed to have been derived from the basal ophiolite of the Great Valley sequence. North of Wilbur Springs the thrust contact between the serpentine and the sediments has been named the Stony Creek fault (Rich, 1971). South and west of Wilbur Springs the Great Valley sequence wraps around the end of the Stony Creek fault. The rocks here, though unmetamorphosed, are tightly folded and severely faulted. In addition, in several places they are in fault contact with isolated serpentinite masses. North of Wilbur Springs and west of the serpentinite band are metamorphosed siltstone and sandstone of uncertain association. These rocks may represent a veneer of Great Valley sequence which is underlain by metamorphosed and deformed volcanic and sedimentary rocks of the Franciscan assemblage (Quinton Aune, oral communication, 1978). On the other hand, they may be part of the Franciscan assemblage (Rich, 1971). In either case, the west boundary of the main serpentinite mass marks the location of the Coast Range thrust, which separates rocks of the Franciscan assemblage from those of the Great Valley sequence. The smaller serpentinite masses west of this boundary probably arise from alteration of mafic or ultramafic bodies within the Franciscan.

GRAVITY SURVEY

Ninety-two gravity stations were occupied in the study area. The overall density of measurements is 4.1 stations per square kilometer, but the stations are in fact more concentrated in the southern part of the area. Owing to the lack of points of known elevation in the area, only two stations are located on bench marks surveyed by the U.S. Geological Survey and the U.S. Coast and Geodetic Survey. Twenty stations are located on unchecked U.S.G.S. spot elevations that have an uncertainty of 3 m. The elevations of the remaining 70 stations are estimated from contours on an advance print of the U.S. Geological Survey topographic map of the Wilbur Springs SW.$7\frac{1}{2}$-minute quadrangle. The estimated accuracy of these stations is ±6 m, which limits the accuracy of the gravity survey to ±1.2 mGal.

Worden Gravity Meter No. 464 was used in this survey. Although this instrument has not been recently calibrated, it is possible to compare the data from six stations in this study with results obtained earlier by the California Division of Mines and Geology (see table 11). The difference between each pair of measurements is consistently less than 1 mGal. All stations in the present survey are tied to the Wilbur Springs Gravity Base Station of the California Division of Mines and Geology (Chapman, 1966).

The initial gravity determinations were first corrected for instrument drift and tidal corrections and were then reduced to a simple Bouguer anomaly for densities of 2.67 g/cm^3 and 2.50 g/cm^3. The higher density is charcteristic of the Franciscan assemblage, and the lower one is characteristic of sediments of the Great Valley sequence and of the volcanic terrane of the Clear Lake area (Isherwood, 1976). The lower density is also consistent with the results of a density log from the deeper geothermal exploration hole at Wilbur Springs.

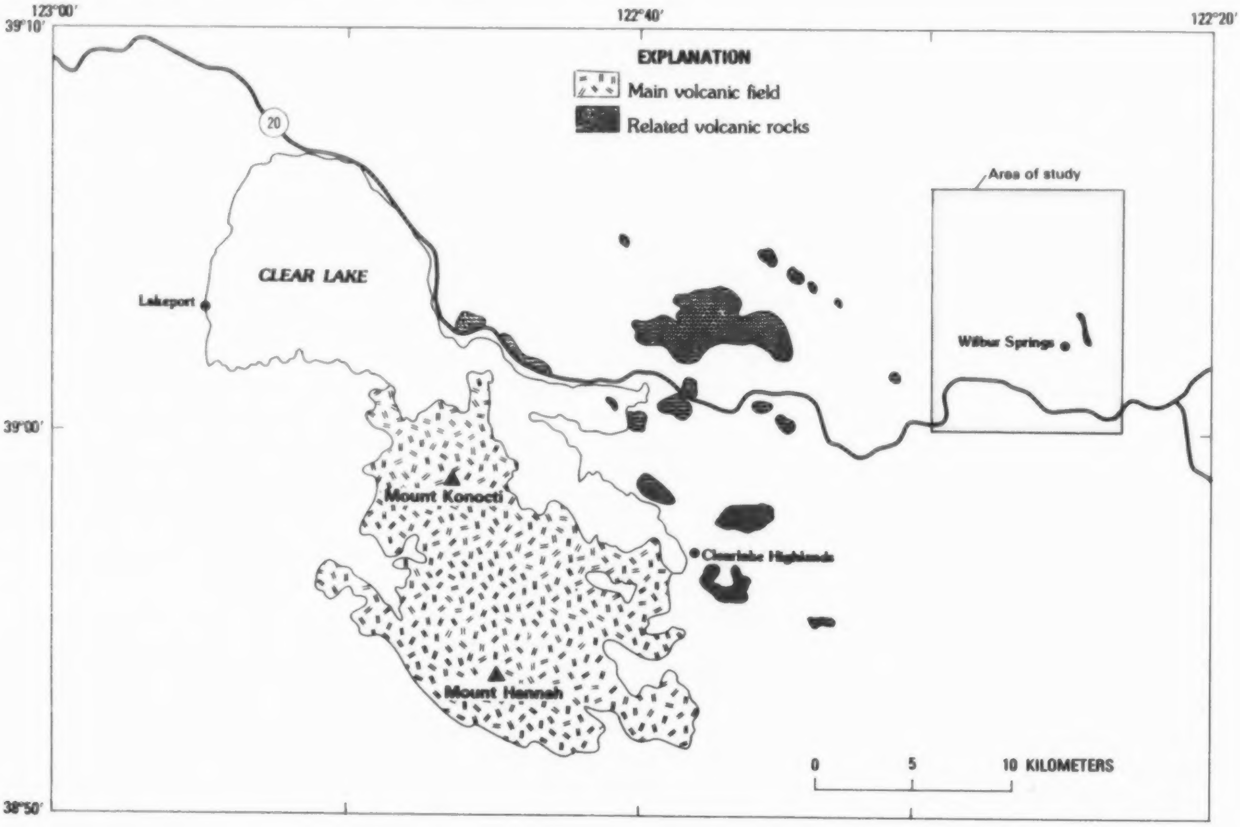

FIGURE 91.—Location of Wilbur Springs study area in relation to the Clear Lake volcanic field.

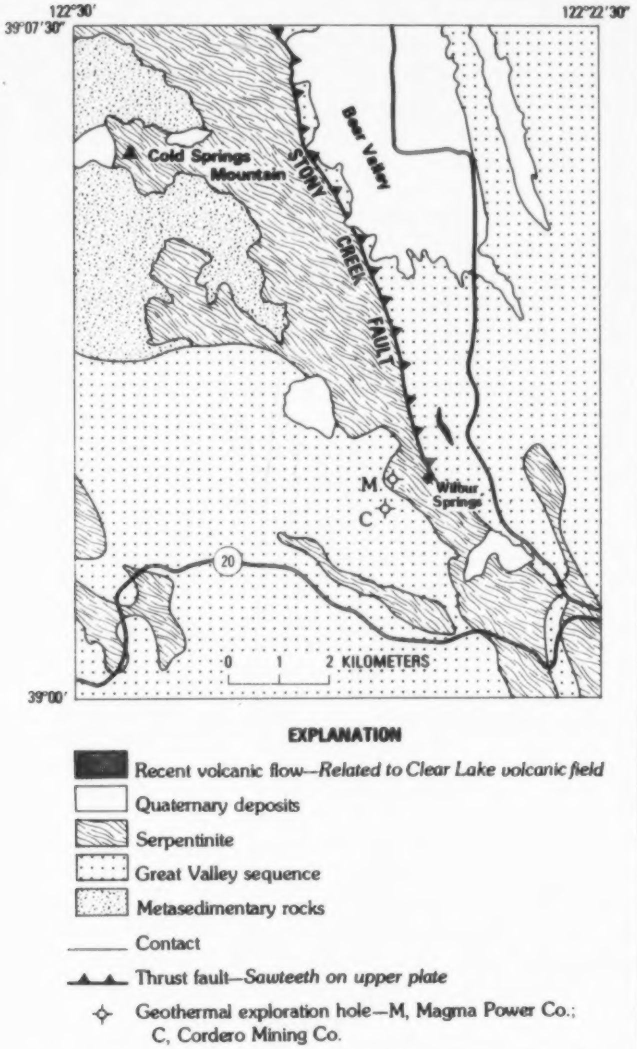
122°30'
122°22'30"
39°07'30"
39°00'
Cold Springs Mountain
STONY CREEK FAULT
Bear Valley
M
C
Wilbur Springs
20
0
1
2 KILOMETERS
EXPLANATION
Recent volcanic flow—Related to Clear Lake volcanic field
Quaternary deposits
Serpentinite
Great Valley sequence
Metasedimentary rocks
Contact
Thrust fault—Sawteeth on upper plate
Geothermal exploration hole—M, Magma Power Co.; C, Cordero Mining Co.

FIGURE 92.—Generalized geology of Wilbur Springs quadrangle, after Rich (1971).

TABLE 11.—*Comparison of gravity stations*

[WS, stations established for this study; CL, G, UB, stations used by the California Division of Mines and Geology in compiling the Ukiah Gravity Sheet (Chapman and others, 1974). Data supplied by R. H. Chapman]

Station	Observed gravity (mGal)	Station	Observed gravity (mGal)
WS 4	979936.61	WS 66	979967.05
CL 85	979935.89	CL 104	979967.09
WS 28	979975.43	WS 81	979832.50
CL 93	979974.55	G 174	979832.07
WS 37	979974.38	WS 85	979976.52
UB 46	97994.12	CL 92	979976.20

Terrane corrections were computed manually for each station using Hayford-Bowie zones out to a distance of 2.29 km (Swick, 1942). At greater distances, out to 166.7 km, terrane corrections were calculated from a computer program developed by the U.S. Geological Survey (Plouff, 1966). Densities of both 2.67 g/cm^3 and 2.50 g/cm^3 were again used. The total terrane corrections ranged from about 1 mGal in the valley north of Wilbur Springs to about 12 mGal on Cold Spring Mountain. The addition of the terrane corrections to the simple Bouguer anomaly resulted in the determination of the complete Bouguer anomaly at the two densities for each station.

INTERPRETATION

The dominant feature of the complete Bouguer anomaly maps (not shown here) is a strong trend of decreasing gravity extending from southwest to northeast. This trend is in fact part of the regional gradient reported by Chapman (1975) for the entire Clear Lake region and attributed by him to the inland thickening of the crust at the continental margin. In the vicinity of Wilbur Springs, this gradient has a constant value of 0.67 mGal/km along a direction N. 30° E. At Wilbur Springs itself, the regional field has a value of 45.3 mGal. In order to isolate the local gravity structure of the Wilbur Springs area, the gradient of Chapman (1975) was removed from the complete Bouguer anomaly maps to obtain two possible maps of the residual gravity, one based on a density of 2.67 g/cm^3, the other on 2.50 g/cm^3. In view of the inherent uncertainty of about ±1 mGal in the accuracy of the measurements, a 1-mGal contour interval did not seem justifiable for the residual-gravity maps. Consequently, the residual-gravity data for each density were independently smoothed and contoured twice at a 2-mGal interval, using first even and then odd integral values for the contours. The four separate maps of residual gravity that result from this procedure are shown in figure 93.

The gravity anomalies in the residual gravity maps are not very pronounced. Indeed, it can be argued that in view of the diversity of rock types and therefore of densities in the study area, the gravity anomalies may be of no geophysical significance. Certainly the small positive anomaly that appears only in the southwest part of figure 93*A* is most likely an artifact arising from the uncertainties in elevation and the choice of contour interval. Also questionable is the suggestion of a positive anomaly on the northeast edge of the study area. The scarcity of stations in this area makes it impossible to draw any definite conclusions concerning the reality of this feature.

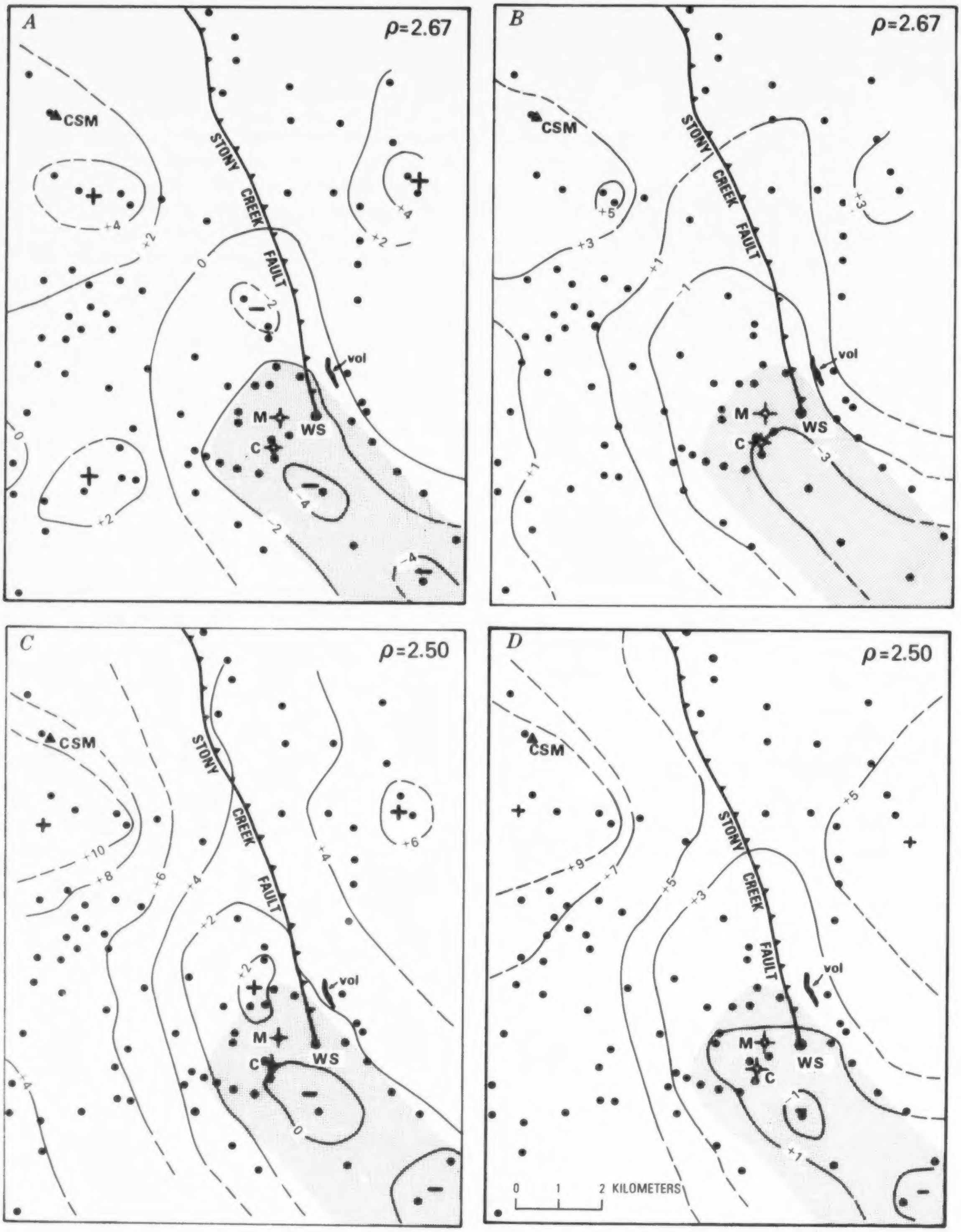
A
ρ=2.67
CSM
STONY CREEK FAULT
vol
M
WS
C
+4
+2
0
-2
-4
B
ρ=2.67
+5
+3
+1
-1
-3
C
ρ=2.50
+10
+8
+6
+4
+2
0
D
ρ=2.50
+9
+7
+5
+3
+1
-1
0 1 2 KILOMETERS

Two features, however, do persist in all the maps, and it is not unreasonable to consider their possible geologic interpretation. The first feature is a 3- to 4-mGal positive anomaly located in the northwest part of the study area and apparently extending and expanding to the west and northwest. Such an anomaly is not difficult to explain, occurring as it does over the Franciscan assemblage. Elsewhere in the Franciscan terrane it has been shown that the serpentinite masses are derived from and often intimately associated with mafic or ultramafic material of relatively high density (Bailey and others, 1964). Therefore, it is plausible that the positive gravity anomaly arises from localized or disseminated masses of such material underlying the metasedimentary rocks.

The other persistent gravity feature is a negative anomaly that encompasses the central part of the study area and extends to the southeast. The maximum amplitude of this anomaly is in the southeast part of the area and has a value of −4 mGal. Geologically the area is quite complex and consists of large serpentinite masses associated with severely deformed (to the west) and slightly deformed (to the east) rocks of the Great Valley sequence. It may be that the gravity anomaly is only a reflection of this structural complexity. On the other hand, the gravity feature persists even with a reduction density of 2.5 g/cm^3. Since the average density of rocks of the Great Valley sequence and of most serpentinite masses is 2.5 g/cm^3, the source of the anomaly must be material of lower density. Furthermore, the area of the negative anomaly includes most of the quicksilver deposits and hot springs in the Wilbur Springs SW. quadrangle. We therefore propose that the gravity anomaly represents a geophysical manifestation of the heat source which gives rise to the thermal anomaly at Wilbur Springs.

If this interpretation is correct, then we can use the amplitude of the anomaly and its dimensions to estimate the depth to the heat source. The maximum amplitude of the gravity anomaly occurs about 1.5 km due south of Wilbur Springs. On a northeast-southwest line through this point, the distance between the two points at which the anomaly falls to half of its maximum amplitude is 3 km, thus the half-width is 1.5 km. Two simple models for the source of the anomaly are a sphere and a horizontal cylinder. In each case the maximum amplitude and half-width can be used to determine values for the depth to the center of the source and the radius of the source (Nettleton, 1976). For a sphere the depth would be 2 km and the radius 1.25 km, based on a density contrast of 0.25 g/cm^3. A similar calculation for the horizontal cylinder gives a depth of 1.5 km and a radius of 0.75 km. For either model the distance from the surface to the top of the heat source is about 0.75 km. Thus if the heat source is responsible for the gravity anomaly, then regardless of the actual geometry, the heat source is likely to be less than a kilometer from the surface.

With regard to the nature of the heat source, there are two possible explanations: a shallow intrusive mass of molten or partially molten low-density (silicic) magma or a steam and (or) hot-water reservoir within fractured or faulted rock. It is unlikely in the case of Wilbur Springs that the heat source itself is a magma intrusion. A temperature of perhaps 1,000°C within a kilometer of the surface would certainly create widespread effects on the surficial geology. Only one such manifestation has been found: an apparent high-temperature hydrothermal alteration at one of the Manzanita group of mines in the vicinity of the deeper geothermal exploration hole (J. M. Donnelly-Nolan and R. J. McLaughlin, oral commun., 1978). The deeper exploration hole (Cordero Mining Co.) in fact provides the strongest evidence against the presence of magma. The site of the hole is within the gravity anomaly, and although the drilling reached a depth of over 1 km, the maximum temperature was only 140°C. Such a result almost requires that the gravity anomaly is related to a steam-hot water reservoir rather than to a magma intrusion. Thus, the most plausible explanation for the source of the negative gravity anomaly is that it arises from a geothermal reservoir whose surficial manifestations are the hot springs and quicksilver deposits of the Wilbur Springs area.

The present survey gives no indication of the ultimate source of heat for the geothermal reservoir. Presumably it is a deeper magma intrusion which is in some way related to the Clear Lake volcanic field. The presence of fractures within the severely deformed rocks of the Great Valley sequence could then provide the porosity necessary for the transfer of heat in the form of hot water or steam from the intrusion to the reservoir. A magma of intermediate density, that is between 2.5 and 2.67 g/cm^3, would be difficult to distinguish from the country rock on the basis of a gravity survey alone. The field observation of basalt of late Pliocene or early Pleistocene age near the northern part of the

FIGURE 93.—Residual Bouger gravity for Wilbur Springs area. *A* and *B*, Even and odd integral contour intervals for a reduction density of 2.67 g/cm^3. *C* and *D*, Even and odd integral contour intervals for a reduction density of 2.50 g/^{3}. Dots represent stations occupied in this survey. Shaded area represents approximate extent of negative gravity anomaly interpreted as a geothermal reservoir. WS, Wilbur Springs; CSM, Cold Spring Mountain; vol, a recent volcanic flow; M and C, geothermal exploration holes of Magma Power Co. and Cordero Mining Co., respectively.

gravity anomaly (J. M. Donnelly-Nolan, oral commun., may, however, represent a small eruption from this intrusion.

The conclusion that the negative gravity anomaly is a manifestation of a geothermal reservoir requires geophysical and geological confirmation. While additional gravity measurements would define the anomaly more accurately, they are unlikely to provide any more definitive information regarding the nature of the heat source. A magnetic survey would also be difficult to interpet since it would be dominated by the effects of the highly magnetic serpentinite masses. The most useful geophysical techniques would probably be seismic (and teleseismic) and electrical (and electromagnetic). Definite confirmation of the presence of a geothermal reservoir would require additional drilling.

SUMMARY

A detailed gravity survey of the Wilbur Springs SW. quadrangle indicates the existence of two gravity features, each with an amplitude of about 4 mGal. The first of these is a positive anomaly associated with a Franciscan terrane and probably related to the presence of mafic or ultramafic material at depth within the Franciscan assemblage. The second feature is a gravity low that encompasses many of the quicksilver deposits and hot springs in the Wilbur Springs area. Although this anomaly may arise from the structural complexity of the area, the available geologic and geophysical data support the inference that the feature arises from a geothermal reservoir at a very shallow depth to the south of Wilbur Spring proper. Additional geophysical studies will be needed to confirm the existence of this reservoir and to evaluate its geothermal potential.

REFERENCES CITED

Bailey, E. H., Irwin, W. P., and Jones, D. L., 1964, Franciscan and related rocks and their significance in the geology of western California: California Division of Mines and Geology Bulletin 183, 177 p.

Chapman, R. H., 1966, The California Division of Mines and Geology gravity base station network: California Division of Mines and Geology Special Report 90, 49 p.

——— 1975, Geophysical study of the Clear Lake region, California: California Division of Mines and Geology Special Report 116, 23 p.

Chapman, R. H., Bishop, C. C., Chase, G. W., and Gasch, J. W., 1974, Gravity map of California, Ukiah sheet: California Division of Mines and Geology, scale 1:250,000.

Isherwood, W. F., 1976, Gravity and magnetic studies of the Geysers-Clear Lake geothermal region, California, U.S.A.: United Nations symposium on the development and use of geothermal resources, 2d, San Francisco, 1975, Proceedings, v. 2, p. 1065-1074.

Moisseeff, A. N., 1966, The geology and geochemistry of the Wilbur Springs quicksilver district, Colusa and Lake Counties, California: Stanford, Calif., Stanford University, Ph. D. thesis, 214 p.

Nettleton, L. L., 1976, Gravity and magnetics in oil prospecting: New York, McGraw-Hill, 464 p.

Plouff, D. L., 1966, Digital terrain corrections based on geographic coordinates: Geophysics, v. 31, p. 1208.

Rich, E. I., 1971, Geologic map of the Wilbur Springs quadrangle, Colusa and Lake Counties, California: U.S. Geological Survey Miscellaneous Geologic Investigations Map I-538, scale 1:48,000.

Swick, C. H., 1942, Pendulum gravity measurements and isostatic reductions: U.S. Coast and Geodetic Survey Special Publication 232, 82 p.

SEISMIC-REFRACTION MEASUREMENTS OF CRUSTAL STRUCTURE NEAR SANTA ROSA AND UKIAH, CALIFORNIA

By David H. Warren

ABSTRACT

Seismic recordings were made in September 1976 along two 150-km profiles subparallel to regional northwest-southeast strike-slip faults. One profile extends from near Fairfield in a northwest direction to the vicinity of Willits, and the other extends from Novato northwest to a point about 20 km southeast of Mendocino. Shots were fired at five locations, and recordings were made by truck-mounted and portable recording systems and by some stations of the Geological Survey's central California microearthquake network. *P*-wave first arrivals recorded on the three types of seismographs were used to determine straight-line segmented traveltime curves. The near-surface velocity ranges from 2.0 to 4.2 km/s in a layer whose thickness ranges from 0.2 to 1.7 km but averages 1 km. Below this layer, seismic basement velocity is about 5.0 to 5.3 km/s in a layer of thickness averaging about 2 km on the northeast line and about 6 km on the southwest line. Underneath, the crustal velocity is about 5.9 km/s. From one shotpoint on the southwest line an apparent velocity of 7.2 km/s was observed for a refractor about 15 km deep. Some prominent later arrivals on the line to the southwest can be interpreted as reflections from the top of the mantle. They suggest a crustal thickness of 20 km and a mean crustal velocity of 5.8 to 5.9 km/s.

INTRODUCTION

On September 22 and 24, 1976, the U.S. Geological Survey fired five shots in the vicinity of the Geysers geothermal area (fig. 94). They were recorded by temporary seismic stations and by the central California seismic telemetry network. The temporary stations were placed along northwest-southeast-trending lines subparallel to the Rodgers Creek, Healdsburg, and Maacama faults. These lines cover an area roughly 170 km long and 40 km wide (more width to the southeast) from Willits to San Pablo Bay.

The purpose of these shots and recordings was to gain knowledge about crustal velocity structure, and to provide master events in order to improve the accuracy of microearthquate locations in this region.

FIELD OPERATIONS

At all five shotpoints (fig. 94; table 12) holes were drilled to emplace the explosive charges. At the Mendocino and Hennessey shotpoints (E-1 and E-3) the holes were located next to water reservoirs.

Recording locations are shown in figure 93. Temporary stations were moved between the two days of shooting. On September 22 shots at Skaggs Springs and Roblar (W-2 and W-3) were recorded along a line just southwest of the Maacama, Healdsburg, and Rodgers Creek faults, and on September 24 shots at Mendocino, Geysers, and Hennessey (E-1, E-2, and E-3) were recorded along a line just northeast of the faults. The fault locations are taken from Jennings (1975) for the Healdsburg and Rodgers Creek faults and from the U.S. Army Corps of Engineers (1978) for the Maacama fault. Just north of Santa Rosa the current seismic activity steps in echelon segments between the Rodgers Creek and Maacama faults. The Healdsburg fault does not seem to be seismically active.

Two types of temporary recording stations were used. One type was truck mounted, with six vertical-component Electrotech EV-17 seismometers connected to cables laid out for 2.5 km at 0.5 km intervals (Warrick and others, 1961). Two horizontal seismometers were placed at the location of one of the vertical seismometers near the center of the spread. An operator recorded events at the times of shots on both recording oscillograph and reel-to-reel 1-inch analog magnetic tape. The other type, the 5-day portable-component system, was left unattended on the ground, with one vertical-component, and sometimes two horizontal-component, Mark Products L-4 seismometers. The system recorded continually on reel-to-reel one-half-inch

Table 12.—*Description of shots and shotpoints*

Name	Key	Lat N.		Long W.		Explosive size (lb)	Date	Pacific daylight time hr:min:sec
Skaggs Springs	W-2	38°	43.48'	123°	1.45'	2,000	Sept. 22, 1976	05:35:00.58
Roblar	W-3	38°	18.16'	122°	46.60'	3,000	Sept. 22, 1976	06:05:00.78
Mendocino	E-1	39°	12.95'	123°	9.43'	3,000	Sept. 24, 1976	05:05:00.79
Geysers	E-2	38°	48.59'	122°	55.59'	2,000	Sept. 24, 1976	05:35:00.64
Hennessey	E-3	38°	29.71'	122°	21.02'	3,000	Sept. 24, 1976	06:05:00.77

analog magnetic tape. The central California network (Lester and others, 1976) usually includes a vertical-component Mark Products L-4C seismometer, a preamplifier, a voltage-controlled oscillator (VCO), and a telemetry interface. The VCO tone is carried by wire (occasionally by radio) to a terminal where it is multiplexed with tones from as many as seven other stations. This multiplexed signal is transmitted by telephone line or radio to the U.S. Geological Survey office in Menlo Park, Calif., where it is demultiplexed and recorded on 16-mm film and 1-inch analog magnetic tape. All systems utilize 1-Hz geophones, and all systems re-

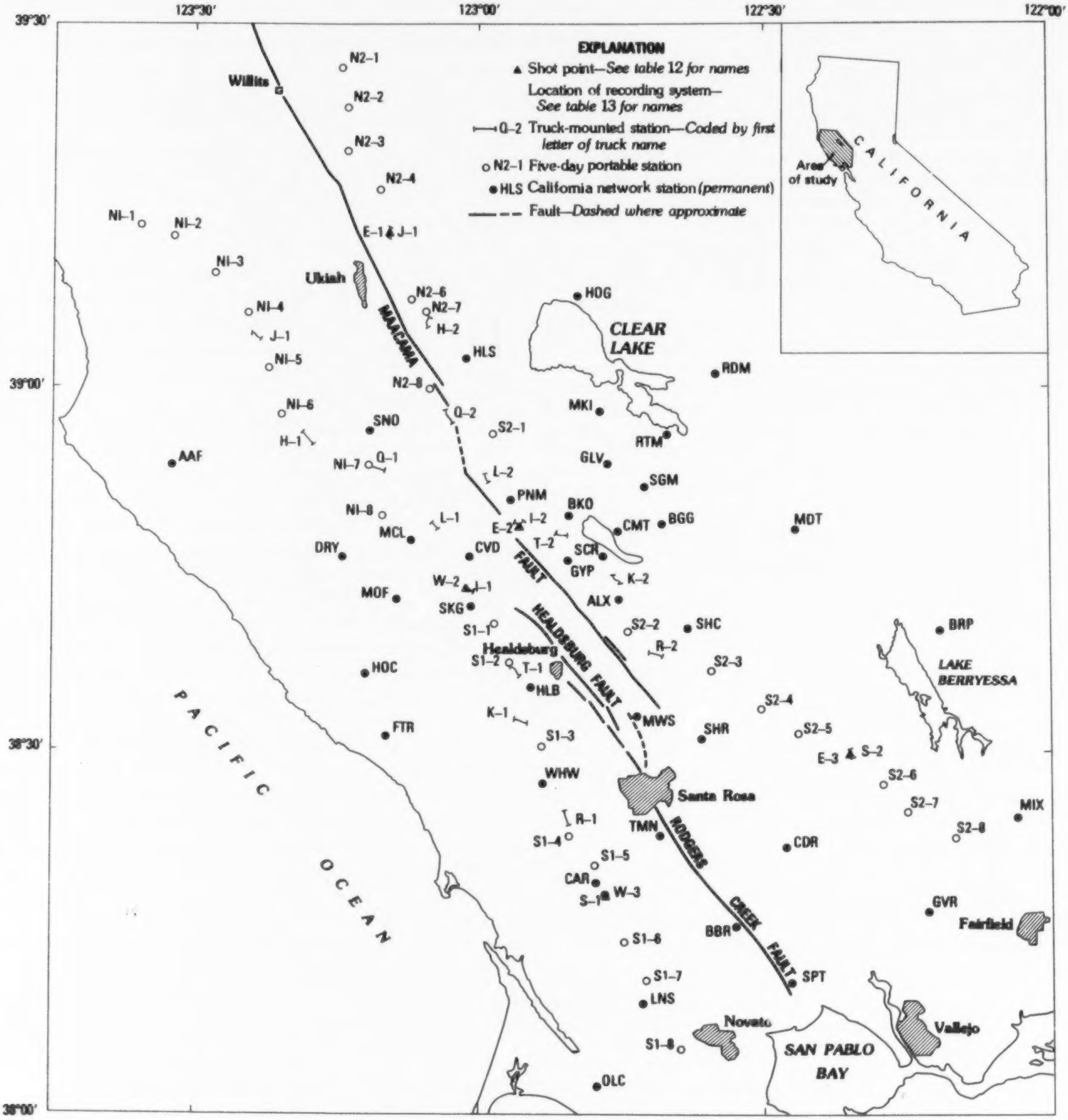
39°30′
123°30′
123°00′
122°30′
122°00′
39°00′
38°30′
38°00′
EXPLANATION
▲ Shot point—See table 12 for names
Location of recording system—See table 13 for names
Q-2 Truck-mounted station—Coded by first letter of truck name
○ N2-1 Five-day portable station
● HLS California network station (permanent)
Fault—Dashed where approximate
Area of study
CALIFORNIA
Willits
Ukiah
Healdsburg
Santa Rosa
Novato
Vallejo
Fairfield
CLEAR LAKE
LAKE BERRYESSA
SAN PABLO BAY
PACIFIC OCEAN
MAACAMA FAULT
HEALDSBURG FAULT
RODGERS CREEK FAULT
N2-1
N2-2
N2-3
N2-4
N2-6
N2-7
N2-8
NI-1
NI-2
NI-3
NI-4
NI-5
NI-6
NI-7
NI-8
E-1
J-1
H-1
H-2
Q-1
Q-2
L-1
L-2
E-2
I-2
T-1
T-2
W-2
I-1
K-1
K-2
R-1
R-2
E-3
S-1
S-2
W-3
S1-1
S1-2
S1-3
S1-4
S1-5
S1-6
S1-7
S1-8
S2-1
S2-2
S2-3
S2-4
S2-5
S2-6
S2-7
S2-8
HOG
HLS
RDM
MKI
RTM
AAF
SNO
GLV
SGM
PNM
BKO
CMT
BGG
MDT
MCL
DRY
CVD
SCR
GYP
MOF
SKG
ALX
SHC
BRP
HOC
HLB
MWS
SHR
FTR
WHW
TMN
CDR
MIX
CAR
GVR
BBR
SPT
LNS
OLC

FIGURE 94.—Locations of seismic recording stations, shotpoints, and faults in the Santa Rosa-Ukiah area, California.

cord the timing signal from WWVB radio. In addition, the truck-mounted system records the radio timing signal from WWV and a 1-second chronometer pulse. The 5-day portable systems and the central California network also record an IRIG time-coded signal.

DATA PROCESSING AND *P*-WAVE FIRST ARRIVALS

The magnetic tapes for the truck-mounted and the 5-day portable systems were digitized in the U.S. Geological Survey playback center. At the time the digitizing was done, a playback of the event was made on an ink recording oscillograph. For data from the truck-mounted system, *P*-wave first arrivals were picked from the monitor records, with occasional use of the playbacks. For data from the five-day portable system, first arrivals were picked on the playbacks. First arrivals were picked on the central California network as part of the normal data processing using the 16 mm film strips (Lester and others, 1976). *P*-wave first-arrival traveltime data are listed in table 13.

TABLE 13.—*Traveltime data*

Station	Trace No	Distance (km)	Traveltime (s)	Reduced traveltime(s)
Skaggs Springs shotpoint				
N1-2		69.61	13.35	1.75
N1-3		61.50	11.94	1.69
N1-4		53.57	10.66	1.73
Juliet-1	1	50.74	10.11	1.65
	6	49.01	9.95	1.78
N1-5		44.96	9.07?	1.58?
N1-6		38.54	7.79	1.37
Hotel-1	1	34.25	7.05	1.34
	5	32.54	6.72	1.30
SNO		28.03	6.04	1.37
N1-7		23.60	4.97	1.04
N1-8		16.66	3.75	.97
Lima-1	1	11.21	2.70	.83
	5	9.70	2.40	.78
MCL		11.12	2.80	.95
MOF		10.47	2.49	.74
CVD		4.99	1.25	.42
India-1	1	.31	.17	.12
	3	.45	.18	.10
	4	.84	.36	.22
	5	1.28	.48	.27
	6	1.61	.58	.31
SKG		2.68	.77	.32
S1-1		6.85	1.60	.46
S1-2		13.14	2.93	.74
Tango-1	1	13.82	3.11	.81
	6	15.83	3.43	.79
HLB		18.06	3.95	.94
Kilo-1	2	21.21	4.61	1.08
	6	22.57	4.84	1.08
S1-3		26.87	5.56	1.08
WHW		32.00	6.69	1.36
S1-5		46.65	9.38	1.60
Sierra-1	1	50.88	10.08	1.60
	6	51.41	10.25	1.68
S1-6		59.11	11.50	1.65
S1-7		65.87	12.69	1.71
S1-8		77.77	14.52	1.56
Roblar shotpoint				
N1-1		124.72	20.56?	−0.23?
N1-2		120.22	20.39	.35
N1-3		112.30	19.20	.48
N1-4		104.44	18.51?	1.10 ?
Juliet-1	1	101.43	17.65	.75
	6	99.80	17.50	.87
Hotel-1	1	84.41	15.18	1.11
	5	82.71	15.00	1.22
N1-7		74.73	13.93	1.47
Quebec-1	2	74.59	13.95	1.52
	6	73.18	13.78	1.58
N1-8		67.15	12.66	1.47
Lima-1	1	62.78	11.99	1.53
	5	61.28	11.79	1.58
MCL		62.00	12.11?	1.78?
CVD		55.78	11.11?	1.81?
MOF		55.39	10.55	1.32
India-1	2	51.40	10.01	1.41
	6	50.51	9.86	1.44
SKG		48.91	9.64?	1.49?
S1-1		45.02	8.81	1.31
S1-2		38.55	7.68	1.25
Tango-1	1	37.85	7.57	1.26
	6	35.93	7.19	1.20
HLB		33.85	6.97?	1.33?
Kilo-1	1	30.48	6.01	.93
	6	29.01	5.68	.84
S1-3		24.72	4.92	.80
WHW		19.69	3.99	.71
S1-4		10.68	2.40	.62
S1-5		4.94	1.30	.48
CAR		2.65	.69	.25
Sierra-1	1	.74	.20	.08
	2	.73	.19	.07
	3	.62	.13	.03
	4	.36	.06	.00
	5	.36	.07	.01
	6	.36	.07	.01
S1-6		7.54	.89	.63
S1-7		14.30	3.22	.84
LNS		17.59	3.93	1.00
S1-8		26.19	5.29	.92
Mendocino shotpoint				
N2-1		26.07	5.45	1.11
N2-2		20.02	4.35	1.01
N2-3		14.00	3.19	.86
N2-4		6.38	1.55	.49
Juliet-2	1	.71	.25	.13
	2	.66	.20	.09
	3	.26	.12	.08
	4	.17	.08	.05
	5	.50	.19	.11
	6	.87	.30	.16
N2-6		10.98	2.39	.56
N2-7		13.66	2.90	.62
Hotel-2	1	14.60	3.09	.66
	6	15.54	3.29	.70
HLS		22.85	4.72	.91
N2-8		24.79	5.23	1.10
Quebec-2	1	28.65	5.96	1.18
	6	30.84	6.31	1.17
S2-1		34.62	6.79	1.02
Lima-2	1	39.62	7.86	1.26
	6	41.22	8.15	1.28
PNM		44.82	8.96?	1.49?
India-2	2	48.56	9.29	1.20
	5	48.96	9.40	1.24
BKO		51.28	9.84?	1.29?
Tango-2	1	52.60	10.05	1.28
	5	53.78	10.15	1.19
Kilo-2	4	63.85	11.86?	1.22?
S2-2		71.05	13.41?	1.57?
Romeo-2	3	76.01	14.27?	1.60?
S2-3		83.12	15.15?	1.30?
Sierra-2	4	106.44	18.96?	1.22?
Geysers shotpoint				
N2-2		69.24	12.92	1.38
N2-3		63.29	12.04	1.49
N2.4		55.57	10.47	1.21
Juliet-2	1	49.98	9.54	1.21
	5	48.86	9.29	1.15
N2-6		38.41	7.56	1.16
N2-7		35.64	7.02	1.08
Hotel-2	1	34.70	6.91	1.13
	6	33.78	6.81	1.18
HLS		26.82	5.58	1.11
N2-8		25.19	5.46	1.26
Quebec-2	2	20.72	4.62	1.17
	6	18.86	4.25	1.10
S2-1		14.83	3.34	.87
Lima	1	9.90	2.43	.78
	6	8.36	2.04	.65
PNM		4.49	1.15	.40
India-2	2	.83	.26	.12
	3	.40	.13	.06
	4	.25	.04	.00
	5	.61	.18	.08
Tango-2	2	5.94	1.53	.54
	6	7.70	1.88	.60
BKO		7.44	1.77	.53
GYP		8.74	2.16	.70
SCR		13.39	2.92	.69
CMT		14.89	3.23	.75
Kilo-2	1	15.76	3.33	.70
	6	17.74	3.74	.78
ALX		18.52	3.90	.81
S2-2		22.88	4.79	.98
Romeo-2	1	27.29	5.42	.87
	6	29.40	5.72	.82
SHC		29.79	5.96?	1.00?
S2-3		36.48	6.84	.76
S2-4		46.29	8.61	.89
S2-5		52.66	9.98	1.20

TABLE 13.—*Traveltime data*—Continued

Station	Trace No	Distance (km)	Traveltime (s)	Reduced traveltime(s)
Geysers shotpoint—Continued				
Sierra-2	1	60.56	11.05	.96
	6	61.56	11.14	.88
S2-6		67.65	12.23	.95
S2-7		73.28	13.74?	1.53?
S2-8		80.28	14.53	1.15
Hennessey shotpoint				
N2-2		124.98	22.16?	1.33?
Juliet-2	3	106.55	19.52?	1.76?
	5	105.98	19.43?	1.77?
N2-6		96.41	17.69?	1.62?
N2-7		93.30	17.13?	1.58?
Hotel-2	2	92.46	16.69	1.28
	6	91.88	16.69	1.38
Quebec-2	1	81.08	15.01	1.50
	6	78.94	14.58	1.42
S2-1		73.34	13.45	1.23
Lima-2	1	70.48	12.95	1.20
	6	69.12	12.68	1.16
India-2	2	61.95	11.24	.92
	5	61.16	11.16	.97
BKO		56.33	10.45	1.06
Tango-2	1	56.14	10.26	.90
	5	54.54	9.96	.87
GYP		52.38	9.82	1.09
CMT		49.31	9.24	1.02
SCR		48.32	9.06	1.01
Kilo-2	2	45.12	8.39	.87
	5	43.75	8.16	.87
ALX		42.61	7.90	.80
S2-2		38.74	7.31	.85
Romeo-2	1	34.56	6.70	.94
	6	32.24	6.25	.88
SHC		31.44	6.32	1.08
S2-3		24.72	4.95	.83
SHR		22.53	4.85	1.09
S2-4		15.00	3.54	1.04
S2-5		8.67	2.22	.78
Sierra-2	1	.84	.26	.12
	2	.59	.20	.10
	3	.32	.14	.09
	4	.12	.04	.02
	5	.31	.08	.03
	6	.52	.15	.06
S2-6		6.56	1.70	.61
S2-7		12.31	2.72	.67
S2-8		19.25	4.17	.96
GVR		26.59	5.36	.93
Skaggs Springs Northeast				
SKG		2.68	0.77	0.32
CVO		4.99	1.25	.42
PNM		15.26	3.73	1.19
GYP		16.27	3.92	1.21
BKO		19.26	4.46	1.25
SCR		21.69	4.82	1.21
CMT		25.06	5.41	1.23
GLV		28.77	6.39	1.59
SGM		31.52	6.98	1.73
BGG		31.57	6.66	1.40
RTM		38.88	7.82	1.34

Station coordinates were read, in degrees and minutes of latitude and longitude, for locations marked in the field on topographic maps. A computer program was used to calculate distances from the shots using Richter's short-distance algorithm (Richter, 1958). These distances are listed in table 12. Also listed are reduced traveltimes wherein a time equal to the distance divided by 6 km/s is subtracted from the traveltime. Thus on a plot of reduced traveltime vs. distance, a line of velocity of 6 km/s appears horizontal, of zero slope.

Reduced traveltimes of the *P*-wave first arrivals are plotted (figs. 95 and 96) for the five shots. Straight line segments were fitted to the points. Each segment corresponds to a layer of an assumed model that consists of constant-velocity layers with sharp boundaries on the top and bottom of each layer and velocity in each layer greater than that in the overlying layer. Models of five layers seem to be indicated by the data, although the shallowest layers are represented sometimes by one layer and sometimes by two layers. Where appropriate the straight line segments were drawn by making reverse points equal. These are points where source and receiver locations can be interchanged with the same ray travel path, with identical traveltime from two different shotpoints. This was appropriate for the approximately 5 km/s and 5.9 km/s layers for shot pairs of Skaggs Springs-Roblar, Mendocino-Geysers, and Geysers-Hennessey. Equations of the traveltime curves are listed in table 14. From these equations, thicknesses and velocities for the layers were calculated using a computer program that utilizes the method of Adachi (1954). These results are listed in table 15. Cross sections of velocity structure plotted from these results are shown in figures 95 and 96. Depth values have been plotted from the surface elevation of each shotpoint, considered zero depth.

On parts of the northeastern profile, Mendocino northwest and Hennessey southeast, there is only one data point, the most distant one in each case, that falls low from the 5 km/s layer. If it is assumed that these points are from the next deeper layer, and further assumed that the velocity of the deeper layer is 5.9 km/s, then a minimum thickness of the 5 km/s layer can be calculated. The results are listed in tables 14 and 15 and shown as dashed lines in figure 96.

A profile was formed for selected stations of the central California network northeast of the Skaggs Springs shotpoint. Traveltimes were used for those stations within 10 km of a line N. 57° E. from the shotpoint. Traveltimes are listed in table 13 and plotted in figure 97. Equations of the traveltime curve are listed in table 14, and the calculated crustal structure is listed in table 15.

RECORD SECTIONS AND REFLECTION ARRIVALS

After the magnetic tapes for the recording truck and the 5-day portable systems were digitized, the digital tapes were sent to a large computer installation. Record sections were made from these data using an extensive program called GEOLAB (J. W. Herriot, written commun., 1977), wherein plotting is done during program execution on both a terminal screen and a permanent copy plotter. Examples of these record sections are shown (figs. 98 and 99) for the Roblar and Geysers shotpoints. First-arrival traveltimes are shown by tick marks next to the individual traces. Although the first arrivals appear to have very low amplitude on

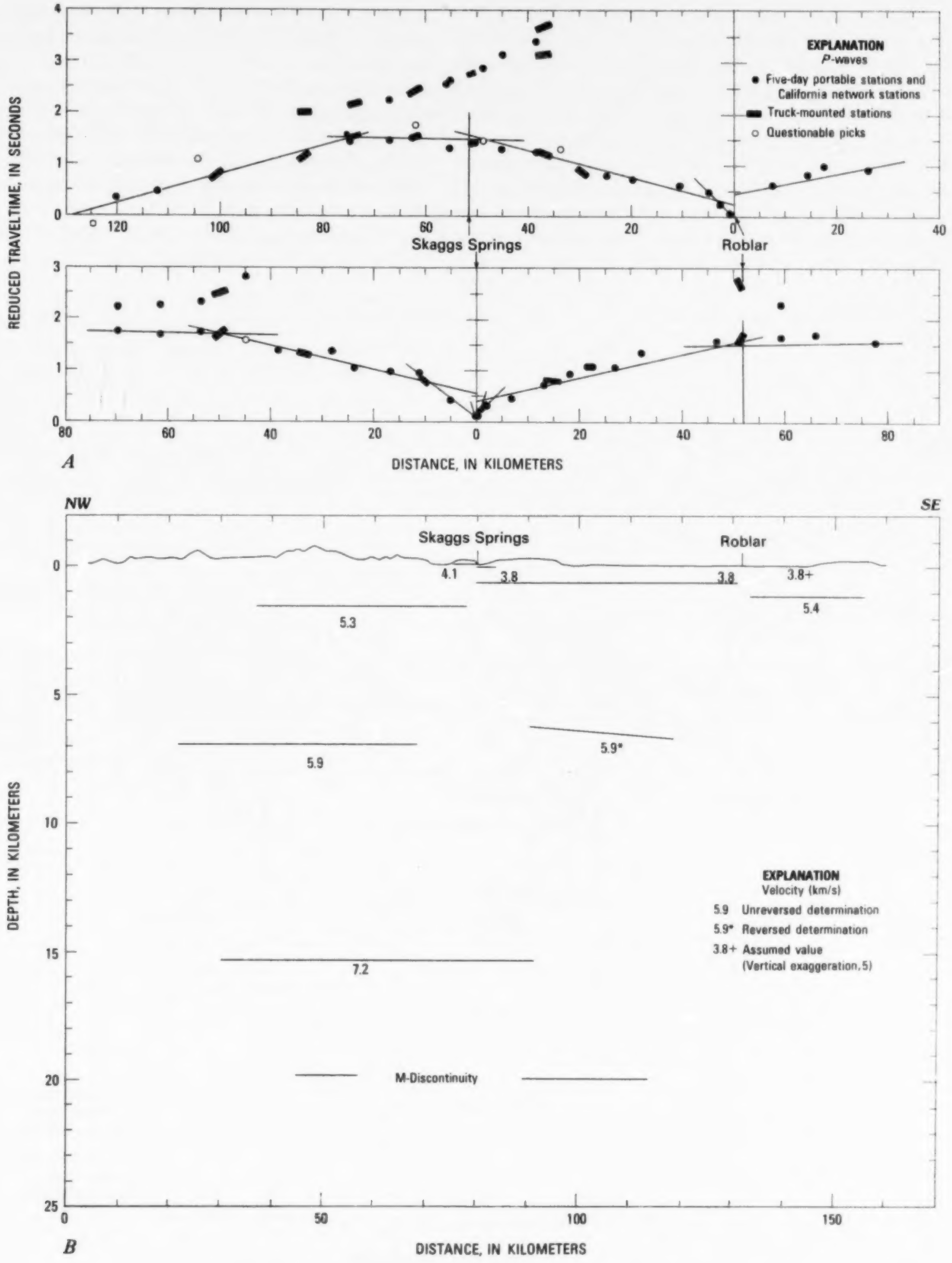

FIGURE 95.—Traveltime plots and velocity profile for southwesterly shots. *A*, Traveltime plots of *P*-wave arrivals. See table 14 for equations of interpreted straight-line segments. *B*, Cross section of velocity (km/s) structure for this profile.

the record sections, they are much clearer on higher gain playbacks or monitor records.

The record sections allow one to study the general character of the seismograms and to correlate arrivals later than the first. Some prominent later arrivals appear on the Roblar northwest record sections (labeled *PmP* in figs. 98*A* and 98*B*). Similar arrivals also appear on the Skaggs Springs northwest and southeast record sections (not included). The reduced traveltimes of the beginnings of these phases were picked from the record sections (table 16), the traveltimes computed, and a plot made of the traveltime squared versus distance squared (fig. 100). These points fit straight lines and therefore are indicative of reflections. The inverse slope of each line gives a measurement of average velocity squared, from the surface to the point of reflection, and the intercept is the two-way traveltime squared for a vertical path assuming that the reflecting interface has no dip. The average crustal velocities are 5.9 km/s for the Roblar reflections and 5.8 km/s for the Skaggs Springs reflections. Crustal thicknesses are 21 km for Roblar northwest and 19 km for Skaggs

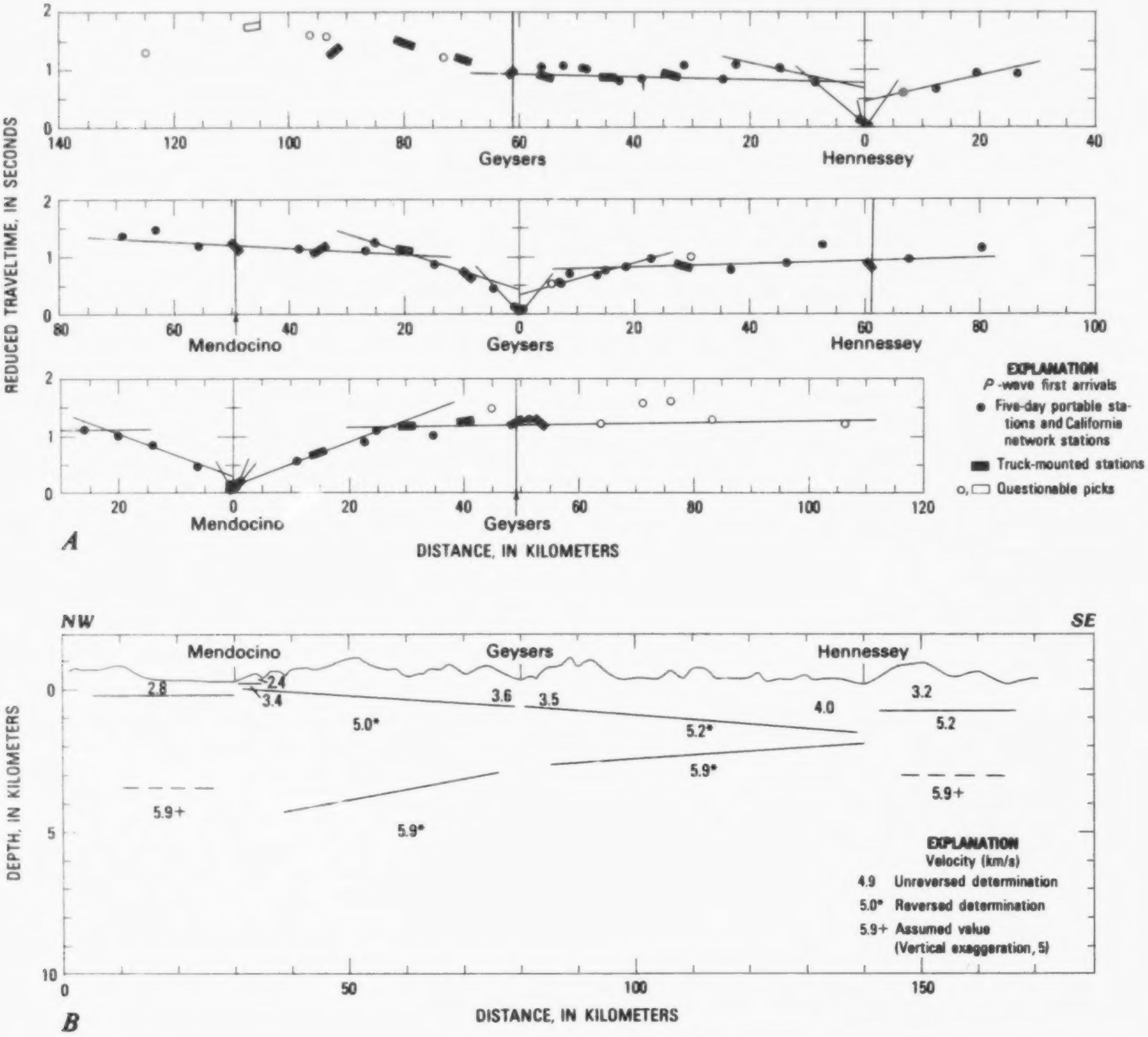

FIGURE 96.—Traveltime plot and velocity profile for northeasterly shots. *A*, Traveltime plots of *P*-wave first arrivals. See table 14 for equations of interpreted straight-line segments. *B*, Cross section of velocity (km/s) structure for this profile.

Springs northwest. These values are within expected errors of about 0.1km/s for the velocity measurements and about 2 km for the crustal thickness measurements. The consistency of these results indicates that the assumption of no dip on the M-discontinuity is valid. Two points on the Skaggs Springs southeast profile are plotted with the data for Roblar northwest (fig. 100*A*). Their reflection points at the base of the crust fall along the same area as the reflections for Roblar northwest.

DISCUSSION

The values of layer thicknesses and velocities as listed in table 15, and the average crustal velocity and crustal thickness as determined from reflections constitute the main results of this survey. Velocity measurements are probably good to about 0.1 km/s for the reversed determinations, and good to several tenths of a kilometer per second for the surficial layering. Velocity models consist of layers of constant velocity separated by sharp discontinuities. In reality, the traveltime curves are smoother, and the transitions between velocity layers are probably gradual. The record sections of Geysers northwest (fig. 99) are typical of most of the other record sections in that there are no later arrivals that can be correlated as phases. If the boundaries between layers were sharp, they would give rise to reflected phases. The lack of strong reflections on the record sections supports the concept of gradual transitions. Some of the *P*-wave first arrival traveltime data (figs. 95 and 96) could be approximated by a gradual transition from the basement layer to the crustal layer of 5.9 km/s. The plot for Skaggs Springs southeast is particularly favorable for a gradual transition.

Although the assumed model of velocity structure has its limitations, a number of conclusions can be drawn from the approximations the values in table 15 represent. The velocity measurements were correlated with the known geology as presented by Jennings (1977), Koenig (1963), and Jennings and Strand (1960).

The uppermost layer usually has an average velocity of 2.8 to 4.2 km/s, and in places there is a thin veneer

TABLE 14.—*Equations of traveltime curves*

Shot	Direction	Intercept (s)	Apparent velocity (km/s)
Skaggs Springs	NW	.00	2.0
		.09	4.1
		.55	5.27
		1.59	5.91
	SE	.00	2.0
		.15	3.8
		.40	5.27
		1.40	5.93
Roblar	NW	.00	3.75
		.26	5.19
		1.42	5.94
		3.6	7.2
	SE	00	3.75+
		.47	5.36
Mendocino	NW	.00	2.8
		.29	4.91
		1.05	5.90+
	SE	.00	2.4
		.06	3.42
		.15	4.88
		1.14	5.96
Geysers	NW	.00	3.6
		.42	5.02
		.92	5.80
	SE	.00	3.5
		.36	5.16
		.77	5.91
Hennessey	NW	.00	2.0
		.06	4.0
		.67	5.30
		.79	5.92
	SE	.00	3.2
		.45	5.25
		.85	5.90+
Skaggs Springs	NE	.00	2.0+
		.09	4.2
		.79	5.2+
		1.10	5.80

+Assumed value.

TABLE 15.—*Calculated crustal structure*

Shot	Direction	Velocity (km/s)	Thickness (km)	Depth (km)
Skaggs Springs	NW	2.0	0.10	0.00
		4.1	1.50	0.10
		5.27	5.45	1.60
		5.91	---	7.1
	SE	2.0	0.18	0.00
		3.8	0.65	0.18
		5.23*	5.4	0.82
		5.93*	---	6.2
Roblar	NW	3.8	0.71	0.00
		5.23*	6.3	0.71
		5.93*	8.5	7.0
		7.2	---	15.4
	SE	3.8+	1.23	0.00
		5.36	---	1.23
Mendocino	NW	2.8	0.50	0.00
		4.91	3.3	0.50
		5.90+	---	3.8
	SE	2.4	0.10	0.00
		3.4	0.19	0.10
		4.95*	4.5	0.29
		5.87*	---	4.8
Geysers	NW	3.6	1.04	0.00
		4.95*	2.0	1.04
		5.87*	---	3.1
	SE	3.5	0.94	0.00
		5.23*	2.1	0.94
		5.92*	---	3.0
Hennessey	NW	2.0	0.07	0.00
		4.0	1.59	0.07
		5.23*	0.3	1.66
		5.92*	---	2.0
	SE	3.2	0.93	0.00
		5.25	2.1	0.93
		5.90+	---	3.1
Skaggs Springs	NE	2.0+	0.10	0.00
		4.2	2.48	0.10
		5.2+	1.1	2.58
		5.80	---	3.7

+Assumed value

*Reversed determination

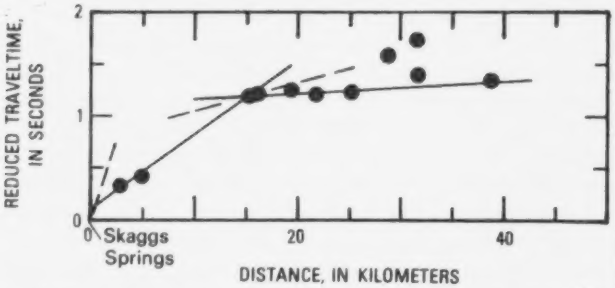

FIGURE 97.—Traveltime plot for northeasterly profile through The Geysers. Dots represent first arrivals of *P* waves at California network and five-day portable stations. See table 14 for equations of interpreted straight-line segments.

TABLE 16.—*Reflection investigation*

Station	Trace No.	Distance X(km)	Reduced travel-time(s)	Travel-time, T(s)	X^2 (÷100)	T^2
			Skaggs Spring, Northwest			
N1-5		44.96	2.80	10.29	20.2	105.9
Juliet-1	6	49.01	2.53	10.70	24.0	114.5
	1	50.74	2.49	10.95	25.7	199.9
N1-4		53.57	2.32	11.25	28.7	126.6
N1-3		61.50	2.27	12.52	37.8	156.8
N1-2		69.61	2.24	13.84	48.5	191.5
			Skaggs Springs, Southeast			
Sierra-1	1	50.88	2.76	11.24	25.9	126.3
	6	51.41	2.67	11.24	26.4	126.3
S1-6		59.11	2.30	12.15	34.9	147.6
			Roblar, Northwest			
Tango-1	6	35.93	3.18	9.17	12.9	84.1
	1	37.85	3.15	9.46	14.3	89.5
	6	35.93	3.75	9.74	12.9	94.9
	1	37.85	3.69	10.00	14.3	100.0
S1-2		38.55	3.43	9.86	14.9	97.2
S1-1		45.02	3.16	10.66	20.3	113.6
SKG		48.91	2.88	11.03	23.9	121.7
India-1	6	50.51	2.80	11.22	25.5	125.9
	2	51.40	2.79	11.39	26.4	129.7
MOF		55.39	2.64	11.87	30.7	140.9
CVD		55.78	2.59	11.89	31.1	141.4
Lima-1	5	61.28	2.50	12.71	37.6	161.5
	1	62.78	2.41	12.87	39.4	165.6
N1-8		67.15	2.29	13.48	45.1	181.7
Quebec-1	6	73.18	2.22	14.42	53.6	207.9
	2	74.59	2.18	14.61	55.7	213.5
Hotel-1	5	82.71	2.03	15.81	68.4	250.0
	1	84.41	2.03	16.10	71.2	259.2

on top with velocity 2.0 to 2.4 km/s. The survey was not designed to study this shallow layering in detail. The material probably consists of sediments, weathered basement, and other unconsolidated material. Its thickness ranges from 0.3 to 1.7 km and averages 1.1 km. There are differences between the two profiles. The northeast profile shows more of a velocity range. From Mendocino northwest the profile crosses a valley where Quaternary sediments occur. If this value is eliminated, the velocity of most of the thickness of the surficial layer ranges from 3.2 to 4.0 km/s. On the southwestern profile, the velocity of most of the thickness of the surficial layer ranges only from 3.8 to 4.1 km/s.

Underneath the surficial material lies seismic basement in which the reversed determinations of true velocity range from 5.0 to 5.2 km/s. This layer is especially well determined by the Skaggs Springs and Roblar profiles southwest of the Healdsburg fault, where its thickness is about 6 km. It is considerably thinner, averaging 2 km, in the profiles to the northeast of the Healdsburg fault. In the profile from the Hennessey shotpoint to the northwest this layer is thin or absent. The southwestern profile is in a terrane of the Franciscan assemblage, Cretaceous-Tertiary marine sedimentary rocks, and, in the southern portion near the Roblar shotpoint, upper Pliocene marine sedimentary rocks. The thicker values of basement determined by the southwest profile may be due to the occurrence of the sedimentary rocks. Most of the northeastern profile is in a terrane of the Franciscan assemblage. Near the Geysers shotpoint, a significant amount of Franciscan volcanic and metavolcanic rocks occur. Near the Hennessey shotpoint, both northwest and southeast, Pliocene volcanic rocks are present. Significant amounts of Mesozoic ultrabasic intrusive rocks outcrop, particularly between the Geysers and Hennessey shotpoints. The occurrence of more basic rocks northwest of Hennessey may correlate with the thinning seismic basement and the shallow depth of the next deeper layer. For such a wide variation of rock types, the velocity in the seismic basement is remarkably uniform.

Underneath the seismic basement lies upper crustal material. The reversed determinations of average velocity remain constant at 5.9 km/s. First arrivals traveling through this layer are called *Pg*. Presumably the layer is composed of crystalline granitic rocks. This is the deepest layer reached by first arrivals from any of the shotpoints except for the Roblar northwest profile, where an apparent velocity of 7.2 km/s was observed at a calculated depth of 15 km, defining the top of an intermediate layer. First arrivals for the layer begin at a distance of about 80 km. On the other long profiles (Mendocino southeast and Hennessey northwest) first arrivals beyond 80 km are very weak, and no information is available for determining this deeper layer.

Reflections from the Mohorovičić discontinuity on the record sections (fig. 98) are up to 1 second in duration. This long reflection time suggests that the base of the crust is a transition zone, or a zone of alternatively higher and lower velocity several kilometers in thickness rather than a sharp step.

The northeast-trending profile formed from California network data (fig. 97) is different in several respects from the other profiles. It passes through the Geysers geothermal field, and through a pronounced low in the Bouguer gravity field (Chapman and Bishop, 1970). In the distance range of 15 to 25 km, where rays reach about 5 km deep, the arrivals fall about 0.3 s later than do arrivals on the other traveltime curves

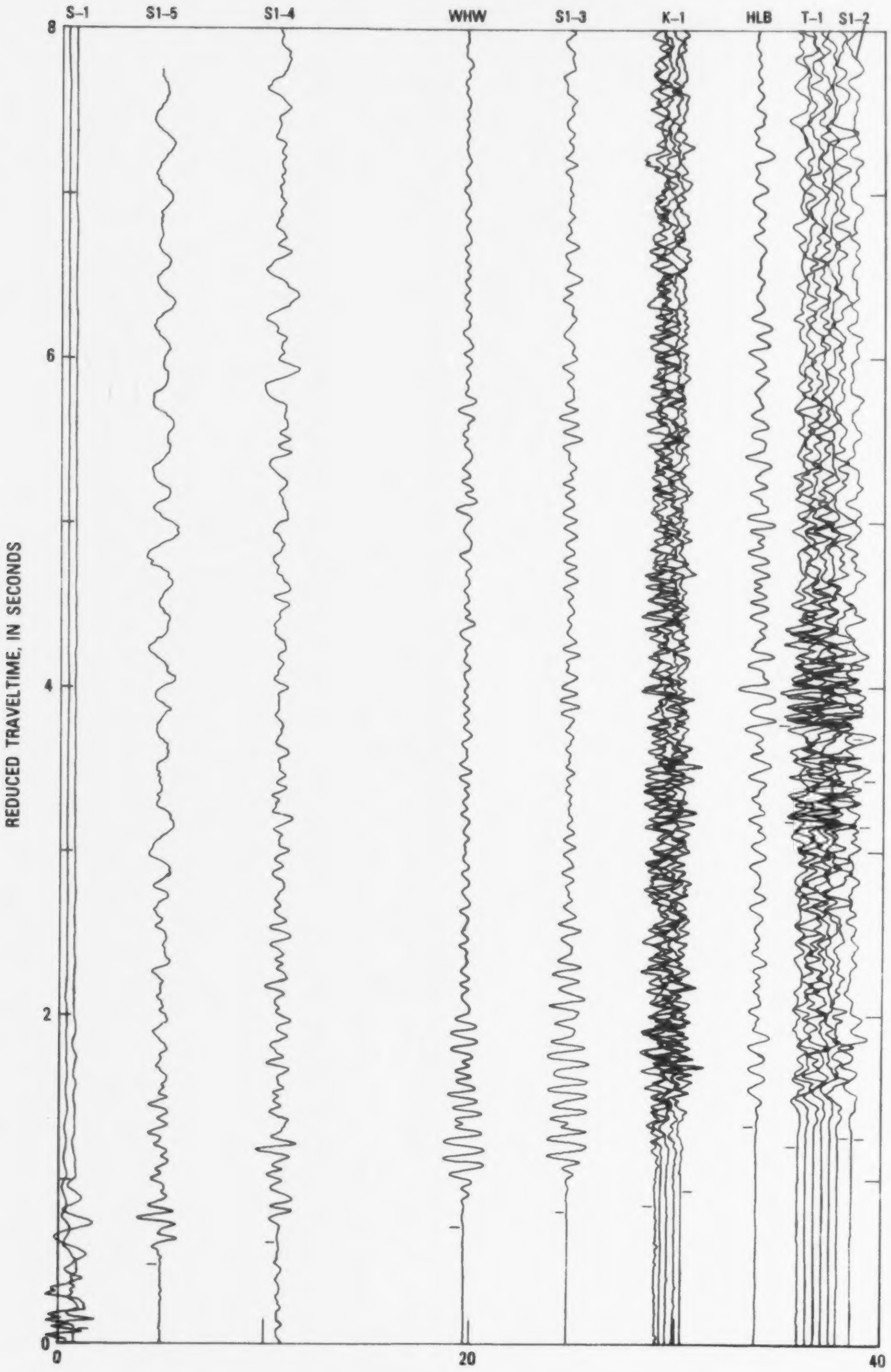

FIGURE 98.—Record sections for Roblar shotpoint, extending northwest. Times of first arrivals and some strong secondary arrivals (*PmP*) shown by tick marks. Traces are alined in a reduced format so that a line of 6-km/s velocity appears horizontal. *A*, Distance range 0 to 40 km. *B*, Distance range 45 to 80 km. *C*, Distance range 85 to 125 km.

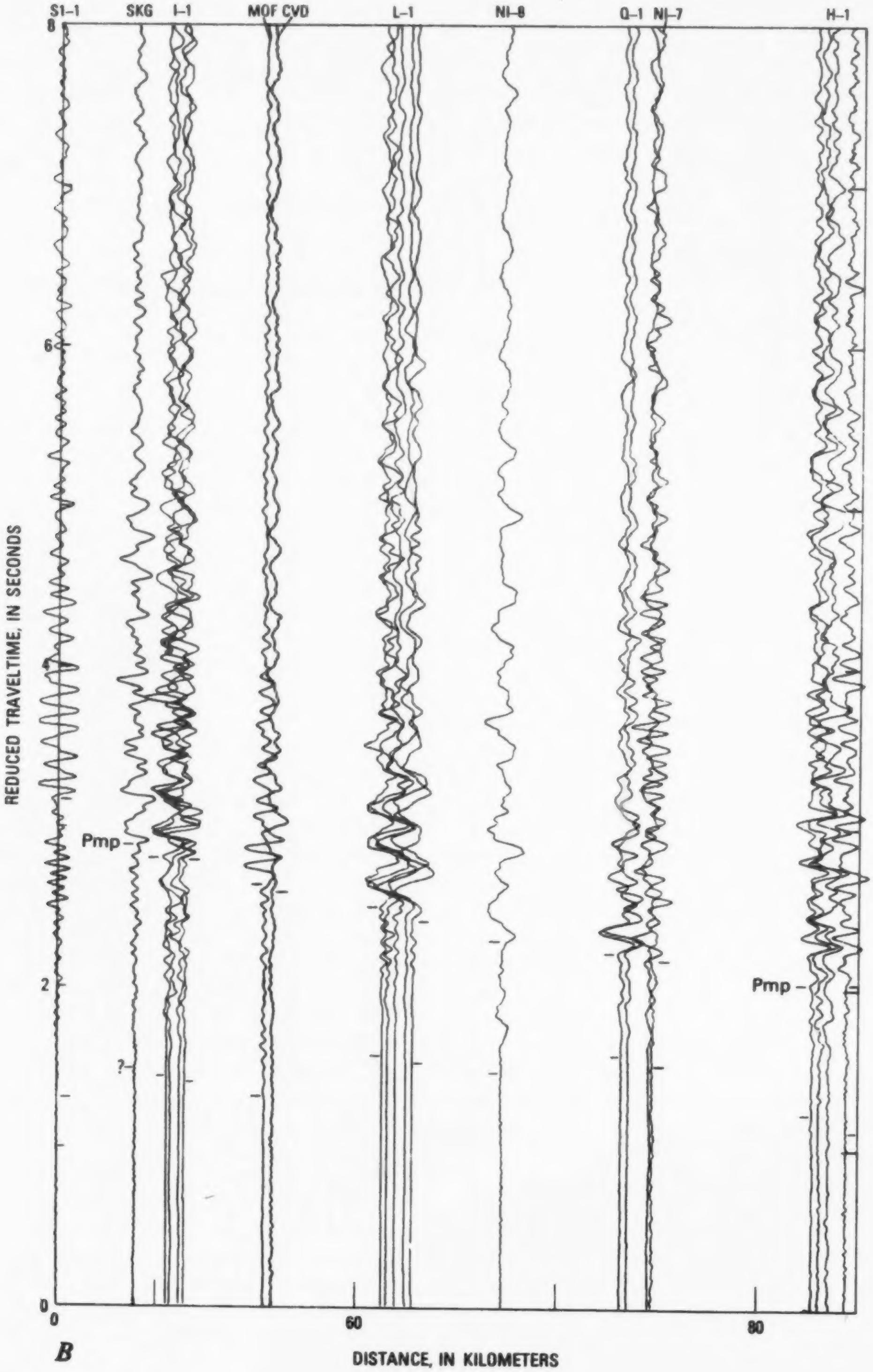

FIGURE 98.—Continued

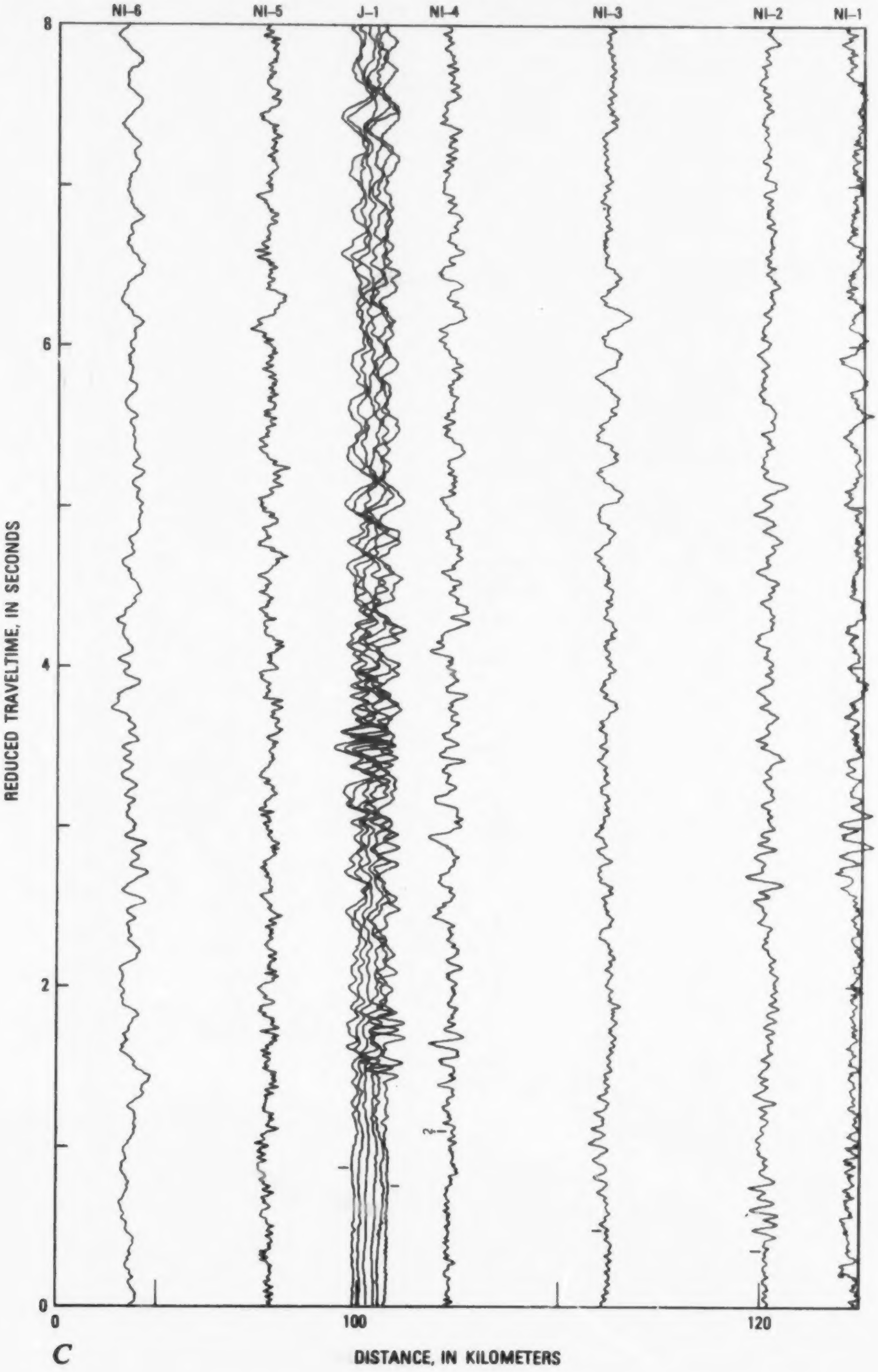

FIGURE 98.—Continued

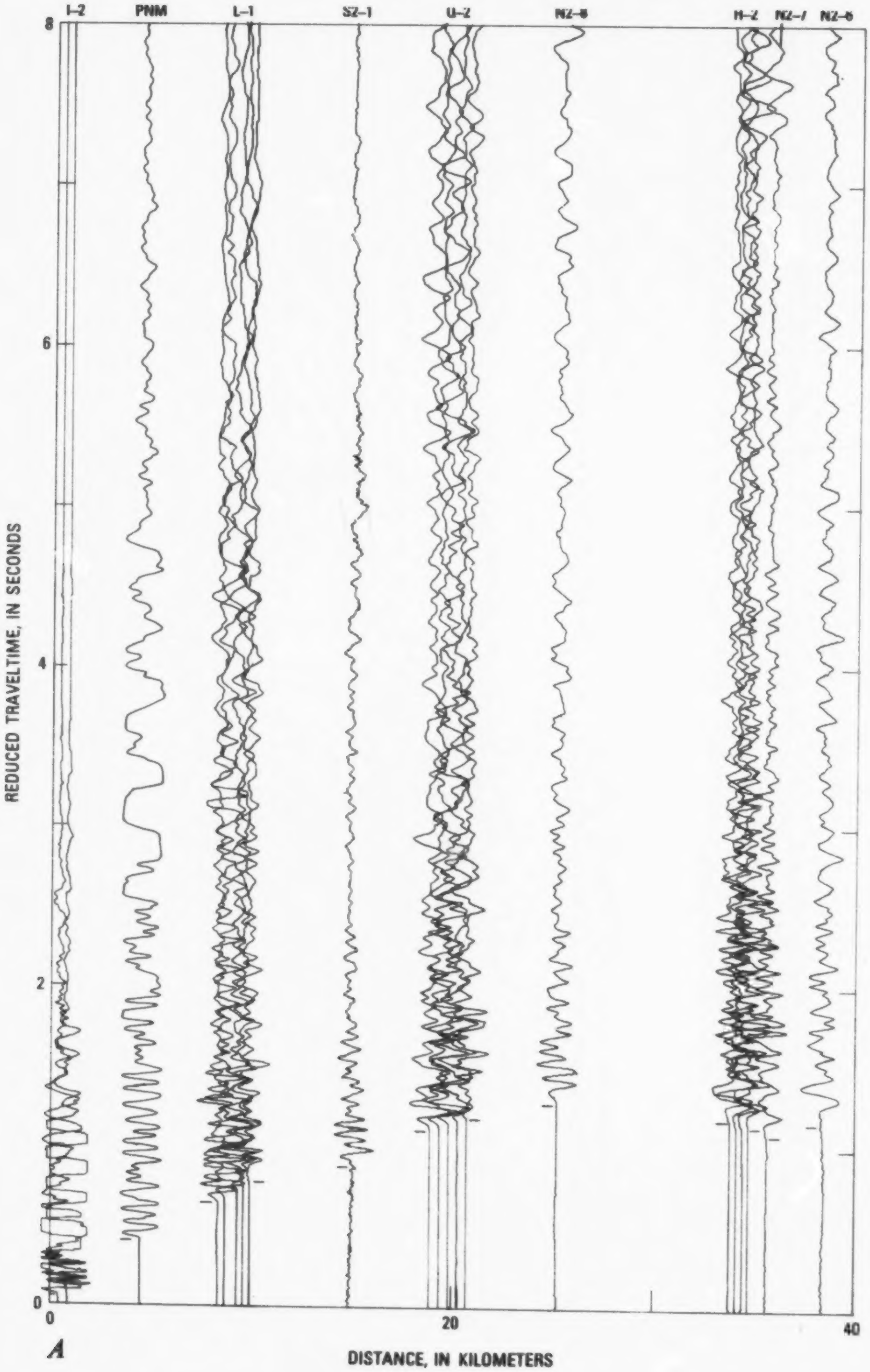

FIGURE 99.—Record sections for Geysers shotpoint, extending northwest. Times of first arrivals shown by *A*. Distance range 0 to 40 km.

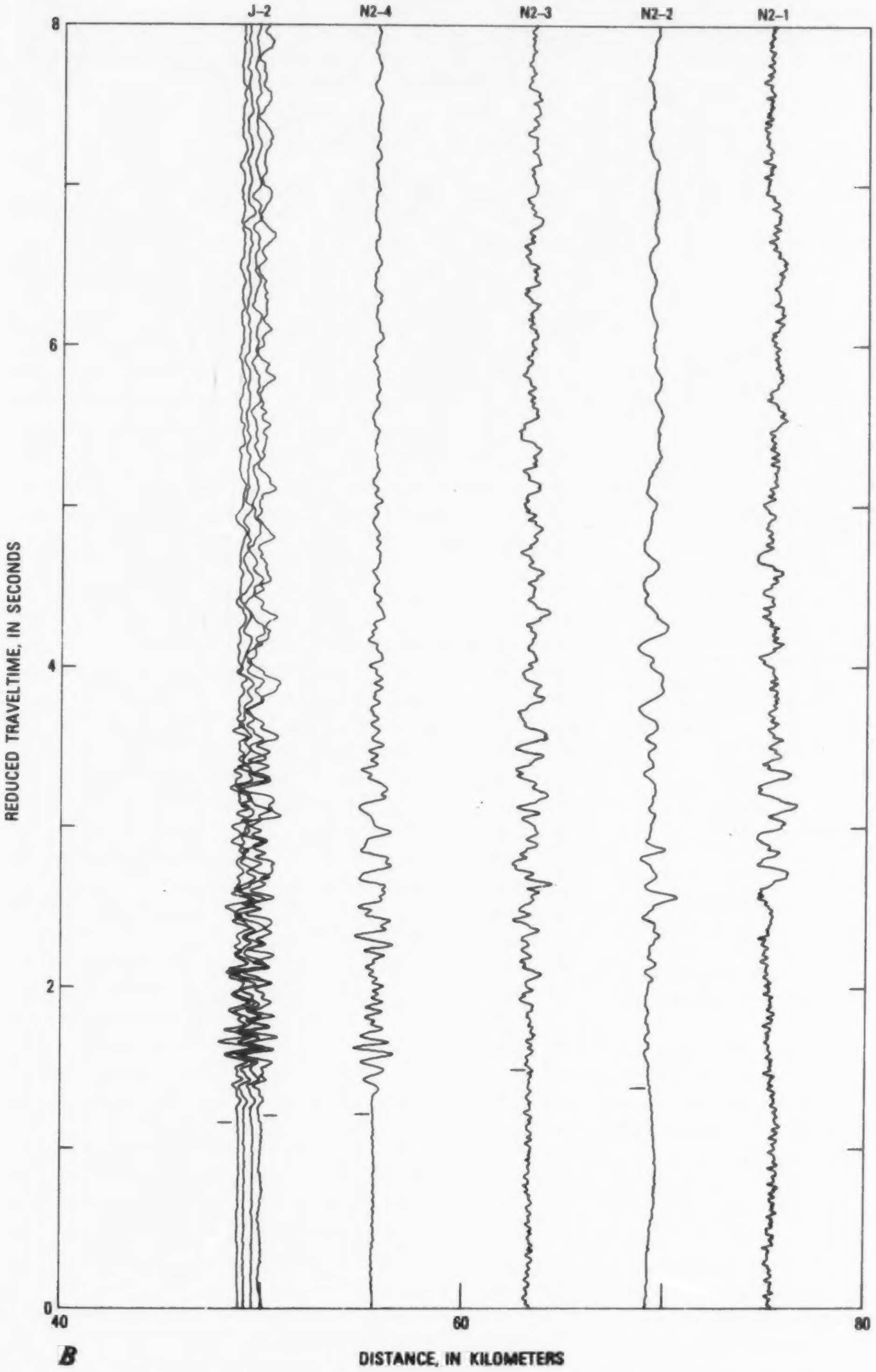

tick marks. Traces are alined in a reduced format so that a line of 6 km/s velocity appears horizontal. *B*, Distance range 40 to 80 km.

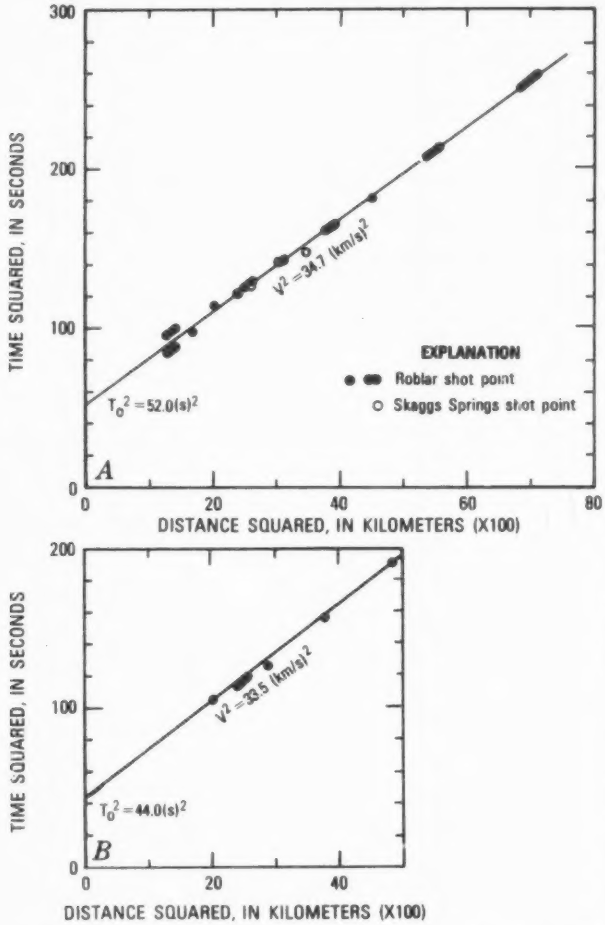

FIGURE 100.—Plots of time squared (T^2) versus distance squared (X^2). V^2, average velocity squared from surface to point of reflection. T_0^2, two-way traveltime squared, for vertical path at zero distance. *A*, Roblar shotpoint, northwest and Skaggs Springs shotpoint, southeast. *B*, Skaggs Springs shotpoint, northwest.

(figs. 95 and 96). This delay suggests that material in the upper crust is somewhat lower in velocity. An alternate interpretation is that the delay occurs in low-velocity material in a fault zone closer to the shotpoint. Healy and Peake (1975) deduced that a vertically oriented low velocity zone, extending to a depth of 12 km, occurs between the San Andreas and San Benito faults near Bear Valley, California. There are three arrivals at a distance range of about 30 km that are as much as 0.4 s later than the line shown in figure 97, suggesting more low-velocity material near the top of the crust. This observation is consistent with results of Iyer and others (this volume), who show large *P*-wave delays in the Geysers geothermal area from teleseismic data.

These profiles are the first to be published for this region, in which Franciscan rocks are widely exposed. The Port Chicago explosion furnishes the closest previous seismic study, just southeast of this survey (Byerly, 1946). From it Byerly concluded that there is 3 km of 5.0-km/s material at the top of the crust, and 11 km of 5.6-km/s velocity from observations of the $\overline{P}$ phase (large-amplitude phase channeled within the crust). Previous work includes studies to the east and south of San Francisco. The most intensive study was by Stewart (1968), who interpreted two seismic-refraction profiles in the Diablo Range and GabilanRange. He distinguished the results as showing differences depending on whether or not they were located in granitic or Franciscan rocks. On the profile in the Diablo Range he concluded that there is no granitic layer, but a thick Franciscan layer extending to 10-km depth, in which the velocity is 5.7 km/s. This is consistent with Byerly's (1939) measurements of the $\overline{P}$ phase, which gave a velocity of 5.6 km/s from stations in Franciscan terrane. Stewart deduced that there is no normal granitic upper crust in the Diablo Range, because he did not find a velocity of about 6.0 km/s; however, this survey shows a *Pg* velocity of 5.9 km/s underneath the 4.9-5.3-km/s layer. Stewart detected 2-3 km of a 4.8-5.0-km/s layer near the top of the crust, which correlates well with the layer called seismic basement in this survey. Stewart's profile in the Gabilan Range, in granitic rocks, showed a *Pg* velocity of 6.0 to 6.3 km/s, with a very thin overlying layer of 4.8 km/s. Eaton (1966) and Healy (1963) similarly reported *Pg* velocities of 6.0 to 6.1 km/s in granitic terranes. Hamilton, Ryall, and Berg (1964) reported a *Pg* velocity of 6.3 km/s to the southwest of the San Andreas fault in the Coast Ranges, although it is unreversed. These results show significant lateral heterogeneity in the upper crust. This survey seems to fit into an intermediate position to the interpretations by Stewart (1968) for the Diablo and Gabilan Ranges.

The occurrence of an intermediate layer agrees with Stewart (1968), who also found it as a first arrival with velocity 6.9 km/s in the Diablo Range, from a depth of about 12 km. The crustal thickness of 20 km southwest of the Healdsburg fault compares with a 22-km-thick crust found by Hamilton, Ryall, and Berg (1964) to the southwest of the San Andreas fault between San Francisco Bay and Monterey Bay, and a thickness of 22 to 24 km by Eaton (1966) near San Francisco. The deepest determination is that by Stewart (1968), who showed a thickness of 30 km under the Diablo Range. In a study of residuals and velocities of *Pn* waves (traveling along the top of the upper mantle) from near regional earthquakes and nuclear explosions, Kind (1972) measured an increase of crustal thickness of 5 to 9 km going from west to east of the San Andreas fault, in the area near the center of the U.S. Geological

Survey's central California seismic network. The 20-km-thick crust found in this survey is less than most previous measurements located east of the San Andreas fault.

REFERENCES CITED

Adachi, Ryutaro, 1954, On a proof of fundamental formula concerning refraction method of geophysical prospecting and some remarks: Kumamoto Journal of Science, ser. A, v. 2, no. 1, p. 18-23.

Byerly, Perry, 1939, Near earthquakes in central California: Seismological Society of America Bulletin, v. 29, no. 3, p. 427-462.

——— 1946, The seismic waves from the Port Chicago explosion: Seismological Society of America Bulletin, v. 36, no. 4, p. 331-348.

Chapman, R. H., and Bishop, C. C., 1970, Bouguer gravity map of California, Santa Rosa sheet: California Division of Mines and Geology, scale 1:250,000.

Eaton, J. P., 1966, Crustal structure in northern and central California from seismic evidence, *in* Bailey, E. H., ed., Geology of northern California: Division of Mines Bulletin 190, p. 419-426.

Hamilton, R. M., Ryall, Alan, and Berg, Eduard, 1964, Crustal structure southwest of the San Andreas fault from quarry blasts: Seismological Society of America Bulletin, v. 54, no. 1, p. 67-77.

Healy, J. H., 1963, Crustal structure along the coast of California from seismic-refraction measurements: Journal of Geophysical Research, v. 68, no. 20, p. 5777-5787.

Healy, J. H., and Peake, L. G., 1975, Seismic velocity structure along a section of the San Andreas fault near Bear Valley, California: Seismological Society of America Bulletin, v. 65, no. 5, p. 1177-1197.

Jennings, C. W., 1975, Fault map of California: California Division of Mines and Geology, scale 1:750,000.

——— 1977, Geologic map of California: California Division of Mines and Geology, scale 1:750,000.

Jennings, C. W., and Strand, R. G., 1960, Geologic map of California, Ukiah sheet, Olaf P. Jenkins edition: California Division of Mines and Geology, scale 1:250,000.

Kind, Rainer, 1972, Residuals and velocities of *Pn* waves recorded by the San Andreas seismograph network: Seismological Society of America Bulletin, v. 62, no. 1, p. 85-100.

Koenig, J. B., compiler, 1963, Geologic map of California, Santa Rosa sheet, Olaf P. Jenkins edition: California Division of Mines and Geology, scale 1:250,000.

Lester, F. W., Kirkman, S. L., and Meagher, K. L., 1976, Catalog of earthquakes along the San Andreas fault system in central California: U.S. Geological Survey Open-File Report 76-732, 32 p.

Richter, C. F., 1958, Calculation of short distances, *in* Elementary seismology: San Francisco, W. H. Freeman, p. 701-705.

Stewart, S. W., 1968, Preliminary comparison of seismic traveltimes and inferred crustal structure adjacent to the San Andreas fault in the Diablo and Gabilan Ranges of central California, *in* Dickinson, W. R., and Grantz, Arthur, eds., Proceedings of conference on geological problems of the San Andreas fault system: Stanford, California, Stanford University Publications in the Geological Sciences, v. 11, p. 218-230.

U.S. Army Corps of Engineers, 1978, Maacama fault study, Sonoma and Mendocino Counties, California: San Francisco, Calif., U.S. Army Engineer District, 156 p.

Warrick, R. E., Hoover, D. B., Jackson, W. H., Pakiser, L. C., and Roller, J. C., 1961, The specification and testing of a seismic refraction system for crustal studies: Geophysics, v. 26, no. 6, p. 820-824.

CHEMICAL ANALYSES OF WATERS FROM SPRINGS AND WELLS IN THE CLEAR LAKE VOLCANIC AREA

By J. M. THOMPSON, F. E. GOFF, and J. M. DONNELLY-NOLAN

INTRODUCTION

In 1971 the Geysers-Clear Lake area was selected by the U.S. Geological Survey geothermal research program as a region for extensive investigation. Studies in that program were designed to determine the origin and structural setting of the geothermal resource, to test and evaluate methods of geothermal prospecting and resource characterization, and to provide background data to be used to evaluate the effects of resource development. This program involved geologic mapping, petrologic studies, isotopic dating, heat-flow measurements, and seismic and other geophysical surveys. The chemical analyses of waters from springs and wells reported here are in support of that program.

Analyses of various thermal water samples from the Clear Lake Volcanics and adjacent areas have been reported by many investigators over nearly 90 years. Winslow Anderson prepared the first detailed compendium of spring waters of this area in 1892; his report was intended to be a reference for medical practitioners in recommending health resorts for their patients. Waring (1915) transformed many of Anderson's earlier analyses from grains per gallon into parts per million and also included a number of important spring analyses not reported by Anderson. Allen and Day (1927) analyzed numerous springs at The Geysers collected during the initial drilling there. Berkstresser (1968) reported analyses of about 41 Lake County springs and 11 springs from surrounding counties. Numerous other investigators have analyzed waters in and near the Geysers-Clear Lake geothermal area in recent years. They included, but are not limited to: White, Brannock, and Murata (1956), White and Roberson (1962), White, Hem, and Waring (1963), Barnes, O'Neil, Rapp, and White (1972), Barnes, O'Neil, Rapp, and White (1973), Vollintine (1975), and Goff, Donnelly, Thompson, and Hearn (1977).

Acknowledgments — We thank Carolyn Kriet Lyon for her assistance in collecting many of the water samples. The cooperation of many property owners is greatly appreciated. The support of B. Carter Hearn was of much help.

SAMPLE COLLECTION

Water samples of springs were collected as close to the main orifice of each spring as possible. Well waters were collected by pumping or discharging water from the well, if possible, or by dropping a weighted bottle attached to a long line. Water samples of streams and lakes were collected at convenient points (docks, piers, and so on). All samples must be considered "grab" samples. No integrated samples from Clear Lake or any major stream or creek were obtained.

Samples were treated in the field as described either by Thompson (1975) or by Thompson, Presser, Barnes, and Bird (1975). The primary difference between the two methods is the method of filtering the samples. The procedure described by Thompson (1975) uses a 50-mL plastic syringe and swennex syringe filter for water filtration; the other procedure (Thompson and others, 1975) uses a large 800-mL plastic filter assembly with an automobile tire pump to force water through the filter. All filtered samples were passed through 0.45-μm membrane filters (Gelman GA-6 metricel). All filtered-acidified (F.A.) samples were acidified with concentrated (12*N*) hydrochloric acid (1 mL of acid per 250-mL sample). A separate sample was collected for silica by pipetting 10 mL of unfiltered sample into about 50 mL of deionized, distilled water in the field and later diluting to a known volume (100 mL) in the laboratory immediately before analysis.

FIELD ANALYSIS

Temperature measurements of springs and wells were made with either a total-immersion maximum-reading mercury-in-glass thermometer or with a conventional mercury-in-glass thermometer. Springs having temperatures near that of ambient air temperature required the use of the latter thermometer. Field determinations were usually made for pH either with a pH electrode or pH strips (colorpHast, EM Laboratories, Inc.), depending upon accessibility of the spring or stream location. A few alkalinity titrations using a pH electrode and standardized sulfuric acid were performed in the field

TABLE 17.—*Chemical analyses of thermal water samples from Clear Lake volcanic field*

[All analyses in milligrams per liter unless otherwise noted. J. M. Thompson, analyst]

Date	Ref. no.	Sample number	Location	Latitude	Longitude	Flow L/min	Temp. °C	Field pH	Lab. pH
--	1	CLW 1	Spring near Bonanza Springs	38°51.9'	122°41.2'	4	--	--	7.38
3 Aug 74	2	2	Spring near Bonanza Springs	51.9'	41.6'	20	18	--	8.45
7 Aug 74	3	3	Howard Spring water supply	51.4'	42.4'	400	15	--	7.35
--	4	4	Well near Seigler Springs	52.8'	41.1'	--	--	--	8.70
5 Dec 74	5	5	Spring off Harrington Flat Road	51.3'	44.2'	4	13	--	7.85
5 Dec 74	6	LJ-74-3	Open well near Seigler Springs	52.9'	41.1'	8	31	6.4	7.40
5 Dec 74	7	CLW 7	Spring at Salminas Resort	52.7'	43.6'	4	16	--	7.20
5 Dec 74	8	LJ-74-2	Spring in pumphouse at Salminas	52.7'	43.6'	Seep	13	6.6	7.10
5 Dec 74	9	1	Cobb Village Water Supply	49.2'	43.1'	320	12	7.5	7.80
5 Dec 74	10	CLW 10	Small spring near Seigler Springs	52.8'	44.0'	4	21	--	6.60
5 Dec 74	11	11	Small spring near Seigler Springs	52.9'	41.1'	160	31	--	6.40
5 Dec 74	12	12	Small cold spring near Seigler Springs	52.4'	42.2'	4	16	7.4	7.40
5 Dec 74	13	13	Seep below andesite of Perini Hill	52.4'	40.9'	8	13	7.6	7.40
5 Dec 74	14	LJ-74-4	Spring on road near Perini Hill	52.7'	41.1'	16	20	7.5	8.13
6 Dec 74	15	5	Horsehoe Spring	59.6'	44.5'	80	41.5	6.6	7.58
6 Dec 74	16	CLW 16	Artesian Well, Konocti Harbor Inn	59.4'	44.3'	--	25	6.8	7.79
6 Dec 74	17	LJ-74-6	Spring, south side Konocti Harbor Inn	59.2'	44.0'	80	35	6.7	7.94
6 Dec 74	18	CLW 18	Spring, south side Konocti Harbor Inn	59.2'	44.0'	4	35	7	7.22
6 Dec 74	19	19	Cold Spring on Wildcat Road at Bridge	54.0'	45.6'	240	18	7.2	7.72
6 Dec 74	20	LJ-74-7	Kip Neasham's Well	56.6'	43.8'	40	11	6.8	6.95
18 Feb 75	21	LJ-75-1	Highland Springs Area	56.1'	54.6'	Seep	15	6.7	6.43
18 Feb 75	22	2	Clear Lake State Park, Drinking Water	39°01.0'	48.4'	--	8.0	7.1	7.54
18 Feb 75	23	3	Little Borax Lake	00.1'	45.2'	--	9.4	9	9.75
19 Feb 75	24	CLW 24	Perini Spring	38°53.0'	38.6'	400	17	6.5	7.06
19 Feb 75	25	25	Bardole Spring	52.3'	38.1'	120	17	6	6.97
19 Feb 75	26	26	Carbonate Pool in Seigler Canyon	52.5'	41.8'	Seep	15	6	6.23
19 Feb 75	27	27	Spring N.W. of Seigler Canyon	53.2'	40.8'	200	15	6	7.06
19 Feb 75	28	28	Thurston Lake	55.7'	40.7'	--	14	--	7.75
19 Feb 75	29	29	Well, Konocti Conservation Camp	54.5'	43.4'	--	25	6	7.24
19 Feb 75	30	30	Spring, Flores Ranch	54.3'	38.6'	20	17	6	6.95
19 Feb 75	31	31	Spring, Diener Ranch	54.0'	42.8'	20	13	6	7.20
19 Feb 75	32	LJ-75-4	Spring, east side Borax Lake	59.2'	40.6'	Seep	15	5.3	5.76
19 Feb 75	33	5	Borax Lake, east side	59.1'	40.8'	--	--	9.3	9.74
19 Feb 75	34	6	Spring on east side of Baylis Point	56.3'	41.6'	4	16.5	7.3	7.18
19 Feb 75	35	7	Well at Riviera (line & bottle)	57.7'	43.0'	--	29.5	6.7	6.38
20 Feb 75	36	8	Beeman Residence, well	58.6'	50.3'	--	13	6	9.34
20 Feb 75	37	9	Bradley Well, N. Shaul Valley	57.2'	48.1'	--	13	6	6.66
20 Feb 75	38	10	Ford Ranch Spring, S. Shaul Valley	56.2'	47.3'	2	16	6	5.86

TABLE 17.—*Chemical analyses of thermal water samples from Clear Lake volcanic field*—Continued

Ref. no.	SiO_2	Ca	Mg	Na	K	Li	HCO_3	SO_4	Cl	F	B	Fe	Mn	Cd	Cu	Zn
1	96	2.9	1.6	5.5	6.0	<0.01	128	4.	4.	--	--	--	--	--	--	--
2	57	2.8	73.	3.5	2.4	<.01	281	48.	4.3	--	--	--	--	--	--	--
3	46	5.4	2.3	4.3	1.4	<.01	125	<.5	2.4	--	--	--	--	--	--	--
4	47	9.9	18.4	5.8	7.5	.13	274	.5	32.	0.22	1.8	--	--	--	--	--
5	48	10.9	7.2	6.5	1.5	<.01	114	1.	3.0	<.1	<.1	0.15	<0.02	--	--	--
6	106	10.3	18.5	13.5	6.5	.12	204	1.	24.	.15	1.6	1.45	.12	--	--	--
7	52	6.2	3.2	6.1	3.7	<.01	67	2.	3.4	.1	<.1	<.02	<.02	--	--	--
8	63	4.7	3.0	6.5	7.9	.02	54	2.	5.0	<.1	<.1	.38	<.02	--	--	--
9	40	6.1	1.8	4.5	2.0	<.01	30	2.	2.0	<.1	<.1	<.02	<.02	--	--	--
10	102	13.8	20.	40.	7.2	.15	225	2.	32.	.12	2.5	2.05	.12	--	--	--
11	106	10.7	20.	35.5	7.1	.13	208	1.	24.	.12	2.0	1.63	.12	--	--	--
12	57	5.4	2.9	7.0	2.6	<.01	76	.5	3.	<.10	<.1	<.02	<.02	--	--	--
13	56	8.7	6.6	6.8	2.5	<.01	96	.5	4.	<.10	<.1	.06	.02	--	--	--
14	74	13.	9.0	7.7	4.1	.01	114	1.3	4.	.10	<.1	<.02	<.02	--	--	--
15	163	155.	144.	125.	21.5	.51	1310	1.0	78.	.37	19.	4.50	.21	--	--	--
16	146	122.	105.	108.	18.	.42	1120	1.0	66.	.29	17.	.12	.24	--	--	--
17	137	100.	82.	84.	13.2	.33	775	<.5	48.	.50	9.	4.51	.23	--	--	--
18	139	105.	85.	87.	13.4	.32	700	1.0	50.	.39	16.5	5.65	.31	--	--	--
19	81	8.6	8.7	8.5	3.0	.05	68	8.	3.3	<.10	<.1	<.02	<.02	--	--	--
20	138	3.6	3.4	11.7	8.5	.02	80	1.0	4.	.24	<.1	1.38	.22	--	--	--
21	87	320.	142.	102.	4.5	.12	2050	1.	8.7	.37	2.1	--	--	--	--	--
22	55	41.	75.	25.5	3.7	.01	612	1.	9.8	<.10	.6	3.10	.77	--	--	--
23	58	1.5	35.	580.	172.	.24	--	7.	130.	.20	58.	<.02	<.02			
24	61	5.5	5.3	7.8	2.9	<.01	69	1.	6.2	<.01	<.1	--	--	--	--	--
25	56	5.5	5.2	7.2	2.6	<.01	60	1.	4.0	<.10	1.0	--	--	--	--	--
26	98	48.	171.	128.	10.8	.36	990	.5	277.	.14	22.	--	--	--	--	--
27	40	2.1	3.5	4.3	1.6	<.01	52	.5	3.7	<.10	<.1	--	--	--	--	--
28	34	3.3	3.8	9.5	4.7	.01	60	1.5	13.	.10	<.1	--	--	--	--	--
29	103	7.0	11.	17.5	4.8	.03	172	--	10.	.18	--	--	--	--	--	--
30	75	75.	4.0	5.5	10.	<.01	77	--	4.8	.12	.2	--	--	--	--	--
31	64	3.2	4.2	9.0	4.3	<.01	67	--	4.8	.11	.2	--	--	--	--	--
32	24	5.0	6.3	5.1	2.4	<.01	86	1.	3.1	<.10	<.1	2.10	.16	--	--	--
33	18	7.0	49.	1900.	195.	.77	4430	36.	3510.	.39	156.	<.02	<.02			
34	49	3.5	6.8	7.8	3.9	.02	69	5.	10.7	.1	<.1	--	<.02	--	--	--
35	120	42.	42.	43.	6.9	.13	447	.5	42.	.22	9.0	8.3	.84	--	--	--
36	64	4.5	15.	26.5	4.8	.66	146	4.	24.	<.10	.7	.02	<.02	--	--	--
37	36	2.1	3.1	6.	3.9	<.01	52	1.	7.8	<.10	<.1	.17	<.02	--	--	--
38	72	4.0	4.8	11.0	6.4	<.01	86	4.0	7.8	<.10	<.1	.15	<.02	--	--	--

TABLE 17.—*Chemical analyses of thermal water samples from Clear Lake volcanic field*—Continued

Date	Ref. no.	Sample number	Location	Latitude	Longitude	Flow L/min	Temp. °C	Field pH	Lab. pH
20 Feb 75	39	LJ-75-11	Well, Honeycutt Ranch (line & bottle)	38°56.4'	122°45.7'	--	23	--	6.48
20 Feb 75	40	12	Well, Kip Neasham (line & bottle)	59.5'	43.7'	--	11	6	7.02
20 Feb 75	41	13	Well, Winter Ranch	55.4'	41.8'	--	7	6	6.32
20 Feb 75	42	14	Gordon Warm Springs	50.1'	43.6'	10	36	7	7.56
12 Jun 75	43	CLW 43	Alder Creek Spring	49.0'	46.1'	240	9.7	6	7.10
15 Jun 75	44	44	Gunning Creek Spring	47.8'	44.2'	120	11.1	6	7.60
22 Jun 75	45	45	Rush Creek Spring	52.8'	44.2'	70	13.3	6	7.90
19 Jun 76	46	46	Ida Clayton Spring	41.9'	38.0'	160	12.5	6	7.31
23 Jun 76	47	LC-76-1	Little Pinnacle Spring	39°09.5'	46.4'	1	11	6	7.98
23 Jun 76	48	2	Upper Bartlett	11.0'	42.0'	6	16	6.5	7.36
23 Jun 76	49	3	Main Bartlett	11.1'	42.1'	8	18.5	7	7.48
23 Jun 76	50	4	Upper Crabtree	17.4'	49.3'	0	36	5.8	6.10
23 Jun 76	51	5	Main Crabtree	17.5'	49.4'	8	41	7.3	7.80
23 Jun 76	52	6	Rice Fork Eel River	17.3'	49.1'	100	25	7	7.97
24 Jun 76	53	7	Gas Spring	11.3'	41.3'	.8	12	5.3	6.61
24 Jun 76	54	8	Newman Spring	11.9'	43.0'	18	34.5	7	7.50
24 Jun 76	55	9	Pseudo Complexion Spring	11.9'	30.3'	4	27	7	8.60
24 Jun 76	56	10	Complexion Spring	10.2'	31.2'	.5	19	12	11.79
24 Jun 76	57	11	Wilbur Springs	02.8'	25.3'	80	50	7.9	8.00
24 Jun 76	58	12	Clear Lake at Clear Lake Highlands	38°56.9'	32.3'	--	24	5.7	7.80
25 Jun 76	59	13	Grizzly Spring	39°00.1'	29.9'	4	20	6.8	7.84
25 Jun 76	60	14	Sulphur Spring	05.8'	31.4'	2	20	6.3	8.07
26 Jun 76	61	CLW 61	Turkey Run Mine	01.0'	26.4'	40	22	7.2	7.62
26 Jun 76	62	62	Jones' Fountain of Life Spring	02.0'	26.7'	60	61	7.5	8.75
26 Jun 76	63	63	Toby's Cold Well (line & bottle)	02.1'	25.6'	--	24.5	7.0	8.46
26 Jun 76	64	64	Hayfield Well (line & bottle)	01.1'	24.2'	--	14.5	6.5	8.47
26 Jun 76	65	65	Blanck's Spring	01.4'	26.0'	20	44.5	7.5	8.39
26 Jun 76	66	66	Eagle Rock Spring	04.1'	26.4'	16	15.5	7.0	8.54
26 Jun 76	67	LC-76-15	Chalk Mountain Spring	04.8'	35.0'	.4	24	6.6	7.58
26 Jun 76	68	16	Cross Spring	02.5'	35.4'	80	18	5.7	7.71
26 Jun 76	69	17	Unnamed Cold Spring	03.2'	35.3'	140	19	5.9	7.84
26 Jun 76	70	18	Quigley Soda Spring	03.2'	35.8'	4	28	7.6	7.72
27 Jun 76	71	19	Herman Pit, Sulfur Bank Mine	00.1'	39.8'	--	21	3.5	2.39
27 Jun 76	72	20	Green Pool, Sulfur Bank Mine	00.2'	39.4'	--	26	5.4	6.27
29 Jun 76	73	CLW 73	Pine Cone Spring	38°51.0'	41.6'	4	25.5	6.5	8.88
29 Jun 76	74	74	Spier's Spring	50.2'	39.2'	8	25.5	6.5	8.60
29 Jun 76	75	75	Bad Creek Spring	51.0'	40.0'	1	27	6.5	8.64
27 Jun 76	76	LC-76-21	Aetna Springs Well #1	39.0'	09.0'	24	34	5.7	8.57

TABLE 17.—*Chemical analyses of thermal water samples from Clear Lake volcanic field*—Continued

Ref. no.	SiO_2	Ca	Mg	Na	K	Li	HCO_3	SO_4	Cl	F	B	Fe	Mn	Cd	Cu	Zn
39	81	6.5	7.0	11.8	8.3	<0.01	43	22.	4.8	< 0.10	<0.1	0.02	<0.02	--	--	--
40	47	3.5	3.6	10.5	3.9	<.01	60	1.	2.8	<.10	<.1	4.0	<.01	--	--	--
41	64	1.0	.5	10.0	6.3	<.01	95	.5	5.7	.11	<.1	1.1	.31	--	--	--
42	126	5.5	21.	54.	5.0	.15	275	.5	41.	<.10	1.3	.04	.03	--	--	--
43	26	1.7	.72	3.	1.5	<.01	15	1.	3.4	<.10	.12	--	--	--	--	--
44	39	4.7	2.1	4.5	1.9	<.01	40	1.	5.1	<.10	.25	--	--	--	--	--
45	43	6.9	5.7	5.	1.4	<.01	57	<.5	2.5	<.1	.16	--	--	--	--	--
46	37	2.1	.5	5.	2.5	<.01	29	1.	7.0	<.1	<.1	--	--	--	--	--
47	28	25.	10.8	5.	1.2	<.01	146	1.*	4.2	.15	<.1	2.	--	--	--	--
48	94	70.	410.	12.	1.4	.02	2420	1.*	8.4	.32	<.1	2.62	.25	<.01	<.01	.04
49	--	89.	470.	14.	1.4	.02	2750	9.	8.4	.39	<.1	.05	<.02	<.01	<.01	.01
50	52	70.	43.	18.	5.2	.015	104	285.	9.8	.34	.10	4.3	1.4	.01	<.01	.08
51	158	51.	198.	1850.	36.5	4.08	3850	1.*	1240.	.34	277.	.31	.06	<.01	<.01	.02
52	27	32.	9.8	10.	1.4	<.01	164	8.*	9.1	2.3	.33	--	--	--	--	--
53	34	65.	32.	17.	1.3	.01	167	120	4.0	.18	.1	.83	.60	<.01	<.01	.02
54	134	162.	520.	2500.	56.5	20.	4290	2.*	3310.	.18	386.	2.31	.12	--	--	--
55	44	5.4	152.	45.	1.8	0.01	786	1.*	115.	<.1	<.1	<.02	<.02	.01	<.01	.01
[1]56	32	.55	.30	13200.	460.	<0.01	384	27.	24100.	.34	31.	.50	.04	--	--	--
57	131	2.5	44.	9200.	445.	8.00	7040	390.	9810.	1.9	280.	.16	.02	.02	.03	.01
58	6	24.	16.	22.	3.	.02	232	1.*	30.	.15	1.55	<.02	<.02	<.01	<.01	.04
59	101	10.	132.	465.	11.9	.70	1225	21	310.	.34	325.	.04	.05	.01	<.01	.01
60	146	23.	12.9	322.	9.2	.28	72	26.	331.	.89	18.	<.02	<.02	<.01	<.01	.03
61	70	21.	770.	1064.	34.8	1.68	2300	2400.	1150.	5.2	34.5	.71	.25	.02	<.01	.04
62	84	2.3	30.	10000.	490.	8.40	4100	80.	11900.	3.2	271.	.41	.05	.04	.03	.02
63	23	25.	162.	200.	6.6	.28	972	170.	140.	.34	4.6	.06	.40	<.01	<.01	<.01
64	19	42.	210.	65.	1.6	.04	1060	200.	28.6	.39	.84	.10	.75	<.01	<.01	<.01
65	113	2.2	70.	7600.	409.	6.48	6800	215.	8050.	2.1	158.	.18	.02	.02	.02	.02
66	78	3.1	172.	222.	17.8	.78	1100	1.	262.	.18	11.0	<.02	<.02	<.01	<.01	.01
67	91	66.	495.	1600.	196.	5.20	3300	32.	2410.	.47	190.	.14	.05	<.01	.01	.01
68	60	17.	12.1	17.	3.8	.02	190	1.*	13.	.18	.1	.10	<.02	<.01	<.01	.01
69	60	16.4	11.2	15.	3.6	<.01	88	1.*	22.	.16	<.1	<.02	<.02	<.01	<.01	<.01
70	89	148.	92.	1040.	162.	4.8	2260	1.*	918.	.32	122.	.10	.22	.01	<.01	.08
[2]71	83	210.	195.	880.	21.6	3.7		4430.	205.	<.10	395.	86.	19.	.015	.08	1.70
72	29	22.	13.8	19.	6.5	.015	173	124.	7.	<.10	.3	.15	.60	<.01	<.01	.10
73	120	28.	210.	580.	13.5	.60	2500	1.*	146.	.32	21.5	.71	.80	<.01	<.01	.04
74	102	24.	290.	295.	16.	.89	1760	1.*	343.	.26	51.2	1.21	.20	<.01	<.01	.02
75	104	37.	450.	52.	3.5	.01	2380	18.	68.	.30	39.	.06	.25	<.01	<.01	.02
76	32	10.	9.8	207.	3.6	.06	610	8.	63.	1.12	2.88	.09	.03	<.01	<.01	.02

[1] No. 56 contained 384 ppm CO_3.

[2] No. 71 contained 19.6 meq/L H^+.

* SO_4 determined by $BaSO_4$ turbidity.

TABLE 17.—*Chemical analyses of thermal water samples from Clear Lake volcanic field*—Continued

Date	Ref. no.	Sample number	Location	Latitude	Longitude	Flow L/min	Temp. °C	Field pH	Lab. pH
27 Jun 76	77	LC-76-22	Aetna Springs Well #2	38°39.0'	122°09.0'	--	33	6.4	7.78
13 Jul 76	78	CLW 78	Magnola Mine Well	43.0'	82.5'	6	19	7.0	8.10
29 Jul 76	79	79	Moki Beach Spring	39°01.0'	48.1'	80	27	6.0	6.87
29 Jul 76	80	80	Hog Hollow Spring	01.4'	35.3'	40	30	5.8	7.26
3 Aug 76	81	81	Unnamed Soda Spring in Cache Formation	38°57.0'	34.3'	8	22	6.8	7.72
4 Aug 76	82	82	Reid's Well	58.2'	38.5'	--	25	5.9	7.23
4 Aug 76	83	83	Kono Tayee Well	39°02.4'	45.7'	--	21.5	5.9	7.97
9 Aug 76	84	84	Old Howard (or Howard Soda) Spring	38°51.4'	40.8'	20	28.5	6.2	7.42
9 Aug 76	85	85	Holm's Warm Well (line & bottle)	58.6'	40.5'	--	40	6.2	7.46
10 Aug 76	86	86	Zem-Zem Spring	45.3'	17.1'	2	21	5.5	8.23
30 Aug 76	87	87	Davis' Soda Spring	59.7'	38.5'	.5	23	6.8	7.46
31 Aug 76	88	88	Spring in Sweet Hollow Creek	39°01.1'	35.0'	--	22	6.1	7.47
3 Sep 76	89	89	Salt Lick Spring	06.0'	36.4'	24	22	5.9	7.96
7 Sep 76	90	90	Hildebrande Spring	38°55.5'	46.2'	8	25	5.3	7.29
8 Sep 76	91	91	Anderson Spring	46.5'	42.4'	2	42	5.6	7.45
16 Sep 76	92	92	Well in Benmore Canyon (line & bottle)	39°01.5'	34.2'	--	21	6.8	7.75
22 Sep 76	93	93	Spring N. of Cache Creek; Magnesite Spr.	04.4'	34.0'	20	22	--	7.52
23 Sep 76	94	94	Garner Sulfur Spring	04.7'	41.9'	0.5	22	6.7	8.00
23 Sep 76	95	95	Garner's Salt Lick	04.6'	42.2'	1	23	7.0	8.01
23 Sep 76	96	96	Garner Cold Spring	05.0'	41.8'	30	16	6.2	7.74
25 Sep 76	97	97	Capped Geyser, Calistoga Hot Spring	38°36.0'	36.0'	80	100	8.4	8.93
30 Sep 76	98	98	Hiway 20 Sulfur Spring	39°01.0'	29.4'	12	23	6.7	7.57
30 Sep 76	99	99	Elgin Mine	03.5'	28.5'	20	54	7.6	7.93
30 Sep 76	100	100	Hough Spring	09.7'	36.8'	1	16	6.0	7.37
1 Oct 76	101	101	Allen Springs, Chalybeate Spring	09.6'	39.9'	20	18	6.1	7.61
1 Oct 76	102	102	Royal Spring	13.8'	44.7'	8	18	5.9	7.80
19 Oct 76	103	103	Riviera Beach Spring	38°57.5'	42.2'	8	34	--	7.55
18 Feb 77	104	104	Little Geysers Hot Spring	46.0'	44.9'	2	99	5.5	6.71
18 Feb 77	105	105	Honeycutt #2 (line & bottle)	56.4'	43.8'	--	49	5.7	6.96
18 Feb 77	106	106	Bennett's Well	56.5'	46.1'	--	46	5.4	6.89
18 Feb 77	107	107	Rouse's Well	56.5'	46.4'	--	43	6.2	7.17
18 Feb 77	108	108	Fitt's Spring	39°00.0'	40.2'	--	16	6.1	8.09
18 Feb 77	109	109	Sulphur Bank Carbonated well	00.0'	40.3'	--	17	5.7	6.77
5 Feb 77	110	LJ-77-1	Siegler Spring, Lithia	38°52.5'	41.5'	4	25	5.9	7.76
5 Feb 77	111	2	Siegler Spring, Hot Sulfur	52.5'	41.5'	88	53.3	6.5	7.77
5 Feb 77	112	3	Siegler Spring, Iron	52.5'	41.5'	24	40.3	5.9	7.41
5 Feb 77	113	4	Siegler Spring, The Geyser	52.5'	41.5'	--	43	5.9	7.28

TABLE 17.—*Chemical analyses of thermal water samples from Clear Lake volcanic field*—Continued

Ref. no.	SiO_2	Ca	Mg	Na	K	Li	HCO_3	SO_4	Cl	F	B	Fe	Mn	Cd	Cu	Zn
77	87	18.4	91.	705.	12.	0.38	2000	1.*	287.	1.5	80.6	0.21	0.12	<0.01	<0.01	<0.01
78	88	22.	33.	40.	2.	.02	324	1.*	9.4	.15	34.2	.18	.20	<.01	<.01	.04
79	129.	79.	104.	90.	13.	.41	936	1.*	58.6	.11	13.5	19.	.40	<.01	<.01	.10
80	136	106.	46.	200.	15.2	.48	862	4.	174.	.33	14.5	4.00	.26	<.01	<.01	<.01
81	98	58.	93.	130.	70.	.24	966	1.*	27.	.21	34.5	.25	.04	<.01	<.01	<.01
82	93	163.	61.	117.	6.6	.13	884	4.	136.	.32	115.	19.	.42	<.01	<.01	.015
83	55	66.	28.	24.	1.6	.01	306	31.	7.3	.21	5.3	21.	.43	<.01	<.01	.05
84	129	52.	320.	166.	20.	.94	1990	2.	187.	.26	125.	1.4	.23	<.01	<.01	<.01
85	124	175	130.	110.	14.8	.50	1440	8.	74.	.21	152.	6.4	.15	<.01	<.01	.08
86	25	34.	25.	252.	2.0	.01	564	4.	157.	.68	8.9	.04	<.02	<.01	<.01	.01
87	86	210.	51.	30.	3.5	.05	644	38.	4.	.16	<.1	6.90	2.43	<.01	<.01	.015
88	96	155.	78.	580.	47.5	1.8	1170	175.	561.	.10	49.	1.5	.40	<.01	<.01	.015
89	100	108.	390.	367.	12.3	.67	2280	4.	419.	.16	48.	3.0	.10	<.01	<.01	.02
90	91	5.0	4.0	12.	6.	.02	76	2.	8.	.11	<.1	.03	.17	<.01	<.01	.03
91	89	120	40.	50.	11.	.17	223	635.	4.	.18	<.1	.65	4.83	<.01	<.01	.01
92	28	100.	360.	2860.	54.	3.4	3050	400	4050.	.71	72.3	4.35	.21	.03	<.01	.01
93	89	183.	735.	950.	47.	3.1	2890	265	1920.	.11	130.	1.3	.20	<.01	<.01	.01
94	23	70.	17.	64.	2.5	.04	420	36.	9.	.37	.42	<.04	.19	<.01	<.01	<.01
95	22	30.	11.	750.	8.0	.30	1610	9.	242.	3.1	225.	<.04	.04	<.01	<.01	<.01
96	29	55.	12.	15.	1.2	.01	228	38.	5.	.55	.1	--	--	--	--	--
97	150	25.	--	193.	8.7	1.90	184	13.	206.	.01	12.	<.04	<.02	<.01	<.01	.01
98	24	3.5	5.0	1550.	34.	.53	498	7.	2080.	6.7	41.5	.15	.05	.01	<.01	.02
99	152	3.6	26.	9950.	580.	12.5	7300	105.	12100.	3.4	220.	.3	1.88	.04	.02	.03
100	75	385.	43.	98.	7.3	.60	831	3.	5.	.9	.27	7.6	.43	<.01	.01	.06
101	100	130.	360.	292.	8.6	2.37	2000	12.	481.	<.1	41.	14.9	.13	<.01	.01	.03
102	94	58.	430.	332.	5.6	.23	2780	3.	300.	.18	28.	5.5	.20	<.01	<.01	.02
103	139	100.	83.	90.	11.	.24	923	38.	31.	.20	13.	6.0	.20	<.01	<.01	.02
104	57	1.3	5.0	20.	.5	<.01	11	97.	3.	<.1	.1	.4	.2	<.01	.01	.04
105	183	20.	19.	115.	29.5	.80	394	41.	101.	.16	16.3	16.7	.5	<.01	<.01	.02
106	183	25.	24.	120.	30.	.77	435	50.	96.	.18	18.	1.8	.84	<.01	<.01	.02
107	136	25.	33.	74.	17.6	.43	401	5.	62.	.25	8.	.5	.50	<.01	<.01	.01
108	25	80.	35.	--	--	--		22.	12.	<.10	<.10	--	--	--	--	--
109	45	80.	91.	50.	3.0	.03	862	10.	19.	.18	.5	--	.92	<.01	.02	1.00
110	125	20.	152.	40.	4.5	.05	941	2.	29.	<.10	2.3	2.10	.08	.01	.03	.02
111	174	35.	230.	175.	21.	.88	1340	1.	289.	<.10	20.	.15	.03	.01	.03	.02
112	151	25.	139.	203.	38.	1.30	982	1.	254.	.11	12.	1.0	.10	<.01	.03	.02
113	159	20.	128.	215.	35.	1.56	831	2.	294	.25	15.	.8	.1	<.01	.02	.02

*SO_4 determined by $BaSO_4$ turbidity.

during the December 1974 and February 1975 collections. Unfortunately, no field analyses for ammonia, hydrogen sulfide, or mercury were obtained. A discharge estimate was made if possible.

LABORATORY ANALYSIS

Silica was determined by a modification of the reduced molybdenum blue method. The procedure used is reported in the Shapiro and Brannock silica procedure (1956). On selected samples silica analyses were performed on those diluted in the field and on nondiluted filtered-acidified (F.A.) samples. The analytical results for the two different methods of preserving silica were within 5 percent for the same sample, although the F.A. samples tended to yield a higher silica value. All water samples from the Geysers-Clear Lake area have silica concentrations less than 250 mg/L (table 17). It is not suggested that field acidification be used on water samples containing higher silica concentrations, owing to problems with silica polymerization. Boron was determined by the carmine procedure as described by Brown, Scougstad, and Fishman (1970). Selected samples were analyzed on a Spectrospan 3 plasma-emission analyzer. The accuracy of the carmine method is within 10 percent of the averaged value.

Sodium, potassium, and lithium determinations were made on either a filtered untreated (F.U.) or, preferably, an F.A. sample. Lithium ion was added to the sample aliquot for sodium and potassium determinations (1,000 mg/L at the concentration analyzed), and sodium ion was added to the lithium sample aliquot (same as above). Calcium and magnesium were determined only on F.A. samples, a very important fact owing to the relatively high concentration of calcium found in many springs of this area. A lanthanum(III) ionization buffer, prepared as described by Brown, Scougstad, and Fishman (1970), was added to each sample aliquot before analysis. Later in the study, iron manganese, cadmium, copper, and zinc were determined by atomic absorption spectrometry. As the samples were only filtered through a 0.45-μm filter, the results must be interpreted carefully.

Major anions were determined only from the raw unacidified (R.U.) samples or, preferably, from the filtered unacidified (F.U.) sample. Alkalinity was determined in the laboratory on all samples. In samples with low HCO_3^- field values (<60 mg/L), the laboratory-determined HCO_3^- content was usually twice that determined in the field. Thus, it is imperative that a field determination for alkalinity be performed if the HCO_3^- content is low (<100 mg/L). For concentrations above 100 mg/L HCO_3^- no significant differences between the field and laboratory values were observed. Water that is cold, dilute, and not buffered can dissolve CO_2 and can react to form HCO_3^- in solution. Thus, waters near the mean annual temperature are likely to have HCO_3^- contents below 60 mg/L and should have alkalinity determined in the field.

Sulfate was determined by the thorin procedure, described by Brown, Scougstad, and Fishman (1970), on all samples above 70 mg/L. The $BaSO_4$ turbidity method (American Public Health Association, 1971) was used for screening, and low values (<10 mg/L) are reported for some samples (table 17). Chloride ion was determined by potentiometric titration using an Ag/AgCl indicating electrode, an Orion double-junction reference electrode, and standardized silver nitrate solution. The conditions are specific for chloride at the pH of the sample aliquot. Flouride was determined electrochemically by a fluoride-specific electrode. All samples and standards were adjusted to an ionic strength of 0.5 and buffered at pH 8 by adding equal volumes of ionic-strength buffer solution and sample or standard. The buffer is described in Thompson, Presser, Barnes, and Bird (1975).

The majority of thermal spring waters in this region may be described as magnesium-calcium bicarbonate. Some water samples, predominantly in the eastern section, are sodium chloride/bicarbonate springs. High concentrations of boron are found in all the thermal waters, with the highest concentrations being found in waters to the east of the Clear Lake volcanic field. The results of the analyses are presented in table 17.

REFERENCES CITED

Allen, E. T., and Day, A. L., 1927, Steam wells and other thermal activity at "The Geysers" California: Carnegie Institution of Washington Publication 378, 106 p.

American Public Health Association, 1971, Standard methods for the examination of water and wastewater [13th ed.]: Washington, D.C., p. 334-335.

Anderson, Winslow, 1892, Mineral springs and health resorts of California: San Francisco, Bancroft, 384 p.

Barnes, Ivan, O'Neil, J. R., Rapp, J. B., and White, D. E., 1973, Silica-carbonate alteration of serpentine: Wall rock alteration in mercury deposits of the California Coast Ranges: Economic Geology, v. 68, p. 388-398.

Barnes, Ivan, Rapp, J. B., O'Neil, J. R., Sheppard, R. A., and Gude, A. V., 1972, Metamorphic fluid in four instances of serpentinization: Contributions to Mineralogy and Petrology, v. 35, p. 263-276.

Berkstresser, C. F., Jr., 1968, Data for springs in the Northern Coast Ranges and Klamath Mountains of California: U.S. Geological Survey open-file report, 49, p.

Brown, Eugene, Skougstad, M. W., and Fishman, M. J., 1970, Methods for collection and analysis of water samples for dissolved minerals and gases: U.S. Geological Survey Techniques of Water Resources Investigations, Book 5, chap. Al, 169 p.

Goff, F. E., Donnelly, J. M., Thompson, J. M., and Hearn, B. C., 1977, Geothermal prospecting in the Geysers-Clear Lake area, northern California: Geology, v. 5, p. 509-515.

Shapiro, Leonard, and Brannock, W. W., 1956, Rapid analysis of silicate rocks: U.S. Geological Survey Bulletin 1036-C, p. 19-56.

Thompson, J. M., 1975, Selecting and collecting thermal springs for chemical analysis: A method for field personnel: U.S. Geological Survey Open-File Report 75-68, 11 p.

Thompson, J. M., Presser, T. S., Barnes, R. B., and Bird, D. B., 1975, Chemical analysis of the waters of Yellowstone National Park, Wyoming from 1965-1973: U.S. Geological Survey Open-File Report 75-25, 59 p.

Vollintine, Larry, ed., 1975, Environmental study of prospective geothermal development in Big Canyon Creek watershed, Lake County, California: Berkeley, University of California Press, 722 p.

Waring, G. A., 1915, Springs of California: U.S. Geological Survey Water-Supply Paper 338, 410 p.

White, D. E., Barnes, Ivan, and O'Neil, J. R., 1973, Thermal and mineral waters of nonmeteoric origin, California Coast Ranges: Geological Society of America Bulletin, v. 84, no. 2, p. 547-559.

White, D. E., Brannock, W. W., and Murata, K. J., 1956, Silica in hot-spring waters: Geochimica et Cosmochimica Acta, v. 10, p. 27-59.

White, D. E., Hem, J. P., and Waring, G. A., 1963, Chemical composition of subsurface water, chap. F *of* Fleischer, Michael, ed., Data of geochemistry (6th ed.): U.S. Geological Survey Professional Paper 440-F, p. 67.

White, D. E., and Roberson, E. E., 1962 Sulphur Bank, California, a major hot-spring quicksilver deposit, *in* Petrologic studies: A volume in honor of A. F. Buddington: New York, Geological Society of America, p. 397-428.

VARIABILITY AND SOURCES OF HYDROGEN SULFIDE AND OTHER GASES IN STEAM AT THE GEYSERS

By CHARLES A. BROOK

ABSTRACT

Hydrogen sulfide is a common constituent of fluids from vapor-dominated geothermal systems throughout the world. In steam at The Geysers, hydrogen sulfide is the second or third most abundant noncondensable gas (after carbon dioxide and methane). Measured hydrogen sulfide concentrations range from less than 0.001 percent to about 0.1 percent by weight of the total steam discharge from individual wells; concentrations of other gases also range by one or two orders of magnitude. Data from wells in the southern part of the Geysers steam field suggest that gas concentrations in individual steam entries are highly variable, both laterally and vertically. The variability in gas contents is apparently unsystematic and is not related to depth, wallrock temperature, gas-to-steam ratio, or location in the steam field.

Three possible sources of hydrogen sulfide in hydrothermal fluids include (1) magmatic exhalation, (2) water-rock reactions (hydrolysis) and (3) thermal metamorphism. Thermal degradation of organic material, especially plant tissue, is favored as the source of much of the hydrogen sulfide at The Geysers. The fracture system in the Geysers reservoir is complex, and fluid passing through fractures in organic-bearing rocks probably is enriched in noncondensable gases including hydrogen sulfide, carbon dioxide, methane, and ammonia. An initial or primary gas-concentration variability can thus be imparted locally to the fluid. Variations in gas concentrations may be secondarily augmented by mixing or by steam condensation and gas enrichment in cooler parts of the reservoir.

INTRODUCTION

Natural steam from known vapor-dominated geothermal systems (The Geysers, Calif.; Larderello, Italy; Matsukawa, Japan) consists mostly of water vapor with small amounts of noncondensable gases (Mori, 1970; White and others, 1971). Water vapor generally accounts for more than 99 weight percent of the steam at The Geysers; the remaining fraction is mostly carbon dioxide (CO_2) with lesser amounts of hydrogen sulfide (H_2S), methane (CH_4), ammonia (NH_3), hydrogen (H_2), nitrogen (N_2), and other gases (table 18).

Noncondensable gas contents in steam have received attention in recent years because of their potentially hazardous environmental effects (for example, U.S. Department of the Interior, 1973; Schieler, 1976). The presence of H_2S has caused much concern because of its foul odor and its toxicity at relatively low concentrations. At The Geysers, wellhead H_2S concentrations range from 5 to more than 1,000 ppm and average about 220 ppm (table 18). These concentrations are within the range of serious health-hazard effects as outlined by Sax (1975, p. 819-820) and can pose immediate problems to drilling crews when H_2S is encountered and vented during drilling operations. Although the characteristics of H_2S in the surface environment have been established, little attempt has been made to document or characterize H_2S occurrences in the subsurface of geothermal systems.

TABLE 18.—*Composition (in weight percent) of steam wells at The Geysers*

[Converted from values in mg/kg reported by Reed and Campbell (1976, p. 1406) for 61 producing steam wells measured from 1972 through 1974. H_2O is added.]

	Low	High	Average
H_2O	96.59	99.88	99.60
CO_2	.029	3.06	.326
H_2S	.0005	.106	.0222
CH_4	.0013	.1447	.0194
C_2H_6	.0003	.0019	.0008
NH_3	.00094	.106	.0194
H_2	.0011	.0218	.0056
N_2	.0006	.0638	.0052
H_3BO_3	.0012	.0223	.0091

The purpose of this report is to (1) document the lateral and vertical variations in H_2S and other noncondensable gas concentrations in steam at The Geysers, (2) discuss possible sources of the gases, and (3) describe possible processes affecting the varied gas concentrations. The investigation of the noncondensable gases began in an attempt to identify the subsurface conditions under which anomalously high H_2S concentrations occur. Much of the well information presented was abstracted from records of wells on Federal leases in secs. 1 and 3, T. 10 N., R. 8 W. (fig. 101). This area is in the southern, unexploited part of the steam field and offers the opportunity to study the geothermal system in a near-pristine state. As used here, the term "gas" is defined as a vapor-phase component of steam other than H_2O.

Acknowledgments.— I thank the Shell Oil Company for permission to release data from wells in the southern part of The Geysers. Review and comments by Donald R. Lindsay of that company greatly improved

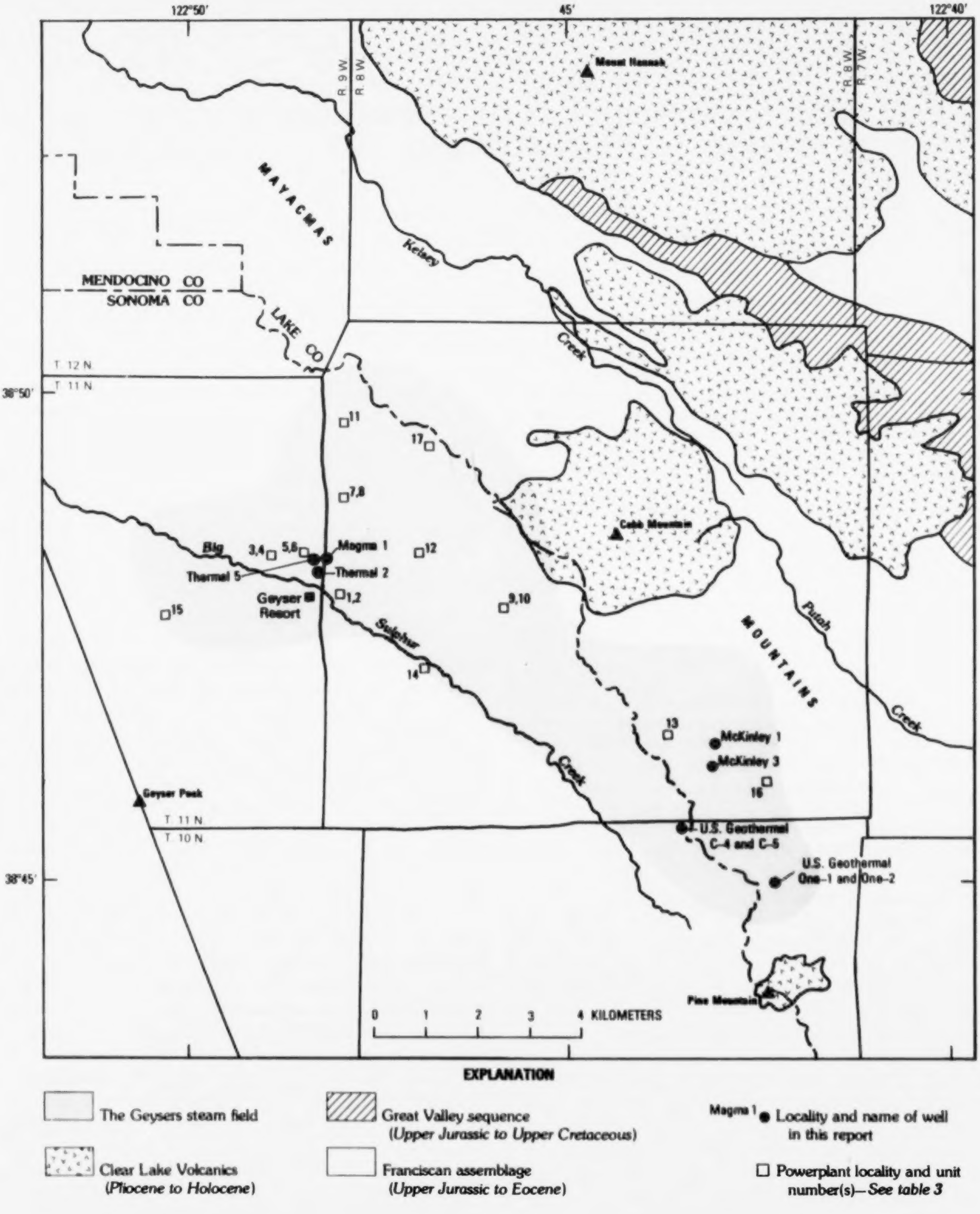
122°50'
45'
122°40'
38°50'
38°45'
R 9 W
R 8 W
R 8 W
R 7 W
T. 12 N.
T. 11 N.
T. 11 N.
T. 10 N.
Mount Hannah
MAYACMAS
MOUNTAINS
Kelsey Creek
MENDOCINO CO
SONOMA CO
LAKE CO
Cobb Mountain
Putah Creek
Big
Sulphur Creek
Magma 1
Thermal 2
Thermal 5
Geyser Resort
3,4
5,6
1,2
7,8
11
12
17
9,10
15
14
13
16
McKinley 1
McKinley 3
U.S. Geothermal C-4 and C-5
U.S. Geothermal One-1 and One-2
Geyser Peak
Pine Mountain
0 1 2 3 4 KILOMETERS
EXPLANATION
The Geysers steam field
Clear Lake Volcanics (Pliocene to Holocene)
Great Valley sequence (Upper Jurassic to Upper Cretaceous)
Franciscan assemblage (Upper Jurassic to Eocene)
Magma 1 ● Locality and name of well in this report
☐ Powerplant locality and unit number(s)—See table 3

FIGURE 101.—Generalized geologic setting of the Geysers steam field, Calif., and locations of selected wells and powerplants.

this report. Discussions with several U.S. Geological Survey colleagues, especially with R. J. McLaughlin. D. E. White, A.H. Truesdell, Ivan Barnes, and M. J. Reed, have contributed to my understanding of The Geysers and of geothermal systems.

EARLIER WORK

Few data on gas concentrations for individual wells at The Geysers are available from the literature. Allen and Day (1927) gave a detailed report on wells drilled during the early 1920's in the area of fumaroles and hot springs near the Geysers Resort (fig. 101). These wells were from 62 m to about 148 m deep. Steam compositions fell within a narrow range, with noncondensable gases making up 1 to 2 percent by volume of the steam. McNitt (1963) reported that noncondensable gases from Magma 1, Thermal 2, and Thermal 5 wells (fig. 101) ranged from 0.68 to 0.83 percent by weight of the steam. These wells were drilled in the 1950's in the same area as the earlier wells and to about the same depths.

MODEL OF STEAM RESERVOIR

As proposed by White, Muffler, and Truesdell (1971), vapor-dominated systems (fig. 102) are believed to develop from hot-water convection systems when a sufficiently potent heat source, or decreasing rate of water recharge, and limited rock permeability cause boiling off of more water than can be replaced by inflow (that is, when net discharge exceeds recharge). Steam boils from a declining water table and flows upward. Most of the steam condenses below the surface and the condensate flows downward to the water table. Some steam and condensate may reach the surface through channels of principal upflow.

Steam and liquid water coexist in the reservoir (White and others, 1971). Steam dominates the largest fractures and is the continuous, pressure-controlling phase; liquid water is relatively immobilized in small pores and fractures. Truesdell and White (1973) concluded that liquid water is the major phase by mass in the reservoir and is held in small pore spaces by surface tension. The liquid water boils as pressure is lowered owing to production; boiling by intergranular vaporization begins adjacent to the well bore and continues with increasing distance away from the bore as the boiling front moves outward with time. At The Geysers, this concept is supported by observed decreases in gravity over the main part of the production field (Isherwood, this volume). Isherwood concluded from mass-balance calculations that the most likely explanation for the observed net mass loss is replacement of hot liquid water by water vapor and removal of the excess fluid. In the unexploited state, vapor-dominated reservoirs are characterized by rather uniform temperatures near 240°C and pressures near 35 kg/cm^2 (White, 1973).

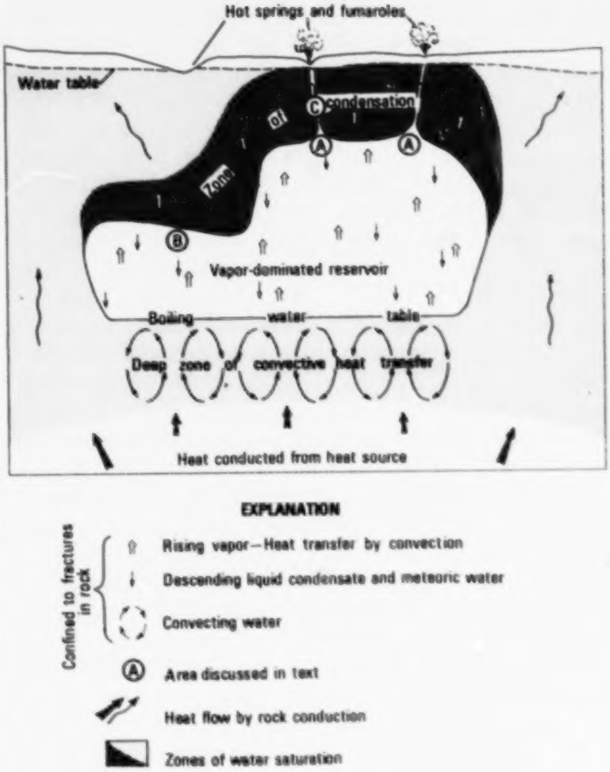
Hot springs and fumaroles
Water table
Zone of condensation
C
A
A
B
Vapor-dominated reservoir
Boiling water table
Deep zone of convective heat transfer
Heat conducted from heat source
EXPLANATION
Confined to fractures in rock
Rising vapor—Heat transfer by convection
Descending liquid condensate and meteoric water
Convecting water
A
Area discussed in text
Heat flow by rock conduction
Zones of water saturation

FIGURE 102.—Conceptual model of fluid movement in a vapor-dominated geothermal system (modified from White and others, 1971). Recharge to vapor-dominated reservoir is supplied by meteoric water from surrounding water-saturated rocks.

The zone of condensation inhibits the free escape of rising vapor. It is believed to be nearly saturated with liquid water derived largely from condensed steam. The zone is probably dominated by downflowing condensate and some surface water, except near major channels of upflowing steam (C, fig. 102). Temperatures in the zone of condensation are probably near the hydrostatic boiling-point curve for pure water (White and others, 1971, p. 86).

Condensation of steam in areas of cooler rock was proposed by White, Muffler, and Truesdell (1971) as a mechanism whereby the noncondensable gas components can be residually concentrated. Areas of condensation would be characterized by increased conductive heat flow and therefore increased temperature gradients. In the reservoir, steam starts to condense near the top and outer margins and continues to condense from all vapor escaping into the zone of condensation. In areas near the reservoir top that are open to the surface (*A*, fig. 102) or that have net upflow of steam which is later condensed in the zone of condensation, any residual gases would be continuously flushed out. Unlike the flushed parts of the reservoir, areas that are poorly flushed and isolated from direct outflow of vapor (*B*, fig. 102) may be enriched in noncondensable gases. These poorly flushed areas would also be expected to have significant thermal gradients. White, Muffler, and Truesdell (1971, p. 93) showed that the lower partial pressure of the remaining water vapor required lower saturation temperatures as steam condenses and gases are residually concentrated. They suggested that temperatures in isolated parts of the reservoir differ little from the main reservoir (about 240°C) until the residual gases are enriched above 5 percent. As residual gas concentrations increase above 5 percent, conductive heat flow and temperature gradients increase, causing more condensation of steam.

In the zone of condensation, temperature gradients in general increase outward and upward; thus, steam is continuously condensing and the rate of mass upflow decreases upward (White and others, 1971, p. 88). Upward increase in steam condensation produces vertical differentiation of gas contents. Upper parts of fractures leading from the reservoir and terminating in the zone of condensation would thus have greatly enriched gas concentrations. Alteration products (mostly clay minerals) and condensed water may clog most of the pore spaces and fractures in the zone of condensation, thus impeding, but in places not prohibiting, the escape of residual gases (White and others, 1971, p.91; James, 1968, p. 715). This process may account for the H_2S odors reported by Yates and Hilpert (1946) in mercury mines in the Geysers area and suggests that some steam-bearing fractures may have a very diffuse subsurface vent area with little or no surface expression.

At The Geysers, the regional structure of the Franciscan assemblage is an important factor controlling the distribution of vapor and liquid water in the steam reservoir. The Franciscan is characterized by imbricate thrust slabs, usually of discrete rock types, dipping at moderate angles to the northeast and southeast. (McLaughlin, this volume). Steam production is mostly from fractures in slabs of otherwise impermeable graywacke, although limited production is also known from fractures in greenstone and melange. Unless interconnected by faults, fracture networks are apparently vertically and laterally isolated by impermeable Franciscan rock types such as serpentinite, shaly melange, sheared greenstone, and metagraywacke (Garrison, 1972; McLaughlin, 1977). Owing to the imbricate structure, geothermal fluids may accumulate at several levels in the reservoir.

VARIABILITY OF GAS CONCENTRATIONS

WELLS IN SOUTHERN PART OF STEAM FIELD

Well records, logs, and cuttings from wells U.S. Geothermal One-1, One-2, C-4, and C-5 (fig. 101) were examined to determine the characteristics of the steam and associated subsurface conditions (lithology, wall-rock temperature) for individual steam entries. (Except for information on these wells reported by Fehlberg (1975) and Hite and Fehlberg (1976), all well records, logs and cuttings are confidential.) The wells are located on two drilling pads (two wells on each pad) about 2 km apart in the southern, unexploited part of the steam field. Steam production is from graywacke of the Franciscan assemblage and occurs both within and below a zone of silicified rock. Commercial steam was first penetrated in well U.S. Geothermal One-1 in mid-1975 (Fehlberg, 1975). Before that year, the nearest producible steam well was about 3 km to the north.

During drilling operations CO_2, H_2S, and hydrocarbon concentrations were monitored continuously at discharge lines using standard gas chromatographic techniques and recorded on lithologic logs by a commercial logging service. Steam entries were also noted on the logs. Gas concentrations for individual steam entries, rather than for total well discharge, could therefore be determined.

Several steam entries were encountered during the drilling of each well. Steam from the different entries had varied flow rates and gas compositions. Carbon dioxide was the dominant gas, followed in order of abundance by CH_4 and H_2S. Small amounts of ethane (C_2H_6) were detected in a few steam entries. All H_2S concentrations were associated with steam entries, but CO_2 and CH_4 concentrations as high as several hundred parts per million were detected in a few wells above the first steam entries. In these instances, CH_4 was associated predominantly with graywacke-argillite assemblages; CO_2 was associated with graywacke and occasionally with greenstone containing abundant calcite veins.

Gas concentrations in individual steam entries for all four wells studied are listed in table 19. The reported gas concentrations are maximum values that represent peak levels at the time of steam entry. Gas concentrations generally declined, sometimes to nearly background levels, and (or) fluctuated widely within a few hours of continued drilling. These declines and fluctuations are probably the result of (1) flushing out of residually concentrated gases and (2) dilution or reactions between the steam and the drilling fluid,

TABLE 19.—*Initial gas concentrations in steam entries encountered during drilling of wells in the southern part of the Geysers steam field*

[ND, not detected]

	Steam entry: True vertical depth of steam entry relative to mean sea level (m)	Maximum gas concentrations (ppm) recorded at steam entry: H_2S	CO_2	CH_4	Flow rate (kg/h)	Estimated wallrock temperature (°C)
1	-139	150	4,200	500	28,600	235
2	-233	200	3,750	490	76,400	240
3	-341	50	3,000	250	20,900	240
4	-347	50	3,000	250	....	240
5	-383	100	1,650	170	6,400	240
6	-506	800	50,000	35,000	5,400	245
7	-513	20	2,800	250	....	245
8	-520 to -536	4	4,000	1,500	Several minor entries	245
9	-530	ND	450	......	92,600	245
10	-538	ND	700	100	33,200	245
11	-555	15	2,100	290	....	245
12	-560	'2	2,100	290	....	245
13	-588	150	7,000	2,200	....	245
14	-597	4	3,400	500	Minor	245
15	-806 to -820	130	45,000	300	Several minor entries	250
16	-820 to -911	200	20,000	4,500	Several minor entries	250
17	-1,095	80	......	......	22,700	255

Fehlberg (1975)

usually compressed air. Recognizing that the chemical character of the steam may change during its ascent to the surface, the concentration values measured at the wellhead may only approximate the actual concentrations in the subsurface. Nevertheless, the values are at least semiquantitative, and relative comparisons therefore are permissible.

Depths, flow rates, and estimated wallrock temperatures for the individual steam entries are also listed in table 19. The depths are corrected to true vertical from the deviations of the bore holes and are reported relative to mean sea level to compensate for different spudding elevations. Flow rates are interpreted from logs and well records. Estimated wallrock temperatures are extrapolated from temperature-depth curves given by Hite and Fehlberg (1976) for wells U.S. Geothermal C-4 and C-5.

As shown in table 19, the variability of gas concentrations with depth is readily apparent. Variations over short vertical and lateral distances are further illustrated by Fehlberg's (1975) descriptions of wells U.S. Geothermal One-1 and One-2. These wells were drilled from the same pad and had both the highest and lowest H_2S, CO_2, and CH_4 concentrations (steam entries 6 and 9, table 19) recorded in the four wells studied. U.S. Geothermal One-1 encountered steam with a potential flow rate of approximately 92,600 kg/h at 1,500 m depth. Analysis of a flow-line sample showed essentially no H_2S. U.S. Geothermal One-2 encountered a steam flow of 22,700 kg/h at a depth of 2,068 m. Steam from this entry contained approximately 80 ppm H_2S. Well One-2 was redrilled directionally beginning at 1,391 m and penetrated a steam entry of about 5,400 kg/h at 1,476 m, within about 17 m laterally of the original borehole. The initial H_2S concentration in this entry was 800 ppm but increased to more than 3,000 ppm with reworking of the borehole. This steam entry was within 180 m laterally and at about the same depth as the steam entry in U.S. Geothermal One-1. Estimated formation temperatures at both entries are about 240°-245°C, yet the gas concentrations of the two steam entries were substantially different.

WELLS IN NORTHERN AND CENTRAL PARTS OF THE STEAM FIELD

Detailed information on individual steam entries is not available for wells north of U.S. Geothermal C-4 and C-5. This area includes the bulk of the Geysers steam field. For the most part, gas analyses are made on total-flow samples collected at wellheads or where steam-collection lines enter powerplants. In either case, total-flow samples represent a mixture of steam from several entries. Even within these limits, total-flow samples show wide ranges of gas concentrations. As shown in table 18 for 61 producing steam wells, concentrations of specific gases may vary by two to three orders of magnitude. Gas concentrations in steam flowing from the McKinley 1 and McKinley 3 wells (fig. 101) differ by 15 to 50 percent (Barnes, Hinkle, and others, 1973, p. A14). These wells are about 425 m apart; McKinley 1 was drilled to 2,220 m and McKinley 3 was drilled to 1,580 m. Average H_2S concentrations in steam entering powerplant units (table 20) also vary from unit to unit, even for nearby units in the main part of the production field (compare units 1 through 6).

CONCENTRATION CHANGES WITH TIME

Fluctuations in gas concentrations with time are known from production data. In general, total gas contents decrease with time in producing wells. These decreases are observed during both short-term drilling and testing (a few hours to several days) and long-term production (several years).

For wells drilled in the main part of the steam field near The Geysers Resort, Truesdell and White (1973, p. 158) noted that the average gas content decreased from about 2 percent to less than 1 percent by weight from 1925 to 1969. Truesdell and White also found that the concentrations of the gases relative to each other changed during the same time; the more water-soluble gases H_2, H_2S, and NH_3 showed an increase in content and the less water-soluble gas CO_2 showed a decrease. Although they compared different wells and assumed that the reservoir is relatively homogeneous, their conclusions are supported by the decrease of noncondensable gas concentrations noted by Finney (1973, p. 158) and Bruce (1970, p. 1517) in wells after several years of production. Bruce reported that noncondensable gases entering powerplant unit 1 decreased from 0.61 to 0.29 percent between 1960 and 1969. The decrease in gas content is probably the result of flushing out of residual gases that have accumulated in the upper parts of the reservoir through repeated condensation and vaporization, as outlined above.

INTERPRETATION OF DATA

Data in table 19 and descriptions of wells U.S. Geothermal One-1 and One-2 indicate that gas concentrations do not vary systematically with depth of steam entry. Wallrock temperatures also seem to have little effect on gas concentrations (6-14, table 19). Furthermore, gas concentrations apparently are not proportionate to the amount of steam in a fracture, as indicated by the variability of the gas component in steam entries with similar flow rates (5 and 6, table 19).

Different gas concentrations in steam flowing from the McKinley 1 and 3 wells (Barnes, Hinkle, and others, 1973) and from the U.S. Geothermal One-1 and One-2 wells (Fehlberg, 1975) illustrate the great variability that can occur over relatively short lateral distances. The wide range of H_2S concentrations in steam entering powerplant units (table 20) also indicates lateral variability of steam composition.

Concentration of gases through repeated vaporization of condensed steam undoubtedly explains some of the variability in gas compositions. The rapid initial decline of gas concentrations in some steam entries does suggest that residually collected gases are being flushed from the steam-bearing fracture. However, the wide variability of gas contents produced from steam entries at similar depths and with similar wallrock temperatures in adjacent wells cannot be so easily explained by this mechanism. Residual concentrations also do not explain the wide variation of gas contents if much of the steam is indeed produced by intergranular vaporization (steam flashed from hot water; Truesdell and White, 1973). The reservoir at The Geysers is apparently nonhomogeneous with respect to gas contents.

Inhomogeneity appears to be a primary feature that exists before any steam condensation or fluid production. The likelihood that gas contents are intrinsically highly variable suggests how fractures even within relatively small areas can carry steam and (or) hot water with considerably different chemical compositions.

POSSIBLE SOURCES OF H_2S IN HYDROTHERMAL SYSTEMS

The ultimate source of H_2S in hydrothermal solutions is a fundamental problem seldom addressed in the literature. There may be, in fact, more than one source for the gas in any given system. Three possibilities are considered for The Geysers: (1) magmatic exhalation, (2) water-rock reactions (hydrolysis), and (3) thermal metamorphism.

TABLE 20.—*Average incoming H_2S concentrations at full steam flow for generating units at the Geysers powerplant*

[Units 13-17 are not in operation (1978); H_2S levels are estimates. Streamflow and H_2S values from Pacific Gas and Electric Co. (1977, p. 100a). Locations of units shown in figure 101]

Unit	Maximum steam flow (kg × 10^6/h)	H_2S (ppm)	Depth range (m) of nearby wells
1	0.11	160	64-1,700
2	.12	150	64-1,700
3	.23	430	65-2,375
4	.23	350	65-2,375
5	.41	310	60-1,260
6	.41	340	60-1,260
7	.41	190	1,355-2,775
8	.41	100	1,355-2,775
9	.41	60	1,480-2,900
10	.41	60	1,480-2,900
11	.82	300	1,260-2,860
12	.82	140	2,150-3,050
13	1.18	90	1,670-2,460
14	.86	140	1,500-2,060
15	.50	370	450-2,685
16	.86	70	1,295-2,335
17	.86	350	1,275-1,665

MAGMATIC ORIGIN

Hydrogen sulfide is commonly reported as a constituent of hot-spring and fumarole gases in areas of recent volcanic activity (White, 1957; White and Waring, 1963). In these areas the gases are often regarded as volatile phases exsolved from magma chambers at relatively shallow depths. At The Geysers, a magmatic source for H_2S and other gases is an attractive hypothesis because of the nearness of the Clear Lake volcanic field. Volcanism in the Clear Lake volcanic field occurred as recently as 10,000 years ago (Donnelly-Nolan and others, this volume); hot-spring and fumarolic activity in the field continues today. A nearly circular 25-mGal negative gravity anomaly, centered on Mount Hannah about 10 km northeast of The Geysers, is interpreted to indicate a magma chamber at depth (Chapman, 1975; Isherwood, this volume). The top of the magma chamber is calculated to be about 6 km below the surface, and the absence of any associated magnetic source is consistent with temperatures above the Curie point, about 550°C (Isherwood, this volume). Whether a magma chamber lies directly beneath The Geysers has not been conclusively demonstrated, although northeast-dipping faults (McLaughlin, this volume) may intersect the magma chamber beneath Mount Hannah and act as conduits for exsolving gases.

WATER-ROCK REACTIONS

Laboratory studies by Ellis and Mahon (1964) showed that the interaction of water at 150°-350°C with graywacke and various volcanic rocks can liberate appreciable quantities of many of the components (NH_3, B, F, Cl, As, alkalis, silica) found in natural thermal waters. Ellis and Mahon suggested that any sulfides in the rock would hydrolyze to H_2S, which in turn would partly oxidize to sulfate.

In Franciscan graywacke and pelitic rocks, pyrite is the only widespread sulfide that may hydrolyze to produce H_2S. However, pyrite occurs in very minor amounts (Bailey and others, 1964, p. 31); where detailed petrographic studies have been made (for example, Taliaferro, 1943), the average pyrite content is generally less that 0.1 percent. Examination of well cuttings substantiates this finding at The Geysers.

Reduction of sulfate in meteoric water in the presence of organic material can also produce H_2S. The sulfate ion SO_4^{2-} is the predominant sulfur species in surface waters (Hem, 1970), and isotopic studies by Craig (1966) indicate that the water phase of steam in geothermal systems is almost entirely meteoric in origin. Recharge for the Geysers geothermal system may be through permeable vent pipes of the Clear Lake volcanic field, specifically at Cobb Mountain (Goff and others, 1977; McLaughlin, this volume). Once the surface water has descended through the volcanic cover and into the underlying organic-bearing sedimentary rocks, and presumably the steam reservoir, reduction of dissolved sulfate could yield H_2S by the reaction:

$$2C_{\text{(organic material)}} + SO_4^{2-} + 2H^+ \longrightarrow H_2S + 2CO_2.$$

This process is promoted by heat and is probably abiogenic because most known sulfate-reducing bacteria (*Desulfovibrio* species) are unable to survive at temperatures exceeding 60°C (ZoBell, 1958).

THERMAL METAMORPHISM

Many thermal and nonthermal springs along the west coast of the United States are characterized by anomalous concentrations of CO_2, H_2S, NH_4^+, B, and hydrocarbons (Barnes, 1970). Increasing evidence indicates that the gases, especially CO_2, in many of these waters are in large part produced by contemporary low-grade thermal metamorphism of marine sedimentary rocks (White and others, 1973; Barnes and O'Neil, 1976). Magmas associated with recent volcanism, as in the Geysers-Clear Lake area, are thought to provide a heat source to facilitate metamorphic reactions but are not considered as sources of the anomalous fluids. Barnes (1970, p. 974) interpreted the origins of the individual components as follows:

> The hydrocarbons frequently found associated with the anomalous waters indicate the presence of organic matter in the metamorphosing materials.* * * The B concentrations have been explained as due to recrystallization of marine clays with the release of B back into solution. The simplest explanation for the hydrocarbon-ammonia association is the breakdown of proteins to yield CO_2, NH_4^+, and some of the hydrocarbons found. The amino compounds may yield some of the H_2S found in the fluids. Abundant nonprotein original sources for H_2S, CO_2, and hydrocarbons also exist but not for the NH_4^+.

Skinner (1967) proposed that H_2S in thermal fluids associated with deposition of Mississippi Valley-type sulfide ores is released from sulfur-bearing organic material by thermal degradation. Sulfur, a fundamental element in proteins, is a common component of organic deposits. Many sulfur-bearing compounds in organic material are thermally unstable and when heated release sulfur in the form of H_2S (Thompson and others, 1965).

DISCUSSION

Allen and Day (1927) believed that the H_2S and other gases at The Geysers have a volcanic origin. In fact, gases from fumaroles and hot-springs in areas of recent volcanic activity are commonly thought to be derived from magmas somewhere in the subsurface. This is often a reasonable assumption, but a few significant differences between the composition of gases at The Geysers and of gases clearly evolved from magmas are worth noting. In volcanic emanations CO_2 is the predominant gas and H_2S is generally present (White and Waring, 1963), as is true at The Geysers. However, CH_4 and NH_3, common at The Geysers, are seldom reported as volcanic gases. Formation of CH_4 and NH_3 by reaction of molecular H_2 with CO_2 and N_2, respectively, in magmatic gases is thermodynamically possible (Ellis, 1957); however, recent investigations support an organic origin for these gases, especially CH_4 (Gunter and Musgrave, 1971). Likewise, carbon isotopic studies of CO_2 in hydrothermal areas (for example, Panichi and Tongiorgi, 1976) suggest that much of the CO_2 in these areas may be products of thermal metamorphism of carbonate and organic material rather than magmatic gases. In further contrast, SO_2 and halogen gases (HCl, HF), common as volcanic emissions, are not detected at The Geysers. Although the dissimilarities between average compositions of volcanic gases and the composition of steam gases at The Geysers are significant enough to support arguments against magmatic origin, one cannot assume that all the steam gases are genetically related and therefore have a singular origin. Thus, a magmatic source for H_2S cannot be completely ruled out.

The contribution of H_2S by hydrolysis of pyrite is not easily evaluated. Sulfate rather than H_2S is the primary sulfur species produced from the reaction of pyrite with water under both aerobic and anaerobic conditions. Raymahashay and Holland (1969) calculated that the concentration of H_2S in a 1 M KCl solution in equilibrium with pyrite-magnetite-hematite, a reasonable heavy-mineral assemblage for Franciscan graywacke, at 250°C and $f_{H_2O} = 36$ atm (3,650 kPa) is only about

$10^{-3.8}$ moles per kilogram of H_2O, or about 5.4 ppm. At 350°C, the amount of dissolved H_2S in solution increases to $10^{+2.7}$ moles per kilogram of H_2O, or about 84.5 ppm. High H_2S concentrations would require highly acidic and reducing conditions, which do not seem reasonable owing to the likely presence of carbonate and silicate buffers and free O_2 from the dissociation of water at elevated (hydrothermal) temperatures. Furthermore, reservoir temperatures at The Geysers are apparently in the range 235°-255°C to at least 3 km depth. The concentration of dissolved H_2S if produced in the reservoir would thus approach Raymahashay and Holland's lower value ($10^{-3.8}$ moles/kg). Higher concentrations would require reactions at higher temperatures presumably occurring at greater depths.

Although a small amount of H_2S might evolve by pyrite hydrolysis, the small quantity of pyrite present in Franciscan rocks and the small amount of H_2S that can be produced by hydrolysis seems inadequate to account for those H_2S concentrations exceeding 100 ppm found in some of the deepest steam entries (steam entries 15-17, table 19), especially where repeated vaporization and condensation are probably minimal. All the pyrite observed in well cuttings appears fresh and unreacted, even in the steam-producing zones, and there appears to be very little wallrock alteration at steam entries. This evidence suggests minimal water-rock reactions in the reservoir but does not exclude the possibility that H_2S is formed by hydrolysis at greater depths and higher temperatures than those in the reservoir. H_2S could be formed beneath a boiling water table as in the vapor-dominated model proposed by White, Muffler, and Truesdell (1971), or sulfate produced by such reactions could subsequently be reduced to H_2S in the presence of organic material.

Organic reduction of ground-water sulfate may contribute H_2S to the hydrothermal fluids. As with hydrolysis of pyrite, however, the significance of this process is not easily determined. The amount of sulfate in solution and thus the amount of sulfate available for reduction is governed by several factors, the most important of these being (1) the original sulfate content in the meteoric water and (2) the amount of sulfate that can be taken into solution either by oxidation of sulfide minerals or by dissolution of sulfate minerals. Sulfate concentrations in nonthermal springs in the Geysers-Clear Lake area are less than 10 mg/L (Goff and others, 1977). The same is true for thermal springs except in areas of fumaroles where sulfate concentrations are commonly several hundred to several thousand mg/L and where much of the sulfate is probably due to oxidized H_2S. Because of the low concentration of ground-water sulfate in the area, only minor amounts of H_2S would be expected to form from reduction of sulfate.

While formation of $H_2S$and other gases may be explained by one or more of the above processes, thermal metamorphism of marine sedimentary rocks, particularly the Franciscan graywacke and pelitic rocks in abundance at The Geysers, can produce most, if not all, of the gases in the steam. Accordingly, H_2S would be produced by thermal degradation of organic material, especially carbonized plant tissue. Arguments supporting this conclusion are given below.

ORGANIC MATERIAL AS SOURCE OF H_2S

Organic material is a common component of sedimentary rocks, although it usually makes up less than 1 percent by weight of the rock and is seldom reported by petrographers. In ordinary sandstone and shale, the organic matter is 90 to 95 percent plant derived (Bostick, 1974, p. 2). In metamorphosed pelitic rocks, carbonaceous matter is equivalent to coal with a rank corresponding to the metamorphic grade (Izawa, 1968).

Considerable quantities of water vapor, CO_2, CH_4, H_2S, and NH_3 are released as volatile matter during thermal decomposition and coalification of organic material (Teichmüller and Teichmüller, 1967). Laboratory tests and experiments show that volatile matter in coal decreases as coal rank increases. For example, there is a greater than 80 percent decrease in volatile matter as coal changes from subbituminous to semianthracite (calculated from data in table 1 of Teichmüller and Teichmüller, 1968). Teichmüller and Teichmüller (1968) concluded that temperature, and time to a lesser extent, are critical factors in the coalification process; the effect of pressure is minimal. Volatile matter is slowly released at temperatures as low as 50°C, but rapidly released at temperatures above 100°C (Teichmüller and Teichmüller, 1968, p. 258). Sulfur compounds, occurring as common components of organic material, are destroyed rapidly because of their thermal instability, with much of the sulfur released as H_2S.

Thermal metamorphism of coal to the rank of anthracite can occur rapidly near intrusive contacts. The occurrence of anthracite in Upper Cretaceous and lower Tertiary rocks of the Glacier coal field, Washington, is believed to be the result of temperature increase brought about by Pleistocene and Holocene magmatic activity related to the Mount Baker volcano (Moen, 1969, p. 16). Mount Baker is about 10 km southeast of the Glacier coal field, roughly the same lateral distance separating The Geysers from the suspected magma chamber beneath Mount Hannah.

At The Geysers, scattered deposits of carbonaceous material are locally found interbedded in Franciscan graywacke (R. J. McLaughlin, oral commun., 1977). The deposits occur as small coaly pods and discontinuous coaly seams a few centimeters thick; relict plant morphology is sometimes recognizable. Carbonaceous material was also reported as rock fragments in the graywacke (McNitt, 1968) and is probably abundant as finely divided fragments in black shale and pelitic rocks. Although the Franciscan rocks at The Geysers have undergone varying grades of metamorphism (McLaughlin and Stanley, 1976), graywacke containing the coaly deposits has only been incipiently metamorphosed. These rocks crop out in the western part of the steam field in McLaughlin's (this volume) "structural unit 2," which underlies much of the field. By analogy to the Glacier coal field in Washington, thermal decomposition and coalification of organic material are believed to be occurring at The Geysers, and these processes are releasing H_2S and other volatiles as separate phases.

The abundance of methane and the traces of ethane in the steam support the conclusion that thermal degradation of organic material plays an important role in the evolution of the gases. Isotopic compositions of carbon in CH_4 and CO_2 are also compatible with an organic source. Craig (1963, p. 43) obtained $\delta^{13}C$ values of 29 to 29.5‰ for CH_4 from The Geysers. These values are within the range of $\delta^{13}C$ values that Craig (1963, p. 39) gave for shale and coal and suggest that the carbon in the CH_4 is of organic origin. Gunter and Musgrave (1971) arrived at a similar conclusion for the methane in hydrothermal gases collected at Lassen Volcanic and Yellowstone National Parks. At The Geysers, carbon dioxide is enriched in ^{13}C compared to the methane; the $\delta^{13}C$ for the CO_2 is about 11‰ (Craig, 1963, p. 42). Craig attributed the enrichment to juvenile carbon; however, the same value can be derived from a mixture of organic carbon from shale with carbon from carbonate minerals in the marine sedimentary rocks.

As already mentioned, CH_4, and to some extent CO_2, entries are associated with graywacke-argillite assemblages above the steam zone. Besides indicating that these gases may be products of thermal metamorphism, this suggests that they can be produced locally from rocks of the appropriate composition. A reasonable assumption is that similar processes and circumstances occur within the steam zone. Thus, any steam-bearing fractures leading from or passing through organic-rich rocks could be enriched in these and other volatile products of thermal degradation and metamorphism.

DISCUSSION AND CONCLUSIONS

Although proof is not yet available, gases in steam at The Geysers may evolve as separate phases from thermal metamorphism of organic material, calcite, and clay contained primarily in Franciscan graywacke and pelite. CH_4, CO_2, H_2S, and NH_3 are released by thermal degradation of organic material during coalification. Metamorphic reactions between calcite and silicate minerals also produce CO_2. Boron compounds result from the breakdown of clay minerals and perhaps from decomposition of organic material. Hydrolysis of pyrite and reduction of sulfate in meteoric waters probably play minor roles in the formation of H_2S.

Gas concentrations vary both vertically and laterally across the steam field. The variability appears to be unsystematic; no relations are recognized between the chemical compositions of steam entries and their depths, wallrock temperatures, gas-to-steam ratios, or position within the steam field. A primary or initial variability probably results from the release of gases from rocks with various amounts of organic matter. Further variability can be brought about by secondary processes such as refluxing of steam condensate and mixing of steam and gas from different source areas.

Residual gas concentrations from condensation in the cooler parts of steam-bearing fractures are temporary and decrease as the fracture is produced. Condensation may cause a chemical zonation of the steam in a fracture, and so the same fracture penetrated at different levels may produce steam of different physicochemical characteristics. The important concept here is whether a fracture, or portion of a fracture, is acting as a steam transporter and is continually flushed out by net movement of steam, or if it is a trap where steam can stagnate and build up residual-gas concentrations. The fracture need not connect with the surface to have continuous fluid movement; a diffuse area of subsurface discharge would have the same result.

Locally meteoric water filtering through the higher parts of a geothermal system may cause dilution or enrichment of certain components, depending on the dissolved constituents and amount of admixture. This mechanism has been identified as one cause of steam composition variability at the Larderello field in Italy (D'Amore and others, 1977).

If the gases are indeed the products of thermal metamorphism, then source rocks are the dominant factor controlling the initial, or primary, gas concentrations. Fractures leading from, or passing through, organic-rich rocks would be expected to carry higher gas concentrations, as opposed to those fractures connecting organic-poor rocks. The amount and kind of gas released into solution depend on the temperature at which organic decomposition is occurring. Mixing of gases from various sources along the path of a fracture or fracture system complicates the picture. The fact that wells drilled from the same pad can encounter steam at about the same depth but with widely differing chemical and physical characteristics suggests that the fractures have limited interconnection, although pressure interference between producing wells indicates just the opposite (Budd, 1973, p. 137). Fracture systems are evidently very complex and reflect the complicated structure of The Geysers. For instance, the redrill of U.S. Geothermal One-2 penetrated first steam almost 600 m above first steam in the original borehole and only 17 m laterally from the original borehole. Steam distribution is controlled by local structure, and imbricate thrust faults suggest the likelihood of several stacked production zones (McLaughlin, this volume). These zones each could have different properties which would influence the gas contents differently. Several factors thus combine to create the wide variations in gas content found in steam at The Geysers. High H_2S concentrations encountered in some steam entries are probably due to a combination of residual-gas concentrations and H_2S-producing source rocks.

REFERENCES CITED

Allen, E. T., and Day, A. L., 1927, Steam wells and other thermal activity at "The Geysers" California: Carnegie Institution of Washington Publication 378, 106 p.

Bailey, E. H., Irwin, W. P., and Jones, D. L., 1964, Franciscan and related rocks, and their significance in the geology of western California: California Division of Mines and Geology Bulletin 183, 177 p.

Barnes, Ivan, 1970, Metamorphic waters from the Pacific tectonic belt of the west coast of the United States: Science, v. 168, p. 973-975.

Barnes, Ivan, Hinkle, M. E., Rapp, J. B., Heropoulos, Chris, and Vaughn, W. W., 1973, Chemical composition of naturally occurring fluids in relation to mercury deposits in part of north-central California: U.S. Geological Survey Bulletin 1382-A, p.

Barnes, Ivan, and O'Neil, J. R., 1976 Metamorphic reactions in flysch rocks, *in* Cadek, J., and Paces, T., eds., International Symposium on Water-Rock Interaction, Czechoslovakia, 1974, Proceedings: Prague, Geological Survey, p. 309-316.

Bostick, N. H., 1974, Phytoclasts as indicators of thermal metamorphism, Franciscan assemblage and Great Valley sequence (upper Mesozoic), California, *in* Dutcher, R. R., Hacquebard, P. A., Schopf, J. M., and Simon, J. A., eds., Carbonaceous materials as indicators of metamorphism: Geological Society of America Special Paper 153, p. 1-17.

Bruce, A. W., 1970, Engineering aspects of a geothermal power plant: Geothermics, Special Issue 2, v. 2, pt. 2, p. 1516-1520.

Budd, C. F., Jr., 1973, Steam production at The Geysers geothermal field, *in* Kruger, Paul, and Otte, Carel, eds., Geothermal energy: Stanford, California, Stanford University Press, p. 129-144.

Chapman, R. H., 1975, Geophysical study of the Clear Lake region, California: California Division of Mines and Geology Special Report 116, 23 p.

Craig, Harmon, 1963, The isotopic geochemistry of water and carbon in geothermal areas, *in* Tongiorgi, E., ed., Nuclear geology on geothermal areas: Pisa, Consiglio Nazionale delle Ricerche, Laboratoria de geologia nucleare, p. 17-53.

_____ 1966, Superheated steam and mineral-water interactions in geothermal areas (abstract): EOS, Transactions of the American Geophysical Union, v. 47, no. 1, p. 204.

D'Amore, F., Celati, R., Ferrara, G. C., and Panichi, Costanzo, 1977, Secondary changes in the chemical and isotopic composition of the geothermal fluids in Larderello field: Geothermics, v. 5, p. 153-163.

Ellis, A. J., 1957, Chemical equilibrium in magmatic gases: American Journal of Science, v. 255, p. 416-431.

Ellis, A. J., and Mahon, W. A. J., 1964, Natural hydrothermal systems and experimental hot-water/rock interactions: Geochimica et Cosmochimica Acta, v. 28, p. 1323-1357.

Fehlberg, E. L., 1975, Shell's activity in The Geysers area, *in* First Workshop on Geothermal Reservoir Engineering, Stanford University: unpublished summaries, 7 p.

Finney, J. P., 1973, Design and operation of The Geysers power plant, *in* Kruger, Paul, and Otte, Carel, eds., Geothermal energy: Stanford, Calif., Stanford University Press, p. 145-161.

Garrison, L. E., 1972, Geothermal steam in The Geysers-Clear Lake region, California: Geological Society of America Bulletin, v. 83, p. 1449-1468.

Goff, F. E., Donnelly, J. M., Thompson, J. M., and Hearn, B. C., Jr., 1977, Geothermal prospecting in The Geysers-Clear Lake area, northern California: Geology, v. 5, p. 509-515.

Gunter, B. D., and Musgrave, B. C., 1971, New evidence on the origin of methane in hydrothermal gases: Geochimica et Cosmochimica Acta, v. 35, p. 113-118.

Hem, J. D., 1970, Study and interpretation of the chemical characteristics of natural water (2d ed.): U.S. Geological Survey Water-Supply Paper 1473, 363 p.

Hite, J. R., and Fehlberg, E. L., 1976, Steam zone temperature gradients at The Geysers, *in* Kruger, Paul and Ramey, H. J., Jr., eds., Second Workshop on Geothermal Reservoir Engineering, summaries: Stanford, California, Stanford University Press, p. 16-20.

Izawa, Eiji, 1968, Carbonaceous matter in some metamorphic rocks in Japan: Journal of the Geological Society of Japan, v. 74, p. 427-431.

James, Russell, 1968, Wairakei and Larderello - Geothermal power systems compared: New Zealand Journal of Science, v. 11, p. 706-719.

McLaughlin, R. J., 1977, The Franciscan assemblage and Great Valley sequence in The Geysers-Clear Lake region of northern California, *in* Field trip guide to The Geysers-Clear Lake area: Geological Society of America, Cordilleran Section, field trip guide, p. 1-24.

McLaughlin, R. J., and Stanley, W. D., 1976, Pre-Tertiary geology and structural control of geothermal resources, The Geysers steam field, California: Second United Nations Symposium on the Devolopment and Use of Geothermal Resources, San Francisco, 1975, Proceedings, v. 1, p. 475-485.

McNitt, J. R., 1963, Exploration and development of geothermal power in California: California Division of Mines and Geology Special Report 75, 44 p.

_____ 1968, Geology of the Kelseyville quadrangle, Sonoma, Lake, and Mendocino Counties, California: California Division of Mines and Geology Map Sheet 9.

Moen, W. S., 1969, Mines and mineral deposits of Whatcom County, Washington: Washington Division of Mines and Geology Bulletin 57, 134 p.

Mori, Y., 1970, Exploitation of the Matsukawa geothermal area: Geothermics, Special Issue 2, v. 2 p. 1150-1156.

Pacific Gas and Electric Co., 1977, Environmental data supplement, Geysers Unit 17: San Francisco, Pacific Gas and Electric Co., 173 p.

Panichi, Costanzo, and Tongiorgi, Ezio, 1976, Carbon isotopic composition of CO_2 from springs, fumaroles, mofettes, and travertines of central and southern Italy: A preliminary prospection method of geothermal area: Second United Nations Symposium on the Development and Use of Geothermal Resources, San Francisco, 1975, Proceedings, v. 1, p. 815-825.

Raymahashay, B. C., and Holland, H. D., 1969, Redox reactions accompanying hydrothermal wall rock alteration: Economic Geology, v. 64, p. 291-305.

Reed, M. J., and Campbell, G. E., 1976, Environmental impact of development in The Geysers geothermal field, USA: Second United Nations Symposium on the Development and Use of Geothermal Resources, San Francisco, 1975, Proceedings, v. 2, p. 1399-1410.

Sax, N. I., 1975, Dangerous properties of industrial materials: New York, Van Nostrand Reinhold, 1258 p.

Schieler, Leroy, 1976, Geothermal effluents, their toxicity and prioritization, *in* Proceedings of the first workshop on sampling geothermal effluents: Las Vegas, Nevada, U.S. Environmental Protection Agency, p. 36-65.

Skinner, B. J., 1967, Precipitation of Mississippi Valley-type ores - A possible mechanism, *in* Brown, J. S., ed., Genesis of lead-zinc-barite-fluorite deposits in carbonate rocks: Economic Geology Monograph 3, p. 363-370.

Taliaferro, N. I., 1943, Franciscan-Knoxville problem: American Association of Petroleum Geologists Bulletin, v. 27, p. 109-219.

Teichmüller, Marlies, and Teichmüller, Rolf, 1967, Diagenesis of coal (coalification), *in* Larson, G., and Chilingar, G. V., eds., Diagenesis in sediments: Amsterdam, Elsevier, v. 8, p. 391-415.

—— 1968, Geological aspects of coal metamorphism, *in* Murchison, D., and Westoll, T. S., eds., Coal and coalbearing strata: Edinburgh, Oliver and Boyd, p. 233-267.

Thompson, C. J., Coleman, H. J., Hopkins, R. L., and Rall, H. T., 1965, Sulphur compounds in petroleum: American Society of Testing and Materials Special Publication 389, p. 329-360.

Truesdell, A. H., and White, D. E., 1973, Production of superheated steam from vapor-dominated geothermal reservoirs: Geothermics, v. 2, p. 154-173.

U.S. Department of the Interior, 1973, Final environmental statement for the geothermal leasing program: v. 1, 421 p.

White, D. E., 1957, Thermal waters of volcanic origin: Geological Society of America Bulletin, v. 68, p. 1637-1658.

—— 1973, Characteristics of geothermal resources, Kruger, Paul, and Otte, Carel, eds., Geothermal energy: Stanford, California, Stanford University Press, p. 69-94.

White, D. E., Barnes, Ivan, and O'Neil, J. R., 1973, Thermal and mineral waters of nonmeteoric origin, California Coast Ranges: Geological Society of America Bulletin, v. 84, p. 547-560.

White, D. E., Muffler, L. J. P., and Truesdell, A. H., 1971, Vapor-dominated hydrothermal systems compared with hot-water systems: Economic Geology, v. 66, p. 75-97.

White, D. E., and Waring, G. A., 1963, Data of geochemistry (6th ed.) - Chapter K, Volcanic emanations: U.S. Geological Survey Professional Paper 440-K, 29 p.

Yates, R. G., and Hilpert, L. S., 1946, Quicksilver deposits of eastern Mayacmas district, Lake and Napa Counties, California: California Journal of Mines and Geology, v. 42, p. 231-286.

ZoBell, C. E., 1958, Ecology of sulfate reducing bacteria: Producers Monthly, v. 22, no. 7, p. 12-29.

GASES FROM SPRINGS AND WELLS IN THE GEYSERS-CLEAR LAKE AREA

By NANCY L. NEHRING

ABSTRACT

Major gases and trace hydrocarbon gases were analyzed from nine springs and one well in and near the Clear Lake volcanic field and from three wells in the Geysers steam field. The Clear Lake samples generally contained 93 to 100 percent CO_2, 0.1 to 6 percent CH_4, and small amounts of H_2; all samples showed some air contamination of probable near-surface origin. Similar patterns in the C_{1-6} hydrocarbon gases indicate a similar origin in sedimentary rocks and a similar history.

The Geysers samples contained 90 to 98 percent CO_2, 0.5 to 2.5 percent H_2S, and lesser amounts of N_2, Ar, CH_4, and H_2. The hydrocarbon patterns suggest an origin similar to that of gases in the Clear Lake area but a somewhat different history. No evidence was found for a magmatic source of gases.

INTRODUCTION

Interpretation of the gaseous composition of geothermal fluids is not as advanced as that of the water composition. Constituents of geothermal gases are thought to be derived from degassing magma or from sedimentary rocks by thermal metamorphism. This study does not entirely support either source; however, the various gaseous components of geothermal fluids, whatever their original source, and their relative amounts may be altered by reaction with rocks, water, and dissolved substances in the reservoir.

METHOD

Gas samples from nine springs and one well in the Clear Lake area (mostly peripheral to the Clear Lake volcanic field, according to Hearn and others, 1976) and from three steam wells in the Geysers area were collected between February and August 1977 (fig. 103). Gases from the springs were collected in a partially submerged funnel held over the bubbles and then transferred to a 300-mL evacuated bottle containing 100 mL of 4*N* NaOH (Giggenbach, 1976). The sample from the Kelseyville methane well was collected by inserting 5 m of stainless-steel tubing through the main valve, sealing the opening as securely as possible, then collecting the gas through the exposed end in a 300-mL bottle containing 4*N* NaOH. Steam samples were collected by cooling to ~30°C the total flow from a bypass on the wellhead and allowing the gases to collect in a 500-mL evacuated bottle containing 100 mL of 4*N* NaOH (Nehring and Truesdell, 1977).

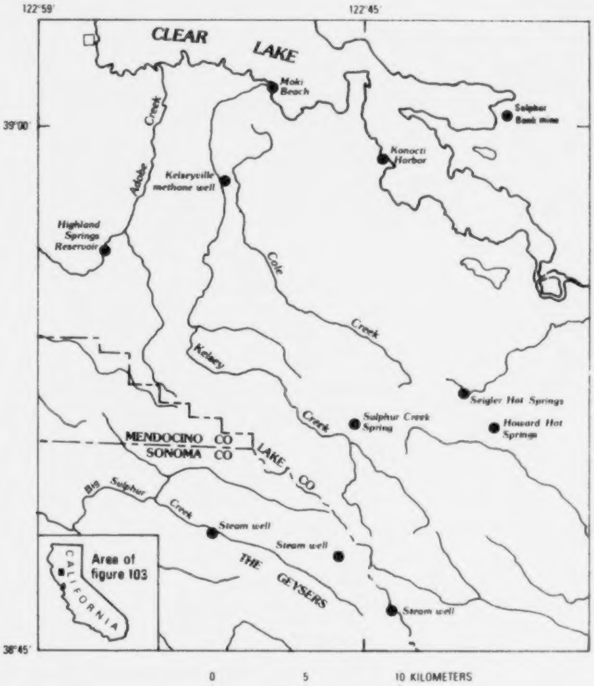
122°59'
122°45'
39°00'
38°45'
CLEAR LAKE
Moki Beach
Sulphur Bank mine
Konocti Harbor
Kelseyville methane well
Adobe Creek
Highland Springs Reservoir
Cole Creek
Kelsey Creek
Seigler Hot Springs
Sulphur Creek Spring
Howard Hot Springs
MENDOCINO CO
SONOMA CO
LAKE CO
Big Sulphur Creek
Steam well
Steam well
Steam well
THE GEYSERS
CALIFORNIA
Area of figure 103
0
5
10 KILOMETERS

FIGURE 103.—Sampling sites in the Geysers-Clear Lake area.

All analyses for each well or spring were carried out on aliquots from the same gas bottle. Analyses of the major residual gases (gases in headspace above NaOH) were done with a gas chromatograph equipped with a Carle thermistor detector and 6-ft Porapak Q and 20-ft molecular sieve 5A columns in series, held at 27°C. Helium carrier gas at an inlet pressure of 60 psi was used for the analyses of O_2, Ar, N_2, and CH_4, and argon carrier gas at 50 psi was used for He and H_2. Hydrocarbon gases were analyzed on the headspace gas with a Hewlett-Packard flame-ionization gas chromatograph; dual 6-ft Porapak Q columns were used with helium carrier gas at 60 psi and an analysis temperature programmed over the range 30°–150°C.

The NaOH solution was analyzed for CO_2, H_2S, and NH_3. Carbon dioxide was determined gravimetrically by precipitation as $SrCO_3$. Hydrogen sulfide was determined gravimetrically by oxidation of S^{2-} to SO_4^{2-} with hydrogen peroxide, acidification to remove carbonate, and precipitation with Ba^{2+}. Ammonia was determined using an ion-specific electrode.

RESULTS AND DISCUSSION

Analyses of all gases are shown in the accompanying tables (tables 21, 22, and 23). Although results are reported to two decimal places, constituents making up more than 1 percent of the total are accurate to only two significant figures. Identification of the hydrocarbon compounds was confirmed on representative samples by gas chromatography/mass spectroscopy by Frank Church and Dave DesMarais of the NASA-Ames Research Center, Mountain View, Calif.

INORGANIC GASES

Carbon dioxide. —Samples from the Clear Lake area contained 93.2 to 99.8 percent CO_2 and those from The Geysers 89.8 to 97.1 percent CO_2. Published $\delta^{13}C$ values of 8 to 15 permil for CO_2 from The Geysers (Craig, 1963; Huebner, this volume) indicate that the CO_2 there, and probably that in the Clear Lake area as well, is derived from decomposition of marine organic matter in the Franciscan Formation.

Hydrogen Sulfide. — Hydrogen sulfide was absent from all Clear Lake samples except those from Sulfur Bank mine and Sulfur Creek Spring. The H_2S at Sulfur Bank mine is probably related to the Quaternary volcanism and ore deposition in the area (White and Roberson, 1962). Sulfur Creek Spring lies on faults postulated to be the boundary between the steam field and the hot-water field (Goff and others, 1977) and may be influenced by the higher temperatures of the steam field, which would cause more extensive decomposition of the organic matter. The gas composition in the Kelseyville methane well has apparently changed in the last few years, showing major decreases in H_2S and CH_4 content. Sulfur-fuming areas were noted in the Clear Lake volcanic field, but an adequate source for gas sampling could not be located. The presence of H_2S at The Geysers, but not in samples from areas peripheral to the volcanic rocks, is probably due to higher-temperature rock-water interactions in the Geysers steam field. The measured reservoir temperature at The Geysers is 250°C versus a predicted 210°C for the Clear Lake area.

Hydrogen. —Hydrogen content is about four orders of magnitude higher at The Geysers than in the Clear Lake area. As with H_2S, higher temperature reaction of water with silicates and ferrous oxides at depth in the reservoir rocks accompanied by rapid transport to the surface may account for this difference. Reaction of the well casing with steam and H_2S may also increase the H_2 content.

TABLE 21.—*Major-gas analyses of the Geysers-Clear Lake area*

[Values, except steam/gas, in mole percent. ND, not determined; * Ar reported in O_2 total]

Locality	CO_2	H_2S	He	H_2	O_2	Ar	N_2	CH_4	NH_3	Steam/gas
Siegler Hot Springs:										
The Geyser Spring	93.23	0	0	0	0.022	0.021	0.65	5.94	ND	ND
Hot Sulfur Spring	98.35	0	0	4.1×10^{-4}	.11	6.6×10^{-3}	.39	1.10	ND	ND
Howard Hot Springs:										
Iron Sulphur Spring	98.96	0	0	6.4×10^{-4}	.91	ND	.61	.12	ND	ND
Magnesia Spring	99.46	0	0	5.9×10^{-4}	.099	(*)	.23	.20	ND	ND
Kelseyville methane well	98.01	0	0	0	.12	5.8×10^{-3}	.60	1.27	ND	ND
Moki Beach—gas near shore	99.23	0	0	2.5×10^{-5}	4.7×10^{-3}	3.3×10^{-4}	.13	.63	ND	ND
Sulphur Bank mine—Herman pit, gas near shore	93.33	0.13	0	0	0	7.2×10^{-4}	1.31	5.46	ND	ND
Konocti Harbor—gas near shore	94.76	0	0	0	.041	.025	1.48	3.76	ND	ND
Sulphur Creek Spring	97.57	.17	0	1.6×10^{-3}	.30	(*)	1.56	.16	ND	ND
Highland Springs Reservoir—gas near shore	99.76	0	0	0	1.6×10^{-4}	1.7×10^{-4}	.030	.20	.0068	ND
The Geysers steam well	97.07	1.22	0	0.68	0	trace	.11	.46	.38	550
The Geysers steam well	95.27	.60	0	2.89	0	4.6×10^{-4}	.091	.60	.86	45
The Geysers steam well	89.82	2.47	0	5.23	0	1.4×10^{-3}	9.0	1.67	.90	325

Nitrogen, oxygen, and argon. —Nitrogen, oxygen, and argon are dissolved or entrained in meteoric water and carried into geothermal systems with the recharge water (Mazor and Wasserburg, 1965). The N_2/Ar ratio for meteoric water normally ranges from 37 in air-saturated water to 84 in entrained air; four out of seven spring samples for which the Ar content was determined lie in this range (table 22). The Geysers well samples have much higher N_2/Ar ratios of 200 to 300 that are probably due to differences in the solubilities of N_2 and Ar in water. As steam flashes from water during production, the less soluble N_2 tends to be carried in the steam phase, and the more soluble Ar tends to remain in the water phase.

Steam is not known to be present at depth in the areas of the Kelseyville methane well, Sulphur Bank mine, or Highland Springs Reservoir. Decomposition of NH_3 (not analyzed in this study) may explain the observed N_2/Ar ratios in the range 100–200.

Oxygen is generally not present in samples containing H_2S because H_2S and O_2 react to form sulfur (or sulfate) until one or the other is consumed. The fact that the sample from Sulphur Creek Spring contains both H_2S and O_2 indicates either near-surface addition of air without sufficient time for the H_2S and O_2 to react or contamination of the sample during collection.

The two samples from Howard Hot Springs are unusual in that they contain an excess of O_2 when compared to the atmospheric ratio of O_2 to N_2 (table 22); no mechanism for this occurrence is known.

TABLE 22.—*Residual-gas analyses (gas over NaOH) of the Geysers-Clear Lake area*

[Values, except N_2/Ar, in mole percent. ND, not determined; *, Ar reported in O_2 total]

Locality	He	H_2	O_2	Ar	N_2	CH_4	N_2/Ar
Seigler Hot Springs:							
The Geyser Spring	0	0	0.32	0.31	9.62	87.79	31
Hot Sulphur Spring	0	.025	6.9	.4	23.95	66.82	60
Howard Hot Springs:							
Iron Sulphur Spring	0	.062	18.65	ND	58.25	11.64	ND
Magnesia Spring	0	.11	18.33	(*)	43.48	36.43	ND
Kelseyville methane well	0	0	5.79	.29	30.07	63.69	103
Moki Beach— gas near shore	0	.0033	.61	.43	16.51	81.49	38
Sulphur Bank mine— Herman pit, gas near shore	0	0	0	.11	20.08	83.43	183
Konocti Harbor— gas near shore	0	0	.78	.47	28.27	71.83	60
Sulphur Creek Spring	0	.0070	15.95	(*)	68.81	7.17	ND
Highland Springs Reservoir— gas near shore	0	0	.067	.073	12.86	86.74	176
The Geysers steam well	0	51.03	0	trace	8.05	34.26	ND
The Geysers steam well	0	87.58	0	.014	2.75	18.12	196
The Geysers steam well	0	76.65	0	.021	6.05	24.45	288

TABLE 23.—*Hydrocarbon-gas analyses of the Geysers-Clear Lake area*

[All values in parts per million of gases other than water]

Locality	Methane	Ethene	Ethane	Propane	?	2-methyl-propane	n-butane	2-methyl-butane	n-pentane	Cyclo-pentane	3-methyl-pentane	2-methyl pentane	n-hexane	Benzene
Seigler Hot Springs:														
The Geyser Spring	59,400	0	560	46	0	1	1	0	0	0	0	0	0	0
Hot Sulphur Spring	11,000	0	160	5	0	0	.1	0	0	0	0	0	0	0
Howard Hot Springs:														
Iron Sulphur Spring	1,200	0	1	0	0	0	0	0	0	0	0	0	0	0
Magnesia Spring	2,000	0	30	2	.04	.1	.1	0	0	0	0	0	0	0
Kelseyville methane well	12,700	0	375	13		4	.4	.5	0	0	0	0	0	0
Moki Beach— gas near shore	6,300	0	6	0	0	0	0	.2	0	0	0	0	0	0
Sulphur Bank mine Herman pit, gas near shore	54,600	0	240	40	.2	1	3	0	0	0	0	0	0	0
Konocti Harbor— gas near shore	37,600	0	150	.8	0	0	0	0	0	0	0	0	0	0
Sulphur Creek Spring	1,600	0	5	.3	0	.5	0	.04	0	0	0	0	0	0
Highland Springs Reservoir— gas near shore	2,000	0	265	13	0	2	.5	.04	.01	0	.2	.3	.2	.5
The Geysers steam well	4,600	0	5	2	0	0	.3	0	0	0	0	0	0	0
The Geysers steam well	6,000	.01	23	5	0	.4	.1	.2	.4	0	0	0	.02	.5
The Geysers steam well	16,700	.5	315	180	0	2	90	2	4	1	0	2	2	45.5

HYDROCARBON GASES

Hydrocarbon gases from The Geysers exhibit chromatographic patterns (fig. 104) similar to those of other geothermal gases from sedimentary rocks (Nehring and Truesdell, 1978). The ratios of ethane, propane, and butane to methane are high in comparison to samples from nonsedimentary geothermal areas. Unsaturated hydrocarbons (other than traces of ethene) are absent, but several branched hydrocarbons are present; pentanes and hexanes also occur. In contrast, samples from igneous rocks are very low in ethane, propane, and butane relative to methane. Unsaturated hydrocarbons usually equal the corresponding saturated hydrocarbons in concentration; branched hydrocarbons are absent, and pentanes and hexanes are seldom present. Samples from degassing magmas (lava flow and dome fumaroles of active volcanoes) are similar to igneous samples, but the methane content is much lower.

The Clear Lake samples are high in ethane and propane relative to methane. 2-methylpropane is present, but butanes are low, and pentanes and hexanes absent. There are no unsaturated hydrocarbons. Apparently the gas profile (fig. 104*B*) has been terminated near five carbon atoms because reservoir temperatures are not high enough to form or transport pentanes and hexanes, or low near-surface temperatures allow condensation of the pentanes and hexanes. The warmest spring temperature was 53°C.

It was hoped that hydrocarbon gas analyses would indicate areas where the Great Valley sequence is concealed beneath the overthrust Franciscan or would give evidence of igneous rocks or degassing magma near Mount Konocti. Barnes and others (1973) found that the major gas in the Great Valley sequence is CH_4, whereas the major gas in the Franciscan is CO_2. Samples from Seigler Hot Springs in the Great Valley sequence and from Sulfur Bank mine, where the Great Valley sequence may be present at depth on the basis of the high chloride content of the thermal water (Goff and others, 1977), have 1 to 6 percent CH_4, which is higher than in most other springs. A high methane content is also found at Konocti Harbor and the Kelseyville methane well, where there is no other evidence for the Great Valley sequence. Both samples are from areas containing lake sediment deposits rich in organic mat-

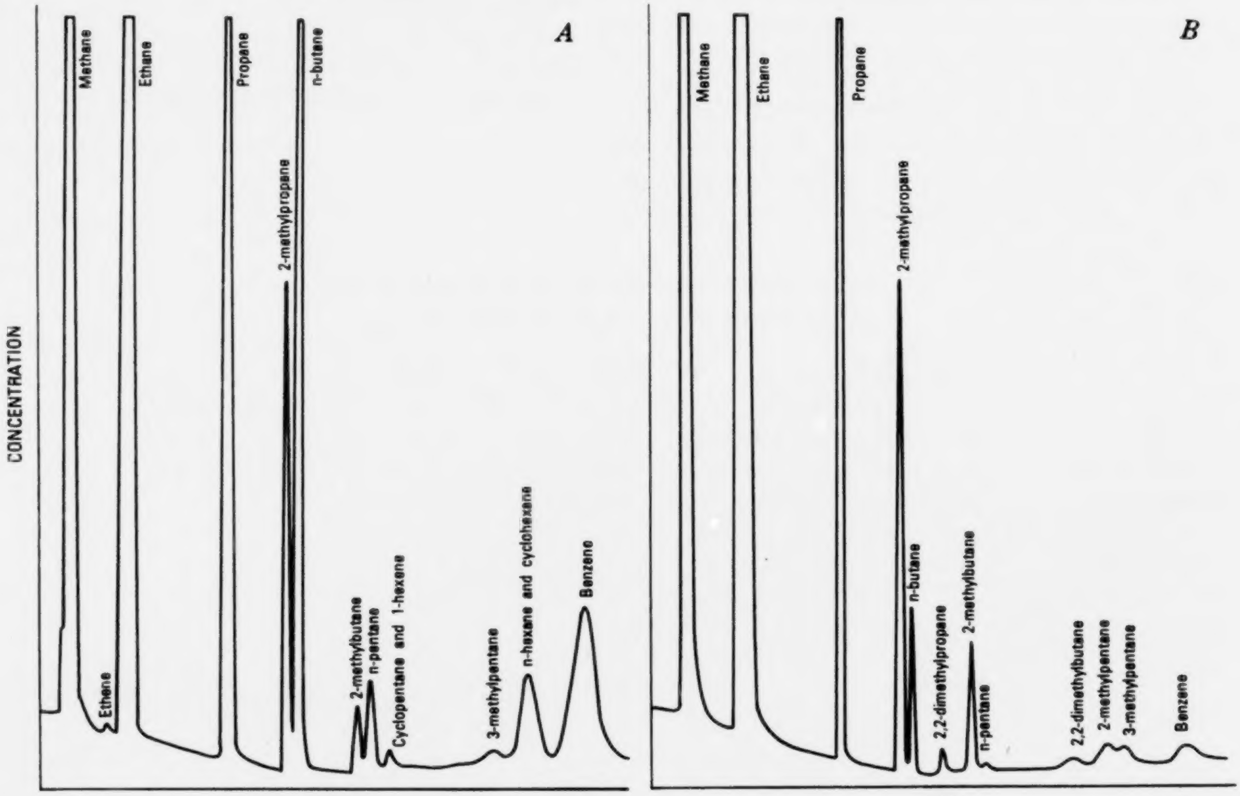

FIGURE 104.—Chromatograms of hydrocarbon gas analyses. *A*, The Geysers steam well. *B*, Highland Springs Reservoir.

ter that may contribute to the CH_4 content, and Moki Beach may be influenced by these deposits to a lesser extent. Several attempts were made to obtain a sample from Sulfur Mound mine and from one of the hot-water wells containing hydrogen sulfide and boron south of Mount Konocti, near Highway 29, but an adequate gas source could not be located.

CONCLUSIONS

Gases of the Geysers-Clear Lake area originate predominantly in the Franciscan Formation, with little or no contribution from magmatic or igneous sources or from the Great Valley sequence. Decomposition of the organic matter in marine sedimentary rocks gives rise to CO_2, H_2S, and hydrocarbon gases. H_2S and H_2, which originate from high-temperature rock-water reactions, are more abundant at The Geysers, where the reservoir temperature is 250°C, than in the Clear Lake area, where the temperature is about 200°C. Oxygen, nitrogen, and argon are brought into these systems by solution in meteoric water entering the thermal fluid reservoir. Overall, the gases from Clear Lake and The Geysers can be considered to result from fluid interaction with rocks of the Franciscan, but they do not indicate any intimate interconnection between the hot-water and steam fields.

REFERENCES CITED

Barnes, Ivan, Hinkle, M. E., Rapp, J. B., Heropoulos, Chris, and Vaughn, W. W., 1973, Chemical composition of naturally occurring fluids in relation to mercury deposits in part of north-central California: U.S. Geological Survey Bulletin 1382-A, 19 p.

Craig, Harmon, 1963, The isotopic geochemistry of water and carbon in geothermal areas, *in* Tongiorgi, Ezio, Nuclear geology on geothermal areas: Pisa, Consiglio Nazionale delle Ricerche, Laboratorio di Geologia Nucleare, p. 17-53.

Giggenbach, W. F., 1976, A simple method for the collection and analysis of volcanic gas samples: Bulletin Volcanologique, v. 39, p. 132-145.

Goff, F. E., Donnelly, J. M., Thompson, J. M., and Hearn, B. C., Jr., 1977, Geothermal prospecting in The Geysers-Clear Lake area, northern California: Geology, v. 5, no. 8, p. 509-515.

Hearn, B. C., Jr., Donnelly, J. M., and Goff, F. E., 1976, Preliminary geologic map and cross-section of the Clear Lake volcanic field, Lake County, California: U.S. Geological Survey Open-File Report 76-751.

Mazor, Fmanuel, and Wasserburg, G. J., 1965, Helium neon, argon, krypton, and xenon in gas emanations from Yellowstone and Lassen Volcanic National Parks: Geochimica et Cosmochimica Acta, v. 29, no. 5, p. 443-454.

Nehring, N. L., and Truesdell, A. H., 1977, Collection of chemical, isotope and gas samples from geothermal wells: Proceedings of the Second Workshop on sampling geothermal effluents, Las Vegas, Nev., 1977, U.S. Environmental Protection Agency Publication EPA-600/7-78-121, p. 130-140.

——— 1978, Hydrocarbon gases in some geothermal and volcanic systems *in* Geothermal energy: A novelty becomes a resource: Geothermal Resources Council Annual Meeting, Hilo, Hawaii, 1978, Transactions, v. 2, p. 483-486.

White, D. E., and Roberson, C. E., 1962, Sulphur Bank, California: A major hot-spring quicksilver deposit, *in* Engel, A. E. J., James, H. L., and Leonard, B. F., eds., Petrologic studies: A volume in honor of A. F. Buddington: New York, Geological Society of America, p. 397-428.

CARBON-13 ISOTOPE VALUES FOR CARBON DIOXIDE GAS AND DISSOLVED CARBON SPECIES IN SPRINGS AND WELLS IN THE GEYSERS-CLEAR LAKE REGION

By MARK HUEBNER

ABSTRACT

Water and gas samples from wells and springs in the Geysers-Clear Lake region have $\delta^{13}C$ values of -11.8 to -19.9 permil for CO_2 (gas) and -9.3 to -11.6 permil for dissolved carbon species. Because $\delta^{13}C$ values from the steam field are more depleted than those in the adjacent hot-water field, carbon dioxide from a deep rock source is probably mixing with carbon dioxide of meteoric origin in the region above the hot-water field. Fractionation between CO_2 (gas) and dissolved carbon species (mainly HCO_3^-) indicate near-equilibrium at measured surface temperatures; however, the data do not agree with reservoir temperatures indicated by chemical geothermometers. The carbon species and the CO_2 (gas) probably reequilibrated during movement of the fluid from the reservoir to the surface.

INTRODUCTION

Carbon isotope compositions can be used to determine the source of CO_2 in gases emanating from hot springs, steam vents, and wells (Craig, 1963; Panichi and Tongiorgi, 1976). Possible major carbon sources include CO_2 outgassed from the mantle, CO_2 dissolved from marine limestone, atmospheric CO_2, and CO_2 from the breakdown of organic matter contained in sedimentary rocks. Craig (1963) and White, Barnes, and O'Neil (1973) reported on carbon isotope geochemistry in the Geysers-Clear Lake region of California. Craig reported $\delta^{13}C$ ranges of -11.0 to -11.5 permil and -6.0 to -10.5 permil for CO_2 (gas) and HCO_3^-, respectively. The bicarbonate samples of White, Barnes, and O'Neil (1973) ranged in $\delta^{13}C$ from $+0.5$ to -10.0 permil.

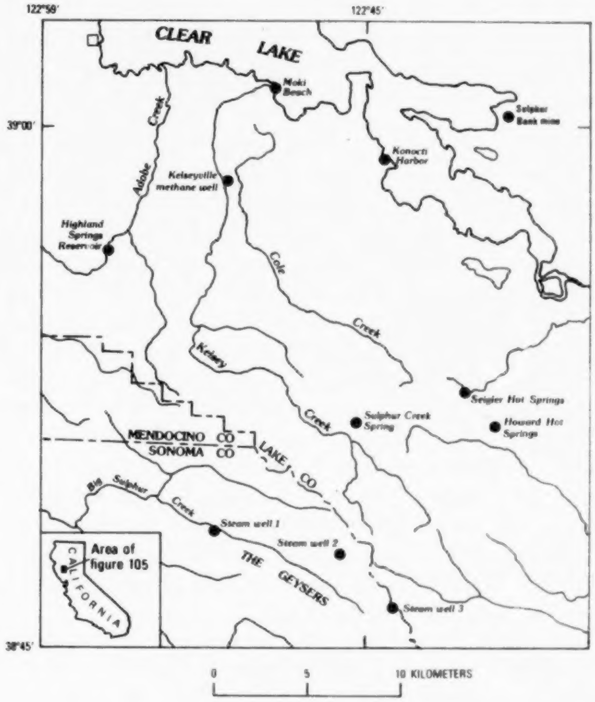
122°59'
122°45'
39°00'
38°45'
CLEAR
LAKE
Moki Beach
Sulphur Bank mine
Konocti Harbor
Kelseyville methane well
Adobe
Creek
Highland Springs Reservoir
Cole
Creek
Kelsey
Creek
Seigler Hot Springs
Sulphur Creek Spring
Howard Hot Springs
MENDOCINO CO
SONOMA CO
LAKE CO
Big Sulphur
Creek
Steam well 1
Steam well 2
Steam well 3
THE GEYSERS
Area of figure 105
CALIFORNIA
0
5
10 KILOMETERS

FIGURE 105.—Sampling sites in the Geysers-Clear Lake region. See table 24 for $\delta^{13}C$ values.

METHODS

Gas samples of CO_2 and water samples containing dissolved carbon species (CO_2, HCO_3^-, CO_3^{2-}) were collected from February to August 1977. Sampling sites included steam wells at the Geysers steam field and warm and hot springs and wells in the Clear Lake region (fig. 105). Total flow (gas + steam condensate) samples were collected at the Geysers steam field through condensing coils connected to a bypass on the wellhead. The condensed steam was cooled to approximately 20°C (Nehring and Truesdell, 1978a) and then allowed into an evacuated 500-mL gas bottle containing 100 mL of 4*N* NaOH. These samples were converted to $SrCO_3$ in the laboratory by adding an excess of a saturated solution of $SrCl_2$ in NH_4OH to 10 mL of the solution in the gas bottle. The $SrCO_3$ was then filtered, washed, and dried.

Gas and water samples were collected at the springs. Gas samples were collected by means of a large funnel connected by Tygon tubing to an evacuated 300-mL gas bottle containing 100 mL of 4*N* NaOH. The funnel was inverted in the spring, the funnel and tubing were filled with water to displace the air, and gas was then collected in the funnel and pumped through the tubing displacing the water before the sample was collected (Nehring and Truesdell, 1978a). These samples were also converted to $SrCO_3$ in the laboratory using the previously described method. Water samples were collected in glass bottles, and the dissolved carbon species were precipitated as $SrCO_3$ in the field, using an excess amount of a saturated solution of $SrCl_2$ in NH_4OH.

Carbon and oxygen isotopic analyses were made on CO_2 liberated from the $SrCO_3$ by the addition of 100 percent H_3PO_4 (McCrea, 1950). All carbon isotope ratios in this chapter are reported as permil deviations from the PDB (Peedee belemnite) standard.

RESULTS

The $\delta^{13}C$ values of the total-flow and gas samples range from –11.8 to –19.9 permil, whereas those of the dissolved carbon species range from –9.3 to –11.6 permil (table 23). The CO_2 in the Geysers steam field shows more depletion in ^{13}C ($\delta^{13}C = -15.9$ to -19.9 permil) than other sample sites except Highland Springs Reservoir (–17.3 permil). These $\delta^{13}C$ values for CO_2 are evidence of an organic source for the carbon and are too light to indicate appreciable contribution from a magmatic source (fig. 106). Further, the trace organic gas compounds do not show a pattern similar to gases from areas associated with igneous magmas (Nehring and Truesdell, 1978b). In the Clear Lake hot-water field, CO_2 (gas) is less depleted in ^{13}C than CO_2 in the Geysers steam field. Mixing of CO_2 from organic sources with CO_2 in meteoric waters could account for these $\delta^{13}C$ values. O'Neil and Barnes (1971) stated that the isotopic composition of carbon species in certain ground waters of California depends on variable contributions of CO_2 from soil, the atmosphere, and marine carbonates.

The area underlying the Clear Lake Volcanics is thought to contain a circulating, dominantly meteoric ground-water system. In such a system, water containing dissolved carbon species from the soil and from the atmosphere would percolate down into deeper sections of the meteoric system, where it picks up CO_2 of organic origin from the underlying hot-water system and then rises to the surface in the springs.

The pH of the springs, which ranges from 5.7 to 7.0, indicates that the major carbon species in the water is bicarbonate (HCO_3^-). O'Neil, Truesdell, and McKenzie (1975) proposed that the carbon isotope fractionation between CO_2 (gas) and HCO_3^- may be a useful indicator of deep temperatures in geothermal systems, but this does not appear to be the case in the Geysers-Clear Lake study area. From the dissolved bicarbonate-carbon dioxide (gas) fractionation curve of Mook, Bommerson, and Staverman (1974) and the differences between $\delta^{13}C$ values of the sampled bicarbonate and CO_2 (gas), calculated isotopic temperatures range from 55° to 88°C. Measured temperatures at the springs ranged from 17° to 52°C (table 24). Although

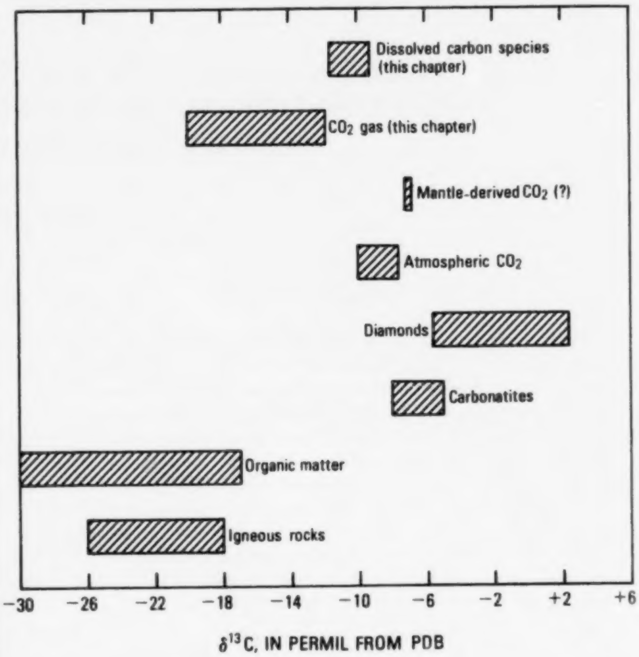

FIGURE 106.—Carbon isotope composition of samples from the Geysers-Clear Lake region compared with isotopic compositions of possible sources. Source data derived from Craig (1963), Taylor, Frenchen, and Degens (1967), and Fuex and Baker (1973). PDB, Peedee belemnite standard.

TABLE 24.—*Carbon-13 isotope values for CO_2 (gas) and dissolved carbon species from springs and wells in the Geysers-Clear Lake region*

	$\delta^{13}C$ (per mil)		pH	Temp. °C	
	Gas	Waters		Observed	Predicted
The Geysers:					
steam well 1	-18.5	--	--	--	--
steam well 2	-19.9	--	--	--	--
steam well 3	-15.9	--	--	--	--
Highland Springs Reservoir	-17.3	--	--	21	--
Moki Beach	-11.8	--	5.7	26	--
Kelseyville methane well	-13.9	--	--	--	--
Sulphur Bank mine	-14.1	--	--	--	--
Konocti Harbor	14.6	-11.4	5.7	74	77
Seigler Hot Springs:					
The Geyser Spring	-15.3	-11.6	5.9	43	70
Hot Sulphur Spring	-13.0	-11.1	6.5-7.0	52	88
Sulphur Creek Spring	-15.2	-10.3	5.7	17	55
Howard Hot Springs:					
Iron Sulphur Spring	-12.9	-9.3	6.5	41	62
Magnesia Spring	-13.0	-10.0	6.5	42	78

the isotopic temperatures are somewhat higher than those measured, the difference is not great, reflecting near-equilibrium at surface temperatures. Subsurface reservoir temperatures of 200°C were inferred by Goff, Donnelly, Thompson, and Hearn (1977) using chemical geothermometry and drill-hole data. The disparity in temperatures indicates that CO_2(gas) $-HCO_3^-$ re-equilibrate during the rise of the geothermal fluids from the deep reservoir.

REFERENCES CITED

Craig, Harmon, 1963, The isotopic geochemistry of water and carbon in geothermal areas, *in* Tongiorgi, Ezio, ed., Nuclear geology on geothermal areas: Pisa, Consiglio Nazionale delle Ricerche, Laboratorio di Geologia Nucleare, p. 17-54.

Fuex, A. N., and Baker, D. R., 1973, Stable carbon isotopes in selected granitic, mafic and ultramafic igneous rocks: Geochimica et Cosmochimica Acta, v. 37, p. 2509-2521.

Goff, F. E., Donnelly, J. M., Thompson, J. M., and Hearn, B. C., Jr., 1977, Geothermal prospecting in The Geysers-Clear Lake area, northern California: Geology, v. 5, p. 509-515.

McCrea, J. M., 1950, On the isotopic chemistry of carbonates and a paleotemperature scale: Journal of Chemical Physics, v. 18, no. 6, p. 849-857.

Mook, W. G., Bommerson, J. C., and Staverman, W. H., 1974, Carbon isotope fractionation between dissolved bicarbonate and gaseous carbon dioxide: Earth and Planetary Science Letters, v. 22, no. 2, p. 169-176.

Nehring, N. L., and Truesdell, A. H., 1978a, Collection of chemical isotope and gas samples from geothermal wells: U.S. Environmental Protection Agency, Workshop on Sampling Geothermal Effluents, 2d, Las Vegas, 1977, Proceedings, document EPA-600/7-78-121, p. 130-140.

—— 1978b, Hydrocarbon gases in some geothermal and volcanic systems, *in* Geothermal energy: A novelty becomes a resource: Geothermal Resources Council Transactions, Hilo, July 1978, p. 483-486.

O'Neil, J. R., and Barnes, Ivan, 1971, ^{13}C and ^{18}O compositions in some fresh carbonates associated with ultramafic rocks and serpentinites: Western United States: Geochimica et Cosmochimica Acta, v. 35, p. 687-697.

O'Neil, J. R., Truesdell, A. H., and McKenzie, W. F., 1975, ΔC^{13} (CO_2-HCO_3^-) as a possible geothermometer: United Nations Symposium on the Development and Use of Geothermal Resources, 2d, San Francisco, May, 1975, Abstracts, no. III-71.

Panichi, Constanzo, and Tongiorgi, Ezio, 1976, Carbon isotopic composition of CO_2 from springs, fumaroles, moffettes and travertines of central and southern Italy: A preliminary prospection method of geothermal areas: United Nations Symposium on Geothermal Energy, 2d, San Francisco, 1975, Proceedings, p. 815-825.

Taylor, H. P., Jr., Frechen, Josef, and Degens, E. T., 1967, Oxygen and carbon isotopic studies of carbonatites from the Laacher See District, West Germany and the Alnö District, Sweden: Geochimica et Cosmochimica Acta, v. 31, p. 407-430.

White, D. E., Barnes, Ivan, and O'Neil, J. R., 1973, Thermal and mineral waters of nonmeteoric origin, California Coast Ranges: Geological Society of America Bulletin, v. 84, p. 547-559.

CHEMICAL COMPOSITION OF WATER AND GAS FROM FIVE NEARSHORE SUBAQUEOUS SPRINGS IN CLEAR LAKE

By J. M. THOMPSON, J. D. SIMS,
SANDHYA YADAV, and M. J. RYMER

ABSTRACT

Gas and water samples can easily be collected from shallow submerged springs by using a peristaltic battery-powered pump. Qualitatively, sulfate, ammonia, chloride, and lithium concentrations may be used to estimate the amount of lake-water contamination. Our deep gas sampling technique, which uses an inverted funnel and long tube to the surface, was employed only where visibility was greater than 2-3 m. Analyses of gas samples collected just under the lake surface compared to samples collected near the lake bottom indicates air contamination in the near-surface samples. Thus, gas samples should be collected deep underwater or as near the spring vent or gas orifice as possible.

INTRODUCTION

In 1971 the Geysers-Clear Lake area was selected by the U.S. Geological Survey geothermal research program as a region for extensive investigation. Under this program, thermal-water samples were first collected in December 1974 during a winter of normal rainfall; the last samples were collected in February 1977 during a period of drought. The drought exposed many springs that normally are submerged by Clear Lake. The collection and analysis of these springs is reported by Thompson, Goff, and Donnelly-Nolan (this volume). The 1977 collection was undertaken to investigate the drought's effect on the previously sampled springs.

Sims and Rymer (1976) mapped numerous springs and gas vents in Clear Lake, both along the shore and in open water. Most springs in open water are located in a line south of Lucerne and along a line across the mouth of Konocti Bay from Wheeler Point to Fraser Point (fig. 107). Goff, Donnelly, Thompson, and Hearn (1976, 1977) indicated that the Konocti Bay fault zone terminates near Little Borax Lake. Chemical analyses of spring waters from across the mouth of Soda and Dorn Bays suggest that the Konocti Bay fault zone curves westward and that these springs are an expression of the fault. Water from Kono Tayee, across the Buckingham Peninsula from Horseshoe Spring, does not appear to be related to other springs along the Konocti Bay fault zone (compare Mg, Na, HCO_3, SO_4, and Cl in samples CLW 15 and 83, table 25).

In 1978 another collection was made of springs from Dorn Bay (the same as Moki Beach) to Wheeler Point when two springs (Moki Beach and Riviera Beach springs) were submerged and three springs (Soda Bay, Horseshoe, and Konocti Bay springs) could be flooded by high windblown waves. The purpose of the 1978 collection was (a) to learn if any springs had changed composition significantly; (b) to test the development of a simple method of collecting water and gas from some submerged springs and gas vents mapped by Sims and Rymer (1976); and (c) to identify one or more dissolved constituents that would allow calculation of the amount of lake-water dilution of the submerged spring-water sample. Owing to the various collectors and changes in lake levels, only three springs (LJ-78-11, 12, and 15) were positively resampled. The others are the nearest active spring to the earlier location. A special effort was made to recollect water samples from currently submerged springs that had been above lake level during the 1976 drought, when the lake was at least 1 m lower than the bottom of the gage at Lakeport, Calif. (E. J. LaCornu, oral commun., 1978).

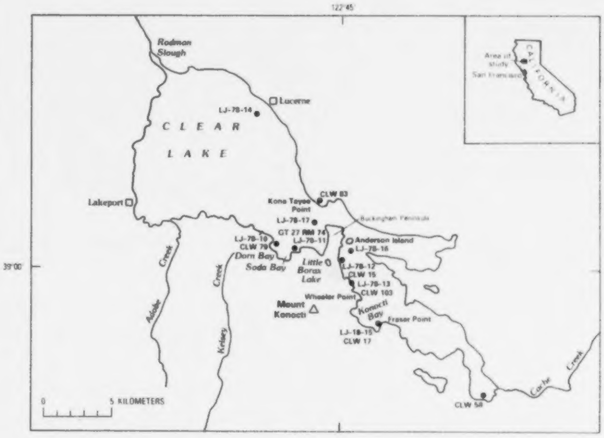

FIGURE 107.—Clear Lake, Calif., and vicinity, showing location of samples listed in table 25.

SAMPLE COLLECTION

Samples were collected and treated using methods of Thompson (1975) and Thompson, Presser, Barnes, and

Bird (1975), which are briefly summarized here. Samples from springs issuing above lake level were collected from as near the orifice as possible in a 1-L plastic bottle attached to a 2-m aluminum pole. All but two of the samples were then decanted into a plastic filter reservoir (1-L capacity) and filtered through a 0.45-μm-pore-size membrane filter. One aliquot was then acidified with $12N$ HCl (4 mL/L) for cation analyses of this filtered sample; another aliquot for anion analysis was not acidified. An additional 10 mL of the unfiltered spring water was transferred by pipette into 50 mL of distilled water for silica analysis. Two samples (CLW 79 and 103) were collected and filtered by use of a syringe filter system. The sample was drawn into the syringe; a 25-mm-diameter filter holder containing a 0.45-μm-pore-size membrane filter was then attached, and the sample was forced through the filter. A filtered-acidified and a filtered-unacidified aliquot were collected. A silica sample also was taken as described above. Samples of Clear Lake waters are "grab" samples that were not filtered.

Water samples from springs at the bottom of Clear Lake were located by feel or visual sighting of exsolved gas bubbles or by a measurable increase in water temperature. Plastic tubing was then positioned in the orifice and attached to a variable-rate peristaltic pump that was powered by a 200-W power inverter connected to a 12-V lead-acid storage battery. After approximately 10 minutes of pumping to thoroughly purge the tubing of lake water, the sample was collected in the plastic filter reservoir described above.

All gas samples except the sample from the bottom of Dorn Bay were collected by the methods described by Nehring (this volume). The Dorn Bay submerged sample was collected by a scuba diver, who filled a funnel and tubing with lake water and placed the funnel over the spring orifice, so that gas displaced the water in the funnel. The tubing extended to a boat on the lake surface. The water remaining in the tubing was removed with a pumping syringe attached to a three-way plastic stopcock. A gas collection bottle was then attached to the tubing, and the gas collected as described by Nehring (this volume).

The funnel technique works well at Clear Lake for springs submerged in 2 or 3 m of water. At deeper locations the pressure of the overlying water column significantly compresses the gases so that the bubbles are too small to be seen under conditions of restricted visibility such as in Clear Lake. However, deep (>10 m) submerged springs are easily located using a combination of visual sightings of the expanding gas bubbles on the surface and a recording fathometer that distinguishes between the difference in density of the gas-charged water and the surrounding lake water. Where underwater visibility exceeds 2-3 m, the method should be feasible to depths of ~25 m.

FIELD DETERMINATIONS

Temperatures of springs were measured using a maximum-reading mercury-in-glass thermometer. The pH of the 1974 to 1977 samples was determined by pH indicator strips; a pH electrode and meter was used on the 1978 samples. Dissolved ammonia species and dissolved hydrogen sulfide species were determined spectrophotometrically with a Bausch and Lomb (B&L) "mini spec 20" and B&L NH_3 and H_2S "spectrokits."

LABORATORY DETERMINATIONS

Cations in the water sample were determined from the filtered-acidified sample on all but the raw acidified 1978 lake-water samples, and anions from the filtered-unacidified sample on all but the 1978 lake samples. Sodium, lithium, rubidium, cesium, strontium, and barium concentrations were determined by flame emission spectroscopy with excess potassium ion (~1,000 mg/L). Potassium was measured similarly but with excess sodium ion (~1,000 mg/L). Magnesium and calcium concentrations were determined by atomic-absorption spectroscopy (AAS) with added lanthanum (1 percent v/v); iron, manganese, and zinc were also measured by AAS but with excess potassium ion (~1,000 mg/L). Silica was determined as described by Shapiro and Brannock (1956), except that 640 nm was used to measure the absorbance. Chloride was determined by potentiometric titration with standardized silver nitrate, a silver indicator electrode, and a double-junction reference electrode. Alkalinity as bicarbonate was measured by a pH titration with standardized sulfuric acid and a combination pH electrode. The starting point of this titration is taken as the laboratory pH. Sulfate and boron were determined as described by Brown, Skougstad, and Fishman (1970). Fluoride was determined by an ion-specific electrode using a tris buffer, as described by Thompson, Presser, Barnes, and Bird (1975). In the 1978 samples fluoride was measured using a CDTA buffer, as described by the manufacturer (Orion Research, Inc., 1976, p. 2-4).

Gas samples were analyzed by gas chromatograph equipped with about 2 m Poropak Q and about 7 m of 5A molecular sieve columns. The sodium hydroxide solution was analyzed for CO_2, H_2S, and NH_3. CO_2 and H_2S were determined gravimetrically–the CO_2 by precipitation as $SrCO_3$, and the H_2S by precipitation as $BaSO_4$ after oxidation with H_2O_2 to sulfate. NH_3 was determined by an ion-selective electrode. The complete procedure is described by Nehring (this volume).

DISCUSSION

The analytical results of the water analyses are shown in table 25. The 1974 Big Soda Spring analysis is courtesy of R. M. Mariner (unpub. data, 1975). Because most samples collected before 1978 contain higher total dissolved solids than those collected in 1978, dilution by Clear Lake is assumed. Qualitatively, sulfate and ammonia concentrations indicate the amount of lake-water dilution: sulfate is in the lake water; ammonia is in the spring water. Using this criterion, it appears that the sample from Dorn Bay is diluted with approximately 50 percent lake water. Chloride and lithium concentrations also can be used to estimate mixing proportions. Most of the springs and possibly all of them may be diluted with various amounts of Clear Lake water (fig. 108). The October 19, 1976 sample from Riviera Beach (CLW 103) contains 34 mg/L Cl. The Riviera Beach sample (LJ-78-13) collected in September 1978 contains 41 mg/L Cl. Because the 1978 sample was collected using the submerged procedure, we would expect its Cl concentration to be lower than the 1976 sample. Possible reasons for this are (a) the same spring was not collected, (b) the 1976 sample was

TABLE 25.—*Chemical analyses of spring water along the shore of Clear Lake*

[All analyses in milligrams per liter. <, less than; --, not measured]

													Kono Tayee	Clear Lake		
Spring name	Moki Beach	Dorn Bay	Big Soda Spring		Horseshoe Spring		Riviera Beach		Konocti Bay				well	Lower Lake	off Lucerne	near Anderson Island
Sample no	CLW 79	LJ-78-10	GT27RM74[1]	LJ-78-11	CLW 15	LJ-78-12	CLW 103	LJ-78-13	CLW 17	LJ-78-15			CLW 83	CLW 58	LJ-78-14	LJ-78-16
Date collected	29 July 76	6 Sept 78	10 Sept 74	6 Sept 78	6 Dec 74	7 Sept 78	19 Oct 76	7 Sept 78	6 Dec 74	8 Sept 78			4 Dec 76	24 Jun 76	7 Sept 78	8 Sept 78
Latitude	39°01.0'		39°00.5'		39°59.6'		38°57.5'		38°59.2'				39°02.4'	38°56.9'	39°04.8'	30°08.0'
Longitude	122°48.1'		122°47.0'		122°44.5'		122°42.2'		122°44.0'				122°45.7'	122°32.3'	122°48.3'	122°44.6'
Temp. (°C)	27	26	30.5	31	41.5	41	34	30	35	33			21.5	24	21	22
Field pH	6.0	5.89	5.81	5.80	6.6	6.13	--	5.7	6.7	5.81			5.9	5.7	5.8	5.9
Laboratory pH	6.87	6.19	--	6.30	7.58	6.74	7.55	6.46	7.94	6.22			7.97	7.80	7.91	7.99
Water depth (m)	--	-2	+.1	+.1	--	.05	--	-.75	--	+.1			--	--	-.1	-.1
Gage height[2]	.65	2.47	2.59	2.53	1.89	2.49	<.00	2.49	1.89	2.47			--	1.37	2.49	2.47
SiO_2	129	83	136	137	163	159	139	104	137	133			55	6	22	21
Fe	194	9.9	12	19	4.5	4.8	5.6	4.1	4.5	3.0			21	<.02	1.2	1.3
Mn	.4	.26	--	.67	.21	.25	.2	.13	.23	.21			.43	<.02	<.05	<.05
Zn	--	.13	--	.02	--	<.01	--	.97	--	<.01			.05	.04	<.01	.01
Ca	79	60	93	89	155	138	100	69	100	83			66	24	30	26
Mg	104	66.9	130	162	144	146	83	110	82	72			28	16	19	17
Sr	--	.4	--	.6	--	1.0	--	.7	--	.6			--	--	.2	.3
Ba	--	1.2	--	1.4	--	1.8	--	1.2	--	1.2			--	--	.3	.4
Na	90	78	100	84	125	106	90	69	84	69			24	22	17	11
K	13	5.7	13	10	21.5	13	11	6.1	13.2	8			1.6	3	2	1
Li	.41	.22	.44	.36	.51	.47	.24	.32	.33	.27			.01	.02	.03	.03
Cs	--	.14	.1	.18	--	.24	--	.22	--	.2			--	--	.2	.14
Rb	--	.08	.04	.11	--	.16	--	.14	--	.12			--	--	.1	.09
NH_4	--	2.4	1.9	3.6	--	2.0	--	1.9	--	.9			--	--	<.1	<.1
HCO_3	936	611	1,190	1,090	1,310	1,420	923	852	775	693			306	232	160	162
SO_4	1	7	1	2	1	1	1	1	<.5	2			31	11	11	11
Cl	59	36	66	65	78	76	34	41	48	44			7.3	3	4	4
F	.11	.2	.3	.45	.37	<.1	.2	.32	.5	<.1			.21	.15	<.1	.11
B	13	10.3	15	12.5	19	15.3	13	9	9	6.5			5.3	1.6	.65	.75
H_2S	--	<0.0	--	<0.0	.	<0.0	--	<0.0	--	<0.0			--	--	--	--

[1] R. M. Mariner, unpub. data, 1975.

[2] At Lakeport gage.

TABLE 26.—*Chemical analyses of spring gases along the shore of Clear Lake*

[Analyses in mole percent. Analyst, Nancy Nehring. Looked for but not detected above 0.001 mol percent: H_2S, He, and C_2H_6; n.d., not detected; —, not determined]

Sample locality	Sample No.	Date of collection	Sample depth (m)	CO_2	NH_3	H_2 ($\times 10^{-[illegible]}$)	Ar ($\times 10^{-[illegible]}$)	O_2	N_2	CH_4	Total
Dorn Bay	LJ-78-10A	Sept 6, 1978	Surface	90.45	0.023	4.58	58	0.634	2.52	5.77	99.45
	LJ-78-10B	do	−2.0	96.13	.0064	n.d.	28.2	.075	.537	3.02	99.79
Moki Beach	([1])	--	--	99.23	--	2.5	3.3	.0047	.13	.63	100.70
Soda Bay	LJ-78-11	Sept. 7, 1978	+.1	99.79	.0119	3.55	.64	.011	.0485	.104	99.92
Horseshoe Spring	LJ-78-12	do	+.05	99.57	n.d.	2.19	1.6	.0271	.124	.189	99.91
Riviera Beach	LJ-78-13	do	−.75	94.73	.0235	n.d.	49	.132	1.16	3.45	99.54
Konocti Bay	LJ-78-15	Sept 8, 1978	+.1	87.02	.0282	n.d.	68	.124	4.45	7.01	98.71
	([1])	--	--	94.76	--	n.d.	25	.041	1.48	3.76	100.07
Shag Rock	LJ-78-17	--	-.05	64.73	.304	n.d.	386	6.34	23.8	n.d.	99.50

[1] From Nehring (this volume).

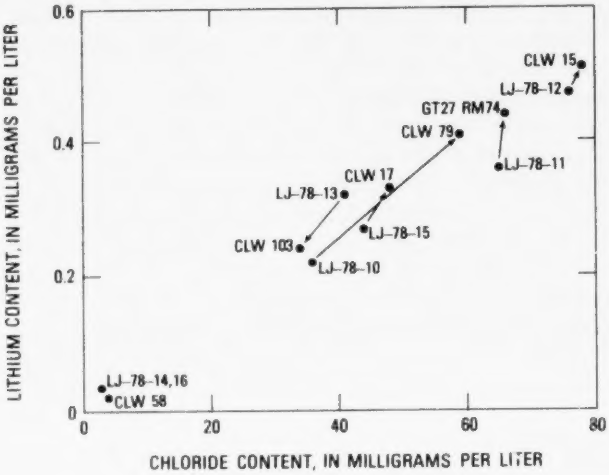

FIGURE 108.—Plot of lithium versus chloride.

diluted by wind-generated waves, or (c) a real change occurred for some unknown reason.

The gas compositions of the various springs are shown in table 26. Two gas analyses from Nehring (this volume) are also listed. The two gas samples from Dorn Bay reveal the influence of the surrounding lake water. The nitrogen and oxygen concentrations in the surface sample are greater than in the bottom sample; furthermore, the N_2:O_2 ratio is 3.97 in the surface sample and 7.17 in the bottom sample. We interpret this difference in N_2:O_2 to result from contamination of the rising gas by air that exsolves from overlying water as the gas passes through it. This same situation is illustrated in the gas from the Shag Rock locality. The surface sample contains 30.1 mol percent air gases. Unfortunately, owing to limited visibility (<1 m) on the bottom and small size of the escaping bubbles, no bottom sample was collected at Shag Rock. It would be interesting to correlate the amount of air gases in surface gas sample of springs or vents with depth of overlying water and the amount of air gases in the bottom sample with bottom depth. Unfortunately, with only two samples, the results here are statistically meaningless.

REFERENCES CITED

Brown, Eugene, Skougstad, M. W., and Fishman, M. D., 1970, Methods for collection and analysis of water samples for dissolved minerals and gases: U.S. Geological Survey Techniques of Water Resources Investigations, Book 5, Chapter Al, 160 p.

Goff, F. E., Donnelly, J. M., Thompson, J. M., and Hearn, B. C., Jr., 1976, The Konocti Bay fault zone, California: Potential areas for geothermal exploration [abs.]: Geological Society of America Abstracts with Programs, v. 8, no. 3, p. 375-376.

——— 1977, Geothermal prospecting in The Geysers-Clear Lake area, northern California: Geology, v. 5, p. 509-515.

Orion Research, Inc., 1976, Instruction manual, fluoride elecrodes: Cambridge, Mass., 32 p.

Shapiro, Leonard, and Brannock, W. W., 1956, Rapid analysis of silicate rocks: U.S. Geological Survey Bulletin 1036-C, p. 19-56.

Sims, J. D., and Rymer, M. J., 1976, Map of gaseous springs and associated faults in Clear Lake, California: U.S. Geological Survey Miscellaneous Field Studies Map MF-721, scale 1:48,000.

Thompson, J. M., Selecting and collecting thermal springs for chemical analysis: A method for field personnel: U.S. Geological Survey Open-File Report 75-68, 12 p.

Thompson, J. M., Presser, T. S., Barnes, R. B., and Bird, D. B., 1975, Chemical analyses of the waters of Yellowstone National Park, Wyoming, 1966-1973: U.S. Geological Survey Open-File Report 75-25, 59 p.

LATE PLEISTOCENE STRATIGRAPHY AND PALYNOLOGY OF CLEAR LAKE

By JOHN D. SIMS, DAVID P. ADAM, and MICHAEL J. RYMER

ABSTRACT

Clear Lake consists of a subcircular main basin with two narrow arms extending to the east-southeast and southeast. Eight continuous cores, from 13.9 to 115.2 m long, taken from the lake sediments were predominantly open-water sapropelic mud similar to the mud currently accumulating in Clear Lake. Also present in the lake sediments are a wedge of sandy and gravelly deltaic sediment, from the southern part of the main basin, shallow-water peat and peaty mud that underlie sapropelic mud in the two arms of the lake, and thin volcanic ash beds that are present in all but one of the cores.

Radiocarbon dates of peat beds and carbonaceous sediments in core 7, from the southeast-trending arm (Highlands Arm) permit the estimation of ages for ash beds and seismotectonic and paleoclimatic events for approximately the last 40,000 years. Chronologic control for core 4 from the main basin of the lake, the other core of major concern in this report, is based on correlations of its ash beds and pollen curves with their radiometrically dated counterparts in core 7. Other Clear Lake cores also contain radiometrically dated horizons, but they have not been analyzed for pollen.

Analyses of pollen from cores 4 and 7 show repeated abrupt changes between high abundance of oak (*Quercus*) and high abundance of pine (*Pinus*) pollen, where oak and pine vary inversely with each other. These changes are interpreted as due to fluctuations in the elevation distribution of oak in the hills surrounding Clear Lake in response to changes in climate. Therefore, the oak-pollen curve from Clear Lake may be considered as an uncalibrated paleoclimatic curve, which strongly resembles curves of deep-sea ^{18}O content in foraminifers, and dates the oldest sediment recovered in the Clear Lake cores at approximately 130,000 years old.

INTRODUCTION

Clear Lake lies in a fault-bounded, seismically active intermontane valley on the north edge of the Clear Lake volcanic field. Eight 12- to 15-cm-diameter cores ranging from 13.9 to 115.2 m in length (fig. 109; table 27) were removed from the lake bottom in 1973. Of major concern in this report are two of these cores (cores 4 and 7), which were described and analyzed by Sims and Rymer (1975a, b). In this report we present new data on ^{14}C age dates, ash-bed correlations, sedimentation rates, and pollen spectra that are used to date the cores. We also present a paleoclimatic record of approximately 130,000 years for the Clear Lake area, as inferred from pollen in core 4.

BACKGROUND

The Clear Lake basin has an area of about 1,370 km², and elevations in the basin range from approximately 400 to 1,475 m. The lake has an area of 114 km², an elevation of about 400 m, an average depth of 9 m, and a maximum depth of 13 m. The lake is not stratified, and on calm summer days the bottom water becomes depleted in oxygen. The Mayacmas Mountains, on the west and south edges of the Clear Lake basin, separate the region from the Russian River drainage and from the Pacific Ocean, some 50-80 km to the west. Elevations along the crest of the Mayacmas Mountains vary between 600 and 1,440 m. To the north, adjacent to the Clear Lake basin, elevations are generally above 1,200 m, and higher ground is commonly above 1,500 m.

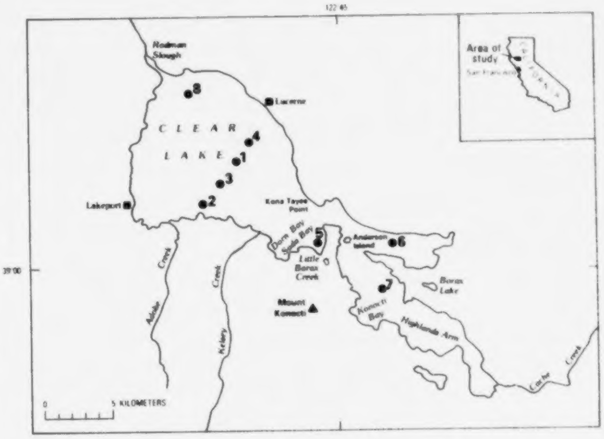

FIGURE 109.—Clear Lake, Calif., showing core sites and geographic features referred to in this chapter.

TABLE 27.—*Total length and recovery and the number of ash beds and estimated maximum age for eight cores from Clear Lake*

[Modified from Sims (1976)]

Core[1]	Water depth (m)	Core length (m)	Recovery (percent)	Number of ash beds	Estimated age of core bottom (yr)
1	8.8	52.6	35.0	6	40,000
2	4.3	13.9	88.0	0	10,000-15,000
3	8.4	69.0	96.0	43	36,000
4	8.4	115.2	92.0	56	130,000
5	7.6	22.6	94.0	7	28,000
6	12.2	21.6	99.0	8	36,000
7	12.8	27.4	94.9	26	40,000
8	5.2	20.5	99.6	5	24,000

[1] Core diameters range from 12 to 15 cm.

The roughly circular main basin of the lake (fig. 109) is bounded on the northeast and east by steep northwest-trending ridges of the Jurassic and Cretaceous Franciscan assemblage of Bailey, Irwin, and Jones (1964). Alluvium-filled valleys and low hills of the Franciscan assemblage bound the rest of the main basin. The Franciscan assemblage also occurs along the north and south shores of the east-west-trending Oaks Arm and part of the north shore of the more southerly Highlands Arm (fig. 109). The southern half of the north shore of the Highlands Arm is bounded by alluvium-filled valleys and low hills of Pleistocene fluvial and lacustrine rocks, the Jurassic and Cretaceous Great Valley sequence, and flows and pyroclastic rocks of the Pliocene to Holocene Clear Lake Volcanics of Hearn, Donnelly, and Goff (1976a, b). Along the south shore of the Highlands Arm the lake is bounded by steep slopes of volcanic constructional features in the Clear Lake Volcanics.

LATE CENOZOIC GEOLOGIC HISTORY

The late Cenozoic geologic history of the Clear Lake region was dominated by faulting and volcanic activity. Northwest-trending faults, which are subparallel to the San Andreas fault zone, are the prominent structural features of the region (McLaughlin, this volume). Local northwest-trending faults are typically contacts between Mesozoic and other units in the Clear Lake area, and similar northwest fault trends are imprinted on the overlying Clear Lake Volcanics (Hearn and others, 1976b) and other Cenozoic deposits. The major north-northwest- and northwest-trending faults that dissect the Clear Lake volcanic field are still active (Hearn and others, this volume). Late Cenozoic faults are also inferred to control shoreline orientation in the Oaks and Highlands Arms of Clear Lake (Hearn and others, 1976a; E. V. Ciancanelli, California Geothermal, Inc., written commun., 1974), as well as the main basin of Clear Lake (Sims and Rymer, 1976). Movement along faults bounding the lake may relate to volcanic activity, which began more than 2 m.y. ago in this region (Donnelly-Nolan and others, this volume). Downdropping along these faults has maintained the lake basin and has allowed the accumulation and preservation of a thick section of sediment which records Quaternary history in the basin.

Pleistocene lacustrine deposits older than those in cores from Clear Lake are found in isolated outcrops and in water wells dug in alluviated valleys near the lake. These older deposits, referred to as the Kelseyville and Lower Lake Formations (Rymer, 1981) are present in Big Valley, south of the main body of the lake, and near the outlet of the lake in the southern part of Highlands Arm, respectively. The Lower Lake and Kelseyville Formations are in part contemporaneous with the Clear Lake Volcanics of Hearn, Donnelly-Nolan, and Goff (1976a) and probably accumulated in fault-controlled subbasins of an ancestral Clear Lake from about 0.6 to between about 0.2 and 0.1 m.y. ago (Rymer, 1981). This interval includes the time of the extrusion of the greatest volume of lava in the Clear Lake volcanic field (0.6 to 0.3 m.y. ago; Donnelly-Nolan, 1977). Late Pleistocene and Holocene lacustrine deposits are present in the Upper Lake area, north of the main body of the lake.

VEGETATION

Vegetation maps that include the Clear Lake area are those of Clark (1937), Kuchler (1964, 1977), Livingston and Shreve (1921), and Knapp (1965); also of interest are the species distribution maps in Little (1971) and Griffin and Critchfield (1972). The maps by Kuchler (1964, 1967) describe the potential natural vegetation; that is, the vegetation that would ultimately prevail under the present climate in the absence of human influence. He recognized four vegetation types in the Clear Lake basin: (1) chaparral, (2) blue oak/digger pine forest, (3) Coast Ranges montane forest, and (4) mixed hardwood forest.

The location of the Clear Lake basin at the south end of the main mountain mass of the inner Coast Ranges has assured that high-elevation plants have always had a ready access to the basin during times of cooler climate. The major potential paths of plant migration to and from lower elevations are to the east through the present canyon of Cache Creek, the present outlet of Clear Lake, and through the Putah Creek drainage to the southeast of the present outlet of Clear Lake. During warm intervals, these routes provided for the rapid reestablishment of plant species, particularly oaks (*Quercus* spp.), that had been displaced from the Clear Lake basin during cool periods. Another access route to low elevations, which was probably of only minor biogeographic importance, is the canyon now occupied by Blue Lakes and Upper Cold Creek through which Clear Lake possibly once drained to the northwest via Cold Creek into the Russian River (Davis, 1933; Hopkirk, 1973).

CORE SEDIMENTS

The sites of the cores were chosen to give a representative sampling of the various parts of the lake. The principal sediment in most cores (table 28) is a fine-grained grayish-brown sapropelic mud similar to sediments currently accumulating in Clear Lake. Extensive bioturbation has greatly disturbed some contained ash beds and primary depositional and deformational structures in the sediments. Gravel and sand are major components in cores 1, 2, and 3, and peat is abundant in the lower sections of cores 6 and 7 (table 28). Volcanic-ash beds are present in all cores except core 2, and range in thickness from 0.5 to 26 cm.

Core 4 is about equidistant from the mouth of Kelsey Creek and Rodman Slough, the major streams entering Clear Lake. The core is 115.2 m long and contains mud throughout its length similar to the mud that is currently accumulating in Clear Lake. Mean grain sizes of sediment samples from core 4 (table 29) range from $5.81 \pm 0.34\phi$ (18 μm) to $6.26 \pm 0.41\phi$ (12 μm). No significant trends in grain-size variation are seen with depth in the core.

Core 7 is a 27.4-m-long section from beneath about 13 m of water in the center of the Highlands Arm. The top 6.7 m of sediment is open-water lake mud that contains abundant remains of large fish (Casteel and others, 1977) and sparse plant remains. Below 6.7 m in the core, the sediments consist of shallow-water lake muds interbedded with sedge peat. Grain-size analyses are difficult in most material of core 7 because of the abundance of macerated plant materials and peat fibers.

Volcanic-ash layers are the only distinctive and widespread marker beds in the cores. Most ash beds were identified only by X-ray radiographic characteristics; the beds were generally not apparent in the split cores (Sims, 1976). All ash beds, except one, are infered to be derived from the Clear Lake volcanic field.

Core 4 contains 56 ash beds or probable ash beds, all but one of which are identified only in X-ray radiographs. The uppermost 16 ash beds have been correlated with similar units in other cores (Sims, 1976; fig. 110). The correlations are based on stratigraphic position, bed thickness, and ^{14}C age of intercalcated organic-rich beds. Sims (1976) pointed out that the tentative chronology derived from ash-bed correlations between core 4 and other cores was not in agreement with the chronology suggested by the pollen curve. These ash-bed correlations are further suspect on the basis of new ^{14}C age dates discussed below.

A distinctive and easily identifiable bed of rhyolitic ash, which has undergone little alteration (ash 36, at a depth of 68.5 m in core 4, fig. 110), is tentatively correlated with the rhyolite of Borax Lake, described by Hearn, Donnelly, and Goff (1976b). The rhyolite of Borax Lake has been K-Ar dated at 91,000±13,000 years by the K-Ar method (Donnelly-Nolan and others, this volume).

Core 7 contains 26 ash beds or probable ash beds, commonly interbedded with peat. Thus the ash beds are easily dated indirectly by ^{14}C methods. In addition to the locally derived ashes of basaltic and andesitic composition in core 7, there is a distinctive ash bed of rhyolitic composition. This bed, dated at 17,500±300

TABLE 28.—*Descriptions of cores from Clear Lake*

[from Sims (1976]

Core No.	Depth interval (m)	Description
1	0-20	Fine, very dark grayish brown to dark-brown (10YR3/2 to 10YR2/2) sapropelic mud.
	20-36	Interbedded greenish-gray (5BG4/1 to 5G45/1) to grayish-green (5G5/4) sand and sandy silt.
	36-52	Mud similar to upper unit; data based on drill cuttings only.
2	0-4.2	Fine, very dark grayish brown (10YR3/2) sapropelic mud.
	4.2-13.9	Interbedded greenish-gray (5G3/1 to 5G4/1) soil (?) and silty or sandy soil (?), and greenish-gray (5BG3/1 to 5BG4/1) gravel.
3	0-9.3	Olive-gray (5Y4/2) sapropelic mud.
	9.3-35.6	Interbedded dark-greenish-gray (5G3/1 to 5G4/1), medium to coarse sand, gravel, sandy gravel, silt, silty mud, and sandy silt interbedded with thin (10 cm) beds of carbonaceous mud and volcanic ash.
	35.6-69.0	Olive-gray (5Y3/2 to 5Y5/2) to gray (N5) silty clay, clay, silty sand, and sand.
4	0-115.2	Gray to dark-gray (5Y5/1 to 5Y4/1), greenish-gray to dark-greenish-gray (5G5/1 and 5BG5/1 to 5GY5/1) and dark-bluish-gray (5B4/1) sapropelic mud with interbedded volcanic ash beds.
5	0-22.6	Olive-gray to dark-olive-gray (5Y4/2 to 5Y3/2) sapropelic mud with seven interbedded volcanic ash beds.
6	0-7.6	Fine, very dark grayish brown to very dark brown (10YR4/2 to 5Y3/2) sapropelic mud.
	7.6-21.6	Interbedded brownish-black (5YR2/1) granular peat, peaty mud, mud, clay and volcanic ash.
7	0-6.7	Fine, very dark grayish brown to very dark brown (10YR3/2 to 10YR2/2) sapropelic mud.
	6.7-27.4	Interbedded fibrous, brown (54R5/3) peat, mud, clay, and volcanic ash.
8	0-20.5	Olive-gray (5Y3/2 to 5Y5/2) sapropelic mud with five interbedded ash beds.

The colors of the type 10YR, 5Y, and 5YR are generally due to oxidation after removal from the ground and during transport and storage prior to study. Other colors, such as greenish gray or dark greenish gray (5GY6/1 or 5BG4/1), are considered to be representative of the unoxidized sediments.

TABLE 29.—*Grain-size analyses from core 4, Clear Lake*

Depth (m)	Phi mean[1] ($\bar{X}_\phi$)	Phi standard deviation (S_ϕ)	Moment 3[2] ($M_{3\phi}$)	Moment 4[3] ($M_{4\phi}$)	Skewness[4] (Sk_ϕ)	Kurtosis[5] (K_ϕ)
10	6.05	0.34	-0.11	0.38	-0.56	3.16
20	5.91	.37	-.07	.41	-.33	3.02
30	6.16	.47	+.02	.55	+.07	2.44
40	5.99	.39	-.13	.43	-.54	2.87
50	5.30	.34	+.03	.30	+.17	2.63
60	6.01	.37	-.12	.36	+.54	2.73
70	5.94	.39	-.11	.39	+.45	2.55
80	6.26	.41	-.03	.45	-.12	2.66
90	5.81	.25	-.06	.22	-.46	3.59
100	6.13	.33	-.08	.29	-.43	2.72
110	6.03	.34	-.07	.30	-.34	2.62
Average	5.96	.36	-.07	.37	-.14	2.82
(σ_ϕ)[6]	.25	.06	.05	.09	.39	.33

[1] Grain size = $2^{-\phi}$ mm.

[2] $M_3 = \frac{1}{n}\sum x_i^3 - \frac{3}{n}\bar{x}\sum x_i^2 + 2x^{-3}$

[3] $M_4 = \frac{1}{n}\sum x_i^4 - \frac{4}{n}\bar{x}\sum x_i^3 + \frac{6}{n}x^{-2} - 3x^{-4}$

[4] $Sk = M_3/(S^2)^{3/2}$

[5] $K = M_4/S$

[6] Phi standard deviation of the individual statistic.

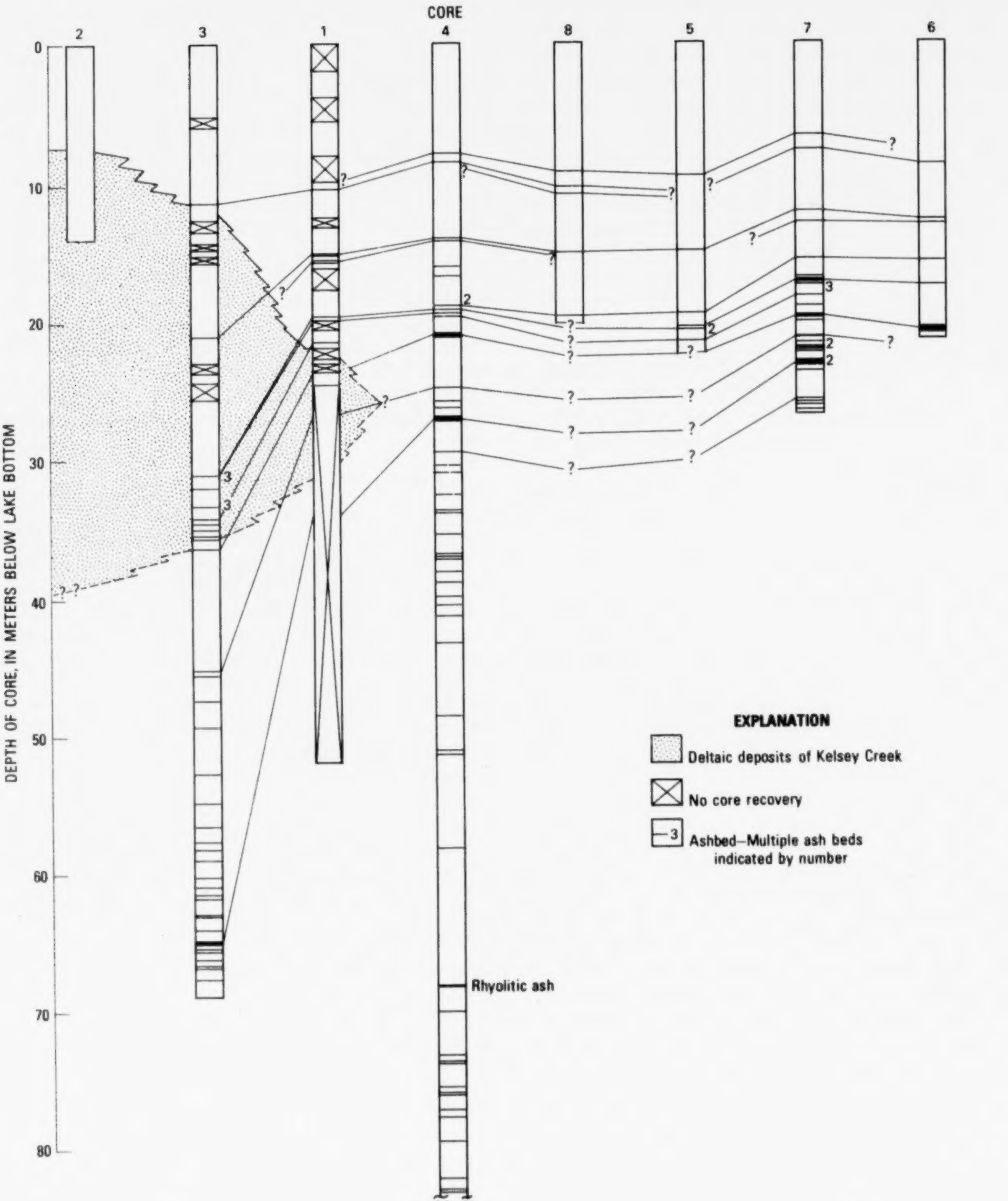
CORE
2
3
1
4
8
5
7
6
DEPTH OF CORE, IN METERS BELOW LAKE BOTTOM
0
10
20
30
40
50
60
70
80
115
Rhyolitic ash
EXPLANATION
Deltaic deposits of Kelsey Creek
No core recovery
Ashbed–Multiple ash beds indicated by number

FIGURE 110.—Ash-bed correlations in eight cores from Clear Lake (modified from Sims, 1976). See figure 109 for location of cores.

B.P., has trace-element affinities with volcanic rocks in the southern Cascade Range (A. M. Sarna-Wojcicki, oral commun., 1975).

Because the ash beds in core 7 are abundant and well dated, they are used as the primary reference in correlations with other cores. These correlations provide the basis for determining the frequency of volcanic eruptions in the Clear Lake basin and help fix the timing of some sedimentologic and paleoclimatic events. In the Highlands Arm, adjacent to the Clear Lake Volcanics, some of the ash beds may have been produced by phreatomagmatic explosive volcanism and, therefore, are probably of local extent (B. C. Hearn, Jr., oral commun., 1975). The geometry of their depositional areas is dependent on the location of the eruptive source with respect to topographic barriers, prevailing winds, and the direction of the explosion itself. However, a number of the local ash beds are widespread enough that correlations within the lake sediments may be made (fig. 110).

Correlation of ash beds, however, is difficult because of the variable number and frequency of occurrence of ash beds in the cores. This is in part because of the various time intervals represented by the different cores. A possible reason for the varying number of ash beds from equivalent time periods is that some of the core sites are near the mouths of Kelsey and Adobe Creeks, which are underlain by several tuffaceous deposits. Erosion and redeposition of these deposits may have produced beds that resemble primary ash beds (Sims, 1976).

CARBON-14 DETERMINATIONS

Radiocarbon-age determinations of carbon-bearing sediment, carbonaceous zones, and peat were done wherever feasible. Fifty-eight ^{14}C-age dates were obtained from the Clear Lake cores (Sims, 1976). The 24 dates for cores 4 and 7 are listed in table 30 and are plotted against depth in figure 111.

Because of the high organic content of the lower part of core 7, it has been well dated (table 30). The dates are in reasonable agreement with their stratigraphic positions, although a few anomalies are present. The date of about 40,000 B.P. at the base of the core is a minimum age, but extrapolation of the sedimentation rate derived from the finite dates in the middle part of the core suggests that the base of the core is not likely to be much older than 40,000 years (Meyer Rubin, oral commun., 1976).

All the age dates from core 4 (table 29) are on carbonaceous sediments containing probably less than 5 percent of very fine grained, disseminated carbon-bearing material. All the samples were acid treated to remove carbonate before ^{14}C analysis. Sample USGS-193 was further prepared by treatment with NaOH to remove humic acid. This sample yielded a ^{14}C age of 23,500±300 yr after acid treatment only and 29,600±580 yr after acid-plus-NaOH treatments. Because NaOH treatments were not done on other samples, their ^{14}C ages must be considered to be minimum ages.

The ^{14}C-age dates in core 4 are at variance with absolute ages suggested by Sims (1976) on the basis of ash-bed correlations from other cores. At the time the correlations were made only one ^{14}C-age date existed for core 4 (W-3217). Later dates from core 4 samples at and above 41 m form a rational sequence of dates. Ages for samples at depths below 41 m do not conform with the sequence of dates from higher positions.

Because all but three ash beds (at 43.7, 68.5, and 77.9 m) in core 4 were identified by their X-ray radiographic characteristics, correlation with visible ash beds in other cores is difficult. Correlations of ash beds in core 4 with ^{14}C-dated ash beds in core 7 yield a rational sequence and age-depth curve for core 4. However, this curve is at variance with ^{14}C-age dates on carbonaceous sediments in core 4 (fig. 111) and with ages

TABLE 30.—*Radiocarbon dates from Clear Lake cores 4 and 7*

Sample[1] No.	Depth (cm)	Type of sediment	Age B.P.
		Core 4	
USGS-446	810	Carbonaceous sediments	6,930±90
USGS-445	1500	do	10,400±80
USGS-319	2000	do	14,120±160
USGS-320	2200	do	14,640±120
W-3217	2545	do	15,010±550
USGS-321	2700	do	16,600±140
USGS-444	4100	do	26,350±440
USGS-193	5800	do	29,600±580
USGS-322	7100	do	29,300±390
USGS-447	8010	do	32,200±750
		Core 7	
I-7719	763-771	Peat	11,330±330
W-3071	820-830	Peaty mud	11,700±250
W-3072	870-880	Peat	12,280±250
W-3073	980-1010	Silty peat	13,160±300
W-3063	1120-1130	Clayey peat	14,900±300
I-7756	1225-1229	Peaty mud	17,660±340
W-3064	1276-1280	do	17,470±300
W-3066	1320-1330	Peat	18,340±300
W-3068	1410-1420	Peaty mud	19,110±300
W-3069	1530-1540	Peat	21,210±400
W-3070	1670-1676	do	26,150±600
I-7928	1715-1720	Carbonaceous mud	23,900±640
I-7932	1727-1733	do	23,300±600
I-7718	2731-2737	Peat	40,000

[1] Sample numbers with a "W" prefix were dated by Meyer Rubin, U.S. Geological Survey. Samples with a "USGS" prefix were dated by Stephen Robinson, U.S. Geological Survey. Samples with an "I" prefix were dated by James Buckley of Teledyne Isotopes, Inc. All dates on core 7 and W-3217 are from Sims (1976).

[2] This sample was acid treated to remove carbonate before analysis and yielded a ^{14}C age date of 23,500±300 B.P. Treatment of a second split of the sample by both acid and base to remove carbonate and humic acids yielded a date of 29,600±580 B.P.

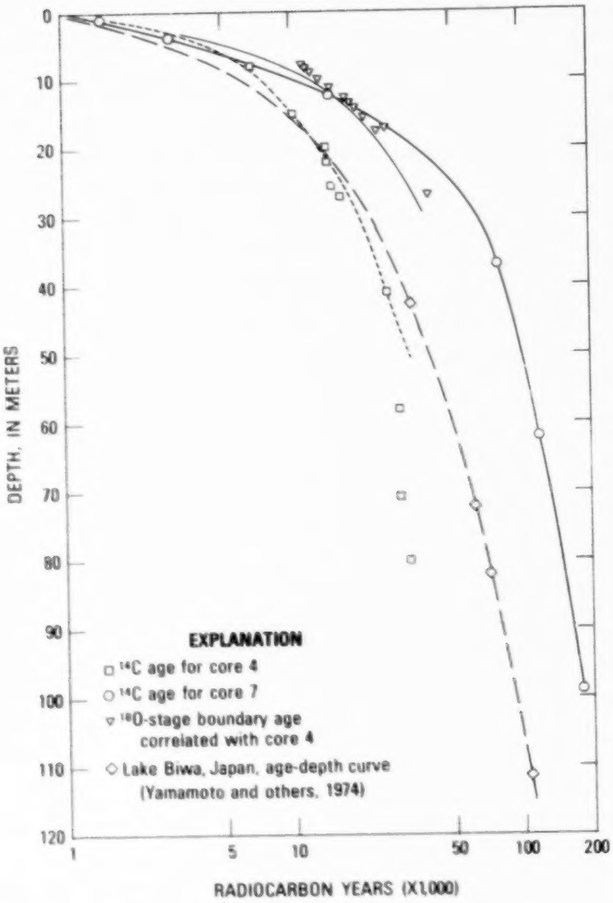

FIGURE 111.—Age-depth relations in cores 4 and 7, Clear Lake and in Lake Biwa, Japan.

derived from correlations of the oak-pollen frequency curve with ^{18}O stages from cores in deep-ocean basins (see below). However, if the three oldest ^{14}C-age dates are assumed to be suspect and not included in a least-squares linear regression of the remaining data, a curve is found similar to that for age dates in Lake Biwa, Japan (Yamamoto and others, 1974). If a further assumption is made that the correlations of the oak-pollen frequency curve with Pacific core V28-268 (Shackleton and Opdyke, 1973) are valid and the stage boundary ages included as data and a power function fitted to the points, another similar curve is obtained. Implicit in the assumptions and curve-fitting techniques is that the long-term sedimentation rates are nearly constant and that compaction is the major controlling age-depth variable.

Lake Biwa, Japan, is in a similar tectonic, geomorphic, and limnological framework (Yokoyama and Horie, 1974; Shoji Horie, oral commun., 1977). Grain sizes of the sediments in Lake Biwa (Yamamoto, 1974) and Clear Lake (table 29) core 4 are also similar. The mean grain size of Clear Lake sediment is about $6.0 \pm 0.25\phi$, and bulk density varies from 1.4 g/cm^3 at 18 m to 1.75 g/cm^3 at 100 m, much like the sediment in Lake Biwa (Yamamoto and others, 1974).

These data all suggest that the power curve fit to the ^{14}C-age dates and ages of correlated ^{18}O zones to core 4 is a reasonable representation of the age of the sediments with depth in core 4.

POLLEN RECORD

The pollen of core 4 is dominated by three types: oak, pine, and TCT[1], which are explained below. The sum of these three types accounts for 76.8 to 99.0 percent of the total arboreal pollen. Variations in the proportions of these types (fig. 112) show repeated changes between samples having high frequencies of oak pollen and samples having high frequencies of pine and TCT pollen. These changes are interpreted in terms of vertical migrations of the vegetation belts of the northern Coast Ranges in response to the climatic changes of the last glacial-interglacial cycle.

The pollen record of core 4 is summarized here by presenting the curves for oak, pine, and TCT; each variable is expressed as a percentage of its sum (fig.112). As noted above, this sum always accounts for at least 76.8 percent of the abnormal pollen in a sample.

The most apparent changes in the core 4 pollen record are the major shifts in oak-pollen frequency. The top 21 m of the core, which is believed to represent the Holocene, has oak-pollen frequencies of between 55 and 77 percent of the modified pollen sum. Between 21.1 and 26 m, oak pollen decreases consistently with depth from 37 to 11 percent. From 27 m down to a depth of 85.3 m, oak-pollen frequencies are less than 11 percent; zones of less than 3 percent oak pollen are found between 28 and 47 m and between 73 and 81 m. Below a depth of 83.5 m, the oak-pollen curve shows a series of complex oscillations. In three major intervals the oak-pollen frequencies are between 20 and 40 percent, and they are separated by intervals having less than 10 percent oak pollen; all oscillations occur between 83.5 and 108 m depth. Near the bottom of the core, between 108 and 112 m, there is a layer of sediment that contains the highest frequencies of oak pollen in the entire sequence, surpassing even the frequencies in the Holocene sediment. This series is underlain by more sediment containing low frequencies of oak pollen that extend to the bottom of the core.

The core 7 pollen record is similar to that of core 4.

---

[1] TCT is an abbreviation for the plant families Taxodiaceae, Cupressaceae, and Taxaceae.

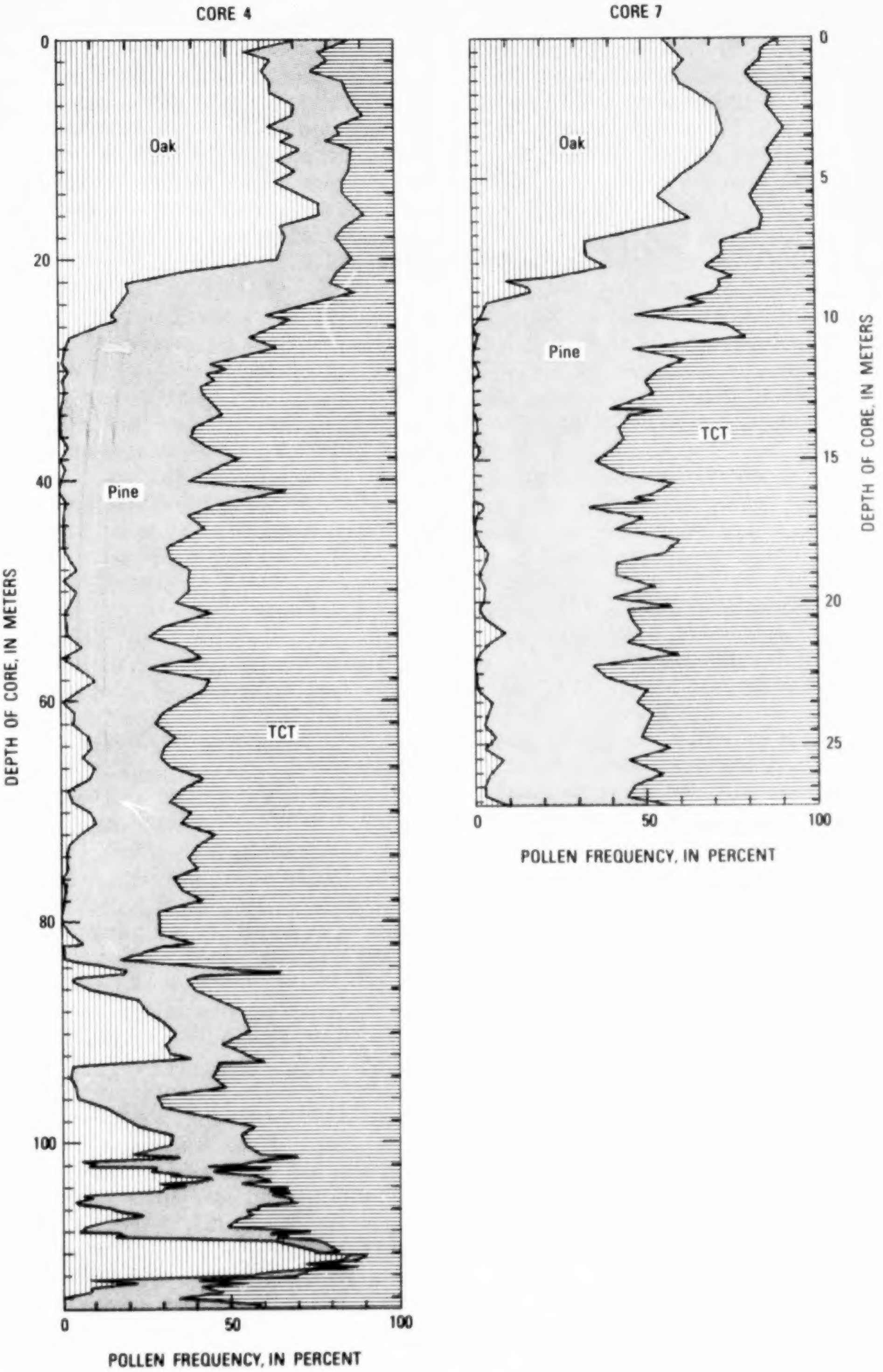

FIGURE 112.—Pollen diagrams for cores 4 and 7. Oak, pine, and TCT pollen are summed and plotted as a ratio of their total. Vertical scale is depth in meters for each core; scales have been adjusted for ease of correlation of the two diagrams. Difference in scales is attributed to differing sedimentation rates and compaction in the two cores.

except that (1) core 7 covers a shorter time interval, (2) the core 7 sedimentation rate is lower than that for core 4, and (3) substantial amounts of locally derived pollen are present in core 7 at depths below 6.7 m; this section also contains seeds of *Brasenia, Nuphar, Zannichellia, Potamogeton,* and *Myriophyllum,* all shallow-water aquatic genera. The summary pollen diagram for core 7 (fig. 112) was prepared using the same pollen sum (oak + pine + TCT) as was used for core 4. This procedure minimizes the differences between the two diagrams and provides the best basis for correlating cores 4 and 7 on the basis of pollen. Above about 6.5 m, oak-pollen frequencies exceed 50 percent, with a pronounced maximum of 73 percent between 2 and 4 m. Below 6.5 m, oak-pollen frequencies decline and reach zero at a depth of 10 m. Almost no oak pollen occurs between 10 and 17.5 m. Below 17.5 m, oak-pollen frequencies vary irregularly between 0 and 10 percent, with an interval of no oak pollen between 22 and 24 m.

DISCUSSION

The source area for the pollen falling into Clear Lake probably includes the entire Clear Lake drainage. The pollen record is thus almost entirely a response to regional rather than local changes and is, therefore, a good record of climatic change. The geographic position of Clear Lake is also important: it is located on the windward edge of North America, several hundred kilometers south of the Wisconsinan continental ice sheets. It is reasonable to expect that the climate in the Clear Lake area has varied primarily in direct response to changes in the climate of the northern Pacific Ocean and not in response to large local masses of ice.

The core 4 pollen record may be considered to represent the relation of the lake pollen rain to the vertical migrations of three climatically controlled vegetation belts, which correspond only in general terms to the vegetation belts described by Kuchler (1977). The lowest of these belts, characterized by high frequencies of oak pollen, surrounds Clear Lake today. Oak pollen, which is the dominant pollen type being deposited in Clear Lake at present, represents primarily species that grow at fairly low elevations. The distribution of oaks appears to be limited in part by high summer soil moisture content, which permits reproduction of root fungus that attacks oaks (N. Hardesty, oral commun., 1978). Therefore oaks are limited to lower elevations where summer soil-moisture content is low. The next highest belt is the lower part of the mixed coniferous forest; it is characterized by low frequencies of oak pollen and by high frequencies of TCT and pine pollen, with TCT dominating. TCT pollen include species such as incense cedar (*Calocedrus decurrens*), juniper (*Juniperus* spp.), cypress (*Cupressus* spp.), and redwood (*Sequoia sempervirens*); redwood pollen may sometimes be identified to the species level. The main pollen producers in the TCT group in the Clear Lake area grow primarily near the lower parts of the montane coniferous forest, above the oak zone. The highest belt is the upper part of the mixed coniferous forest and is dominated by pine pollen. The pines (*Pinus* spp.) may be found growing at nearly all elevations, but pine pollen tends to reach maximum proportions of the total pollen rain at the highest elevations.

Because Clear Lake is so large, the pollen being deposited in it represents an integrated response of the vegetation of a very large area. Also, because Clear Lake is a unique depositional site in the Coast Ranges, it is not possible to obtain modern pollen samples from different elevations and vegetation types that approximate late Pleistocene assemblages for direct comparison with the Clear Lake fossil types. Although no surface pollen samples are available from the northern Coast Ranges to support the above description, it is in agreement with two pollen surface transects across the Sierra Nevada, described by Adam (1967), and there are broad similarities in the vegetation of the two areas.

The balance between oak-pollen-dominated and conifer-pollen-dominated pollen spectra is the most important single measure of climatic history in the Clear Lake pollen record. The relative proportions of oak versus conifer pollen are a measure of the relative importance of oak-woodland and conifer-forest plant communities within the source area for the Clear Lake pollen rain. The upper 21 m of core 4, having high frequencies of oak pollen, is interpreted to be Holocene deposits. Between 22 and 26 m, frequencies of 10-20 percent for oak pollen indicate a transitional period between the maximum cold conditions of the full glacial stage and the establishment of modern vegetation in early Holocene time. Between 26 and 83 m there are two broad intervals of minimum oak-pollen frequency, from 26 to 43 m and from 73 to 83 m; these intervals are taken herein to represent late and early Wisconsinan time, respectively. They are separated by about 25 m of sediment at depths from 47 to 72 m in which there are systematic fluctuations of oak-pollen frequency from 0 to 10 percent. This entire interval of 47-72 m is interpreted to correspond to the middle Wisconsinan interstadial interval of the midcontinent, but the changing oak-pollen frequencies therein indicate that the climate was not uniform throughout the interval.

The set of oscillations in oak-pollen abundance between 83 and 112 m depth cannot be easily interpreted in terms of classic continental glacial stratigraphy. This interval contains the only pre-Holocene sediments having oak-pollen frequencies as high as those of the

Holocene; these sediments occur between 108 and 112 m and, by analogy with the Holocene deposits, are interpreted to represent the last interglacial interval. The series of oak-pollen maxima between 83 and 108 m do not exceed values of 45 percent, while Holocene values are nearly all over 55 percent. These lower sediments therefore represent interstadial rather than interglacial conditions. It is not at all clear where the climatic oscillations shown by these sediments should be placed in terms of North American continental glacial stratigraphy.

When the Clear Lake oak-pollen curve is compared with an oxygen-isotope curve from the deep sea, however, there is a remarkable correspondence. Figure 113 shows the Clear Lake oak-pollen curve of core 4 and Shackleton and Opdyke's (1973) ^{18}O curve for core V28-238 from the equatorial Pacific, some 5,000 km southwest of Clear Lake. The degree of similarity between the curves is, we think, a sufficient basis for applying the chronologic controls available for the deep-sea curves to the Clear Lake core. The work of Shackleton and Heusser (1977) has placed this correlation on a firmer basis. They studied the pollen and the oxygen-isotope records in a core taken from the eastern Pacific off the coast of Oregon and found that the first pre-Holocene sediments that contain pollen spectra resembling those of the Holocene (in their case, sediments having high abundance of alder pollen) are from their oxygen-isotope stage 5e. This is the same correlation as is suggested using direct comparison of the two curves in figure 113.

Also of interest, although not shown, is the scarcity of spruce (*Picea*) pollen throughout cores 4 and 7. Spruce apparently is limited in its distribution by summer drought, and the rarity of spruce throughout the last full glacial cycle in core 4 indicates that summers were dry even during full glacial conditions (Adam, 1973).

In contrast, the wedge of gravel found in cores 1, 2, and 3 (fig. 110) suggests that streamflows into Clear Lake must have been considerably higher in order to transport the gravel. The core sediments show no sign of having dried out at any time, so the gravels were apparently deposited subaqueously by running water and not by prograding subaerial alluvial fans.

When the scarce spruce pollen and the gravel deposits are considered together, they suggest that during the late Pleistocene there was a greater seasonal contrast in precipitation than there is at present; late Pleistocene summers were dry and winters were very wet.

This interpretation is in general agreement with the regional synthesis by Johnson (1977). However, the Clear Lake pollen record offers a substantial improvement over that synthesis for the past 130,000 years because of the continuity of the record. Most of the evidence analyzed by Johnson either was of a discontinuous or short-term nature or was from marine deposits; only by studying continuous sequences of continental sediments can the nature of the California Quaternary record be fully understood.

SUMMARY

The sediments in Clear Lake vary in composition, rate of accumulation, and in the type of pollen they contain. Present-day sediments uniformly consist of sapropelic mud. In the past, coarser clastic sediments have been deposited in a wedgelike mass in the southern part of the main lake basin near the present mouths of Kelsey and Adobe Creeks, probably as the result of late Pleistocene climatic variations. During the period between about 40,000 and 10,000 B.P., peat and peat-rich sediments accumulated in Highlands Arm and, to a lesser extent, in Oaks Arm of Clear Lake (fig. 110). Ash beds are common in all cores except core 2. Many ash beds are correlated between cores by stratigraphic position, bed thickness, and ^{14}C-age dates of enclosing sediments (Sims, 1976). At least 12 ash beds may be correlated between the various cores (fig. 110). Only one ash bed is known to have been derived from a source outside the Clear Lake volcanic field. Thus, a minimum record for volcanic eruptions in the Clear Lake area may be determined for the last 40,000 years. Thirty-three additional ash beds are present in core 4 because of its greater length, but an undetermined number of these are redeposited volcaniclastic debris that mimic air-fall ash beds. The ash beds and associated radiocarbon dates in cores 4 and 7 form the basis for calibration of the oak-pine-TCT pollen curves for approximately the last 40,000 years.

Analyses of pollen from cores 4 and 7 suggest that during the last glacial interval, the occurrence of oak was displaced downward in the hills surrounding the lake, causing the virtual disappearance of oak from the basin; thus at depths below 10 m in core 7 and between 27 and 83 m in core 4 there is little oak pollen present. The highest oak-pollen frequencies found in core 4 are between 108 and 112 m deep (fig. 113). This interval is correlated with the last interglaciation (about 128,000 B.P.). At the top of this interval, oak pollen decreases abruptly from more than 60 percent to less than 5 percent of arboreal pollen over a stratigraphic interval of 80 to 180 cm; this decline is attributed to a sudden change in climate at the end of the last interglacial period (Sangamon interglaciation of the midcontinental region).

Near the base of core 4, between 83 and 108 m, is a series of five oscillations in oak-pollen percentages (fig. 113) that are interpreted to have occurred between the

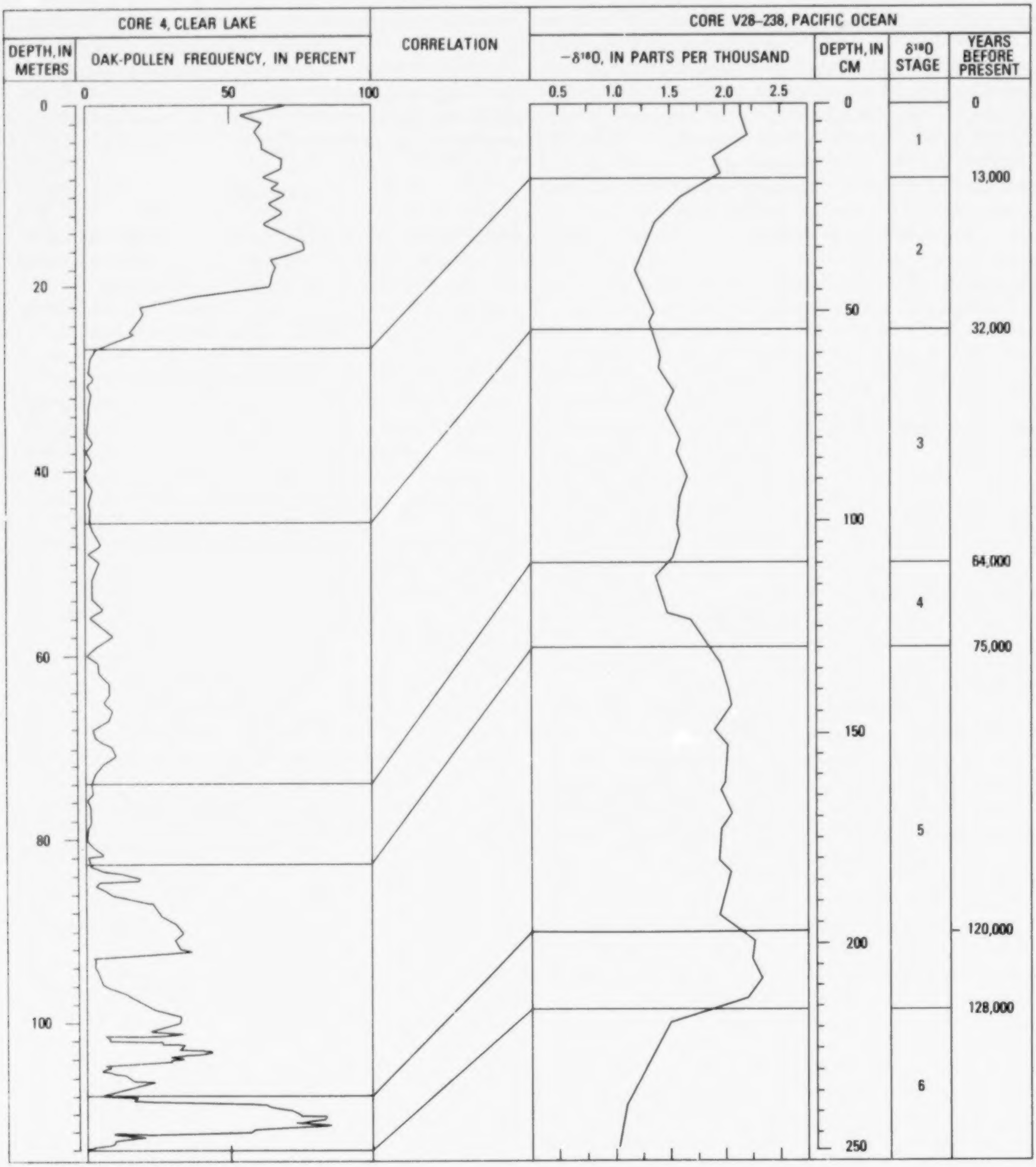

FIGURE 113.—Oak-pollen frequency curve (percent age of oak-pine-TCT total) versus depth for core 4, Clear Lake and ^{18}O curve from Pacific Ocean deep-sea core V28-238 (Shackleton and Opdyke, 1973). ^{18}O stage numbers and age dates from Shackleton and Opdyke (1973).

end of the last interglacial and the onset of the most severe climatic conditions of the early Wisconsinan (about 75,000 to 120,000 B.P.). The abrupt changes in oak-pollen frequency in this 25-m interval are exceeded only by the changes at the beginning of the present and last interglacials (about 13,000 and 128,000 B.P.). There are three separate intervals that have oak-pollen frequencies between 20 and 30 percent (fig. 113); these are interpreted to represent conditions warmer than during the middle Wisconsinan (about 32,000 to 64,000 B.P.),but cooler than the Holocene. Two other intervals characterized by oak-pollen frequencies of between 10 and 20 percent are between 74 and 83 m, and 27 and 44 m depth, respectively (fig. 113). The wide variations in oak-pollen frequency are interpreted as primarily a response of oak to temperature, although moisture variations also were involved. Thus, the oak-pollen curve may be considered as an uncalibrated paleotemperature curve. This curve also strongly resembles curves of deep-sea ^{18}O content in foraminifers.

REFERENCES CITED

Adam, D. P., 1967, Late Pleistocene and Recent palynology in the central Sierra Nevada, California, *in* Cushing, E. J., and Wright, H. E., Jr., eds., Quaternary paleoecology: New Haven, Conn., Yale University Press, p. 275-301.

——— 1973, Early Pleistocene(?) pollen spectra from near Lake Tahoe, California: U.S. Geological Survey Journal of Research, v. 1, no. 6, p. 691-693.

Bailey, E. H., Irwin, W. P., and Jones, D. L., 1964, Franciscan and related rocks, and their significance in the geology of western California: California Division of Mines and Geology Bulletin 183, 177 p.

Casteel, R. W., Adam, D. P., and Sims, J. D., 1977, Late Pleistocene and Holocene remains of Hysterocarpus traski (Tule perch) from Clear Lake, California, and inferred Holocene temperature fluctuations: Quaternary Research, v. 7, p. 133-143.

Clark, H. W., 1937, Association types in the north Coast Ranges of California: Ecology, v. 18, p. 214-230.

Davis, W. M., 1933, The lakes of California: California Journal of Mines and Geology, v. 29, p. 175-236.

Donnelly, J. M., 1977, Geochronology and evolution of the Clear Lake volcanic field: Berkeley, University of California, Ph. D. thesis, 48 p.

Donnelly, J. M., McLaughlin, R. J., Goff, F. E., and Hearn, B. C., Jr., 1976, Active faulting in The Geysers-Clear Lake area, northern California: Geological Society of America Abstracts with Programs, v. 8, p. 369-370.

Goff, F. E., Donnelly, J. M., Thompson, J. M., and Hearn, B. C., Jr., 1976, The Konocti Bay fault zone, California: Potential area for geothermal exploration: Geological Society of America Abstracts with Programs, v. 8, p. 375-376.

Griffin, J. R., and Critchfield, W. B., 1972, The distribution of forest trees in California: U.S. Department of Agriculture, Forest Service Research Paper PSW-82, 114 p.

Hearn, B. C., Jr., Donnelly, J. M., and Goff, F. E., 1976a, Geology and geochronology of the Clear Lake Volcanics, California: United Nations Symposium on the Development and Use of Geothermal Resources, 2d, San Francisco, 1975, Proceedings, v. 1, p. 423-428.

——— 1976b, Preliminary geologic map and cross section of the Clear Lake volcanic field, Lake County, California: U.S. Geological Survey Open-File Report 76-751.

Hopkirk, J. D., 1973, Endemism in fishes of the Clear Lake region of central California: California University Publications in Zoology, v. 96, 135 p.

Jenkins, O. P., and Strand, R. G., 1960, Geologic map of California, Ukiah sheet: California Division of Mines and Geology, scale 1:250,000.

Johnson, D. L., 1977, The late Quaternary climate of coastal California: Evidence for an Ice Age refugium: Quaternary Research, v. 8, p. 154-179.

Knapp, Rudinger, 1917, Die Vegetation von Nord- und Mittelamerika und der Hawaii-Inseln: Stuttgart, Gustav Fischer Verlag, 373 p.

Koenig, J. B., compiler, 1963, Geologic map of California, Santa Rosa sheet: California Division of Mines and Geology, scale 1:250,000.

Kuchler, A. W., 1964, Manual to accompany the map "Potential natural vegetation of the conterminous United States": American Geographical Society, Special Publication 36, 39 p.

——— 1977, The map of the natural vegetation of California, *in* Barbour, M. G., and Major, J., eds., Terrestrial vegetation of California: New York, Wiley-Interscience, p. 909-928.

Little, E. L., Jr., 1971, Atlas of United States trees, v. 1, Conifers and important hardwoods: U.S. Department of Agriculture, Miscellaneous Publication 1146, 8 p., 200 maps.

Livingston, B. E., and Shreve, F., 1921, The distribution of vegetation in the United States as related to climatic conditions: Carnegie Institution of Washington Publication 284, 590 p.

Rymer, M. J., 1981, Stratigraphy revision of the Cache Formation (Pliocene and Pleistocene), Lake County, California: U.S. Geological Survey Bulletin 1502-C [in press].

Shackleton, N. J., and Heusser, L. F., 1977, Oxygen isotope and pollen stratigraphy of a deep-sea core from the Pacific Coast of North America: International Quaternary Association Congress, 10th, Birmingham, England, 1977, Abstracts, p. 416.

Shackleton, N. J., and Opdyke, N. D., 1973, Oxygen isotope and paleomagnetic stratigraphy of equatorial Pacific core V-28-238 - Oxygen isotope temperatures and ice volumes on a 10^5-year and 10^6-year scale: Quaternary Research, v. 3, p. 39-55.

Sims, J. D., 1976, Paleolimnology of Clear Lake, California, U.S.A., *in* Horie, Shoji, ed., Paleolimnology of Lake Biwa and the Japanese Pleistocene: Kyoto, Japan, Kyoto University, v. 4, p. 658-702.

Sims, J. D., and Rymer, M. J., 1975a, Preliminary description and interpretation of cores and radiographs from Clear Lake, Lake County, California - core 4: U.S. Geological Survey Open-File Report 75-666, 19 p.

——— 1975b, Preliminary description and interpretation of cores and radiographs from Clear Lake, Lake County, California - core 7: U.S. Geological Survey Open-File Report 75-144, 21 p.

——— 1976, Map of gaseous springs and associated faults, Clear Lake, California: U.S. Geological Survey Miscellaneous Field Studies Map MF-721.

Yamamoto, Atsuyuki, 1974, Grain size analysis of sediments and its application to the paleoclimatology in Lake Biwa; in Horie, Shoji, ed., Paleolimnology of Lake Biwa and the Japanese Pleistocene: Kyoto, Japan, Kyoto University, v. 2, p. 113-134.

Yamamoto, Atsuyuki, Kanari, Seiichi, Fukuo, Yoshiaki, and Horie, Shoji, 1974, Consolidation and dating of the sediments in core samples from Lake Biwa, *in* Horie, Shoji, ed., Paleolimnology of Lake Biwa and the Japanese Pleistocene: Kyoto, Japan, Kyoto University, v. 2, p. 135-144.

Yokoyama, Takuo, and Horie, Shoji, 1974, Lithofacies in a 200-m core sample from Lake Biwa, *in* Horie, Shoji, ed., Paleolimnology of Lake Biwa and the Japanese Pleistocene: Kyoto, Japan, Kyoto University, v. 2, p. 31-37.

PLIOCENE AND PLEISTOCENE FISHES FROM THE CLEAR LAKE AREA

By RICHARD W. CASTEEL and MICHAEL J. RYMER

ABSTRACT

The remains of six genera of fossil fish were found in the Cache, Lower Lake, and Kelseyville Formations in Lake County, Calif. The fishes range in age from late Pliocene to late Pleistocene. These remains include the first fossil occurrence of Tule perch, which is the second embiotocid genus known from the late Pliocene freshwater record of California. Our findings add three new fish genera to the taxa known from the Cache, Lower Lake, and Kelseyville Formations and suggest lacustrine environments like present-day Clear Lake. The presence of the fossil fishes suggests increased precipitation and runoff during deposition of the upper part of the Pleistocene Kelseyville Formation.

INTRODUCTION

This report describes six genera of fossil fish that were recovered from Pliocene and Pleistocene rocks in the Cache, Lower Lake, and Kelseyville Formations, Lake County, Calif. The fossils came from nine vertebrate localities (fig. 113) in the three formations. These formations are briefly summarized below to provide a stratigraphic and temporal framework for the contained fossil fish.

The oldest of these formations is the Cache Formation. The Cache is composed of nonmarine sandstone, conglomerate, and siltstone, and is at least 1,500 m thick. These rocks were deposited predominantly in streams, but partly in a lacustrine environment. Terrestrial vertebrate fossils, identified by C. A. Repenning (Rymer, 1981), suggest an age range for the Cache Formation of approximately 1.8-3.0 m.y. (Blancan). Locally overlying the Cache is a basalt flow that

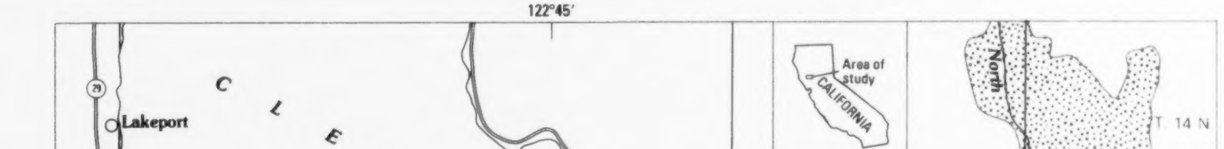
122°45'
39°00'
29
Lakeport
C
L
E
A
R
Creek
Kelsey
Core 6
Core 7
L
A
K
E
Mount Konocti
Kelseyville
20
53
Area of study
CALIFORNIA
North
Fork
Cache
Creek
Cache Creek
M-1350
20
M-1354
T. 14 N.
T. 13 N.
T. 12 N.
M-1353
M-1351
29
M-1352
M-1356
M-1355
M-1349
M-1239
Lower Lake
EXPLANATION
Kelseyville Formation
Lower Lake Formation
Cache Formation
0
5 KILOMETERS
29
R. 10 W.
R. 9 W.
R. 8 W.
R. 7 W.
R. 6 W.

FIGURE 114.—Fossil-fish localities in the Cache, Lower Lake, and Kelseyville Formations, Lake County, Calif.

was mapped by Hearn, Donnelly, and Goff (1976) and dated by the K-Ar method at 1.66±0.10 m.y. (Donnelly-Nolan and others, this volume).

The Lower Lake Formation is composed of siltstone and sandstone with minor limestone, calcareous siltstone, diatomite, and interbedded tuff beds, which were all deposited in a lacustrine environment (Rymer, 1981). The Lower Lake Formation is at least 130 m thick and is Pleistocene in age. This formation locally overlies the dacite of Diener Drive, which has a K-Ar age of 0.92±0.03 m.y. (Donnelly-Nolan and others, this volume). Interbedded near the top of the Lower Lake Formation is the dacite of Cache Creek, dated at 0.40±0.04 m.y. (Donnelly-Nolan and others, this volume).

The Kelseyville Formation consists of sandstone, siltstone, and less common conglomerate. This member is predominantly of lacustrine origin and contains near its base a bed of lapilli tuff that may be correlative with the nearby part of the rhyolite of Thurston Creek, dated at 0.64±0.03 m.y. (Donnelly-Nolan and others, this volume). The age of the exposed top of the Kelseyville Formation is approximately 0.13-0.20 m.y. The Lower Lake and Kelseyville Formations are partly coeval and may have been deposited in different subbasins of a lake that was ancestral to Clear Lake (Rymer, 1981).

All skeletal identifications of the fish reported herein were made with the aid of comparative skeletons, and scales were identified on the basis set forth by Casteel (1972). Pharyngeal teeth of the catostomids were identified by using the criteria of Eastman (1977). Nomenclature of the fishes follows that of the American Fisheries Society (1970).

LOCALITIES AND FOSSIL FISHES

Fossil-fish remains from the Cache Formation are from two vertebrate localities (M-1354 and M-1350). USGS vertebrate locality M-1354 (lat 38°59'43" N., long 122°31'47" W.) is located in a south-facing gully near the top of the ridge between Grizzly and Middle Creeks at an elevation of approximately 387 m (Lower Lake 7.5' quadrangle). The remains of two genera of freshwater fish (table 31) were found in siltstone. The presence of *Hysterocarpus* at this locality represents the first reported fossil occurrence of this genus and indicates that the genus is at least late Pliocene in age. USGS vertebrate locality M-1350 (lat 38°59'33" N., long 122°32'38" W.) is in a streambank exposure along the North Fork of Cache Creek, approximately 0.7 km northwest of BM 1006 on the State Highway 20 bridge over the North Fork of Cache Creek. The remains of a single taxon (table 31) were recovered from a siltstone bed that is approximately 100 m stratigraphically above locality M-1354.

Of two USGS vertebrate localities associated with the Lower Lake Formation (M-1239 and M-1349), one yielded a genus of fish (*Hysterocarpus*) not previously known in the formation. USGS vertebrate locality M-1239 (lat 38°54'46" N. long 122°37'11" W.) is in a roadcut 0.3 km north of the intersection of Highways 29 and 53. Earlier sampling of a bed of diatomaceous tuffaceous claystone dipping 65° N. yielded the remains of three genera of freshwater fish: *Orthodon* cf. *O. microlepidotus* (Ayres), *Gasterosteus* cf. *G. aculeatus* Linnaeus, and *Archoplites* cf. *A. interruptus* (Girard) (Casteel and Rymer, 1975). Resampling of the claystone yielded additional remains of two of the above taxa (table 31). USGS vertebrate locality M-1349 (lat 38°56'17" N., long 122°36'52" W.) is along 19th Avenue in Clearlake Highlands, Calif., approximately 10 m west of Garner Avenue (Lower Lake 7.5' quadrangle), in a bed of calcareous siltstone that also contains the remains of gastropods and ostracodes. The sample locality lies at approximately the same stratigraphic horizon as the claystone in locality M-1239. The fossil fishes from locality M-1349 are listed in table 31.

Five localities within the Kelseyville Formation have yielded fish remains. All genera were not previously known in the Kelseyville and two genera (*Catostomus* and *Mylopharodon*) were not previously known from Pleistocene rocks of either the Lower Lake or Kelseyville Formations. USGS vertebrate locality M-1352 (lat 38°56'11" N., long 122°52'30" W.) is in lacustrine siltstone located in a west-facing gully on the northwest side of hills in sec. 33, T. 13 N., R. 9 W., approximately 0.48 km south of BM 1569 along Wight Way (Kelseyville 7.5' quadrangle). Fossil leaves from this locality, identified by J. A. Wolfe (Rymer, 1981), indicate that deposition here and at localities M-1355 and M-1356, in the lower part of the Kelseyville Formation, occurred during an interglacial period that may be correlative with oxygen-isotope stage 7 (Rymer,

TABLE 31.—*Location, specific distribution, and listing of fossil fish parts recovered in the Cache, Lower Lake, and Kelseyville Formations*

USGS vert. loc. No.	Family	Genus and species	Material recovered	USNM sample No.
		Cache Formation		
M-1354	Centrarchidae	*Archoplites* cf. *A. interruptus* (Girard) (Sacramento Perch).	Five scales	252775
	Embiotocidae	*Hysterocarpus* cf. *H. traski* Gibbons (Tule perch).	Two scales and one dentigerous pharyngeal plate.	264246
M-1350	Embiotocidae	*Hysterocarpus* cf. *H. traski* Gibbons	One scale fragment and an isolated pharyngeal tooth.	252776

1981). The plants identified include *Plantanus racemosa* Nutt. (California sycamore), *Quercus douglasii*, Hook. and Arn. (blue oak), *Q. wislinzenii* A. DC (interior live oak), *Populus trichocarpa* Torr. and Gray (black cottonwood), and at least three species of *Salix* (willow). The flora was interpreted as interglacial, with mean annual temperatures above 13°C (J. A. Wolfe, written commun., 1976). In addition to fish remains (table 31), this siltstone also locally contains the remains of gastropods and ostracodes. USGS vertebrate locality M-1356 (lat 38°55'59" N., long 12252'22" W.) is located in a west-facing gully in the NW1/4 sec. 33, T. 13 N., R. 9 W. Fish remains (table 31) occur in lacustrine siltstone that is approximately at the same stratigraphic horizon as the siltstone at locality M-1352. USGS vertebrate locality M-1355 (lat 38°55'30" N., long 122°52'17" W.) is located in a northwest-trending gully, 1.76 km south of BM 1569 on Wight Way, at an elevation of approximately 530 m (Kelseyville 7.5' quadrangle). Fish remains from this locality (table 31) are from lacustrine siltstone. USGS vertebrate locality M-1351 (lat 38°56'46" N., long 122°48'45" W.) is located in a road-cut exposure along Highway 29, approximately 4 km (by air) south-southeast of Kelseyville (Kelseyville 7.5' quadrangle). Five subsamples from this locality, all within 1.5 m of one another, were removed from a bed of vitric tuff that lies approximately 20 m above the Kelsey Tuff Member of the Kelseyville Formation, near the top of the exposed section of the Kelseyville Formation. The presence of *Mylopharodon* at this locality (table 31) represents the second reported occurrence of this genus in California; the other occurrence was from USGS vertebrate locality M-1242 and University of California Museum of Paleontology (UCMP) locality V-5834 in Alameda County, Calif., dating from the early Pleistocene (Irvingtonian) (Casteel and Adam, 1977). Also of interest is the presence of *Catostomus*, which represents the first reported fossil occurrence of this genus in California. Fossil leaves and cones, identified by J. A. Wolfe, from localities near M-1351 and M-1353, the upper part of the Kelseyville Formation, suggest deposition during a climatically cool (glacial) period, which may be correlative with oxygen-isotope stage 6 (Rymer, 1981). The megafossil plant assemblage identified by J. A. Wolfe also indicates that there may have been increased precipitation during deposition of this part of the Kelseyville Formation (J. A. Wolfe, written commun., 1976). USGS vertebrate locality M-1353 (lat 38°57'04" N., long 122°50'24" W.) is located in the bank of Kelsey Creek, approximately 3.5 km (by air) south of Kelseyville (Kelseyville 7.5' quadrangle). Fish remains (table 31) occur in silty sandstone at this locality.

TABLE 31.—*Location, specific distribution, and listing of fossil fish parts recovered in the Cache, Lower Lake, and Kelseyville Formations*—Continued

USGS vert. loc. No.	Family	Genus and species	Material recovered	USNM sample No.
Lower Lake Formation				
M-1239	Gasterosteidae	*Gasterosteus* cf. *G. aculeatus* Linnaeus (Three-spine stickleback).	Two Scute fragments, one of which represents a lateral scute.	252777
	Centrarchidae	*Archoplites* cf. *A. interruptus* (Girard)	Two scales	264247
M-1349	Cyprinidae	*Orthodon* cf. *O. microlepidotus* (Ayres) (Sacramento blackfish).	Six pharyngeal tooth fragments	252778
		Gen. et sp. indeterminate	One right homandibular and a posterior fragment of a left dentary.	264248
	Gasterosteidae	*Gasterosteus* cf. *G. aculeatus* Linnaeus	One left frontal	264249
	Centrarchidae	*Archoplites* cf. *A. interruptus* (Girard)	Five scales	264250
		Hysterocarpus cf. *H. traski* Gibbons	Four scales	264251
Kelseyville Formation				
M-1352	Centrarchidae	*Archoplites* cf. *A. interruptus* (Girard)	One scale	252779
	Embiotocidae	*Hysterocarpus* cf. *H. traski* Gibbons	Twenty-four scales and two otoliths (one left, one right).	264252
M-1356	Embiotocidae	*Hysterocarpus* cf. *H. traski* Gibbons	Thirteen scales	252780
	Cyprinidae Catostomidae	Gen. et sp. indeterminate	One caudal vertebra	264253
M-1355	Centrarchidae	*Archoplites* cf. *A. interruptus* (Girard)	Five scales	252781
	Embiotocidae	*Hysterocarpus* cf. *H. traski* Gibbons	Thirteen scales	264254
M-1351	Cyprinidae	*Mylopharodon* cf. *M. conocephalus* (Baird and Girard) (hardhead).	One molariform pharyngeal tooth	252782
		Gen. et sp. indeterminate	Nine isolated pharyngeal teeth and forty-eight vertebral centra.	264255
	Catostomidae	*Catostomus* cf. *C. occidentalis* Ayres (Sacramento sucker).	Seventy-six isolated pharyngeal teeth and and a fragment of a left operculum.	264256
	Gasterosteidae	*Gasterosteus* cf. *G. aculeatus* Linnaeus	Four vertebrae (two caudal, two ultimate).	264257
	Centrarchidae	*Archoplites* cf. *A. interruptus* (Girard)	One fragment of a right operculum and three vertebrae (one precaudal, two caudal).	264258
	Embiotocidae	*Hysterocarpus* cf. *H. traski* Gibbons	Eighty-four scales, six isolated pharyngeal teeth, three vertebrae (one thoracic, two caudal), two opercular fragments (one left, one right), and one urohyal.	264259
M-1353	Centrarchidae Embiotocidae	Gen. et sp. indeterminate	One spiny ray	252783

DISCUSSION

The fossil fish collected from various localities within the Cache, Lower Lake, and Kelseyville Formations reflect an essentially lacustrine environment. As tables 31 and 32 indicate, the late Pliocene and Pleistocene(?) fish fauna of the Cache Formation consists of *Archoplites* and *Hysterocarpus*. Both of these fishes are characteristic of the Hitch ecological zone (Hopkirk, 1975), which includes the fast- to slow-moving and standing waters in the present-day Lower Sonoran, and occasionally Upper Sonoran, Life Zones of California. The taxa from the Pleistocene Lower Lake Formation, *Orthodon*, *Gasterosteus*, *Archoplites*, and *Hysterocarpus*, are also characteristic of the Hitch zone and indicate a similar environment of deposition. The fish fauna of the Pleistocene Kelseyville Formation includes two additional taxa, *Mylopharodon* and *Catostomus*. Both of these fishes are most characteristic of the Sucker zone, which includes large sluggish creeks, small rivers, and the upper reaches of large rivers in today's Upper Sonoran Life Zone (Hopkirk, 1974). These two fishes are present only in the upper part of the Kelseyville Formation and may be further indicators of increased precipitation and, therefore, large permanent streams that entered the lake during deposition of the upper part of the Kelseyville Formation. Nonetheless, the fauna as a whole is still dominantly lacustrine. A lacustrine and sluggish lowland stream environment has been invoked by others to describe present-day Clear Lake. Hopkirk (1974), for example, stated that Clear Lake is similar to the oxbow lakes of the Sacramento Valley because Clear Lake is a warm shallow lake that has a low influx of cold water and a high loss of water due to evaporation.

Comparison of these essentially lacustrine fossil-fish faunas from the Cache, Lower Lake and Kelseyville Formations with the fish fauna of Clear Lake seems appropriate. Subfossil-fish remains in cores 6 and 7 (fig. 114) of Clear Lake sediment date back to approximately 36,000 and 40,000 B.P., respectively (Sims and others, this volume). On the basis of published reports on the fish faunas of these two cores (Casteel and others, 1975, 1977), as well as unpublished data on two additional cores of Clear Lake sediment, we find a great similarity between the fish remains in the sediments of Clear Lake and those of the Cache, Lower Lake, and Kelseyville Formations (table 32). This similarity extends to faunal composition, as well as to the types and condition of the fish remains themselves. The fossil-fish fauna of these Pliocene and Pleistocene formations also correlate strongly with the fish fauna observed in a recent survey of Clear Lake (Cook and others, 1966) (table 32). The few gaps in this faunal correlation may be due to the sparse fossil record or to variations in fossil preservation.

TABLE 32.—*Specific distribution of fossil fishes in the Cache, Lower Lake, and Kelseyville Formations and in cores from Clear Lake, and in present-day Clear Lake*

[Fish species from Clear Lake cores from Casteel and others (1975, 1977); present-day species from Cook and others (1966). Zone designations from Hopkirk (1974). +, species present; —, species absent; 0 species formerly present]

Taxon	Cache Formation	Lower Lake Formation	Kelseyville Formation	Clear Lake			Zone
				Core 6	Core 7	Recent survey	
Salmonidae:							
Salmo gairdneri Indeterminate salmonid	—	—	—	+	+	+	Trout roach
Cyprinidae:							
Hesperoleucus symmetricus	—	—	—	—	—	+	Roach
Mylopharodon cf. *M. conocephalus*	—	—	+	—	—	—	Sucker
Orthodon cf. *O. microleplidotus*	—	+	—	+	+	+	Hitch
Lavinia exilicauda	—	—	—	+	—	+	Hitch
Pogonichthys macrolepidotus	—	—	—	—	+	+	Hitch
Ptychocheilus grandis	—	—	—	—	+	+	Sucker
Gila crassicauda	—	—	—	—	—	0	Hitch
Catostomidae:							
Catostomus cf. *C. occidentalis*	—	—	+	+	+	+	Sucker
Gasterosteidae:							
Gasterosteus cf. *G. aculeatus*	—	+	+	+	+	+	Hitch
Centrarchidae:							
Archoplites cf. *A. interruptus*	+	+	+	+	+	+	Hitch
Embiotocidae:							
Hysterocarpus cf. *H. traski*	+	+	+	+	+	+	Hitch
Cottidae:							
Cottus asper	—	—	—	+	+	+	Hitch

A point of zoogeographic interest should also be noted concerning the presence of *Mylopharodon* in the Kelseyville Formation. This fish was not reported as a member of the recent fish fauna of Clear Lake in the early survey of Jordan and Gilbert (1894) or in later surveys (for example, Cook and others, 1964; 1966). Hopkirk (1974) stated that the absence of *Mylopharodon* from Clear lake might well be the result of local extinction within the last few thousand years. Our findings support this view.

A second point of zoogeographic interest concerns the occurrence of *Gasterosteus* in Clear Lake. This genus was reported to be not only present but common in the Clear Lake fauna before the turn of the century (Jordan and Gilbert, 1894); however, it was not recovered in the later survey of Cook, Moore, and Conners (1966), who considered its occurrence in Clear Lake doubtful. The present fossil data indicate that *Gasterosteus* was a part of the fauna of the lake(s) of the Pleistocene Lower Lake and Kelseyville Formations, which may be ancestral to Clear Lake. Furthermore, the remains of *Gasterosteus* are very abundant in the sediments of present-day Clear Lake that are older than approximately 11,000 B.P. (Casteel and others, 1975, 1977). The absence of *Gasterosteus* in Clear Lake since the turn of this century may well be due to human alteration of both its physical and chemical environments.

Another point of interest deals with the two otoliths found at USGS vertebrate locality M-1352 in the Kelseyville Formation. The otoliths (fig. 115) both measure 7 mm in length and appear to be from the same individual. From the size of these otoliths it is possible to estimate the length and weight of the fish. Weight may be estimated in this species by the following relation:

$$\log \text{weight (g)} = -0.90 + 3.15\,(\log \text{otolith length mm})\quad (n = 12,\quad r = 0.96).$$

Similarly, the standard length (Casteel, 1976) may be estimated by the following relation:

$$\log \text{standard length (mm)} = 1.22 + 1.14\,(\log \text{otolith length mm})\quad (n = 14,\quad r = 0.97).$$

The estimated weight of the fish is 116 g and its estimated standard length is 153 mm. These estimates correspond to the sizes of *H. traski* at the end of their third year of life (Moyle, 1976) in living faunas.

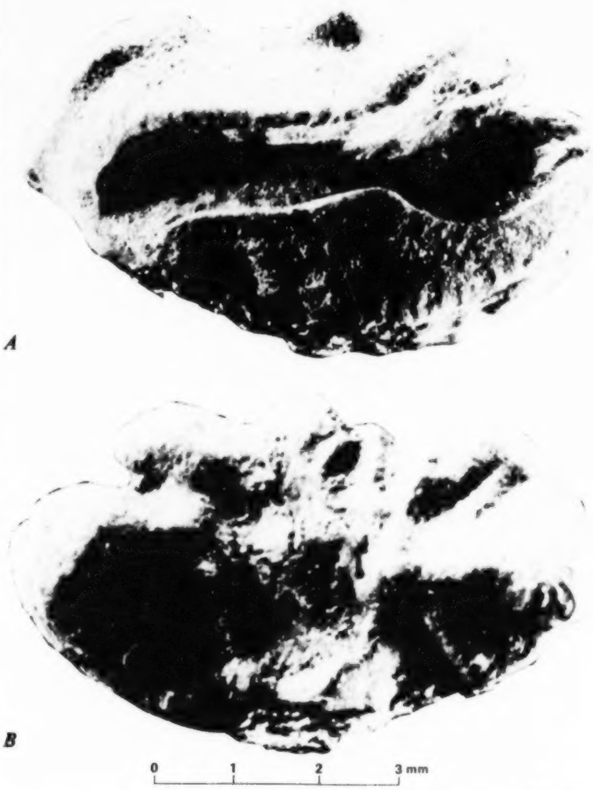

FIGURE 115.—Fossil otoliths from the Kelseyville Formation (USGS vertebrate loc. M-1352), represent *Hysterocarpus* cf. *H. traski* Gibbons (USNM 264252). *A*, Right otolith. *B*, Left otolith.

REFERENCES CITED

American Fisheries Society, 1970, A list of common and scientific names of fishes from the United States and Canada: Special Publication 6, 150 p.

Casteel, R. W., 1972, A key, based on scales, to the families of native California freshwater fishes: California Academy of Sciences Proceedings: v. 39, p. 75-86.

——— 1976, Fish remains in archaeology and paleo-environmental studies: London, Academic Press, 180 p.

Casteel, R. W., and Adam, D. P., 1977, Pleistocene fishes from Alameda County, California: U.S. Geological Survey Journal of Research, v. 5, p. 209-215.

Casteel, R. W., Adam, D. P., and Sims, J. D., 1975, Fish remains from Core 7, Clear Lake, Lake County, California: U.S. Geological Survey Open-File Report 75-173, 67 p.

Casteel, R. W., Beaver, C. K., Adam, D. P., and Sims, J. D., 1977, Fish remains from Core 6, Clear Lake, Lake County, California: U.S. Geological Survey Open-File Report 77-639, 154 p.

Casteel, R. W., and Rymer, M. J., 1975, Fossil fishes from the Pliocene or Pleistocene Cache Formation, Lake County, California: U.S. Geological Survey Journal of Research, v. 3, p. 619-622.

Cook, S. F., Jr., Conners, J. D., and Moore, R. L., 1964, The impact of the fishery upon the midge populations of Clear Lake, Lake County, California: Entomological Society of America Annals, v. 57, p. 701-707.

Cook, S. F., Jr., Moore, R. L., and Conners, J. D., 1966, The status of the native fishes of Clear Lake, Lake County, California: Wasmann Journal of Biology, v. 24, p. 141-160.

Eastman, J. T., 1977, The pharyngeal bones and teeth of catostomid fishes: American Midland Naturalist, v. 97, p. 68-88.

Hearn, B. C., Jr., Donnelly, J. M., and Goff, F. E., 1976, Preliminary geologic map and cross section of the Clear Lake volcanic field, Lake County, California: U.S. Geological Survey Open-File Report 76-751.

Hopkirk, J. D., 1974, Endemism in fishes of the Clear Lake region of central California: University of California Publications in Zoology, v. 96, 135 p.

Jordan, D. S., and Gilbert, C. H., 1894, List of the fishes inhabiting Clear Lake, California: U.S. Bureau of Fisheries Bulletin, v. 14, p. 139-140.

Moyle, P. B., 1976, Inland fishes of California: Berkeley, University of California Press, 405 p.

Rymer, M. J., 1981, Stratigraphic revision of the Cache Formation (Pliocene and Pleistocene), Lake County, California: U.S. Geological Survey Bulletin 1502-C [in press].

MERCURY IN THE SEDIMENTS OF CLEAR LAKE

By JOHN D. SIMS and DONALD E. WHITE

ABSTRACT

Two cores 21.6 and 6 m long were taken in Clear Lake 3.5 and 1.2 km east-northeast of the Sulphur Bank mercury mine, respectively. Sediments in the cores are mostly bioturbated olive-gray sapropelic mud. The longer core contains interbedded peat, carbonaceous sediments, and ash beds between 7.6 and 21.6 m depth. Six zones of peat and carbonaceous sediments have been ^{14}C dated and the ash beds correlated with ^{14}C-dated ash beds in a core 2.5 km to the south.

The mercury content of the sediments in the longer core is much higher than the local background (0.4 parts per million or less), ranging from 0.4 to 75 ppm. The lowest values are generally below 13 m, and the highest value is at the top of the core. Above 13 m depth, the mercury content varies between 1 and 65 ppm and averages 12.1 ppm. Below 13 m (about 17,500 B.P.), the mercury content of the sediments varies between 0.4 and 9.2 ppm (at 21 m) and averages 1.4 ppm. Carbon-14 dates in this core and correlations with ash beds dated in other nearby cores indicate irregular episodes of a high rate of supply of Hg, reaching peak levels at about 34,000, 23,300, 18,000, 9,500, 7,400, and 3,600 B.P. Andesite at Sulphur Bank mine is mineralized with cinnabar and is ^{14}C dated at younger than 44,500±800 B.P. Present-day high values (75 ppm) of Hg are interpreted to be related to mining activity. Older high values are attributed to the flow of Hg-bearing fluids, which, although variable, were probably continuous; Hg not deposited in the Sulphur Bank ore body presumably passed into Clear Lake and was adsorbed on organic material by mechanisms not fully understood.

INTRODUCTION

Of eight continuous sediment cores taken from the bottom of Clear Lake (Sims and others, this volume), one, core 6, was located in Oaks Arm near the Sulphur Bank mercury mine (fig. 116). Another core, core 10, was later taken even nearer to the mine, but because it was not useful to their study, Sims, Adam, and Rymer (this volume) do not describe it. The ore deposit of the Sulphur Bank mine was emplaced by hydrothermal processes which included springs probably similar to those present near the mine today (Everhart, 1946; White and Roberson, 1962). We therefore tested the sediments of cores 6 and 10 for mercury in an effort to detect the late Pleistocene events or processes associated with the Sulphur Bank ore body.

The principle constituent of cores 6 and 10 is a uniform fine-grained sapropelic mud similar to the sediment accumulating today in Clear Lake (Sims and others, this volume). Core 6 contains numerous ash beds, some of which correlate with others in nearby core 7 of Sims, Adam, and Rymer (this volume). Core 10 contains no ash beds or other datable features.

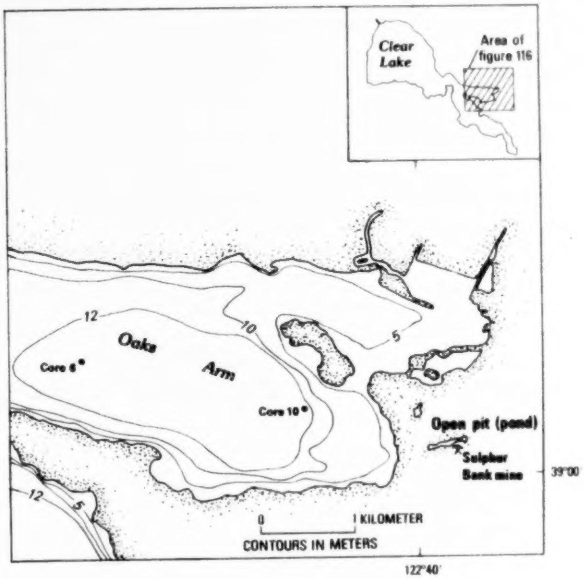

FIGURE 116.—Location of cores 6 and 10 in Oaks Arm of Clear Lake with respect to Sulphur Bank mercury mine.

Sediment transport from the main basin to the arms of the lake probably occurs as the result of regular afternoon northwesterly winds. These winds probably also cause stirring and mixing of water; however, there are few data on current patterns in Clear Lake. The drainage areas of streams flowing into the Oaks Arm of Clear Lake are small. Because this arm of the lake is somewhat isolated, and because it is alined with the dominant northwesterly wind direction, it is likely that sediment derived from the nearby drainage area remains in the Oaks Arm.

ACKNOWLEDGMENTS

We are indebted to Ivan Barnes for initially suggesting that a look at the mercury content of core 6 might be enlightening and for the useful discussions we had with him concerning the data. Michael J. Rymer provided expert field and technical assistance. Analyses by Peter Buseck and David Phelps at Arizona State University, Tempe, Arizona, were made under U.S.G.S. Geothermal Research Grant 14-08-0001-G-383.

SUMMARY OF DATA FROM THE SULPHUR BANK MERCURY MINE

The Sulphur Bank mercury mine, on the Oaks Arm of Clear Lake (fig. 115), is the most productive mineral deposit in the world that is clearly related to hot springs (White and Roberson, 1962; White, 1967). The mineralization is entirely of late Quaternary age and is localized in rocks immediately below the natural water table that existed prior to mining. The hydrothermal alteration and mineralogy of the ore and gangue are controlled to a major extent by the water table. The upper part of an augite andesite lava flow has probably been above the water table throughout the period of introduction of mercury and is extensively leached by sulfuric acid formed by oxidation of H_2S from the active hydrothermal system (White and Roberson, 1962).

Native sulfur was abundant near the surface and was mined commercially from 1865 to 1868, when sulfur ceased because of decreasing grade downward (Veatch, 1883; Everhart, 1946). Mercury, in contrast, increased downward, resulting in an objectionable color to the sulfur. The mine was reopened in 1873 for mercury, which was produced continuously until 1897. Mining by underground methods became increasingly difficult because of abundant objectionable gases (H_2S, CO_2, and CH_4) and high temperatures (up to 80°C). Ore was then mined intermittently from small open pits in 1899-1902, 1915-18, and, on a larger scale, in 1927-47 and 1955-57. Recorded production from the mine is 129,418 flasks of mercury; the total original content of the deposit, allowing for mining and furnace losses and metal still in the ground, must have been equivalent at least to 200,000 flasks, or about 7,000 metric tons (White and Roberson, 1962).

The principal ore bodies were at and below the water table in the middle and lower parts of the augite andesite lava flow and in immediately underlying lacustrine sediments and landslide deposits. Thin films of cinnabar, associated with sulfur, were found on acid-leached rock above the water table. Some commercial-grade ore was deposited in the Franciscan assemblage, but in decreasing concentrations with depth; no mercury mineralization was identified in drill cuttings from geothermal exploration wells from depths below 100 m (White and Roberson, 1962; White, 1967). A carbonized log in lacustrine and landslide deposits 1.6 m below the base of the augite andesite gave a ^{14}C date of >33,000 B.P. (White and Roberson, 1962; p. 401); reanalysis of the same log (analysis QL-190) later yielded an age of 44,500±800 B.P. (Minze Stuiver, written commun., 1975). Potassium-argon dating of the augite andesite yielded only 0.1 to 0.2 percent radiogenic argon (Donnelly, 1977, p. 28). The indicated age, 40,000 ±100 B.P., is useful only in indicating relative youthfulness.

Faults, including a normal fault that displaces the augite andesite at least 10 m, and associated fractures provided the principal structural control for ore deposition. Everhart (1946, p. 136-137) concluded that the major structural features were older than the Quaternary rocks, but White and Roberson (1962, p. 403) found positive evidence for significant postandesite movement.

The thermal system in the Sulphur Bank mine is still discharging mineralized water exceedingly high in B, NH_3, and CO_2 and with considerable Cl, H_2S, hydrocarbon gases, and other constituents (White and Roberson, 1962). Veatch (1883, p. 17-18) estimated a discharge of 300 gallons per minute (1.1 m^3/min) from the springs, but possible contributions from recent rain and near-surface dilution cannot be evaluated because the chemical composition of the discharge was not determined. White and Roberson (1962, p. 418) calculated an average discharge of deep saline water of 0.15 to 0.2 m^3/min. The chemical and isotopic composition of the saline water points to a metamorphic origin for the thermal fluid (White and others, 1973) rather than volcanic, connate, or meteoric origins. The anomalous heat flow of the area, however, is related to the late Tertiary and Quaternary volcanism (Isherwood, this volume).

Whether mercury is still being actively transported in significant quantities in the Sulphur Bank system has been debated (Dickson and Tunell, 1968, p. 1685-1688; White and Roberson, 1962; White, 1967). Positive evidence had been found for deposition of small amounts of cinnabar and metacinnabar as coatings on pebbles previously rounded by agitation in spring pools (White and Roberson, 1962), but Dickson and Tunnel (1968, p. 1685-1688) questioned the significance of the small quantities involved. However, one of us (White) found copious new deposits of mercury in 1975 in active spring vents in the pond that occupies the abandoned mine pit; the pond level was temporarily lowered by evaporation in 1975 below its outlet to Clear Lake, revealing cinnabar, marcasite, pyrite, and native sulfur in loosely cemented rubble emplaced on the north bank of the pond during and after drilling of the eastern of two geothermal exploration wells in 1961-62 (White and Roberson, 1962, p. 425). The time the pond first filled to this level, after the period of dewatering and mining in 1955-57, is not precisely known but was about 1964. Since then, probably a kilogram or more of mercury has been deposited in the nearshore vents, and unknown but probably much larger quantities have precipitated elsewhere in the pond.

Prior to mining, the natural system had no deposits of sinter because temperatures and silica contents were too low. Travertine was absent above the general level of Clear Lake, but inconspicuous travertine occurs along the shore of the lake near and below the high-water line, thus indicating some discharge, presumably thermal, into the lake in addition to the natural discharge from the mine area prior to exploitation (Veatch, 1883).

CORE DATA

Core 6 (fig. 117) was taken in October 1973 from a barge-mounted rotary drilling rig stationed where the water depth was 12.2 m; and is 21.64 m long. Core 6 is located at the west end of the flat floor of the Oaks Arm about 3.5 km from Sulphur Bank mine. Core 10 (fig. 115) was taken subsequently in February 1976 by a gas-operated piston corer (Mackereth, 1958) in about 12 m of water and is 3.87 m long. Core 10 is from the east end of the floor of the Oaks Arm approximately at the break in slope.

The sediments in core 6 consist of bioturbated interbedded sapropelic mud, peat, peaty mud, and volcanic ash (fig. 117). The upper 7.57 m consists of fine, very dark grayish brown to very dark brown (10YR4/2 to 5Y3/2) sapropelic mud. At 7.57 m depth the first peaty bed appears; it is 9.5 cm thick and is composed of clayey peat. Between 7.57 and 13.0 m are several peat-rich horizons and two ash beds. The lower ash bed, between 12.93 and 12.95 m, is rhyolitic in composition and is correlated with a similar ash between 12.29 and 12.34 m in nearby core 7 (Sims and others, this volume). Radiocarbon analyses on carbonaceous material 5 cm above and 40 cm below the core 7 ash bed yield dates of 17,660±340 and 17,470±300 B.P., respectively (See table 30). Below 13.0 m the sediments are

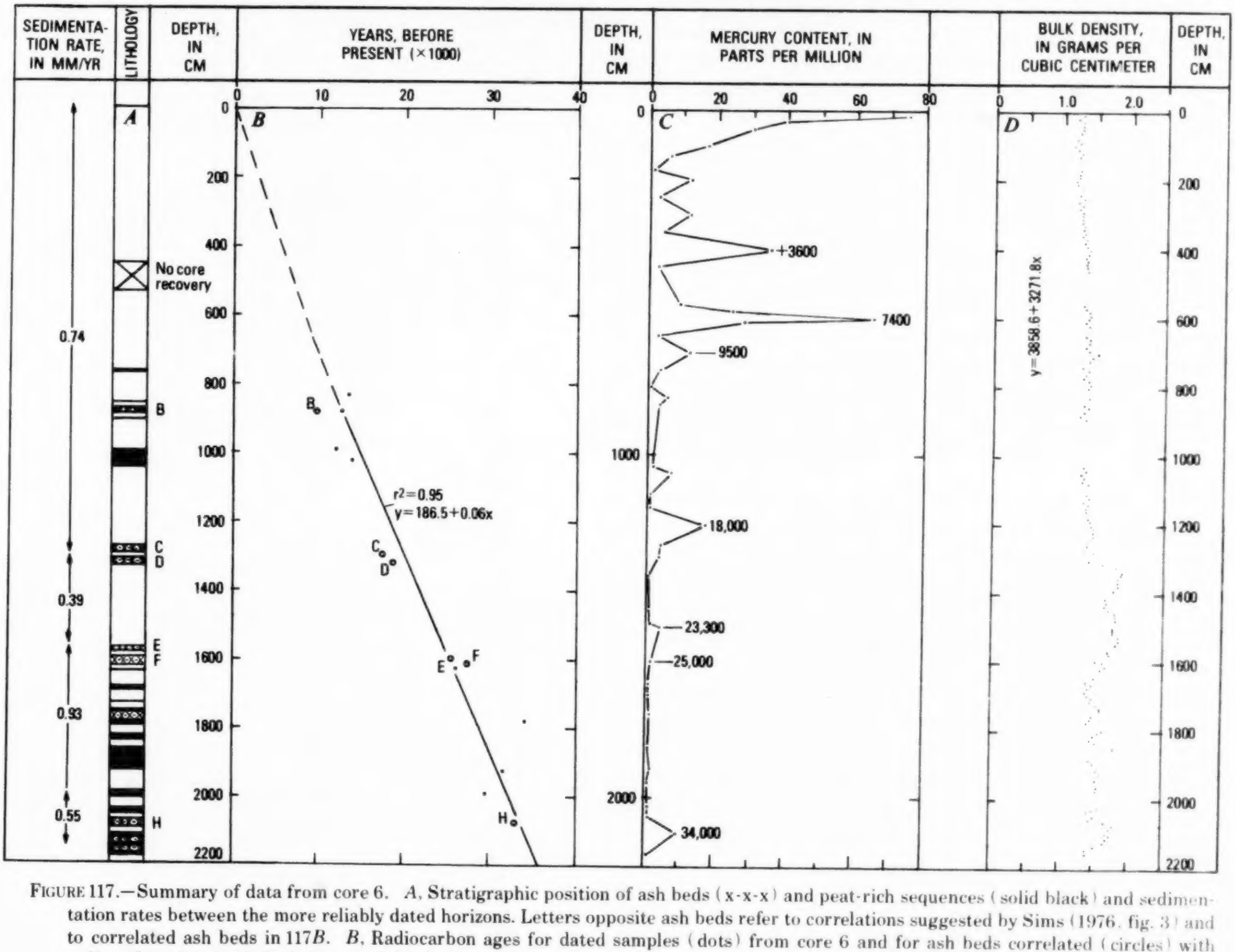

FIGURE 117.—Summary of data from core 6. *A*, Stratigraphic position of ash beds (x-x-x) and peat-rich sequences (solid black) and sedimentation rates between the more reliably dated horizons. Letters opposite ash beds refer to correlations suggested by Sims (1976, fig. 3) and to correlated ash beds in 117*B*. *B*, Radiocarbon ages for dated samples (dots) from core 6 and for ash beds correlated (circles) with radiocarbon-dated ash beds in core 7 (data from Sims, 1976). *C*, Mercury content and estimated radiocarbon ages of selected maxima. *D*, Bulk density versus depth.

more clay rich and compact (fig. 117) and contain numerous interbedded peat or peaty beds and six additional ash beds. Most of the beds interpreted as volcanic ash are clay-rich units that have a mottled texture in X-ray radiographs; fresh glass is rare or absent. These units are interpreted as altered basaltic, andesitic, or dacitic pyroclastic material (Sims and Rymer, 1975a).

Radiocarbon dates of carbonaceous components of the sediments yield an absolute chronology for the core (fig. 117). Between these dated horizons sedimentation rates may be estimated for the intervals. For core 6, sedimentation rates average about 0.66 mm/yr. Incremental sedimentation rates between some of the more reliably dated horizons range from 0.39 to 0.93 mm/yr (fig. 117).

Sedimentation rates for core 10 cannot be calculated because no datable horizons were identified. The sedimentation rate for core 10 is probably higher than that for a comparable time span in core 6 because of proximity to the shore and the waste dumps of the Sulphur Bank mine. These dumps, which are unvegetated and susceptible to severe seasonal erosion, were emplaced after 1927, when mechanized open-pit mining started.

These data provide the lithologic and time framework for the mercury analyses of the sediments. Samples were taken at intervals ranging from 30 to 109 cm and air dried. Those from core 6 were analyzed in 1975 by Kam Leong of the U.S. Geological Survey by a mercury vapor technique (Vaughn, 1967), and samples from core 10 plus a few from core 6 were analyzed in 1978 by Peter Buseck and David Phelps, Arizona State University, Tempe, by a similar technique (Matlick and Buseck, 1976). The results of the analyses are given in table 33.

The lower 5 m of core 6 (16.6-21.6 m) is characterized by Hg contents less than 1 ppm (range, 0.4-0.85 ppm). Between 16 m and the top of the core Hg contents are variable but are markedly higher than in the lower 5 m (fig. 116); however, clear anomalies occur at 21.0 m (9.2 ppm Hg, 34,000 B.P.) and at 19.1 m (1.2 ppm Hg, 30,600 B.P.). The two highest levels of Hg are at 6 m (65 ppm) and 10 cm, the shallowest sample (75 ppm). The first sample above 20 m showing increased Hg levels is at 15.98 m having a value of 1.3 ppm. The interpolated age of this sample from ^{14}C age dates is about 25,000 B.P. Stratigraphically higher maxima of Hg content and their interpolated ages are shown in figure 117.

DISCUSSION

Mercury contents vary with depth in core 6 from Clear Lake, but the variation in core 10 is not clearly defined, perhaps because the core does not represent a long enough time span to show the episodic variations found in core 6. The Hg contents are not related in any simple way to variations in lithology or organic content of sediments (fig. 117). Peat and peat-rich beds and compaction (density) increase downward, but there is no other obvious change in the sediment. We interpret the variations in Hg content in most of core 6 as reflecting variations in the amount of Hg escaping into the lake while the Sulfur Bank mercury deposit was being formed. However, the Hg contents of the upper 0.3 to 1.0 m of core 6 are probably related in part to mining activities and erosion of the waste dumps that accumulated on and near the lakeshore. Unfortunately, we cannot determine with certainty the specific depth of sediments that reflect human activity, but we believe that the upper 50 cm is so affected and that the deeper anomalies are natural.

TABLE 33.—*Mercury analyses for cores 6 and 10, Clear Lake*

[All analyses from core 6 except samples at 30, 400, 579, 609, 1,490, 1,910, and 2,020 cm depth by Kam Leong, U.S. Geological Survey; the rest are by Peter Buseck and Dave Phelps, Arizona State University, Tempe, Ariz., >, greater than]

Depth (cm)	Sample No.	Hg (ppm)
	Core 6	
10	303	75.0
30	305	>40.0
50	307	30.0
100	311	17.0
130	314	6.0
170	368	1.3
200	371	12.0
250	317	2.8
300	322	12.0
350	327	4.4
400	332	>35.0
450	337	2.8
559	338	9.0
579	340	24.0
599	342	65.0
609	343	27.5
650	345	2.8
701	350	12.0
749	355	3.4
800	360	.9
830	361	5.4
851	363	3.4
1030	374	1.8
1051	376	7.0
1111	380	.9
1151	384	.85
1201	388	17.0
1262	393	3.8
1294	396	3.4
1352	403	.4
1452	411	.4
1490	413	1.15
1502	414	3.8
1598	422	1.3
1663	426	.4
1693	430	.5
1753	435	.85
1801	462	.76
1851	457	.4
1910	466	1.2
1953	439	.4
2020	442	.57
2057	446	.85
2100	451	9.2
2159	456	.4
	Core 10	
0	10-001	44.0
40	10-005	50.0
80	10-009	63.0
120	10-013	14.25
160	10-017	35.5
200	10-021	6.5
240	10-025	15.0
280	10-029	27.5
320	10-033	7.5
360	10-037	17.5
387	10-040	>40.0

The Hg-mineralized andesite is known by independent ^{14}C-age dating to be younger than 44,000 B.P., and the formation of the ore body postdates the flow. The first notable increase in Hg levels in the sediments over background levels occurred about 34,000 B.P. We speculate that the andesite flow was cut by a fault at this time, thereby providing permeable channels for discharge of the mercury-bearing ore fluids.

The chemical state of Hg in the sediments is unknown. The mercury mineral deposited in the Sulphur Bank mine was mainly cinnabar (HgS); however, the Hg contained in the sediments below the upper meter of core 6 is probably not detrital cinnabar because the cinnabar of the ore deposit was precipitated near and below the local water table and not directly exposed to erosion before mining began in the 1800's. Other alternatives for transporting Hg from the present mine area to the offshore sediments include (1) HgS precipitating in the discharging spring waters along the edge of the altered andesite flow, perhaps as colloidal HgS not fixed in the ore deposit; or (2) elemental Hg that, because of its high volatility, escaped from the water table and from spring vents, eventually dissolving in the nearby lake water and becoming adsorbed on organic detritus.

REFERENCES CITED

Dickson, F. W., and Tunnell, George, 1968, Mercury and antimony deposits associated with active hot springs in the western United States, *in* Ridge, J. D., ed., Ore deposits in the United States 1933-1967, Graton-Sales Volume: American Institute of Mining and Metallurgical Engineering, v. 2, p. 1673-1701.

Everhart, D. L., 1946, Quicksilver deposits at the Sulphur Bank mine, Lake County, California: California Journal of Mines and Geology, v. 42, p. 125-153.

Mackereth, F. J. H., 1958, A portable core sampler for lake deposits: Limnology and Oceanography, v. 3, p. 181-191.

Matlick, J. S., III, and Buseck, P. R., 1976, Exploration for geothermal areas using mercury: A new geochemical technique: United Nations Symposium on the Development and Use of Geothermal Resources, 2d, San Francisco, 1975, Proceedings, v. 1, p. 785-792.

Reimers, R. S., Krenkel, P. A., Eagle, Margaret, and Tragitt, Gregory, 1975, Sorption phenomenon in the organics of bottom sediments, *in* Krenkel, P. A., ed., Progress in Water Technology: v. 7, p. 117-130.

Sims, J. D., 1975, Determining earthquake recurrence intervals from deformational structures in young lacustrine sediments: Tectonophysics, v. 29, p. 141-152.

Sims, J. D., 1976, Paleolimnology of Clear Lake, California, U.S.A., *in* Horie, Shoji, ed., Paleolimnology of Lake Biwa and the Japanese Pleistocene: Kyoto, Japan, Kyoto University, v. 4, p. 658-702.

Sims, J. D., and Rymer, M. J., 1975a, Preliminary description and interpretation of cores and radiographs from Clear Lake, Lake County, California: Core 7: U.S. Geological Survey Open-File Report 75-144, 70 p.

——— 1975b, Preliminary description and interpretation of cores and radiographs from Clear Lake, Lake County, California: Core 6: U.S. Geological Survey Open-File Report 75-569, 47 p.

——— 1976, Map of gaseous springs and associated faults in Clear Lake, California: U.S. Geological Survey Miscellaneous Field Studies Map MF-721, scale 1:48,000.

Vaughn, W. M., 1967, A simple mercury vapor detector for geochemical prospecting: U.S. Geological Survey Circular 540, 8 p.

Veatch, J. A., 1883, Letter from Dr. John A. Veatch to the Borax Company of California, June 28, 1857: California State Mining Bureau, Third Annual Report of State Mineralogist, pt. 2, p. 15-20.

White, D. E., 1967, Mercury and base-metal deposits with associated thermal and mineral waters, *in* Barnes, H. L., ed., Geochemistry of hydrothermal ore deposits: New York, Holt, Rinehart and Winston, p. 575-631.

White, D. E., Barnes, Ivan, and O'Neil, J. R., 1973, Thermal and mineral waters of non-meteoric origin, California Coast Ranges: Geological Society of America Bulletin, v. 84, p. 547-560.

White, D. E., and Roberson, C. E., 1962, Sulphur Bank, California, a major hot spring quicksilver deposit: Geological Society of America, Buddington Volume, p. 397-428.

FAULTING AND ORE CONTROLS AT THE CULVER-BAER MINE, SONOMA COUNTY, CALIFORNIA

By Eugene V. Ciancanelli

ABSTRACT

The Culver-Baer mercury mine is located in the Mayacmas quicksilver district on the northwest-trending Mercuryville fault zone, a part of the San Andreas fault system. A zone of hydrothermal alteration occurs along the strike of the Mercuryville fault zone, which was the principal conduit for hydrothermal ore fluids in this area. The hydrothermal fluids selectively altered large blocks of serpentinite to silica-carbonate rock, the host rock for the mercury mineralization. Within the fault zone the serpentinite and silica-carbonate rock are faulted into large blocks surrounded by fault gouge. The fault gouge consists of mylonitized shale enclosing sheared and brecciated blocks of hydrothermally altered graywacke. The regional and local structural relations suggest right-lateral displacement of the faulted blocks of serpentinite and silica-carbonate rock within the Mercuryville fault zone. The variation in location and the specific type of hydrothermal alteration indicate that hydrothermal alteration occurred in three stages at the Culver-Baer mine. Specific structures such as rolls along fault planes, fault intersections, and tension fractures were permeable zones for the circulation of hydrothermal fluids and structurally favorable sites for mercury mineralization.

INTRODUCTION

The Culver-Baer mercury mine is located in the Mayacmas quicksilver district in Sonoma County, Calif., at the south edge of the Geysers steam field (fig. 118). The Culver-Baer was first mined in 1872 and has operated intermittently during periods of high mercury prices. The mine was last operated during the late 1960's and early 1970's by the Sulphur Creek Mining Company and is currently owned by Thermogenics Corporation. Approximately 20,000 flasks of mercury has been produced. The workings consist of an open pit developed by the Sulphur Creek Mining Company and several levels of older underground workings, all of which are now inaccessible except for the #3 adit level. The #3 adit level was the lowest level mined in the Culver-Baer mine. The portal for the #3 adit is located near the bottom of Devils Den Canyon, and in 1969 the workings extended in an east to southeast direction for 1,013.5 m.

The surface and accessible underground workings of the Culver-Baer mine were mapped during the fall of 1968 and the spring of 1969 in conjunction with a geothermal exploration program conducted by Geothermal Resources International in the Geysers-Clear Lake region. The detailed study of the Culver-Baer mine had two objectives; the first was to gain an understanding of the behavior of hydrothermal systems in the Geysers area. During the late 1960's it was known that mercury mineralization was associated with thermal springs (White and Roberson, 1962; White, 1967; and Dickson and Tunell, 1968), and the association of mercury with geothermal fields was also documented in other areas (Koenig, 1969; Tonani, 1970; White, 1970). It was thought that a detailed study of the Culver-Baer mine would provide the opportunity to study a "fossil" hydrothermal system similar to the active hydrothermal system in the Geysers steam field. It was hoped that the relation of the fractures in the Culver-Baer mine to the older hydrothermal system would provide a better understanding of the relation of the fracture system to the steam reservoir in the Geysers steam field.

In the late 1960's the demand for mercury was very high, and the second objective for the Culver-Baer mine study was to evaluate the potential for developing additional mercury ore. Several promising underground exploration targets were conceived but never tested. One surface orebody was suggested to the Sulphur Creek mining Company, and this ore was mined.

Acknowledgments.—I am grateful for the field assistance of Dave Wood and Arthur R. Brown in the preparation of the underground maps. Joseph Gallacci of the Sulphur Creek Mining Company provided access to the property, and Tom O'Connor, a mining engineer, provided a survey of the #3 adit-level mine workings. The geologic map of the #3 adit level was tied to O'Connor's survey. S. A. Williams provided petrographic descriptions of several rock samples. The late George Gall and the late J. Q. Anderson provided the benefit of their experience to the project. Geothermal Resources International provided the financial support for this study. Dennis Sorg and Robert J. McLaughlin kindly reviewed the manuscript.

GEOLOGIC SETTING OF THE CULVER-BAER MINE

The Culver-Baer mine is located along the northwest-trending Mercuryville fault zone, which forms the southwest edge of the Geysers steam field

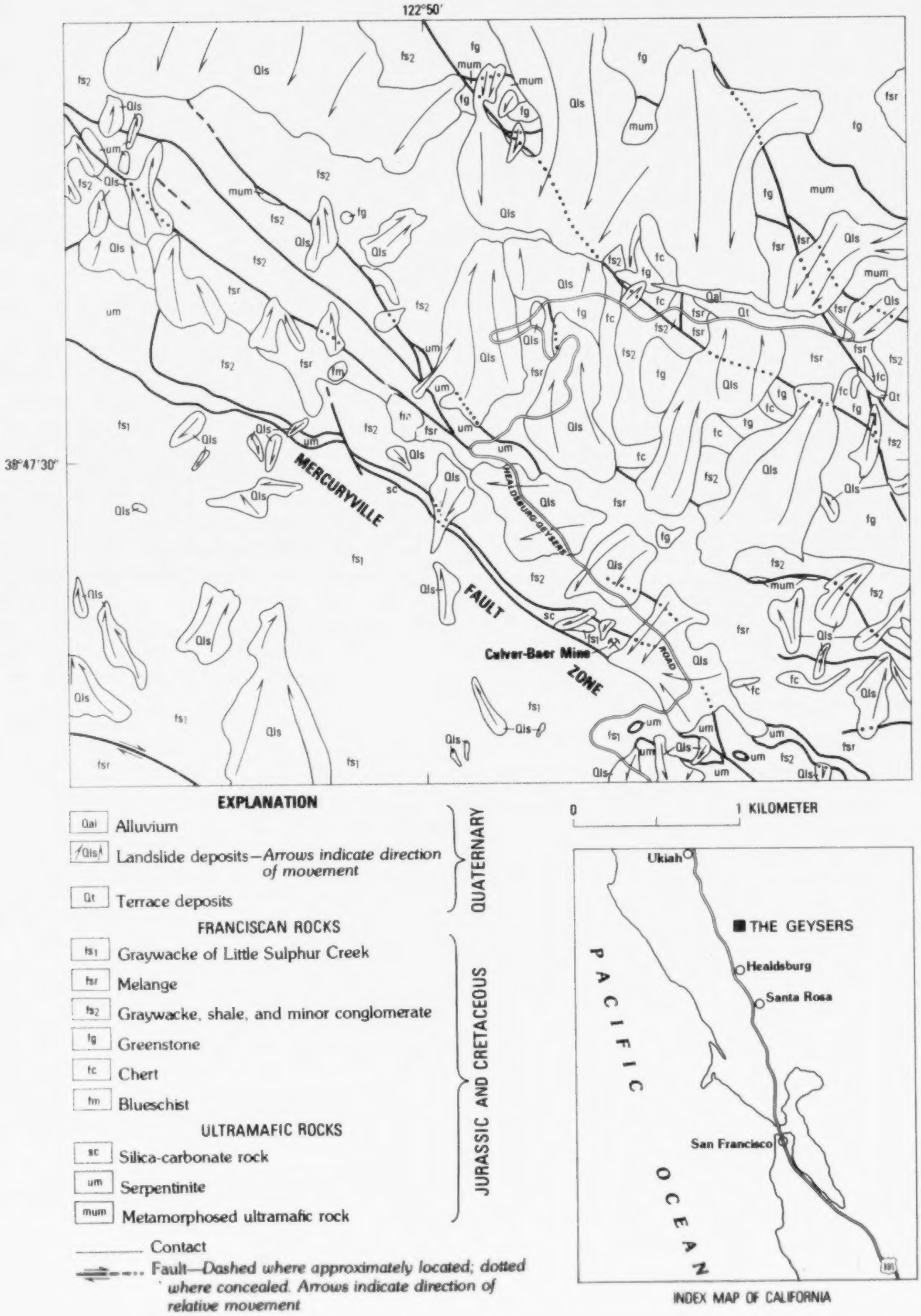
122°50′
38°47′30″
MERCURYVILLE FAULT ZONE
HEALDSBURG-GEYSERS ROAD
Culver-Baer Mine
Qls
Qal
Qt
fs1
fsr
fs2
fg
fc
fm
sc
um
mum
EXPLANATION
Qal Alluvium
Qls Landslide deposits—Arrows indicate direction of movement
Qt Terrace deposits
QUATERNARY
FRANCISCAN ROCKS
fs1 Graywacke of Little Sulphur Creek
fsr Melange
fs2 Graywacke, shale, and minor conglomerate
fg Greenstone
fc Chert
fm Blueschist
ULTRAMAFIC ROCKS
sc Silica-carbonate rock
um Serpentinite
mum Metamorphosed ultramafic rock
JURASSIC AND CRETACEOUS
Contact
Fault—Dashed where approximately located; dotted where concealed. Arrows indicate direction of relative movement
0
1 KILOMETER
Ukiah
THE GEYSERS
Healdsburg
Santa Rosa
San Francisco
PACIFIC OCEAN
101
INDEX MAP OF CALIFORNIA

FIGURE 118.—Geologic map of the Geysers-Culver-Baer mine area (from McLaughlin, 1975a).

(Goff and others, 1977). The geology of the area (fig. 118) has been mapped and described by Bailey (1946), NcNitt (1968), McLaughlin (1975a), and McLaughlin and Stanley (1975). A discussion of the gravity and magnetic studies in the area was published by Isherwood (1975). The rocks in the immediate area of the Culver-Baer mine consist of intensely sheared and faulted graywacke and shale of the Franciscan assemblage and minor conglomerate, chert, and metabasalt (greenstone). An elongate northwest-trending block of serpentinite within the Mercuryville fault zone has been selectively altered to silica-carbonate rock. The serpentinite may be part of an ophiolite sequence that was underthrust by the Franciscan assemblage and subsequently tectonically emplaced in its present position by high-angle faulting and infolding along the Mercuryville fault zone (McLaughlin, 1975b, 1977a, b). The serpentinite is possibly related to the ophiolite section exposed 1½ km to the south at Black Mountain and Geyser Peak.

The Mercuryville fault zone apparently forms the south edge of the Geysers steam reservoir. Geothermal wells drilled high on the Mercuryville structure by Pacific Energy Corporation and Geothermal Kinetics Corporation have been unsuccessful. As a result of the Culver-Baer mine study it was predicted in the late 1960's that the steam field would end against the Mercuryville structure because significant amounts of hydrothermal alteration and mineralization did not occur to the south of the structure. Geothermal Resources International therefore decided not to obtain geothermal leases south of the Mercuryville fault.

STRUCTURE

The Mercuryville fault zone strikes northwest, dips steeply northeast, and appears to have both vertical and horizontal components of movement. Detailed mapping of the #3 adit level indicated that silica-carbonate rock in the fault zone is displaced in a right-lateral sense. Right-lateral movement characterizes the northwest-trending fault zones in the region.

The Mercuryville fault zone dips generally 40°-90° NE., although dips measured on faults and shear zones in the underground workings range from 17° to 90° NE. The fault zone ranges from 10 to 100 m in width, and it is composed of blocks 1cm to 10 m in size of hydrothermally altered brecciated Franciscan graywacke in a grayish-black shalelike mylonitic matrix. The mylonite matrix may have originally formed from shale interbeds within the graywacke that were less competent than the graywacke and were, therefore, more readily mylonitized by fault movement. It is also possible that the mylonite matrix was formed from graywacke, as no recognizable bodies of shale occur as breccia blocks in the mylonite zone. There are likewise very few fragments of serpentinite or silica-carbonate rock in the fault zone. More than 99 percent of all breccia fragments consist of hydrothermally altered graywacke. The altered graywacke is light gray and contains numerous ocher limonite-rich veins. The hydrothermal alteration of the graywacke is confined to the breccia fragments within the fault zone. At the borders of the fault zone, the altered graywacke breccia fragments are in contact with relatively unfractured silica-carbonate wallrocks (fig. 119). The contact surface between the brecciated rock of the fault zone and the wallrock is a zone of highly polished jetblack mylonite 5 to 30 cm thick. During the course of mapping, this material was referred to as metamylonite. The metamylonite is a jetblack lustrous material resembling anthracite and consists of numerous highly polished microfracture surfaces.

The Mercuryville fault is a rather wide shear zone that encompasses large blocks of relatively unfaulted rock. These included blocks may be compared to large horses or large-scale boudins where brittle rock was torn apart and included within the more plastic mylonite of the fault zone (fig. 120). The large blocks of relatively unfaulted serpentinite, silica-carbonate rock, and graywacke included with the mylonite are often cut by small faults that generally strike north or northeast.

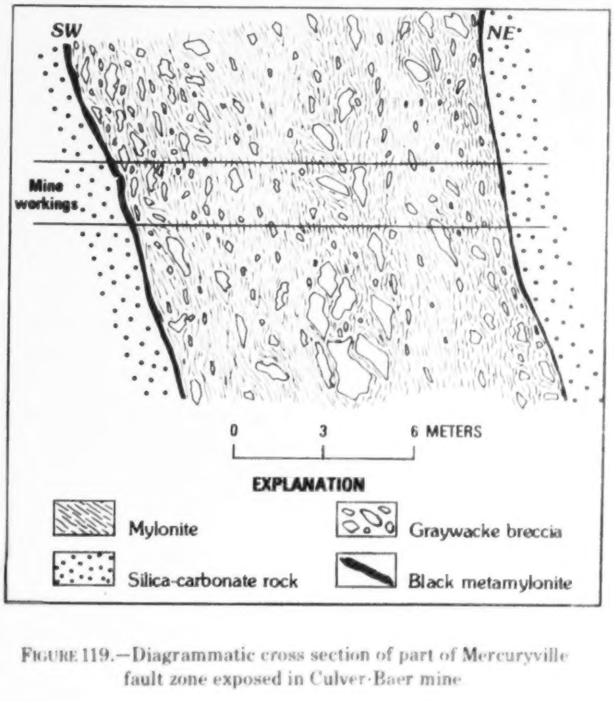

FIGURE 119.—Diagrammatic cross section of part of Mercuryville fault zone exposed in Culver-Baer mine

Only rarely do these secondary faults cut the mylonitized rocks of the Mercuryville fault.

The mylonite and breccia blocks exhibit a planar fabric that trends northwest and dips steeply northeast parallel to the plane of the Mercuryville fault. The planar fabric is locally deflected and runs parallel to the edges of the included blocks of serpentinite, silica-carbonate rock, and hydrothermally altered graywacke (fig. 120).

ALTERATION AND MERCURY MINERALIZATION

The zone of hydrothermal alteration at the Culver-Baer mine is localized along the Mercuryville fault zone. Serpentinite has been altered to silica-carbonate rock, and the graywacke has been selectively altered at several scattered locations.

The alteration of the graywacke is very feeble and consists of local sericitization, alteration of mafic minerals to limonite, replacement of feldspar and mica by clay minerals and hydromicas, and by veining by calcite and limonite after iron sulfides. The hydrothermally altered graywacke crops out as light-gray areas cut by thin veins of limonite. Mercury ore was produced from similar hydrothermally altered graywacke at other mines in the Mayacmas quicksilver district. Bailey (1946) noted the occurrence of cinnabar and native mercury in the sandstone near serpentinite and silica-carbonate rock at the mines on the ridge between Big Sulphur and Little Sulphur Creeks, one of which is the Culver-Baer mine. Mercury ore was mined in a small open pit located to the north of the Healdsburg-Geysers road (near the letters "Qls" on the second bend in this road proceeding north from south edge of area, fig. 118). The mercury occurred as cinnabar in the silica-carbonate rock and as native mercury in the hydrothermally altered graywacke.

The principal host rock for mercury mineralization in the Mayacmas quicksilver district is hydrothermally altered serpentinite, locally referred to as silica-carbonate rock. The silica-carbonate rock associated with mercury mineralization in the Mayacmas quicksilver district has been described by Bailey (1946), Yates and Hilpert (1946), and Henderson (1969). The alteration of serpentinite to silica-carbonate rock is believed to postdate the Sonoma Volcanics (Bailey, 1946; Yates and Hilpert, 1946). The age of the Sonoma Volcanics ranges from 5.3 m.y. to about 2.9 m.y. (Mankinen, 1972). Conversion of serpentinite to silica-carbonate rock may still be occurring in this region as the Geysers steam field is an active hydrothermal system.

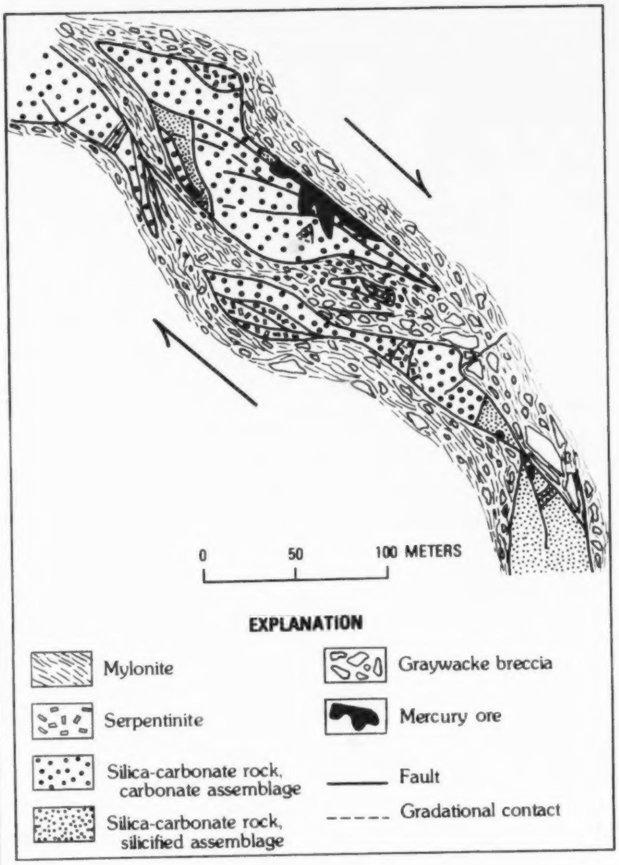

FIGURE 120.—Geologic sketch map of Field stope area of Culver-Baer mine. Large blocks of serpentinite and silica-carbonate rock have been torn apart and displaced in a right-lateral sense (arrows) by movement along Mercuryville fault, which encloses these blocks.

At the Culver-Baer mine the silica-carbonate rock was divided into two types on the basis of the mineral assemblage. The first, a carbonate mineral assemblage, consists of dolomite, calcite, ankerite, siderite, magnesite, kaolinite, and variable amounts of quartz and chalcedony. The second type, a harder silicified mineral assemblage, is composed largely of chalcedony, quartz, and opal. The two types of silica-carbonate rock could be distinguished in the mud-covered mine workings by the sound they make when struck by a pick. The carbonate assemblage gives a dull thud while the silicified assemblage has a clear ring. The softer carbonate assemblage tends to form smooth rounded faces during mining, and the harder silicified assemblage has a regular fracture pattern that forms blocky faces during mining. The carbonate assemblage is a poor host rock for mercury mineralization and usually does not contain ore-grade concentrations of cinnabar. The siliceous silica-carbonate rock and the carbonate assemblage with veins and patches of silicification are the main host rocks for ore deposition in the Culver-Baer mine.

Bailey (1946, p. 217) observed the opposite relation for the western Mayacmas quicksilver district: "chalcedony is the most abundant mineral in the silica-carbonate rock generally, but the ore seems to be chiefly associated with rock rich in carbonates."

The contacts between the two types of silica-carbonate rock are always faults. No gradational contacts were noted. There are gradational types of silica-carbonate rock; these include a carbonate assemblage with siliceous patches and bands and a silica assemblage with occasional patches or bands of the softer carbonate assemblage. The gradational types of silica-carbonate rock are separated from the strictly carbonate or strictly siliceous assemblages by faults. No exposures were observed where a strictly carbonate assemblage or a strictly siliceous assemblage are in unfaulted contact with a gradational silica-carbonate assemblage. If such gradational contacts did exist, they have become fault contacts by subsequent tectonic activity. Gradational contacts were noted between the serpentinite and the carbonate assemblage but not between the serpentinite and the siliceous assemblage.

The silica-carbonate rock exhibits a sequence of hydrothermal alteration and mineralization that occurred in several stages. Stage 1 was the selective conversion of serpentinite to a carbonate-rich silica-carbonate rock. Stage 2 was a period of localized silicification along fracture zones. Mercury mineralization may have occurred during stage 2. At the end of stage 2 serpentinite coexisted with both the carbonate and silicified assemblages of silica-carbonate rock. Following stage 2 a period of faulting occurred during which silicified silica-carbonate rocks were moved adjacent to the softer carbonate assemblage. During this period of faulting any gradational contacts that may have existed between the various types of silica-carbonate rock were probably faulted. Stage 3 was a second later period of silicification and ore deposition when veinlets of quartz, 1 cm or less in thickness, were deposited in open fractures. Cinnabar is commonly found in these quartz veinlets and the quartz veinlets generally occur with disseminated cinnabar. The silicified silica-carbonate rock of stage 2 was more brittle than the carbonate assemblage silica-carbonate rock of stage 1. Zones of permeable breccia were developed when the silicified assemblage was fractured, which gave access to the ore deposition. Hydrothermal alteration and brecciation of graywacke in the Mercuryville fault zone could not be correlated with any of the three stages of alteration and mineralization.

The major ore mineral at the Culver-Baer mine is cinnabar, which commonly occurs as euhedral crystals along fracture surfaces and within veinlets. Native mercury occurred in altered graywacke mined from the small open pit located to the north of the Healdsburg-Geyser road. Bailey (1946) reported metacinnabar from the now inaccessible Oakland workings of the Culver-Baer mine. The ore from the Oakland workings is reported to have been purple in contrast to the Geyser workings and the Field stope which have scarlet cinnabar. This purple ore at the Oakland workings may have been a mixture of dark metacinnabar with cinnabar.

The #3 adit level was driven toward the downward projection of the Oakland ore body, but the workings appear to have stopped just short of intersecting the projected downward extension of the Oakland mineralization. On the #3 adit level the Field stope ore body is approximately 250 m northwest of that possible intersection. Iron oxide, pyrite, and marcasite occur with cinnabar in the Field stope. Iron oxides are present in the interval from the Field stope to the end of the #3 adit level. In the final 100 m of the #3 adit level, iron oxides after sulfides increase sharply. The increase could indicate that the extension of the Oakland mineralization is nearby.

The presence of iron oxide near the Oakland ore body may explain the presence of metacinnabar in the ore. Dickson and Tunell (1959) showed that pure metacinnabar is stable above 344°C at atmospheric pressure, but in the presence of Fe and Zn in solid solution the inversion temperature may be 240°C or even lower. They stated that a progression of metacinnabar to cinnabar could be the result of either a decrease in temperature or a decrease, at constant temperature, in concentration of some substance such as iron until cinnabar predominated. The authors suggest that it is probably more reasonable to explain continuous deposition of HgS by decreasing temperature rather than variations in the composition of the ore fluids, otherwise reverse relationships (early cinnabar and late metacinnabar) should be observed more commonly. Field relations at the Culver-Baer mine suggest that the ore fluids had a higher iron content in the vicinity of the main ore bodies with possibly the highest iron content in the Oakland ore body. The presence of metacinnabar in the Oakland ore was perhaps controlled by the iron concentration in the ore fluids.

STRUCTURAL ORE CONTROLS

The major structural ore control at the Culver-Baer mine is faulting. Faults serve as the channelways along which the hydrothermal fluids circulated. It is a rule of thumb in exploring for mercury in the Mayacmas quicksilver district to explore flexures in the fault plane, especially where the dip of the fault flattens appreciably. These flattened "rolls" create inverted troughs, and it is along these troughs that ore often forms (fig. 121). The ore in the Field stope is an excellent example of ore localized along a roll in a fault plane. The wallrocks along the zone of flexure are intensely fractured, and as a result the silica-carbonate rock along the zone of flexure became a conduit for later stages of silicification and mercury mineralization.

Mercury ore may also be localized at the intersection

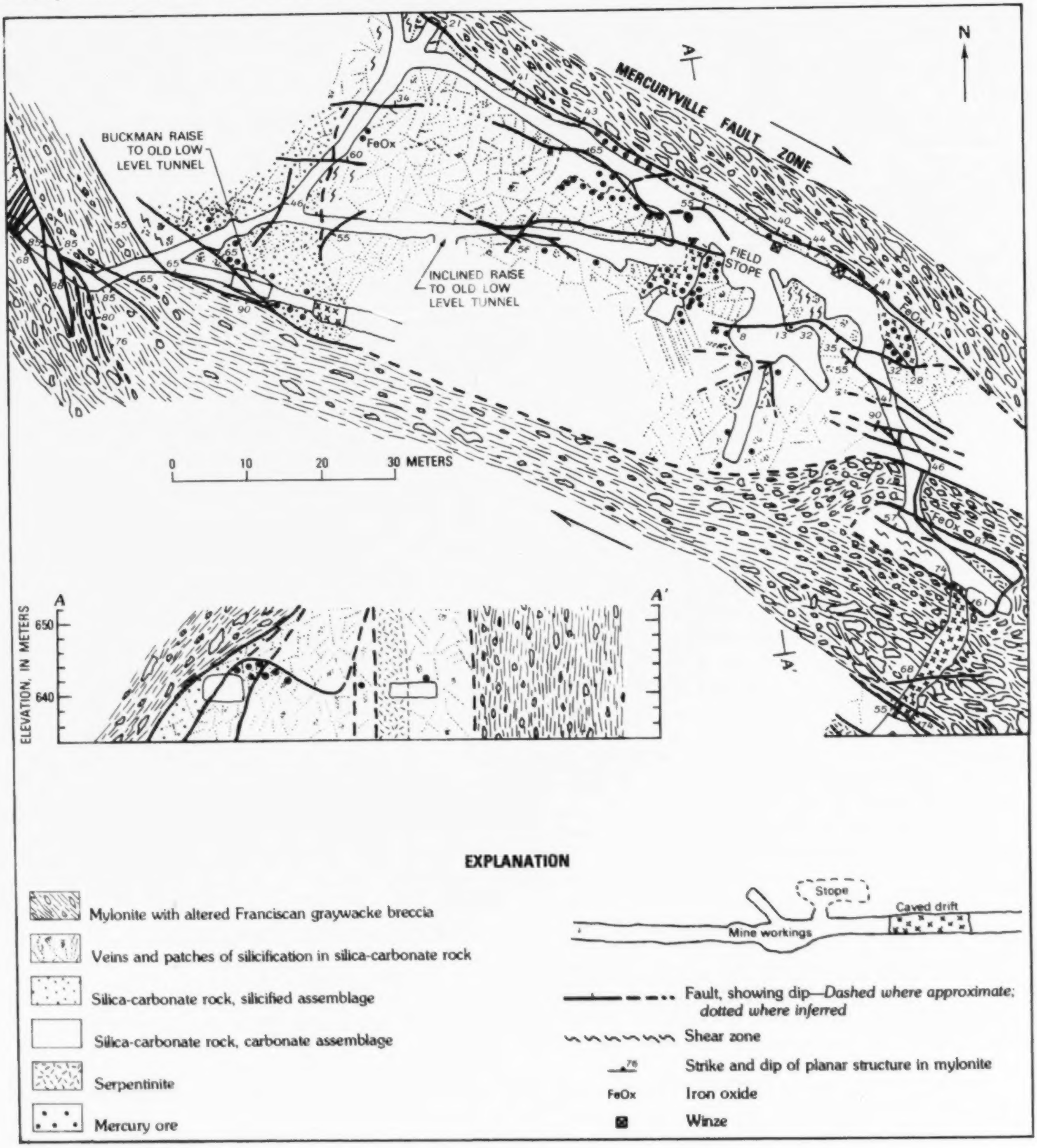
N
A
A'
MERCURYVILLE FAULT ZONE
BUCKMAN RAISE TO OLD LOW LEVEL TUNNEL
INCLINED RAISE TO OLD LOW LEVEL TUNNEL
FIELD STOPE
FeOx
0 10 20 30 METERS
ELEVATION, IN METERS
650
640
EXPLANATION
Mylonite with altered Franciscan graywacke breccia
Veins and patches of silicification in silica-carbonate rock
Silica-carbonate rock, silicified assemblage
Silica-carbonate rock, carbonate assemblage
Serpentinite
Mercury ore
Stope
Caved drift
Mine workings
Fault, showing dip—Dashed where approximate; dotted where inferred
Shear zone
Strike and dip of planar structure in mylonite
FeOx Iron oxide
Winze

FIGURE 121.—Geologic map and cross section of Culver-Baer mine #3 adit level.

of two or more fault planes. The ore in the vicinity of the Buckman raise appears to be of this type (fig. 121). The area could not be thoroughly studied because of dangerous ground conditions and loose timbering in the Buckman raise. One miner was seriously injured during efforts to rehabilitate this part of the mine. A vertical fault (fig. 121) separates mylonite and altered Franciscan graywacke breccia on the south and silica-carbonate rock on the north. This vertical fault is intersected by another fault dipping 65° NE. The footwall of this second fault is carbonate assemblage silica-carbonate rock with scattered patches of silicification. The hanging wall is silicified assemblage silica-carbonate rock with later stage veinlets of a second period of silicification. At the intersection of the two faults mercury ore occurs in the hanging-wall silicified assemblage of silica-carbonate rock.

Tension fractures along a fault plane or between two fault planes can localize ore, as has occurred near the southeast end of the #3 adit level. Two small mercury ore bodies in silicified assemblage silica-carbonate rock occur near the south end of the area shown in figure 120. The silica-carbonate rock is two wedge-shaped slabs formed by a tearing apart of the silica-carbonate rock by right-lateral movement along the Mercuryville fault zone. Small tension fractures and breccia occur near the tip of both wedge-shaped slabs formed from movement along the fault. The open fractures provided a favorable environment for ore formation. A high concentration of iron oxides and intense silicification accompany the mercury mineralization in this part of the mine.

IMPLICATIONS FOR MERCURY EXPLORATION

Four structural and mineralogical features are significant in controlling mercury ore deposition at the Culver-Baer mine and may be useful for locating future ore:

1. Faults and secondary tensional fractures associated with faulting, especially flexures and fault intersections, are sites of ore deposition.
2. Silicified assemblage silica-carbonate rocks represent a second period of alteration of silica-carbonate rock that resulted in a brittle, easily fractured rock favorable to ore deposition.
3. Late quartz veining along secondary fractures appears to have accompanied one of the major periods of mercury deposition.
4. Iron oxides after pyrite and marcasite may accompany or form a halo around mercury ore bodies.

IMPLICATIONS FOR GEOTHERMAL EXPLORATION

1. At the Culver-Baer mine, selective and spotty distribution of hydrothermal alteration and mineralization suggests that hydrothermal fluids are not evenly distributed along fault or fracture planes. There may be impermeable zones along faults that do not readily transmit hydrothermal fluids, and thus by analogy, steam production from several wells located within the same fault may vary greatly. It is, therefore, suggested that differences in the steam production of individual wells in close proximity can be controlled by the nature of the fracturing in the vicinity of the well bore.
2. The most favorable locations for the occurrence of hydrothermal fluids are fault intersections and flexures along fault planes. The rock in such areas is more intensely fractured and therefore is a more permeable reservoir rock.
3. Hard brittle rocks are most easily fractured and can maintain open fractures for maximum transmission of hydrothermal fluids.
4. The degree of hydrothermal alteration and the presence of sulfides can be used during the drilling of geothermal wells to indicate fractured intervals and possibly to indicate the approach of a potential steam zone. I have found this method useful in predicting fracture reservoir locations in the Roosevelt steam field in Utah.
5. In the Geysers area, the fault planes are highly irregular, and so projections of the strike and dip of faults to depth are rarely accurate.
6. The main northwest-trending fault zones in the Geysers region, such as the Mercuryville fault zone, are not as significant to the steam reservoir as secondary north-northwest-, northeast-, and north-south-trending faults. These secondary faults and related fractures may be either "open" reservoir faults or tight. Movement along the main northwest-trending fault zones tends to maintain open secondary faults, and the density of secondary faulting is greater along and adjacent to the northwest-trending zones.

REFERENCES CITED

Bailey, E. H., 1946, Quicksilver deposits of the Western Mayacmas District, Sonoma County, California: California Journal of Mines and Geology, v. 42, no. 3, p. 199-230.

Dickson, F. W., and Tunell, George, 1959, The stability relations of cinnabar and metacinnabar: American Mineralogist, v. 44, p. 471-487.

—— 1968, Mercury and antimony deposits associated with active hot springs in the western United States, *in* Ridge, J. D., ed., Ore deposits of the United States, 1933-1967: American Institute of Mining, Metallurgical, and Petroleum Engineers, Graton-Sales Volume, v. 2, p. 1675-1701.

Goff, F. E., Donnelly, J. M., Thompson, J. M., and Hearn, B. C., 1977, Geothermal prospecting in The Geysers-Clear Lake area, northern California: Geology, v. 5, p. 509-515.

Henderson, F. B., III, 1969, Hydrothermal alteration and ore deposition in serpentinite type mercury deposits: Economic Geology, v. 64, no. 5, p. 489-499.

Isherwood, W. F., 1975, Gravity and magnetic studies of The Geysers-Clear Lake geothermal region, California, USA: United Nations Symposium on the Development and Use of Geothermal Resources, 2d, San Francisco, Proceedings, v. 2, p. 1065-1073.

Koenig, J. B., 1969, Mercury distribution at two geothermal fields: Coso Hot Springs, California and Ahuachapan, El Salvador [abs.]: Geological Society of America, Abstracts with Programs, p. 33.

Mankinen, E. A., 1972, Paleomagnetism and potassium-argon ages of the Sonoma Volcanics, California: Geological Society of America Bulletin, v. 83, no. 7, p. 2063-2072.

McLaughlin, R. J., 1975a, Preliminary field compilation of in-progress geologic mapping in The Geysers geothermal area, California: U.S. Geological Survey Open-File Report 75-198.

____ 1975b, Structure of Franciscan rocks in the central Mayacmas Mountains, Sonoma and Lake Counties, California: Geological Society of America Abstracts with Programs, v. 7, no. 3, p. 345.

____ 1977a, The Franciscan assemblage and Great Valley sequence in the Geysers-Clear Lake region of northern California: Geological Society of America, Cordilleran Section, Field Trip Guide to The Geysers-Clear Lake Area, p. 3-24.

____ 1977b, Late Mesozoic-Quaternary plate tectonics and The Geysers-Clear Lake geothermal anomaly, northern Coast Ranges, California: Geological Society of America Abstracts with Programs, v. 9, no. 4, p. 464.

McLaughlin, R. J., and Stanley, W. D., 1975, Pre-Tertiary geology and structural control of geothermal resources, The Geysers steam field, California: United Nations Symposium on the Development and Use of Geothermal Resources, 2d, San Francisco, Proceedings, v. 1, p. 475-485.

McNitt, J. R., 1968, Geology of the Kelseyville quadrangle, Sonoma, Lake and Mendocino Counties, California: California Division of Mines and Geology, Map Sheet 9.

Tonani, Franco, 1970, Geochemical methods of exploration for geothermal energy: Geothermics, Special Issue 2, v. 2, part 1, p. 492-515.

White, D. E., 1967, Mercury and base metal deposits with associated thermal and mineral waters, *in* Barnes, H. L., Geochemistry of hydrothermal ore deposits: New York, Holt, Rinehart and Winston, p. 575-627.

____ 1970, Geochemistry applied to the discovery, evaluation and exploitation of geothermal energy resources: Geothermics, Special Issue 2, v. 1, p. 58-80.

White, D. E., and Roberson, C. E., 1962 Sulphur Bank, California, a major hot spring quicksilver deposit: Geological Society of America, Buddington Volume, p. 397-428.

Yates, R. G., and Hilpert, L. S., 1946, Quicksilver deposits of eastern Mayacmas district, Lake and Napa Counties, California: California Journal of Mines and Geology, v. 42, no. 3, p. 231-286.

PRELIMINARY INVESTIGATION OF ACCESSORY ZIRCONS FROM VOLCANIC AND SEDIMENTARY ROCKS FROM CLEAR LAKE

By FREDERICK A. WILSON

ABSTRACT

A preliminary study was made of zircons from five samples of sedimentary and volcanic rocks from the Clear Lake volcanic field. The distributions of crystal types, size, degree of idiomorphism, and inclusions for each sample population were compared graphically and statistically.

The Franciscan assemblage and the Great Valley sequence underlie the volcanic field. Samples of Franciscan metagraywacke and Great Valley sandstone yield similar tan-colored zircon concentrates composed of colorless individual zircons that fluoresce. The two concentrates, however, have different size distributions. The andesite of Perini Hill yielded a pale-pink zircon concentrate made up of colorless, pale-pink, and pink zircons. Part of a large schistose xenolith from this andesite contains similar zircons, but many xenolith zircons show substantial overgrowths, and the size distribution is similar to that of the Franciscan sample. The pink zircon concentrate from a younger, coarsely porphyritic dacite of Horseshoe Bend contains pink, inclusion-filled, mainly euhedral zircons with a broad distribution of three crystal types that differ markedly from the other samples.

Although the number of samples in this study is limited, it is tentatively concluded that the Franciscan sample was deposited closer to its source than the Great Valley sample; the andesite of Perini Hill illustrates an intermediate stage in an assimilation process where the source of xenocryst zircons and the contaminant rock are still identifiable; and the broad distribution of zircon types in the dacite of Horseshoe Bend suggests a complex origin for the zircon population and the lava.

INTRODUCTION

Zircon studies provide an inexpensive method of exploring genetic relations between igneous rocks. The method is ideally suited to laboratories with limited facilities. The essential equipment consists of a microscope fitted with a mechanical stage, sieves, and rock crushers. The heavy liquids, bromoform and methylene iodide, may be substituted for by careful panning (Karakida, 1961, p. 62).

Most zircon studies of sedimentary rocks have dealt mainly with criteria for distinguishing between zircons of sedimentary and igneous origin (Poldervaart, 1955, 1956; Yamamoto and Matsukuma, 1964) and provenance of the sediments (Callender and Folk, 1958). The intensive investigations into the origin of granites (Reed and Gilluly, 1932; Taylor, 1937) led to the application of various quantitative analytical techniques to the study of zircons in plutonic rocks (Tomita, 1954; Larsen and Poldervaart, 1957; Yamamoto and Matsukuma, 1964) and subsequently to studies of zircons in volcanic and metamorphic rocks (Yamamoto, 1960; Karakida, 1961; Murthy, 1969).

Many of the previous studies are based on the assumption that in differentiating calc-alkaline magmas, zircon crystallizes early for a short period of time, yielding a characteristic zircon population throughout the entire pluton. The reduced major axis (RMA) is a statistical line fitted to a scatter plot of zircon measurements. According to Larsen and Poldervaart (1957, p. 547), the RMA is assumed to come nearest to expressing growth trends of zircons in some calc-alkaline rocks.

However, studies of hafnium-zirconium ratios (Hf/Zr) in zircons by Gottfried and Waring (1964) indicate that zircon crystallizes continuously throughout magmatic differentiation. Studies of xenoliths and contact zones of plutons (Gillson, 1925; Karakida, 1954; Taubeneck, 1957; Yamamoto and Matsukuma, 1964; Davis and others, 1968; Lee and others, 1968) show that secondary metamorphic zircons can form in country rock and different zircon populations can evolve in the marginal zones of plutons.

Because the origins of zircon populations in igneous rocks can be quite complex, it appears unlikely that the RMA's of most zircon populations represent only their growth trends. The RMA is, however, a valid description of the distribution of size in a zircon population and provides a graphical method of making comparisons with other zircon populations (Murthy, 1969, p. 42).

The methods of analysis most frequently described in the literature were employed in order to make the data comparable to previously published zircon studies. These preliminary results have revealed interesting trends that suggest hypotheses for further investigation.

ACKNOWLEDGMENTS

The sample of an inclusion from the andesite of Perini Hill was provided by C. B. Hearn, Jr. I thank D. Gottfried for many helpful discussions and suggestions which led to the formulation of this study, C. B. Hearn,

Jr., for his interest and advice during this study, and G. Mason for assistance with computer problems.

CLEAR LAKE VOLCANIC ROCKS

The volcanic rocks of Clear Lake, Calif., chronicle about 2.0 m.y. of quiet repetitive extrusion of basalt, andesite, dacite, and rhyolite. Pyroclastic deposits are a minor part of the total exposed volcanic section. All these rocks overlie the Franciscan assemblage of Late Jurassic to Eocene age and the Great Valley sequence of Late Jurassic to Late Cretaceous age.

Volcanic activity has generally migrated northward (Hearn and others, this volume). Some of the oldest andesites from the south-central part of the field contain numerous xenoliths, thus making contamination an important consideration in the theory of the origin of some Clear Lake lavas (Eichelberger, 1974; Brice, 1953; Anderson, 1936).

SAMPLES AND METHODS

Fifteen samples of volcanic and sedimentary rocks from the Clear Lake area (fig. 122) were collected from outcrops and float. Each sample of volcanic rock weighed approximately 40 kg; sedimentary samples were smaller.

SEPARATION METHODS

Rock samples were crushed using jaw crushers and rollers. They were then sieved, and the fraction larger than 40 mesh was recrushed by rollers and resieved. The total fraction of less than 40 mesh size was then processed on a Wilfley table to concentrate the heavy minerals. Further concentration by bromoform and (or) methylene iodide reduced the sample to minerals above specific gravity 3.3. Magnetite was removed with a hand magnet and the Frantz isodynamic separator was used to separate weakly magnetic minerals. The nonmagnetic sulfides and unwanted silicates were removed by gentle heating in a mixture of nitric and hydrofluoric acids. This process resulted in a relatively clean zircon concentrate.

Zircons, generally, are most abundant in coarse-grained acid igneous rocks; therefore, preliminary separations were made to determine which volcanic rocks would produce sufficient zircons for analysis. Obsidian from rhyolite of Borax Lake, basalt of Arrowhead Road, a vesicular glassy dacite of Clear Lake Park, and andesite of Boggs Mountain all yielded no zircons. Andesite of Seigler Canyon and hornblende andesite of Grouse Springs produced a few pink zircons. Coarsely porphyritic dacite of Horseshoe Bend, xenolith-rich andesite of Perini Hill, and the sedimentary rocks supplied sufficient zircons. These rocks, therefore, form the basis of this report. Only those samples which yielded zircons are listed in table 34 and shown in figure 124.

CLASSIFICATION

The zircon concentrates were immersed in a high-index-of-refraction liquid on a microscope slide and then placed under a cover glass. Linear traverses by mechanical stage were designed so that at least 200 zircons would be observed during a traverse of the entire slide. Each doubly terminated crystal falling under the crosshair was classified and its length and breadth was measured. Where this method failed to include approximately 200 zircons, all doubly terminated crystals on the entire slide were used (see table 35). Each crystal was classified according to its (1) crystal type, (2) size, (3) degree of idiomorphism, and (4) types of in-

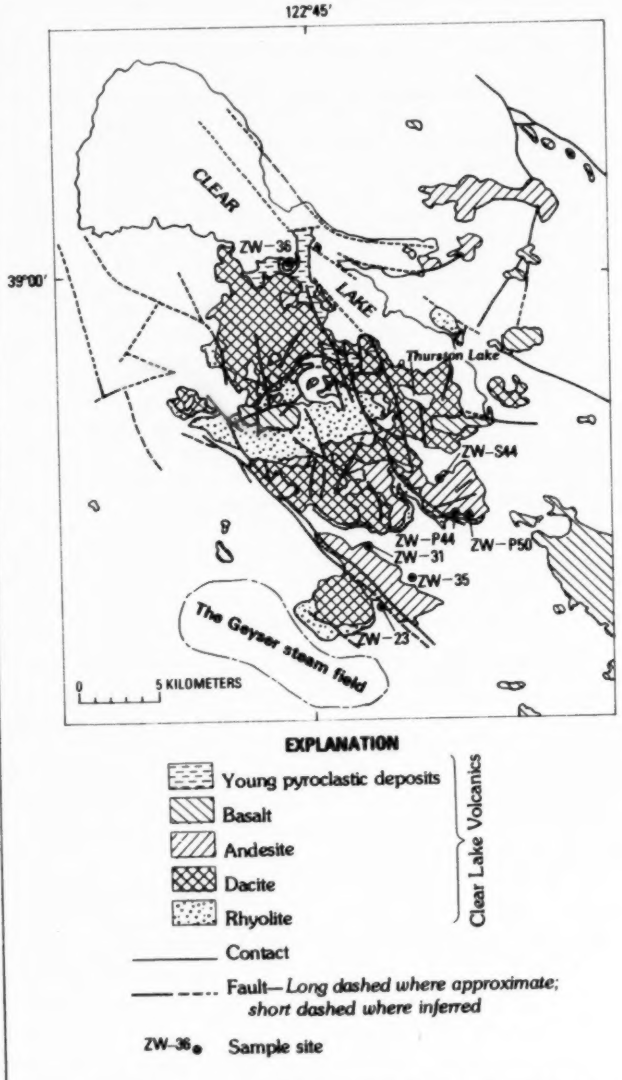

FIGURE 122.—Geologic map showing location of samples, Clear Lake, Calif., after Hearn, Donnelly, and Goff (1975) (see table 30).

clusions contained (figs. 123, 124). Other features such as color, fluorescence, zonation, and distinctive crystallographic structures such as basal edges (Murthy, 1969, p. 33) were noted but not quantitatively analyzed.

CRYSTAL TYPE

The following five crystal types are modifications of six crystal types devised by Yamamoto (1960, p. 87) which incorporate all the forms formerly used in classifications by Tomita and Karakida (1958) in studies of granitic rocks:

a. First-order prism with simple or complex dipyramid.

b. Second-order prism with simple or complex dipyramid.

c. Combination first- and second-order prisms and simple dipyramid.

d. Complex prism and complex dipyramid.

e. Crystal in which the C axis is the shortest.

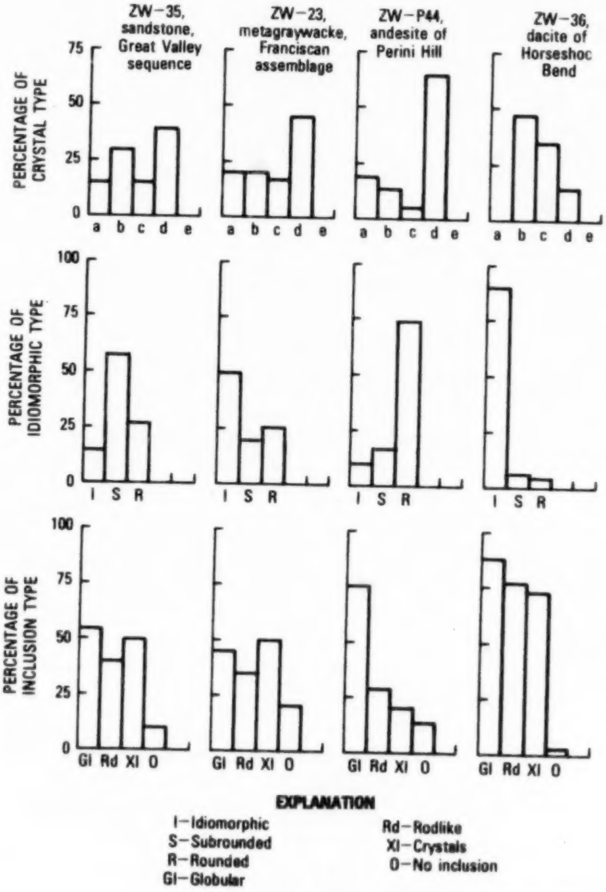

For explanation of crystal types see text

FIGURE 123.—Histograms of crystal type, idiomorphism, and inclusions of zircons from rocks from Clear Lake, Calif.

SIZE

Size data were analyzed by scatter plots, size-frequency curves, and reduced major axis (RMA), all of which have been widely used in studies to compare zircon populations visually. The RMA is a simple statistical method of identifying and comparing bivariate data which was described by Kermack and Haldane (1950, p. 30-41). Imbrie (1956) used RMA to describe growth trends in paleontologic populations, and Larsen and Poldervaart (1957) subsequently applied it to zircon populations. The RMA is used in this study solely as a line fitted to a scatter plot of length and breadth measurements to identify and compare zircon sample populations and not as an indicator of growth trends (Larsen and Poldervaart, 1957). Statistical data in table 35 were used to construct RMA's and make sample comparisons in table 36. The presence of more than one distinct zircon population in a sample is suggested by a bimodal or irregularly skewed size-frequency curve.

Calculations for the RMA were described by Imbrie (1956), Larsen and Poldervaart (1957), and Murthy (1969). An abbreviated description of these statistics is as follows:

1. Mean length, $\bar{x} = \Sigma(x)/N$, where N is the number of grains.
2. Mean breadth, $\bar{y} = \Sigma(y)/N$.
3. Mean elongation, $\bar{x}/\bar{y}$.

TABLE 34.—*Sample locations*

Sample	Rock type and map unit[1]	Age (m.y.)[2]	Location	Coordinates
ZW-36	Dacite of Horseshoe Bend.	.35	Soda Bay Road along Horseshoe Bend.	Long 122°46.00′ lat 39°00.30′
ZW-S44	Andesite of Seigler Canyon.	.96	Northwest side of Seigler Canyon Road 0.8 km north of Hobergs Airport.	Long 122°40.30′ lat 38°52.85′
ZW-P44	Andesite of Perini Hill.	.94 (approx)	North side of Perini Road at Diamond Flat 1 km south of Perini Hill.	Long 122°38.93′ lat 38°52.07′
ZW-31	Andesite of Grouse Spring.	1.49 to 1.60 (approx)	Grouse Spring, Boggs Mountain.	Long 122°40.54′ lat 38°50.70′
ZW-35	Unit IVb, sandstone, Great Valley sequence.	Late Cretaceous	Road 100, above quarry, Boggs Mountain.	Long 122°40.66′ lat 38°49.75′
ZW-23	Conglomeratic metagraywacke, Franciscan assemblage.	Jurassic to Cretaceous	0.5 km north of Whispering Pines.	Long 122°42.49′ lat 38°49.30′
ZW-P50	Xenolith in andesite of Perini Hill.	?	1.5 km south-southwest of Perini Hill.	Long 122°38.60′ lat 38°51.75′

[1] Volcanic units from Hearn, Donnelly, and Goff (1976a); Great Valley unit from Swe and Dickinson (1970); Franciscan unit from McLaughlin (1978).

[2] Ages of volcanic rocks from Donnelly-Nolan, Hearn, Curtis, and Drake (this volume).

TABLE 35.—*Statistical size data for zircon samples, Clear Lake*

	$\bar{x}$ (mm)	$\bar{y}$ (mm)	$\bar{x}/\bar{y}$	S_x (mm)	S_y (mm)	a	σa	θ	r	Dd (percent)	b	Number of zircons
ZW-23, metagraywacke, Franciscan assemblage	0.109	0.053	2.057	0.029	0.016	0.552	0.050	28.9°	0.650	22.9	−0.007	69
ZW-35, sandstone, Great Valley sequence	.107	.052	2.058	.029	.012	.414	.023	22.5°	.300	30.9	.008	295
ZW-36, dacite, Horseshoe Bend	.160	.067	2.388	.060	.024	.400	.018	21.8°	.682	29.7	.003	269
ZW-44, andesite, Perini Hill	.135	.066	2.045	.052	.022	.423	.021	22.9°	.609	33.2	.009	255
ZW-P50, inclusion, Perini Hill	.109	.053	2.056	.042	.021	.500	.046	22.6°	.828	22.7	−.001	37

TABLE 36.—*Z tests of reduced major axes of zircons from Clear Lake*

	ZW-23		ZW-35		ZW-36		ZW-P44	
	Z_a	Z_p	Z_a	Z_p	Z_a	Z_p	Z_a	Z_p
ZW-23, metagraywacke, Franciscan assemblage	--	--	--	--	--	--	--	--
ZW-35, sandstone, Great Valley sequence	2.51	--	--	--	--	--	--	--
ZW-36, dacite of Horseshoe Bend	2.86	--	0.48	1.32	--	--	--	--
ZW-P44, andesite of Perini Hill	2.38	--	.29	.53	0.83	2.16	--	--
ZW-P50, inclusion in andesite of Perini Hill	.77	.80	1.67	1.63	2.02	--	1.52	1.37

4. Standard deviation of length,

$$S_x = \sqrt{\Sigma(x-\bar{x})^2/N}.$$

5. Standard deviation of breadth,

$$S_y = \sqrt{\Sigma(y-\bar{x})^2/N}.$$

6. Correlation coefficient,

$$r = \Sigma(x-\bar{x})(y-\bar{y}) / \sqrt{\Sigma(x-\bar{x})^2\Sigma(y-\bar{y})^2},$$

which is a measure of how closely the two variables are related.

7. Correlation of relative dispersion about the RMA,

$$Dd = 100\sqrt{2(1-r)\,(S_x^2+S_y^2)\,/\,(\bar{x}^2+\bar{y}^2)}$$

which expresses the percentage of relative scatter of points about the RMA.

8. Tangent of the angle at which the RMA is drawn through point $(\bar{x},\bar{y})$, $a = S_y/S_x$.
9. The angle of slope in degrees, θ.
10. RMA intercept of the y axis, $b = \bar{y} - a\bar{x}$.
11. Standard error of slope,

$$\sigma_a = a\sqrt{(1-r^2)/N},$$

which is a measure of the sample slope reliability as an estimate of the actual population. The smaller the standard error, the more reliable the estimate.

Because the samples are large, Z tests are employed to compare RMA's at a 95-percent confidence level. The essential elements of the RMA are slope and position.

12. Comparison of slope:

$$Z_a = a_1 - a_2 / \sqrt{\sigma_{a_1}^2 + \sigma_{a_2}^2}$$

where a_1 and a_2 are the RMA slopes of the compared samples. If $Z_a > 1.96$, the difference is considered significant, and a comparison of position need not be made. If $Z_a < 1.96$, a comparison of position is to be calculated.

13. Comparison of position:

$$\mathrm{Zp} = \frac{x_0(a_1 - a_2) + (b_1 - b_2)}{\sqrt{\sigma_{a_1}^2 (x_0 - x_1)^2 + \sigma_{a_2}^2 (x_0 - x_2)^2}}$$

In this study the value of x_0 has been arbitrarily set at 0.4. If $Z_p > 1.96$, there is a significant difference between the two RMA's and, therefore, between the two populations.

The RMA's are presented in figure 124. Other data presented are scatter plots (fig. 125), elongation-frequency curves (fig. 126), length-frequency curves (fig. 127), and breadth-frequency curves (fig. 128).

DEGREE OF IDIOMORPHISM

Zircons were classified according to their degree of idiomorphism as (1) euhedral, if the edges were straight and corners were sharp; (2) subrounded, if the edges were rounded to any degree and if the crystal type could be identified, and (3) rounded, if no identification of the crystal type could be made.

Rounding in zircon populations has been ascribed to both sedimentary and magmatic processes. Karakida (1964, p. 140-141) concluded, when comparing igneous and sedimentary zircon populations, that the rounding of smaller zircons in a population may serve as a criterion for magmatic corrosion; but the rounding of zircon in xenoliths is directly related to the degree of alteration of the xenolith. According to Yamamoto and Matsukuma (1964, p. 51), rounded zircons in plutonic rocks are derived from "foreign rocks." Intrusive granites which contain a high proportion of rounded zircons may be highly contaminated (Poldervaart, 1956, p. 532). In this study, the andesite of Perini Hill, which contains numerous xenoliths and predominantly rounded zircons, may illustrate an intermediate stage in the contamination process where the sources of xenocryst zircons and contaminant rocks are still identifiable.

INCLUSIONS

Zircons from the volcanic rocks are characterized by numerous rodlike crystals, fluid inclusions, and globular masses of black or brown opaque material. Although zonation by color or by difference in refractive index is lacking, parallel orientation of rodlike inclusions in some crystals outlines zones of crystal growth. Zircon populations from the sedimentary rocks contain fewer inclusions per zircon, and most of these inclusions are minute crystals; distinct zonation is common.

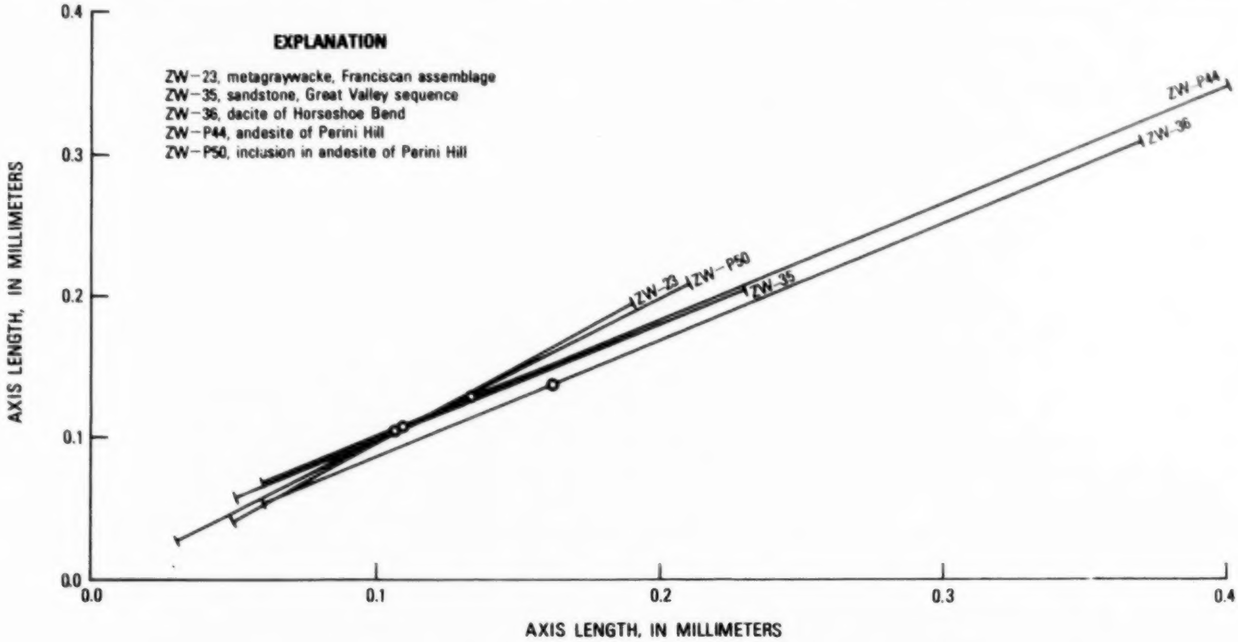

FIGURE 124.—Reduced major axes (RMA) of zircons from rocks from Clear Lake, Calif.

and some crystals have clear overgrowths; and there is a higher frequency of clear zircons with no inclusions. Zircons from dacite are crowded with numerous randomly oriented rodlike inclusions.

RESULTS

SEDIMENTARY ROCKS

Sample ZW-23 is light-brown conglomeratic metagraywacke from the Franciscan assemblage taken from about 25 m below the contact with andesite on the south side of Boggs Mountain (fig. 122). The zircon concentrate contains 90 percent angular zircon fragments and only yielded 69 doubly terminated predominantly euhedral zircons (table 35). Sample ZW-35 is brown fine-grained graywacke in the Great Valley sequence from the north side of Boggs Mountain (fig. 122). It yielded a concentrate with 70 percent zircon fragments.

The high proportion of zircon fragments in these

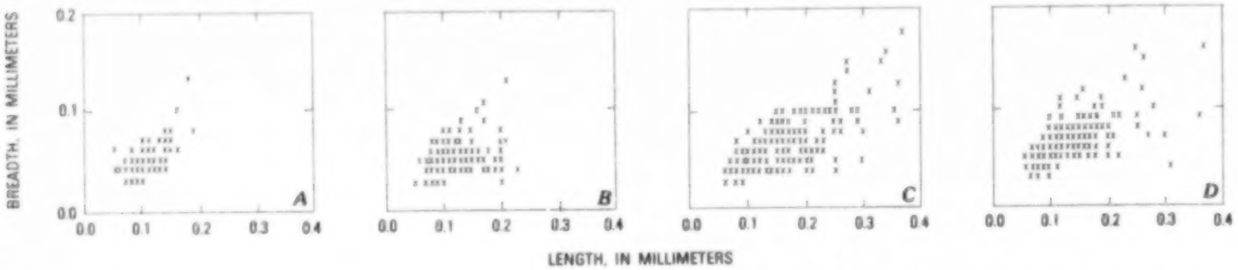

FIGURE 125.—Scatter plots of zircon sample populations, Clear Lake, Calif. *A*, Franciscan assemblage. *B*, Great Valley sequence. *C*, Dacite of Horseshoe Bend. *D*, Andesite of Perini Hill.

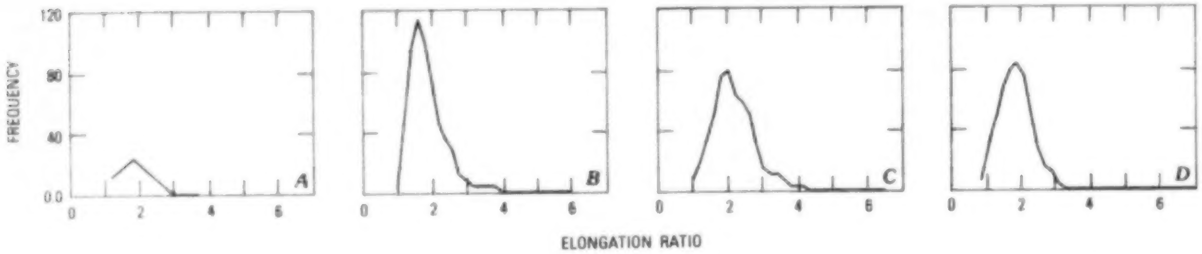

FIGURE 126.—Elongated-frequency curves of zircon sample populations, Clear Lake, Calif. *A*, Franciscan assemblage. *B*, Great Valley sequence *C*, Dacite of Horseshoe Bend. *D*, Andesite of Perini Hill.

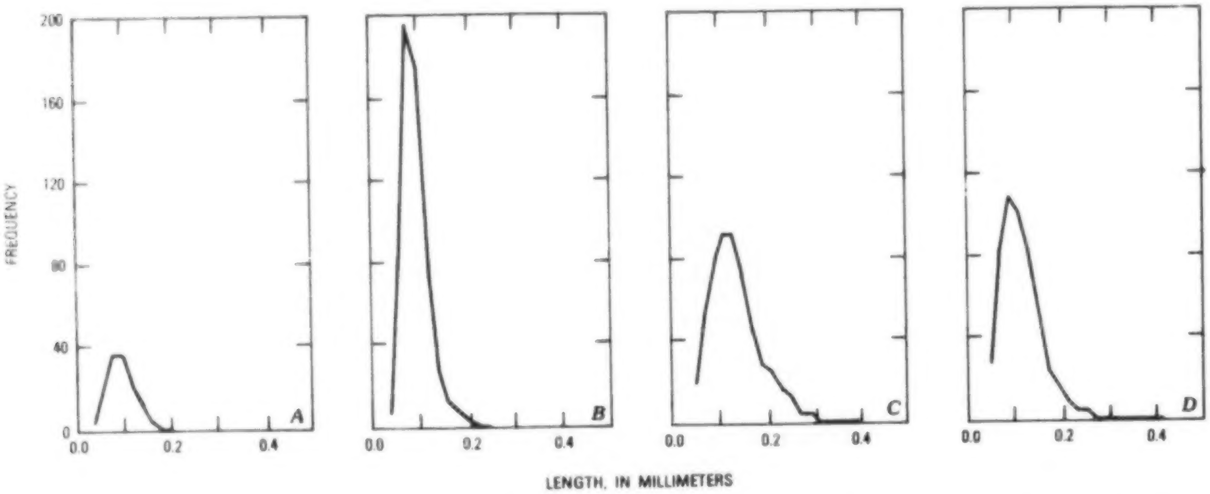

FIGURE 127.—Length-frequency curves of zircon sample populations, Clear Lake, Calif. *A*, Franciscan assemblage. *B*, Great Valley sequence. *C*, Dacite of Horseshoe Bend. *D*, Andesite of Perini Hill.

samples raises the question whether the zircon crystals were broken in the crushing process, during transportation and deposition, or by processes operating on the source rock. Larsen and Poldervaart (1957, p. 551, 553) investigated the effect of the extraction process. They found that the largest zircons of high elongation are broken during crushing, but these crystals are generally few in number. Finer crushing liberated 3-4 times as many zircons with no significant difference in the proportion of broken crystals. In sedimentary processes, zircons are broken and rounded until a size is reached where further fragmentation is ineffective (Poldervaart, 1968, p. 7). Viswanathan (1968, p. 133-137) concluded that there was no significant difference in the number of broken zircon crystals in the sheared and the unsheared areas of soda granite of the Singhbum District, Bihar, India. Sedimentary processes appear to be the major agent affecting the proportion of fragments in these zircon populations.

Both Great Valley (ZW-35) and Franciscan (ZW-23) samples yielded tan-colored zircon concentrates of colorless individual zircons that fluoresce. These concentrates also have a large proportion of crystal inclusions, some opaque cores with clear overgrowths, and many inclusion-free zircons. Maxima of size-frequency curves (figs. 126-128) and the distribution of crystal types (fig. 123) are similar. Both populations contain dominantly *D*-type crystals. These factors could indicate a similar source area for both populations, but *Z* tests of RMA slopes (Za = 2.51, table 36) indicate dissimilar size distributions. The scatter plot (fig. 125) and the elongation frequency curve of the Great Valley sample (fig. 126) show a substantial number of zircons of relatively high elongation; these are not present in the Franciscan sample. The Great Valley population is composed of mainly subrounded zircons with a smaller mean length and breadth, whereas the Franciscan population is dominantly euhedral with a greater mean length and breadth. This appears to be a reflection of the depositional environment and could indicate that the Franciscan sample was closer to its source than the Great Valley sample. Zircon studies involving systematic sampling from Franciscan and Great Valley sedimentary rocks may result in a better identification of formation units and a better understanding of sediment sources.

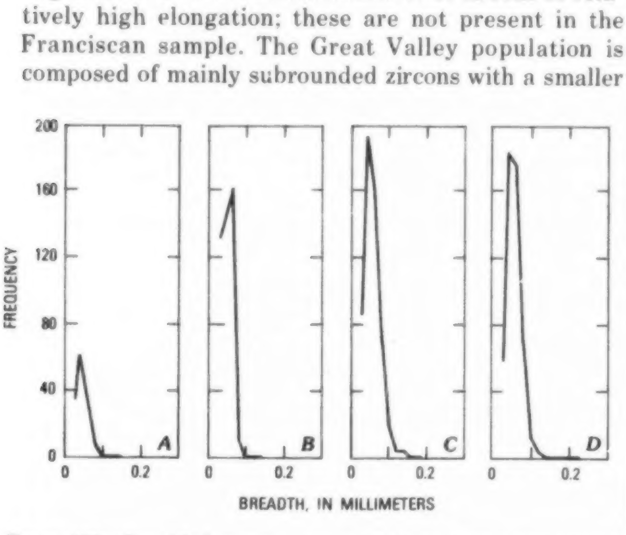

FIGURE 128.—Breadth-frequency curves of zircon sample populations, Clear Lake, Calif. *A*, Franciscan assemblage. *B*, Great Valley sequence. *C*, Dacite of Horseshoe Bend. *D*, Andesite of Perini Hill.

Z tests (table 36) show a statistical relationship between the Great Valley sample (ZW-35) and all of the volcanic rocks. The Franciscan sample (ZW-23) is only similar to the inclusion (ZW-P50) in andesite of Perini Hill.

ANDESITE

The andesite of Perini Hill (ZW-P44, table 34) was the only andesite sampled that yielded abundant zircons. It is a dark-gray rock, about 0.94 m.y. old, characteristically rich in schistose to granular tabular and rounded xenoliths 1-15 cm in size. The pale-pink zircon concentrate from this rock is a mixture of predominantly rounded colorless, pale-pink, and pink zircons. The distribution of crystal types, predominance of *D*-type crystals, size-frequency maxima (figs. 126-128), RMA slope (fig. 124), *Z* tests (table 36), and large proportion (15 percent) of inclusion-free zircons (fig. 123) are remarkably similar to the underlying sandstone populations.

Brice (1953, p. 41) described a large xenolith composed of $2\frac{1}{2}$-cm lenses and bands of quartz separated by finer grained garnetiferous red and gray laminae. A 152-g sample (ZW-P50) of a similar xenolith yielded 37 predominantly rounded zircons that are colorless, pale pink, and pink. Most of the zircons (34 of 37) are rounded. There is a large proportion of inclusion-free zircons. Many zircons have substantial overgrowths with rounded and irregular outlines. *Z* tests (table 36) show that the inclusion's zircon size distribution is statistically the same as the Franciscan ($Z_a = 0.77$, $Z_p = 0.80$; ZW-23), the andesite ($Z_a = 1.52$, $Z_p = 1.37$; ZW-P44), and the Great Valley ($Z_a = 1.67$, $Z_p = 1.63$; ZW-35) samples; the Franciscan sample shows the closest comparison to the inclusion.

The mineral assemblage of this type of xenolith places it in the pyroxene hornfels facies (Brice, 1953, p. 41). Taubeneck (1957) observed that zircons in argillaceous sediments developed euhedral overgrowths in the pyroxene hornfels facies. All zircon concentrates recovered from the Clear Lake Volcanics contained pink zircons, and only colorless zircons were recovered from sedimentary rocks. Therefore, the variation in color in the zircons from the xenolith and the Perini

Hill sample may be the result of some zircons reaching equilibrium with the environment of the enclosing magma (Karakida, 1967, p. 422).

It has been suggested by Brice (1953, p. 42) that quartz-rich inclusions, such as those studied, may account for the numerous quartz xenocrysts in Clear Lake basic lavas. Since other xenoliths may be as rich in zircon as the sampled xenolith and because zircon is a highly refractory mineral, residual zircons may also be localized near quartz xenocrysts. Although the data are limited, it appears that the andesite of Perini Hill is an intermediate stage in the assimilation of zircon xenocrysts into a magma.

DACITE

The dacite of Horseshoe Bend (ZW-35, table 34) is located low on the north side of Mount Konocti. Mount Konocti is underlain by the Franciscan assemblage, and the Great Valley sequence is absent (Goff and others, 1977, p. 513). The sample is from pink, massive, porphyritic dacite 0.35 m.y. old with 1-10-mm feldspar and quartz phenocrysts. Its zircon concentrate is pink and contains pink inclusion-filled euhedral zircons with a broad distribution of three crystal types (fig. 123) that differ markedly from other samples.

The high percentage of euhedral zircons (fig. 123) may appear to be an indication of uncontaminated lava (Yamamoto, 1960, p. 96-97), but the broad distribution of zircon types suggests contributions of zircons from more than one origin. One would expect a single crystal type to be dominant in an uncontaminated lava (Yamamoto and Matsukuma, 1964).

The RMA of the dacite parallels the slope of the andesite ($Z_a = 0.53$, ZW-P44, table 36; fig. 124) and the Great Valley sample ($Z_a = 0.48$, ZW-35) but the comparison of position ($Z_p = 1.32$, ZW-35) indicates that only the Great Valley sample has a similar zircon size distribution. However, the distribution of crystal types, degree of idiomorphism, and inclusions (fig. 123) are dissimilar to the Great Valley and andesite samples. The inclusions and high degree of idiomorphism show limited similarity to the Franciscan sample.

This preliminary sample suggests that the zircon population of the dacite of Horseshoe Bend has a complex origin and could include zircon xenocrysts from adjacent rocks or magmas. According to Anderson (1936, p. 647), the dacite lavas of Mount Konocti contain large phenocrysts of quartz with reaction rims and phenocrysts of sanidine, but sanidine is not present in the groundmass. The reaction rims on quartz represent disequilibrium. The absence of sanidine in the groundmass indicates that sanidine did not crystallize from the melt. Anderson proposed a mixing of magmas to account for the dual character of the lavas. This theory could explain the mixed population of zircons in the dacite of Horseshoe Bend. However, if the zircon population is largely influenced by zircon xenocrysts, size statistics could indicate that assimilation of Great Valley sandstone may have been involved in producing the dacite lava.

CONCLUSIONS

In view of the limited number of samples described in this report, only tentative conclusions may be drawn:

1. Silicic rocks of the Clear Lake Volcanics that contain coarse quartz and feldspar phenocrysts, and basic lavas that contain abundant zircon-rich xenoliths, are most likely to yield abundant zircons.
2. The size distribution of zircons in the Franciscan and Great Valley samples may reflect depositional environment and could indicate that the Franciscan sample was closer to its source than the Great Valley sample.
3. The andesite of Perini Hill appears to illustrate an intermediate stage in an assimilation process where the source of xenocryst zircons and the contaminant rock are still identifiable.
4. A predominance of rounded zircons of various colors in volcanic rock may be an indication of contamination.
5. The broad distribution of zircon types in the dacite of Horseshoe Bend suggests a complex origin for the zircon population and the lava.

REFERENCES CITED

Anderson, C. A., 1936, Volcanic history of the Clear Lake, California: Geological Society of America Bulletin, v. 47, p. 629-664.

Brice, J. C., 1953, Geology of Lower Lake quadrangle, California: California Division of Mines Bulletin 166, 72 p.

Callender D. L., and Folk, R. L., 1958, Idiomorphic zircon, key to volcanism in the lower Tertiary sands of Central Texas: American Journal of Science, v. 256, p. 257-269.

Davis, G. L., Hart, S. R., and Tilton, G. R., 1968, Some effects of contact metamorphism on zircon ages: Earth and Planetary Science Letters, v. 5, no. 1, p. 27-34.

Eichelberger, J. C., 1974, Magma contamination within the volcanic pile: Origin of andesite and dacite: Geology, v. 2, no. 1, p. 29-33.

Gillson, J. L., 1925, Zircon, a contact-metamorphic mineral in the Pend Oreille district, Idaho: American Mineralogist, v. 10, p. 187-194.

Goff, F. E., Donnelly, J. M., Thompson, J. M., and Hearn, B. C., Jr., 1977, Geothermal prospecting in The Geysers-Clear Lake areas, northern California: Geology, v. 5, p. 509-515.

Gottfried, David, and Waring, C. L., 1964, Hafnium content and Hf/Zr ratio in zircon from the southern California batholith: U.S. Geological Survey Professional Paper 501-B, p. B88-B91.

Hearn, B. C., Jr., Donnelly, J. M., and Goff, F. E., 1975, Preliminary geologic map of the Clear Lake volcanic field, Lake County, California: U.S. Geological Survev Open-File Report 75-391, scale 1:24,000.

____ 1976a, Geology and geochronology of the Clear Lake Volcanics, California: U.N. Symposium on the Development and Use of Geothermal Resources, 2nd, San Francisco, 1975, Proceedings, v. 1, p. 423-428.

—— 1976b, Preliminary geologic map and cross-section of the Clear Lake volcanic field, Lake County, California: U.S. Geological Survey Open-File Report 76-751.

Imbrie, John, 1956, Biometrical methods in the study of invertebrate fossils: American Museum of Natural History Bulletin, v. 108, pt. 2, p. 211-252.

Karakida, Y., 1954, The presence of "Zircon Zone" along a Cretaceous granodiorite-granite contact in North Kyushu: Geological Society of Japan Journal, v. 60, no. 711, p. 517-532.

—— 1961, Zircon overgrowths in the Ryoke metamorphic zone of the Yana area, southwest Japan: Kyushu University, Faculty of Science Memoirs, ser. D., Geology, v. 10, no. 2, p. 59-72.

—— 1964, Magmatic corrosion, Petrological studies of naturally heated zircons, part III: Studies in Literature and Science, Seinan Gakuin University, v. 4, no. 2, p. 121-143.

—— 1967, Color changes in xenolith zircons, petrological studies of naturally heated zircons, Part IV: Geological Society of Japan Journal, v. 73, no. 9, p. 419-428.

Kermack, K. A., and Haldane, J. B. S., 1950, Organic correlation and allometry: Biometrika, v. 37, Parts 1 and 2, p. 30-41.

Larsen, L. H., and Poldervaart, Arie, 1957, Measurement and distribution of zircons in granitic rocks of magmatic origin: Mineralogical Magazine, v. 31, no. 238, p. 544-564.

Lee, D. C., Stern, T. W., Mays, R. E., and Van Loenen, R. E., 1968, Accessory zircons from granitoid rocks of the Mount Wheeler Mine area, Nevada: U.S. Geological Survey Professional Paper 600-D, p. D197-D203.

McLaughlin, R. J., 1978, Preliminary geologic map and structural sections of the central Mayacmas Mountains and the Geysers steam field, Sonoma, Lake, and Mendocino Counties, California: U.S. Geological Survey Open-File Report 78-389.

Murthy, M. V. N., ed., 1969, Zircon: Geological Survey of India Miscellaneous Publication 9, 236 p.

Poldervaart, Arie, 1955, Zircons in rocks; 1, Sedimentary rocks: American Journal of Science, v. 253, p. 433-461.

—— 1956, Zircons in rocks; 2, Igneous rocks: American Journal of Science, v. 254, p. 521-554.

—— 1963, Zircons in rocks, *in* Murthy, M. V. N., ed., Zircon: Geological Survey of India Miscellaneous Publication 9, p. 1-24.

Reed, J. C., and Gilluly, James, 1932, Heavy mineral assemblages of some of the plutonic rocks of eastern Oregon: American Mineralogist, v. 17, no. 6, p. 201-220.

Smithson, F., 1939, Statistical methods in sedimentary petrology: Geological Magazine, v. 76, pt. 2, p. 348-361.

Swe, Win, and Dickinson, W. R., 1970, Sedimentation and thrusting of Late Mesozoic rocks in the Coast Ranges near Clear Lake, California: Geological Society of America Bulletin, v. 81, p. 165-189.

Taubeneck, W.H., 1957, Zircons in the metamorphic aureole of the Bald Mountain batholith, Elkhorn mountains, northeastern Oregon [abs.]: Geological Society of America Bulletin, v. 68, p. 1803.

Taylor, J. H., 1937, A contribution to the study of accessory minerals of igneous rocks: American Mineralogist, v. 22, p. 686-700.

Tomita, T., 1954, Geologic significance of the color of granite zircon: Kyushu University Faculty of Science Memoirs Series D., Geology, v. 6, no. 2.

Tomita, T., and Karakida Y., 1958, Source identification of some granitic xenoliths in volcanic rocks: Kyushu University Faculty of Science Memoirs, Series D, Geology, v. 8, no. 2, p. 25-34.

Viswanathan, T. V., 1968, Zircon studies of soda granite from Mosaboni Mines, Singhbhum District, Bihar, *in* Murthy, M. V. N., ed., Zircon: Geological Survey of India Miscellaneous Publication 9, p. 130-137.

Yamamoto, Takashi, 1960, A study of andesite zircons from Hisatsu volcanic area, Kyushu: Bulletin of the Kyushu Institute Technology (Mathematics and Natural Sciences), no. 6, pt. 3, p. 81-97.

Yamamoto, Takashi, and Matsukuma, K., 1964, A study of zircons in granites and granitic rocks: Bulletin of the Kyushu Institute Technology (Mathematics and Natural Sciences), no. 11, p. 33-53